EFFECT OF STACKING SEQUENCE AND FIBER ORIENTATION ON THE STRESS-STRAIN BEHAVIOR OF CFRP CONFINED CONCRETE CYLINDERS

by
Ahmed Sulaiman

Thesis submitted to the
Faculty of Graduate Studies and Research
in partial fulfillment of the requirements for the degree of
Master of Applied Sciences
in Civil Engineering

Under the auspices of the Ottawa-Carleton Institute for Civil Engineering

uOttawa

University of Ottawa
February 2016

Abstract

A limited number of studies have been conducted in the literature to examine the effect of stacking sequence and fiber orientation on the compressive behavior of fiber reinforced polymer (FRP) confined concrete. This thesis presents the results of an experimental investigation examining the effect of parameters such as fiber orientation, amount of confinement, and specimen size on the behavior of FRP-confined concrete. As part of the experimental study, a large set of concrete cylinders having two different sizes (100 mm x 200 mm and 150 mm x 300 mm) were jacketed with carbon fiber reinforced polymer (CFRP) sheets having various orientations and tested under pure axial compressive loading. The specimens were confined using various CFRP stacking sequences, with fibers oriented at 0°, 90°, and ±45° (both unidirectional and woven). Furthermore, within each stacking sequence, the numbers of layers was varied between 4, 6, and 8 to examine the impact of number of plies on the behavior of the FRP-confined concrete cylinders. In addition, the research program included a large number of CFRP coupons made from CFRP laminates having the same properties as the CFRP jackets used in the strengthening of the cylinder series. The analytical program assesses the accuracy and suitability of using various FRP confinement models in the literature to predict the stress-strain response of the confined cylinders tested in the experimental program. The results indicate that parameters such as fiber orientation, stacking sequence, number of confinement layers and specimen size have a direct impact on the strength, ductility and stress-strain behavior of CFRP confined concrete. However, the level of influence varies from one parameter to the other, with the results demonstrating that fiber orientation has a more noticeable effect when compared to the other parameters. The results of the analytical program demonstrate the need to develop reliable confinement models which can take into account the effects of fiber orientation.

Acknowledgement

I would like to express my deepest and sincere gratitude to my supervisors Dr. Hassan Aoude, and Dr. Husham Almansoor (Associate Researcher at the NRC), for their continued guidance, advice, helpful criticism and patience throughout the course of this research project.

A large amount of work presented in this thesis was conducted at the National Research Council Canada (NRC). I am grateful for the opportunity to have benefited from this experience and for the support provided by the NRC during my research study.

The experimental program was conducted in the structural laboratories of the National Research Council Canada (NRC), University of Ottawa, and McGill University. Help and instructions from Dr. Muslim Majeed and Dr. Gamal Elnabelsya (UOttawa), Mr. Jim Margeson and Dr. Omran Maadani (NRC), and Dr. William D. Cook (McGill) are gratefully acknowledged.

I would like to thanks the help, advice and friendship of many friends at the University of Ottawa. Special thanks go to Omar Algassem, Tommy Hains, Corey Guertin-Normoyle, and Yang Li, thank you all for all kind of supports.

This thesis is dedicated to my family especially my wife and my lovely children. This thesis won't be completed without their love and support in every minute of my research. Finally, I would like to express my gratitude to my parents whom encouraged me always.

Table of contents

List of Figures

List of Tables

Notations

Notations	Definition
a_1	Coefficient in the model by Miyauchi et al. (1999)
b_1	Coefficient in the model by Miyauchi et al. (1999)
c_1	Constant in the stress enhancement expression
c_2	Constant in the stress enhancement expression
D	Diameter of circular specimens
E_1	The first slope of the FRP confined concrete stress-strain curve
E_2	The second slope of the FRP confined concrete stress-strain curve
E_{FRP}	Elastic modulus of FRP jacket
E_c	Concrete modulus of elasticity
E_{co}	Initial tangent modulus of concrete
E_l	Lateral confining stiffness = $2.E_{FRP}.n_{FRP}/D$
f_{FRP}	Ultimate tensile stress of FRP jacket
$f_{cc'}$	Peak axial compressive stress of FRP confined concrete
f_c	Axial compressive stress of concrete
f_{c1}	Axial compressive stress of FRP confined concrete at first peak
f_{co}	Peak axial compressive stress of unconfined concrete
f_{cu}	Axial compressive stress of FRP confined concrete at ε_{cu}
f_l	Lateral confining pressure
$f_{lu,a}$	Actual lateral confining pressure at ultimate
f_o	Concrete axial stress at kink point of stress-strain curve
K_1	FRP confinement stiffness
k_1	Axial stress enhancement coefficient
k_2	Axial strain enhancement coefficient

k_{lo}	FRP stiffness threshold
k_{ε}	Hoop strain reduction factor
m	Parameter in model proposed by Youssef et al. (2007)
m_1	Parameter in model proposed by Fahmy and Wu (2010)
m_2	Parameter in model proposed by Fahmy and Wu (2010)
n	Parameter in the expression for predicting confined concrete stress
n_{FRP}	Total thickness of FRP jacket
ε_c	Axial strain of concrete
ε_{c1}	Axial strain of FRP confined concrete at f_{c1}
ε'_{cc}	Maximum axial strain of FRP confined concrete
ε_{co}	Axial strain of unconfined concrete
ε_{cu}	Ultimate axial strain of FRP confined concrete
ε_{FRP}	Ultimate tensile strain of FRP jacket
$\varepsilon_{h,rup}$	Hoop rupture strain of FRP jacket
ε_{l1}	Lateral strain of concrete at f_{l1}
ε_o	Axial strain corresponding ε_o
ε_t	Transition strain
μ_{tu}	Average tangent dilation rate of FRP confined concrete at ε_{cu}
λ	Parameter in model proposed by Miyauchi et al. (1999)

1 Chapter 1: Introduction

1.1 Introduction

1.1.1 FRP jacketing - an innovative solution to retrofit reinforced-concrete columns

Extensive research and numerous earthquakes have demonstrated the vulnerability of poorly detailed reinforced concrete columns under seismic loads, the failure of which can cause structural collapse and catastrophic failures. **Figure 1-1** shows typical column failures observed in past earthquakes, where large tie spacing and poor detailing, leads to loss of column capacity under cyclic load reversals. The 1989 Loma Prieta earthquake, the 1994 Northridge earthquake and the 1995 great Hanshin earthquake provide clear examples of the human and economic losses that can result from the failure of critical concrete infrastructure during such events. It is now well understood that performance of reinforced concrete columns, in terms of strength and ductility, is strongly influenced by the detailing of internal steel reinforcement. As a result of this understanding, modern codes impose stringent requirements for the detailing of transverse reinforcement in columns in seismic regions. Unfortunately, a large stock of existing buildings and bridges in seismic regions were designed prior to the development of such codes, and there exists an important need to develop methods to retrofit the columns in such vulnerable structures.

Strength and ductility of concrete columns increases by improving lateral confinement. In the past steel and concrete jackets were utilized to improve the confinement of columns in existing structures. These jacketing techniques can result in significant improvement in column behavior, however these methods are not always ideal because they are labor-intensive, in addition to issues related to corrosion and deterioration.

In the past three decades the popularity of fiber reinforced polymers (FRP) has increased in civil engineering applications due to their favorable properties which include: high strength-to-weight ratio, corrosion resistance, and high versatility which allows for ease of constriction. Structural members which can be strengthened externally with FRP include columns, beams, slabs, walls, and joints, and the strengthening is applicable to concrete, steel, masonry, and timber structures.

In the case of reinforced concrete columns, application of externally-bonded FRP jacketing results in significant enhancement in strength and overall energy-dissipation capacity due to the ability of FRP to enhance confinement of the concrete cross-section (Sheikh et al. 2007). Over the years, a large number of studies have been conducted to examine the behavior of FRP-confined concrete, ranging from a large number of studies on small-scale cylinders as well as larger-scale reinforced concrete columns. The research has allowed for the development of numerous FRP confinement models and the development of design guidelines in codes of practice such as the Canadian CSA S806 Standard (Design and construction of building structures with fiber-reinforced polymers).

Figure 1-1 Typical concrete column failure due to poor confinement

1.1.2 Research motivation

The models and design equations related to FRP confinement have been calibrated based on extensive data generated in previous research studies. Unfortunately many of these studies have only considered a limited number of test variables, which have typically including FRP material type (e.g. CFRP or GFRP), number of FRP plies and concrete strength (with most data related to normal-strength concrete). The majority of studies have also only considered the effect of unidirectional FRP, applied in the hoop direction. With the development of new manufacturing methods and technologies more complex FRP composite systems are now possible, where fiber alignment within the FRP matrix can be optimized for improved performance. The behavior of concrete columns reinforced with such innovative FRP systems is unclear and there is a need to explore the effect of fiber orientation and FRP layup configuration on the stress-strain behavior of FRP-confined concrete. There is also a need to examine the applicability of existing FRP confinement models to predict the stress-strain response of concrete sections retrofitted with such systems.

1.2 Research objectives

The primary objective of this thesis is to examine the effect of fiber orientation and FRP layup configuration and sequence on the stress-strain performance of concrete specimens confined with external carbon fiber reinforced polymer (CFRP) jacketing. This objective is achieved by studying the influence of fiber orientation and FRP stacking sequence on CFRP laminate behavior in tension and the stress-strain behavior of CFRP confined concrete cylinders under compressive axial loading. A secondary objective is to examine the suitability of existing FRP confinement models to predict the stress-strain response of cylinders confined with CFRP jackets

having variable fiber orientation and layup configurations. The details of the research program are summarized below.

1.2.1 Experimental program

As part of this study a total of 169 concrete cylinders are externally confined with CFRP jackets and tested under uniaxial compression loading. Parameters considered in this study include the effect of fiber orientation (0^o, 45^o, 90^o), fabric type (unidirectional and woven), number of FRP layers (4, 6 and 8 layers), stacking/layup sequence and concrete cylinder size (100 mm and 150 mm diameter). In addition the study includes a companion set of 195 CFRP coupons, made from laminates having the same properties as the CFRP jackets used in the cylinder series, which are tested under uniaxial tension load. The cylinder and coupon specimens were batched into 9 different groups based on their fiber orientation, with the number of CFP layers varied within each series.

The effectiveness of the various FRP confinement layups is assessed by comparing the stress-strain response of the FRP-confined cylinders to the response of control cylinders without confinement. The effect of the test parameters (effect of number of layers, specimen size, fiber orientation, and stacking sequence) is examined by comparing the stress-strain response of the specimens qualitatively and quantitatively using various stress-strain indicators such as the increase in peak stress, peak strain, toughness and ductility. In addition, the effect of the parameters is also assessed by examining the failure modes of companion specimens having different FRP layup configurations.

1.2.2 Analytical program

The design of columns retrofitted with FRP jacketing requires reliable and accurate modeling of the stress-strain behavior of FRP-confined concrete (Cui, 2009). The majority of existing models have been calibrated based on data which does not include specimens having FRP jackets with varying fiber orientations or complex layups. The analytical program of this thesis assesses the applicability of existing FRP confinement models to predict the stress-strain response of the large set of cylinders tested in the experimental program. As part of the study a total of 11 models are first described and then used to predict the experimental stress-strain curves of the cylinders in the 9 series considered in this research study.

1.2.3 Organization

This thesis is organized in 7 chapters:

- Chapter 1 introduces the significance of this thesis, describes the objectives and scope of the research program;
- Chapter 2 provides a literature review which summarizes previous research that has been conducted on the stress-strain behavior of FRP-confined concrete. After reviewing the effect of important variables which affect stress-strain response previous studies which have examined the effect of FRP fiber orientation are also summarized;
- Chapter 3 describes the experimental program which and provides information on the test matrix, specimen properties, materials properties, construction, instrumentation, and test setup for both CFRP-confined concrete cylinders and CFRP coupons;

- Chapter 4 presents the details of the experimental results , organized by series for both CFRP-confined concrete cylinders and CFRP coupons, and summarizes the stress-strain responses and failure modes of all specimens tested in the research program;
- Chapter 5 provides further discussion on the test results, with emphasis on the effect of the test variables (number of layers, specimen size, fiber orientation and stacking sequence) on stress-strain response and failure mode;
- Chapter 6 summarizes the analytical program and compares the experimental and analytical stress-strain curves obtained using various prediction models from the literature;
- Chapter 7 provides conclusions and final remarks highlighting the research findings with recommendations for future research.

2 Chapter 2: Literature review

2.1 Chapter overview

This chapter provides a literature review related to the behavior of FRP-confined concrete under compressive loading. The chapter begins with a general review of FRP applications in civil engineering and an overview of the effect of FRP jacketing on the stress-strain response of concrete in compression. The chapter then summarizes existing research which has focused on FRP confinement, with a review of various parameters which affect the stress-strain response of FRP-confined concrete, such as FRP type, number of FRP layers, concrete strength, specimen cross section and specimen size. The second part of the chapter is more relevant to the current study, and reviews research which has examined the effect of FRP fiber orientation and FRP stacking sequence on the behavior of FRP-confined concrete.

2.2 Introduction to FRP confinement

2.2.1 An overview on FRP materials

Fiber reinforced polymers (FRP), also termed fiber reinforced plastics, are a category of innovative material with high strength to weight ratio made by embedding continuous fibers (carbon, glass, aramid) in a polymer matrix which binds the fibers together. The most common FRP types in civil engineering applications include carbon fiber reinforced polymers (CFRP), glass fiber reinforced polymers (GFRP), and aramid fiber reinforced polymers (AFRP), while common polymers include epoxy, polyester thermosetting plastic, and vinyl ester.

CFRP, GFRP, and AFRP are widely used in both civil engineering practice and research; however, the first two composite types are more commonly used in strengthening applications. CFRP materials show superior tensile properties when compared to GFRP, while GFRP

composites are generally cheaper. Typical stress-strain behavior of different FRP types are compared with steel in **Figure** 2-1, it can be noticed that FRP show high strength and overall toughness (area under curve), but show linear-elastic response until brittle failure, with failure typically caused by tensile rupture of the FRP fibers in the composite matrix.

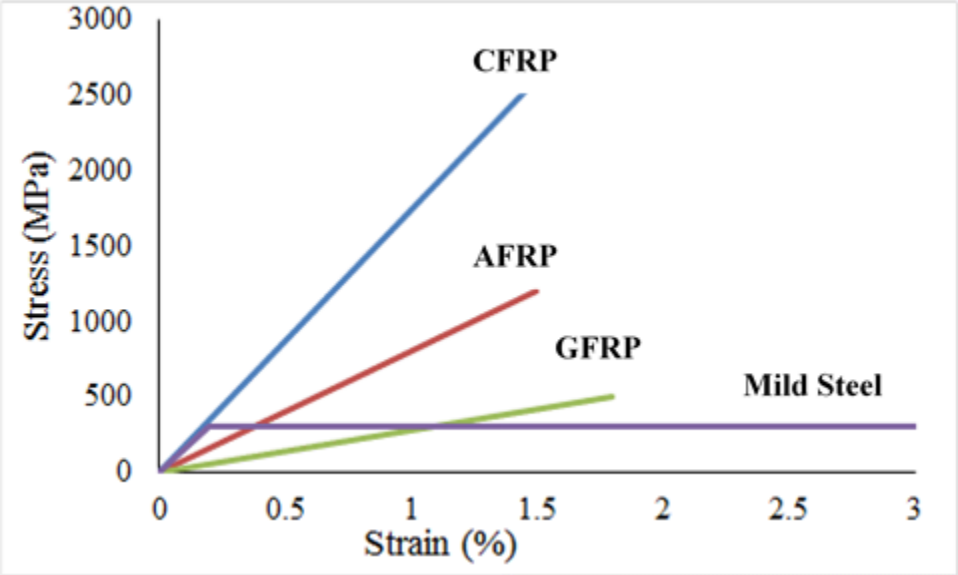

Figure 2-1 Stress-strain curve of FRP types against steel

FRP materials can be used to improve the structural behavior of both new and existing structures. In the case of new construction, FRP bars (typically made of GFRP) can be used to replace conventional steel reinforcement in reinforced concrete (RC) beams and columns, resulting in corrosion-resistant construction. In the latter, FRP composites (sheets or plates) are used to strengthen or repair structural components such as beams, columns, walls and joints, where FRP is used to enhance confinement, shear strength or flexural capacity as it is presented in **Figure 2-2**. It is noted that the orientation of the fibers in the FRP composites varies based on the strengthening application (e.g. FRP wrapped around columns for confinement with fibers aligned in the hoop direction, while FRP is placed on the tension face of members for flexural strengthening with fibers aligned along the longitudinal direction).

Figure 2-2 Strengthening of existing structures and orientation of fibers

Two methods are used in the FRP-strengthening of RC structures: first, the wet-layup method involves the in-situ application of epoxy to fibers to produce FRP sheets to confine columns, strengthen beams, slabs, walls or joints. The second method involves the prefabrication of FRP tubes (which are also used as cast-in place formwork) to confine columns, or pre-manufactured FRP plates which are attached to structural components. In the case of columns the wet-layup method is more versatile as the CFRP sheet can be adapted to various cross-sectional shapes, while prefabricated tubes result in improved quality-control (this method is also advantageous in the strengthening of non-circular cross-sections as the circular tubes can be used as cast-in place formwork).

Based on extensive research, the use of FRP for the design of new and strengthening of existing structures has been recognized by various design codes, including: ACI 440.1R "Guide for the design and construction of structural concrete reinforced with FRP bars" and ACI 440.2R "Guide for the design and construction of externally bonded FRP systems for strengthening concrete structures" (USA); FIB Bulletins "FRP reinforcement in RC structures" and "Externally bonded FRP reinforcement for RC structures" (Europe); and CSA S806-12 (Canada).

2.2.2 Mechanism of FRP confinement in circular columns

FRP-confinement is an innovative and effective retrofit method which can significantly improve the strength and energy-dissipation capacity of reinforced concrete columns. Over the years, a large number of studies have been conducted to examine the structural behavior of FRP-confined concrete. In addition to research on large-scale columns (under axial and/or simulated earthquake loads), extensive research has been conducted on smaller-scale specimens to study the compressive behavior of FRP-confined concrete. **Figure 2-3** shows the effect of FRP jacketing on the stress-strain behavior of plain concrete. It can be seen from **Figure 2-3** that confinement provided by the FRP jacket results in significant improvement in strength, strain capacity and overall toughness.

In the case of cylinders or columns having circular cross-section, the lateral confining pressure provided by the FRP (f_l) is assumed to be uniformly distributed around the circumference (see **Figure 2-4**). The confinement action provided by the FRP jacket is "passive"; that is the pressure is activated and increases with the lateral expansion of concrete due to Poisson's effect under axial compression. Failure occurs when the lateral expansion of the concrete core results in tensile failure of the FRP jacket. Based on this assumption the lateral confining pressure applied to the concrete core can be calculated using the following expression:

$$f_l = \frac{2\,.\,f_{FRP}\,.\,n_{FRP}}{D} \qquad \textbf{Eq. 2-1}$$

Wh*ere*. $\boldsymbol{n_{FRP}}$ = Total number of FRP layers (number of layers multiply by thickness of one layer) and $\boldsymbol{D}$ = diameter of the concrete cross-section.

The tensile strength of the FRP material ($\boldsymbol{f_{FRP}}$) can be calculated using the following expression which assumes linear-elastic behavior (Hooke's law):

$$f_{FRP=}\, E_{FRP}.\, \varepsilon_{FRP} \qquad \textbf{Eq. 2-2}$$

Where E_{FRP} =Modulus of elasticity of FRP jacket and ε_{FRP} =Rupture strain of FRP jacket.

Researchers have reported that ultimate strain of the FRP jacket can be lower than the ultimate tensile strain of the FRP material (i.e. as obtained by coupons). Therefore some researchers have proposed factors and equations for the expected ultimate strain of the FRP material (Lam and Teng 2003; Liu et al. 2013). This strain is then used to adjust the ideal maximum confining pressure to reflect the "actual" lateral confinement pressure expected in the circular jacket at failure.

Based on extensive experimental data and this confinement pressure concept, researchers have proposed a large number of models to predict the stress-strain response of FRP-confined concrete. Further discussion related to these models is provided in Chapter 6 of this thesis.

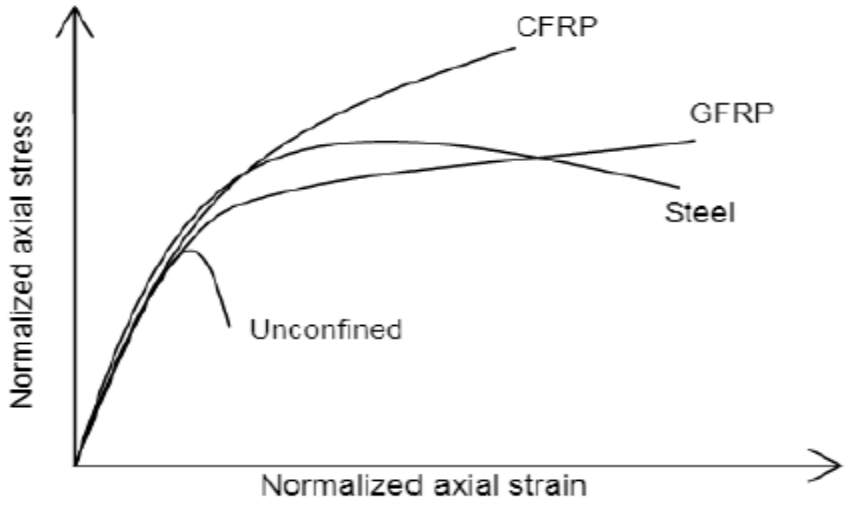

Figure 2-3 Normalized axial stress-strain behavior of confined concrete (Spoelstra and Monti (1999))

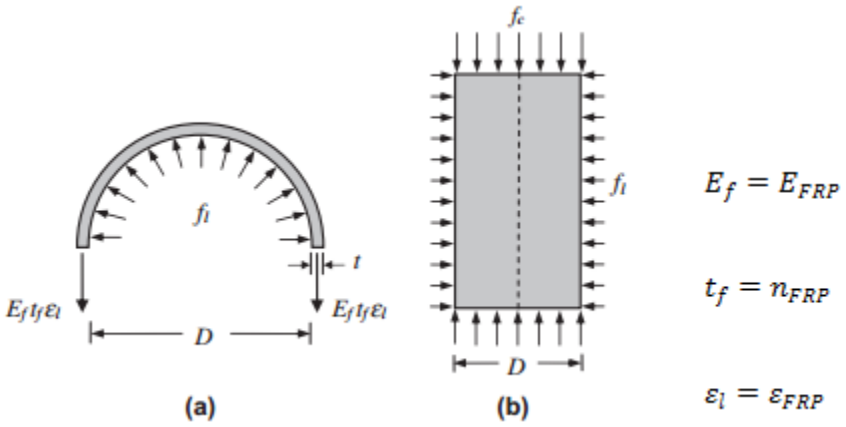

Figure 2-4 confining action of FRP shell on concrete core*:* a) FRP shell, b) concrete core

2.2.3 Influential parameters affecting the stress-strain behavior of FRP-confined concrete

Numerous studies have shown that FRP confinement leads to significant increase in both strength and ductility of concrete in compression (Karbhari and Gao, 1997).

In this section the impacts of parameters which affect the stress-strain behavior of FRP confined concrete, such as FRP type, number of FRP layers, concrete strength, specimen cross section and specimen size, are discussed.

2.2.3.1 Effect of FRP type

FRP type is one of the basic parameters which affect the strength and strain enhancement of FRP-confined concrete. In general three primary types of FRP sheets are used in civil engineering applications: carbon fiber reinforced polymer (CFRP), glass fiber reinforced polymer (GFRP), and aramid fiber reinforced polymer (AFRP). The majority of researchers have found that CFRP has a more effective impact on improving the stress response of confined concrete compared to GFRP and AFRP composites. Saafi et al. (1999) tested a total of 30 cylindrical specimens having dimensions of 152 x 435 mm under axial compression load. Details of the testing program are presented in **Table 2-1**. As it is shown in **Table 2-2**, two types of FRP materials were used in the experiments, namely glass-FRP and carbon-FRP. As shown in **Table 2-2**, specimens confined with carbon-FRP resulted in maximum gain in strength, while specimens confined with glass-FRP achieved the maximum increase in strain. In another study, Xiao and Wu (2003) tested over 200 small size cylinders with CFRP and GFRP. Although no comparison was made between two different types of confinement, examination of the results shows that better strength enhancements were achieved in specimens confined with CFRP while in the case of strain better results were achieved in GFRP confined specimens. Cui and Sheikh

(2010) tested a total of 112 normal and high-strength cylindrical specimens having dimensions of 150 x 300 mm under monotonic uniaxial compression load. The specimens in this study were reinforced with CFRP and GFRP composites. It was found that specimens in confined with CFRP showed a higher increase in both strength and strain compared to those confined with GFRP sheets. For example, normal strength concrete specimens confined with 1 layer of CFRP/GFRP exhibited an increase of about 68.2%/23.74% in strength, and 580%/508% in strain, respectively. A similar observation was made for a companion series of specimens confined with high-strength concrete. Ghernouti and Rabehi (2010) tested a total of nine 160 x 320 mm normal strength concrete (43 MPa) cylinders confined with CFRP and GFRP under axial compression load. The specimens confined with CFRP showed enhancement in strength and axial strain of about 48 % and 262 %, while the specimens confined with the same amount of GFRP showed a gain in strength and axial strain of about 11 % and 242 %, respectively. In another study, Aire et al. (2010) conducted an experimental and analytical study on the behavior of normal and high strength (30 MPa and 70 MPa) concrete cylinders (150 x 300 mm) wrapped with GFRP or CFRP composites. As noted in previous studies, cylinders confined with CFRP showed a more significant increase in strength when compared to specimens confined with GFRP, however, the failure of GFRP confined cylinders was observed to be more gradual, while the failure of CFRP confined cylinders was sudden and explosive. In summary, research demonstrates that FRP type has a strong influence on the response of FRP-confined concrete, with research indicating that CFRP is more effective in increasing confined strength when compared to other types of composites. **Figure 2-5** shows an example of the stress-strain behavior of CFRP and GFRP confined concrete cylinders compared to unconfined concrete.

Table 2-1 Test Program

	No. of specimens tested					
	GFRP tube thickness, mm			CFRP tube thickness, mm		
	GE1	GE2	GE3	C1	C2	C3
Specimens	0.8	1.6	2.4	0.11	0.23	0.55
Confined	3	3	3	3	3	3
Plain	2	2	2	2	2	2

Table 2-2 Experimental Results

Specimen	Ultimate strength, MPa	Ultimate strain, percent	Increase in strength, percent	Increase in strain, percent
Plain	35	0.25	—	—
GE1	52.8	1.9	51	660
GE2	66	2.47	89	888
GE3	83	3	137	1100
C1	55	1	57	300
C2	68	1.6	94	540
C3	97	2.22	177	788

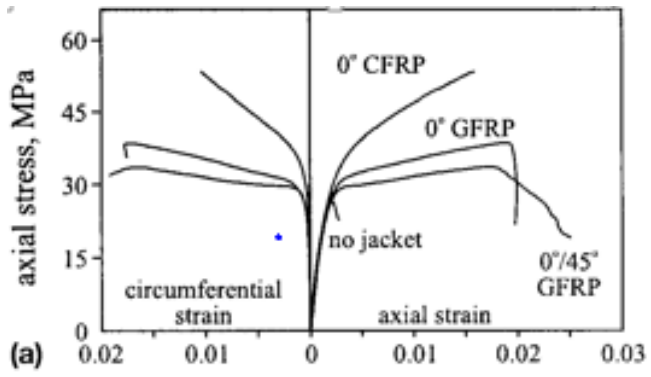

Figure 2-5 stress-strain curve of unconfined and confined concrete

[Adapted from Pessiki et al. 2001]

2.2.3.2 Effect of the number of FRP layers

The amount of FRP confinement layers is one of the most important factors that affect the behavior of FRP-confined concrete. Based on the literature review, both strength and strain of

FRP-confined concrete samples increase by increasing the amount of confinement layers. Ilki et al. (2002) tested a total of twelve 150 x 300 mm cylindrical concrete specimens which were confined with 2, 4 and 6 layers of CFRP. While the concrete in this study had relatively low compressive strength (6.2 MPa) the results showed that by adding more layers of CFRP, the compressive strength and axial strain increased proportionally. The confined strength of specimens wrapped with 2, 4, and 6 layers of CFRP increased to 6.6, 12.4, and 17.5 times the unconfined concrete strength, while corresponding axial strains increased by 2100, 3200, and 3700 %. Han et al. (2012) tested a total of 10 square FRP-confined normal strength concrete specimens with dimensions of 100 x 100 x 300 mm under compressive axial load. Specimens confined with 1 and 3 layers of CFRP displayed an increase in compressive strength by multiples of 2.0 and 4.2, while confined strains increased by factors of 5.5 and 11.6, respectively. Abbasnia and Holakoo (2012) investigated the behavior of FRP-confined concrete under cyclic compressive loading. In this study, 18 concrete cylinders (152 x 305 mm) were prepared and batched in 2 groups based on the amount of confinement (Groups 1 and 2 were wrapped with 2 and 3 layers of CFRP, respectively). The average compressive strength of specimens confined with 3 layers of CFRP increased by 45 % while specimens wrapped with 2 layers of CFRP had an increase in compressive strength of 24 %. In a comprehensive study which examined multiple parameters, Vincent and Ozbakkaloglu (2013) tested a total of 55 concrete cylindrical specimens that casted from normal, high and ultra-high (35 MPa, 65 MPa, and 100 MPa) concrete with dimensions of 152 x 305 mm under monotonic axial compression. As in previous studies, specimens with more layers of CFRP showed greater gains in strength and ductility. For example, specimens with 1 layer of CFRP showed 5% & 123% gains in strength and strain, while specimens with 4 layers of CFRP experienced gains of 58% and 413%, respectively. In

summary, the amount of FRP confinement has an important effect on the stress-strain behavior of FRP confined concrete, with strength and ductility increasing with an increase in the number of FRP layers.

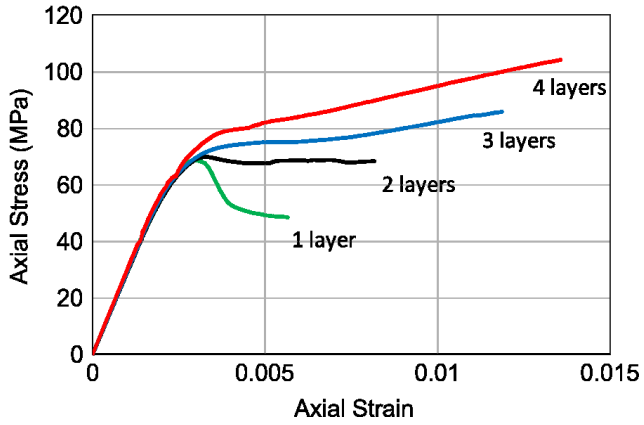

Figure 2-6 influence of amount of confinement on FRP-wrapped HSC

[Adapted from Vincent and Ozbakkaloglu (2013)]

2.2.3.3 Effect of concrete strength

Several researchers have examined the effect of unconfined concrete strength on the stress-strain behavior of FRP-confined concrete. Li et al. (2003) conducted a large series of uniaxial compression tests on 108 specimens confined with CFRP. The specimens were divided into three groups based on concrete strength (17.2, 20.6, and 27.5 MPa) and each group had 36 cylinders sorted into three sets of 12 specimens based on their dimensions (100 x 200 mm, 120 x 240 mm, and 150 x 300 mm). The results showed that the influence of FRP confinement is relatively more noticeable on specimens with lower unconfined concrete strength. For example, cylinders with layer of CFRP sheet with unconfined compressive strength of 17.2 MPa showed a 111 % increase in strength, while specimens with same amount of confinement and unconfined concrete compressive strength of 27.5 MPa showed a 93 % increase in strength. Xiao et al. (2010) tested a total of twelve 152 x 305 mm high strength concrete (HSC) cylinders confined with

unidirectional CFRP. Two different batches of concrete were studied with unconfined strengths of 70.8 MPa and 111.6 MPa for Batch 1 and 2, respectively. Specimens confined with three layers of CFRP sheets in Batches 1 and 2 exhibited an increase in strength of approximately 155% and 53% under the same amount of confinement. Vincent and Ozbakkaloglu (2013) tested three groups of FRP-confined specimens casted using the wet layup method and cast-in place FRP, having unconfined concrete strength of 35 MPa (NSC), 65 MPa (HSC) and 100 MPa (UHSC). As shown in **Figure 2-7**, the strength enhancement and strain enhancement was found to be more substantial as the unconfined compressive strength of concrete decreased. Specimens cast from NSC and confined with one layer of FRP showed a 16% increase in strength and 254% increase in strain, while specimens cast from UHSC and confined with one layer of FRP displayed a 6 % increase in strength and a 65 % increase in strain. Song et al. (2013) tested a total of 16 normal strength concrete specimens with different dimensions and cross sections. Specimens were wrapped with either 1, 2, or 3 layers of FRP sheets. Details of the test specimens are tabulated in **Table 2-3**. It was observed that confined strength decreased linearly with increased load eccentricity and exponentially with increased concrete compressive strength.

In summary research demonstrates that the effect of FRP confinement is affected by the unconfined strength of concrete, with the effect on confined strength being less substantial as the unconfined strength is increased.

Table 2-3 Details of FRP-strengthened concrete columns

Specimen ID	Specimen dimension (mm^2)	Concrete grade	FRP type	FRP wraps	Load eccentricity (mm)	Replicate
		Circular plain (CP) concrete column specimens[a]				
SCP-1	100 × 300	C20	I	0, 1, 2, and 3	0	2
SCP-2	150 × 450	C20	I	0, 1, 2, and 3	0	2
SCP-3	100 × 300	C40	I	0, 1, 2, and 3	0	2
SCP-4	150 × 450	C40	I	0, 1, 2, and 3	0	2
		Square plain (SP) concrete column specimens[b]				
SSP-1	100 × 300	C20	I	1, 2, and 3	0	2
SSP-2	150 × 450	C20	I	1, 2, and 3	0	2
		Square reinforced (SR) concrete column specimens[b]				
SSR-1	250 × 1,500	C30	II	0 and 1	20	1
SSR-2	250 × 1,500	C30	II	0 and 1	60	1
SSR-3	250 × 1,500	C30	II	0 and 1	100	1
SSR-4	250 × 1,500	C30	II	0 and 1	150	1

[Adapted from Song et al. (2013)].

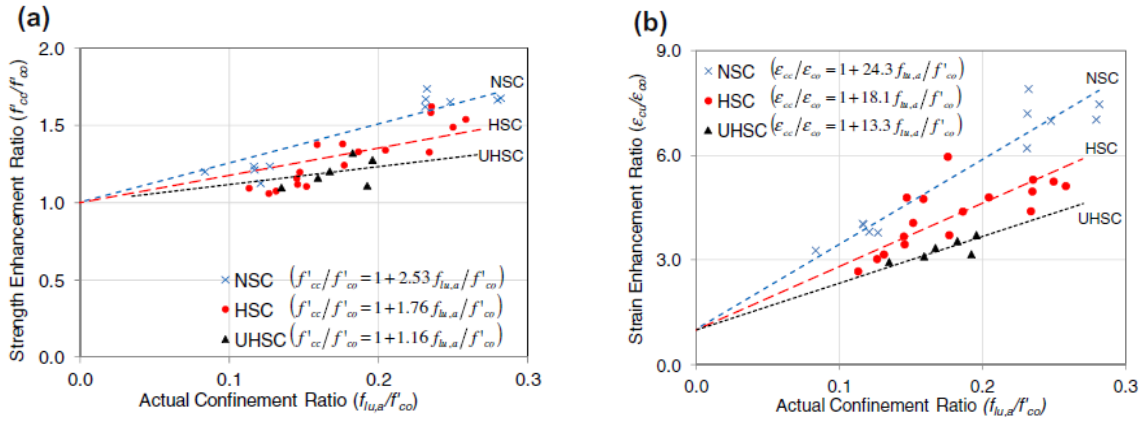

Figure 2-7 Influence of concrete strength on strength and strain enhancement ratios of test specimens: (a) Strength enhancement ratio, (b) Strain enhancement ratio.

[Adapted from Vincent and Ozbakkaloglu (2013)]

2.2.3.4 Effect of specimen cross-section

Research on concrete columns confined with conventional transverse reinforcement has shown that confinement becomes less effective as the column cross-section shape changes from circular to rectangular as it is shown in **Figure 2-8**. This is because the "effectively confined area" in rectangular specimens is smaller than in circular specimens, where confinement is generally uniform. Similar observations have been made on specimens with external FRP confinement.

Youssef et al. (2007) proposed a stress-strain model for concrete confined by FRP composites based on the results of a comprehensive experimental program on large-scale columns and short height specimens having square (S), rectangular (R) and circular (C) sections. A total of 117 large specimens (R: 254 x 381 x 762 mm; S: 381 x 381 x 762 mm; C: 406 x 813 mm and 152 x 305 mm) were tested under pure axial load. The study found that cross sectional shape affected both strength and strain enhancement of the confined specimens. The degree of enhancement of stress and strain of square columns was related to the corner radius of the specimen cross section. Although specimens with a 50 mm corner radius displayed the best behavior among all square columns in the program, they did not perform as well as the cylindrical columns. Ilki et al. (2008) tested a total of 68 small size concrete columns under uniaxial compression. Specimens were casted in circular, rectangular, and square cross sections (C 250 x 500 mm, R 150 x 300 x 500 mm, and S 250 x 250 x 500 mm). Circular specimens showed more enhancement in strength compared to square and rectangular specimens, while square and rectangular specimens exhibited more gain in ductility. For example, the average increase in stress for circular, square and rectangular specimens was found to be 5.5, 3.6, and 2.8 for specimens confined with 3 layers of FRP, respectively. All specimens with different cross sections experienced an increase in strength and strain when confined with FRP materials. Nevertheless, circular specimens showed a maximum increase in strength and specimens with rectangular or square cross sections underwent higher axial deformations. El-Hacha and Mashrik (2012) tested a total of 84 circular and square normal strength concrete specimens which were confined by steel fiber reinforced polymer (SFRP). The stress-strain curve of square specimens after reaching unconfined peak stress showed a descending trend, while an ascending trend was observed in the stress-strain curve of circular specimens. This indicates that the load carrying capacity in FRP confined

circular specimens is much higher than in FRP confined square specimens. Regardless of concrete compressive strength and number of SFRP layers, as shown in **Figure 2-9**, the axial stress-circumferential strain curves of confined circular specimens show an ascending branch after reaching the unconfined compressive strength of concrete, while a post-peak descending branch can be observed for confined square specimens. In summary, research demonstrates that specimens with circular sections show a better response to FRP confinement when compared to specimens with rectangular sections; this is a result of the uniformity of confinement that can be achieved on specimens with circular sections.

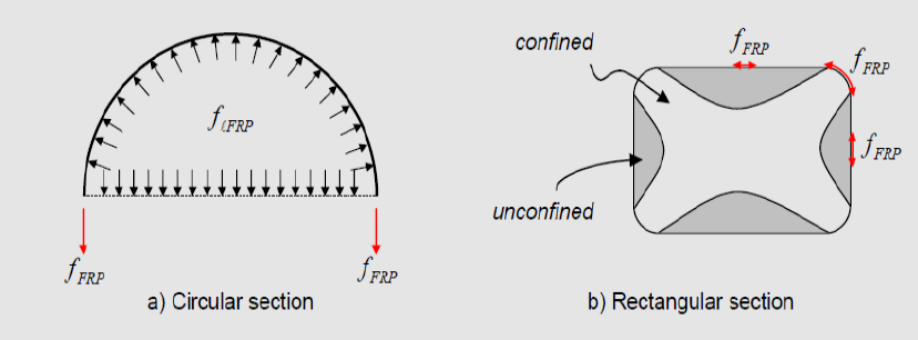

Figure 2-8 External confinement with FRP

[Adapted from Rahai et al. 2008]

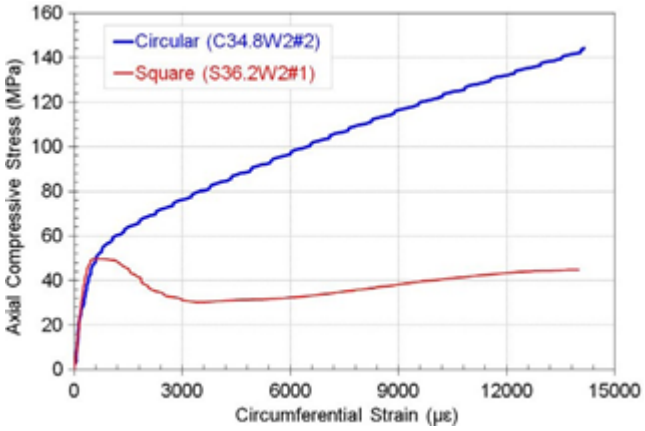

Figure 2-9 Typical Axial Stress-Circumferential Strain Curves of SFRP Wrapped Circular and Square Specimens

[Adopted from R. El-Hacha,M.A. Mashrik]

2.2.3.5 Effect of cross-section aspect ratio

The cross-sectional aspect-ratio, *a/b* (where *a* and *b* represent the longer and shorter cross-section dimensions), is another parameter that can affect the stress-strain behavior of concrete of FRP-confined specimens with rectangular cross-sections. Kumutha et al. (2007) tested a total of nine concrete reinforced concrete column specimens which were reinforced with 4 - 10 mm longitudinal bars and 6 mm steel ties with a spacing of 125 mm in the lateral direction. The specimens had either 0, 1 or 2 layers of external FRP confinement. As shown in **Figure 2-10**, the ultimate strength was found to decrease when the sectional shape is changed from square (a/b = 1) to rectangular (a/b = 1.25 and 1.66) for both the control and FRP-confined specimens. Specimens with aspect ratio of 1.66 experienced smaller ultimate axial and lateral strain compared to those with an aspect ratio of 1.25. Tao et al (2008) studied the compressive behavior of CFRP-confined concrete specimens with cross sections of 150 x 150 mm, 150 x 230 mm, and 150 x 300 mm and corner radiuses of 20, 35, and 50 mm. The amount of FRP confinement varied from 0 to 2 layers. The effect of aspect-ratio was related to the theory of "effective confinement" where in rectangular sections, only the "effectively confined" concrete core and corners are well confined while confinement in rest of the section is negligible. Thus, by increasing the aspect ratio, the ratio of effectively confined area to total area will be reduced resulting in reduced confinement efficiency. Wu and Wei (2010) studied the effect of cross-sectional aspect ratio on the strength of FRP-confined specimens with aspect-ratios which varied between 1.0 and 2.0 and reinforced with 1 or 2 plies of CFRP. **Table 2-4** shows that the specimens with smaller aspect-ratios experienced a higher gain in confined strength when compared to those with larger aspect ratios. The results show that gain in strength gradually decreases as the aspect ratio increases from 1 to 2, and becomes insignificant once the aspect

ratio reaches a value of 2. Ozbakkaloglu and Oehlers (2008) tested a total of 23 concrete-filled fiber reinforced polymer tubes having two different cross sections of 200 x 200 mm and 150 x 300 mm under concentric compression. The authors found that the influence of confinement decreased when the cross-section aspect ratio was increased from 2 to 1. Abbasnia et al. (2012) tested a total of 18 FRP-confined concrete prisms under monotonic and cyclic loading. The specimens had three different cross sections of 152 x 152 mm, 152 x 120 mm, and 152 x 90 mm. The corner radius of the specimens varied from 17 to 29 mm. In this investigation, the effect of aspect ratio on the plastic strain behavior of FRP confined concrete specimens was considered. It was observed that the cross sectional aspect-ratio does not have an impact on the plastic strain of confined specimens. Kumutha and Palanichamy (2006) tested a total of nine concrete columns under concentric compression. Specimens were casted in constant square cross-section area and height between two capitals of 750 mm. It was noticed that overall confinement effectiveness (in terms of peak confined strength) was decreased with the increase of the cross sectional aspect-ratio. However, in most cases, an increase in aspect ratio led to an increase in both axial and lateral strain values. In summary, research shows that the cross-sectional aspect ratio has a considerable effect on the behavior of FRP wrapped concrete, where an increase in aspect-ratio results in reduced confinement efficiency.

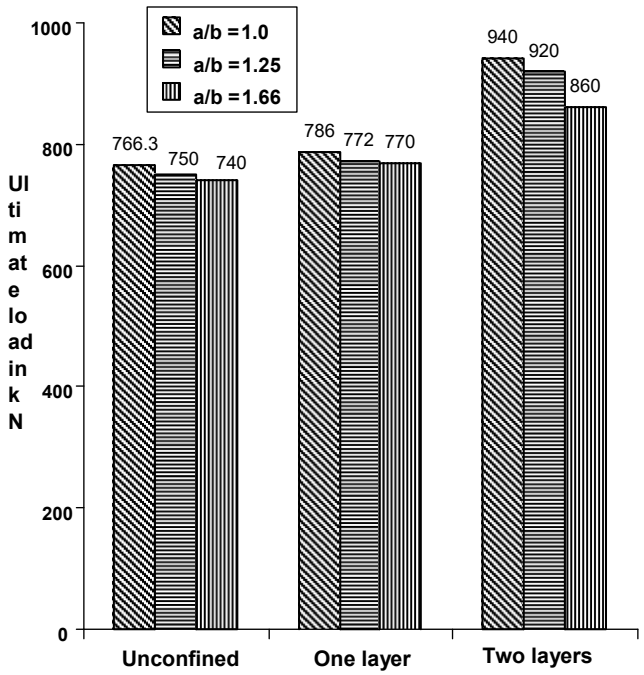

Figure 2-10 Effect of Aspect Ratio on Ultimate Load

[Adapted from Kumutha et al (2007)]

Table 2-4 Mean Compressive Strength and Corresponding fcc'/fco

Aspect ratio h/b	Unconfined (MPa)	1-ply (MPa)	f_{cc}/f_{co}	2-ply (MPa)	f_{cc}/f_{co}
1.0	35.30	41.23	1.17	60.37	1.71
1.25	35.30	38.77	1.10	51.36	1.45
1.5	35.30	38.39	1.09	43.87	1.24
1.75	35.30	37.68	1.07	40.51	1.15
2.0	35.30	37.44	1.06	38.97	1.10

[Adapted from Wu and Wei (2010)]

2.2.3.6 Effect of specimen size

Specimen size is another parameter that can affect the response of FRP-confined concrete. Masia et al. (2004) tested thirty concrete prisms with three different sizes of 100 x 100 x 300 mm, 125 x 125 x 375 mm, and 150 x 150 x 450 mm (small, medium, and large, respectively) in order to examine the size effect in axially loaded FRP-confined specimens with square cross-sections. It

was observed that the impact of confinement is more significant on specimens with smaller cross section. For example, small specimens wrapped with one layer of CFRP had an increase in strength & strain of 119% & 669%, while large specimens confined with the same amount of CFRP showed an increase in strength & strain of 45% & 360%, respectively. Wang and Wu (2011) performed a study on the size effect of concrete short columns confined with aramid FRP (AFRP) jackets. A total of 135 specimens were tested under axial compressive loading and specimens were wrapped with different amounts of AFRP layers. The unconfined compressive strength of the concrete in this study varied between 29 and 51 MPa. There was no clear size effect on the failure modes of the AFRP confined concrete short columns, however specimen size had a significant effect on the transitional and ultimate strength ratios of the specimens with lower AFRP confinement (with an insignificant effect on the transitional and ultimate strain ratios). Elsanadedy et al. (2012) completed an experimental and numerical investigation of the size effects in FRP-wrapped concrete cylinders. A total of 37 specimens batched in three groups based on specimen size (50 x 100 mm, 100 x 200 mm, 150 x 300 mm) were tested under pure compressive load. In the case of 50, 100, and 150 mm diameter specimens wrapped with one layer of CFRP, the axial stress increased by 172 %, 92 %, and 86 %, respectively. In the case of axial strain, specimens with a diameter of 50, 100, and 150 mm wrapped with 1 layer of CFRP showed an increase of 354 %, 203 %, and 161 %, respectively. Long and Zhu (2014) have noted that the peak stress FRP-confined normal and high strength concrete decreases with an increase in specimen size. In summary, research demonstrates that effectiveness of FRP confinement, in terms of strength and strain enhancement, is more important in specimens with small cross sections.

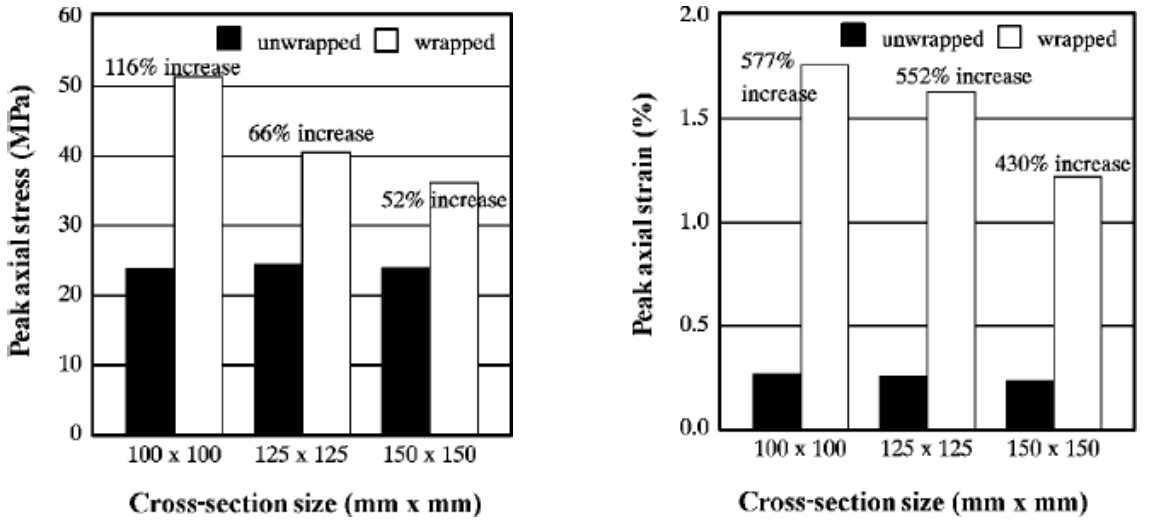

a) Effect of specimen size on peak stress

b) Effect of specimen size on peak strain

Figure 2-11 Size effect on peak stress and corresponding peak strain

[Adapted from Masia et al. (2004)]

2.2.3.7 Effect of corner radius

Another important factor which influences the stress-strain behavior of FRP confined specimens with rectangular and square sections is the corner radius. Research shows that rectangular and square specimens that have sharp corners fail in a premature manner by a rupture of the FRP jacket in these regions of stress concentration. Based on the concept of uniform confinement, specimens with larger corner radius are confined more uniformly and therefore experience greater strength gained when compared to specimens with small corner radius or sharp corners. Wang and Wu (2008) tested a total of 108 specimens with dimensions of 150 x 150 x 300 mm having corner radiuses varying between 0 and 75 mm under compressive loading. Specimens with sharp corners confined with one layer of CFRP exhibited an increase of approximately 2 % in strength, while specimens with the same properties but a corner radius of 75 mm showed an increase in strength of about 80 %. **Figure 2-12** shows a similar result from tests conducted by

Al-Salloum (2007) on circular and square specimens (150 x 300 mm and 150 x 150 x500 mm) where an increase in corner radius results in more effective confinement and greater strength gain. In the Ozbakkaloglu and Oehlers (2008) study, FRP confined specimens with different corner radiuses were also tested. The experimental results showed that the effect of confinement in both rectangular and square specimens is influenced by the corner radius, where an increase in corner radius provides greater FRP confinement efficiency. For instance, the increase in strength of rectangular specimens with a corner radius of 40 mm were recorded as 177 % compared to unconfined specimens, whereas specimens with a 10 mm corner radius showed approximately the same behaviour as unconfined specimens. Ilki et al. (2008) tested a total of 68 FRP-confined specimens under pure axial loading, including 21 circular (250 x 500 mm), 23 squares (250 x 250 x 500 mm), and 24 rectangular (150 x 300 x 500 mm) specimens. For the square and rectangular series, specimens with larger corner radius showed additional increase in strength, although the specimens showed no significant difference in axial strain compared to the other confined specimens. For example, the compressive strengths of specimens with corner radii of 20 and 40 mm were 17 % and 51 % higher than that of the specimens with the corner radius of 10 mm (Ilki et al. 2008). In summary, research shows that FRP confinement efficiency in square and rectangular concrete sections is improved with an increase in corner radius.

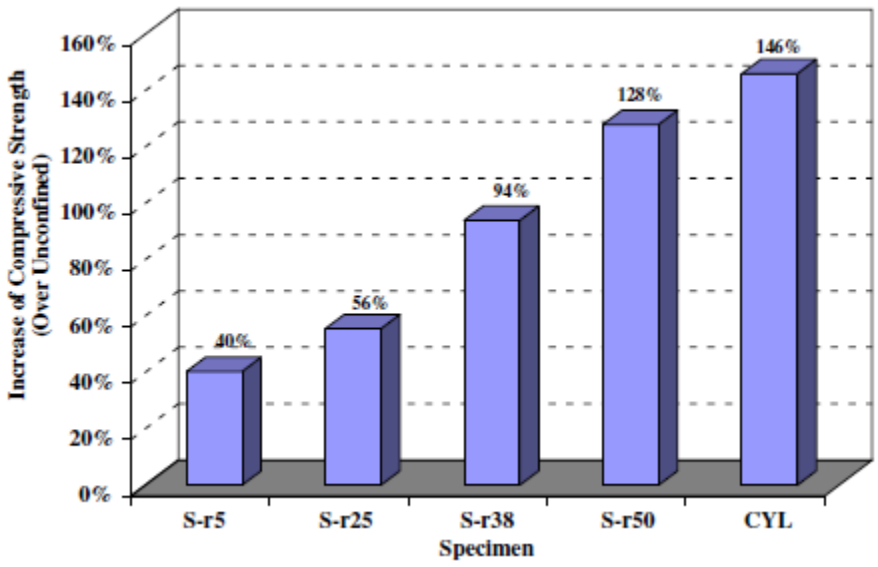

Figure 2-12 Effect of Corner Radius on Confined Square Columns

[Adapted from Al-Salloum (2007)]

2.2.3.8 Effect of FRP confinement on the behavior of columns

While most of the previous review of the literature has focussed on unreinforced FRP-confined specimens it is worth mentioning that important research has also been conducted to examine the effect of FRP confinement in reinforced concrete columns. A limited number of studies are mentioned in this section. Wang et al. (2012) conducted an experimental and analytical study examining the behaviour of large circular RC columns confined with CFRP under axial loading. Thirty specimens, divided into two different groups based on size (C1: 305 x 915 mm and C2: 204 x 12 mm) were tested under monotonic or cyclic axial compression loading. Both plain concrete and reinforced concrete columns were included in each group. The results showed that CFRP-confined specimens experienced enhancement in both axial stress and strain when compared to unconfined specimens. For instance, reinforced concrete specimens in group C1 (305 x 915 mm), which contained 8 - 12 mm longitudinal bars and 6 mm ties at 80 mm spacing,

experienced an increase in peak compressive strength of approximately 115 % when wrapped with 2 layers of CFRP when compared to the control specimens. Similarly the provision of 2 layers of CFRP resulted in an increase in peak strain by factors of 16.1 and 7.3 when compared to the plain and reinforced concrete controls specimens without FRP confinement.

Researchers have also found that by increasing the number of FRP sheets, the ultimate strength of RC columns will increase accordingly. It is worthwhile mentioning that the effect of confinement is more obvious on specimens with a lower percentage of internal reinforcing.

Rousakis and Karabinis (2012) investigated the response of FRP confined square reinforced concrete columns under axial compressive monotonic or cyclic loading. A total of 37 specimens with dimensions of 200 x 200 x 320 mm, with unconfined strength of 26 MPa, and wrapped with 1 to 9 layers of CFRP. The results showed that specimens with large tie spacing experienced relatively larger increase in strength and strain due to FRP confinement when compared to more heavily reinforced specimens with smaller tie spacing. Similarly the enhancement in strength improved with an increase in the number of CFRP layers. For example, columns with tie spacing 200 mm and one layer of CFRP experienced an increase in strength of roughly 47 %, when compared to control specimens, while provision of 5 layers of CFRP resulted in a strength increase of approximately 135 %. On the other hand, columns with tie spacing of 95 mm and wrapped with one layer of CFRP displayed a 16 % rise in strength (compared to 47% in the previous series), while 5 layers of CFRP demonstrated a 36 % increase in strength (compared to 135% in the previous series). It can be concluded from the above discussion that the effect of FRP confinement is more noticeable on reinforced concrete specimens with lower transverse reinforcement ratio. In summary, FRP confinement has a considerable impact on the axial strength of reinforced concrete columns, although the effect is more significant on plain concrete

specimens. Furthermore, the effectiveness of FRP confinement increases with an increase in the number of FRP layers and is more evident in columns with low transverse reinforcement ratio.

2.2.3.9 Effect of cast in place FRP tubes on the behavior of concrete specimens:

In the last two decades, the study of the behavior of concrete filled FRP tubes (CFFTs) has attracted more interest from researchers. An FRP tube can act as formwork, as a barrier to environmental effects, as confinement and as shear and flexural reinforcement. Mirmiran and Shahawy (1997) tested a total of 30 cylindrical (152.5 x 305 mm) concrete filled FRP tubes. Unidirectional E-glass fiber with a winding angle of ±15° was applied to build the tubes and the unconfined compressive strength of the concrete used was of approximately 31 MPa. As shown in **Figure 2-13**, an increase in the number of FRP layers resulted in an improvement of both strength and strain. For instance, the compressive strength increased from 62 MPa to 86 MPa when the number of FRP layers increased from 6 to 14 layers. In addition, the strain of the aforementioned specimens increased from 0.035 to 0.043.

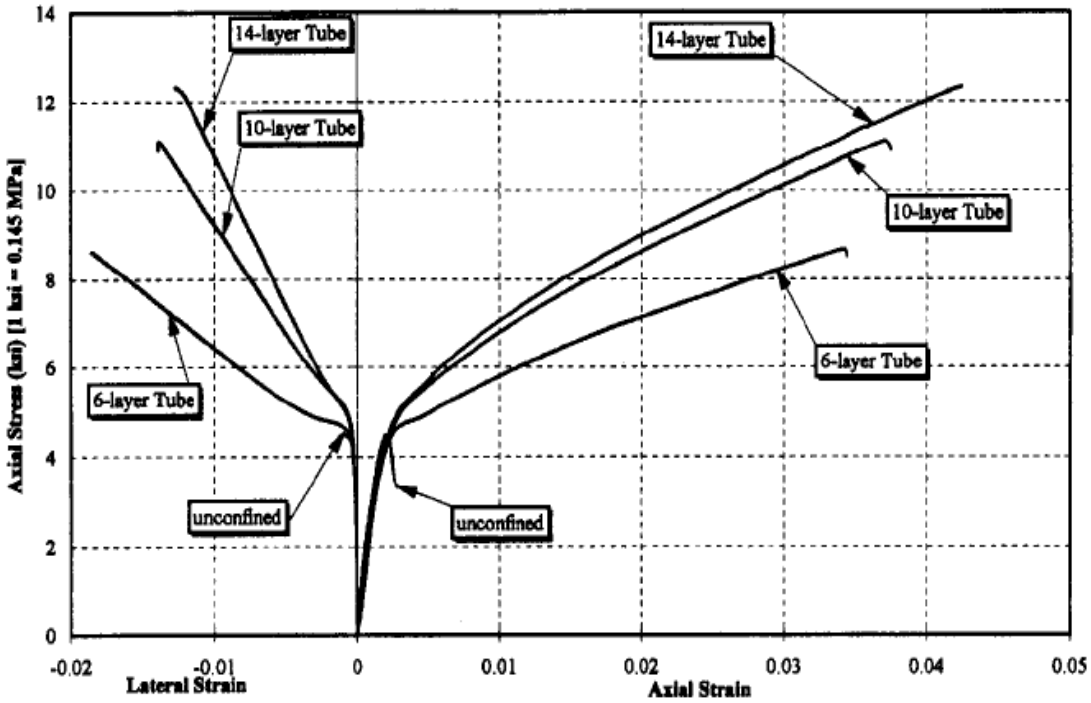

Figure 2-13 Experimental Stress-Strain Curves of Specimens

[Adapted from Mirmiran and Shahawy (1997)]

Ozbakkaloglu and Oehlers (2008) tested a total of 55 cylindrical specimens with dimension of 152 x 305 mm under monotonic axial compression; 35 of the specimens were confined by FRP tubes and the remaining 20 cylinders were confined by wrapping the FRP sheets with the hand wet lay-up method. Three different concrete mixes with compressive strengths of 35, 65, and 100 MPa were used in the program and the amount of confinement for both FRP tubes and wrapped specimens varied from 1 to 6 layers. The results from both series demonstrated that both the strength enhancement ratio (f'_{cc}/f_{co}) and the strain enhancement ratio ($\varepsilon'_{cc}/\varepsilon_{co}$) decreased when the compressive strength of concrete increased. Both Ozbakkaloglu (2013) and Vincent and Ozbakkaloglu (2013) claimed that, in the range of compressive strength of concrete and amount of confinement that was tested, no significant difference was observed in ultimate stress and ultimate strain when comparing specimens confined with wet-layup method or using premade

CFFT. However, a noticeable difference was observed in the transition zone, the area located between the first and second branch of the stress-strain curve, where specimens confined with the hand lay-up method showed a wider transition zone compared to those that were tube-encased. The aforementioned difference was ascribed to the shrinkage of concrete inside the FRP tube during curing. Therefore, concrete confined by FRP tubes can be expected to react in the same manner as discussed in the previous sections regarding the type of FRP, number of layers, compressive strength of concrete, size of specimens as well as the cross section shape, aspect ratio and corner radius.

Table 2-5 Summary of Existing Studies on FRP-confined Concrete

Study(Author name)	# of Specimens	Fc' (MPa)	Specimen Properties				Reinforcement		FRP Properties		
			Cross section	Size (mm)	Height (mm)	Corner Radius (mm)	Longitudinal	Transverse	FRP Type	# of Layers	Orientation
Specimens (Circular)											
Fardis & Khalili (1981,1982)	46	35	C	75	150	0	P	P	GFRP	1 - 5	–
		31	C	100	200						
Kestner et al. (1998)	16	26	C	152	610	0	P	P	CFRP , GFRP	0 - 2	0^0, $\pm45^0$
Toutanji (1999)	18	30	C	76	305	0	P	P	CFRP1, CFRP2	2	0^0
									GFRP		
Xiao & Wu (2000)	12	28	C	152	305	0	P	P	CFRP	0 - 3	0^0
	12	38									
	12	48									
Harries & Kharel (2002)	–	32	C	152	305	0	P	P	GFRP	1 - 15	–
									CFRP	1-3	
Ilki et al. (2002)	12	6	C	150	300	0	P	P	CFRP	0 - 6	–
Li et al. (2003)	36	17	C	100	200	0	P	P	CFRP	0 - 3	–
	36	21		120	240						
	36	28		150	300						
	18	17	C	300	600				CFRP	0 - 2	–
Li et al. (2005)	27	46	C	152	305	0	P	P	GFRP	0 - 4	0^0, 30^0, $\pm45^0$, 60^0, 90^0
Au & Buyukozturk (2005)	24	24	C	150	375	0	P	P	GFRP	1 - 2	0^0, $0^0/90^0$, $\pm45^0$
Li (2006)	24	46	C	–	–	0	P	P	GFRP	2 , 4	0^0, 30^0, $\pm45^0$, 60^0, 90^0
Youssef et al.(2007)	27	28	C	406	813	0	P	P	GFRP, CFRP	1 - 13	0^0
	30			152	305						
Wu et al. (2009)	60	46	C	100	300	0	P	P	AFRP	1 - 3	–
		79									
		101									
Cui & Sheikh (2010)	112	45 - 112	C	152	305	0	P	P	CFRP, GFRP	1 - 5	–
Ghernouti & Rabehi (2010)	9	22	C	160	320	0	P	P	GFRP	–	–
						0			CFRP		

Study(Author name)	# of Specimens	Fc' (MPa)	Specimen Properties				Reinforcement		FRP Properties		
			Cross section	Size (mm)	Height (mm)	Corner Radius (mm)	Longitudinal	Transverse	FRP Type	# of Layers	Orientation
Sadeghian et al. (2010)	30	35 - 45	C	150	300	0	P	P	CFRP	1 - 4	0^0, 90^0, $\pm45^0$
Aire et al. (2010)	18	30 & 70	C	150	300	0	P	P	CFRP	0 - 12	0^0
									GFRP		$90/10^0$
Xiao et al. (2010)	6	71	C	152	305	0	P	P	–	1 - 5	0^0
	6	112									
Wang & Wu (2011)	72	29,51	C	70	210	0	P	P	AFRP	–	–
			C	105	315						
			C	194	582						
Ozbakkaloglu & Akin (2012)	24	39 & 103	C	152.5	305	0	P	P	AFRP	2 - 6	0^0
									CFRP		
Liang et al. (2012)	24	34	C	100	200	0	P	P	CFRP	0 - 3	0^0
				200	400						
				300	600						
Abbasnia &Holakoo (2012)	18	46	C	152	305	0	P	P	CFRP	2, 3	0^0
El-Hacha &Mashrik(2012)	36	35,41	C	150	300	0	P	P	SFRP	0 - 3	$0^0/90^0$
Elsanadedy et al. (2012)	37	41	C	50	100	0	P	P	CFRP	0 - 3	0^0
				100	200						
				150	300						
Vincent &Ozbakkaloglu (2013)	20	36-112	C	152	305	0	P	P	CFRP	1 - 6	0^0
Song et al. (2013)	16	20 - 40	C	100	300	0	P	P	CFRP	0 - 3	0^0
				150	450						
Vincent&Ozbakkaloglu (2013)	6	50 & 80	C	152	305	0	P	P	AFRP	1 - 3	90^0
Long & Zhu (2014)	20	35,53	C	100	200	0	P	P	BFRP, CFRP	0 - 3	–
				200	400						
				300	600						
Specimens (Rectangular)											
Kestner et al. (1998)	12	26	R	152²	610	0	P	P	CFRP , GFRP	0 - 2	0^o, $\pm45^o$
Youssef et al.(2007)	27	28	R	254 X 381	762	0	P	P	GFRP, CFRP	1 - 13	0^o
	27			381²	762						
R.Benzaid et al. (2008)	24	55	R	100²	300	0, 8, 16	P	P	GFRP	1 - 2	–

Study(Author name)	# of Specimens	Fc' (MPa)	Specimen Properties				Reinforcement		FRP Properties		
			Cross section	Size (mm)	Height (mm)	Corner Radius (mm)	Longitudinal	Transverse	FRP Type	# of Layers	Orientation
Wang & Wu (2011)	63	29,51	R	70²	210	7	P	P	AFRP	–	–
			R	100²	300	10					
			R	150²	450	15					
Han et al. (2012)	10	21	R	100²	300	0	P	P	CFRP	–	–
El-Hacha & Mashrik(2012)	36	36,39	R	150²	300	0	P	P	SFRP	0 - 3	0°/90°
	12	25	R	150²	300	3, 6, 10, 25				1	
R.Abbasnia et al. (2013)	18	30	R	150²	300	25.2, 33.6, 42	P	P	CFRP	2	0°
				120X 180	300						
				90X 180	300						
Song et al. (2013)	6	20 - 40	R	100²	300	0	P	P	CFRP	0 - 3	0°
				150²	450						
Columns(Circular)											
Kestner et al. (1998)	4		C	508	1830	0	8 Φ22	#3 @ 356 mm	CFRP , GFRP	3	0^0, ±45^0
Parretti & Nanni (2002)	5	20	C	200	914	0	8 Φ 10	Φ6 @ 50 mm	CFRP	1	±45^0, 0^0
Ilki et al. (2008)	21	9-30	C	250	500	0	6 Φ 10	Φ8 @ 145 mm	CFRP	0 - 4	0^0
Wang et al. (2012)	10	24	C	305	915	0	8 Φ12	Φ6 @40 or 60 or 80 or 120mm	CFRP	0 - 2	0^0
	20			204	612		6 Φ10				
Changdong (2013)	25	34,41	C	300	525	0	6 Φ25 or 8 Φ22	Φ6 @ 60mm	CFRP, BFRP	1, 2	0^0
Columns(Rectangular)											
Kestner et al. (1998)	4	33	R	457²	1830	0	8 Φ22	#3 @ 356 mm	CFRP , GFRP	3	0^0, ±45^0
Parretti & Nanni (2002)	3	35	R	178²	914	0	4 Φ 13	Φ6 @ 178 mm	CFRP	1	±45^0
Ilki et al. (2008)	23	21	R	250²	500	10, 20, 40	4 Φ 14	Φ8 @ 175 mm	CFRP	0 - 4	0^0
	24			150x300	500	10, 20, 40	4 Φ 12	Φ8 @ 200 mm			
Rousakis & Karabinis (2012)	42	26	R	200²	320	30	4 Φ14	Φ8 @95 or 200mm	CFRP	1, 5	–
									GFRP	3, 9	
Gajdosova & Bilcik (2013)	8	32	R	210 X 150	4100	20	2 X 4 Φ10	4 X Φ6 @ 150	CFRP	1	0^0
Pham et al. (2013)	16	40	R	150²	800	0	4 Φ12	Φ6 @ 60mm	CFRP	3	–
Song et al. (2013)	8	20 - 40	R	250²	1500	0	4 Φ14	Φ6 @200mm	CFRP	0 - 3	0^0
Hadi & Le (2014)	12	40	R	200²	800	32	4 Φ12	Φ12 @ 100 mm	CFRP	0 - 3	0^0, 45^0. 90^0

2.3 Effect of fiber orientation

In this section, the impact of fiber orientation on the behavior of FRP-confined concrete specimens and columns will be reviewed. Researchers have generally shown that specimens confined with fibers in the hoop direction (0^o) show the best overall enhancement in stress-strain behavior (in terms of overall strength and toughness) when compared to other orientations, while confinement with angular FRP fibers (e.g. $\pm 45^o$) results in relatively more ductile behavior.

2.3.1 Rajappa (2004)

Rajappa (2004) investigated various parameters affecting the behavior FRP-confined concrete. Parameters considered in the study included concrete strength, fiber orientation, size effect, and number of layers, and the experiments included both plain and reinforced concrete specimens. Two batches of concrete were prepared with unconfined strength of 31 and 55 MPa for batches 1 and 2, respectively. A total of 16 specimens (plain and reinforced) were cast in batch 1, with 22 specimens (plain and reinforced) cast in batch 2. The cylindrical specimens were jacketed with CFRP sheets that had fiber orientation of 0^0, 45^0, or $\pm 45^0$ with the number of layers varied from 1 to 3. The following conclusions can be drawn from this study:

- As expected, internal reinforcement increased the strength of both batches of concrete, with the reinforced specimens in batch 2 showing an average increase in peak strength of 11 % compared to the plain concrete specimens, while the reinforced specimens in batch 1 (lower concrete strength) experienced an average increase in peak strength of 17 % when compared to the companion plain concrete specimens.

- Plain cylinders wrapped with 1 layer of FRP having fibers oriented in the hoop direction (0^o) showed an average enhancement of 44 % in strength while reinforced concrete specimens wrapped with same amount of FRP in the same orientation showed an increase in strength of 45 %. On the other hand, plain concrete specimens confined with 3 layers of FRP in the hoop direction showed an average gain in strength of 161 % while reinforced concrete cylinders confined with 3 layers of FRP achieved an average increase in strength of 150 %;
- In addition to the greater increase in strength, specimens confined with 3 layers of CFRP (hoop direction) gained more stiffness compared to those confined with 1 layer of CFRP. Similarly, specimens wrapped with 3 layers of CFRP were able to withstand 8 times more axial strain than the unconfined specimens.
- Confined specimens (both plain and reinforced) with FRP having 45^o fibers showed a smaller increase in strength than specimens confined with FRP sheets oriented at 0^o. A similar observation was made in the case of specimens with FRP oriented at $\pm 45^o$;
- Plain cylinders wrapped with 2 layers of CFRP at $\pm 45^o$ showed a rise in strength of 14% in strength while companion reinforced concrete specimens wrapped with the same CFRP sheets experienced an average increase of 12% in strength (compared to 44% and 45% for specimens with fibers at 0^o);
- Specimens (plain and reinforced) wrapped with $\pm 45^o$ fiber orientation showed a high increase in hoop strain when compared to other FRP orientations;
- Plain and reinforced specimens cast using batch 1 (lower unconfined strength) and wrapped with $\pm 45^o$ CFRP demonstrated relatively greater increase in strength when compared to companion specimens in batch 2;

- In terms of the effect of size, the increase in strength of the 76 x 152 mm, 102 x 203 mm and 152 x 305 mm unconfined concrete cylinders was about 28 %, 35 % and 17 %, respectively.
- Specimens with dimensions of 76 x 152 mm and 102 x 203 mm, wrapped with 3 layers of CFRP, showed increases in strength of 131 % and 115 %, respectively.
- Similarly, specimens with different sizes experienced different gains in axial and hoop strain. For example, cylinders having dimensions of 76 x 152 mm, 102 x 203 mm and 152 x 305 mm, and confined with 1 layer of 0^{o} FRP showed strain enhancements of 2.8, 3.4, and 3.6, respectively. The increase in hoop strain for the same specimens was 1.6, 22.9, and 20.1, respectively.

2.3.2 Au and Buyukozturk (2005)

Au and Buyukozturk (2005) examined the effect of fiber orientation on FRP-confined concrete by testing a total of 24 concrete cylinders (with dimensions of 150 x 375mm), 18 of which were confined with E-glass FRP with the remaining 6 without any confinement (used as control specimens). All specimens were tested under uniaxial compression, and the unconfined compressive strength of concrete was 24 MPa. As shown in **Figure 2-14**, three different types of FRP fabric (0^0 hoop, $0^0/90^0$ and $\pm 45^0$) were used to produce six different wrap configurations (see **Table 2-6**). The following conclusions can be drawn from this study:

- Angular fiber wraps ($\pm 45^{o}$) showed ductile behavior at failure when compared to other fiber orientations; however, the peak stress of specimens confined with hoop direction

fiber (0^0) was much higher than for other fiber orientations. These behaviors can be observed from the comparison of **Figure 2-15**.

- Specimens confined with a combination of an inner layer of FRP with angular fibers (WA) and an outer layer of FRP with fibers at 0^o (UC) produced excellent behavior improvements, with gains of 99 % gain in strength, as well increases by factors of 14 and 17 times in lateral and axial strains when compared to the control unconfined specimens.

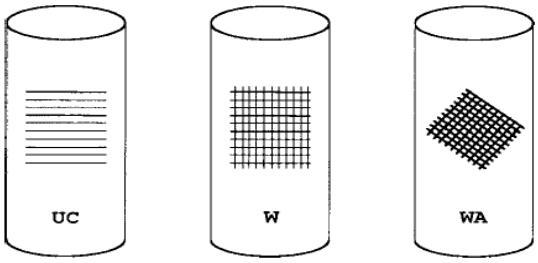

Figure 2-14 Basic Fabric Designation

[Adopted from Au and Buyukozturk (2005)

Table 2-6: Wrap Configurations

Configuration	Designation	Description
1	C1-UC1	1 layer of UC fabric
2	C1-W1	1 layer of W fabric
3	C1-WA1	1 layer of WA fabric
4	C2-W1-WA1	1 inner layer of W + 1 outer layer of WA
5	C2-UC1-WA1	1 inner layer of UC + 1 outer layer of WA
6	C2-WA1-UC1	1 inner layer of WA + 1 outer layer of UC

[Adopted from Au and Buyukozturk (2005)]

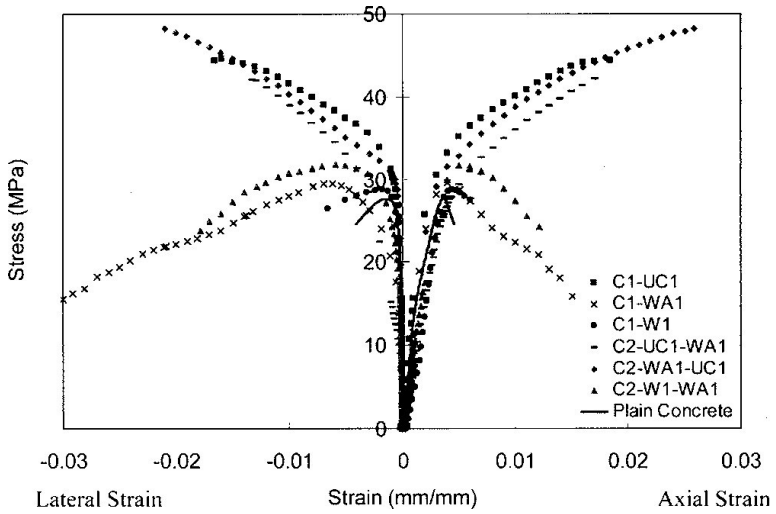

Figure 2-15 Load deformation plot of each configuration

[Adopted from [Adopted from Au and Buyukozturk (2005)]

2.3.3 Li et al. (2005)

Li et al. (2005) tested 27 FRP-confined concrete cylinders having dimensions of 152 x 305 mm and wrapped with different fiber configurations to examine the effect of fiber orientation. The series included 3 control cylinders (unconfined strength of 46 MPa), with 18 specimens wrapped with two layers of unidirectional E-glass FRP having six different orientations, and the remaining 6 cylinders wrapped with four layers of unidirectional E-glass FRP in the (90^0) or hoop direction (0^0) only.

Table 2-7 presents the different fiber orientations that were used for all 8 groups. Coupon tests were conducted to determine the tensile strength of the E-glass FRP with fibers oriented at 0^0, 45^0 and 90^0. The coupon tests tconfirmed that FRP coupons with fibers orientation in the hoop direction (0^0) will have more tensile strength, which in turn leads to better confinement when the

FRP is used as a jacket for concrete cylinders. The following points can be drawn from the summary of the test results displayed in **Table 2-8** and **Figure 2-16**:

- Specimens confined with angular fibers ($45^0/45^0$, $90^0/90^0/90^0/90^0$, $60^0/30^0$) did not behave as desired because of the low tensile strength of the E-glass FRP sheets with fibers at an angled orientation (one can see that the FRP confined specimens with an angled fiber orientation failed at a strength which is relatively close to the compressive strength of the unconfined concrete);
- Fiber orientation and jacket thickness have a considerable effect on the total stress-strain behavior of confined specimens having FRP oriented in the hoop direction. For example, the compressive strength of the confined cylinders with two layers of $0^0/0^0$ FRP increased by 8% compared to the control specimens, while the compressive strength of specimens confined with four layers of $0^0/0^0/0^0/0^0$ was enhanced by 19 %. On the other hand, cylinders wrapped with sheets having angular fibers did not show an efficient enhancement in the compressive strength of concrete, regardless of the number of layers;
- Specimens wrapped with 2 layers of 45° sheets displayed a more ductile behavior when compared to specimens wrapped with 4 layers of 90° sheets. However the greatest overall toughness was attributed to specimens with fibers oriented at 0°.

Table 2-7: Fiber Orientation for each Group of Concrete Columns

Group no.	1	2	3	4	5	6	7	8
Fiber orientation	0°/0°	0°/90°	90°/90°	60°/30°	45°/45°	–45°/45°	0°/0°/0°/0°	90°/90°/90°/90°

[Adapted from Li et al. (2005)]

Table 2-8 Summary of Test Results

Fiber orientation	Compressive strength (MPa)
0°/0°	49.40
0°/90°	48.67
90°/90°	47.61
60°/30°	46.12
45°/45°	46.72
−45°/45°	46.75
90°/90°/90°/90°	48.91
0°/0°/0°/0°	54.62
Control	45.60

[Adapted from Li et al. (2005)]

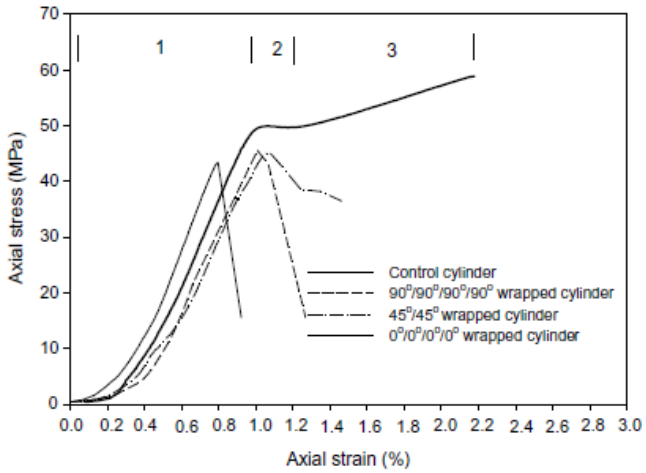

Figure 2-16 Typical Axial Stress-Axial Strain Behaviors of Various Types of Cylinders

[Adapted from Li et al. (2005)]

2.3.4 Sadeghian et al. (2009)

Sadeghian et al. (2009) studied the effect of fiber orientation by testing a series of CFRP coupons having different fiber configurations. A total of 24 coupon specimens (cross-section of 30 x 350mm) were prepared and tested under axial tension load, with eight wrap configurations prepared from fibers oriented at 0^0, $\pm45^0$ and 90^0, with the number of layers varied from 1 to 4.

The test program and specimen properties are presented in **Table 2-9**. The following conclusions are drawn from this study (see **Table 2-10**):

- The increase in the number of CFRP layers having the same orientation enhanced the stiffness and maximum load capacity, while the maximum elongation remained relatively unchanged;
- Coupons with fibers oriented at 0^0 (and matrix orientation 90^0) behaved in a fully linear manner and experienced a brittle rupture at failure;
- Coupons with a CFRP fiber orientation of $\pm 45^0$ showed nonlinear behavior and more ductile failure response. The authors noted that non-linear behavior is an important characteristic, especially in cases when ductility is critical. Based on this behavior, the authors proposed an analytical model to predict the non-linear stress-strain behavior of specimens with fibers at $\pm 45^0$;
- As the fiber angle approached 90^o, the ultimate strength of the FRP sheet reduced substantially. In this study, FRP sheets with a 0^o fiber orientation had an ultimate tensile strength of 303 MPa while FRP sheets with a 90^o fiber orientation had an ultimate strength of only 29 MPa.

Table 2-9: Test Program and Coupon Properties

Coupon series	Coupon number	Number of plies	Fiber orientation	Gauge width (mm)	Gauge length (mm)	Gauge thickness (mm)	Thickness per ply (mm)
L	L-1	1	0°	29.0	150	0.92	0.92
	L-2			29.4	148	0.90	0.90
	L-3			29.1	150	0.92	0.92
T	T-1	1	90°	28.5	150	0.88	0.88
	T-2			29.2	152	0.88	0.88
	T-3			26.9	155	0.97	0.97
LT	LT-1	2	0°/90°	30.7	150	1.85	0.93
	LT-2			29.2	152	1.83	0.91
	LT-3			28.9	150	1.83	0.91
LL	LL-1	2	0°/0°	28.9	150	1.78	0.89
	LL-2			28.7	150	1.85	0.93
	LL-3			29.2	150	1.78	0.89
LLL	LLL-1	3	0°/0°/0°	29.7	150	2.70	0.90
	LLL-2			31.9	152	2.58	0.86
	LLL-3			29.7	153	2.64	0.88
DD′	DD′-1	2	±45°	29.6	146	1.58	0.79
	DD′-2			25.8	150	1.68	0.84
	DD′-3			30.0	152	1.60	0.80
DLD′	DLD′-1	3	+45°/0°/−45°	31.4	150	2.43	0.81
	DLD′-2			34.0	150	2.43	0.81
	DLD′-3			32.4	150	2.40	0.80
LDD′L	LDD′L-1	4	0°/±45°/0°	29.8	151	3.13	0.78
	LDD′L-2			30.4	152	3.20	0.80
	LDD′L-3			29.1	152	3.07	0.77

[Adapted from Sadeghian et al**. (**2009**)**]

Table 2-10: Average Results of CFRP Coupon Tests

Fiber orientation	Ultimate strength (MPa)	Initial modulus (MPa)	Ultimate strain (%)	Strain ductility
Longitudinal orientation (0°)	303	41,000	0.74	1.0
Matrix orientation (90°)	29	2,400	0.72	1.0
Orthotropic orientation (0°/90°)	100	17,000	0.97	1.6
Angle orientation (±45°)	47	3,750	3.50	3.5
Angle orientation (0°/±45°/0°)	140	22,000	3.20	3.7
Angle orientation (+45°/0°/−45°)	117	17,000	3.10	4.1

[Adapted from Sadeghian et al. (2009)]

2.3.5 Sadeghian et al. (2010)

In a follow-up study, Sadeghian et al. (2010) examined the effect of fiber orientation by testing a series of 30 cylinders having dimensions of 150 x 300 mm and confined with CFRP having different fiber orientations under uniaxial compression loading. The series including various stacking sequences with fibers oriented in the longitudinal (90^o: L), transverse (0^o: T) and diagonal directions (±45^o: DD'), while the number of layers was varied between 1 and 4 (see

Table 2-11). Based on 7 unconfined specimens, the compressive strength of the unconfined concrete was found to vary between 35 and 45 MPa. The various configurations were used to examine the effect of wrap thickness and fiber orientation on the stress-strain behavior of CFRP confined cylinders. The following points can be gathered from the results of this study:

- Specimens with a 1 layer of CFRP in the hoop direction (0^o) had a significant increase in ultimate strength (102 %) and ultimate strain (181 %) when compared to the unconfined specimens;
- Specimens with FRP oriented in the longitudinal direction (90^o) did not show an effective increase in strength or ductility. However, when combined with FRP sheets at 0^o, the behavior of the specimens became similar to that of specimens with FRP fibers oriented in the hoop direction;
- Specimens confined with 4 layers of angled FRP ($\pm 45^o$) demonstrated an effective enhancement in ductility, an improvement by a factor of 10 in ductility, compared to unconfined cylinders, while specimens confined with 4 layers of 0^o FRP sheets had an increase of 8 times;
- Specimens confined with a combination of FRP sheets with fibers oriented in transverse and angled directions (0^o and $\pm 45^o$) behaved in a similar fashion to cylinders confined purely with FRP in the transverse (0^0) direction.
- The authors of this study also proposed an analytical model for predicting the ultimate stress and strain of FRP-confined cylinders with fibers aligned in hoop direction.

Table 2-11: Test Program and Specimen Properties

Specimen	Number of layers	Fiber orientation	Number of specimen
P	–	Plain	7
T	1	0°	1
TT	2	0°/0°	2
TTT	3	0°/0°/0°	2
TTTT	4	0°/0°/0°/0°	1
L	1	90°	1
LL	2	90°/90°	1
LLL	3	90°/90°/90°	1
TL	2	0°/90°	2
LT	2	90°/0°	2
LLT	3	90°/90°/0°	1
DD′	2	±45°	1
DD′DD′	4	±45°/±45°	1
DD′T	3	±45°/0°	2
TDD′	3	0°/±45°	1
LDD′	3	90°/±45°	1
DD′TT	4	±45°/0°/0°	1
TDD′T	4	0°/±45°/0°	1
LTDD′	4	90°/0°/±45°	1

[Adapted from Sadeghian et al. (2010)]

Table 2-12 Experimental results

Specimen	Fiber orientation	f'_{cc} (MPa)	ε_{cc} (%)	f_r (MPa)	f_r/f'_{co}	f'_{cc}/f'_{co}
T	0	79.0	0.62	3.6	0.09	1.98
TT	0/0	91.9	0.96	7.2	0.18	2.30
TT	0/0	96.4	0.86	7.2	0.18	2.41
TTT	0/0/0	124.9	1.61	10.8	0.27	3.12
TTT	0/0/0	125.7	1.32	10.8	0.27	3.14
TTTT	0/0/0/0	143.3	1.76	14.4	0.36	3.58
LT	90/0	83.2	0.55	3.6	0.09	2.08
LT	90/0	78.2	0.72	3.6	0.09	1.96
TL	0/90	78.8	0.67	3.6	0.09	1.97
TL	0/90	77.2	0.79	3.6	0.09	1.93
LLT	90/90/0	84.9	0.74	3.6	0.09	2.12

[Adapted from Sadeghian et al. (2010)]

2.3.6 Vincent and Ozbakkaloglu (2013B)

Vincent and Ozbakkaloglu (2013B) investigated the effect of fiber orientation and specimen end-condition on the compressive behavior of FRP-confined concrete cylinders by testing a total of 24 circular specimens confined with Aramid-FRP (AFRP). Two different concrete mixes with average compressive strengths of 50 MPa and 80 MPa were used. The influence of fiber orientation was taken into consideration by preparing 12 concrete-filled FRP tubes (CFFTs) having dimensions of 100 x 200 mm and with fiber orientations of 45^0, 60^0, 75^0, and 88^0, with respect to the longitudinal axis. Three cylinders were fabricated for each of the different fiber angles studied in the research program. For the purpose of comparison, specimens confined with fibers orientated in the hoop direction were also prepared. The remaining 12 specimens (152 x 305 mm) were used to examine the influence of specimen end-condition on the stress-strain behavior of FRP-confined concrete. For these specimens, the FRP fiber orientation was placed in the hoop direction (90^0 from axial axis). Details on the specifications of test specimens are presented in **Table 2-13**. The following points can be drawn from this study (see **Table 2-14)**:

- CFFT specimens with fibers aligned in the hoop direction (90^o with respect to the loading axis) displayed a greater increase in strength and an ascending trend in the second branch of their stress-strain response, while specimens with fiber orientations of 45^o and 60^o showed a descending trend in the second branch of their stress-strain response with little or no increase in strength;
- CFFT specimens with 45^o and 60^o fiber orientations behaved in a more ductile fashion than the other cylinders. In addition, specimens with fibers at a 75^0 angle behaved similarly to those with 45^o and 60^o fiber orientations;

- All other 12 cylinders which wrapped in hoop direction had failure by rupturing of FRP jacket at mid height of specimens in hoop direction.
- Specimen end conditions did not have a significant effect on the stress-strain behavior of the FRP-confined cylinders.

Table 2-13 Details of Test Specimens

D (mm)	H (mm)	Confinement type	Concrete type	Total fiber thickness of FRP jacket, t_f (mm)	Fiber angle (degrees)	Loading arrangement	Number of specimens
100	200	CFFT, filament winding	HSC	0.6	45	Concrete and FRP jacket	3
					60		3
					75		3
					88		3
152	305	FRP-wrapped, wet lay-up	NSC	0.6	90	Concrete	3
						Concrete and FRP jacket	3
		CFFT, wet lay-up	NSC	0.6	90	Concrete	3
						Concrete and FRP jacket	3
						Total	24

[Adapted from Vincent and Ozbakkaloglu (2013B)]

Table 2-14: Test Results

Group	Specimen	f'_{co} (MPa)	ε_{co} (%)	θ_f (degrees)	f'_{cc} (MPa)	f'_{cu} (MPa)	ε_{cu} (%)	$\varepsilon_{h,rup}$ (%)	f'_{cc}/f'_{co}	$\varepsilon_{cu}/\varepsilon_{co}$	k_ε
HSCFFTs with inclined fibers	H-T-45-1[a]	70.0	0.28	45	70.5	56.4	0.63	0.54	1.02	1.58	0.21
	H-T-45-2[a]	79.5	0.30	45	80.9	64.7	0.37	0.72			
	H-T-45-3[a]	85.5	0.31	45	87.6	70.1	0.40	0.53			
	H-T-60-1[a]	80.5	0.30	60	82.4	65.9	1.40	1.25	1.01	4.02	0.44
	H-T-60-2[a]	78.0	0.30	60	79.1	63.3	1.48	1.89			
	H-T-60-3[a]	74.0	0.29	60	74.5	59.6	0.71	0.73			
	H-T-75-1	83.0	0.31	75	108.3		1.25	0.95	1.35	4.35	0.38
	H-T-75-2	83.0	0.31	75	111.6		1.42	1.01			
	H-T-75-3	85.9	0.31	75	117.3		1.48	1.38			
	H-T-88-1	85.9	0.31	88	176.2		2.89	2.36	1.99	8.91	0.75
	H-T-88-2	83.0	0.31	88	154.9		2.53	1.74			
	H-T-88-3	85.9	0.31	88	176.6		2.89	2.42			
NSCFFTs	N-TE-90-1	49.4	0.24	90	104.6		3.15	2.19	2.15	14.32	0.93
	N-TE-90-2	49.4	0.24	90	107.9		3.55	2.42			
	N-TE-90-3	49.4	0.24	90	106.3		3.47	2.38			
	N-T-90-1	49.4	0.24	90	109.9		3.01	2.11	2.23	12.92	0.89
	N-T-90-2	49.4	0.24	90	109.9		3.18	2.33			
	N-T-90-3	49.4	0.24	90	110.7		2.98	2.24			
NSC FRP-wrapped	N-WE-90-1	49.4	0.24	90	109.0		3.73	2.54	2.14	14.79	0.90
	N-WE-90-2	49.4	0.24	90	103.4		3.40	2.10			
	N-WE-90-3	49.4	0.24	90	105.3		3.37	2.08			
	N-W-90-1	49.4	0.24	90	107.7		3.41	2.18	2.17	14.24	0.87
	N-W-90-2	49.4	0.24	90	104.0		3.22	2.12			
	N-W-90-3	49.4	0.24	90	110.1		3.48	2.22			

[a] Indicates specimens with ultimate conditions defined by an axial stress drop below $0.8f'_{cc}$.

[Adapted from Vincent and Ozbakkaloglu (2013B)]

2.3.7 Hadi and Le (2014)

Hadi and Le (2014) performed a study on the behaviour of square reinforced concrete columns wrapped with CFRP placed in different fiber orientations. A total of 12 specimens, having dimensions of 200 x 200 x 800 mm with an 80 mm square hollow section, were tested under centric and eccentric compression loading. To prevent premature failure of the FRP jacket, specimen corners were rounded to a radius of 32 mm. The columns were reinforced in both the longitudinal and transverse directions with 4 - 12 mm longitudinal bars and 6 mm ties spaced at 100 mm (see **Figure 2-17**). The unconfined compressive strength of concrete for all columns was 40 MPa and the specimens were jacketed with CFRP oriented in the hoop direction (0^o), longitudinal direction (90^o), and at $\pm 45^o$ (**Table 2-15** shows the CFRP thickness and configurations used in the various specimens). The following conclusions can be drawn from the findings of this study:

- The effect of confinement was more noticeable in specimens wrapped with 3 layers of CFRP in the hoop direction;
- In terms of ductility, fibers oriented in the hoop directions resulted in a more noticeable increase in column axial and lateral strain. The axial strain of specimens confined with 3 layers of CFRP in the hoop direction under concentric loading (HF-0) increased by 4.7 times compared to the reference specimens without FRP (RC-0), and 2.4 times compared to columns confined with one vertical & two hoop layers (VHF-0) and those with two ±45° & one hoop layers (AHF-0). The relative increases in axial strain were even more significant in the case of eccentric loading;

- The largest ductility was expected from specimens wrapped with a combination of angled and hoop layers, however the increase in ductility in those specimens was only found to be approximately 1.6-2.1 times the enhancement in the reference specimens.
- In the case of eccentric loading, the influence of vertical and angled fiber was beneficial in resisting the bending moment, especially as the eccentricity was increased.

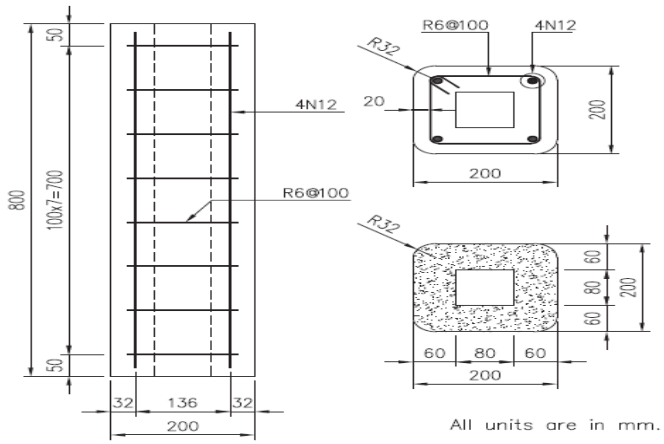

Figure 2-17 Details of the Test Specimens and Reinforcement

[Adapted from Hadi and Le (2014)]

Table 2-15 Summary of testing results

Specimen	Max. load	Corresponding displacement at max. load		Ultimate displacement		Corr. axial load at ultimate displacement (kN)	Normalised max. load
	kN	Axial mm	Lateral mm	Axial mm	Lateral mm		
RC-0	1341	3.32	N/A[a]	3.58	N/A	1139	1
HF-0	1485	21.99	N/A	–	–	–[b]	1.11
VHF-0	1525	4.03	N/A	8.07	N/A	1287	1.14
AHF-0	1417	3.81	N/A	7.02	N/A	1174	1.06
RC-25	998	2.99	1.71	3.15	1.99	848	1
HF-25	1245	3.75	1.48	–	–	–	1.25
VHF-25	1189	3.80	1.57	8.17	6.14	911	1.19
AHF-25	1083	3.73	2.29	7.60	7.01	759	1.09
RC-50	755	3.06	2.20	3.38	2.70	641	1
HF-50	825	3.67	2.56	26.96	27.94	697	1.09
VHF-50	889	4.13	3.23	10.32	8.34	737	1.18
AHF-50	862	3.78	2.50	8.79	6.65	696	1.14

[a] The lateral displacement is not applicable in cases of concentric loading.
[b] Data was lost due to an accident during testing.

[Adapted from Hadi and Le (2014)]

2.3.8 Parretti and Nanni (2002)

Parretti and Nanni (2002) conducted a study examining the effect of fiber orientation on CFRP-confined reinforced concrete columns. Five circular specimens (200 x 914 mm) and three rectangular specimens (178 x 178 x 914 mm) were tested under pure axial compression. Both types of columns had a cap enlargement of 610 x 610 x 254mm in the end regions to force failure in the specimen gage length. Longitudinal reinforcement consisted of 4 - 13 mm and 8 - 10 mm bars for the rectangular and circular specimens, respectively, while lateral reinforcement consisted of 6 mm ties at 178mm and 50mm for rectangular and circular columns, respectively. One circular column was wrapped with $\pm 45^{0}$ CFRP, and three were confined with unidirectional CFRP in the hoop direction (0^{o}). As for the rectangular specimens, one was wrapped with $\pm 45^{0}$ CFRP and one in the hoop direction (0^{o}). All specimens were confined with one layer of CFRP. The following conclusions were drawn from this study:

- Circular columns confined with FRP sheets with the fibers in the hoop direction (0^{o}) experienced sudden an explosive failures due to rupture of the FRP jacket, however these specimens experienced a substantial increase in strength, whereas the specimens wrapped with fibers oriented at ±45° showed more ductile and gradual failures, with more significant strength enhancement (for example see **Figure 2-18**, where specimen DB450-C [confined in ±45°] behaves in a more ductile fashion compared to L200-C and L300-C which were confined in the hoop direction).
- In the case of the rectangular columns, use of unidirectional fibers (0^{o}) showed greater ductility and overall gain in strength compared to those confined with $\pm 45^{o}$ FRP sheets (see **Figure 2-19**)

- Overall, circular specimens performed better in terms of strength and ductility enhancement when compared to companion specimen having rectangular cross-sections, which was attributed to the reduction in effectively confined concrete area in specimens with a rectangular cross section.

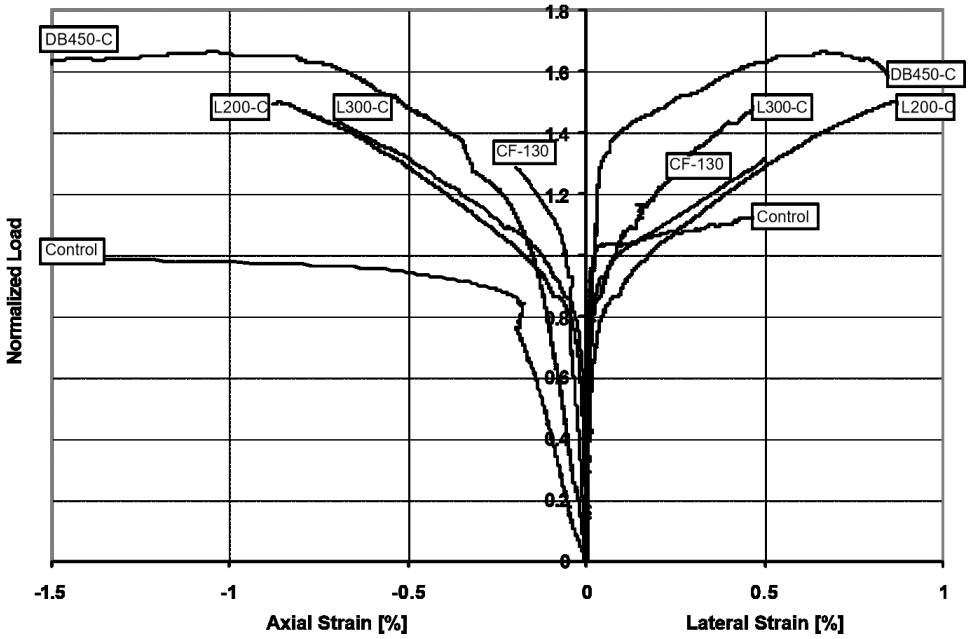

Figure 2-18 Normalized Load-Strain Envelopes for Circular Columns

[Adapted from Parretti and Nanni (2002)]

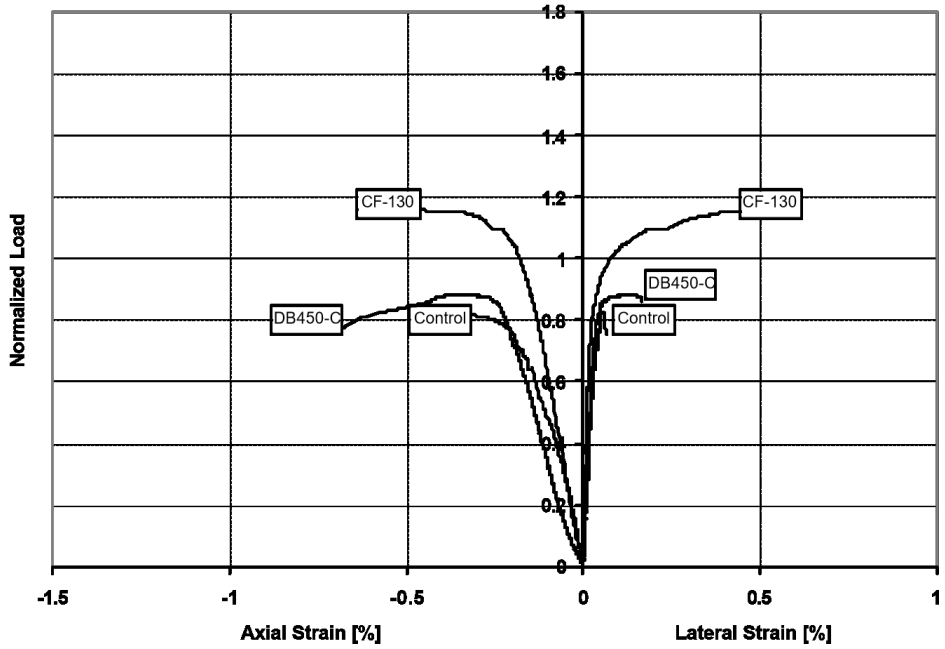

Figure 2-19 Normalized Load-Strain Envelopes for Rectangular Columns

[Adapted from Parretti and Nanni (2002)]

2.3.9 Hong and Kim (2004)

Hong and Kim (2004) tested 14 circular (300 x 600 mm) and 4 square columns (250 x 250 x 600 mm) confined by carbon composite tubes under monotonically increasing axial loading. The tubes were made of filament-wound carbon composite with $90^o + 90^o$, $90^o \pm 60^o$, $90^o \pm 45^o$, and $90^o \pm 30^o$ winding angles with respect to the longitudinal axis. In the case of the circular specimens, significant improvement was noticed in both ultimate strength and ductility. However, the square specimens did not show considerable enhancement compared to the cylinders. The circular specimens with winding angles of $90^0 + 90^0$, $90^0 \pm 60^0$, $90^0 \pm 45^0$, and $90^0 \pm 30^0$ showed a rise in strength of 4.58, 5.00, 3.30, and 2.61 times the strength of unconfined concrete, respectively. On the other hand, the square specimens with winding angles of $90^0 \pm 45^0$

and $90^0 \pm 30^0$ displayed an increase in compressive strength of approximately 1.27 and 1.64 times the strength of unconfined specimens

2.4 Summary

This chapter provided a review of existing studies related to the behavior of FRP-confined concrete. The influence of parameters such as FRP types, amount of confinement, unconfined concrete strength, specimen cross section, size effect, aspect ratio, and corner radius were discussed. The literature review demonstrates these parameters can affect the stress-strain behavior of FRP-confined concrete. A brief review of the influence of FRP on the behavior of reinforced concrete columns and a review of research related to cast in place FRP jacketing was also summarized. The chapter also summarizes a number of studies which have examined the influence of fiber orientation on the stress-strain behavior of FRP-confined cylinders and columns. In general, the results show that confinement with FRP fibers oriented in the hoop direction (0^o) results in the maximum increase in strength among other fiber orientations. However, specimens confined angular fibers oriented at $\pm 45^0$ can show relatively more significant enhancements in ductility (although this is not always the case from all experiments in the literature). A limited number of studies have also examined the effect of stacking sequence and combination of FRP orientations on the stress-strain behavior of FRP-confined concrete, however the conclusions from these limited studies are not conclusive on the benefits of combining transverse, longitudinal and angular fiber orientations, and the effects of complex FRP confinement configurations (combination of different orientations and in different sequences) on the behavior of FRP-confined concrete has yet to be thoroughly investigated.

3 Chapter 3: Experimental Program

3.1 Chapter Overview

This research program was undertaken to gain understanding into various parameters that affect the behavior of concrete confined with carbon fiber-reinforced polymers (CFRP). As part of the study a large set of cylindrical CFRP-confined concrete specimens are tested under monotonic uniaxial compression. Test variables considered in the study include CFRP fiber orientation, CFRP stacking sequence, number of CFRP layers, and concrete cylinder specimen size. To examine the effect of the test parameters on CFRP laminate behavior, the experimental program also includes a companion set of CFRP coupons which are tested under uniaxial tension. This chapter describes the details of the experimental testing program, material properties, specimen construction, specimen instrumentation, and testing procedures.

3.2 Testing Program

3.2.1 CFRP confined cylinders

To gain a better understanding of the effect of CFRP retrofitting on the behavior of concrete in compression, a total of 169 concrete cylinders, including 161 wrapped specimens and 8 unwrapped control specimens, were tested under uniaxial compression to failure. Variables considered in this study include: CFRP fiber orientation, CFRP stacking sequence (lay-up), number of CFRP layers and concrete cylinder specimen size. As shown in **Table 3-1** the research program includes one control set of unconfined (unwrapped) concrete specimens (*Series 0*) and nine (9) series of CFRP-confined specimens (*Series 1, 2, 3, 4A, 4B, 5A, 5B, 6, 7*) with various CFRP lay-ups. Each lay-up (stacking sequence) had varying combinations and orientations of unidirectional and woven CFRP. Two different types of CFRP fabrics were used

to manufacture the nine stacking sequences shown in **Table 3-1**: 1) unidirectional CFRP; and 2) woven ±45 CFRP. The unidirectional CFRP is called UD [0˚] in the series nomenclature when the fibers in the ply are running parallel to the hoop direction of the cylinder, and is called UD [90˚] when the fiber is running parallel to the longitudinal direction of the cylinder. This CFRP type is also referred to as UD [-45˚] or UD [+45˚] when the unidirectional fiber orientation is slanted by an angle -45 or +45 with respect to the hoop direction (see **Figure 3-2**). The woven CFRP fabric had woven fibers aligned in ±45° directions and is called W [±45^0] in the series nomenclature. Within each series two standard sizes of concrete cylinders specimens were manufactured and tested: the "small" specimens had a diameter, d = 100 mm and height, h = 200 mm, while the "large" specimens had a diameter, d = 150 mm and height, h = 300 mm (see **Figure 3-1**). In general the specimens within each series were confined with 4, 6 or 8 layers of CFRP in order to examine the effect of the number of layers on the behavior of CFRP-confined concrete. A total of five replicates were tested for most "small" specimen configurations, while three replicates were tested in the case of the "large" specimen configurations.

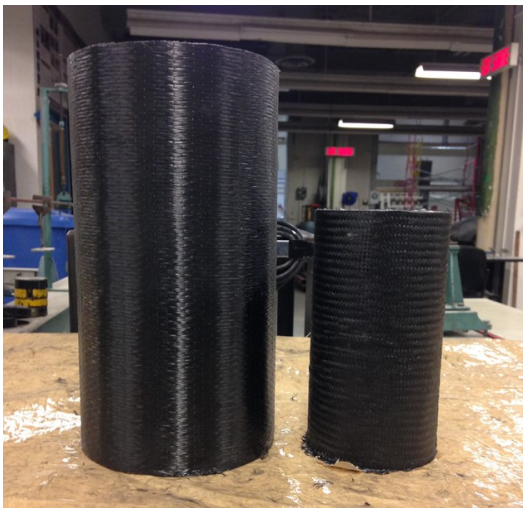

Figure 3-1 Two sizes of concrete cylinders considered in this study

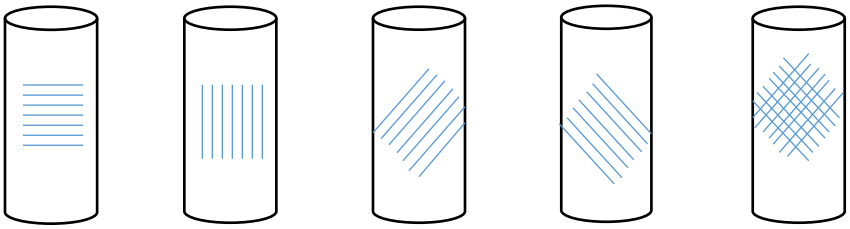

(a) UD [0°] (b) UD [90°] (c) UD [+45°] (d) UD [-45°] (e) W [±45°]

Figure 3-2 Unidirectional (UD) & woven (W) CFRP nomenclature description

Table 3-1CFRP-confined concrete cylinder test matrix

Series	Orientation	# of Layers	# of 100 mm Specimens	# of 150 mm Specimens
0	Control	0	5	3
1	UD $[0]_4$	4	5	3
	UD $[0]_6$	6	5	3
	UD $[0]_8$	8	5	3
2	UD$[90\ ^\circ/0^\circ]_2$	4	5	3
	UD$[90\ ^\circ/0^\circ]_3$	6	5	3
	UD$[90\ ^\circ/0^\circ]_4$	8	5	3
3	UD $[+45^\circ/-45^\circ]_2$	4	4	3
	UD $[+45^\circ/-45^\circ]_3$	6	5	3
	UD $[+45^\circ/-45^\circ]_4$	8	5	3
4A	UD$[90^\circ/0^\circ]$W$[\pm45^\circ]_2$	4	4	3
	UD$[90^\circ/0^\circ]_2$W$[\pm45^\circ]_2$	8	4	3
4B	UD$[90^\circ]$W$[\pm45^\circ]_2$UD$[0^\circ]$	4	4	3
	UD$[90^\circ]_2$W$[\pm45^\circ]_4$UD$[0^\circ]_2$	8	4	3
5A	UD$[0^\circ]_2$W$[\pm45^\circ]_2$	4	4	2
	UD$[0^\circ]_4$W$[\pm45^\circ]_4$	8	4	3
5B	W$[\pm45^\circ]_2$UD$[0^\circ]_2$	4	4	3
	W$[\pm45^\circ]_4$UD$[0^\circ]_4$	8	4	2
6	UD$[90^\circ_2/0^\circ_2]$	4	5	3
	UD$[90^\circ_3/0^\circ_3]$	6	5	3
	UD$[90^\circ_4/0^\circ_4]$	8	5	3
7	W$[\pm45^\circ]_4$	4	4	-
	W$[\pm45^\circ]_6$	6	4	-
	W$[\pm45^\circ]_8$	8	4	-

3.2.2 CFRP tension coupons

In order to gain further understanding into the effect of FRP stacking sequence on laminate behavior, the experimental program also included a companion set of 195 carbon fiber-reinforced polymer (CFRP) laminated specimens, otherwise referred to as coupons in this thesis, were tested under uniaxial tension in accordance with the ASTM D3039//D3039M standard (ASTM, 2015). The coupons had dimensions of 25 mm x 250 mm and were manufactured in nine (9) series using the same lay-ups considered in the cylinder testing program (see Table 3-2). Within each series test variables included the number of CFRP layers (4, 6 or 8 layers) and coupon orientation with respect to loading (X or Y axis - see **Section 3.5.1**).

Table 3-2 CFRP tension coupon test matrix

Series	Orientation	# of Layers	X Direction	Y Direction
1	UD $[0^\circ]_4$	4	5	0
	UD $[0^\circ]_6$	6	5	0
	UD $[0^\circ]_8$	8	5	0
2	UD$[90^\circ/0^\circ]_2$	4	5	5
	UD$[90^\circ/0^\circ]_3$	6	5	5
	UD$[90^\circ/0^\circ]_4$	8	5	5
3	UD $[+45^\circ/-45^\circ]_2$	4	5	5
	UD $[+45^\circ/-45^\circ]_3$	6	5	5
	UD $[+45^\circ/-45^\circ]_4$	8	5	5
4A	UD$[90^\circ/0^\circ]$W$[\pm45^\circ]_2$	4	5	5
	UD$[90^\circ/0^\circ]_2$W$[\pm45^\circ]_2$	8	5	5
4B	UD$[90^\circ]$W$[\pm45^\circ]_2$UD$[0^\circ]$	4	5	5
	UD$[90^\circ]_2$W$[\pm45^\circ]_4$UD$[0^\circ]_2$	8	5	5
5A	UD$[0^\circ]_2$W$[\pm45^\circ]_2$	4	5	5
	UD$[0^\circ]_4$W$[\pm45^\circ]_4$	8	5	5
5B	W$[\pm45^\circ]_2$UD$[0^\circ]_2$	4	5	5
	W$[\pm45^\circ]_4$UD$[0^\circ]_4$	8	5	5
6	UD$[90^\circ_2/0^\circ_2]$	4	5	5
	UD$[90^\circ_3/0^\circ_3]$	6	5	5
	UD$[90^\circ_4/0^\circ_4]$	8	5	5
7	W$[\pm45^\circ]_4$	4	5	5

3.3 Layup Description

This section provides further description on the nine layups considered in the study. As noted previously, the layups are composed of various combinations of unidirectional (UD) and woven ±45° (W) CFRP fabric. **Table 3-3** illustrates the stacking sequence used in each layup series as well as the order of the CFRP sheet application, starting with the innermost sheet, which is applied to the concrete cylinder surface, and ending with the outermost sheet.

Table 3-3 Layup Description of CFRP Confined Specimens

Series	Orientation	# of Layers	Stacking Sequence Description
1	UD[0˚]	4	(0)-(0)-(0)-(0)
		6	(0)-(0)-(0)-(0)-(0)-(0)
		8	(0)-(0)-(0)-(0)-(0)-(0)-(0)-(0)
2	UD[90 ˚/0˚]	4	(90)-(0)-(90)-(0)
		6	(90)-(0)-(90)-(0)-(90)-(0)
		8	(90)-(0)-(90)-(0)-(90)-(0)-(90)-(0)
3	UD [+45˚/-45˚]	4	(+45)-(-45)-(+45)-(-45)
		6	(+45)-(-45)-(+45)-(-45)-(+45)-(-45)
		8	(+45)-(-45)-(+45)-(-45)-(+45)-(-45)-(+45)-(-45)
4A	UD[90˚/0˚]W[±45˚]	4	(90)-(0)-(±45)-(±45)
		8	(90)-(0)-(90)-(0)-(±45)-(±45)-(±45)-(±45)
4B	UD[90˚]W[±45˚]UD[0˚]	4	(90)-(±45)-(±45)-(0)
		8	(90)-(90)-(±45)-(±45)-(±45)-(±45)-(0)-(0)
5A	UD[0˚]W[±45˚]	4	(0)-(0)-(±45)-(±45)
		8	(0)-(0)-(0)-(0)-(±45)-(±45)-(±45)-(±45)
5B	W[±45˚]UD[0˚]	4	(±45)-(±45)-(0)-(0)
		8	(±45)-(±45)-(±45)-(±45)-(0)-(0)-(0)-(0)
6	UD[90˚$_x$/0˚$_x$]	4	(90)-(90)-(0)-(0)
		6	(90)-(90)-(90)-(0)-(0)-(0)
		8	(90)-(90)-(90)-(90)-(0)-(0)-(0)-(0)
7	W[±45˚]	4	(±45)-(±45)-(±45)-(±45)
		6	(±45)-(±45)-(±45)-(±45))-(±45)-(±45)
		8	(±45)-(±45)-(±45)-(±45) (±45)-(±45)-(±45)-(±45)

3.3.1.1 Series 0:

Specimens in this series were tested without CFRP confinement in order to obtain the strength of unconfined concrete at the time of testing. The series includes 8 specimens, including 5 "small" (100 x 200 mm) and 3 "large" (150 x 300 mm) cylinders.

3.3.1.2 Series 1:

All specimens in this series were confined with unidirectional (UD) CFRP sheets with fibers oriented at 0° with respect to the cylinder horizontal axis (i.e. hoop direction). The series includes "small" (100 x 200 mm) and "large" (150 x 300 mm) cylinders confined with 4, 6, or 8 layers of CFRP. For each configuration, 5 replicates were included for the "small" cylinders and 3 replicates were included for the "large" cylinders.

3.3.1.3 Series 2:

Specimens in this series were confined with unidirectional (UD) CFRP sheets placed in both 0° and 90° orientations with respect to the cylinder horizontal axis. As shown in **Table 3-3**, one layer of CFRP with fibers aligned at 90° was first applied on the concrete cylinder surface, followed by a second CFRP sheet with fibers aligned at 0° (hoop direction). This sequence was repeated a second, third or fourth time for the specimens with 4, 6 or 8 layers, respectively. Both "small" and "large" cylinders were tested for each configuration, including 5 & 3 replicates for the 100 & 150 mm cylinders, respectively.

3.3.1.4 Series 3:

In this series, specimens were confined with unidirectional (UD) CFRP with fibers at +45° and -45°. In order to obtain this fiber orientation the unidirectional sheets where slanted at an angle of +45° or -45° (see **Figure 3-2**). As shown in **Table 3-3**, the specimens were manufactured by

installing a first layer of UD sheet at +45°, followed by a second layer with fibers at -45°. This sequence was repeated a 2nd, 3rd or 4th time for the specimens with 4, 6 or 8 layers, respectively. Both "small" and "large" cylinders were tested for each configuration, including 5 & 3 replicates for the 100 & 150 mm cylinders, respectively.

3.3.1.5 Series 4:

Series 4 was divided into 2 subseries, 4A and 4B, based on the order of the layup sequence. Specimens in series 4A were wrapped with 4 and 8 layers of unidirectional (UD) and woven (W) CFRP sheets at 90^0, 0^0, and $\pm45^0$ (see **Table 3-3**). For specimens having 4 layers, UD fabric was first applied at 90^0 and 0^0 (layer 1 and 2, respectively) followed by 2 layers of woven $\pm45^0$ CFRP. For specimens confined with 8 layers, the sequence of unidirectional CFRP at 90^0-0^0 was repeated two times (i.e. 90^0- 0^0 -90^0- 0^0) followed by 4 l layers of woven $\pm45^0$ CFRP fabric. For series 4B the sequence was changed to UD [90°] - W [±45°] - UD [0°]. For specimens confined with 4 layers, the first layer of unidirectional CFRP had fibers aligned at 90°, and this was followed by two layers of woven $\pm45^0$ CFRP, and a final layer of UD with fibers aligned in the 0^0 direction. In the case of specimens confined with 8 layers of CFRP, the first 2 layers of unidirectional CFRP were applied at 90^0, followed by 4 layers of W [±45°] CFRP and 2 layers of unidirectional CFRP with fibers aligned at 0^0. Both "small" and "large" cylinders were tested for each configuration in Series 4A/4B, including 4 & 3 replicates for the 100 & 150 mm cylinders.

3.3.1.6 Series 5:

Series 5 was divided into 2 subseries, 5A and 5B, based on the order of the layup sequence. Specimens in series 5A were wrapped with 4 and 8 layer of 0^0 unidirectional and woven $\pm45^0$ CFRP (see **Table 3-3**). For specimens confined with 4 layers of CFRP, the first two layers of

unidirectional CFRP were applied in the 0^0 direction, followed by two layers of woven $\pm45^0$ CFRP. The same procedure was used for specimens confined with 8 layers of CFRP; specimens were first confined with 4 layers of unidirectional CFRP at 0^0, followed by 4 layers of woven $\pm45^0$ CFRP. The stacking sequence was changed to W [±45°] - UD [0°] for series 5B. The specimens were first wrapped with 2 or 4 layers of W [±45°] CFRP followed by 2 or 4 layers of UD [0°] CFRP. Both "small" and "large" cylinders were tested for each configuration in Series 5A/5B, including 4 & 3 replicates for the 100 & 150 mm cylinders, respectively.

3.3.1.7 Series 6:

Specimens in this series were confined with unidirectional CFRP sheets placed in both 90° and 0° orientations. As shown in **Table 3-3**, this series differs from series 2, in that the first 2 layers were applied at 90° before the application of 2 layers at 0° for specimens having 4 layers of CFRP. The same procedure was used for specimens confined with 6 and 8 layers; first multiple layers having 90° orientation were applied, followed by the application of multiple layers having 0° orientation. Both "small" and "large" cylinders were tested for each configuration in this series, including 5 & 3 replicates for the 100 & 150 mm cylinders.

3.3.1.8 Series 7:

The final series, which was a companion to series 3, was designed to examine the effect of woven vs. unidirectional fibers on the behavior of CFRP-confined concrete. Specimens in this series were confined with 4, 6, or 8 layers of woven ±45° CFRP fabric. Both "small" and "large" cylinders were tested for each configuration in this series, including 4 replicates for the 100 mm cylinders. However, 150 mm cylinders were not include in this series.

3.4 Material Properties

3.4.1 Concrete

In order to fully explore the influence of CFRP wrap on concrete behavior tested under uniaxial compression load, concrete of a relatively low compressive strength was used to fabricate the cylinders. Concrete with a specified strength of 25 MPa was provided by a local ready-mix company (see **Figure 3-3**); the mix proportions are shown in **Table 3-4**. The concrete used commercially available Type I Portland Cement; 14 mm maximum size crushed limestone aggregate complying with ASTM C33-2013; sand conforming to the graduation requirement of ASTM C33-2013; and did not contain any dry or liquid admixtures. The properties of the fresh concrete, in terms of slump, density and air content are reported in **Table 3-5**.

Table 3-4 Concrete Mix Design

Materials	Mass (kg/m³)	Weight fraction
Cement	256	1
Water	128	0.5
Sand	781	3.0
Aggregate	1077	4.2

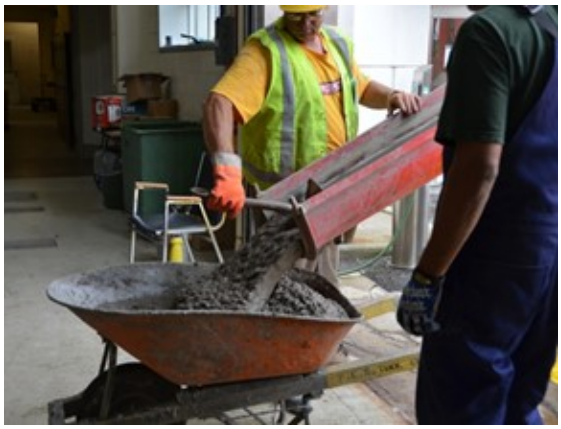

(a) Ready-mix concrete

(b) Preparation of standard cylinders

Figure 3-3 Concrete ready-mix supply and casting of cylinders

Two standard concrete cylinder sizes were adopted in this study: as noted previously the "small" and "large" size cylindrical specimens had dimensions (d x h) of 100 x 200 mm and 150 x 300 mm, respectively. In total 169 "small" and "large" cylinders, including 161 wrapped and 8 unwrapped cylinders were cast to manufacture the specimens in *Series 0-9* (see **Figure 3-3**). All cylinders were prepared and cured according to the ASTM C31 Standard (ASTM, 2015). Molds were removed after 16 hours and concrete cylinders were left to cure for 28 days. Curing was achieved by covering the specimens with a layer of wet burlap followed by another layer of plastic sheet. When the curing period was over, the cylinders were wrapped with different CFRP lay-ups. The wrapped and companion control (unwrapped) specimens were tested approximately one year after the initial casting date (335 days).

An additional set of "small" size cylinders were also cast to track the concrete strength gain with time, with three additional samples tested at 7, 28, 56 and 90 days. All cylinders were tested under uniaxial compression in accordance with the ASTM C39 Standard (ASTM, 2015). The strength gain results are summarized in **Table 3-6** and **Figure 3-6**. All cylinders were tested using a *STATEC* 2000 KN universal testing machine at the National Research Council of Canada (NRC) as shown in **Figure 3-5**. For the specimens tested at 28 days only, the modulus of elasticity (Ec) and Poisson's ratio (ν) of the concrete were also determined using a compressometer in accordance with the ASTM C469 Standard (ASTM, 2015) (see **Figure 3-5c**). As shown in **Table 3-5** the average modulus of elasticity and Poisson's ratio at 28 days were found to be 26.8 GPa and 0.22, respectively. The control (unwrapped) series 0 specimens were tested at 335 days. A total of 5 "small" and 3 "large" cylinders were tested and the concrete was determined to have an average unconfined concrete compressive strength of 43 MPa at this age. Complete stress-strain relationships for the unconfined concrete were also determined (where

strain was adjusted using readings obtained from the testing frame machine head-displacement - see **Section 3.6.1**); typical stress-strain curves for the series 0 "small" and "large" size specimens are shown in **Figure 3-6**.

Table 3-5 Fresh and hardened concrete properties at 28 days

Fresh Concrete Properties at 28 days				
Slump (mm)	Volume weight (Kg)	Density (Kg/m³)	Air (%)	Temperature ºC
65	16.873	2380	3.5	22.5
Compressive properties at 28 days				
Peak Load (KN)	Strain at Peak (µm/m)	Stress at Peak (MPa)	Modulus of Elasticity (GPa)	Poisson's
256.5	3656	30.78	26.81	0.22

Table 3-6 Average compressive strength of concrete at different ages

Age (Days)	7	28	56	90	335
Compressive Strength (MPa)	22.79	30.78	35.89	38.95	43.00
% of 28d Compressive Strength	74.1	--	116.6	126.5	139.7

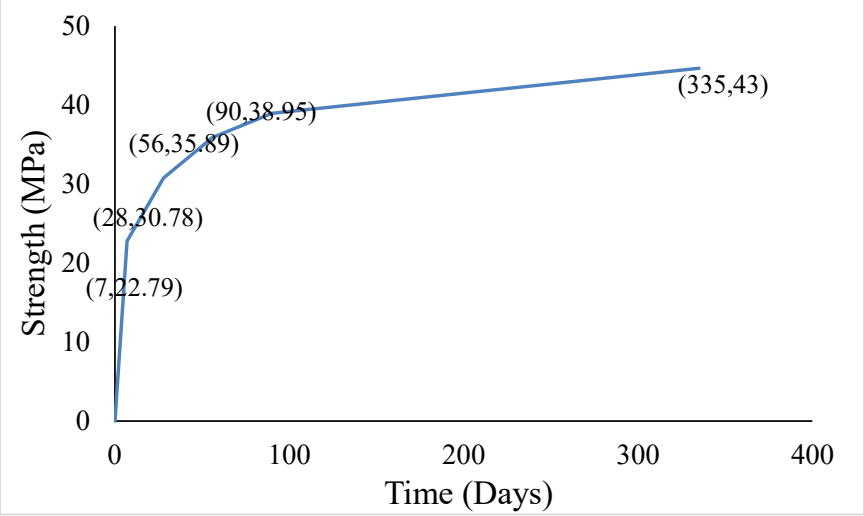

Figure 3-4 Concrete strength gain with time

(a) *STATEC* 2000 KN universal testing machine with cylinder ready for testing

(b) Cylinder in testing compartment

(c) Compressometer setup

Figure 3-5 Concrete cylinder test setup

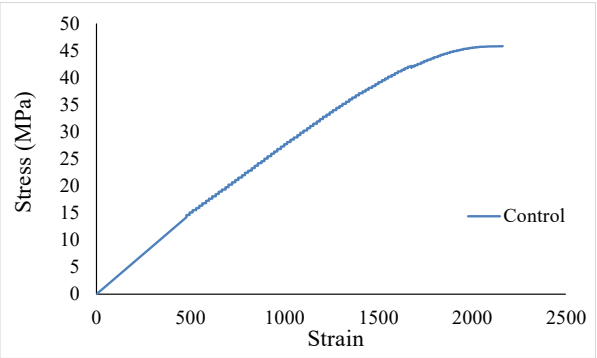

(a) 100 mm control specimens

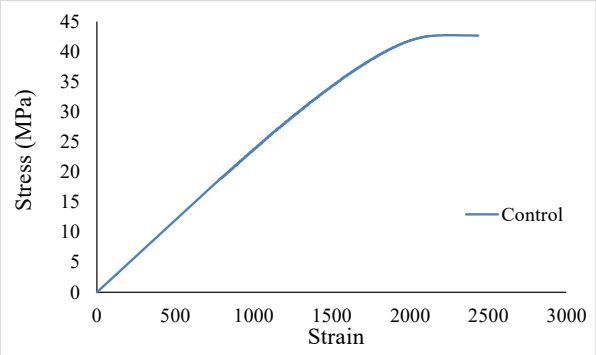

(b) 150 mm control specimens

Figure 3-6 Typical stress-strain curves for control (series 0) cylinders at 335 days.

3.4.2 Fiber Reinforced Polymer (FRP)

Two types of carbon fiber reinforced polymer (CFRP) fabric, with (1) unidirectional CFRP fibers and (2) woven ±45 CFRP fibers, were used in the experimental program (see **Figure 3-7**). The unidirectional fabric, which is coded as *TC-09-U* by the manufacturer, consists of concentrated fibers at 0° with sparsely spaced fibers at 90° for linking (at a warp-weft ratio of 97%-3%), and has a nominal thickness of 0.34 mm/ply with a wet lay-up thickness of 0.7 mm/ply. The woven ±45 CFRP, coded as *TC-06-T* by the manufacturer, consists of 2:2 twill fabric with fibers aligned in ±45° (at a warp-weft ratio of 50%-50%), and has a nominal thickness of 0.2 mm/ply with a wet lay-up thickness of 0.38 mm/ply. The manufacturer-specified properties of both types of CFRP are presented in **Table 3-7**. It is noted that the stress-strain properties of the composite layups used to the wrap the cylinders were determined experimentally by testing coupons in accordance to ASTM D3039/D3039M Standard.

Figure 3-8 shows the resin and hardener that were used for the epoxy matrix in this study. The epoxy consisted of *ProBuild MM55538* epoxy resin and *ProBuild MM55729* hardener at a ratio of 3:1 by weight, and was mixed manually for about 1 minute before saturating the CFRP fabric.

According to the manufacturer, the mixed epoxy has a working life of about 30 minutes at 25 ºC. This guideline was followed during the manufacture of all CFRP-confined cylinder samples.

Table 3-7 CFRP properties as specified by the manufacturer

FRP Type	Modulus of Elasticity (GPa)	Rupture Strength (MPa)	Nominal Thickness (mm)	Wet Lay-up Thickness (mm)
TC-09-U	131	1605	0.34	0.70
TC-06-T	60	861	0.20	0.38

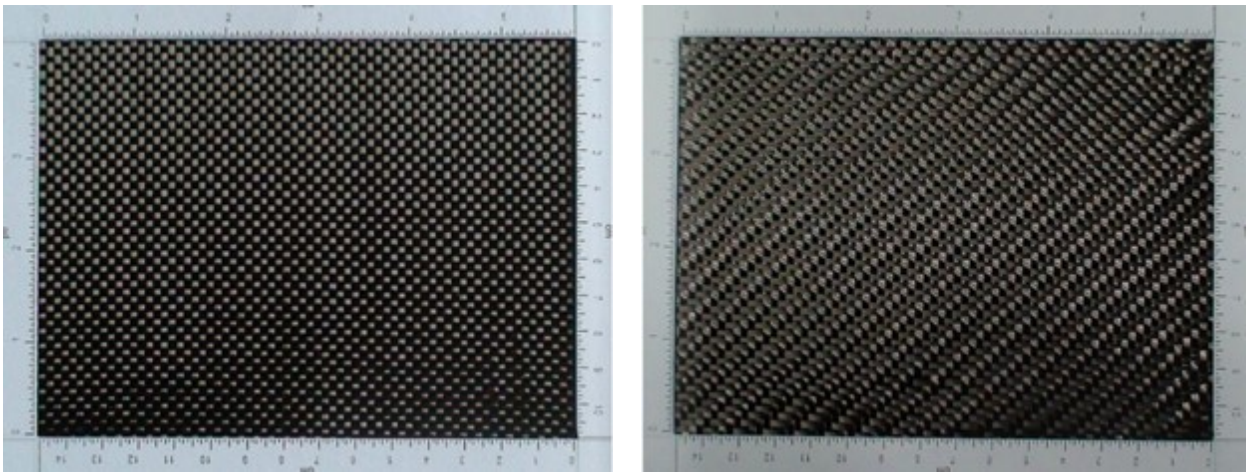

(a) Unidirectional (UD) fabric (b) Woven (W) fabric

Figure 3-7 Two types of CFRP fabric considered in this study

(a) Resin (b) Hardener

Figure 3-8 Epoxy mixture components

3.5 Preparation and Testing of Specimens

This section describes the construction, test set-up and testing procedure for the CFRP confined concrete cylinders and CFRP coupons.

3.5.1 Construction of Specimens

3.5.1.1 CFRP-confined Concrete Cylinders

The majority of the CFRP-confined specimens were wrapped immediately following the initial 28 day curing period of the concrete cylinders (the exception being the specimens in Series 4, 5 and 7 which were wrapped 1037 days after casting). After wrapping, the specimens were left to cure under normal dry laboratory conditions until the start of the testing program which began approximately one year after the initial concrete cast date. As noted previously, the compressive strength of the unconfined concrete had increased to 42 MPa at this time.

Before wrapping, the concrete cylinders were ground flat at both ends using a cylinder grinder to ensure a smooth and uniform test surface for loading. The ends were then tapped with duct tape to avoid having epoxy residue on the surface of the specimens (this tape was removed prior to testing). The sheets were applied to the concrete surface by the wet layup method. As noted previously the epoxy-resin ratio was 1:3. All cylinders were wrapped over their entire height and the CFRP plies were extended as close as possible to the ends of the cylinders to minimize the likelihood of premature failure of the unconfined concrete at the specimen ends. It is noted that an overlap of 70 mm was used in between each layer of CFRP to prevent de-bonding during testing. This overlap has been found to be sufficient from previous testing conducted at the NRC and is in line with the recommendations of other researchers (Shahawy et al.2000, Benzaid et al.2010, Li, G.2006, etc.).

The jacketing process is illustrated in **Figure 3-9**. First, the CFRP sheets for each layer were cut into separate sheets of 203.2 mm x 389 mm and 304.8 mm x 548.5 mm for the 100 mm and 150 mm cylinders, respectively. After cutting the sheets, the jacketing began by applying a layer of epoxy on the dry surface of the concrete cylinders as shown in **Figure 3-9a**, and this was followed by impregnating one layer of CFRP sheet with epoxy as shown in **Figure 3-9b**. Thereafter the fully saturated CFRP sheet was applied on the surface of the concrete cylinder as shown in **Figure 3-9c**. Finally, the applied CFRP sheet was pressed using a *Matt Roller* in the fiber direction to extract any entrapped air bubbles and excess epoxy as demonstrated in **Figure 3-9d**. The remaining layers were applied immediately after application of the first layer following the same procedure until the stacking sequence was completed. A sufficient amount of epoxy was applied for all CFRP layers to ensure a fully saturated CFRP jacket. A few days after wrapping, the extra edges of the CFRP at the ends of the cylinders were flattened flush with the

cylinder ends using a sanding machine. The specimens were then left to cure under normal laboratory conditions until testing. In all cases the CFRP had cured for a minimum of 7 days before cylinder testing.

(a) Surface preparation (b) Sheet impregnation (c) Cylinder wrapping (d) Rolling

Figure 3-9 Step by Step Jacketing of Concrete Cylinders

3.5.1.2 CFRP Coupons

Laminated carbon fiber-reinforced polymer (CFRP) free-film sheets having dimensions of 450 mm x 450 mm were used to manufacture the tension coupon specimens in this study. The laminated plates for each series had the same CFRP stacking sequences used in the companion cylinder testing program. A total of 10 coupons of 250 mm in length and 25 mm width were cut from each individual laminated plate, resulting in 2 sets of 5 coupons for each laminated system. It is noted that the second set of 5 specimens was cut in the perpendicular direction (X direction) in order to examine the effect of test orientation on laminate behavior.

Figure 3-10 shows the steps used to manufacture the coupons. The steps consist of (a) cutting the dry CFRP fabric for all layers into 450 mm x 450 mm sheets; (b) impregnating the sheets with epoxy, layer by layer, using the same wet-layup technique described previously; (c) casting

the laminate plates, and (d) cutting the coupons in both X and Y directions (completed using a water jet cutting machine). It is noted that the sheets were cast on release plastic film to ensure as flat a surface as possible. A typical coupon after manufacture is shown in **Figure 3-10e**.

To avoid premature failure of the coupon at the machine grip locations, aluminum tabs were glued to the ends of each coupon in accordance with the recommendations of the ASTM D3039//D3039M standard. The dimensions of the coupons and tabs, as well as a typical coupon with tabs attached, are shown in **Figure 3-11**. It is noted that the coupon thickness shown in the figure corresponds to that of the Series 1 specimens with 4 layers; the actual coupon thickness varied depending on the series and number of layers and was measured and recorded at three different locations along the coupon length prior to testing.

(a) Cutting sheets into 450 x 450 mm sheets

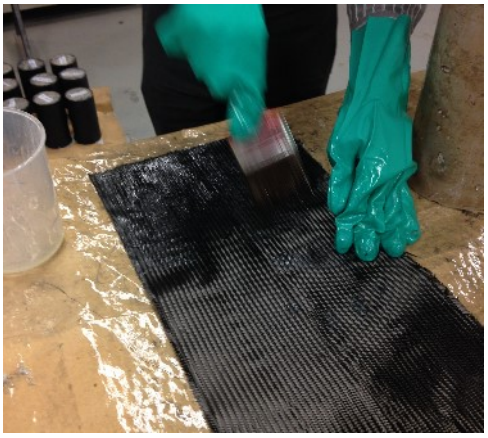

(b) Impregnation with epoxy

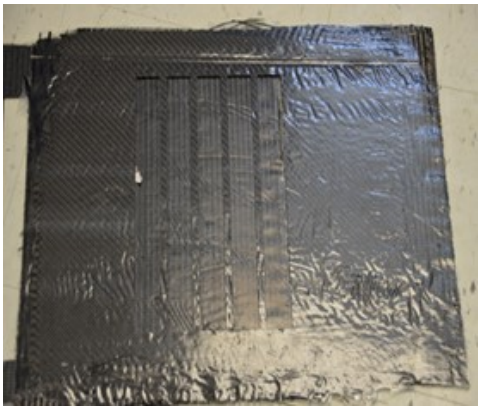

(c) CFRP laminated free-film cast and cured

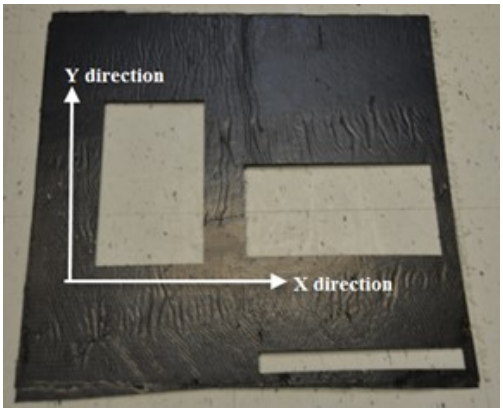

(d) Cast free-film showing where 5 specimens were cut in 2 orientations to produce 2 sets of 5 specimens

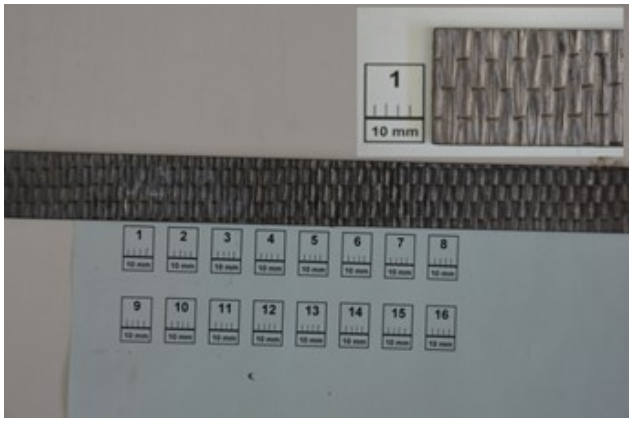

(e) Single coupon specimen cut from free-film with fiber orientation clearly visible for top layer of laminate

Figure 3-10 FRP Coupons Manufacturing Steps

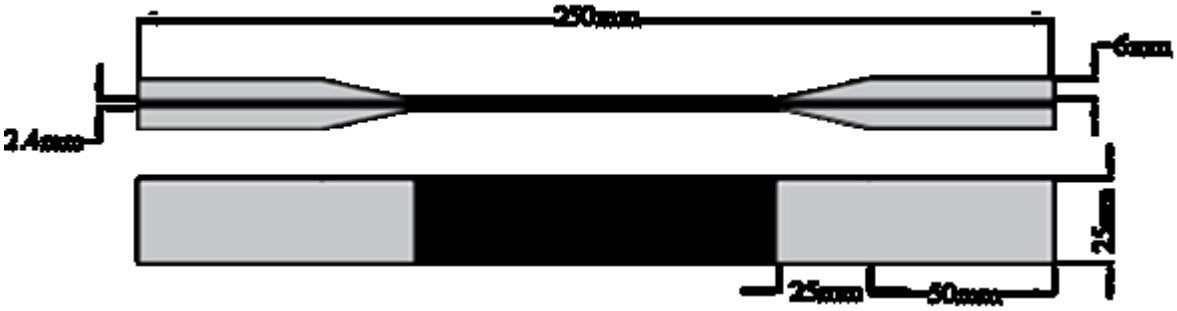

(a) Coupon and tab dimensions

(b) Typical CFRP coupon with tabs attached

Figure 3-11 CFRP tab dimensions and typical manufactured sample ready for testing

3.6 Instrumentation and Test Set-up

3.6.1 CFRP-confined concrete cylinders

Two different machines were used to test the CFRP-confined concrete cylinders in this study. The majority of the "small" 100 mm specimens were tested using an *Instron SATEC* 2000 KN universal testing machine at the National Research Council of Canada. Specimens with an estimated capacity exceeding 2000 KN were tested using a 4500 KN *MTS Rockframe* machine at

McGill University. This included the majority of the "large" 150 mm specimens and the following 100 mm specimens: *series-1* 8 layers.

Figure 3-12 and **Figure 3-13** show the *SATEC* 2000 KN and *MTS* 4600 KN test set-ups used during the cylinder tests. Both machines are equipped with load cells and computers which also serve as a data acquisition systems. In the case of both machines, the bottom steel platen moves while the top compression platen stays in place. For this study the top compression platen in both machines had a spherical seat (pin) support in order to improve alignment and ensure even pressure across the top surface of the cylinder specimens. After placing the cylinders in between the top and bottom platens, the specimens were subjected to uniaxial compressive loading to failure. Displacement controlled loading at a rate of 0.5 mm/min was adopted for all tests except for specimens purely confined with ±45° (*series 7*), where a rate of 2.5 mm/min was used. Load/ displacement histories were recorded by the test frame computers.

A High definition Nikon D7000 camera with 30 frames per second (fps) and 8 megapixel resolution and high speed camera with 3000 fps and resolution of 720 x 460 dpi were used to record the status of specimens at different loading stages and to capture the failure mode of specimens. As noted previously 5/3 replicates were typically tested for the "small"/"large" cylinder configurations in each series.

(a) SATEC Testing Frame

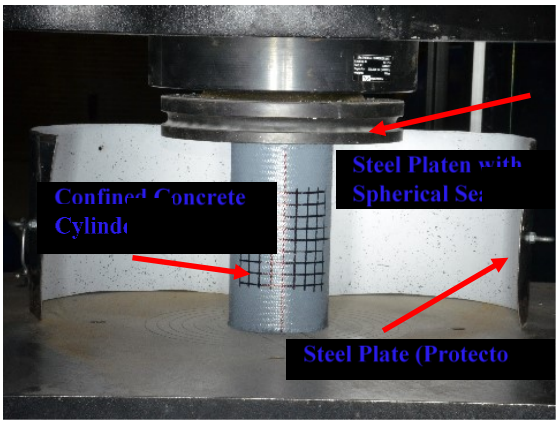

(b) Typical CFRP specimen ready for testing

Figure 3-12 SATEC 2000 KN machine and test set-up

(a) *MTS* testing machine

(b) Typical specimen ready for testing

Figure 3-13 MTS 4600 KN Instrumentation and Test Set-Up

Since explosive and brittle failures were expected, the majority of the cylinder specimens were tested without external LVDTs or extensometers (see **Figure 3-14**). The axial strains on the specimens were obtained by adjusting the displacements recorded by the machine test frames.

Figure 3-14 Typical explosive failure of CFRP Confined Specimens

In the case of the *SATEC* machine, a calibration factor was used to adjust the machine-recorded displacements; this factor was determined based on previous testing conducted at the NRC where concrete cylinders were tested with extensometers (the factor represents the average ratio of machine and extensometer recorded displacements obtained during these tests).

In the case of the *MTS* machine, the following compliance equation was used to correct the machine recorded axial displacements:

$$\boldsymbol{Corrected\ diplacement = Machine\ axial\ dipslacament - 0.000032334 * (load\ in\ KN)} \quad \textbf{(Eq. 3-1)}$$

This compliance formula was determined based on previous testing at McGill University. In order to verify the accuracy of the compliance formula, one large and one small size specimen from Series 1 were also tested with a pair of MTS extensometers with 100 mm gauge length (see

Figure 3-15). The extensometers were used up to the 50% of ultimate stress, after which they were removed in order to avoid damaging them. **Figure 3-16** shows the strain readings for one of these samples, as determined from the machine, before and after adjustment. Also shown are the extensometer recorded strain readings for the same sample - it can be seen that the machine-adjusted and extensometer readings match well.

(a) 100 mm specimen with extensometers

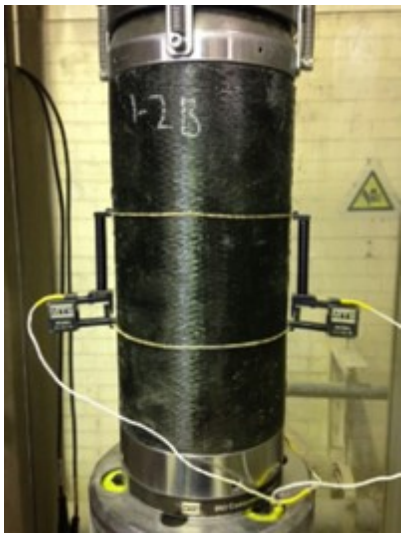

(b) 150 mm specimen with extensometers

Figure 3-15 Sample specimens from Series 1 with extensometers attached

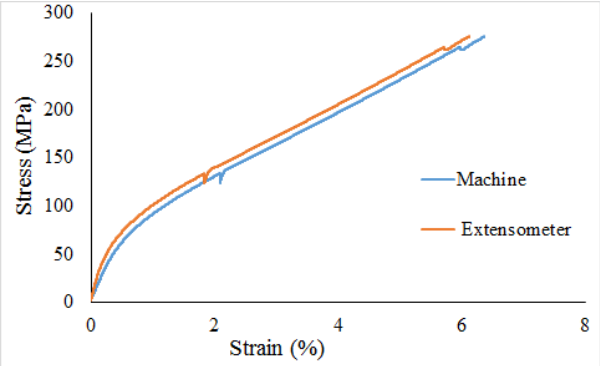

(a) Extensometer and raw machine axial displacement for sample CFRP-confined cylinder.

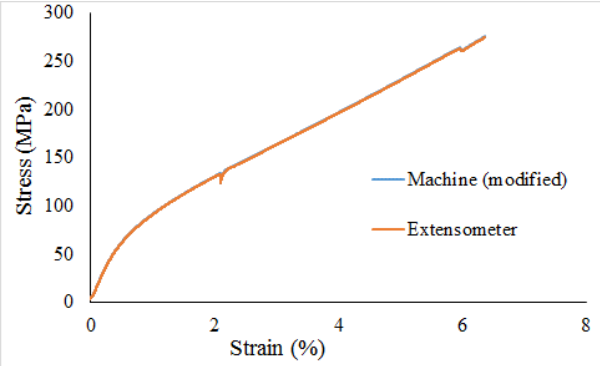

(b) Comparison of machine-adjusted and extensometer axial displacements for sample CFRP-confined cylinder

Figure 3-16 Calibration of axial displacements for cylinders tested using MTS machine

3.6.2 FRP Coupons:

A 600 KN capacity *GALDABINI* displacement-control testing machine equipped with pneumatic grips was used to examine the tensile behavior of the CFRP coupons. It is noted that the testing machine had only one grip pressure which could not be adjusted. As noted previously, aluminum tabs were glued to both ends of the coupons in accordance to ASTM D3039/D3039M standard to avoid premature failure of the coupons at the end regions. The same epoxy with the same mix ratio used in the cylinder preparation was used to glue the tabs onto the surface of the coupons. The typical length of the coupons between the upper and lower grips was 150 mm. Testing of the specimens was conducted under displacement control at a rate of 0.5 mm/min for all test samples. Axial displacements were measured by equipping the specimens with an MTS extensometer with 25 mm gauge length. Five replicates were tested for each coupon configuration. **Figure3-17** shows the *GALDABINI* testing frame and a typical coupon ready for testing.

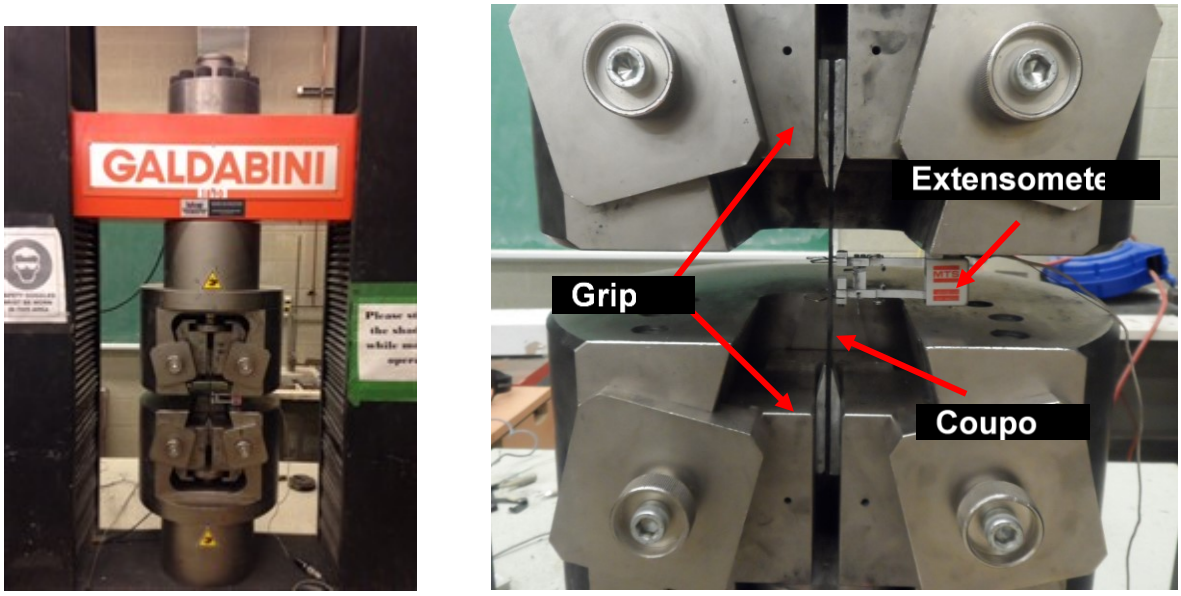

(a) *GALDABINI* Testing Frame (b) Sample FRP coupon ready for testing

Figure3-17 *GALDABINI* Testing Frame and typical CFRP coupon ready for testing

4 Chapter 4: Experimental Results

4.1 General:

As part of this study, a total of 169 concrete cylinders were tested under uniaxial compression in order to understand the influence of various parameters such as fiber orientation, stacking sequence, number of layers and specimen size on the behavior of CFRP-confined concrete. In addition, the testing program included a series of 195 coupons which were tested under uniaxial tension to further examine the effect of these parameters on laminate behavior. This chapter summarizes the detailed results provided by the experimental program. Results from the CFRP coupons and confined cylinders are presented for each series (1-7). For the coupons, the results include stress-train behavior for the samples tested in each orientation as well as the failure mode. It should be noted that the stress-strain curves are presented from the 3 best specimens in each series. In the case of the cylinders, the results for the "small" and "large" size specimens for each series are presented in terms of failure mode and stress-strain behavior.

4.2 Series 1

4.2.1 Coupons

Series 1 included a total of 15 coupons manufactured using 4, 6 or 8 layers of unidirectional CFRP aligned at 0^{o} (UD [0°]). Five replicates were produced for each layer configuration. The specimens were tested under uniaxial tension at a constant rate of 0.5 mm/min until rupture. During the initial test calibration process, the first two coupons with four layers failed prematurely due to problems with the test setup and therefore the results from these tests are not included in the discussion that follows.

4.2.1.1 Mode of Failure

All of the coupons failed in an abrupt manner regardless of the number of layers. However, the failures were more brittle and violent as the numbers of CFRP layers increased (for example the noise generated at failure was more pronounced for the specimens with 8 layers). The post failure photos of the coupons in this series can be seen in **Figure 4-1**.The failure mode designations in accordance with the ASTM D3039 standard are listed in **Table 4-1.** Lateral failures at the grips (LAT) and in the middle gage region (LGM) were observed for most specimens, although the failures to move to the grips as the number of layers increased to 6 and 8, which may be due to the large forces required to cause failure in these samples. The coupons also experienced longitudinal splitting failures in the middle gage region (SGM), which may be due to the sudden failures in the specimens of this series.

4.2.1.2 Stress-Strain behavior

The stress-strain behavior of CFRP coupons are presented in **Figure 4-2**, where the results from the 3 representative replicates are presented. The peak stress & strain (at rupture) and modulus of elasticity for all samples are summarized in **Table 4-1**. All coupons showed linear-elastic behavior up to the final rupture. **Table 4-1** shows that the peak tensile stress of the laminate reduced as the number of layers increased (although overall tensile load increased). As shown in **Table 4-1** and **Figure 4-2**, the load carrying increasing proportionally with number of layers. For instance, average load carried by coupons with 4, 6, and 8 layers of CFRP was recorded as 57.2, 72.3, and 84.4 KN, respectively. On the other hand, the tensile stress decreased from an average of 961 MPa to 777 MPa as the number of layers increased from 4 to 8. In the case of energy absorption capacity, which is calculated from area under the stress-strain curve, the values

increased from 3.20 to 3.92 as the number of layers increased from 4 to 8 layers. No clear trend emerges when examining the effect of laminate thickness on failure strain. The results show that the laminate modulus of elasticity decreased from 97 GPa to 75 GPa as the number of CFRP layers increased from 4 to 8. In terms of the consistency of the results, **Figure 4-2** shows that the laminates with a greater number of layers displayed more uniform results when compared to those with a lesser amount of CFRP sheets.

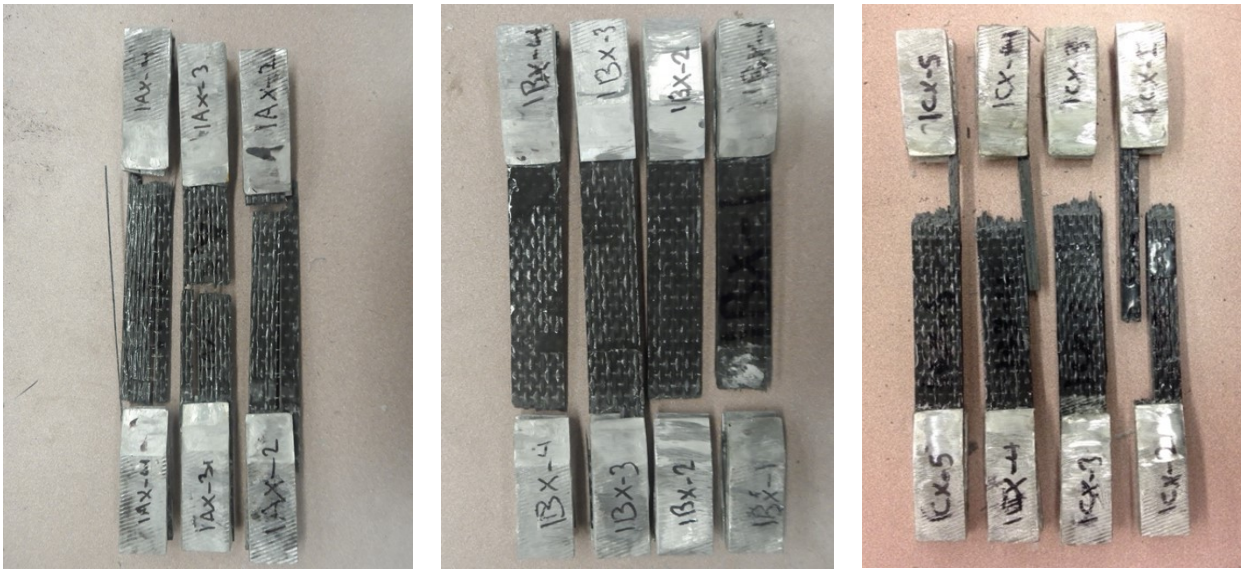

(a) 4 layers (b) 6 layers (c) 8 layers

Figure 4-1 Final failure modes of CFRP coupons (Series 1)

Table 4-1 Laminate properties and failure mode (Series 1)

Series	Specimen	Thickness (mm)	Width (mm)	Area (mm^2)	Properties at Peak			e_{cu}	Modulus E (GPa)	Failure Mode
					Load (KN)	Stress (MPa)	Strain (mm/mm)			
$UD[0^\circ]_4$	**2**	2.33	25.15	58.59	54.5	933.9	0.0090	3.76	103.77	LGM, SGM
	3	2.61	25.14	65.61	57.3	880.7	0.0120	2.56	73.39	LGM, SGM
	4	2.24	25.04	56.08	59.9	1067.3	0.0087	3.27	122.68	LAT, LGM
	AVG.	**2.41**	**25.11**	**60.09**	**57.2**	**960.6**	**0.0099**	**3.20**	**97.04**	-
$UD[0^\circ]_6$	**1**	3.79	25.09	95.09	75.1	764.0	0.0076	2.88	100.52	LIT
	2	3.86	25.09	96.97	77.0	794.3	0.0066	2.57	120.34	LIT
	3	3.83	25.07	96.02	71.2	741.7	0.0075	2.75	98.90	LIT
	4	3.87	25.22	97.6	65.8	673.9	0.0063	2.10	106.96	LIT
	AVG.	**3.83**	**25.12**	**96.34**	**72.3**	**743.5**	**0.0070**	**2.58**	**106.69**	-
$UD[0^\circ]_8$	**2**	4.31	25.02	107.84	80.2	744.2	0.0093	3.27	80.02	LIT,SGM
	3	4.33	25.07	108.55	78.0	718.8	0.0096	3.30	74.88	SGM
	4	4.31	25.04	107.92	88.4	818.7	0.0110	4.24	74.43	LIT, SGM
	5	4.41	24.99	110.21	91.22	826.4	0.0120	4.88	68.86	LIT,SGM
	AVG.	**4.34**	**25.03**	**108.6**	**84.4**	**777.0**	**0.0105**	**3.92**	**74.55**	-

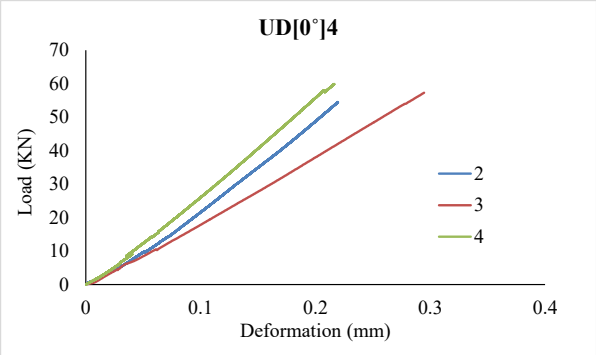

4 Layers

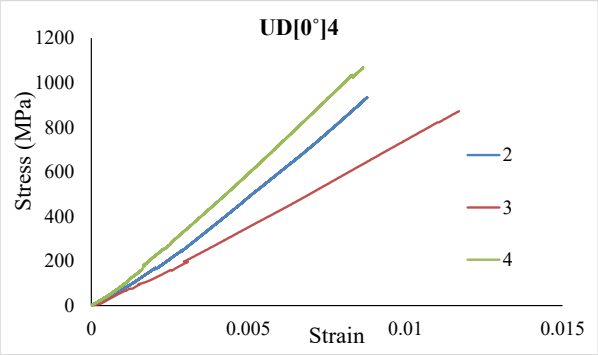

4 Layers

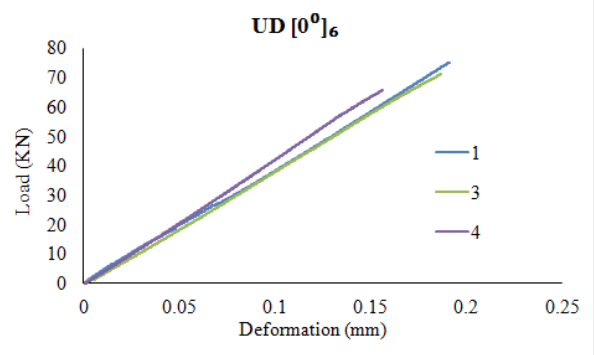

6 Layers

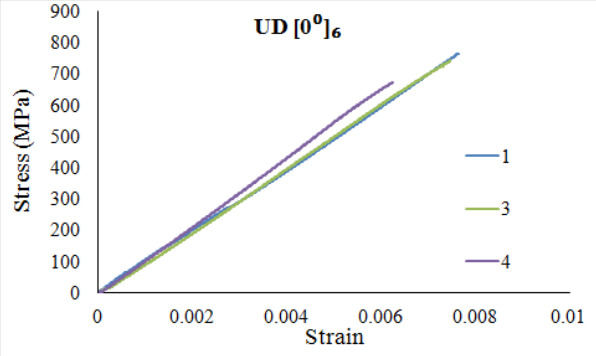

6 Layers

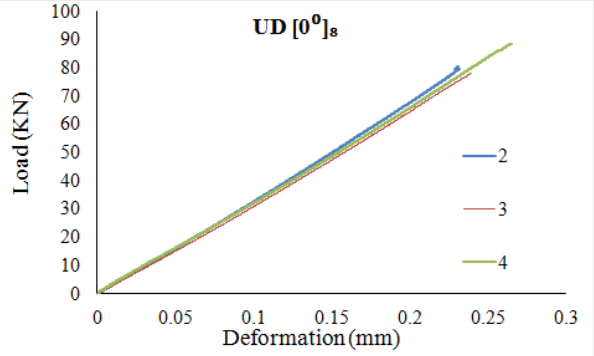

8 Layers

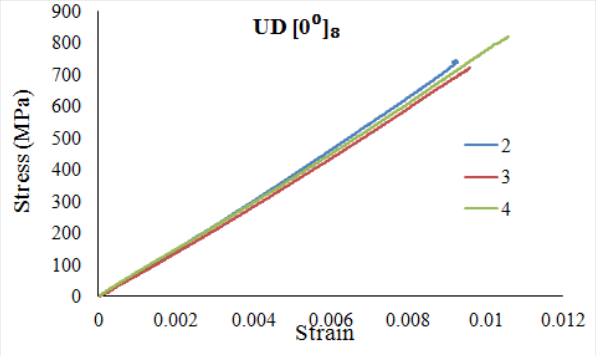

8 Layers

Figure 4-2 Load-deformation and stress-strain behavior of CFRP coupons in Series 1

4.2.2 Cylinders

The specimens in this series were wrapped with unidirectional CFRP sheets that have fibers aligned in the 0° direction. Two sizes of cylinders having dimensions of 100 x 200 mm ("small") and 150 x 300 mm ("large") were tested, with each type confined by either 4, 6 or 8 layers of CFRP. Five replicates were tested for each "small" cylinder configuration, while three replicates were tested for each "large" cylinder configuration. The failure mode and post-test photos of all tested specimens in this series can be found in **Figure 4-3**. The stress-strain curves of all tested specimens for both sizes are presented in **Figure 4-5**. The peak stress and peak strain of the tested specimens in *Series 1* are summarized in **Table 4-2** and **Table** 4-3.

.

4.2.2.1 Mode of Failure

The failure mode of all specimens in this series, regardless of cylinder size or number of layers, was caused by the sudden rupture of the unidirectional FRP jacket in the hoop (0°) direction. The CFRP jacket began being active as the axial stress neared the unconfined strength of the concrete. Upon reaching this stress level, the sound of concrete crushing could be heard during the rest of the loading process. High-speed video shows that lateral expansion became more predominant (when compared to vertical shortening) after this stage which indicates the activation of hoop tension on the fibers in the CFRP jacket. As the specimens continued to gain strength, no sign of distress was observed before failure. In all cases, the fracture of the FRP jacket and the failure of the specimens occurred suddenly with a large release of energy. In the case of the specimens with 4 layers of CFRP, some cracking noises were heard a few seconds prior to failure, while the failure of the specimens with 6 and 8 layers of CFRP occurred without

warning. **Figure 4-3** shows representative post-failure photos of the specimens in this series. It can be observed that the specimens confined with a greater amount of CFRP showed more explosive failures. For example, the cylinders confined with 8 layers resulting in more severe crushing and spalling. In all cases, the failure of the CFRP jacket occurred due to rupture of fibers in the hoop direction, with failure generally concentrating over a length of ~ h/3 near the ends. In all the cases, the core concrete had a "cone" type failure at fracture; this failure mode is expected due to the ability of the CFRP to restrain lateral expansion of the concrete as the vertical compressive force is applied. A thin layer of concrete remained attached to the FRP jacket after failure which indicates a good bond between the concrete surface and the FRP jacket (see **Figure 4-4**). No pre-mature failures were observed and the rupture of the jackets did not occur in the overlap areas.

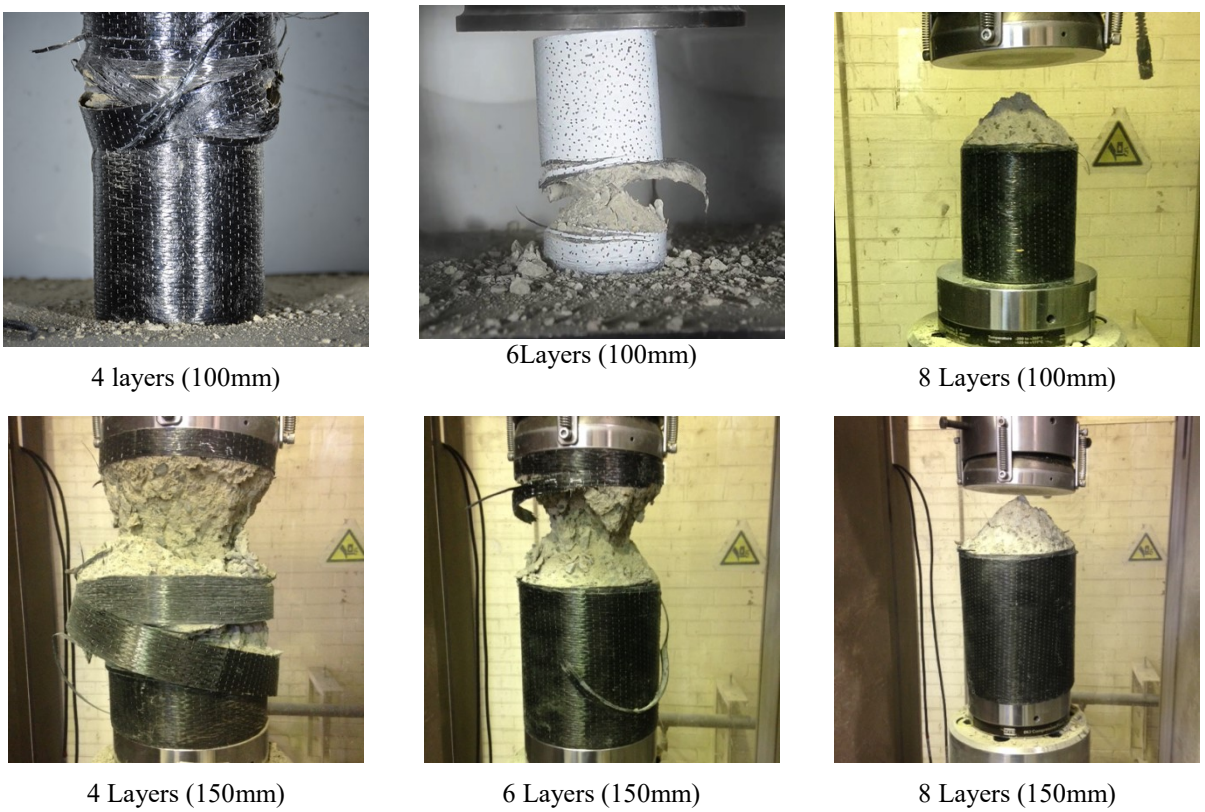

Figure 4-3 Final failure modes of CFRP confined concrete cylinders (Series 1)

Figure 4-4 Perfect bond between concrete and CFRP jacket

4.2.2.2 Stress-Strain Behavior

The stress-strain results of the CFRP-confined concrete cylinders in Series 1 are shown in **Figure 4-5**. The results in terms of peak stress ($f_{cc}{}'$) and peak strain ($\varepsilon_{cc}{}'$) are tabulated in **Table 4-2** and **Table 4-3** for the 100 mm and 150 mm specimens, respectively. A substantial increase in both stress and strain of CFRP confined concrete cylinders is evident. For the "small" cylinders, the average increase in stress (f'_{cc}/f_{co}) was 4.13, 4.99 and 6.13 for specimens confined with 4, 6 and 8 layers of CFRP. The average increase in strain ($\varepsilon'_{cc}/\varepsilon_{co}$) was found to be 29.71, 20.77 and 20.61 for specimens confined with 4, 6 and 8 layers of CFRP. Stress and strain was found to rise as the number of CFRP sheets increased, however the relative increase in stress and strain was more pronounced for the first 4 layers of confinement.

Similar observations were made for the "large" size specimens where peak stress and strain were obtained by increasing the number of CFRP layers. The large cylinders showed an average increase in stress of 3.13, 4.17 and 4.91 for specimens confined with 4, 6 and 8 layers of CFRP respectively, while values of 10.11, 15.25 and 17.93 were found in the case of average increase in strain in the same order. It should be noted that the increase in stress and strain are more

pronounced for the small size specimens. For example at 4 layers, the increase in stress is 24% lower for the larger cylinders.

Figure 4-5 In terms of the consistency of results, more uniform results between replicates are observed for the "small" specimens with lesser amount of confinement (i.e. 4 layers vs. 8 layers). With exception of the result at 4 layers, the larger cylinders showed more uniform results when compared to the smaller companion specimens.

Table 4-2 Experimental results 100 mm specimens (Series 1)

Specimen	# of Layer	Specimen Size (mm)	f'_{cc} (MPa)	(f'_{cc}/f_{co})	ε'_{cc}	$(\varepsilon'_{cc}/\varepsilon_{co})$
1	4	100	180.72	4.20	0.048	35.56
2	4	100	173.63	4.03	0.047	23.12
3	4	100	181.89	4.23	0.053	37.16
4	4	100	175.60	4.08	0.054	33.01
5	4	100	177.68	4.13	0.059	19.71
AVG.	**4**	**100**	**177.91**	**4.13**	**0.052**	**29.71**
1	6	100	176.94	4.11	0.057	19.23
2	6	100	229.65	5.34	0.068	23.03
3	6	100	217.98	5.06	0.063	21.26
4	6	100	229.28	5.33	0.062	20.83
5	6	100	220.04	5.11	0.058	19.52
AVG.	**6**	**100**	**214.78**	**4.99**	**0.062**	**20.77**
1	8	100	245.02	5.69	0.067	22.35
2	8	100	257.35	5.98	0.059	19.86
3	8	100	280.94	6.53	0.058	19.48
4	8	100	259.42	6.03	0.059	20.04
5	8	100	275.72	6.41	0.064	21.32
AVG.	**8**	**100**	**263.69**	**6.13**	**0.062**	**20.61**

Table 4-3 Experimental results 150 mm specimens (Series 1)

Specimen	# of Layers	Specimen Size (mm)	(f'_{cc}) (MPa)	(f'_{cc}/f_{co})	(ε'_{cc})	$(\varepsilon'_{cc}/\varepsilon_{co})$
1	4	150	129.78	3.05	0.033	10.98
2	4	150	131.57	3.09	0.024	7.97
3	4	150	138.53	3.25	0.034	11.38
AVG.	**4**	**150**	**133.29**	**3.13**	**0.030**	**10.11**
1	6	150	179.16	4.21	0.048	15.98
2	6	150	173.59	4.07	0.041	13.74
3	6	150	180.41	4.23	0.048	16.02
AVG.	**6**	**150**	**177.72**	**4.17**	**0.046**	**15.25**
1	8	150	220.25	5.17	0.056	18.76
2	8	150	197.55	4.64	0.050	16.82
3	8	150	209.09	4.91	0.054	18.22
AVG.	**8**	**150**	**208.96**	**4.91**	**0.054**	**17.93**

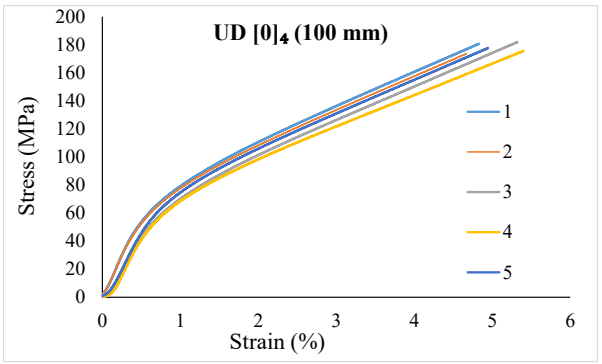

4 Layers

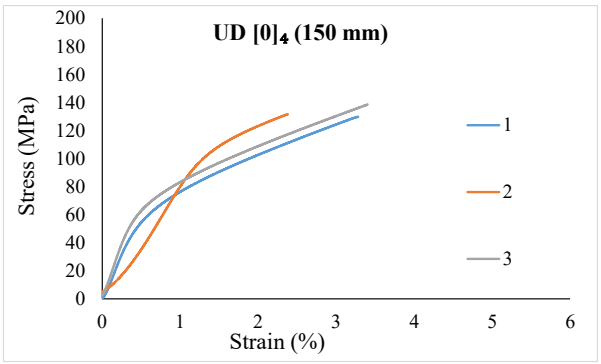

4 Layers

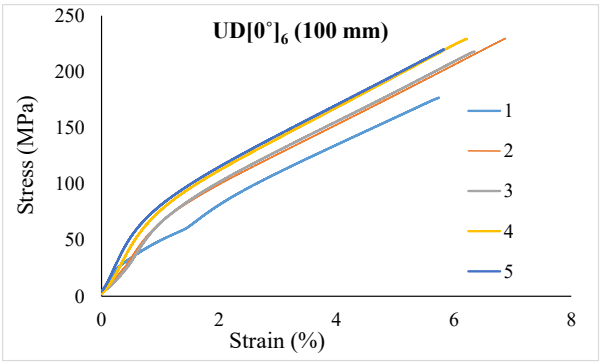

6 Layers

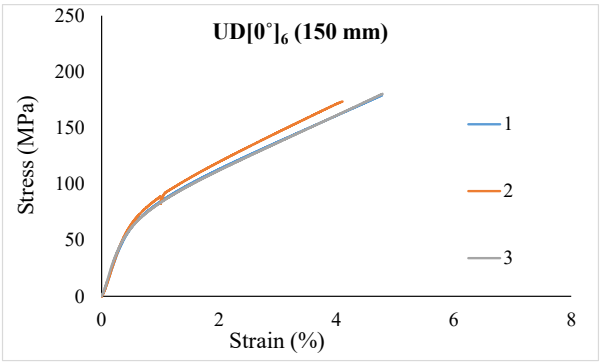

6 Layers

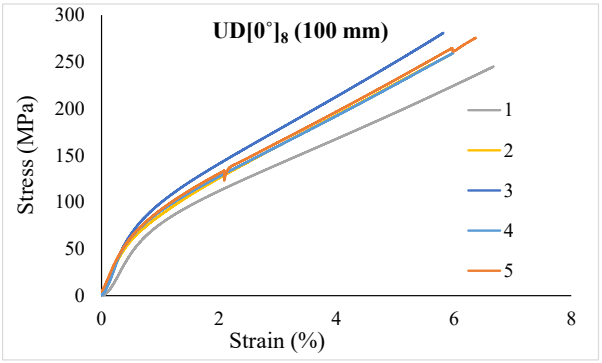

8 Layers

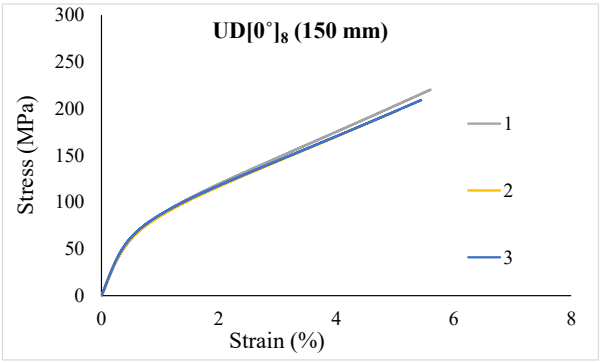

8 Layers

Figure 4-5 Stress-strain responses of tested specimens (Series 1)

4.3 Series 2

4.3.1 Coupons

Series 2 included a total of 30 coupons manufactured using 4, 6 or 8 layers of unidirectional CFRP aligned at 90-0^{o} (UD [90-0˚]). The specimens were tested under uniaxial tension. Five replicates were produced for each layer configuration in both X and Y directions. Mode of failure and post failure photos of coupons can be seen in **Figure 4-6.** Results of peak stress and peak strain as well as failure mode of the coupons are presented in **Table** 4-4**.** As part of the initial testing procedure, the first few coupons suffered non-representative failures due to errors in test setup and therefore are not included when discussing average properties.

4.3.1.1 Mode of Failure

All of the coupons showed brittle rupture disregarding the number of layers. However, the sudden mode of failure was more pronounced in coupons with a higher number of CFRP layers. Since the coupons are tested in direct tension the strength of the coupons can be attributed to the CFRP sheets in the 0^{o} direction because the longitudinal CFRP sheets only carry load with the weak fibers used to join the main fibers together. Modes of failure of each coupon in accordance to the ASTM D3039 (2015) specification are tabulated in **Table** 4-4**.** Both lateral failures at the grips (LAT) and in the middle gage region (LGM) were observed (see **Figure 4-6**).

4 layers (X direction)

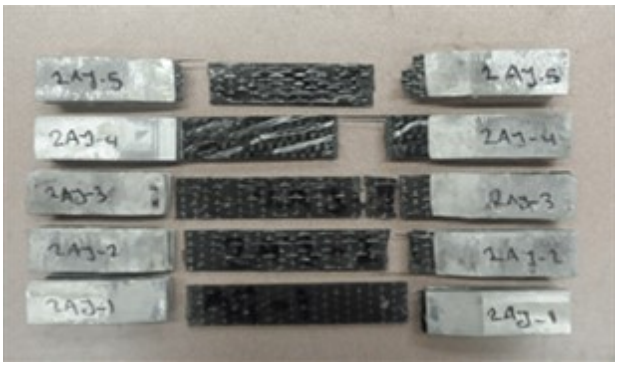

4 layers (Y direction)

6 layers (X direction)

6 layers (Y direction)

8 layers (X direction)

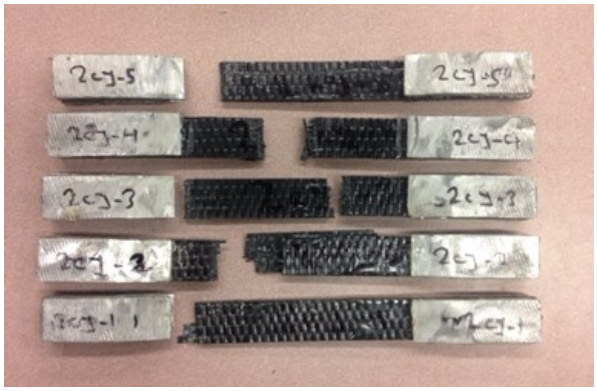

8 layers (Y direction)

Figure 4-6 Final failure modes of CFRP coupons (Series 2)

Table 4-4 CFRP coupon properties and failure mode (Series 2)

Series	Specimen	Thickness (mm)	Width (mm)	Area (mm²)	Properties at peak				E (Gpa)	Failure Mode
					Load (KN)	Stress (MPa)	Strain	e_{cu}		
$UD[90^{\circ}/0^{\circ}]_2$ X direction	1	2.77	24.95	69.03	-	-	-		-	GAT
	2	2.41	25.09	60.56	23.2	382.6	0.0092	1.80	41.59	LAT
	3	2.67	25.17	67.20	28.4	422.4	0.0120	2.50	35.20	LAT,LGM
	4	2.58	25.08	64.63	29.0	448.5	0.0108	2.70	41.53	LIT
	5	2.73	25.06	68.51	29.5	430.9	0.0137	2.80	31.45	LAT
	AVG	**2.60**	**25.10**	**65.23**	**27.5**	**421.1**	**0.0159**	**2.45**	**37.44**	
$UD[90^{\circ}/0^{\circ}]_2$ Y direction	1	2.70	25.07	67.68	32.5	480.2	0.0073	1.68	65.78	LAT
	2	2.47	25.09	61.97	29.0	468.6	0.0142	3.09	33.00	LAT,LGM
	3	2.75	25.00	68.83	32.9	477.5	0.0137	3.17	34.86	LAT,LGM
	4	2.57	25.25	64.99	30.9	476.3	0.0123	2.90	38.72	LGM
	5	2.69	25.15	67.65	28.3	418.3	0.0111	2.23	37.69	LAT,LGM
	AVG	**2.64**	**25.11**	**66.22**	**30.7**	**464.2**	**0.0117**	**2.61**	**42.01**	
$UD[90^{\circ}/0^{\circ}]_3$ X direction	1	3.70	25.07	92.83	44.9	484.2	0.0147	4.82	32.94	LGM
	2	3.68	25.00	92.10	44.9	488.3	0.0150	3.73	32.55	LGM
	3	3.71	25.05	92.94	34.5	371.1	0.0100	1.86	37.11	LAT
	4	3.70	25.08	92.89	39.1	421.1	0.0112	2.43	37.60	LGM
	5	3.72	25.15	93.63	47.9	511.5	0.0139	3.57	36.80	LGM
	AVG	**3.70**	**25.07**	**92.88**	**42.3**	**455.2**	**0.0130**	**3.28**	**35.40**	
$UD[90^{\circ}/0^{\circ}]_3$ Y direction	1	3.41	25.29	86.25	40.2	465.7	0.0134	3.12	34.76	LAT
	2	3.64	25.21	91.86	39.6	430.9	0.0116	2.35	37.15	LGM
	3	3.71	25.12	93.12	42.9	461.4	0.0124	2.82	37.21	LAT
	4	3.54	25.09	88.91	39.6	445.8	0.0105	2.36	42.46	LAT
	5	3.71	25.06	92.90	40.6	436.8	0.0122	2.65	35.80	LGM
	AVG	**3.60**	**25.16**	**90.61**	**40.6**	**448.2**	**0.0120**	**2.66**	**37.48**	
$UD[90^{\circ}/0^{\circ}]_4$ X direction	1	4.25	24.96	106.08	50.1	472.4	0.0110	2.55	42.94	LAT
	2	4.23	24.98	105.75	55.6	525.9	0.0122	3.27	43.11	LGM
	3	4.23	24.97	105.55	51.4	487.0	0.0110	2.61	44.28	LGM
	4	4.37	24.93	108.88	56.2	516.0	0.0126	3.25	40.95	LGM
	5	4.18	24.96	104.40	62.2	595.4	0.0146	4.06	40.78	LAT
	AVG	**4.25**	**24.96**	**106.13**	**55.1**	**519.4**	**0.0123**	**3.15**	**42.41**	
$UD[90^{\circ}/0^{\circ}]_4$ Y direction	1	4.40	25.00	110.00	52.4	476.6	0.0113	2.60	42.18	LAT
	2	4.63	25.03	115.99	50.0	430.7	0.0102	2.19	42.23	LGM
	3	4.40	24.97	109.85	55.3	503.2	0.0123	3.01	40.91	LAT,LGM
	4	4.17	25.00	104.17	69.1	663.2	0.0144	4.81	46.05	LGM
	5	4.20	25.10	105.42	44.2	419.3	0.0112	2.47	37.44	LAT
	AVG	**4.36**	**25.02**	**109.09**	**54.2**	**498.6**	**0.0119**	**3.02**	**41.76**	

4.3.1.2 Stress-Strain behavior

For all coupons linear-elastic behavior up to the rupture as seen in the load-deformation graphs presented in **Figure 4-7**. Coupons with more CFRP layers displayed more uniform results. The stress-strain behavior of CFRP coupons in both the X and Y directions are presented in **Figure 4-8.** A summary of results consisting of maximum load, stress, strain and calculated maximum modulus of elasticity for each coupon is presented in **Table** 4-4. Based on the average test results of the 3 best specimens in the series, both load and stress are found to have gradually increased by adding more layers of CFRP sheets, while strain of the same specimens displayed decrease with increasing the number of CFRP sheets. Coupons in X direction showed increase in stress from 421.1 to 519.4 MPa and decrease in strain from 0.0159 to 0.0123 by increasing the number of layers from 4 to 8 layers. Results presented in **Table** 4-4 shows that energy absorption capacity increased as the number of layers from 4 to 6, while this toughness decreased slightly as the layers went from 6 to 8, with values of 2.45, 3.28, and 3.15 for 4, 6, and 8 layers of CFRP sheets in X direction. The modulus of elasticity of coupons remained in the same range regardless of the number of layers for both the X and Y directions. **Figure 4-7** and **Figure 4-8** show that coupons with a higher number of layers displayed the most uniform results. In terms of the effect of cur direction, coupons in the Y direction showed higher stress and modulus of elasticity compared to those in the X direction. However, X direction coupons displayed a larger strain compared to those in the Y direction. For instance, the average stress and modulus of elasticity at 4 layers were of 421.1 MPa and 37.44 GPa, respectively, which are 16% and 10% lower than for the X direction coupons. However, the average strain in the X direction coupons are of 0.0159 which is 26% higher compared to those of the Y direction coupons.

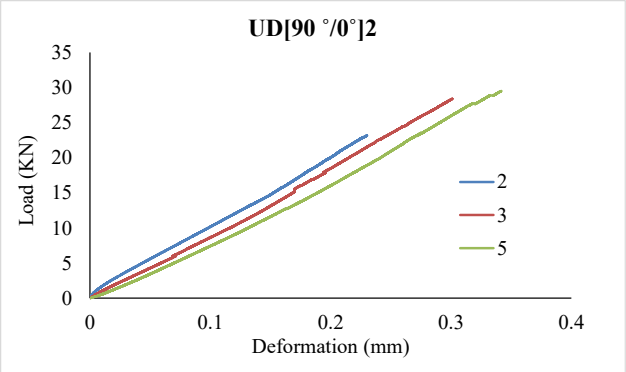

4 layers (X direction)

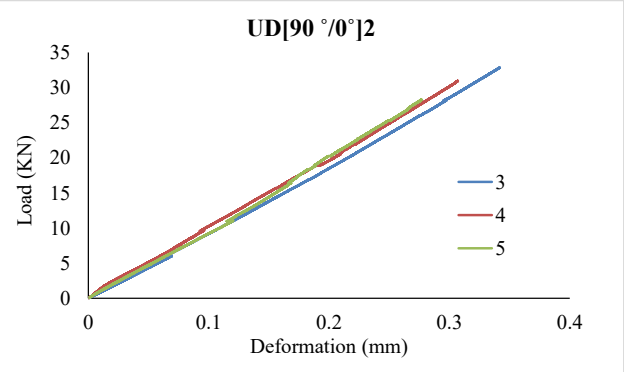

4 layers (Y direction)

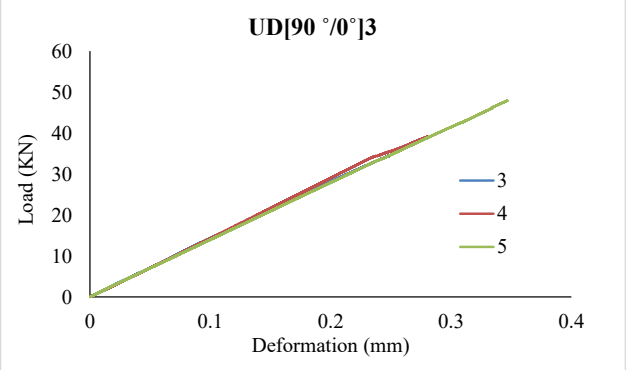

6 layers (X direction)

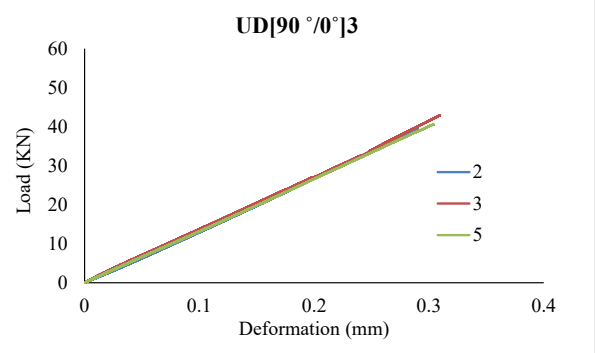

6 layers (Y direction)

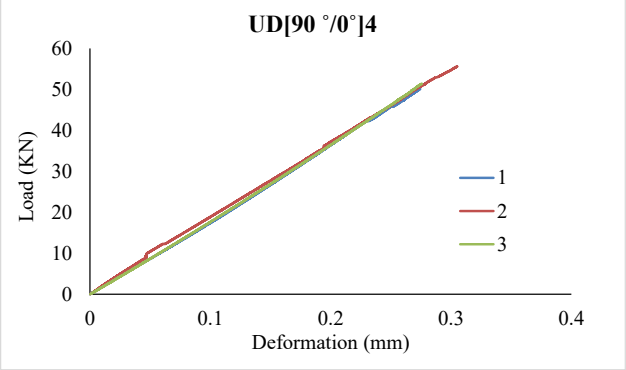

8 layers (X direction)

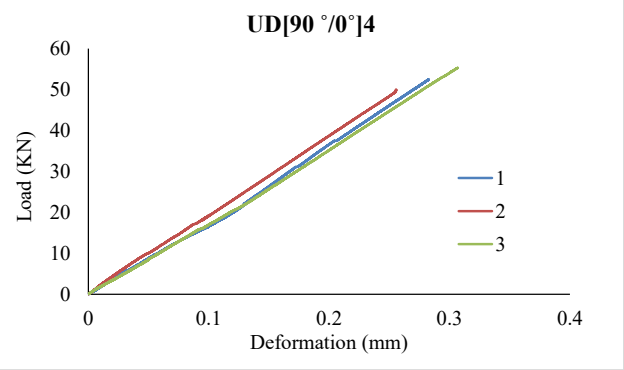

8 layers (Y direction)

Figure 4-7 Load-deformation curves of CFRP coupons (Series 2)

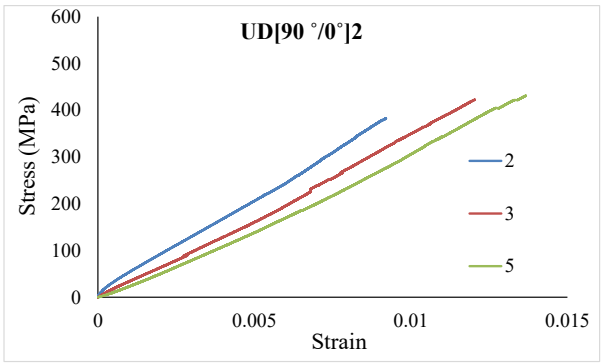

4 layers (X direction)

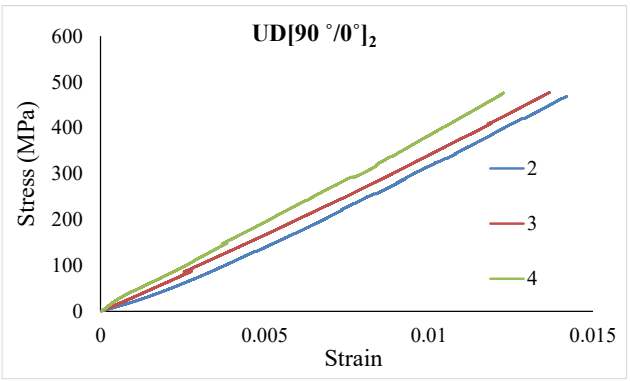

4 layers (Y direction)

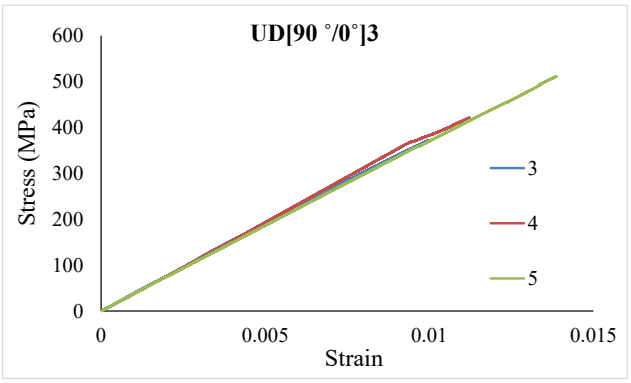

6 layers (X direction)

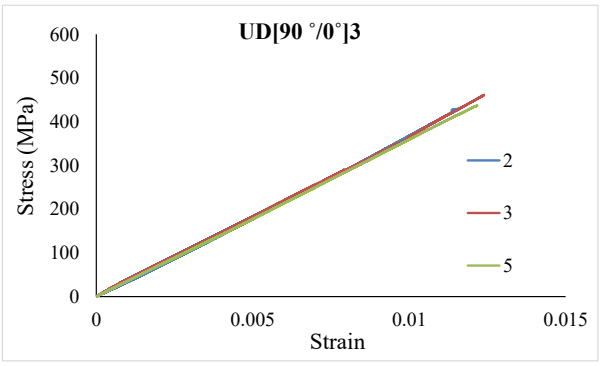

6layers (Y direction)

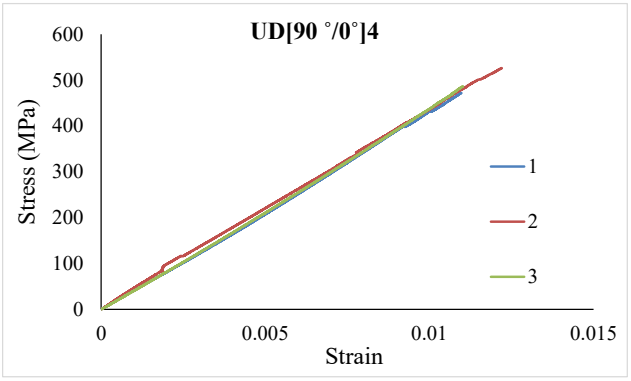

8 layers (X direction)

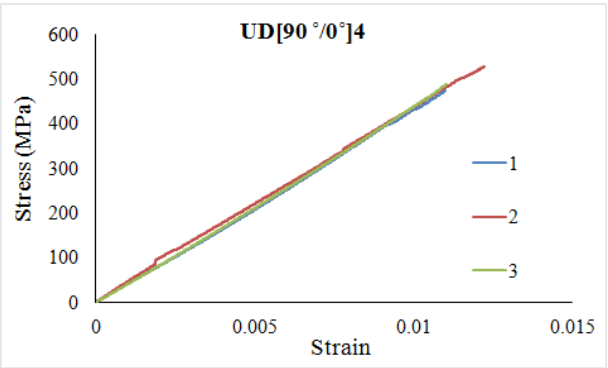

8 layers (Y direction)

Figure 4-8 Stress-strain curves of CFRP coupons (Series 2)

4.3.2 Cylinders

The specimens in this series were wrapped with unidirectional CFRP sheets that have fibers aligned in both 0° and 90° directions. Five replicates were tested for each configuration in the case of the "small" cylinders, while three replicates were tested for the "large" cylinders. The stress-strain curves of all tested specimens for both sizes are presented in **Figure 4-10**. The peak stress and peak strain of the specimens in *Series 2* are summarized in **Table 4-5** and **Table 4-6**.

4.3.2.1 Mode of Failure

At approximately 80% of loading, rupture of the outer layer of the jacket was initiated, which resulted in a softening of the response and an increase in load until the final rupture. Rupture of the jacket occurred in both the 90° and 0° directions. The failure was initiated by bulging of the jacket in the 90^0 direction leading to rupture of fibers in the hoop direction (0^0). This led to final rupture of the jacket with a tear along the height of the specimens, resulting in spalling of concrete pieces out of the jacket. The failure mode and post-test photos of all tested specimens in this series can be found in **Figure 4-9**. One can see that the damage of the concrete core and jacket rupture were more somewhat more pronounced in “large” size specimens (see **Figure 4-9**). Jacket rupture in “small” size specimens initiated in the hoop direction and extended in the longitudinal direction to either the top or bottom of the cylinder (but not over the entire cylinder height), while in “large” size specimens, rupture started in the hoop direction and led to the rupture of the jacket in the longitudinal direction over the entire height, and became severe in the case of cylinders with 8 layers. Cone and shear failure was observed in most of cases with concrete crushing more severe for larger specimens with greater number of layers.

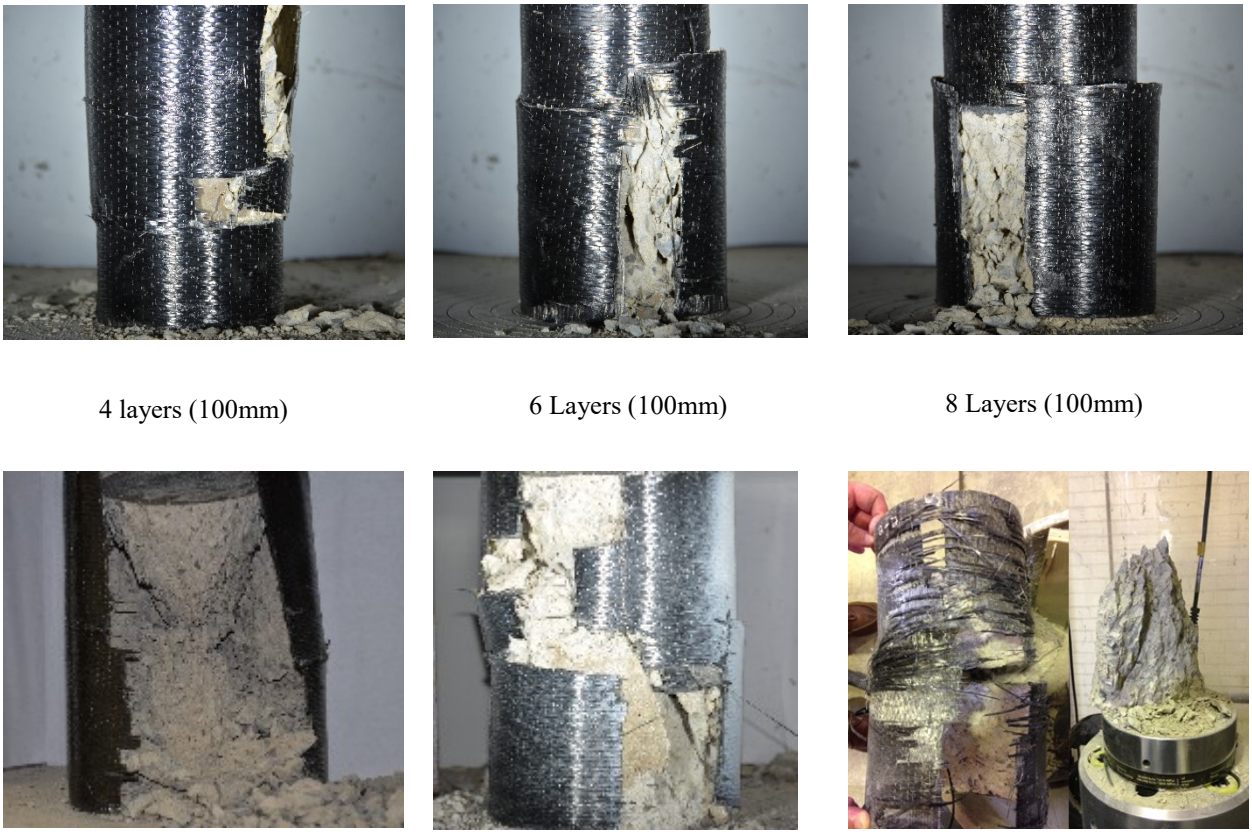

4 layers (100mm) | 6 Layers (100mm) | 8 Layers (100mm)

4 Layers (150mm) | 6 Layers (150mm) | 8 Layers (150mm)

Figure 4-9 Final failure modes of CFRP confined concrete cylinders (Series 2)

4.3.2.2 Stress-Strain Behavior

The stress-strain behavior of the CFRP-confined concrete cylinders in *Series 2* is shown in **Figure 4-10**. A summary of the results which consist of peak stress ($f_{cc}{}'$) and peak strain ($\varepsilon_{cc}{}'$) are tabulated for the 100 mm and 150 mm specimens in **Table 4-5** and **Table 4-6** respectively. A substantial increase in both stress and strain of CFRP confined concrete cylinders is obvious. The "small" cylinders displayed an average increase in stress (f'_{cc}/f_{co}) of 2.34, 2.95 and 3.44 for specimens confined with 4, 6 and 8 layers of CFRP, respectively. The average increase in strain ($\varepsilon'_{cc}/\varepsilon_{co}$) was found to be 7.64, 10.47 and 12.05 for specimens confined with 4, 6, and 8 layers of

CFRP, respectively. Both stress and strain were increased by adding more layers of CFRP sheets, however the relative increase in stress and strain was more pronounced for the first 4 layers of confinement.

Similarly, both stress and strain of the "large" size specimens were increased by adding more layers of CFRP sheets. However, the resulting values were different than those obtained from “small” size specimens. For example, values of 1.96, 2.36 and 2.71 were obtained in the case of average increase in stress, while values of 6.88, 7.54 and 8.60 were found in the case of average increase in strain for specimens confined with 4, 6 and 8 layers of CFRP sheets, respectively.

Table 4-5 Experimental results 100 mm specimens (Series 2)

Specimen	# of Layer	Specimen Size	$(f_{cc}{}')$	(f'_{cc}/f_{co})	(ε'_{cc})	$(\varepsilon'_{cc}/\varepsilon_{co})$
1	4	100	101.26	2.35	0.025	8.29
2	4	100	105.88	2.46	0.023	7.69
3	4	100	90.65	2.11	0.024	7.97
4	4	100	101.66	2.36	0.023	7.80
5	4	100	105.00	2.44	0.019	6.45
AVG.	**4**	**100**	**100.89**	**2.34**	**0.023**	**7.64**
1	6	100	125.71	2.92	0.033	10.97
2	6	100	129.17	3.00	0.031	10.43
3	6	100	127.05	2.95	0.033	11.06
4	6	100	126.77	2.95	0.030	10.05
5	6	100	126.07	2.93	0.029	9.83
AVG.	**6**	**100**	**126.96**	**2.95**	**0.031**	**10.47**
1	8	100	141.52	3.28	0.035	11.58
2	8	100	139.61	3.24	0.033	11.13
3	8	100	159.20	3.70	0.033	11.17
4	8	100	149.18	3.47	0.038	12.84
5	8	100	150.97	3.51	0.040	13.54
AVG.	**8**	**100**	**148.09**	**3.44**	**0.036**	**12.05**

Table 4-6 Experimental results 150 mm specimens (Series 2)

Specimen	# of Layer	Specimen Size (mm)	(f'_{cc})	(f'_{cc}/f_{co})	(ε'_{cc})	$(\varepsilon'_{cc}/\varepsilon_{co})$
1	4	150	83.71	1.96	0.022	7.30
2	4	150	85.52	2.01	0.021	6.99
3	4	150	81.74	1.92	0.019	6.36
AVG.	**4**	**150**	**83.66**	**1.96**	**0.021**	**6.88**
1	6	150	93.00	2.18	0.022	7.28
2	6	150	107.24	2.52	0.026	8.74
3	6	150	101.40	2.38	0.020	6.60
AVG.	**6**	**150**	**100.55**	**2.36**	**0.022**	**7.54**
1	8	150	118.64	2.78	0.027	9.00
2	8	150	115.35	2.71	0.029	9.73
3	8	150	112.27	2.64	0.021	7.06
AVG.	**8**	**150**	**115.42**	**2.71**	**0.026**	**8.60**

Overall, more uniform results were obtained from larger size specimens. The increase in stress and strain was more pronounced in small size specimens as it is clearly shown in the results that were presented in both **Table 4-5** and **Table 4-6.**

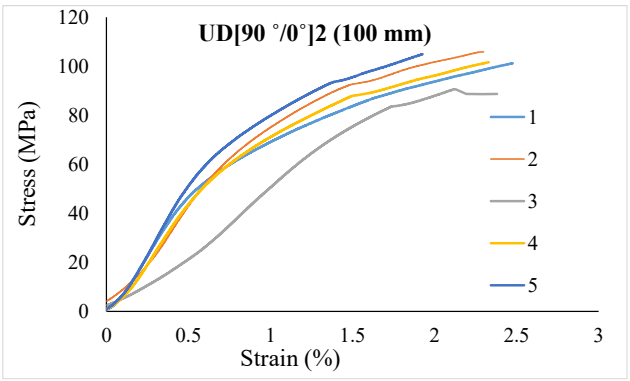

4 Layers

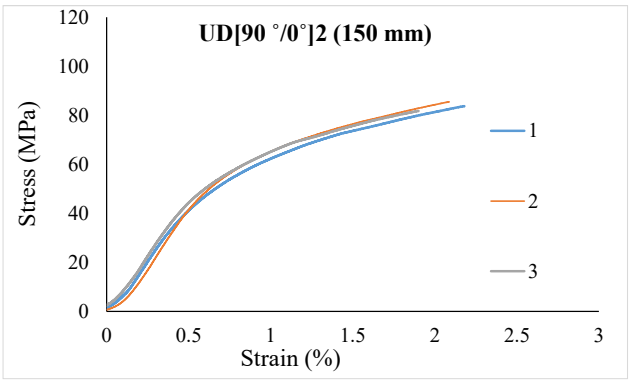

4 Layers

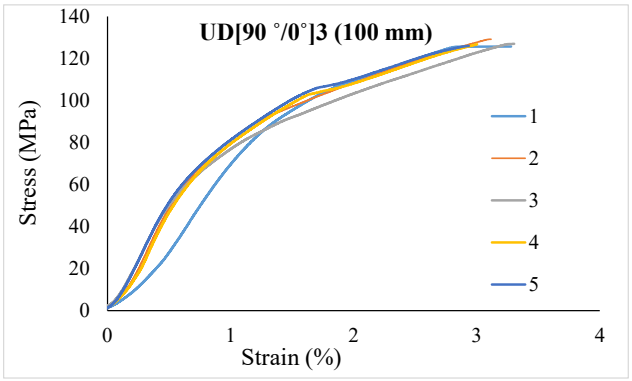

6 Layers

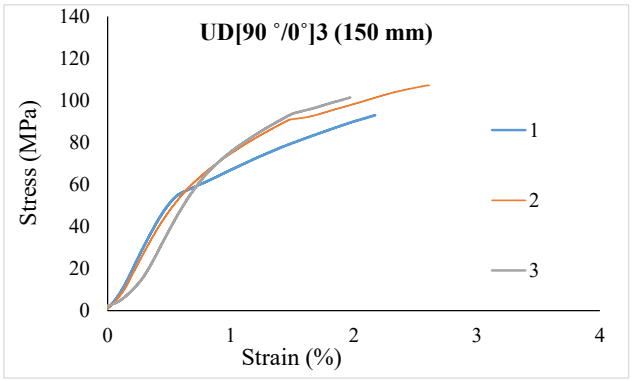

6 Layers

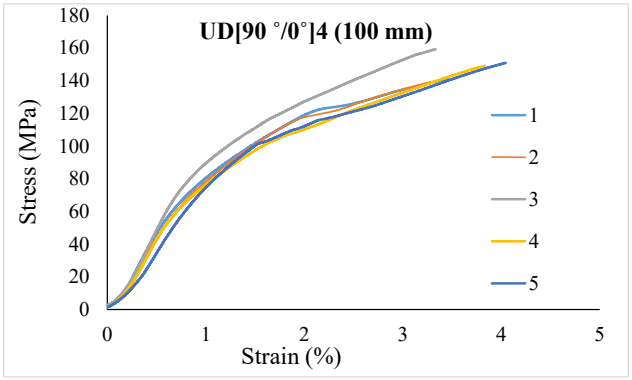

8 Layers

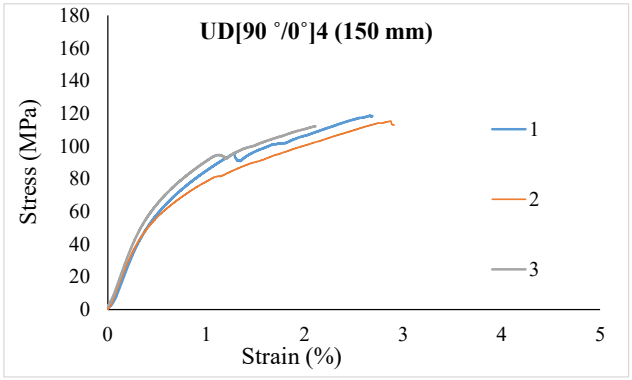

8 Layers

Figure 4-10 Stress-strain responses of tested specimens (Series 2)

4.4 Series 3

4.4.1 Coupons

Series 3 included a total of 30 coupons manufactured using 4, 6 or 8 layers of unidirectional CFRP aligned at +45-45º (UD [+45-45˚]). The specimens were tested under uniaxial tension. Five replicates were included for each layer configuration in both X and Y directions. Mode of failure and post failure photos of coupons can be seen in **Figure 4-11.** Results of peak stress and peak strain as well as failure modes are presented in **Table 4-7.**

4.4.1.1 Mode of Failure

All of the coupons showed very ductile failure disregarding the number of layers. Coupons sustained large deformation while small loads were carried. The modes of failure for each coupon in accordance to ASTM D3039/D3039M (2015) specification are tabulated in **Table** 4-7**.** Angular failures of the CFRP coupons were observed to occur in the middle gage regions (AGM) for all coupons disregarding the number of layers (see **Figure 4-11**). The failure angle was in both $+45^0$ and -45^0 due to having CFRP sheets with fibers aligned in both angles.

4 layers (X direction)

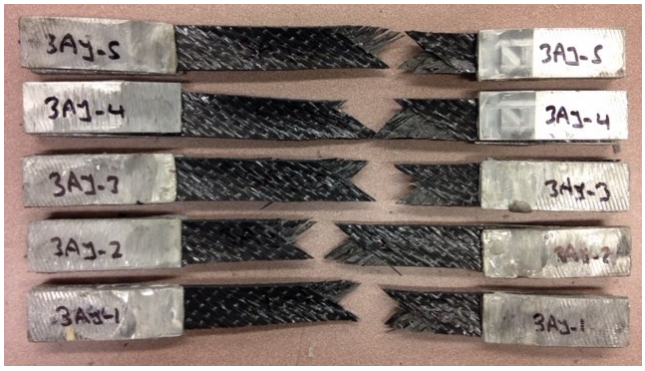

4 layers (Y direction)

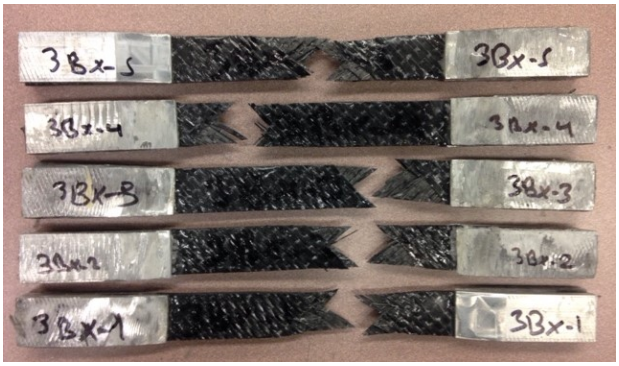

6 layers (X direction)

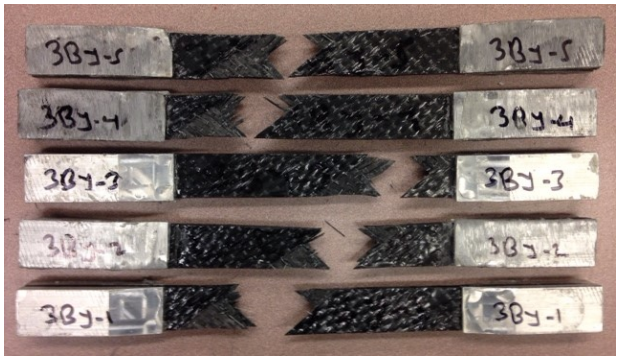

6 layers (Y direction)

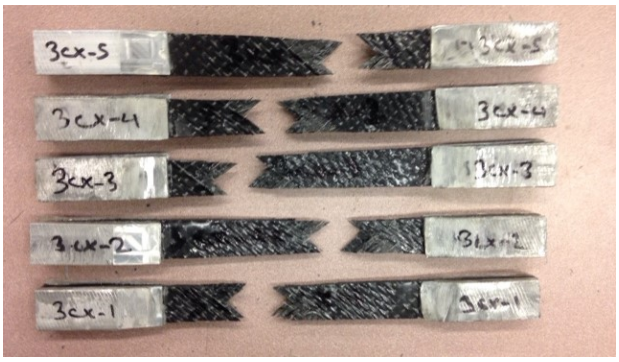

8 layers (X direction)

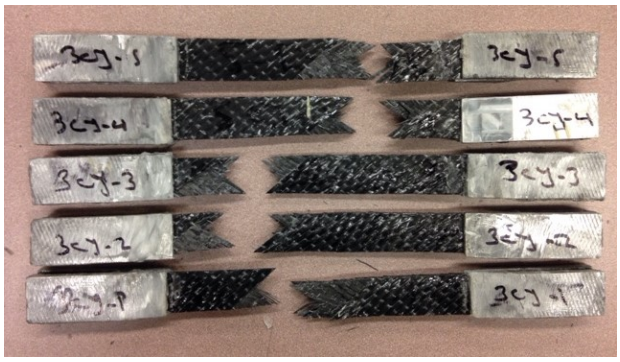

8 layers (Y direction)

Figure 4-11 Final failure modes of CFRP coupons (Series 3)

Table 4-7 CFRP coupon properties and failure mode (Series 3)

Series	Specimen	Thickness (mm)	Width (mm)	Area (mm²)	Properties at peak				E (GPa)	Failure Mode
					Load (KN)	Stress (MPa)	Strain	e_{cu}		
UD [+45°/-45°]$_2$ X direction	1	2.35	24.82	58.33	4.7	81.1	0.0833	6.06	0.97	AGM
	2	2.37	24.92	59.06	4.6	77.8	0.0461	2.95	1.69	AGM
	3	2.35	24.91	58.54	4.8	83.3	0.0965	7.24	0.86	AGM
	4	2.42	24.84	60.11	4.7	77.6	0.0446	2.90	1.74	AGM
	5	2.47	24.90	61.50	5.3	86.3	0.0387	2.88	2.23	AGM
	AVG	**2.39**	**24.88**	**59.51**	**4.8**	**81.2**	**0.0618**	**4.41**	**1.50**	
UD [+45°/-45°]$_2$ Y direction	1	2.45	24.80	60.76	6.92	113.7	0.1313	12.65	0.87	AGM
	2	2.38	24.78	58.48	7.35	124.4	0.1463	16.27	0.85	AGM
	3	2.38	24.80	59.02	6.62	112.3	0.1287	12.48	0.87	AGM
	4	2.33	24.76	57.69	7.06	122.2	0.1118	11.69	1.10	AGM
	5	2.36	24.74	58.39	7.13	122.2	0.1268	13.63	0.96	AGM
	AVG	**2.38**	**24.78**	**58.87**	**7.02**	**119.0**	**0.1289**	**13.34**	**0.93**	
UD [+45°/-45°]$_3$ X direction	1	3.68	24.91	91.67	9.8	106.8	0.0431	3.60	2.48	AGM
	2	3.66	25.08	91.79	10.1	110.4	0.0423	3.79	2.61	AGM
	3	3.65	24.94	91.03	10.5	115.3	0.0539	5.02	2.14	AGM
	4	3.59	24.83	89.14	10.4	117.2	0.0483	4.56	2.43	AGM
	5	3.50	24.75	86.63	10.1	116.7	0.0572	5.56	2.04	AGM
	AVG	**3.61**	**24.90**	**90.05**	**10.2**	**113.3**	**0.0489**	**4.51**	**2.34**	
UD [+45°/-45°]$_3$ Y direction	1	3.79	24.87	94.26	9.9	104.8	0.0231	1.70	4.54	AGM
	2	3.76	24.96	93.85	9.3	99.0	0.0378	2.99	2.62	AGM
	3	3.63	24.91	90.42	9.6	106.7	0.0266	2.16	4.01	AGM
	4	3.75	24.92	93.45	9.6	102.7	0.0323	2.69	3.18	AGM
	5	3.74	24.94	93.28	9.5	102.3	0.0371	3.00	2.76	AGM
	AVG	**3.73**	**24.92**	**93.05**	**9.6**	**103.1**	**0.0314**	**2.51**	**3.42**	
UD [+45°/-45°]$_4$ X direction	1	4.45	24.95	111.03	9.6	86.5	0.0214	1.35	4.04	AGM
	2	4.46	24.98	111.41	10.2	91.7	0.0227	1.50	4.04	AGM
	3	4.48	24.97	111.86	10.4	92.8	0.0256	1.74	3.62	AGM
	4	4.37	24.96	109.07	10.2	93.7	0.0261	1.80	3.59	AGM
	5	4.40	24.96	109.82	9.7	88.2	0.0190	1.16	4.64	AGM
	AVG	**4.44**	**24.96**	**110.64**	**10.0**	**90.6**	**0.0230**	**1.51**	**3.99**	
UD [+45°/-45°]$_4$ Y direction	1	4.92	25.06	123.29	16.4	133.3	0.1097	12.66	1.22	AGM
	2	4.94	25.05	123.75	17.1	137.9	0.0756	8.76	1.82	AGM
	3	4.89	25.07	122.59	17.0	138.7	0.0735	8.38	1.89	AGM
	4	4.89	25.08	122.64	15.6	127.6	0.0844	9.02	1.51	AGM
	5	4.96	25.05	124.25	16.6	133.9	0.0653	7.12	2.05	AGM
	AVG	**4.92**	**25.06**	**123.30**	**16.6**	**134.3**	**0.0817**	**9.19**	**1.69**	

4.4.1.2 Stress-Strain behavior

Non-linear behavior, disregarding the amount of layers and cutting direction, is obvious from the load-deformation graphs presented in **Figure 4-12**. The stress-strain behavior of CFRP coupons in both the X and Y directions are presented in **Figure 4-13.** A summary of the test results which consists of maximum stress and strain as well as the calculated maximum modulus of elasticity of each coupon is presented in **Table 4-7.** In general, both the load and stress increased by increasing the number of layers from 4 to 6, while no noticeable impact (and in some cases or decrease in values) was observed by increasing the number of layers to 8. The strain of the same specimens was decreased by adding more layers of CFRP sheets. For example, values of (4.8, 81.2, and 0.0618), (10.2, 113.3, and 0.0489), and (10, 90.6, and 0.0230) were observed in the case of load, stress, and strain for coupons with 4, 6, and 8 layers of CFRP sheets. Energy absorption capacities showed small increase by increasing the number of layers from 4 to 6, while decrease in values was experienced by increasing the number of layers to 8 layers. Energy absorption capacity for coupons with 4, 6, and 8 layers of CFRP sheets were 4.41, 4.51, and 1.51. The results presented in **Table 4-7** showed increase in modulus of elasticity as the number of CFRP layers increases. **Figure 4-12** and **Figure 4-13** show that coupons with more layers displayed more uniform results. In most of the cases, coupons in the Y direction showed a larger stress and strain compared to those in the X direction. However, the X direction coupons displayed larger modulus of elasticity compared to those in the Y direction.

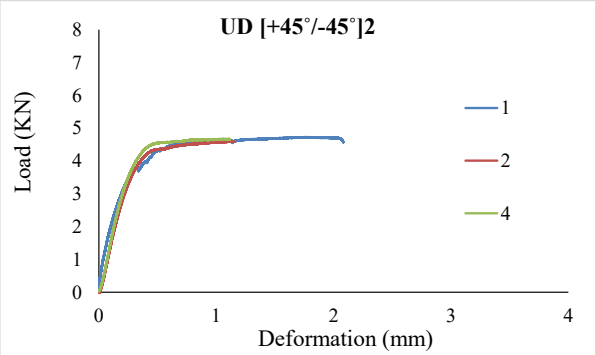

4 layers (X direction)

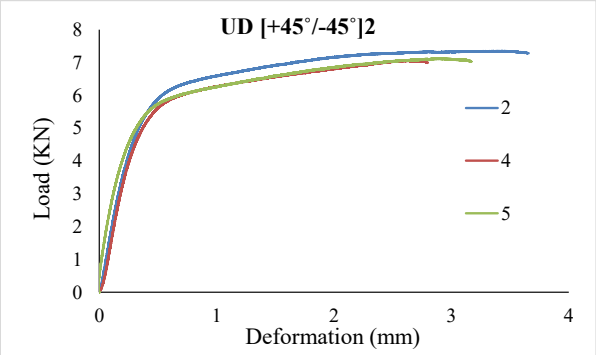

4 layers (Y direction)

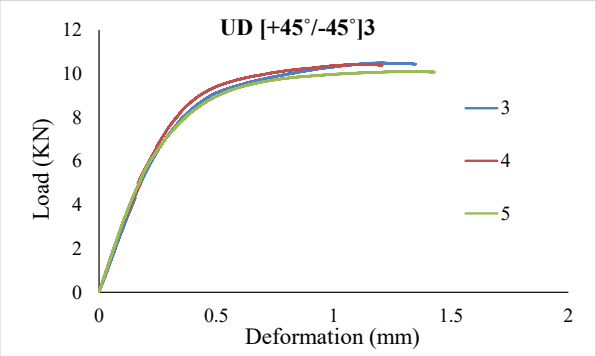

6 layers (X direction)

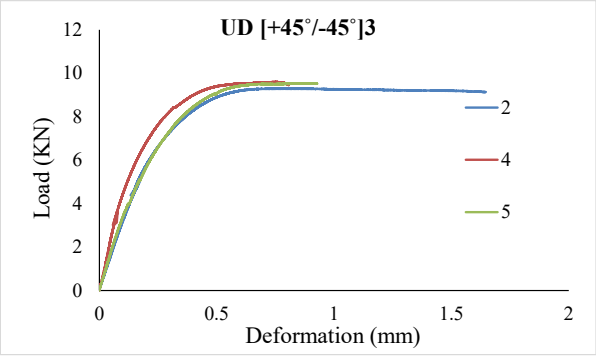

6 layers (Y direction)

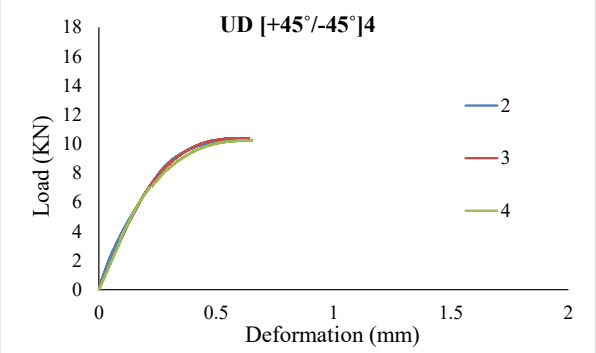

8 layers (X direction)

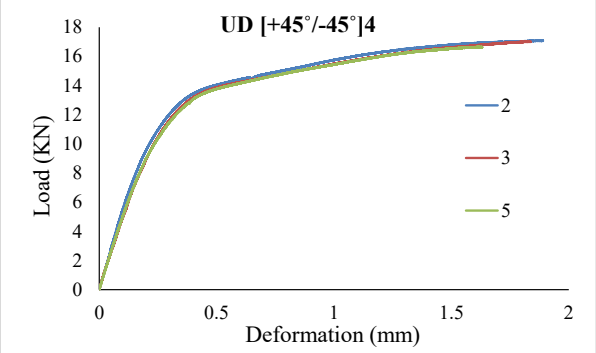

8 layers (Y direction)

Figure 4-12 Load-deformation curves of CFRP coupons (Series 3)

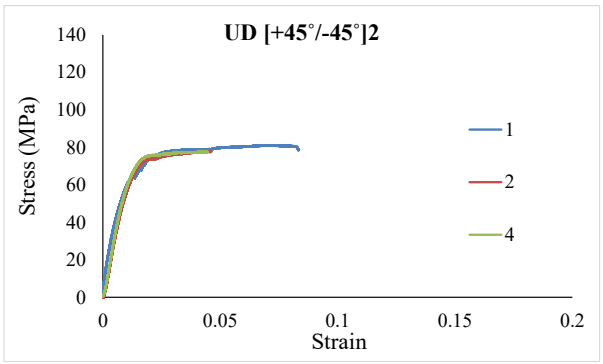

4 layers (X direction)

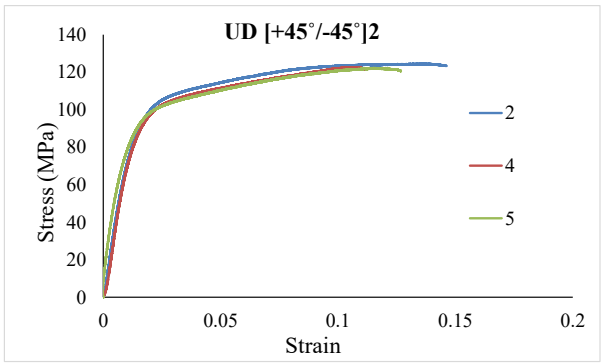

4 layers (Y direction)

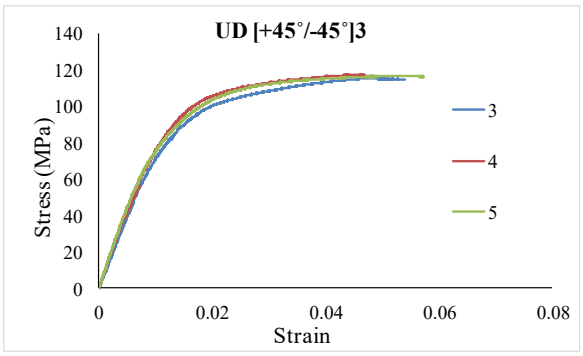

6 layers (X direction)

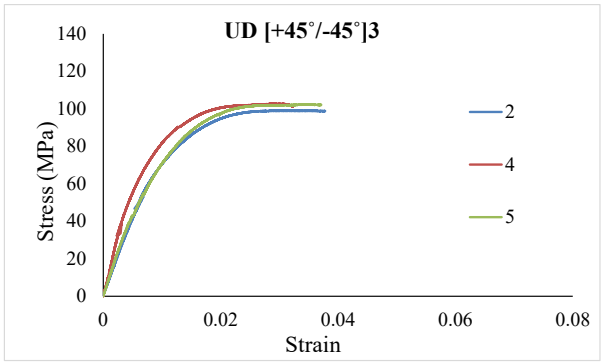

6layers (Y direction)

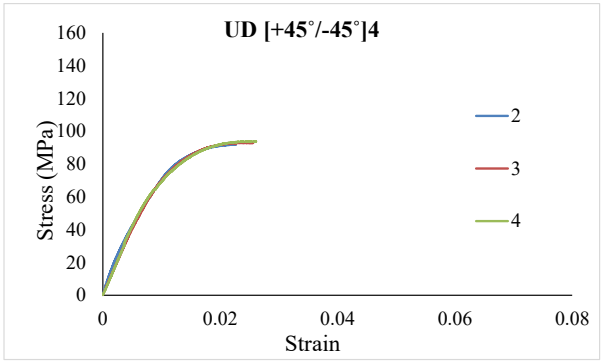

8 layers (X direction)

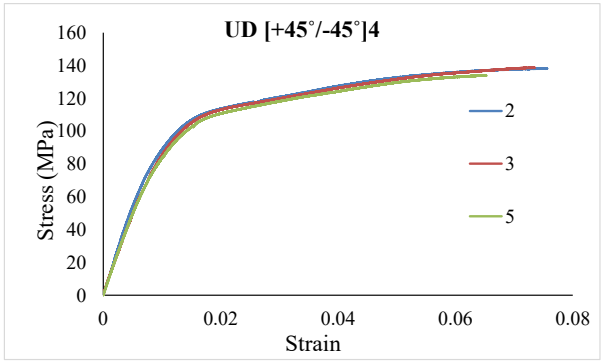

8 layers (Y direction)

Figure 4-13 Stress-strain curves of CFRP coupons (Series 3)

4.4.2 Cylinders

The specimens in this series were wrapped with unidirectional CFRP sheets that have fibers aligned in both the +45° and -45° directions as described in chapter 3. Two sizes of cylinders having dimensions of 100 x 200 mm ("small") and 150 x 300 mm ("large") were tested, with

each type confined by either 4, 6 or 8 layers of CFRP. Five replicates were tested for each "small" cylinder configuration, while three replicates were tested for each "large" cylinder configuration. The stress-strain curves of all tested specimens for both sizes are presented in **Figure 4-14**. The peak stress and peak strain of the tested specimens in *Series 3* are summarized in **Table 4-8** and **Table 4-9**.

4.4.2.1 Mode of Failure

Figure 4-14 shows the failure modes of both small and big specimens with different amounts of confinement. The same mode of failure was observed for all specimens. Disregarding the size and the amount of confinement, the specimens in this series sustained large shortening and axial deformations before failure. Rupture of the jacket in both small and big specimens occurred in a zigzag manner with tears at angles of 45 degrees. Crushing was controlled with only 1% to 5% of the crushed concrete being ejected out of the jacket, while global shear cracks were noticed in the concrete core. The rupture of the jacket was from bottom to top. Overall, specimens failed in a very ductile manner.

The CFRP jackets became active very slowly compared to those in *series 1* and *series 2*. The CFRP confined concrete cylinders started to gain stress with a slight increase in strain up until the maximum strength of unconfined concrete, from there the confined cylinders started to display a huge increase in strain with a small increase in stress up to the final failure.

4 layers (100mm)

6 Layers (100mm)

8 Layers (100mm)

4 Layers (150mm)

6 Layers (150mm)

8 Layers (150mm)

Figure 4-14 Final failure modes of CFRP confined concrete cylinders (Series 3)

4.4.2.2 Stress-Strain Behavior

The stress-strain results of the CFRP-confined concrete cylinders in Series 2 are shown in **Figure 4-15**. A summary of the results which consist of peak stress ($f_{cc}{}'$) and peak strain ($\varepsilon_{cc}{}'$) are tabulated in **Table 4-8** and **Table 4-9** for the 100 mm and 150 mm specimens, respectively. A substantial increase in strain of CFRP confined concrete cylinders can be clearly observed. However, no significant changes were seen for the increase in stress compared to those of unconfined concrete, although the small increase in stress was found to be proportional to the number of CFRP layers. The "small" cylinders displayed an average increase in stress (f_{cc}/f_{co}) of approximately 1.21, 1.47 and 1.70 for specimens confined with 4, 6 and 8 layers of CFRP,

respectively. The average increase in strain ($\varepsilon_{cc}/\varepsilon_{co}$) was found to be 18.62, 30.21 and 33.35 for specimens confined with 4, 6 and 8 layers of CFRP. Both the stress and strain were increased by adding more layers of CFRP sheets, however the relative increase in stress and strain was more pronounced for the first 4 layers of confinement.

Similarly, both the stress and strain of the "large" size specimens were increased by adding more layers of CFRP sheets. However, the values were different than those obtained from the “small” size specimens. For example, values of 1.05, 1.28 and 1.46 were obtained in the case of average increase in stress, while values of 9.23, 22.25 and 25.78 were found for the average increase in strain for specimens confined with 4, 6 and 8 layers of CFRP sheets, respectively.

Table 4-8 Experimental results 100 mm specimens

Specimen	# of Layer	Specimen Size	(f_{cc}')	(f_{cc}/f_{co})	(ε_{cc}')	$(\varepsilon_{cc}/\varepsilon_{co})$
1	4	100	56.60	1.31	0.067	22.60
2	4	100	49.26	1.14	0.040	13.45
3	4	100	48.35	1.12	0.063	21.24
5	4	100	54.87	1.27	0.051	17.17
AVG.	**4**	**100**	**52.27**	**1.21**	**0.056**	**18.62**
1	6	100	53.57	1.24	0.033	10.98
2	6	100	57.05	1.33	0.108	36.02
3	6	100	71.25	1.66	0.109	36.79
4	6	100	79.33	1.84	0.101	33.81
5	6	100	55.14	1.28	0.100	33.47
AVG.	**6**	**100**	**63.27**	**1.47**	**0.090**	**30.21**
1	8	100	59.59	1.38	0.079	26.62
2	8	100	88.84	2.06	0.129	43.16
3	8	100	87.35	2.03	0.119	39.92
4	8	100	64.35	1.50	0.082	27.62
5	8	100	66.84	1.55	0.088	29.43
AVG.	**8**	**100**	**73.39**	**1.70**	**0.099**	**33.35**

Table 4-9 Experimental results 150 mm specimens

Specimen	# of Layer	Specimen Size	(f_{cc}')	(f_{cc}/f_{co})	(ε_{cc}')	$(\varepsilon_{cc}/\varepsilon_{co})$
1	4	150	43.12	1.01	0.038	12.70
2	4	150	44.98	1.06	0.020	6.57
3	4	150	46.14	1.08	0.025	8.42
AVG.	**4**	**150**	**44.75**	**1.05**	**0.028**	**9.23**
1	6	150	50.69	1.19	0.045	15.10
2	6	150	59.57	1.40	0.089	29.69
3	6	150	53.41	1.25	0.066	21.97
AVG.	**6**	**150**	**54.56**	**1.28**	**0.066**	**22.25**
1	8	150	58.68	1.38	0.055	18.31
2	8	150	64.06	1.50	0.072	24.01
3	8	150	63.56	1.49	0.105	35.02
AVG.	**8**	**150**	**62.10**	**1.46**	**0.077**	**25.78**

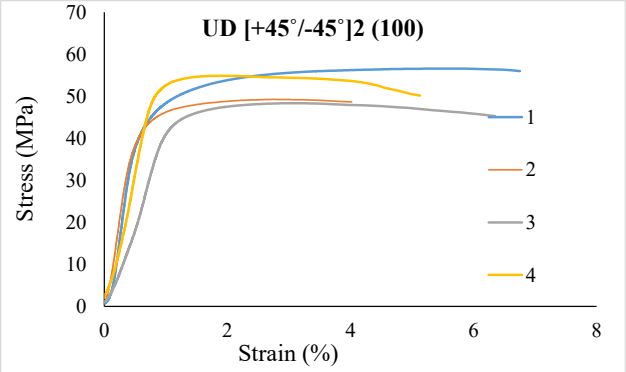

4 Layers

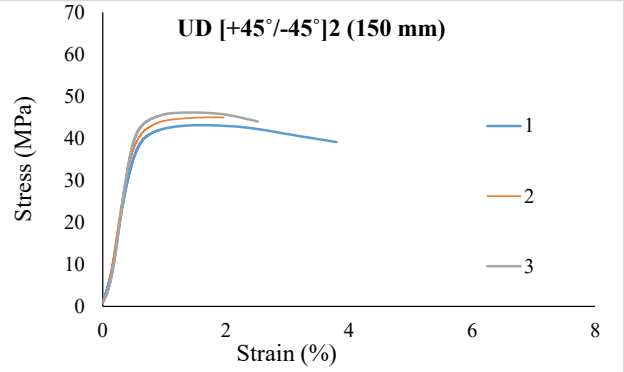

4 Layers

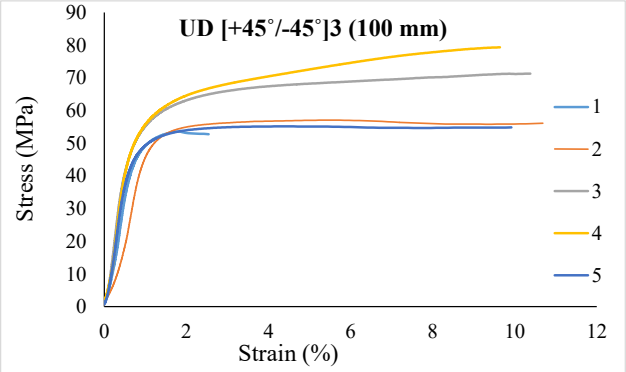

6 Layers

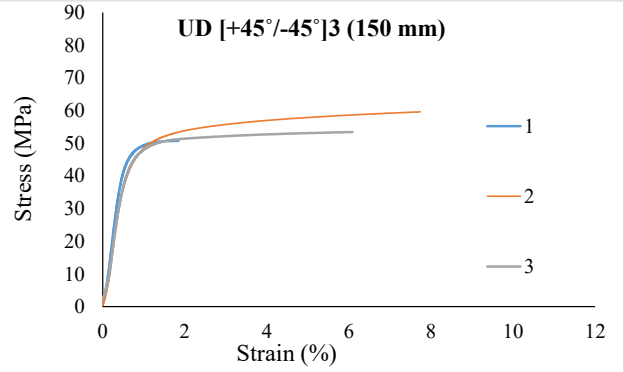

6 Layers

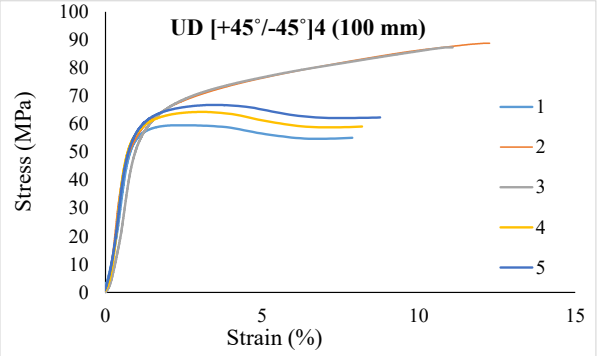

8 Layers

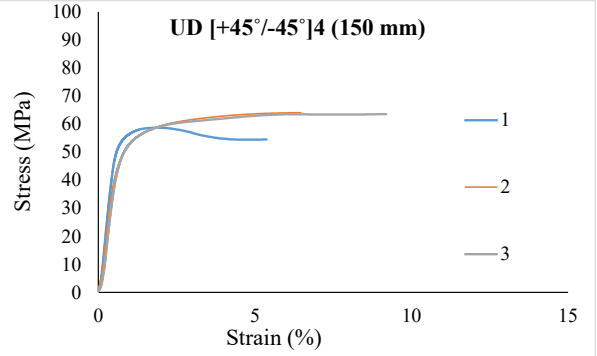

8 Layers

Figure 4-15 Stress-strain responses of tested specimens (Series 3)

4.5 Series 4

4.6 Series 4A

4.6.1 Coupons

Series 4A included a total of 20 coupons manufactured using 4 or 8 layers of both unidirectional and woven CFRP sheets which consist of fibers aligned at 90, 0 and $\pm 45^0$ (UD[90˚/0˚]W[±45˚]) directions. This series was divided into 2 subseries, 4A1 and 4A2 based on the stacking sequence of CFRP sheets. Five replicates were included for each layer configuration in both the X and Y directions. Mode of failure and post failure photos of the coupons can be seen in **Figure 4-16** and **Figure 4-21.** The results of peak stress, peak strain and the failure nomenclature of the coupons are presented in **Table 4-10.**

4.6.1.1 Mode of Failure

All of the coupons showed ductile failure due to having more layers of CFRP sheets aligned in the $\pm 45^0$ direction compared to CFRP sheets applied in other directions The modes of failure of each coupon in accordance to ASTM D3039/D3039M (2015) specification are tabulated in **Table 4-10.** In most of the coupons, lateral rupture occurred in the middle gage region (LGM), except those with 8 layers of CFRP, which showed delamination of the other $\pm 45^0$ sheets (DGM) as shown in **Figure 4-16**. Delamination of the coupons occurred between unidirectional and woven CFRP sheets.

4 layers (X direction)

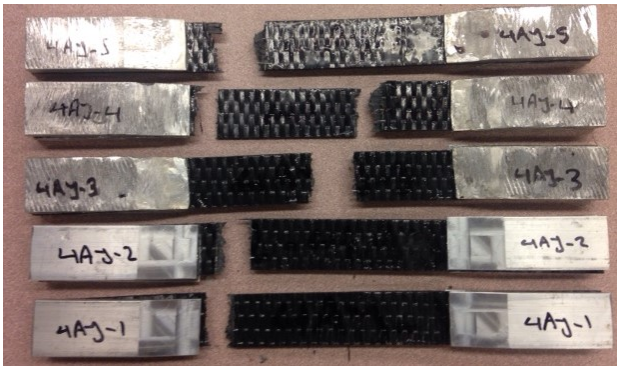

4 layers (Y direction)

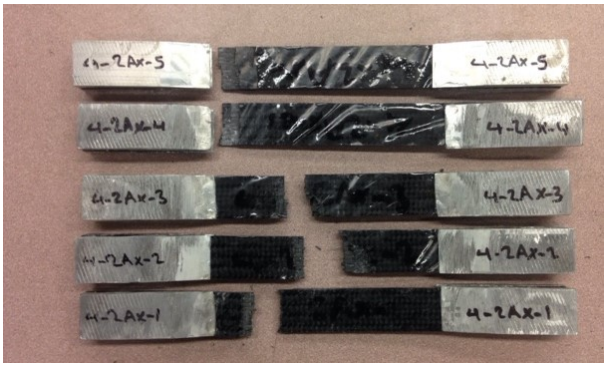

8 layers (X direction)

8 layers (Y direction)

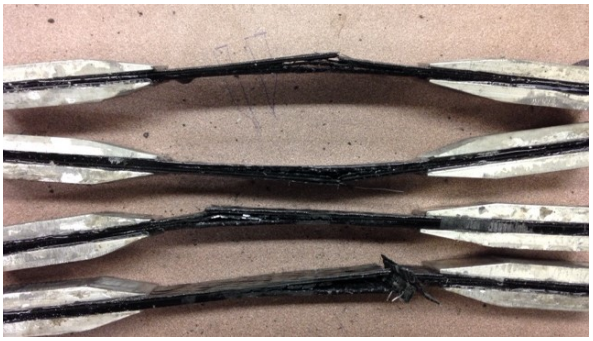

Figure 4-16 Final failure modes of CFRP coupons (Series 4A)

Table 4-10 CFRP coupon properties and failure mode (Series 4A)

Series	Specimen	Thickness (mm)	Width (mm)	Area (mm²)	Properties at peak				E (GPa)	Failure Mode
					Load (KN)	Stress (MPa)	Strain	e_{cu}		
UD[90°/0°]W[±45°]$_2$ X direction	1	2.53	24.94	63.10	18.4	290.7	0.0340	1.88	8.55	LGM
	2	2.44	24.98	60.95	18.2	299.2	0.0350	1.94	8.55	LGM
	3	2.55	25.01	63.77	19.2	301.5	0.0397	2.17	7.60	LGM
	4	2.51	24.91	62.52	13.6	217.1	0.0251	0.94	8.65	LGM
	5	2.55	24.90	63.49	18.5	291.7	0.0127	1.80	22.97	LGM
	AVG	**2.51**	**24.95**	**62.77**	**17.6**	**280.1**	**0.0293**	**1.75**	**11.26**	
UD[90°/0°]W[±45°]$_2$ Y direction	1	2.08	25.06	52.12	17.6	337.6	0.0117	2.09	28.86	LGM
	2	2.37	25.06	59.39	14.7	246.8	0.0110	1.36	22.43	LGM
	3	2.36	24.98	58.95	18.5	313.3	0.0123	1.82	25.47	LGM
	4	2.23	25.04	55.84	19.0	340.2	0.0150	2.63	22.68	LGM
	5	2.25	25.21	56.72	19.1	337.8	0.0142	2.35	23.79	LGM
	AVG	**2.26**	**25.07**	**56.60**	**17.8**	**315.1**	**0.0128**	**2.05**	**24.65**	
UD[90°/0°]$_2$W[±45°]$_4$ X direction	1	4.40	25.07	110.31	39.9	362.0	0.0141	2.56	25.67	LGM
	2	4.46	25.04	111.68	35.9	321.5	0.0141	2.28	22.80	LGM
	3	4.31	25.00	107.75	38.7	359.2	0.0138	2.55	26.03	LGM
	4	4.46	25.02	111.59	36.3	325.7	0.0119	1.93	27.4	LAT
	5	4.36	24.98	108.91	36.9	338.5	0.0125	2.08	27.08	LAT
	AVG	**4.40**	**25.02**	**110.05**	**37.5**	**341.4**	**0.0133**	**2.28**	**25.80**	
UD[90°/0°]$_2$W[±45°]$_4$ Y direction	1	4.52	25.04	113.18	39.2	346.5	0.0138	2.43	25.11	DGM
	2	4.42	25.02	110.59	36.7	332.4	0.0127	2.05	26.17	DGM
	3	4.64	25.07	116.32	37.4	321.9	0.0145	2.34	22.20	DGM
	4	4.41	24.94	109.98	33.8	307.8	0.0138	1.94	22.30	DGM
	5	4.21	24.89	104.79	34.5	329.5	0.0137	2.27	24.05	DGM
	AVG	**4.41**	**24.99**	**110.97**	**36.3**	**327.6**	**0.0137**	**2.21**	**23.97**	

4.6.1.2 Stress-Strain behavior

The coupons showed some limited non-linear behavior due to the presence of ±45^0 CFRP sheets. Close inspection of the load-deformation and stress-strain behavior shows the response is comprised of two different branches. Based on the observed results in Series 2 and 3, the first branch of behavior in the curve can be attributed to the ±45^0 CFRP sheets, while the second branch of behavior is attributed to the effect of the 90-0^0 CFRP sheets. A summary of the test

results consisting of maximum stress and strain as well as calculated maximum modulus of elasticity of each coupon are presented in **Table 4-10.** The increase in load and stress increase when increasing the number of layers while opposite behavior was noticed in the case of peak strain. The load and stress were increased from 17.6 and 280.1 to 37.5 and 341.4 by increasing the number of layers from 4 to 8. However, the strain of the same specimens decreases from 0.0293 to 0.0133 by increasing the number of layers from 4 to 8 layers. The energy absorption capacity and the modulus of elasticity showed increase by adding layers with values of 1.75 and 11.26, 2.28 and 25.79 for coupons with 4 and 8 layers of CFRP sheets (X direction). In most of the cases, Y direction coupons showed larger peak tress compared the X direction, although X direction coupons displayed larger rupture strains compared to the Y direction.

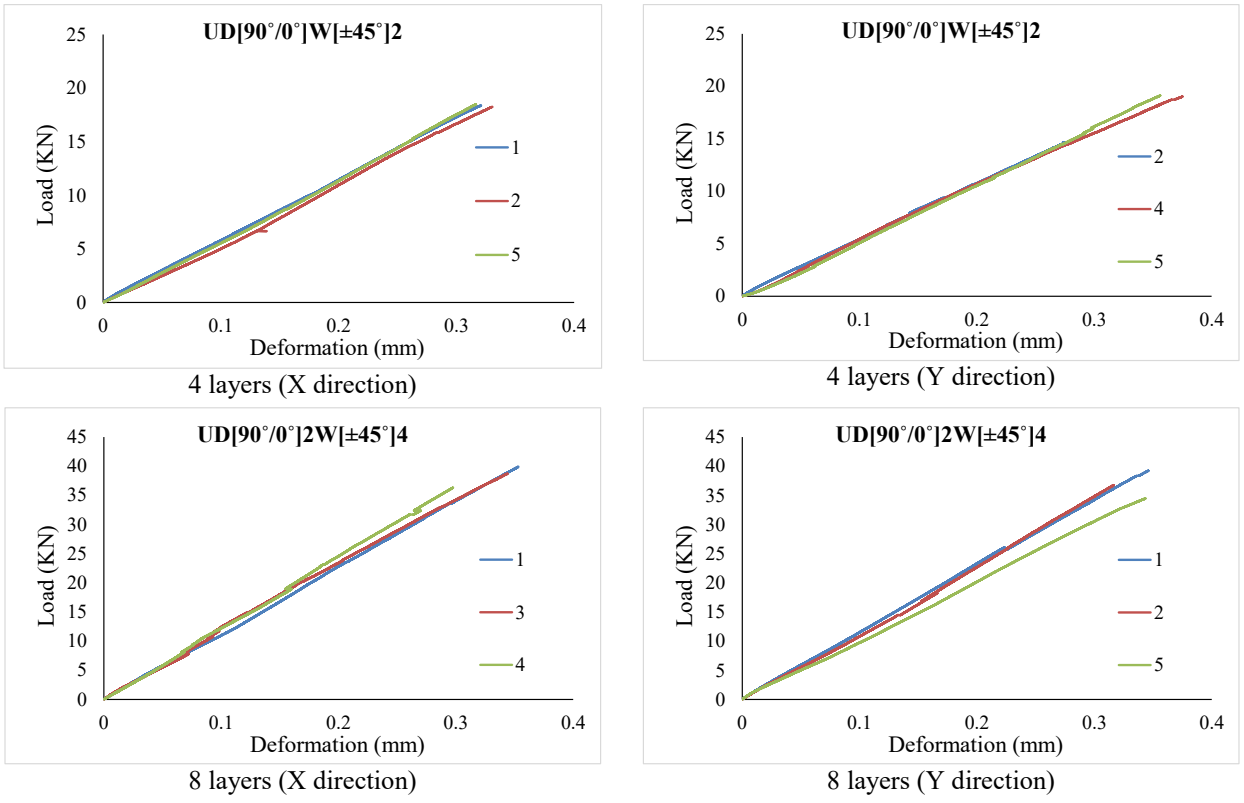

Figure 4-17 Load-deformation curves of CFRP coupons (Series 4A)

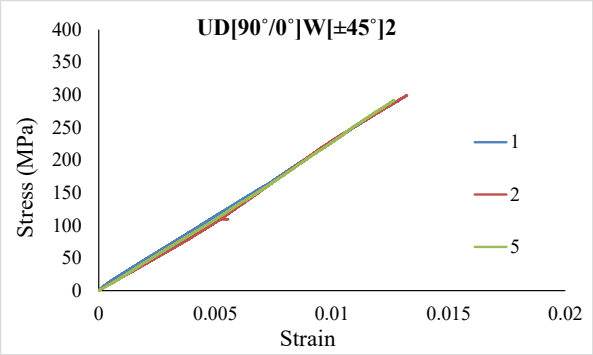

4 layers (X direction)

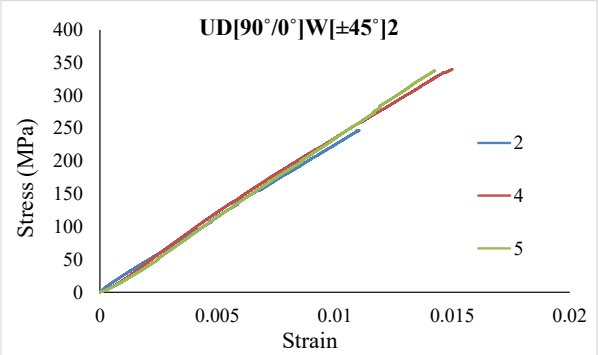

4 layers (Y direction)

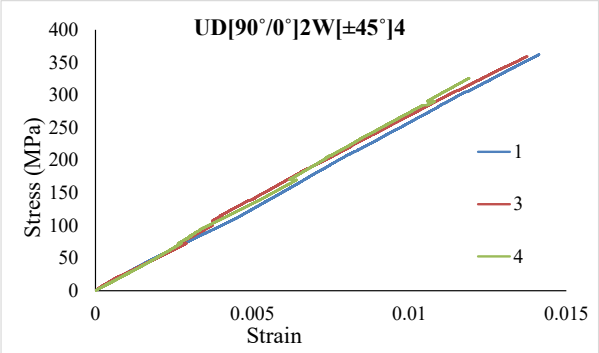

8 layers (X direction)

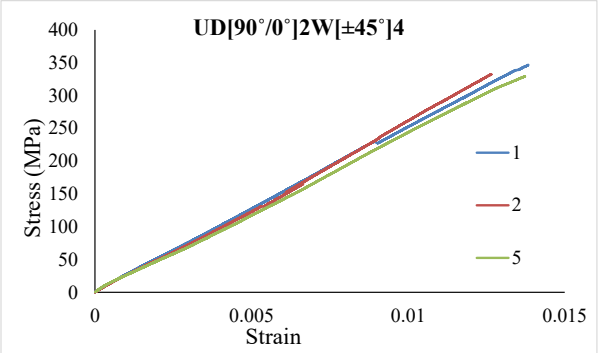

8 layers (Y direction)

Figure 4-18 Stress-strain curves of CFRP coupons (Series 4A)

4.6.2 Cylinders

The specimens in this series were wrapped with unidirectional and woven CFRP sheets that have fibers aligned in 0°, 90° and ±45° directions as described in chapter 3. Specimens were divided into 2 subseries based on the stacking configuration. Each subseries were further divided into 2 batches based on their size and each batch was then split into 2 sub-batches based on the amount of confinement. Four replicates were tested for each "small" cylinder configuration, while three replicates were tested for each "large" cylinder configuration. The stress-strain curves of all

tested specimens for both sizes are presented in Figure 4-20. The peak stress and peak strain of the tested specimens in *Series 4A* are summarized in **Table 4-11** and **Table 4-12**.

4.6.2.1 Mode of Failure

Figure 4-19 shows the failure mode of both small and big specimens with 4 and 8 layers of CFRP confinement. Rupture of the jacket consisted of fiber failures in the hoop and longitudinal direction with a zigzag pattern in the tear of the jackets. Delaminating of the layers was not observed. Rupture of the jacket was found to be more pronounced in the larger specimens. The concrete core showed cone, cone and shear, as well as columnar types of failure. It is worth mentioning that the ratio of crushing to cracking of concrete core was very low for the smaller specimens. As it is evident from **Figure 4-19**, the failed concrete remained in the jacket which indicates gradual failure of the confined specimens in this series.

4 layers (100mm)

8 Layers (100mm)

4 Layers (150mm)

8 Layers (150mm)

Figure 4-19 Final failure modes of CFRP confined concrete cylinders (Series 4A)

4.6.2.2 Stress-Strain Behavior

The stress-strain results of the CFRP-confined concrete cylinders in Series 4A are shown in Figure 4-20. A summary of the results, which consists of the peak stress ($f_{cc}{}'$) and peak strain ($\varepsilon_{cc}{}'$) are tabulated in **Table 4-11** and **Table 4-12** for the 100 mm and 150 mm specimens, respectively. A substantial increase in both stress and strain of CFRP confined concrete cylinders is clearly shown. The "small" cylinders displayed an average increase in stress (f_{cc}/f_{co}) of 2.07 and 2.99 for specimens confined with 4 and 8 layers of CFRP, respectively. The average increase in strain ($\varepsilon_{cc}/\varepsilon_{co}$) was found to be 7.83 and 11.55 for specimens confined with 4 and 8 layers of CFRP, respectively. Both stress and strain were increased by adding more layers of CFRP sheets,

however the relative increase in stress and strain was more pronounced for the first 4 layers of confinement. Similarly, both stress and strain of the "large" size specimens were increased by adding more layers of CFRP sheets. Values of 1.67 and 2.34 were obtained in the case of average increase in stress, while values of 7.01 and 6.48 were found in the case of average increase in strain for specimens confined with 4 and 8 layers of CFRP sheets, respectively. More uniform results were achieved from specimens with a larger amount of confinement.

Table 4-11 Experimental results 100 mm specimens

Specimen	# of Layer	Specimen Size	(f_{cc}')	(f_{cc}/f_{co})	(ε_{cc}')	$(\varepsilon_{cc}/\varepsilon_{co})$
1	4	100	92.31	2.14	0.024	8.18
2	4	100	84.42	1.96	0.024	7.85
3	4	100	87.34	2.03	0.021	6.90
4	4	100	92.50	2.15	0.025	8.37
AVG.	**4**	**100**	**89.14**	**2.07**	**0.023**	**7.83**
1	8	100	129.05	2.99	0.035	11.78
2	8	100	127.04	2.95	0.038	12.72
3	8	100	133.96	3.11	0.030	10.02
4	8	100	125.07	2.91	0.035	11.69
AVG.	**8**	**100**	**128.78**	**2.99**	**0.034**	**11.55**

Table 4-12 Experimental results 150 mm specimens

Specimen	# of Layer	Specimen Size	(f_{cc}')	(f_{cc}/f_{co})	(ε_{cc}')	$(\varepsilon_{cc}/\varepsilon_{co})$
1	4	150	76.36	1.79	0.021	6.94
2	4	150	65.09	1.53	0.020	6.79
3	4	150	72.37	1.70	0.022	7.30
AVG.	**4**	**150**	**71.27**	**1.67**	**0.021**	**7.01**
1	6	150	100.52	2.36	0.022	7.50
2	6	150	100.12	2.35	0.018	6.01
3	6	150	98.70	2.32	0.018	5.91
AVG.	**6**	**150**	**99.78**	**2.34**	**0.019**	**6.48**

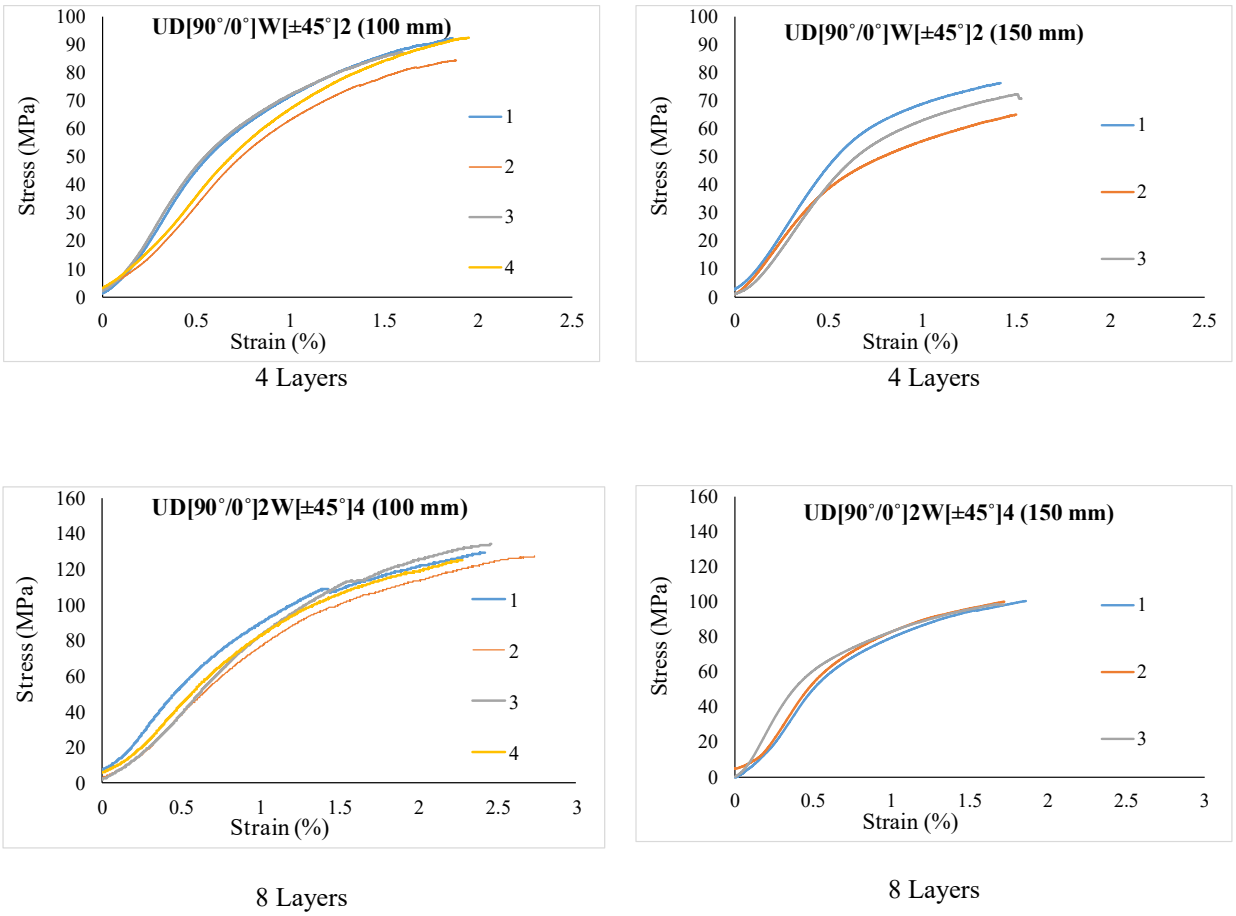

Figure 4-20 Stress-strain responses of tested specimens (Series 4A)

4.7 Series 4B

4.7.1 Coupons

Series 4B included a total of 20 coupons manufactured using 4 or 8 layers of both unidirectional and woven CFRP sheets which consist of fibers aligned at 90^0, 0^0 and $\pm45^0$ (UD[90˚]W[±45˚]UD[0˚]) directions. This series was divided into 2 subseries, 4B1 and 4B2 based on the stacking sequence of CFRP sheets. Five replicates were produced for each layer configuration in both the X and Y directions. Mode of failure and post failure photos of the

coupons can be seen in **Figure 4-21.** Results of peak stress and peak strain as well as the failure nomenclature of coupons are presented in **Table 4-13**.

4.7.1.1 Mode of Failure

All of the coupons showed ductile failure due to having more layers of CFRP sheets aligned in the $\pm 45^0$ direction than CFRP sheets applied in other directions. The mode of failure of each coupon in accordance to the ASTM D3039/D3039M (2015) specification is tabulated in **Table 4-13.** In most of the coupons, lateral failures occurred in middle gage regions (LGM). A few of the coupons showed lateral failures near the grips (LAT) as shown in **Figure 4-21**.

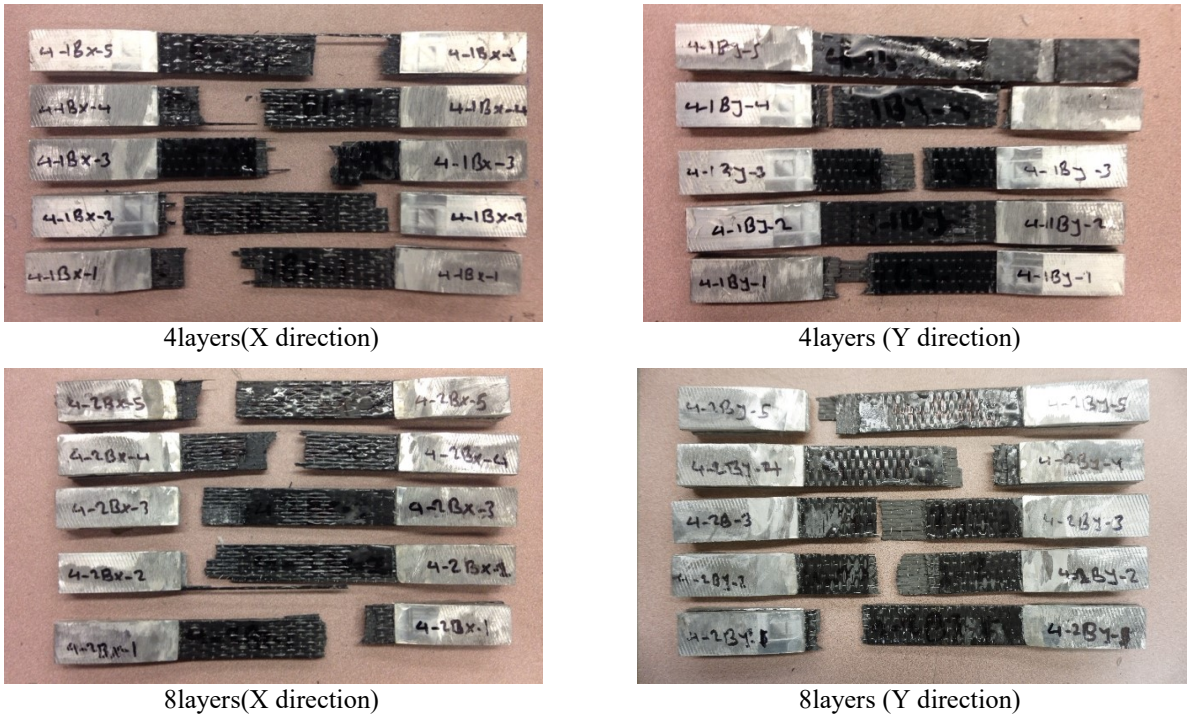

4layers(X direction) 4layers (Y direction)

8layers(X direction) 8layers (Y direction)

Figure 4-21 Final failure modes of CFRP coupons (Series 4B)

Table 4-13 CFRP coupon properties and failure mode (Series 4B)

Series	Specimen	Thickness (mm)	Width (mm)	Area (mm²)	Properties at peak				E (GPa)	Failure Mode
					Load (KN)	Stress (MPa)	Strain	e_{cu}		
UD[90˚]W[±45˚]$_2$UD[0˚] X direction	1	2.48	24.90	61.75	18.50	299.5	0.0187	2.38	16.02	LGM
	2	2.34	24.99	58.48	17.45	298.4	0.0142	2.05	21.01	LGM
	3	2.37	25.03	59.32	18.61	313.7	0.0142	2.11	22.09	LGM
	4	2.43	25.08	60.94	19.40	317.9	0.0142	2.26	22.39	LGM
	5	2.46	24.98	61.45	19.34	315.1	0.0133	2.07	23.69	LGM
	AVG	**2.42**	**24.99**	**60.39**	**18.66**	**308.9**	**0.0149**	**2.17**	**21.04**	
UD[90˚]W[±45˚]$_2$UD[0˚] Y direction	1	2.64	25.22	66.58	21.65	324.8	0.0152	2.60	21.36	LGM
	2	2.58	25.32	65.33	16.95	259.5	0.0119	1.64	21.81	LGM
	3	2.70	25.39	68.55	20.98	306.4	0.0139	2.20	22.04	LGM
	4	2.58	25.24	65.12	20.50	314.2	0.0182	2.65	17.27	LGM
	5	2.81	25.15	70.67	17.82	251.8	0.0122	1.76	20.64	LAT
	AVG	**2.66**	**25.26**	**67.25**	**19.58**	**291.3**	**0.0143**	**2.17**	**20.62**	
UD[90˚]$_2$W[±45˚]$_4$UD[0˚]$_2$ X direction	1	3.96	25.01	99.04	19.7	199.5	0.0068	0.66	29.33	LGM
	2	3.90	25.15	98.08	27.3	278.6	0.0122	1.61	22.83	LAT
	3	3.94	25.10	99.40	33.7	340.8	0.0124	1.93	27.49	LAT
	4	3.97	24.94	99.01	38.8	392.3	0.0154	2.92	25.48	LGM
	5	3.96	24.97	98.88	33.5	339.6	0.0157	2.73	21.63	LGM
	AVG	**3.94**	**25.03**	**98.88**	**30.6**	**310.2**	**0.0125**	**1.97**	**25.35**	
UD[90˚]$_2$W[±45˚]$_4$UD[0˚]$_2$ Y direction	1	4.33	25.17	108.98	25.4	233.3	0.0092	1.11	25.36	LGM
	2	4.15	25.19	104.54	39.9	382.1	0.0142	2.80	26.91	LGM
	3	4.21	25.28	106.43	36.6	344.2	0.0153	2.51	22.49	LGM
	4	3.65	25.25	92.16	26.2	284.5	0.0143	2.21	19.89	LGM
	5	4.03	25.22	101.64	31.2	306.7	0.0123	1.99	24.94	LAT
	AVG	**4.07**	**25.22**	**102.75**	**31.9**	**310.2**	**0.0131**	**2.12**	**23.92**	

4.7.1.2 Stress-Strain behavior

A summary of the test results which consists of maximum stress and strain as well as the calculated maximum modulus of elasticity of each coupon is presented in **Table 4-13**. The stress-strain behavior of CFRP coupons in both the X and Y directions are presented in **Figure 4-18.** The coupons showed limited non-linear behavior due to the presence of $\pm 45^0$ CFRP sheets. The load carrying capacity of coupons were increased by increasing the number of layers, while

no noticeable increase in stress was observed. Load increased from 18.66 to 30.6 KN by increasing the number of layers from 4 to 8, while obtained stress values were 308.9 and 310.2 MPa for the same coupons. Conversely maximum strains dropped by increasing the number of layers. **Table 4-13** shows strains decreased from 0.0149 to 0.0125 by increasing the number of layers from 4 to 8 layers. The energy absorption capacity did not show noticeable change by increasing the number of layers. A small increase was observed in modulus of elasticity of coupons by increasing the number of layers from 4 to 8 layers. In most cases, coupons in the Y direction showed larger stress values compared to those in the X direction. However, X direction coupons showed larger failure strains compared to those in the Y direction

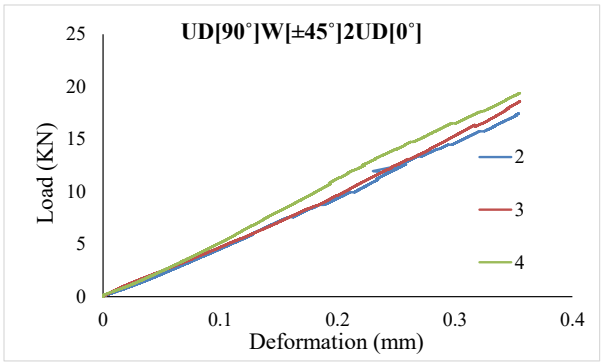

4 layers (X direction)

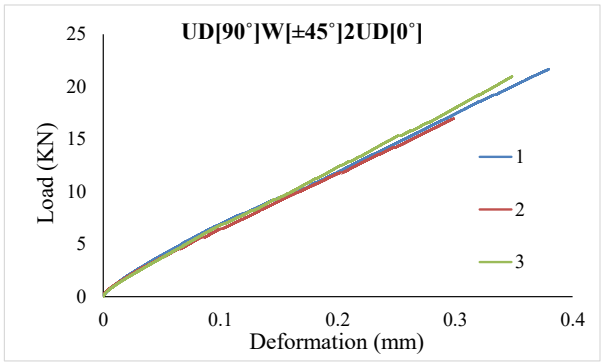

4 layers (Y direction)

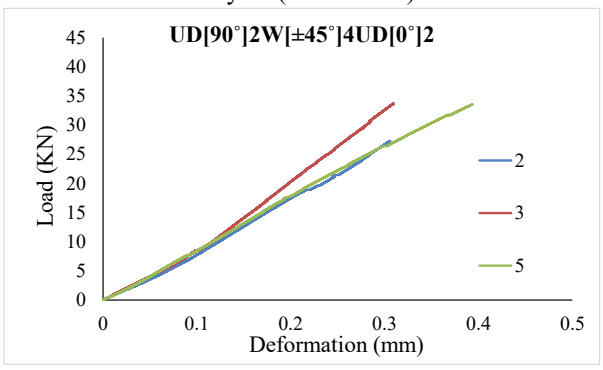

8 layers (X direction)

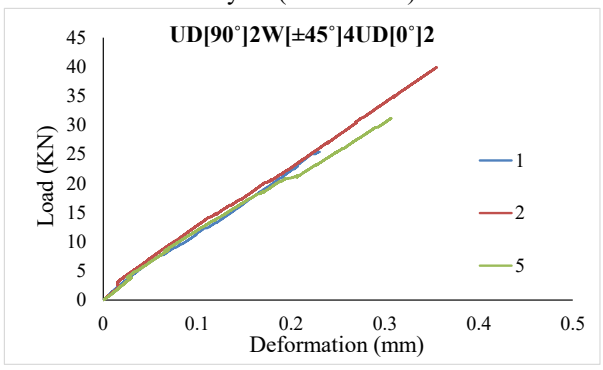

8 layers (Y direction)

Figure 4-22 Load-deformation curves of CFRP coupons (Series 4B)

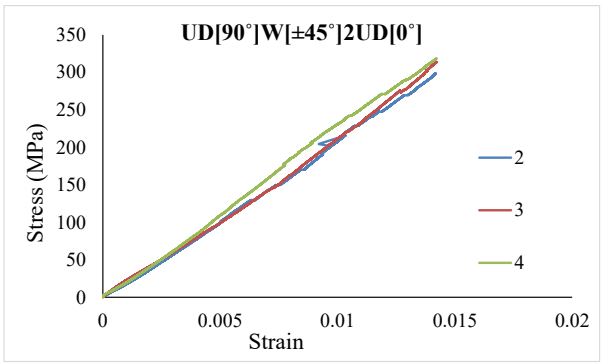

4 layers (X direction)

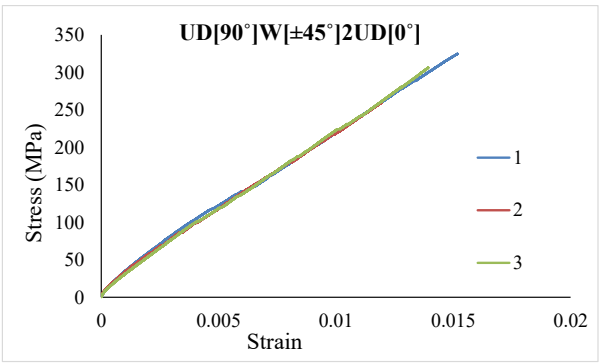

4 layers (Y direction)

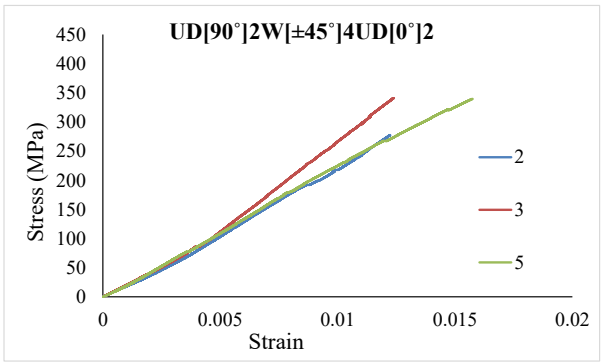

8 layers (X direction)

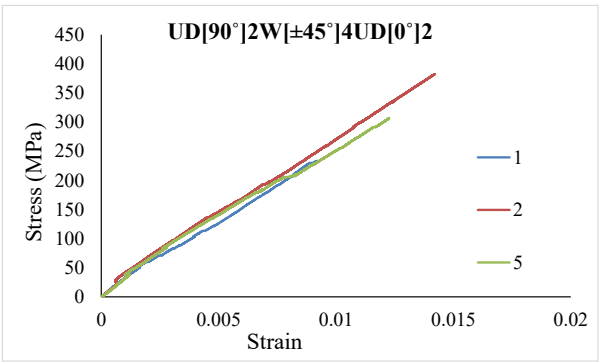

8 layers (Y direction)

Figure 4-23 Stress-strain curves of CFRP coupons (Series 4B)

4.7.2 Cylinders

The stacking sequence of this series varied from *Series 4-A* simply by the order of application of the layers. Four replicates were tested for each "small" cylinder configuration, while three replicates were tested for each "large" cylinder configuration. The stress-strain curves of all tested specimens for both sizes are presented in **Figure 4-25**. The peak stress and peak strain of the tested specimens in *Series 4A* are summarized in **Table 4-11** and **Table 4-12**.

4.7.2.1 Mode of Failure

The failure of all specimens were the same, delamination occurred between the outer layers and the middle layers, while the inner layers and middle layers remained attached up to the final failure. **Figure 4-24** shows a typical failure of small and large specimens with 4 and 8 layers of CFRP. Generally fiber ruptures occurred in the outer layer which had fibers aligned in the hoop direction while the inner layers sustained less damage. As a result the crushed concrete remained confined in the jacket except in the case of large specimens with 4 layers of CFRP where cone and columnar modes of failure were observed. A larger compressive load is required to break big size specimens compared to small size cylinders, and the confinement provided in the specimens with 4 layers may be insufficient to prevent complete failure of the hoop direction fibers due to the huge pressure release at failure. Nonetheless the confined specimens in this series showed gentle and ductile failures due to the combination of unidirectional and angular fibers, as well as the order of CFRP layers (angular CFRP as innermost, and unidirectional CFRP as outermost).

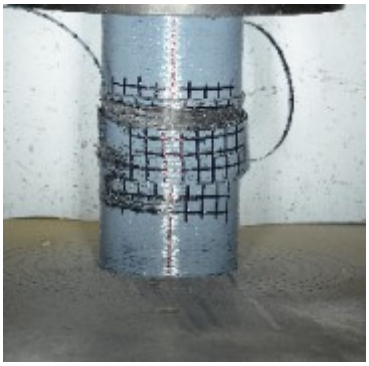

4 layers (100mm)

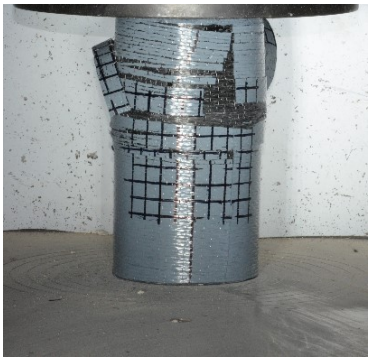

8 Layers (100mm)

4 Layers (150 mm)

8 Layers (150 mm)

Figure 4-24 Final failure modes of CFRP confined concrete cylinders (Series 4B)

4.7.2.2 Stress-Strain Behavior

The stress-strain behavior of the CFRP-confined concrete cylinders in Series 4B is shown in **Figure 4-25**. A summary of the results which consist of peak stress (f_{cc}') and peak strain (ε_{cc}') are tabulated in **Table 4-14** and **Table** 4-15 for the 100 mm and 150 mm specimens, respectively. An increase in both stress and strain of CFRP confined concrete cylinders is apparent. The "small" cylinders displayed an average increase in stress (f_{cc}/f_{co}) of approximately 1.89 and 2.65 for specimens confined with 4 and 8 layers of CFRP, respectively. The average increase in strain ($\varepsilon_{cc}/\varepsilon_{co}$) was found to be 7.74 and 11.65 for specimens confined with 4 and 8 layers of CFRP, respectively. The relative increase in stress and strain was more pronounced for the first 4 layers of confinement. Similarly, both stress and strain of the "large"

size specimens was increased by adding more layers of CFRP sheets. However, the values were different than those obtained from "small" size specimens. Values of 1.70 and 2.20 were found in the case of average increase in stress, while values of 8.02 and 6.86 were obtained in the case of average increase in strain for specimens confined with 4 and 8 layers of CFRP.

Table 4-14 Experimental Results 100 mm Specimens (4B)

Specimen	# of Layer	Specimen Size (mm)	(f_{cc}') (MPa)	(f_{cc}/f_{co})	(ε_{cc}')	$(\varepsilon_{cc}/\varepsilon_{co})$
1	4	100	78.60	1.83	0.025	8.50
2	4	100	75.83	1.76	0.024	7.93
3	4	100	87.22	2.03	0.022	7.36
4	4	100	83.67	1.94	0.021	7.18
AVG.	**4**	**100**	**81.33**	**1.89**	**0.023**	**7.74**
1	8	100	115.85	2.69	0.033	11.14
2	8	100	119.94	2.79	0.026	8.77
3	8	100	103.75	2.41	0.042	14.21
4	8	100	115.88	2.69	0.037	12.49
AVG.	**8**	**100**	**113.86**	**2.65**	**0.035**	**11.65**

Table 4-15 Experimental Results 150 mm Specimens (4B)

Specimen	# of Layer	Specimen Size(mm)	(f_{cc}') (MPa)	(f_{cc}/f_{co})	(ε_{cc}')	$(\varepsilon_{cc}/\varepsilon_{co})$
1	4	150	72.16	1.69	0.024	8.08
2	4	150	72.75	1.71	0.024	7.89
3	4	150	72.66	1.71	0.024	8.08
AVG.	**4**	**150**	**72.52**	**1.70**	**0.024**	**8.02**
1	6	150	97.17	2.28	0.023	7.78
2	6	150	88.29	2.07	0.017	5.93
3	6	150	95.67	2.25	0.020	6.88
AVG.	**6**	**150**	**93.71**	**2.20**	**0.020**	**6.86**

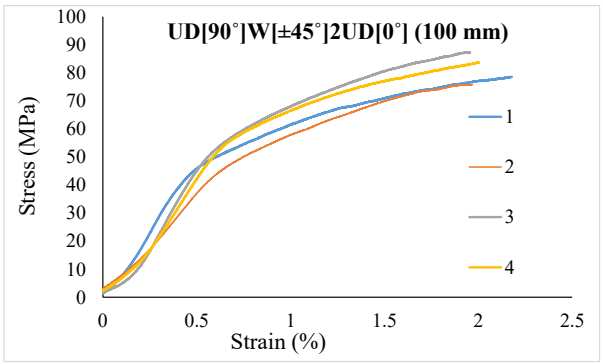

4 Layers

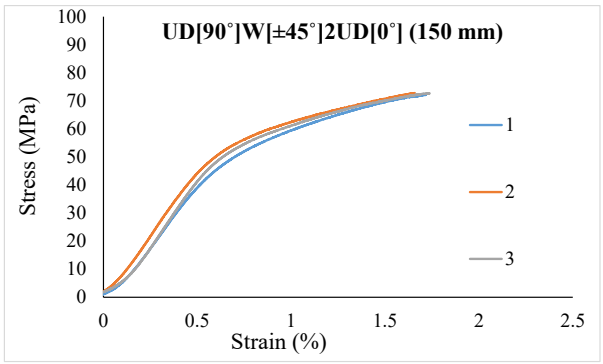

4 Layers

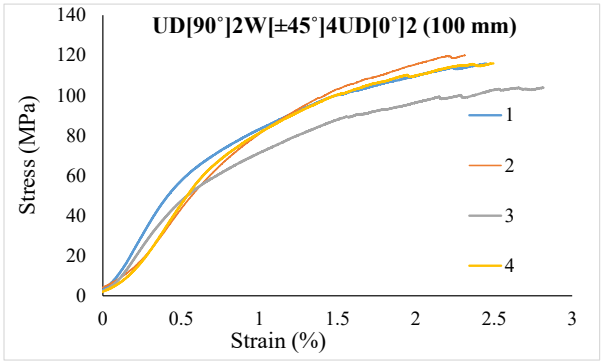

8 Layers

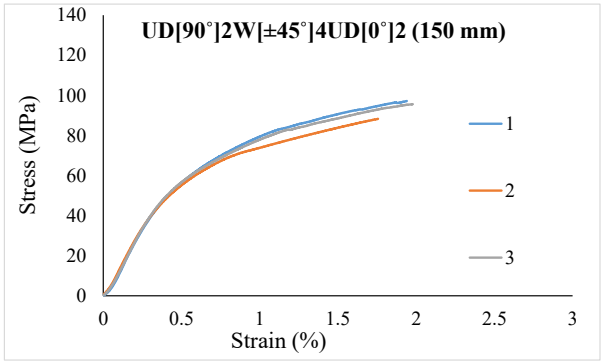

8 Layers

Figure 4-25 Stress-Strain Responses of Tested Specimens (Series 4B)

4.8 Series 5

4.9 Series 5A

4.9.1 Coupons

Series 5A included a total of 20 coupons manufactured using 4 or 8 layers of both unidirectional and woven CFRP sheets with the fibers aligned in the 0^0 and $\pm 45^0$ directions (UD[0˚]W[±45˚]). The coupons were tested under uniaxial tension. Five replicates were prepared for each layer configuration in both the X and Y directions. Mode of failure and post failure photos of the coupons can be seen in **Figure 4-26 .** Results of the peak stress and peak strain as well as the failure nomenclature of the coupons are presented in **Table 4-16.**

4.9.1.1 Mode of Failure

All of the coupons showed ductile failure disregarding the number of layers. The mode of failure of each coupon in accordance to the ASTM D3039/D3039M (2015) specification is tabulated in **Table 4-16**. Two failure modes types were observed in most specimens due to the combination of 0 and 45 degree fibers, where lateral failures (LGM) combined with delamination (DGM) were observed in the middle gage regions (see **Figure 4-26**).

4 layers (X direction)

4 layers (Y direction)

8 layers (X direction)

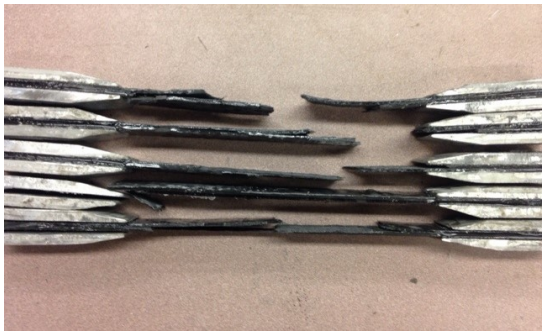

8 layers (Y direction)

Figure 4-26 Final failure modes of CFRP coupons (Series 5A)

Table 4-16 CFRP coupon properties and failure mode (Series 5A)

Series	Specimen	Thickness (mm)	Width (mm)	Area (mm²)	Properties at peak				E (GPa)	Failure Mode
					Load (KN)	Stress (MPa)	Strain	e_{cu}		
$UD[0^\circ]_2W[\pm45^\circ]_2$ X direction	1	2.44	25.08	61.19	32.30	528.47	0.0137	3.67	38.57	LGM,DGM
	2	2.58	25.18	64.96	28.16	433.97	0.0100	2.33	43.40	LGM,DGM
	3	2.56	25.11	64.28	30.53	475.00	0.0141	3.17	33.69	LGM,DGM
	4	2.42	25.18	60.94	30.17	494.40	0.0104	2.82	47.53	LGM,DGM
	5	2.64	25.10	66.26	33.73	509.74	0.0134	3.52	38.04	LGM,DGM
	AVG	**2.53**	**25.13**	**63.53**	**30.98**	**488.31**	**0.0123**	**3.10**	**40.25**	
$UD[0^\circ]_2W[\pm45^\circ]_2$ Y direction	1	2.14	24.96	53.41	4.32	80.99	0.0156	0.81	5.19	LGM,DGM
	3	2.48	24.93	61.83	4.87	78.76	0.0236	1.36	3.34	LGM,DGM
	4	2.54	24.94	63.35	4.41	69.61	0.0219	1.03	3.18	LGM,DGM
	5	2.32	24.92	57.81	4.42	76.44	0.0176	0.88	4.34	LGM,DGM
	AVG	**2.37**	**24.94**	**59.11**	**4.50**	**76.45**	**0.0197**	**1.02**	**4.01**	
$UD[0^\circ]_4W[\pm45^\circ]_4$ X direction	1	4.17	25.12	104.75	49.71	474.62	0.0113	2.53	42.00	LGM,DGM
	2	4.07	25.15	102.36	64.72	631.67	0.0144	4.43	43.86	LGM,DGM
	3	4.26	25.30	107.78	60.63	562.54	0.0135	3.48	41.67	LGM,DGM
	4	4.01	25.16	100.89	50.75	502.53	0.0118	2.83	42.59	LGM,DGM
	5	4.11	25.16	103.41	66.24	639.88	0.0166	4.89	38.55	LGM,DGM
	AVG	**4.13**	**25.18**	**103.84**	**58.41**	**562.25**	**0.0135**	**3.63**	**41.73**	
$UD[0^\circ]_4W[\pm45^\circ]_4$ Y direction	1	4.21	25.16	105.92	7.95	75.90	0.0143	0.69	5.31	LGM,DGM
	2	4.12	25.21	103.86	7.81	76.23	0.0144	0.67	5.29	LGM,DGM
	3	4.42	25.24	111.56	8.06	74.78	0.0140	0.63	5.34	LGM,DGM
	4	4.00	25.06	100.24	7.40	73.27	0.0113	0.47	6.48	LGM,DGM
	5	4.20	25.10	105.42	7.89	76.22	0.0131	0.58	5.82	LGM,DGM
	AVG	**4.19**	**25.15**	**105.40**	**7.82**	**75.28**	**0.0134**	**0.61**	**5.65**	

4.9.1.2 Stress-Strain behavior

In general most coupons showed non-linear behavior, although this is more obvious in the Y direction coupons (see **Figure 4-27**). It can be seen that, coupons with more CFRP layers displayed more uniform results. A summary of the test results which consists of the maximum stress and strain as well as the calculated maximum modulus of elasticity for each coupon is presented in **Table 4-16.** Based on the average test results of the 3 best specimens in the series, maximum load, stress, strain gradually increased by adding more layers of CFRP sheets while

small changes were observed in energy absorption capacity and modulus of elasticity of the same coupons. Load, stress, strain, energy absorption capacity, and modulus of elasticity values of (30.98, 488.31, 0.0123, 3.10, and 40.25), and (58.41, 562.25, 0.0135, 3.63, and 41.73) were found for coupons with 4 and 8 layers of CFRP sheets, respectively. The stress-strain behavior of CFRP coupons in both the X and Y directions are presented in **Figure 4-28.** Coupons that were cut in the X direction showed larger maximum stress. X direction coupons showed lower maximum strains at 4 layers of CFRP sheets, while no difference is observed at 8 layers.

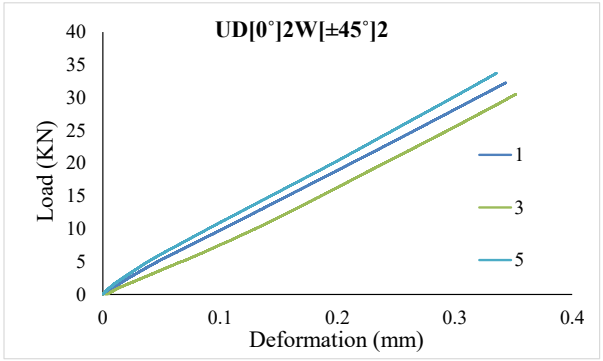

4 layers (X direction)

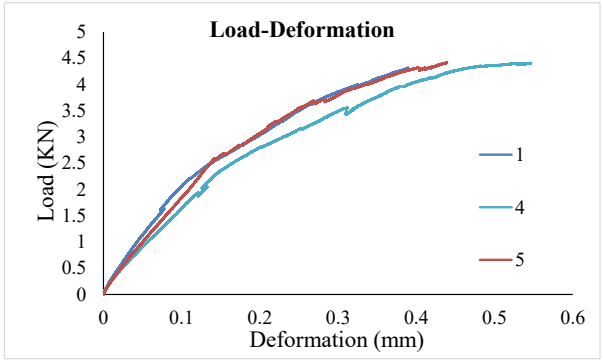

4 layers (Y direction)

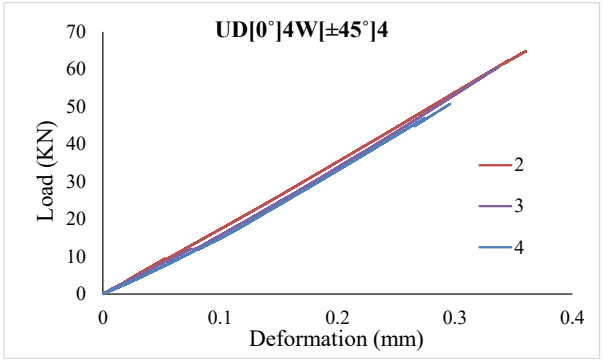

8 layers (X direction)

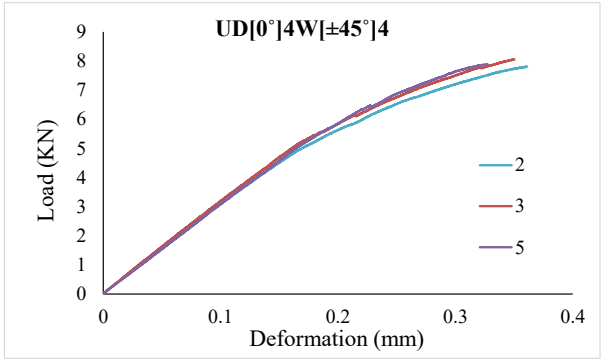

8 layers (Y direction)

Figure 4-27 Load-deformation curves of CFRP coupons (Series 5A)

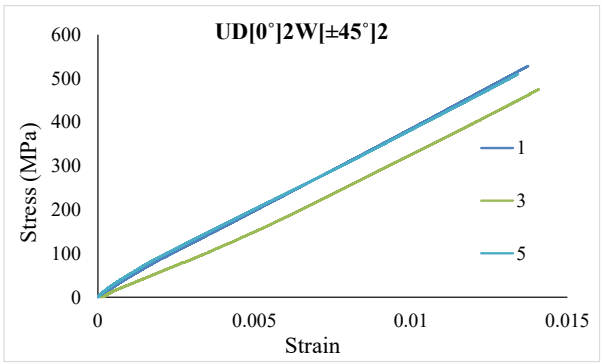

4 layers (X direction)

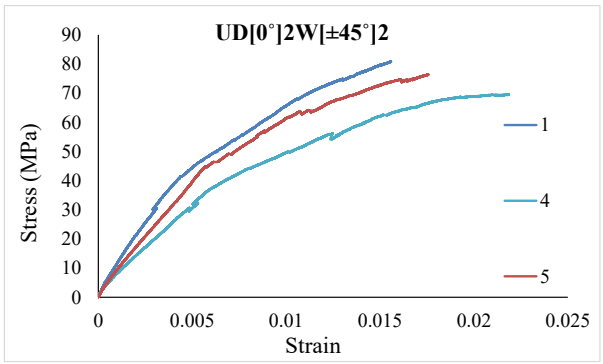

4 layers (Y direction)

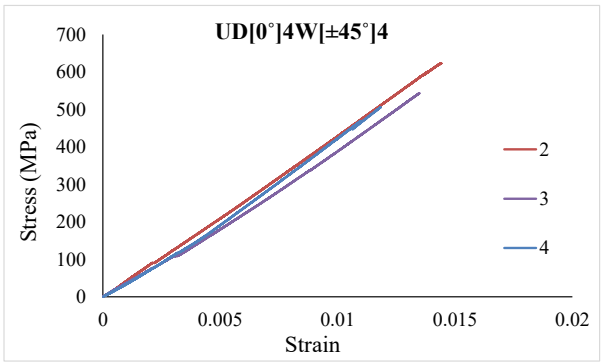

8 layers (X direction)

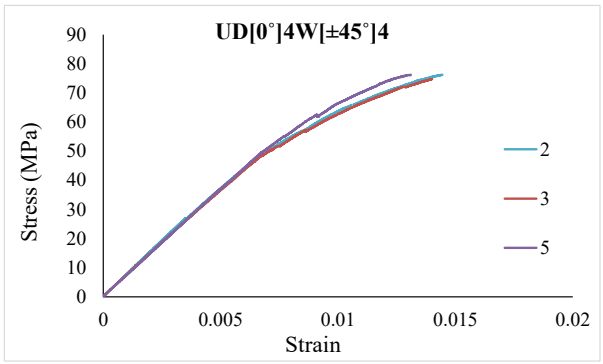

8 layers (Y direction)

Figure 4-28 Stress-strain curves of CFRP coupons (Series 5A)

4.9.2 Cylinders

The specimens in this series were wrapped with unidirectional and woven CFRP sheets that have fibers aligned in both the 0° and ±45° directions as described in chapter 3. The concrete cylinders were confined with either 4 or 8 layers of CFRP sheets. Four replicates were tested for each "small" cylinder configuration, while three replicates were tested for each "large" cylinder configuration. The stress-strain curves of all tested specimens for both sizes are presented in **Figure 4-30**. The peak stress and peak strain of the tested specimens in *Series 5A* are summarized in **Table 4-17** and **Table 4-18**.

4.9.2.1 Mode of Failure

Figure 4-29 presents the failure modes of both small and big specimens with different amounts of confinement layers. Confined concrete cylinders with 4 layers of CFRP sheets experienced more damage compared to those with 8 layers, regardless of the specimen size.

High speed video shows rupture of the jackets started at around the mid height of the cylinders with a tendency to then extend to the upper third of the specimens. After the vertical rupture ended, the failure began to stretch horizontally, with final rupture of the jacket in a "wing" type pattern. The observed failure was sudden and catastrophic. A small noise was heard prior to the final jacket failure followed by a huge noise upon jacket rupture. No delamination occurred except at localized regions which indicate that the bond remained intact between different CFRP types. No clear shear cracking was found in the concrete of the failed specimens. The cone was however observed in some specimens, and this was more obvious in the specimens with a smaller number of CFRP layers (see **Figure 4-29**). In the case of small specimens, roughly about 5% of the crushed concrete got out of the jacket in specimens confined with more CFRP layers, while this percentage reached 10% in specimens with less CFRP layers. The failures were more severe for larger specimens with 4 layers of CFRP with complete disintegration of concrete at failure in some samples (see **Figure 4-29**).

4 layers (100mm)

8 Layers (100mm)

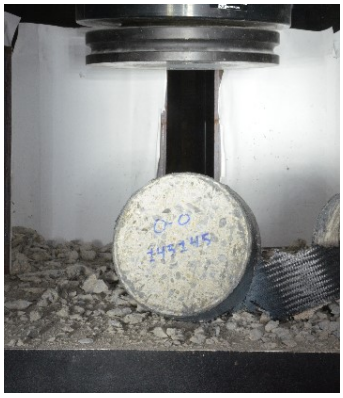

4 Layers (150mm)

8 Layers (150mm)

Figure 4-29 Final Failure Mode of CFRP Confined Concrete Cylinders (Series 5A)

4.9.2.2 Stress-Strain Behavior

The stress-strain performance of the tested CFRP-confined concrete cylinders in Series 5A is shown in **Figure 4-30**. A summary of the results which consist of peak stress (f_{cc}') and peak strain (ε_{cc}') are tabulated in **Table 4-17** and **Table 4-18**, for the 100 mm and 150 mm specimens, respectively. An increase in both stress and strain of CFRP confined concrete cylinders is evident. The "small" cylinders displayed an average increase in stress (f_{cc}/f_{co}) of approximately 2.82 and 4.16 for specimens confined with 4 and 8 layers of CFRP, respectively. The average increase in strain ($\varepsilon_{cc}/\varepsilon_{co}$) was found to be roughly 14.80 and 19.58 for specimens confined

with 4 and 8 layers of CFRP, respectively. Both stress and strain were increased by adding more layers of CFRP sheets, however the relative increase in stress and strain was more pronounced for the first 4 layers of confinement.

Similarly both stress and strain of the "large" size specimens were increased by adding more layers of CFRP sheets. However, the values were different than those obtained from “small” size specimens. For example, values of 2.28 and 3.46 were obtained for the average increase in stress, while values of 24.05 and 12.23 were found in the case of average increase in strain for specimens confined with 4 and 8 layers of CFRP sheets, respectively.

Overall, more uniform results were obtained from specimens confined with a higher number of CFRP layers.

Table 4-17 Experimental Results 100 mm Specimens

Specimen	# of Layer	Specimen Size (mm)	(f_{cc}') (MPa)	(f_{cc}/f_{co})	(ε_{cc}')	$(\varepsilon_{cc}/\varepsilon_{co})$
1	4	100	121.98	2.83	0.0392	13.13
2	4	100	122.47	2.85	0.0402	13.44
3	4	100	117.72	2.73	0.0361	12.08
4	4	100	123.54	2.87	0.0614	20.55
AVG.	**4**	**100**	**121.43**	**2.82**	**0.0442**	**14.80**
1	8	100	177.06	4.11	0.0536	17.94
2	8	100	169.48	3.94	0.0595	19.90
3	8	100	174.57	4.06	0.0627	20.98
4	8	100	194.50	4.52	0.0583	19.51
AVG.	**8**	**100**	**178.90**	**4.16**	**0.0585**	**19.58**

Table 4-18 Experimental Results 150 mm Specimens

Specimen	# of Layer	Specimen Size (mm)	(f_{cc}') (MPa)	(f_{cc}/f_{co})	(ε_{cc}')	$(\varepsilon_{cc}/\varepsilon_{co})$
1	4	150	98.49	2.31	0.0772	25.84
2	4	150	95.99	2.53	0.0665	22.27
AVG.	**4**	**150**	**97.24**	**2.28**	**0.0719**	**24.05**
1	8	150	141.32	3.32	0.0355	11.88
2	8	150	151.05	3.55	0.0370	12.37
3	8	150	149.98	3.52	0.0372	12.44
AVG.	**8**	**150**	**147.45**	**3.46**	**0.0365**	**12.23**

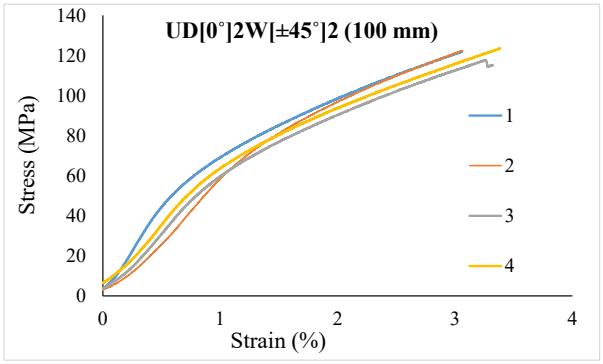

4 Layers

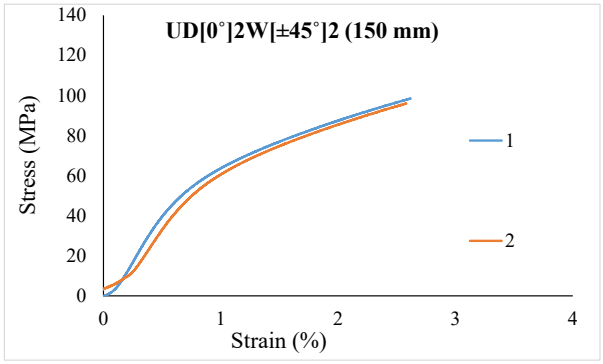

8 Layers

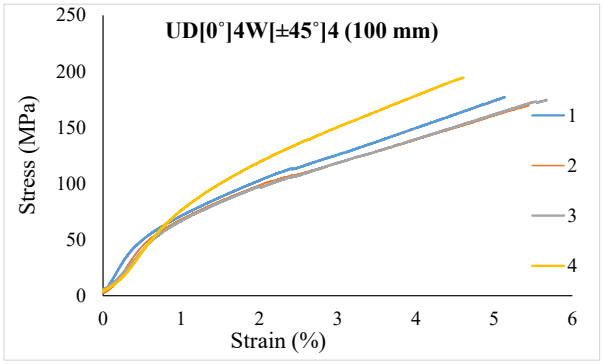

8 Layers

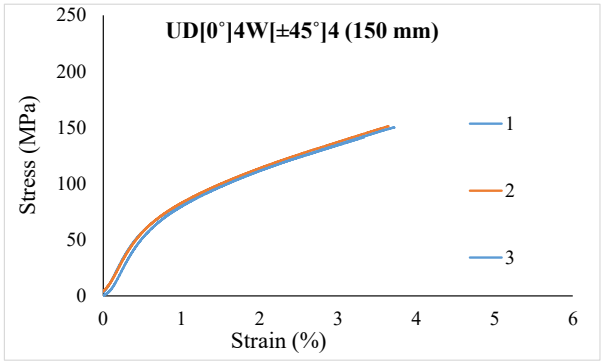

8 Layers

Figure 4-30 Stress-Strain Responses of Tested Specimens (Series 5A)

4.10 Series 5B

4.10.1 Coupons

No coupons were tested for this series as it was assumed behavior would correspond to the behavior observed in Series 5A.

4.10.2 Cylinders

The specimens in this series were wrapped with woven and unidirectional CFRP sheets that have fibers aligned in both the ±45° and 0° directions as described in chapter 3. Concrete cylinders were confined with either 4 or 8 layers of CFRP sheets. Four replicates were tested for each "small" cylinder configuration, while three replicates were tested for each "large" cylinder configuration. The stress-strain curves of all tested specimens for both sizes are presented in **Figure 4-31**. The peak stress and peak strain of the tested specimens in *Series 5B* are summarized in **Table 4-19** and **Table 4-20**.

4.10.2.1 Mode of failure

Figure 4-31 presents the failure mode of both “small” and “large” size specimens. The failure was initiated by opening of the jacket in a wing type pattern with fiber rupture in the hoop direction at the mid-height. The failure was very sudden. De-bonding between the unidirectional and woven CFRP sheets occurred. High speed video shows delamination of CFRP sheets started right after wing development and opening of the jacket, which took place in an accelerated pace with a large peeling noise. After the peeling, the wings stopped opening and the cylinders failed. In almost all of the specimens in this series, no concrete fragments were released and no fracture was detected in the inner layers (woven CFRP layers). It was found that the final failure fracture of the jacket occurred in the hoop direction fibers at mid height due to hoop tension failure. In

the specimens inspection it was found that woven CFRP sheets (inner sheets) remained in place as if nothing had happened.

4 layers (100mm)

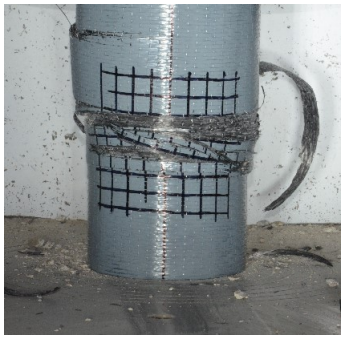

8 Layers (100mm)

4 Layers (150 mm)

8 Layers (150 mm)

Figure 4-31 Final failure modes of CFRP confined concrete cylinders (Series 5B)

4.10.2.2 Stress-Strain Behavior

The stress-strain performance of the CFRP-confined concrete cylinders in Series 5B is shown in **Figure 4-32**. A summary of the results which consist of peak stress (f_{cc}') and peak strain (ε_{cc}') are tabulated in **Table 4-19** and **Table 4-20**, for the 100 mm and 150 mm specimens, respectively. A significant increase in both stress and strain of CFRP confined concrete cylinders is evident. The "small" cylinders displayed an average increase in stress (f_{cc}/f_{co}) of

approximately 2.42 and 3.80 for specimens confined with 4 and 8 layers of CFRP, respectively. The average increase in strain ($\varepsilon_{cc}/\varepsilon_{co}$) was found to be 10.03 and 20.76 for specimens confined with 4 and 8 layers of CFRP, respectively. Both stress and strain were increased by adding more layers of CFRP sheets, however the relative increase in stress and strain was more pronounced for the first 4 layers of confinement.

Similarly both stress and strain of the "large" size specimens were increased by adding more layers of CFRP sheets. However, the values were different than those obtained from “small” size specimens. For example, values of 1.90 and 3.27 were obtained for the average increase in stress, while values of 7.64 and 12.83 were found in the case of average increase in strain for specimens confined with 4 and 8 layers of CFRP sheets, respectively.

Table 4-19 Experimental Results 100 mm Specimens (5B)

Specimen	# of Layer	Specimen Size (mm)	(f_{cc}') (MPa)	(f_{cc}/f_{co})	(ε_{cc}')	$(\varepsilon_{cc}/\varepsilon_{co})$
1	4	100	106.20	2.47	0.0291	9.73
2	4	100	103.41	2.40	0.0269	9.01
3	4	100	107.87	2.51	0.0299	10.02
4	4	100	98.96	2.30	0.0340	11.40
AVG.	**4**	**100**	**104.12**	**2.42**	**0.0300**	**10.03**
1	8	100	170.76	3.97	0.0496	16.60
2	8	100	150.02	3.49	0.0573	19.17
3	8	100	158.89	3.69	0.0498	16.67
4	8	100	174.22	4.05	0.0915	30.61
AVG.	**8**	**100**	**163.47**	**3.80**	**0.0620**	**20.76**

Table 4-20 Experimental Results 150 mm Specimens (5B)

Specimen	# of Layer	Specimen Size (mm)	(f_{cc}') (MPa)	(f_{cc}/f_{co})	(ε_{cc}')	$(\varepsilon_{cc}/\varepsilon_{co})$
1	4	150	78.21	1.84	0.0211	7.05
2	4	150	78.21	1.84	0.0204	6.82
3	4	150	86.46	2.03	0.0270	9.04
AVG.	**4**	**150**	**80.96**	**1.90**	**0.0228**	**7.64**
1	6	150	140.38	3.29	0.0327	10.94
2	6	150	138.02	3.24	0.0440	14.71
AVG.	**6**	**150**	**139.20**	**3.27**	**0.0383**	**12.83**

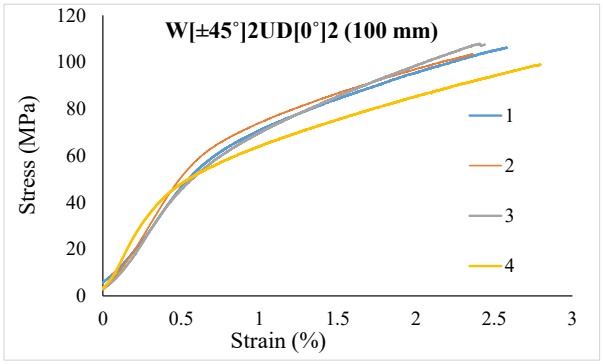

4 Layers

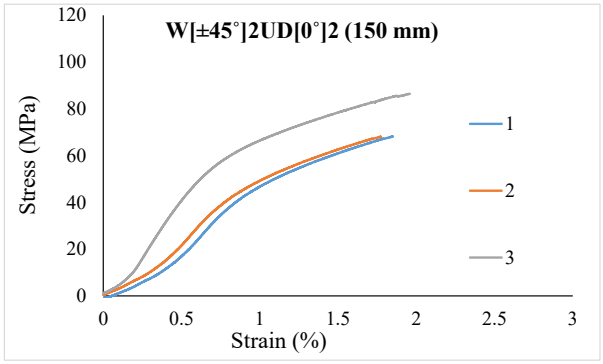

4 Layers

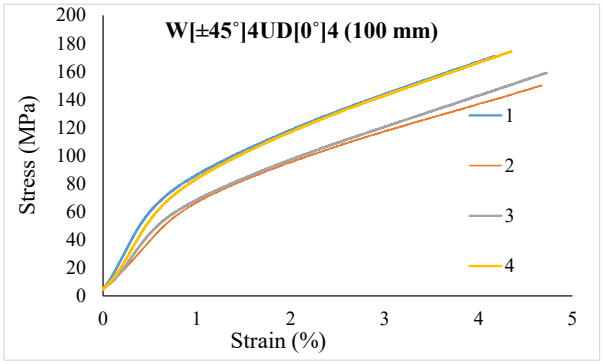

8 Layers

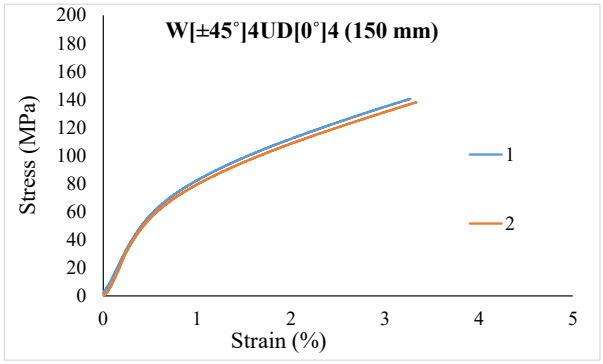

8 Layers

Figure 4-32 Stress-Strain Responses of Tested Specimens (Series 5B)

4.11 Series 6

4.11.1 Coupons

Series 6 included a total of 30 coupons manufactured using 4, 6 or 8 layers of unidirectional CFRP aligned at 90-0^{o} (UD [90-0°]). The specimens were tested under uniaxial tension. Five replicates were produced for each layer configuration in both the X and Y directions. Mode of failure and post failure photos of the coupons can be seen in **Figure 4-33.** Results of peak stress and peak strain as well as failure nomenclature of coupons are presented in **Table** 4-21**.**

4.11.1.1 Mode of Failure

All of the coupons showed brittle rupture disregarding the number of layers. However, a more sudden failure was observed in coupons with more CFRP layers. The modes of failure of each coupon in accordance to the ASTM D3039 (2015) specification are tabulated in **Table 4-21.** Both lateral failures at the edges (LAT) and in the middle (LGM) were observed (see **Figure 4-33**).

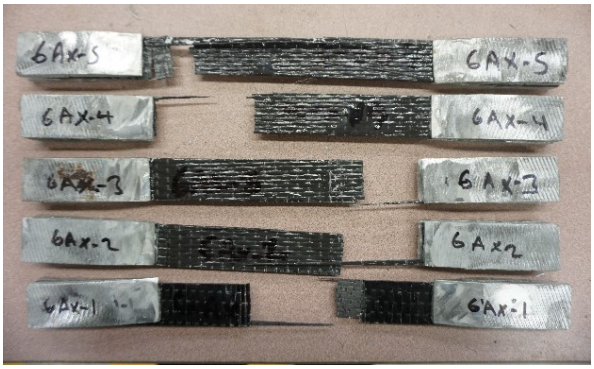

4 layers (X direction)

4 layers (Y direction)

6 layers (X direction)

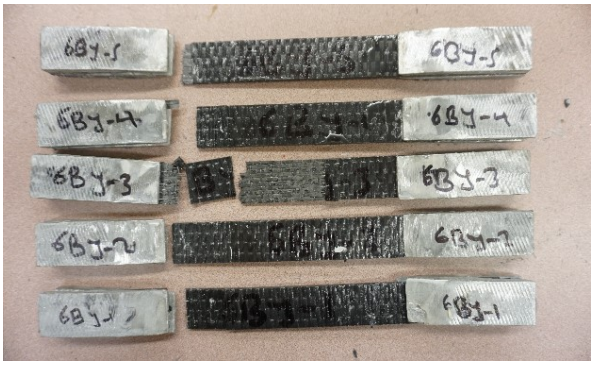

6 layers (Y direction)

8 layers (X direction)

8 layers (Y direction)

Figure 4-33 Final failure modes of CFRP coupons (Series 6)

Table 4-21 CFRP coupon properties and failure mode (Series 6)

Series	Specimen	Thickness (mm)	Width (mm)	Area (mm²)	Properties at peak					
					Load (KN)	Stress (MPa)	Strain	e_{cu}	E (Gpa)	Failure Mode
UD[90°₂/0°₂] X direction	1	2.54	24.85	63.12	27.35	433.25	0.0133	2.94	32.57	LGM
	2	2.54	24.76	62.89	27.10	430.79	0.0128	2.76	33.65	LIT
	3	2.50	25.12	62.80	26.15	416.46	0.0153	3.24	27.22	LIT
	4	2.63	24.66	64.85	25.63	395.68	0.0168	3.56	23.55	LIT
	5	2.41	24.88	59.96	25.89	432.44	0.0128	2.72	33.78	LGM
	AVG	**2.52**	**24.85**	**62.72**	**26.42**	**421.72**	**0.0142**	**3.04**	**30.16**	
UD[90°₂/0°₂] Y direction	1	2.62	25.03	65.58	23.52	358.70	0.0107	1.86	33.52	LIT
	2	2.44	24.96	60.90	26.68	437.54	0.0128	2.81	34.18	LGM
	3	2.31	25.14	58.07	20.98	361.79	0.0108	1.96	34.50	LIT
	4	2.47	25.07	61.02	29.63	477.79	0.0139	3.16	34.37	LIT
	5	2.51	25.32	63.55	28.43	446.69	0.0134	2.98	33.35	LGM
	AVG	**2.47**	**25.10**	**309.12**	**25.85**	**416.50**	**0.0123**	**2.55**	**33.78**	
UD[90°₃/0°₃] X direction	1	3.38	24.97	84.40	40.47	479.51	0.0132	2.88	36.33	LAT
	2	3.28	24.92	81.74	34.27	419.64	0.0110	2.21	38.15	LAT
	3	3.35	24.97	83.65	47.93	573.06	0.0125	3.46	45.84	LAT
	4	3.38	24.96	84.36	37.79	448.38	0.0119	2.63	37.68	LIT
	5	3.31	24.95	82.58	42.53	515.06	0.0124	3.15	41.54	LAT
	AVG	**3.34**	**24.95**	**83.35**	**40.60**	**487.13**	**0.0122**	**2.87**	**39.91**	
UD[90°₃/0°₃] Y direction	1	3.57	24.95	89.07	37.45	420.78	0.0119	2.50	35.36	LIT
	2	3.68	25.15	92.55	47.15	509.51	0.0137	3.30	37.19	LIT
	3	3.62	25.08	90.79	51.16	563.43	0.0151	4.25	37.31	LAT
	4	3.55	24.96	88.61	35.96	406.16	0.0118	3.19	34.42	LIT
	5	3.75	25.10	94.12	46.27	491.51	0.0139	3.50	35.36	LIT
	AVG	**3.63**	**25.05**	**91.03**	**43.60**	**478.28**	**0.0133**	**3.35**	**35.93**	
UD[90°₄/0°₄] X direction	1	4.60	24.93	114.68	55.15	480.85	0.0126	2.82	38.16	LIT
	2	4.63	24.87	115.15	58.56	508.26	0.0121	2.90	42.00	LGM,SGM
	3	4.43	24.93	110.44	49.00	443.29	0.0114	2.62	38.88	LGM,SGM
	4	4.47	25.10	112.20	62.38	556.40	0.0096	2.63	57.96	LGM,SGM
	5	4.47	25.00	111.75	56.23	503.55	0.0118	2.84	42.67	LGM,SGM
	AVG	**4.52**	**24.97**	**112.84**	**56.26**	**498.47**	**0.0115**	**2.76**	**43.94**	
UD[90°₄/0°₄] Y direction	1	4.00	24.97	99.88	50.47	505.37	0.0115	2.72	43.94	LGM,SGM
	2	4.10	24.93	102.21	50.59	494.88	0.0113	2.86	43.79	LGM
	3	4.23	25.03	105.88	50.11	472.85	0.0097	2.24	48.75	LGM,SGM
	4	4.30	25.03	107.63	59.58	553.49	0.0134	3.70	41.30	LGM
	5	4.40	24.90	109.56	64.08	584.88	0.0156	4.40	37.49	LGM,SGM
	AVG	**4.21**	**24.97**	**105.12**	**54.97**	**522.30**	**0.0123**	**3.18**	**43.05**	

4.11.1.2 Stress-Strain behavior

A linear-elastic behavior up to the rupture, regardless the number of layers and cutting direction is seen in the load-deformation graphs shown **Figure 4-34**. The stress-strain behavior of CFRP coupons in both the X and Y directions are presented in **Figure 4-35.** . It is clear from **Figure 4-34** and **Figure 4-35** that coupons with more layers of CFRP displayed the more uniform results compared to those with fewer sheets. Based on the average test results of the 3 best specimens in the series, the load and stress were found to gradually increase by adding more layers of CFRP sheets, while the strain of the same specimens showed opposite behavior. For example, the load and stress were increased from 26.42 KN to 56.26 and from 421.72 to 498.47 MPa by increasing the number of layers from 4 to 8 layers, respectively. Energy absorption capacity showed decrease as the number of CFRP sheets increased with values of 3.04, 2.87, and 2.76 for coupons with 4, 6, and 8 layers of CFRP sheets, respectively. Modulus of elasticity increased from 30.16 GPa to 43.93 GPa as number of layers increased from 4 to 8 layers. Coupons in the X direction showed larger maximum stress compared to those in the Y direction up to 6 layers of CFRP sheets, while the behavior changed for coupons with 8 layers of CFRP. However, in most of cases the Y direction coupons displayed larger failure strains compared to those in the X direction. For instance, the average stress with 4 layers is of 421.72 MPa which is 1.24% lower than for the Y direction coupons. However, the average strain in the Y direction coupons with 6 layers of CFRP is 0.0133 which is 8% higher than for the X direction coupons.

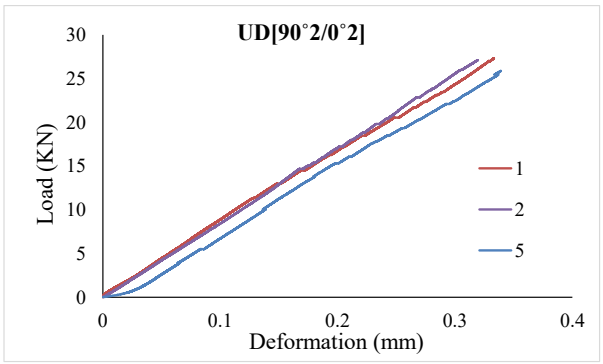

4 layers (X direction)

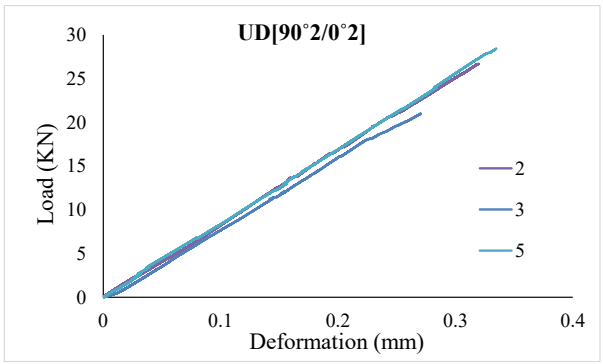

4 layers (Y direction)

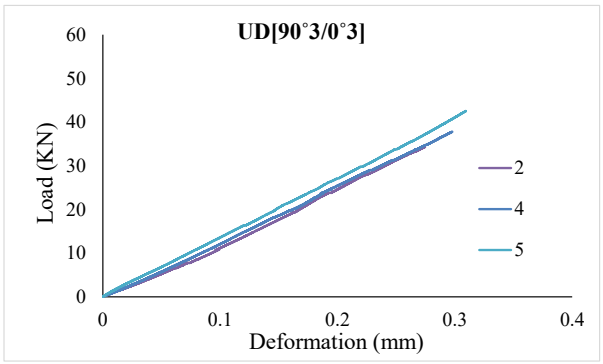

6 layers (X direction)

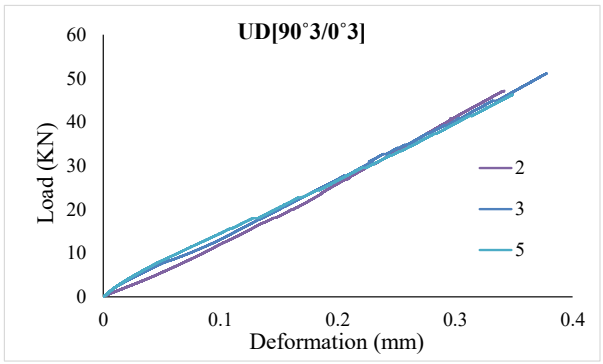

6 layers (Y direction)

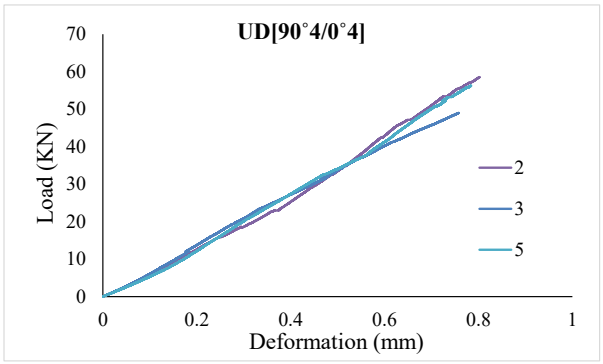

8 layers (X direction)

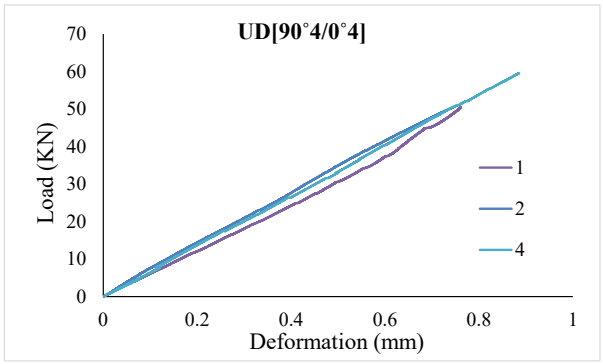

8 layers (Y direction)

Figure 4-34 Load-deformation curves of CFRP coupons (Series 6)

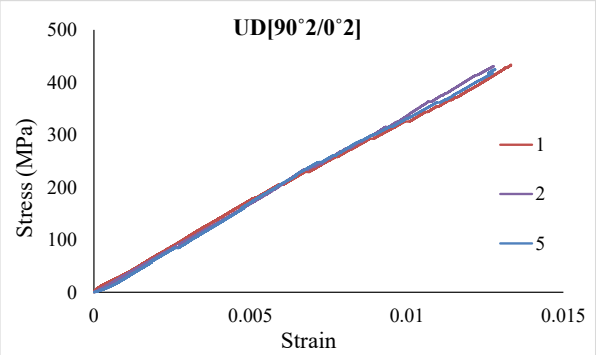

4 layers (X direction)

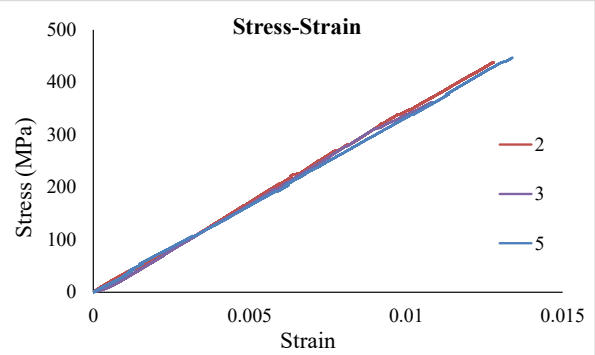

4 layers (Y direction)

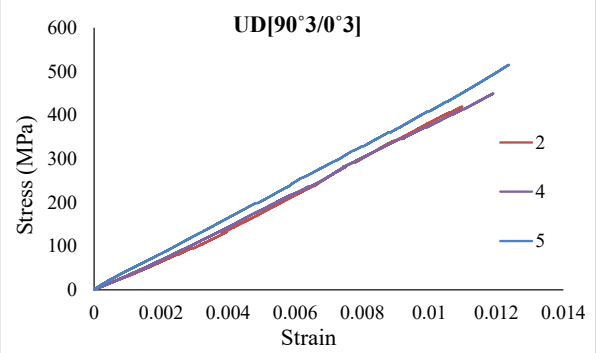

6 layers (X direction)

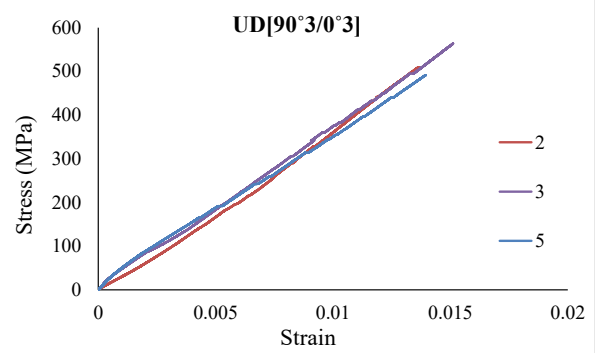

6layers (Y direction)

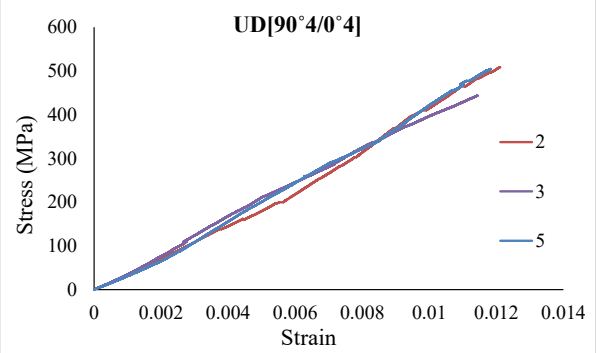

8 layers (X direction)

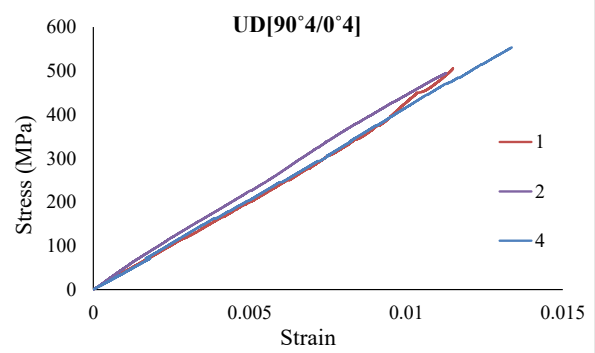

8 layers (Y direction)

Figure 4-35 Stress-strain curves of CFRP coupons (Series 6)

4.11.2 Cylinders

The specimens in this series were wrapped with unidirectional CFRP sheets that have fibers aligned in both the 0^o and 90^o directions as described in chapter 3. Five replicates were tested for each "small" cylinder configuration, while three replicates were tested for each "large" cylinder configuration. The stress-strain curves of all of the tested specimens for both sizes are presented in **Figure 4-37**. The peak stress and peak strain of the tested specimens in *Series 6* are summarized in **Table 4-22** and **Table 4-23**.

4.11.2.1 Mode of Failure

Prior to the final failure, jacket rupture occurred in the hoop direction followed softening of response as load increased until final failure. Rupture of the jacket occurred in both the 90^o and 0^o directions. Failure was initiated by the bulging of the jacket in the 90^o direction followed by a wrinkling of the jacket producing large tensile strains in the hoop direction (0^0) fibers. Final fracture of the jacket occurred in the hoop direction followed by rupture in the longitudinal direction (90^0) fibers. Small fragments of concrete were released from the jacket at rupture. The amount of spalled concrete was less than that of series 2. Failure mode and post-test photos of all tested specimens in this series can be found in **Figure 4-36**. Damage of the concrete core and the CFRP jacket was more pronounced in specimens with less layers regardless of the specimen size. After inspection, cone and shear failures occurred in the concrete core of most specimens.

4 layers (100mm) 6 Layers (100mm) 8 Layers (100mm)

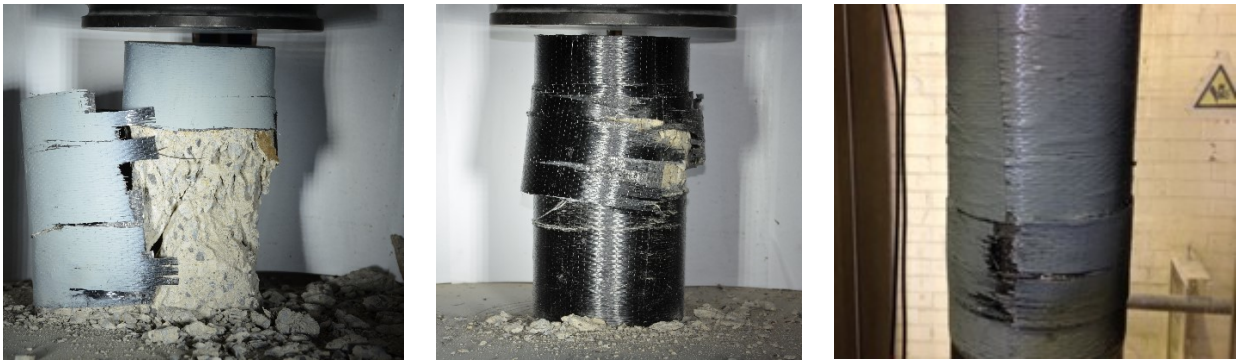

4 Layers (150mm) 6 Layers (150mm) 8 Layers (150mm)

Figure 4-36 Final failure modes of CFRP confined concrete cylinders (Series 6)

4.11.2.2 Stress-Strain Behavior

The stress-strain behavior of the CFRP-confined concrete cylinders in Series 6 is shown in **Figure 4-41**. A summary of the results which consists of the peak stress ($f_{cc}{}'$) and peak strain ($\varepsilon_{cc}{}'$) are tabulated in **Table 4-22** and **Table 4-23**, for the 100 mm and 150 mm specimens, respectively. A substantial increase in both stress and strain of CFRP confined concrete cylinders is evident. The "small" cylinders displayed an average increase in stress (f'_{cc}/f_{co}) of roughly 2.45, 2.81, and 3.30 for specimens confined with 4, 6 and 8 layers of CFRP, respectively. The average increase in strain ($\varepsilon'_{cc}/\varepsilon_{co}$) was found to be 11.07, 13.12 and 14.55 for specimens confined with 4, 6 and 8 layers of CFRP, respectively. Both stress and strain increased by adding

more layers of CFRP, however the relative increase was more pronounced for the first 4 layers of confinement.

Similarly, both stress and strain of the "large" size specimens were increased by adding more layers of CFRP sheets. However, the values were different than those obtained from “small” size specimens. For example, values of 1.83, 2.37 and 2.53 were obtained for the average increase in stress, while values of 10.21, 10.51 and 8.01 were found in the case of average increase in strain for specimens confined with 4, 6 and 8 layers of CFRP sheets, respectively.

Overall, more uniform results were obtained from bigger size specimens. The increase in stress and strain were more pronounced in small size specimens as it is apparent from the results presented in both **Table 4-22** and **Table 4-23**.

Table 4-22 Experimental Results 100 mm Specimens (Series 6)

Specimen	# of Layer	Specimen Size (mm)	$(f_{cc}{}')$	(f'_{cc}/f_{co})	(ε'_{cc})	$(\varepsilon'_{cc}/\varepsilon_{co})$
1	4	100	104.70	2.43	0.0324	10.84
2	4	100	100.93	2.34	0.0324	10.84
3	4	100	106.08	2.46	0.0336	11.24
4	4	100	108.75	2.53	0.0341	11.42
5	4	100	106.63	2.48	0.0329	11.00
AVG.	**4**	**100**	**105.42**	**2.45**	**0.0331**	**11.07**
1	6	100	121.65	2.83	0.0347	11.61
2	6	100	122.58	2.85	0.0390	13.04
3	6	100	107.96	2.51	0.0368	12.32
4	6	100	129.78	3.02	0.0468	15.67
5	6	100	122.20	2.84	0.0387	12.94
AVG.	**6**	**100**	**120.83**	**2.81**	**0.0392**	**13.12**
1	8	100	137.60	3.20	0.0470	15.74
2	8	100	141.08	3.28	0.0409	13.67
3	8	100	148.83	3.46	0.0434	14.52
4	8	100	142.87	3.32	0.0403	13.50
5	8	100	139.30	3.24	0.0458	15.32
AVG.	**8**	**100**	**141.94**	**3.30**	**0.0435**	**14.55**

Table 4-23 Experimental Results 150 mm Specimens (Series 6)

Specimen	# of Layer	Specimen Size (mm)	(f'_{cc})	(f'_{cc}/f_{co})	(ε'_{cc})	$(\varepsilon'_{cc}/\varepsilon_{co})$
1	4	150	73.39	1.72	0.0260	8.66
2	4	150	87.95	2.06	0.0400	13.39
3	4	150	72.38	1.70	0.0256	8.58
AVG.	**4**	**150**	**77.91**	**1.83**	**0.0305**	**10.21**
1	6	150	98.73	2.32	0.0301	10.09
2	6	150	100.56	2.36	0.0322	10.78
3	6	150	104.22	2.45	0.0318	10.65
AVG.	**6**	**150**	**101.17**	**2.37**	**0.0314**	**10.51**
1	8	150	109.50	2.57	0.0245	8.19
2	8	150	108.62	2.55	0.0252	8.44
3	8	150	105.32	2.47	0.0221	7.38
AVG.	**8**	**150**	**107.81**	**2.53**	**0.0239**	**8.01**

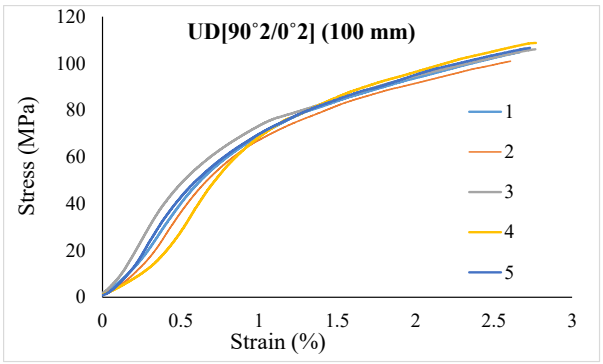

4 Layers

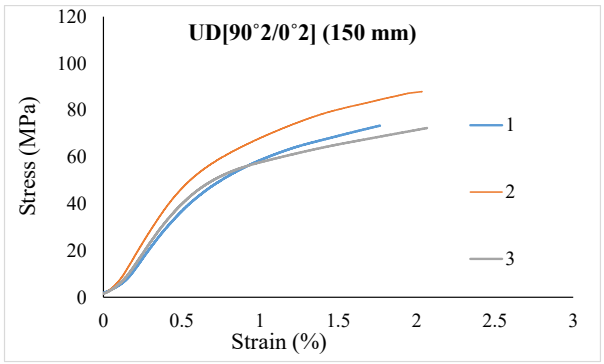

4 Layers

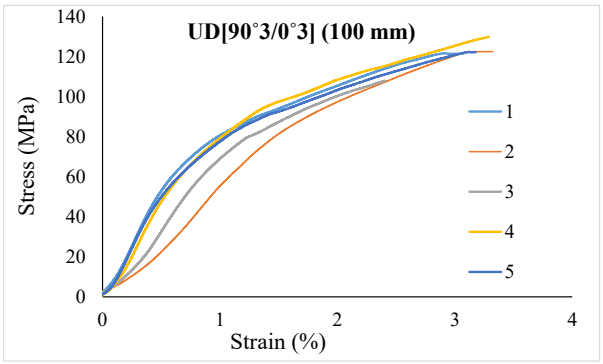

6 Layers

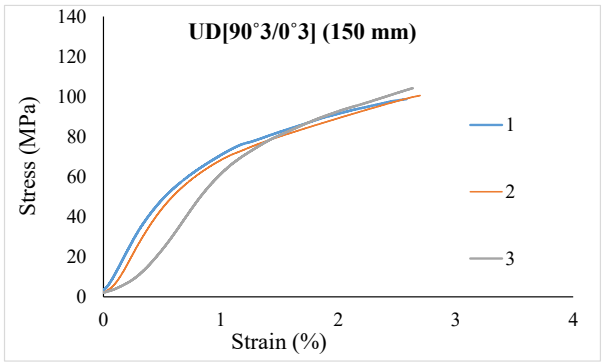

6 Layers

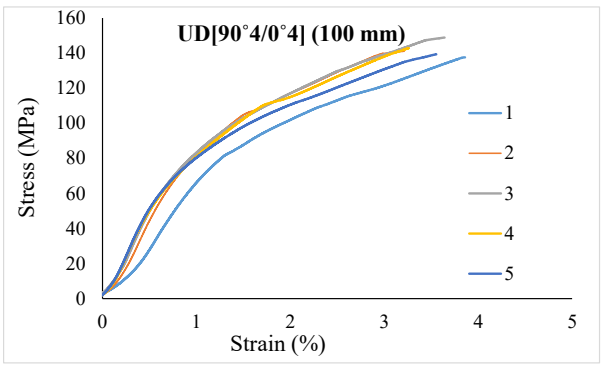

8 Layers

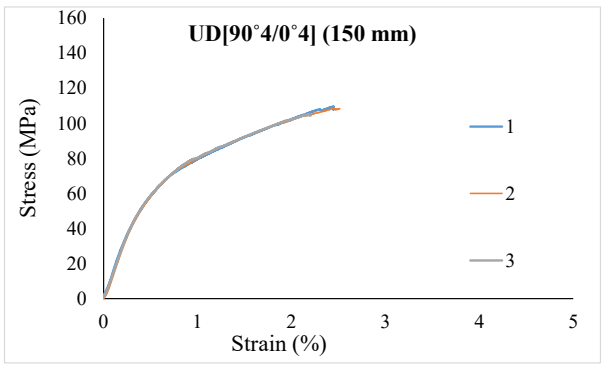

8 Layers

Figure 4-37 Stress-Strain Responses of Tested Specimens (Series 6)

4.12 Series 7

4.12.1 Coupons

Series 7 included a total of 10 coupons manufactured using 4 layers of woven CFRP aligned at ±45° (W $[\pm 45^{\circ}]_4$). The specimens were tested under uniaxial tension. Five replicates were prepared for each layer configuration in both the X and Y directions. Mode of failure and post failure photos of the coupons can be seen in **Figure 4-38.** Results of the peak stress and peak strain as well as the failure nomenclature of coupons are presented in **Table 4-24.** It is worthwhile mentioning that the test results data for two of the coupons in the Y direction were not collected successfully.

4.12.1.1 Mode of Failure

All of the coupons showed very ductile behavior, coupons experiencing very large deformations before final rupture. The modes of failure of each coupon in accordance to the ASTM D3039 (2015) specification are tabulated in **Table 4-24.** A stretching sound in the coupons was heard prior to final rupture. Lateral failures in the middle gage region (LGM) were observed in most specimens (see **Figure 4-38**).

4 layers (X direction) 4 layers (Y direction)

Figure 4-38 Final failure modes of CFRP coupons (Series 7)

Table 4-24 CFRP coupon properties and failure mode (Series 7)

Series	Specimen	Thickness (mm)	Width (mm)	Area (mm²)	Properties at peak					
					Load (KN)	Stress (MPa)	Strain	e_{cu}	E (Gpa)	Failure Mode
UD[90°₂/0°₂] X direction	1	2.21	24.85	54.92	6.35	115.78	0.0521	5.00	2.22	LGM
	2	2.14	24.88	53.24	6.84	128.47	0.0726	7.57	1.77	LGM
	3	2.17	24.80	53.82	7.33	136.20	0.0613	6.42	2.22	LGM
	4	2.12	24.97	52.94	7.19	135.82	0.0697	7.57	1.95	LGM
	5	2.10	25.01	52.52	7.58	144.09	0.0786	8.40	1.83	LGM
	AVG	**2.15**	**24.90**	**53.54**	**7.06**	**132.07**	**0.0669**	**7.01**	**2.00**	
UD[90°₂/0°₂] Y direction	1	2.28	24.87	56.70	6.78	119.57	0.0616	5.53	1.94	LGM
	2	2.19	24.98	54.71	-	-	-	-	-	LGM
	3	2.32	24.97	57.93	-	-	-	-	-	LGM
	4	2.55	25.08	63.95	6.75	105.68	0.0563	4.68	1.88	LGM
	5	2.52	24.90	62.75	7.18	114.26	0.0576	5.12	1.98	LGM
	AVG	**2.37**	**24.96**	**59.15**	**6.90**	**113.17**	**0.0585**	**5.11**	**1.93**	

4.12.1.2 Stress-Strain behavior

Non-linear stress-strain behavior was observed as expected, regardless of the cutting direction, this characteristic is clear in the load-deformation graphs presented in **Figure 4-39**. Coupons with a higher number of CFRP layers displayed more uniform results. The stress-strain behavior of CFRP coupons in both the X and Y directions are presented in **Figure 4-40.** A summary of the test results which consists of the maximum load, stress, strain and the calculated maximum modulus of elasticity of each coupon is presented in **Table 4-24**. Based on the average test results of the 3 best specimens in the series, the stress and strain gradually were increased by adding more layers of CFRP sheets. Slightly higher maximum stress and strain values were recorded for coupons in the X direction. For instance, the average stress and strain are of 132.07 MPa and 0.0669 which is 14% and 12.5% higher than for the X direction coupons, respectively

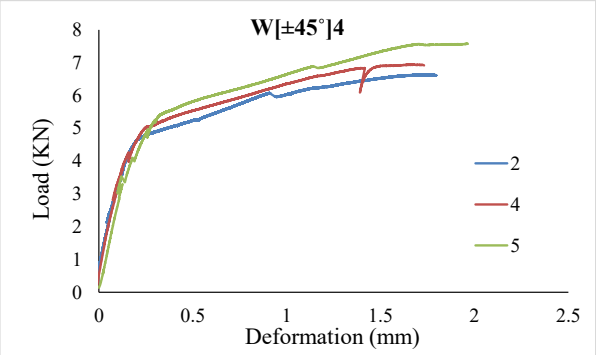

4 layers (X direction)

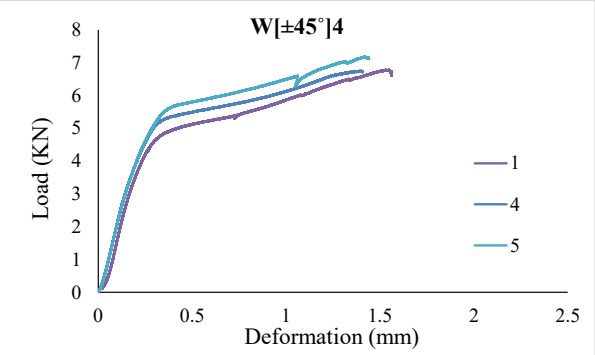

4 layers (Y direction)

Figure 4-39 Load-deformation curves of CFRP coupons (Series 7)

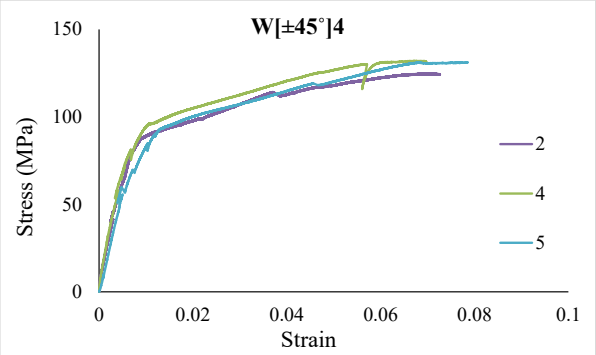

4 layers (X direction)

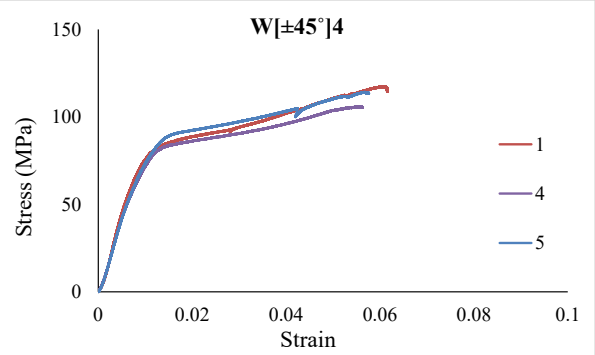

4 layers (Y direction)

Figure 4-40 Stress-strain curves of CFRP coupons (Series 7)

4.12.2 Cylinders

The specimens in this series were wrapped with woven CFRP sheets that have fibers aligned in the ±45° direction as described in chapter 3. Four replicates were tested for each "small" cylinder configuration, while no "large" size cylinders were considered in this series. The stress-strain

curves of all tested specimens are presented in **Figure 4-42**. The peak stress and peak strain of the tested specimens in *Series 7* are summarized in **Table 4-25**.

4.12.2.1 Mode of Failure

The specimens in this series failed in a very ductile manner. No severe fiber fracture was noticed in the plastic deformation stage before final failure. Fiber reorientation at the mid-height was observed in most of the specimens disregarding the number of CFRP layers. After inspection, shear cracks were noticed in the concrete core. It is obvious from **Figure 4-41** that all specimens failed similarly.

High-speed video shows rupture of the jacket started from the bottom in all specimens. The fiber failures were spread in the $+45^0$ direction to about half of the specimen height, then the rupture orientation changed to the vertical direction at mid-height and returned to -45^0. Bulging was observed and no significant concrete fragmentation was observed, indicating that the CFRP jacket allowed for large energy absorption. Concrete cylinders experienced significant shortening in height and swelled in circumference. The absorbed energy was released in a very gentle manner during the final rupture of the jacket at which point a small amount of concrete spalled out of the jacket (with spalling being greater at 8 layers).

4 layers (100mm) 6 Layers (100mm) 8 Layers (100mm)

Figure 4-41 Final Failure Mode of CFRP Confined Concrete Cylinders (Series 7)

4.12.2.2 Stress-Strain Behavior

The stress-strain behavior of the CFRP-confined concrete cylinders in Series 7 is shown in **Figure 4-42**. A summary of the results which consists of the peak stress ($f_{cc}{}'$) and peak strain ($\varepsilon_{cc}{}'$) are tabulated in **Table 4-25** for the 100 mm specimens. A substantial increase in both stress and strain of CFRP confined concrete cylinders is evident. The "small" cylinders displayed an average increase in stress (f'_{cc}/f_{co}) of 1.02, 1.15 and 1.31 for specimens confined with 4, 6 and 8 layers of CFRP, respectively. The average increase in strain ($\varepsilon'_{cc}/\varepsilon_{co}$) was found to be 13.60, 47.81 and 51.71 for specimens confined with 4, 6 and 8 layers of CFRP, respectively. The increase in strain was enhanced by adding more layers of CFRP sheets. Overall, more uniform results were obtained from the specimens with more CFRP layers.

Table 4-25 Experimental Results 100 mm Specimens (Series 7)

Specimen	# of Layer	Specimen Size (mm)	(f_{cc}')	(f'_{cc}/f_{co})	(ε'_{cc})	$(\varepsilon'_{cc}/\varepsilon_{co})$
1	4	100	42.09	0.98	0.0276	9.24
2	4	100	41.52	0.96	0.0389	13.02
3	4	100	48.30	1.12	0.0388	12.98
4	4	100	43.13	1.00	0.0572	19.16
AVG.	**4**	**100**	**43.76**	**1.02**	**0.0406**	**13.60**
1	6	100	46.90	1.09	0.1662	55.62
2	6	100	55.22	1.28	0.1367	45.76
3	6	100	48.63	1.13	0.1434	47.99
4	6	100	46.94	1.09	0.1251	41.88
AVG.	**6**	**100**	**49.2**	**1.15**	**0.1429**	**47.81**
1	8	100	56.94	1.32	0.1665	55.72
2	8	100	62.03	1.44	0.1820	60.91
3	8	100	54.58	1.27	0.1756	58.76
4	8	100	52.34	1.22	0.0940	31.45
AVG.	**8**	**100**	**56.47**	**1.31**	**0.1545**	**51.71**

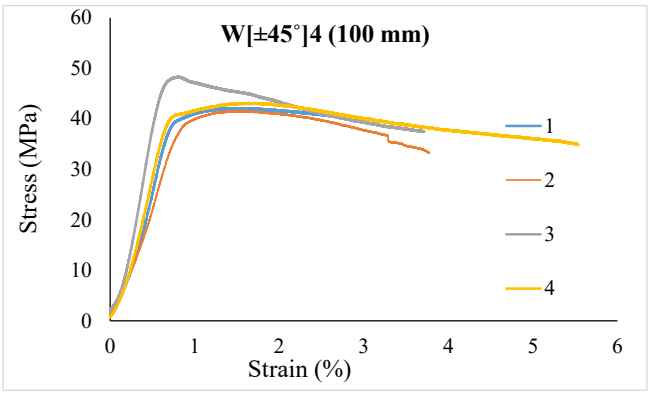

4 Layers

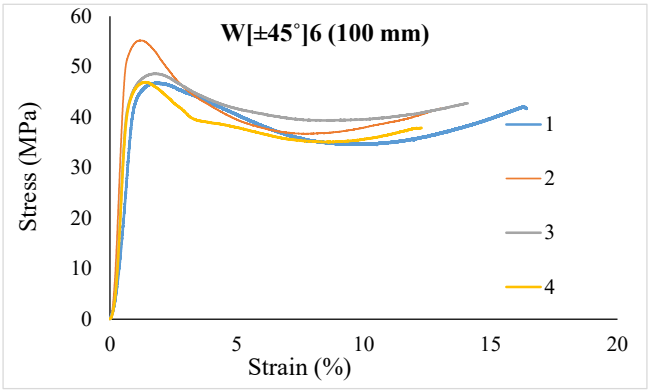

6 Layers

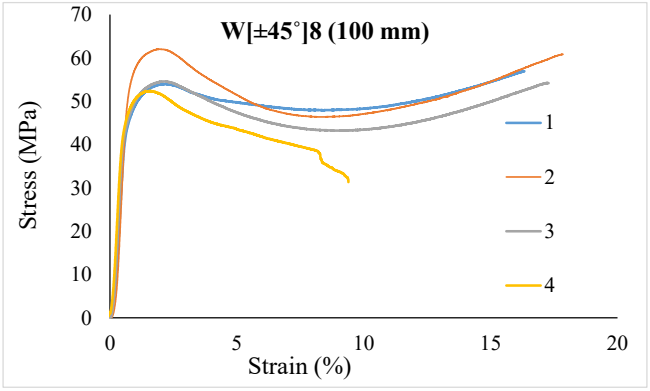

8 Layers

Figure 4-42 Stress-Strain Responses of Tested Specimens (Series 7)

5 Chapter 5: Discussion of Results

5.1 General

In this chapter the stress-strain performance of the CFRP confined concrete cylinders are analyzed to examine the influence of the various parameters considered in the research program which include: number of CFRP layers, specimen size and fiber orientation. The influence of the test parameters on stress-train response is assessed by comparing various quantitative indicators related to strength, ductility and toughness.

5.2 Parameters and Summary of Results

The effect of the test variables on the behavior of the CFRP confined concrete cylinders is examined by comparing the stress-strain response of the specimens. In addition to comparing the relative increase peak stress $\left(\frac{f'_{cc}-f_{co}}{f_{co}}\right)$ and strain $\left(\frac{\varepsilon'_{cc}-\varepsilon_{co}}{\varepsilon_{co}}\right)$, various quantitative indicators related to strength, ductility and toughness as defined by Cui and Sheikh (2010) are also compared. These include: a strength enhancement effectiveness factor (k_1), a ductility factor (μ_{cu}), an energy absorption capacity factor (e_{cu}), and a work index (w_{cu}).

5.2.1 Strength effectiveness factor (k_1)

The strength enhancement factor (k_1) is calculated using the expression shown in **Eq. 5-1** which consists of the ratio of maximum increase in concrete stress and the maximum confining pressure of the FRP jacket.

$$k_1 = (f'_{cc} - f_{co})/f_l \qquad \textbf{Eq. 5-1}$$

Where f'_{cc}= peak confined concrete stress, taken as the greater of f_o (concrete stress at kink point of stress-strain curve) and f_{cu} (ultimate stress); f_l = maximum confining pressure provided by the FRP jacket; where $f_l = 2.f_{FRP}.n_{FRP}/D$ and where n_{FRP} = total thickness of FRP jacket; f_{FRP} = tensile strength of FRP material in fiber direction (with units of MPa), as obtained from the tension coupon tests reported in Chapter 4, and D = diameter of the specimen.

5.2.2 Ductility factor (μcu)

Figure 5-1 shows the ductility factor which is the ratio of the rupture strain and the axial strain corresponding to the maximum confined concrete stress on the initial tangent and is calculated using the expression shown in **Eq. 5-2**:

$$\mu_{cu} = \varepsilon_{cu}/\varepsilon_1 \qquad \textbf{Eq. 5-2}$$

Where ε_{cu}= axial strain corresponding to rupture of the FRP jacket and ε_1 = axial strain corresponding to the maximum confined concrete stress on the initial tangent E_t.

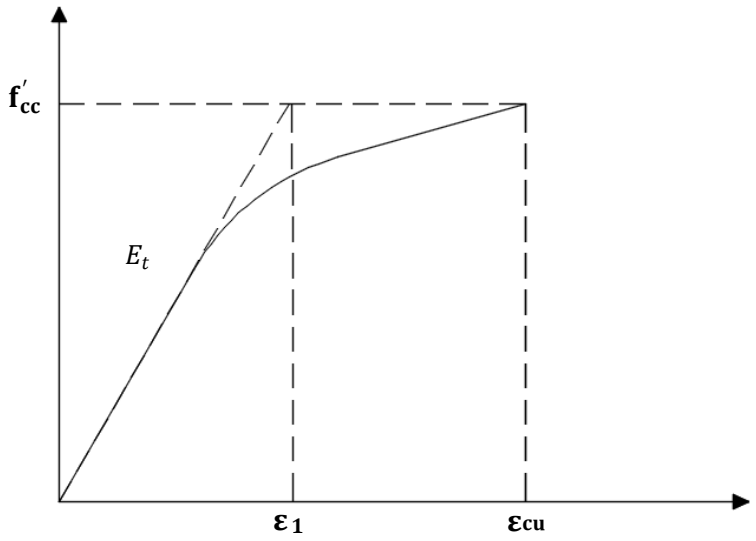

Figure 5-1 Definition of the ductility factor

5.2.3 Energy absorption capacity factor (e_{cu})

Energy absorption capacity is defined as the area under the stress-strain curve up to the rupture of FRP jacket and is graphically presented in **Figure 5-2**.

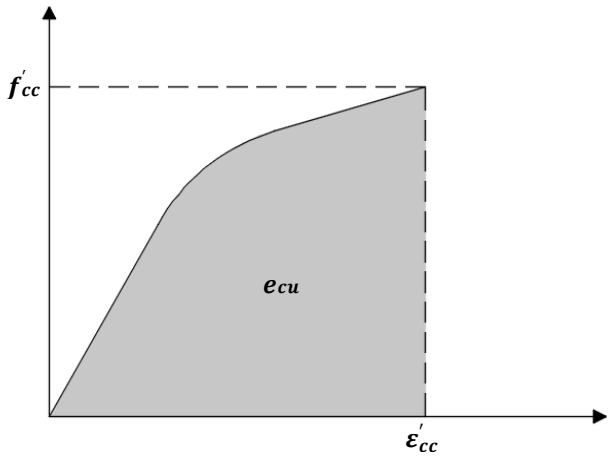

Figure 5-2 Definition of energy absorption capacity

5.2.4 Work index (w_{cu})

The last indicator that is used to evaluate stress-strain response is the Work index, a dimensionless parameter which is calculated by normalizing the energy absorption capacity as shown in **Eq. 5-3**:

$$w_{cu} = e_{cu}/(f'_{cc}\, x\, \varepsilon_1) \qquad \textbf{Eq. 5-3}$$

5.2.5 Summary of results

The summary of the test results including peak stress (f'_{cc}), peak strain (ε'_{cc}), increase in peak stress $\left(\frac{f'_{cc}-f_{co}}{f_{co}}\right)$, increase in peak strain $\left(\frac{\varepsilon'_{cc}-\varepsilon_{co}}{\varepsilon_{co}}\right)$ as well as the various stress-train indicators defined in the previous sections are presented in **Table 5-1**. It is noted that the data presented in **Table 5-1** represents the average results from the various cylinders tested within each series. The effect of the various test parameters are discussed in detail in the sections that follow. The effect of the number of layers and size effect in each series are reviewed in **Sections 5.2** and **5.3**, respectively. The effect of fiber orientation and stacking sequence is discussed in **Section 5.4**.

Table 5-1 Summary of average results

Experiment			%Increase in strength	f_l	$\varepsilon_{cc}{}'$	%Increase in strain	ε_1	k_1	μ_{cu}	e_{cu}	w_{cu}
Orientation	Size (mm)	$f_{cc}{}'$ (MPa)	$\left(\frac{f'_{cc}}{f_{co}}\right)$	(MPa)		$\left(\frac{\varepsilon'_{cc}}{\varepsilon_{co}}\right)$					
UD[0˚]$_4$	100.0	177.9	313.4	46.4	0.052	2043.168	0.018	2.91	2.92	5.96	1.87
UD[0˚]$_6$	100.0	214.8	399.1	57.7	0.062	2447.025	0.028	2.98	2.29	10.40	1.76
UD[0˚]$_8$	100.0	263.7	512.8	68.1	0.062	2427.141	0.460	3.24	2.07	7.59	0.92
UD[0˚]$_4$	150.0	133.3	212.9	30.5	0.030	1139.595	0.013	2.97	2.61	2.69	1.75
UD[0˚]$_6$	150.0	177.7	317.2	38.2	0.046	1769.436	0.013	3.54	3.42	3.73	1.53
UD[0˚]$_8$	150.0	209.0	390.5	45.1	0.054	2098.687	0.017	3.69	3.23	7.08	2.04
UD[90˚/0˚]$_2$	100.0	100.9	134.4	22.2	0.023	836.725	0.013	2.60	1.84	1.98	1.58
UD[90˚/0˚]$_3$	100.0	127.0	195.0	34.0	0.031	1183.874	0.014	2.47	2.29	3.55	2.07
UD[90˚/0˚]$_4$	100.0	148.1	244.1	44.3	0.036	1377.144	0.017	2.37	2.13	4.86	1.95
UD[90˚/0˚]$_2$	150.0	83.7	96.4	14.8	0.021	743.797	0.010	2.77	2.12	2.42	2.95
UD[90˚/0˚]$_3$	150.0	100.5	136.0	22.7	0.023	824.228	0.011	2.56	2.09	3.43	3.06

UD[90˚/0˚]$_4$	150.0	115.4	170.9	29.5	0.026	954.050	0.009	2.47	2.99	2.09	2.11
UD [+45˚/-45˚]$_2$	100.0	52.3	21.5	4.4	0.056	2182.622	0.008	2.08	7.08	2.45	6.04
UD [+45˚/-45˚]$_3$	100.0	63.3	47.0	8.3	0.090	3604.514	0.010	2.45	9.14	5.27	8.28
UD [+45˚/-45˚]$_4$	100.0	73.4	70.5	8.1	0.100	3989.044	0.011	3.74	9.15	6.54	8.03
UD [+45˚/-45˚]$_2$	150.0	44.7	5.0	3.0	0.028	1032.221	0.006	0.73	4.85	1.29	5.10
UD [+45˚/-45˚]$_3$	150.0	54.6	28.1	5.5	0.066	2628.537	0.007	2.17	9.60	3.26	8.50
UD [+45˚/-45˚]$_4$	150.0	62.1	45.8	5.4	0.077	3060.585	0.008	3.60	9.58	4.39	8.72
UD[90˚/0˚]W[±45˚]$_2$	100.0	89.1	107.1	16.6	0.023	859.581	0.011	2.78	2.17	1.43	1.49
UD[90˚/0˚]$_2$W[±45˚]$_4$	100.0	128.8	199.3	30.1	0.035	1316.188	0.005	2.85	8.91	3.04	6.06
UD[90˚/0˚]W[±45˚]$_2$	150.0	71.3	67.3	11.1	0.021	759.800	0.008	2.59	2.50	1.08	1.80
UD[90˚/0˚]$_2$W[±45˚]$_4$	150.0	99.8	134.2	20.1	0.019	694.254	0.009	2.85	2.19	1.32	1.50
UD[90˚]W[±45˚]$_2$UD[0˚]	100.0	81.3	89.0	15.2	0.023	849.477	0.002	2.52	13.07	1.32	9.17
UD[90˚]$_2$W[±45˚]$_4$UD[0˚]	100.0	113.9	164.6	25.0	0.035	1328.344	0.015	2.83	2.45	2.70	1.69
UD[90˚]W[±45˚]$_2$UD[0˚]	150.0	72.5	70.3	10.1	0.024	882.902	0.008	2.96	2.87	1.24	2.05
UD[90˚]$_2$W[±45˚]$_4$UD[0˚]	150.0	93.7	120.0	16.7	0.021	741.679	0.009	3.07	2.36	1.39	1.70
UD[0˚]$_2$W[±45˚]$_2$	100.0	121.4	182.2	25.0	0.044	1714.885	0.017	3.13	2.62	3.75	1.83

$UD[0^\circ]_4W[\pm45^\circ]_4$	100.0	178.9	315.7	46.6	0.059	2300.800	0.022	2.92	2.72	6.74	1.75
$UD[0^\circ]_2W[\pm45^\circ]_2$	150.0	97.2	128.3	16.7	0.072	2849.393	0.013	3.27	5.40	3.57	2.77
$UD[0^\circ]_4W[\pm45^\circ]_4$	150.0	147.5	246.1	31.1	0.037	1399.670	0.013	3.38	2.74	3.60	1.83
$W[\pm45^\circ]_2UD[0^\circ]_2$	100.0	104.1	141.9	25.0	0.030	1130.201	0.011	2.44	2.78	2.13	1.91
$W[\pm45^\circ]_4UD[0^\circ]_4$	100.0	163.5	279.9	46.6	0.062	2445.702	0.017	2.59	3.76	6.22	2.27
$W[\pm45^\circ]_2UD[0^\circ]_2$	150.0	81.0	90.1	16.7	0.023	836.671	0.012	2.30	1.88	1.24	1.25
$W[\pm45^\circ]_4UD[0^\circ]_4$	150.0	139.2	226.8	31.0	0.038	1472.576	0.015	3.11	2.66	3.43	1.73
$UD[90^\circ_2/0^\circ_2]$	100.0	105.4	145.0	24.2	0.033	1257.037	0.013	2.58	2.58	2.48	1.84
$UD[90^\circ_3/0^\circ_3]$	100.0	120.8	180.8	32.5	0.039	1508.248	0.015	2.39	2.79	3.25	1.92
$UD[90^\circ_4/0^\circ_4]$	100.0	141.9	229.8	45.7	0.043	1684.243	0.016	2.17	2.70	4.47	1.96
$UD[90^\circ_2/0^\circ_2]$	150.0	77.9	82.9	16.1	0.031	1152.040	0.009	2.19	3.47	1.55	2.23
$UD[90^\circ_3/0^\circ_3]$	150.0	101.2	137.5	21.7	0.031	1188.378	0.013	2.70	2.58	2.25	1.85
$UD[90^\circ_4/0^\circ_4]$	150.0	107.8	153.1	30.5	0.024	881.775	0.008	2.00	3.10	1.85	2.22
$W[\pm45^\circ]_4$	100.0	43.8	1.7	5.7	0.041	1567.727	0.008	0.13	5.13	1.47	4.22
$W[\pm45^\circ]_6$	100.0	49.4	14.8	8.6	0.143	5762.074	0.009	0.74	16.49	5.56	13.01
$W[\pm45^\circ]_8$	100.0	56.5	31.2	11.5	0.155	6240.224	0.009	1.17	17.38	7.43	14.62

5.3 Effect of the number of layers

The effect of the number of layers on the stress-strain behavior of CFRP confined concrete cylinders tested in this research program is investigated in this section. A total of 9 stacking sequences where considered in this study, and the number of layers varied within each series. The discussion in this section will focus on the 100 mm cylinder specimens.

5.3.1 Series 1 (UD [0˚])

The specimens in Series 1 (UD [0˚]) were confined with 4, 6, and 8 layers of unidirectional CFRP with fibers aligned in the hoop direction. **Figure 5-3** compares the typical stress-strain response of the specimens with 4, 6 and 8 layers in this series (UD $[0^\circ]_4$, UD $[0^\circ]_6$ and UD $[0^\circ]_8$). In all cases, the stress-strain curves show an initially steep parabolic ascending branch followed by a quasi-linear second branch up to failure. **Figure 5-3** demonstrates that the number of CFRP layers has a noticeable influence on stress-strain behavior, with specimens having additional layers exhibiting a larger gain in strength and overall toughness. Cylinders with 4, 6, and 8 plies had average increase in stress (f'_{cc}/f_{co}) of 313%, 399%, and 512%, respectively. The effect of increasing the number of layers is less important in the case of the increase in strain ($\varepsilon'_{cc}/\varepsilon_{co}$) with average values of 2043%, 2447%, and 2427%, for the same set of specimens. It is noted that while there is a significant increase in stress when going from 6 to 8 layers, the strain does not increase with the two additional layers of CFRP. The stress-train behavior can be further investigated by comparing the strength, ductility and toughness parameters defined in **Section 5.2** and reported in **Table 5-2** (the parameters are also compared graphically in **Figure 5-5**).

The number of plies is found to have an insignificant influence on the strength effectiveness factor (k_1) with values of 2.91, 2.98, and 3.24 for cylinders with 4, 6, and 8 layers of CFRP. The result indicates that while overall stress increases with additional layers of FRP, the incremental

increase in stress is not directly proportional to the number of applied layers (i.e. doubling the number of FRP layers does not double the peak confined stress). Examination of the data in **Table 5-2**, shows that the energy absorption capacity (e_{cu}) increases proportionally with the amount of external confinement. Specimens confined with 4, 6, and 8 plies of CFRP had average energy absorption capacity factors of 5.9, 10.4, and 9.7, respectively. It is important to note that energy absorption doubles when going from 4 to 6 layers, whereas no further increase is observed when going to 8 layers of CFRP. The improvement in toughness and ductility due to the increase in CFRP layers is not as obvious when evaluated in terms of work index factor (w_{cu}) or ductility factor (μ_{cu}). Ductility factors (μ_{cu}) of 2.92, 2.29, and 2.07, as well as work index factors (w_{cu}) of 1.87, 1.76 and 1.24 were obtained for specimens confined with 4, 6, and 8 layers of CFRP sheets, respectively. The ductility factor decreases with the increase in the number of layers and this can be explained by the fact that strain ε_1 (0.018 to 0.46) increases proportionally to the number of plies, while the associated increase in maximum strain ε_{cc}' (0.052 to 0.062) is relatively small.

As reported in Chapter 4, all specimens in this series failed in a brittle manner, however the failures were found to be more explosive for cylinders with a greater number of CFRP plies (see **Figure 5-4**).

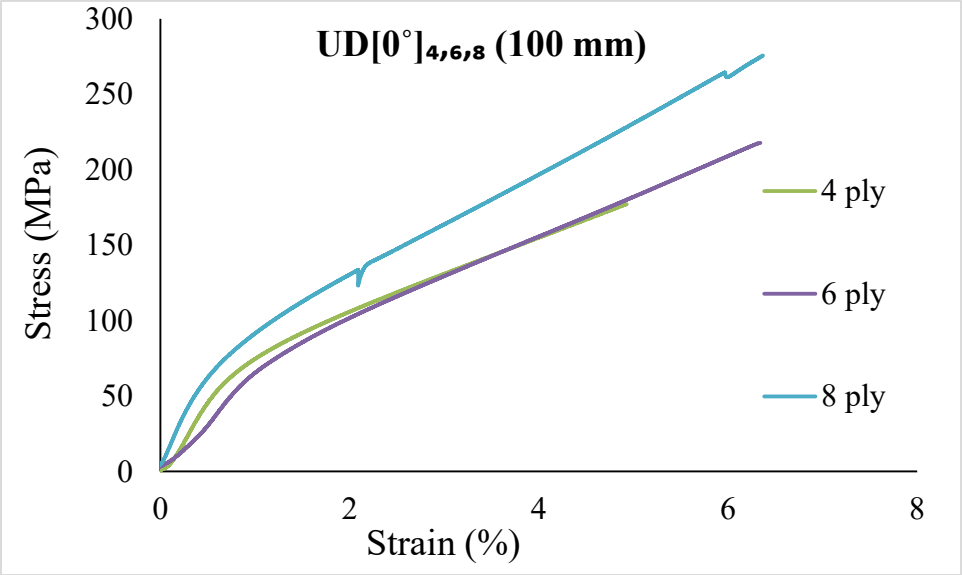

Figure 5-3 Stress-Strain Curves (UD [0˚] 100 mm)

4 layers 6 layers 8 layers

Figure 5-4 Post failure photos of CFRP confined cylinders (series 1 (100 mm))

Table 5-2 Results of specimens tested in series 1

Orientation	Experiment			%Increase in Strength			%Increase in Strain					
	Specimen #	Size(mm)	f_{cc}'	$\left(\frac{f'_{cc}}{f_{co}}\right)$	f_l (MPa)	ε_{cc}'	$\left(\frac{\varepsilon'_{cc}}{\varepsilon_{co}}\right)$	ε_1	k_1	μ_{cu}	e_{cu}	w_{cu}
$UD[0^\circ]_4$	1.0	100.0	180.7	319.9	46.4	0.048	1882.971	0.017	2.97	2.83	5.58	1.81
	2.0	100.0	173.6	303.5	46.4	0.047	1816.496	0.013	2.81	3.62	5.19	2.32
	3.0	100.0	181.9	322.7	46.4	0.053	2084.858	0.020	2.99	2.62	5.98	1.62
	4.0	100.0	175.6	308.1	46.4	0.054	2117.481	0.023	2.86	2.38	5.88	1.47
	5.0	100.0	177.7	312.9	46.4	0.059	2314.034	0.019	2.90	3.14	7.18	2.15
	AVG	**100.0**	**177.9**	**313.4**	**46.4**	**0.052**	**2043.168**	**0.018**	**2.91**	**2.92**	**5.96**	**1.87**
$UD[0^\circ]_6$	1.0	100.0	176.9	311.2	57.7	0.057	2258.022	0.021	2.32	2.74	6.73	1.81
	2.0	100.0	229.6	433.6	57.7	0.069	2723.348	0.034	3.24	2.01	12.15	1.55
	3.0	100.0	218.0	406.5	57.7	0.064	2506.894	0.032	3.03	2.02	10.28	1.50
	4.0	100.0	229.3	432.8	57.7	0.062	2453.549	0.030	3.23	2.09	11.80	1.72
	5.0	100.0	220.0	411.3	57.7	0.058	2293.311	0.023	3.07	2.59	11.02	2.23
	AVG	**100.0**	**214.8**	**399.1**	**57.7**	**0.062**	**2447.025**	**0.028**	**2.98**	**2.29**	**10.40**	**1.76**
$UD[0^\circ]_8$	1.0	100.0	245.0	469.4	68.1	0.067	2639.844	0.026	2.97	2.53	9.67	1.50
	2.0	100.0	257.4	498.0	68.1	0.059	2335.110	0.023	3.15	2.61	9.15	1.56
	3.0	100.0	280.9	552.8	68.1	0.058	2288.844	0.023	3.49	2.54	9.83	1.52
	4.0	100.0	259.4	502.8	68.1	0.060	2357.276	2.205	3.18	0.03	9.32	0.02
	5.0	100.0	275.7	540.7	68.1	0.064	2514.632	0.024	3.42	2.62	0.00	0.00
	AVG	**100.0**	**263.7**	**512.8**	**68.1**	**0.062**	**2427.141**	**0.460**	**3.24**	**2.07**	**7.59**	**0.92**

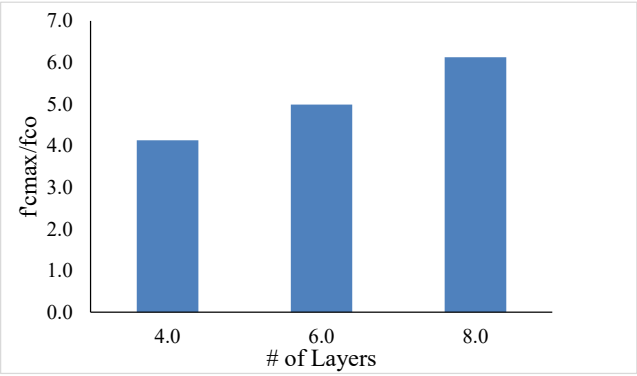

Increase in stress

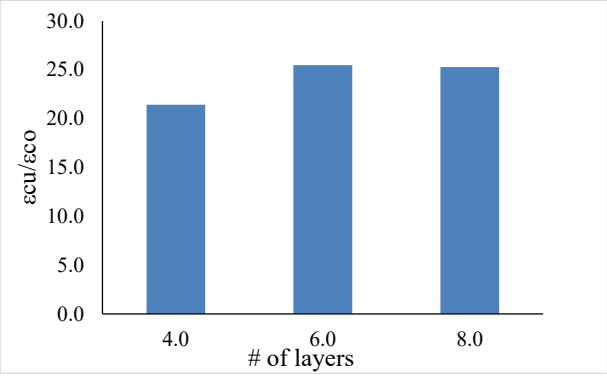

Increase in strain

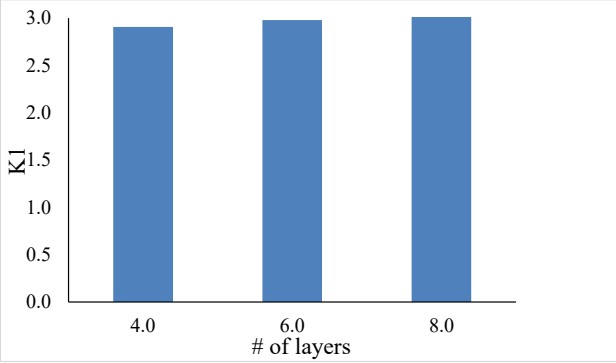

Strength effectiveness

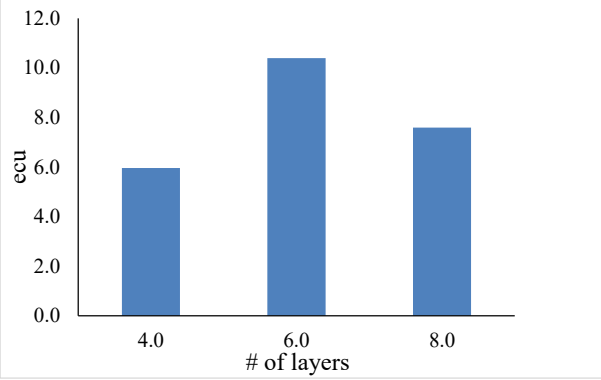

Energy absorption capacity

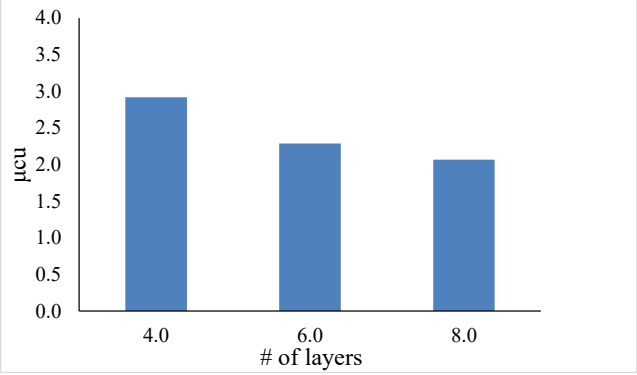

Ductility factor

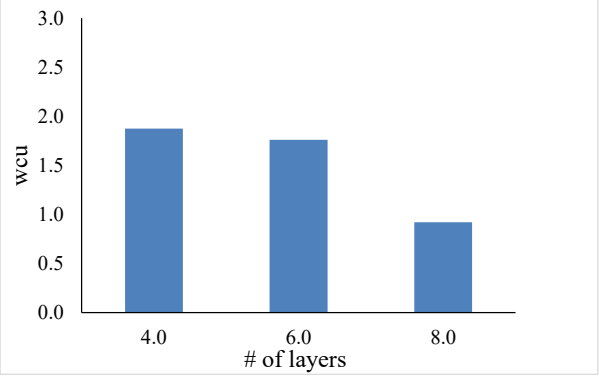

Work index

Figure 5-5 Effect of number of layers on different factors (series 1 (100 mm))

5.3.2 Series 2 (UD [90˚/0˚])

Figure 5-6 presents the stress-strain response of typical specimens tested in Series 2 (UD [90˚/0˚]) which were wrapped with 4, 6, and 8 layers of unidirectional CFRP in a 90°/0° pattern (UD $[90˚/0˚]_2$, UD $[90˚/0˚]_3$ and UD $[90˚/0˚]_4$). The stress-strain indicators defined in **Section 5.2** are reported in **Table 5-3** and compared in **Figure 5-8**. Failure photos for typical cylinders in this series are shown in **Figure 5-7**.

Previous researchers have noted that the impact of the amount of confinement is generally more important on a specimen's ability to withstand strain than it is on its strength (Cui and Sheikh 2010). It is noted that this observation comes from studies where cylinders are wrapped with a moderate amount of FRP layers. Results from this series confirm this observation, where specimens show average strength gains (f'_{cc}/f_{co}) of 134.4% to 244.1% when the number of layers increased from 4 layers to 8 layers. The gain in strain for the same specimens is more substantial, where specimens confined with 4 and 8 layers of CFRP are found to have $\varepsilon'_{cc}/\varepsilon_{co}$ ratios of 836% and 1377%, respectively. It is noted that while these specimens are wrapped with 4 and 8 total layers, the 90˚ layers are not expected to influence strength in specimens tested under pure axial compression, therefore the result is more influenced by the increase in the number of 0° plies which goes from 2 to 4.

It can be seen from **Figure 5-8** that the amount of confinement proved to be unimportant in regards to the strength effectiveness factor (k_1), with average values of 2.60, 2.47, and 2.37 were obtained for specimens confined with 4, 6, and 8 layers of CFRP, respectively. On the other hand overall energy absorption capacity (e_{cu}) increases by increasing the number of layers with average values of 1.69, 1.52, and 1.26 obtained for these same specimens. The effect of the number of layers on both the work index (w_{cu}) and ductility factor (μ_{cu}) is not as apparent as on

other properties, particularly as the number of layers increases from 6 to 8. For instance, average work index factors of 1.58, 2.07 and 1.95 as well as average ductility factors of 1.84, 2.29, and 2.13 were determined for specimens confined with 4, 6 and 8 layers of CFRP. These results demonstrate that an increase in the amount of confinement layers has a less significant effect when evaluated in terms of ductility or normalized energy absorption capacity.

In terms of shape of the stress-strain curves, the response is similar to that observed in Series 1, however the transition between the initial parabolic branch and second quasi-linear branch is less obvious and more rounded, which can be attributed to the influence of the 90˚ layers.

In terms of the effect of the number of plies on failure modes, it was noticed that rupture of the FRP jacket happened with rupture initiating in 0 degree followed by opening up of the jacket along the 90 degree axis, disregarding the amount of CFRP layers, however, the jacket opening at failure was more significant in cylinders with a greater number of CFRP layers (see **Figure 5-7**).

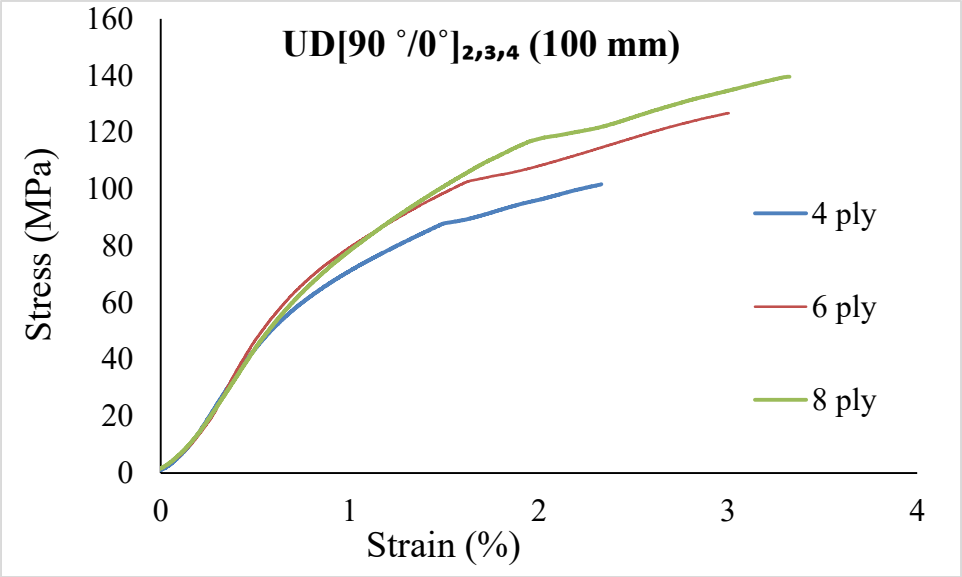

Figure 5-6 Stress-Strain Curves (UD [90˚/0˚] 100 mm)

4 layers 6 layers 8 layers

Figure 5-7 Post failure photos of CFRP confined cylinders (series 2 (100 mm))

Table 5-3 Results of specimens tested in series 2

Orientation	Experiment			%Increase in Strength			%Increase in Strain					
	Specimen #	Size(mm)	$f_{cc}{}'$	$\left(\frac{f'_{cc}}{f_{co}}\right)$	f_l (MPa)	$\varepsilon_{cc}{}'$	$\left(\frac{\varepsilon'_{cc}}{\varepsilon_{co}}\right)$	ε_1	k_1	μ_{cu}	e_{cu}	w_{cu}
UD[90˚/0˚]$_2$	1.0	100.0	101.3	135.3	22.2	0.025	916.208	0.011	2.62	2.36	2.16	2.03
	2.0	100.0	105.9	146.0	22.2	0.023	843.168	0.013	2.83	1.76	2.10	1.52
	3.0	100.0	90.6	110.6	22.2	0.024	877.021	0.018	2.14	1.34	1.92	1.19
	4.0	100.0	101.7	136.2	22.2	0.023	856.299	0.012	2.64	1.96	2.12	1.75
	5.0	100.0	105.0	144.0	22.2	0.019	690.931	0.011	2.79	1.81	1.59	1.42
	AVG	**100.0**	**100.9**	**134.4**	22.2	**0.023**	**836.725**	**0.013**	**2.60**	**1.84**	**1.98**	**1.58**
UD[90˚/0˚]$_3$	1.0	100.0	125.7	192.1	34.0	0.033	1245.917	0.018	2.43	1.79	2.96	1.28
	2.0	100.0	129.2	200.2	34.0	0.031	1179.442	0.013	2.53	2.35	3.73	2.18
	3.0	100.0	127.1	195.2	34.0	0.033	1256.381	0.012	2.47	2.74	4.01	2.62
	4.0	100.0	126.8	194.6	34.0	0.030	1132.458	0.013	2.46	2.24	3.44	2.03
	5.0	100.0	126.1	193.0	34.0	0.029	1105.170	0.013	2.44	2.34	3.59	2.27
	AVG	**100.0**	**127.0**	**195.0**	**34.0**	**0.031**	**1183.874**	**0.014**	**2.47**	**2.29**	**3.55**	**2.07**
UD[90˚/0˚]$_4$	1.0	100.0	141.5	228.9	44.3	0.035	1319.984	0.015	2.22	2.27	4.43	2.05
	2.0	100.0	139.6	224.4	44.3	0.033	1264.177	0.016	2.18	2.09	4.35	1.95
	3.0	100.0	159.2	270.0	44.3	0.033	1267.870	0.017	2.62	2.02	5.13	1.95
	4.0	100.0	149.2	246.7	44.3	0.038	1473.861	0.017	2.40	2.23	5.31	2.07
	5.0	100.0	151.0	250.8	44.3	0.040	1559.828	0.020	2.44	2.05	5.09	1.71
	AVG	**100.0**	**148.1**	**244.1**	**44.3**	**0.036**	**1377.144**	**0.017**	**2.37**	**2.13**	**4.86**	**1.95**

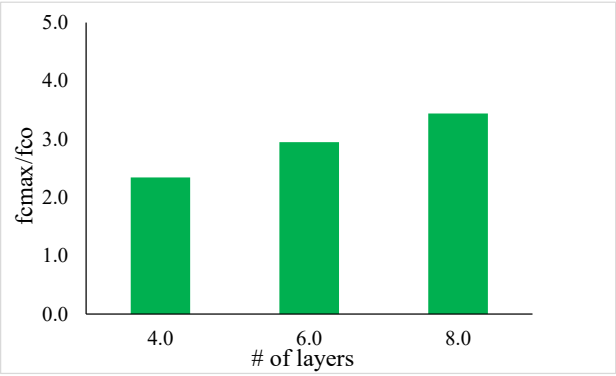

Increase in stress

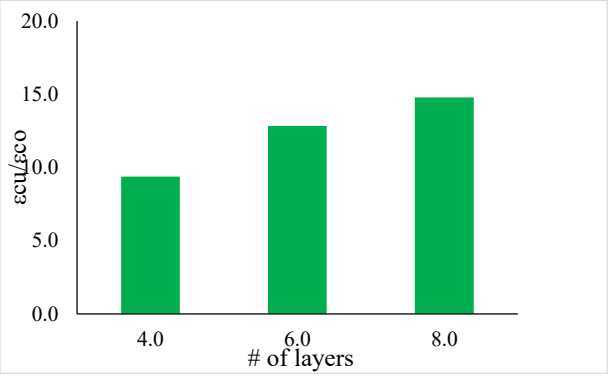

Increase in strain

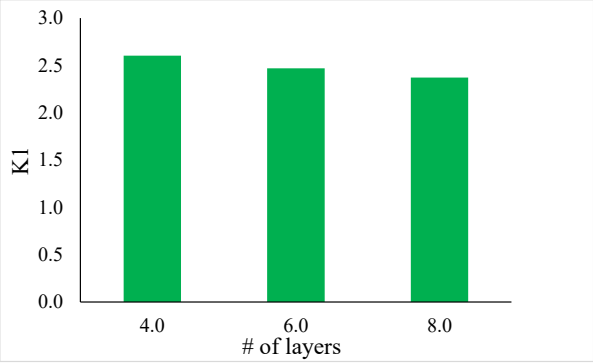

Strength effectiveness

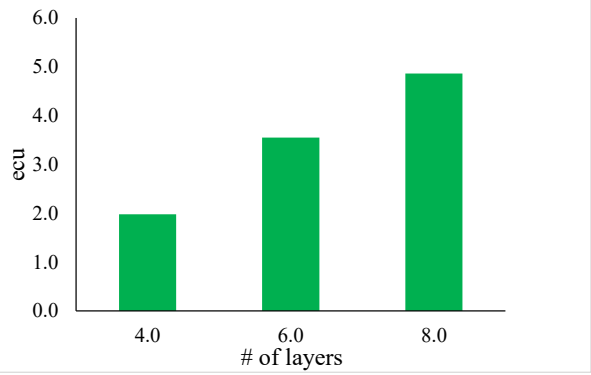

Energy absorption capacity

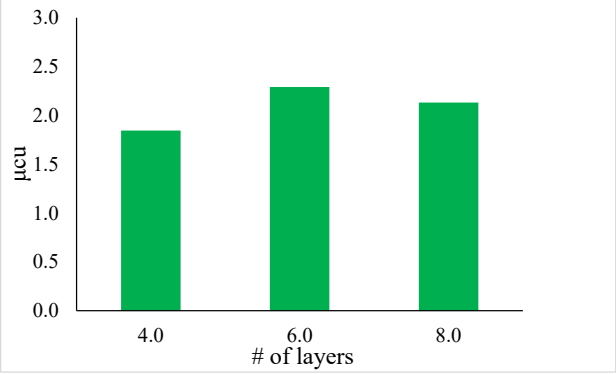

Ductility factor

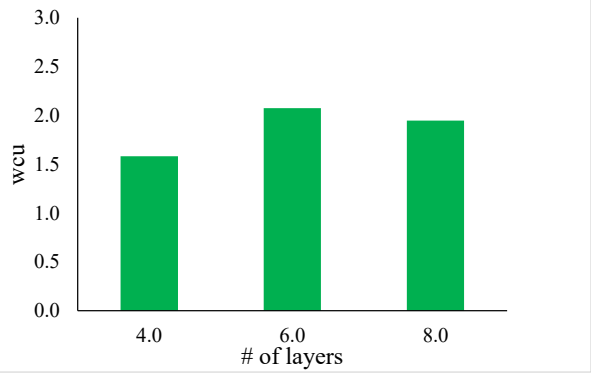

Work index

Figure 5-8 Effect of number of layers on different factors (series 2 (100 mm))

5.3.3 Series 3 (UD [+45˚/-45˚])

The series 3 specimens (UD [+45˚/-45˚]) were wrapped with 4, 6, and 8 layers of unidirectional CFRP angled in a +45˚/-45˚ pattern (UD $[+45^{\circ}/-45^{\circ}]_2$, UD $[+45^{\circ}/-45^{\circ}]_3$ and UD $[+45^{\circ}/-45^{\circ}]_4$). The stress-strain response of specimens in this series are shown in **Figure 5-9** and the strength, toughness and ductility indicators are reported in **Table 5-4** and compared in **Figure 5-11**. Failure photos for typical cylinders in this series are shown in **Figure 5-10**.

Previous researchers have noted that the use of 45° angular FRP fibers has an important effect on increasing strain capacity and ductility, with much lesser effect on increasing stress. Average data from this series shows that cylinders wrapped with 4 layers of angular CFRP showed a small enhancement in strength (f'_{cc}/f_{co}) of roughly 21.5%, while a considerable increase in strain ($\varepsilon'_{cc}/\varepsilon_{co}$) of approximately 2183% was reached. Specimens confined with 6 layers of angular CFRP shows average strength and strain ratios of 47% and 3605%, while specimens with 8 layers shows further increases in stress and strain of 70.5% and 3989%. Based on these results 6 layers of angular CFRP seems to provide the greatest relative improvement in overall performance, with significant enhancement in strain capacity when going from 4 to 6 layers. Further increase in strength and modest enhancement in strain is observed when additional layers of CFRP are added (8 layers). As will be shown in subsequent comparisons, the improvement in stress-strain response and overall confinement is not only a function of the number of FRP layers provided, but it is also a function of the use of an optimal fiber orientation (Li et al. 2006).

Examination of the data in **Table 5-4** shows that the strength effectiveness factor (k_1) obtained in the UD [+45˚/-45˚] series shows fluctuation for the different samples tested within each sub-series, although average values increase from 2.08, to 2.45 to 3.74 for specimens with 4, 6 and 8 layers of angular CFRP. The trend is more clear when examining the energy absorption capacity

(e_{cu}) in this series, which doubled from 2.45 to 5.27 as the number of CFRP layers is increased from 4 to 6. However, only a minor improvement in energy absorption capacity is obtained when the jacket layers were increased to 8 layers (e_{cu} = 6.54), pointing to limited CFRP contribution as the number of layers is increased beyond 6. This observation is also apparent when comparing the work index and ductility factors (μ_{cu}) which show no significant increase for specimens with 6 and 8 layers, while both factors increased as the number of layers goes from 4 to 6 layers (see **Table 5-4** and **Figure 5-11**).

Examination of the curves in **Figure 5-9** shows that specimens confined with +45˚/-45˚ CFRP show a completely different stress-strain response when compared to specimens confined with unidirectional fibers in the hoop direction, where the initial parabolic branch transitions to a plateau after the confined stress reach a peak, with large increase in strain until failure. This characteristic plastic response can potentially be of use to enhance the ductility of seismically-deficient columns and allow for the dissipation of greater seismic energy during hysteretic response (Sadeghian et al. 2010).

The effect of using angular fibers was also clearly evident in the failure mode of the specimens in this series, which were gradual and ductile, in contract to the brittle and explosive failures observed in the UD [0º] series. The CFRP jackets in this series opened up at 45º angles regardless of the number of layers, although the jackets tended to open up more in cylinders with a greater number of CFRP layers (see **Figure 5-10)**.

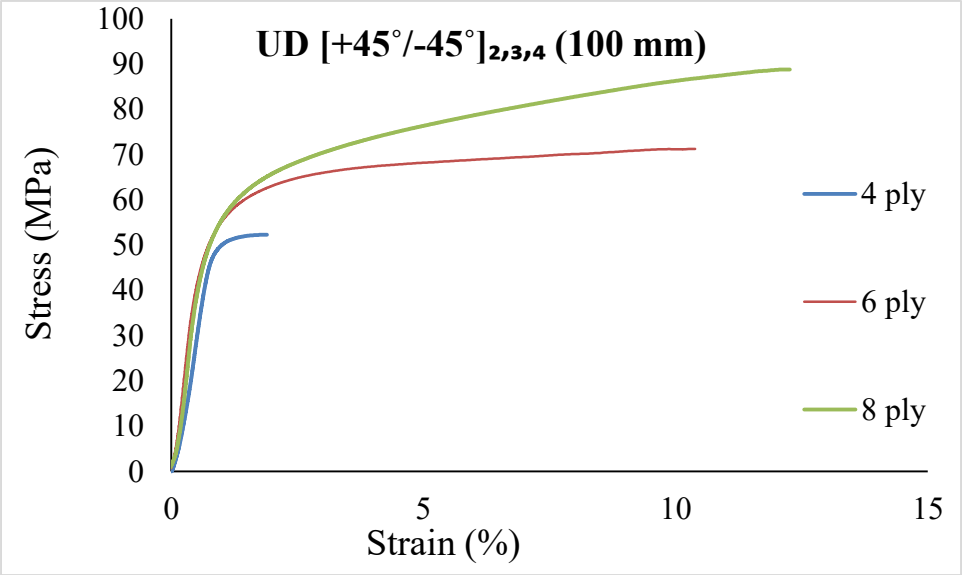

Figure 5-9 Stress-Strain Curves (UD [+45°/-45°] 100 mm)

4 layers 6 layers 8 layers

Figure 5-10 Post failure photos of CFRP confined cylinders (series 3 (100 mm))

Table 5-4 Results of specimens tested in series 3

Orientation	Experiment			%Increase in Strength			%Increase in Strain					
	Specimen #	Size(mm)	f_{cc}'	$\left(\frac{f'_{cc}}{f_{co}}\right)$	f_l (MPa)	ε_{cc}'	$\left(\frac{\varepsilon'_{cc}}{\varepsilon_{co}}\right)$	ε_1	k_1	μ_{cu}	e_{cu}	w_{cu}
UD [+45°/-45°]$_2$	1.0	100.0	56.6	31.5	4.4	0.068	2671.235	0.007	3.06	9.37	3.76	9.22
	2.0	100.0	49.3	14.5	4.4	0.040	1549.364	0.006	1.40	7.27	1.99	7.30
	3.0	100.0	48.4	12.4	4.4	0.063	2504.432	0.012	1.20	5.37	2.91	5.10
	5.0	100.0	54.9	27.5	4.4	0.051	2005.458	0.008	2.67	6.31	1.13	2.53
	AVG	**100.0**	**52.3**	**21.5**	**4.4**	**0.056**	**2182.622**	**0.008**	**2.08**	**7.08**	**2.45**	**6.04**
UD [+45°/-45°]$_3$	1.0	100.0	53.6	24.5	8.3	0.033	1245.917	0.009	1.27	3.70	1.48	3.11
	2.0	100.0	57.1	32.6	8.3	0.108	4316.701	0.013	1.69	8.15	5.65	7.50
	3.0	100.0	71.2	65.6	8.3	0.110	4410.464	0.010	3.41	11.06	7.13	10.07
	4.0	100.0	79.3	84.3	8.3	0.101	4045.671	0.011	4.39	9.59	6.90	8.25
	5.0	100.0	55.1	28.1	8.3	0.100	4003.816	0.008	1.46	13.19	5.21	12.45
	AVG	**100.0**	**63.3**	**47.0**	**8.3**	**0.090**	**3604.514**	**0.010**	**2.45**	**9.14**	**5.27**	**8.28**
UD [+45°/-45°]$_4$	1.0	100.0	59.6	38.5	8.1	0.080	3163.439	0.008	2.04	10.18	4.29	9.22
	2.0	100.0	88.8	106.4	8.1	0.129	5191.957	0.012	5.64	10.50	9.67	8.86
	3.0	100.0	87.4	103.0	8.1	0.119	4794.748	0.016	5.46	7.24	8.66	6.02
	4.0	100.0	64.3	49.5	8.1	0.083	3286.130	0.010	2.62	8.36	4.77	7.51
	5.0	100.0	66.8	55.3	8.1	0.088	3508.945	0.009	2.93	9.45	5.31	8.54
	AVG	**100.0**	**73.4**	**70.5**	**8.1**	**0.100**	**3989.044**	**0.011**	**3.74**	**9.15**	**6.54**	**8.03**

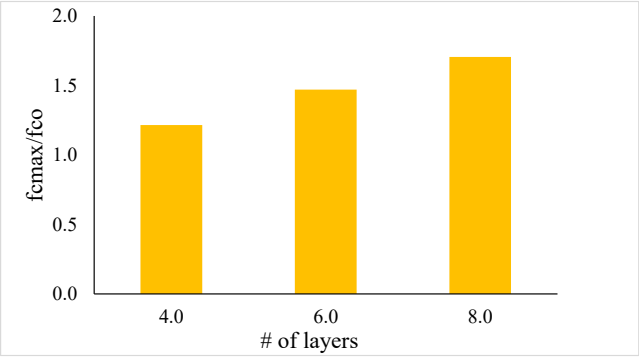

Increase in stress

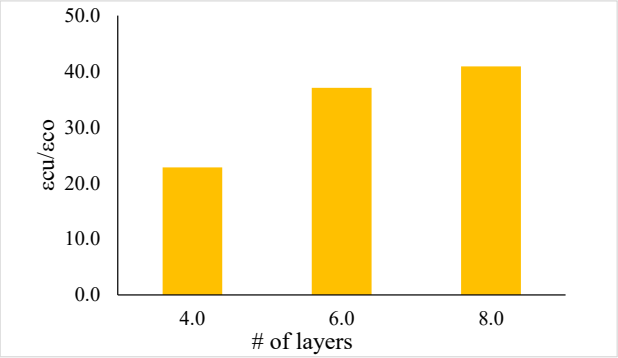

Increase in strain

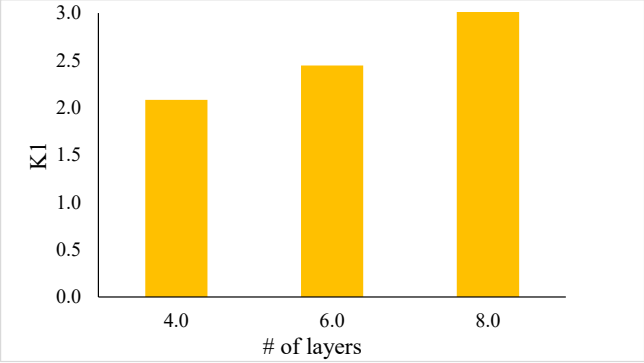

Strength effectiveness

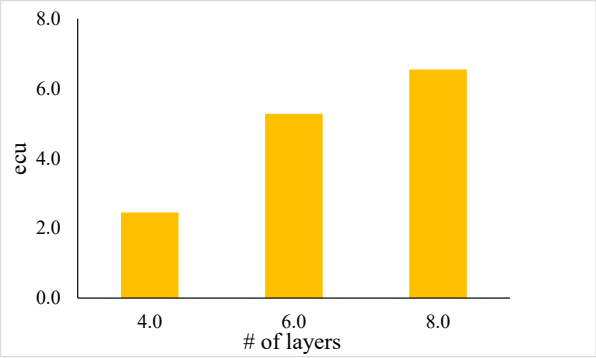

Energy absorption capacity

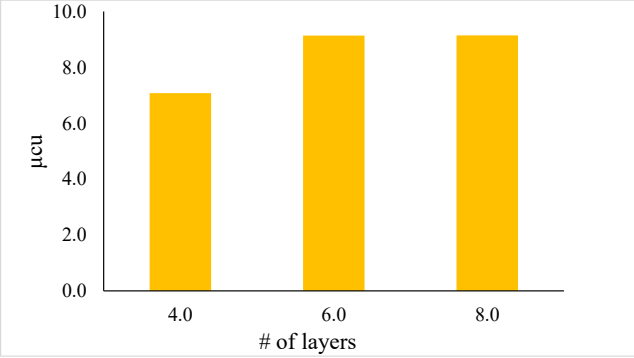

Ductility factor

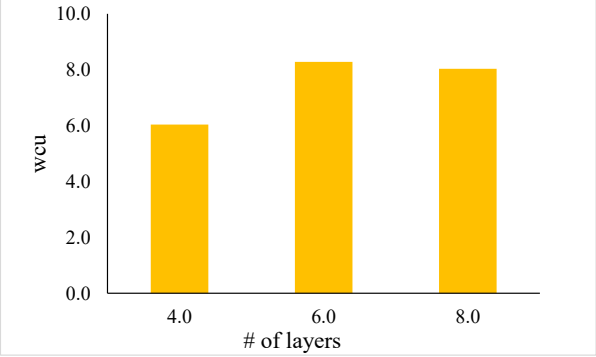

Work index

Figure 5-11 Effect of number of layers on different factors (series 3 (100 mm))

5.3.4 Series 4A (UD [90˚/0˚] W [±45˚]$_2$)

The series 4 specimens (UD [90˚/0˚] W [±45˚]$_2$) had either 4 or 8 plies of CFRP. Specimens with 4 plies were wrapped with two layers of unidirectional CFRP at 90˚/0˚ followed by woven CFRP fabric having angular ±45˚ fibers (this pattern was doubled for specimens with 8 plies). The stress-strain response of specimens in this series is shown in **Figure 5-12** and the various stress-strain indicators for this series are reported in **Table 5-5** and **Figure5-14**. Failure photos for typical cylinders in this series are shown in **Figure 5-13**.

Provision of unidirectional fibers in the hoop direction in this series resulted in some incremental increase in stress. Similarly, provision of woven CFRP with angular fibers led to increase in strain capacity. Cylinders wrapped with 4 layers of CFRP showed enhancement in strength (f'_{cc}/f_{co}) of roughly 107.1%, while a considerable increase in strain ($\varepsilon'_{cc}/\varepsilon_{co}$) of approximately 859.6% was reached which is significant, but somewhat smaller when compared to companion specimens in Series 3 which were wrapped with purely angular (+45/-45) CFRP sheets. Specimens with 8 plies showed further increases in strength and strain with average values of 199.3% and 1316.2%. When examining the strength enhancement in terms of the strength effectiveness factor (k_1) the values fluctuate between 2.75 and 2.85, with average values reducing from 1.75 to 1.56 as the number of plies is increased from 4 to 8, an indicator of reduced CFRP efficiency as the number of plies is doubled . However, the effect of the number of plies is evident when evaluated in terms of energy absorption capacity (e_{cu}), where average values double from 1.43 to 3.04 when increasing the number of plies from 4 to 8. This effect is also clear when comparing the work index (w_{cu}) and ductility factor (μ_{cu}) for these specimens, with a fourfold increase as the number of layers goes from 4 to 8 layers (see **Table 5-5** and **Figure5-14**).

Examination of the stress-strain curves in **Figure 5-12** shows a hybrid between the responses observed in series 1, 2 and 3, with an initially parabolic ascending branch followed by a second branch with relatively lower stiffness with large plastic deformations until failure. As with series 2, the transition point between the two branches is rounded and not as clear as in Series 1 (particularly for the series with 8 plies).

In terms of failure mode, the specimens showed relatively less explosive failures when compared to specimens in series 1 due to the provision of angular fibers. Failure of the jackets occurred in a ±45˚ pattern, with the jacket opening up more evidently and over most of the specimen height in cylinders confined with 4 plies, while the jacket opening was more controlled in cylinders with 8 plies of CFRP.

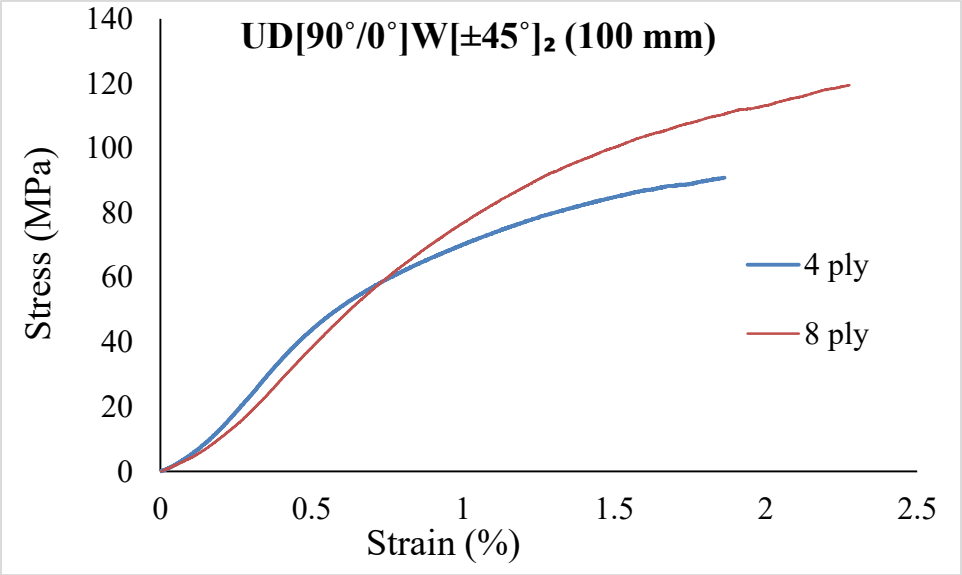

Figure 5-12 Stress-Strain Curves (UD [90˚/0˚] W [±45˚]$_2$ 100 mm)

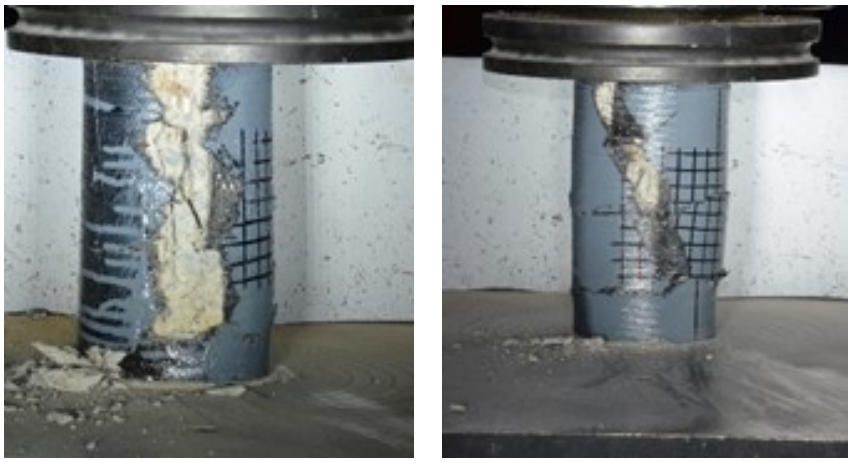

4 layers 8 layers

Figure 5-13 Post failure photos of CFRP confined cylinders (series 4A (100 mm))

Table 5-5 Results of specimens tested in series 4A

Orientation	Experiment			%Increase in strength $\left(\frac{f'_{cc}}{f_{co}}\right)$			%Increase in strain $\left(\frac{\varepsilon'_{cc}}{\varepsilon_{co}}\right)$					
	Specimen #	Size(mm)	$f_{cc}{}'$		f_l (MPa)	$\varepsilon_{cc}{}'$		ε_1	k_1	μ_{cu}	e_{cu}	w_{cu}
UD[90˚/0˚]W[±45˚]$_2$	1.0	100.0	92.3	114.5	16.6	0.024	903.283	0.010	2.97	2.56	1.57	1.78
	2.0	100.0	84.4	96.2	16.6	0.023	862.864	0.012	2.49	1.89	1.34	1.27
	3.0	100.0	87.3	103.0	16.6	0.021	745.507	0.009	2.67	2.18	1.23	1.49
	4.0	100.0	92.5	114.9	16.6	0.025	926.672	0.012	2.98	2.05	1.58	1.40
	AVG	**100.0**	**89.1**	**107.1**	**16.6**	**0.023**	**859.581**	**0.011**	**2.78**	**2.17**	**1.43**	**1.49**
UD[90˚/0˚]$_2$W[±45˚]$_4$	1.0	100.0	129.0	199.9	30.1	0.035	1344.809	0.011	2.86	3.06	3.20	2.16
	2.0	100.0	127.0	195.2	30.1	0.038	1459.499	0.003	2.79	13.04	3.20	8.65
	3.0	100.0	134.0	211.3	30.1	0.030	1128.560	0.003	3.02	9.25	2.67	6.15
	4.0	100.0	125.1	190.6	30.1	0.035	1331.883	0.003	2.72	10.27	3.10	7.29
	AVG	**100.0**	**128.8**	**199.3**	**30.1**	**0.035**	**1316.188**	**0.005**	**2.85**	**8.91**	**3.04**	**6.06**

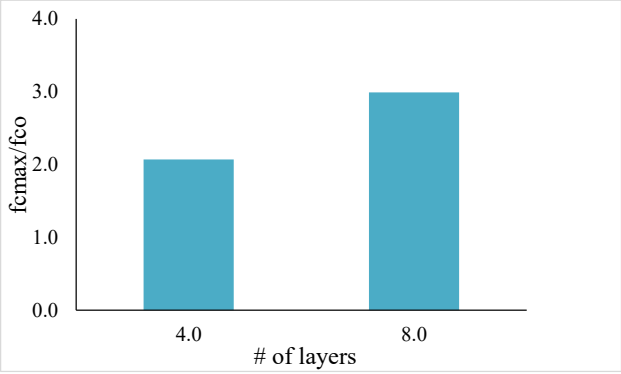

Increase in stress

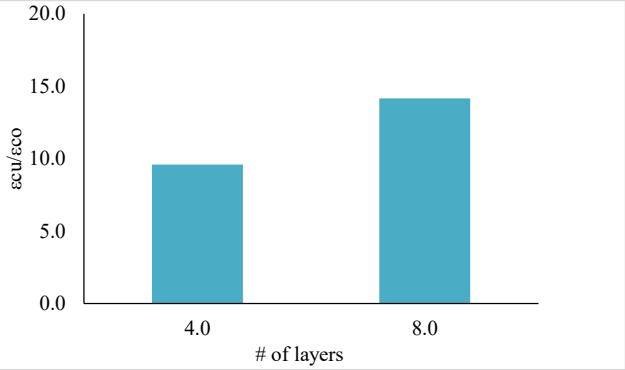

Increase in strain

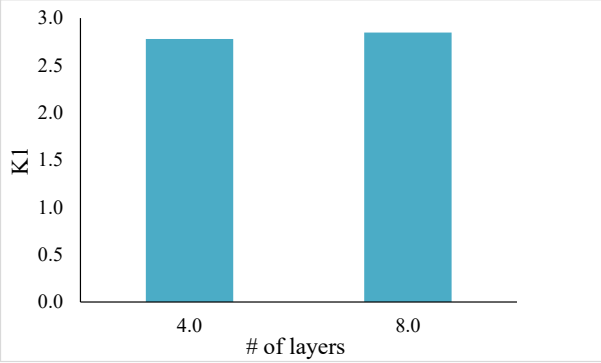

Strength effectiveness

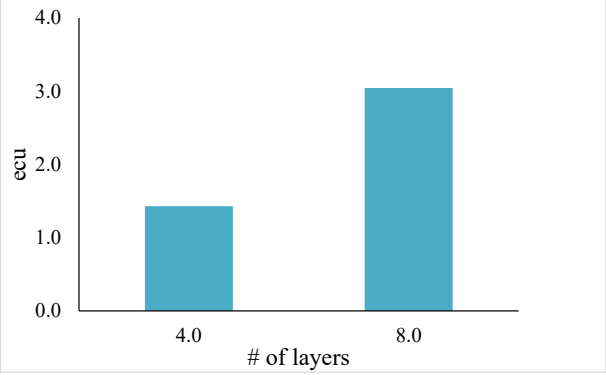

Energy absorption capacity

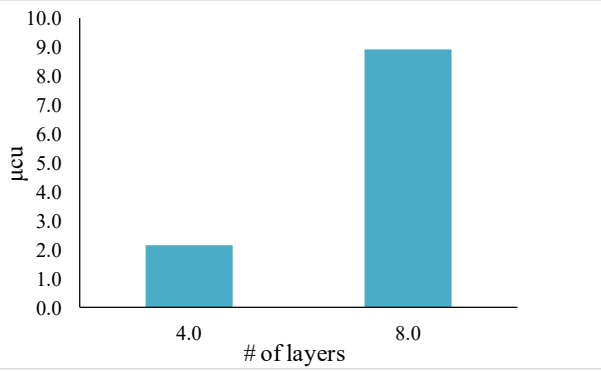

Ductility factor

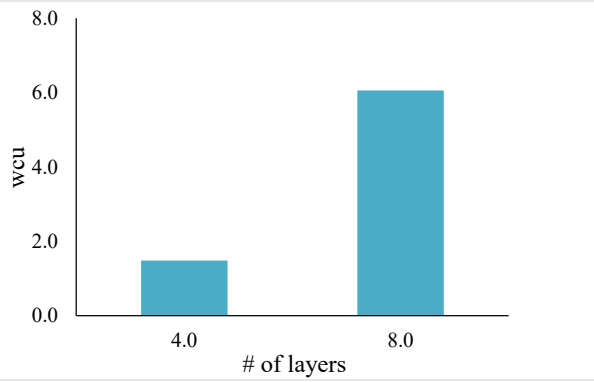

Work index

Figure5-14 Effect of number of layers on different factors (series 4A (100 mm))

5.3.5 Series 4B (UD [90˚] W [±45˚]$_2$ UD [0˚])

The Series 4B specimens where reinforced with the same number and type of CFRP plies used in Series 4A, however the order of the plies was different in this series, with the woven CFRP fabric sandwiched in between 90^o and 0^o plies of unidirectional CFRP. The stress-strain response of specimens with 4 and 8 plies are shown in **Figure 5-15** and the strength, toughness and ductility parameters are reported in **Table 5-6** and in **Figure 5-17**. Failure photos for typical cylinders in this series are shown in **Figure 5-16**.

As with its companion series, the provision of unidirectional fibers aligned in the hoop direction allowed for an increase in peak stress for this series. The strength enhancement ratios (f'_{cc}/f_{co}) increase as the number of layers goes from 4 to 8 layers, with average values of 18.1 % and 34.7 %. It is noted that strength ratios are comparatively lower than the values for companion specimens in Series 4A. The provision of woven $\pm 45^0$ fibers also resulted in a significant improvement in strain capacity, with average $\varepsilon'_{cc}/\varepsilon_{co}$ ratios of 849.5% and 1328.3% for specimens with 4 and 8 plies in this series. Examining the results in **Table 5-6**, the strength effectiveness factor (k_1) reaches average values of 2.52 and 2.83 for the specimens with 4 and 8 plies, respectively which indicates a slight reduction in confinement efficiency with the doubling of FRP layers. On the other hand the effect of increasing the number of plies is clear when examining the energy absorption capacity (e_{cu}) in this series, which doubles from 1.32 to 2.70 as the number of CFRP layers is increased from 4 to 8. However unlike the previous series, the opposite trend is observed when comparing the average work index (w_{cu}) and ductility factor (μ_{cu}) for this series, where both parameters decrease by factors of over 5 as the number of plies goes from 4 to 8.

The stress-strain response in **Figure 5-15** follows similar response to the behavior observed in Series 4A, where the response shows a hybrid of the characteristic responses observed in Series 1-3. As in the previous series, the transition zone and is more rounded and less clear for the specimen with 8 plies of CFRP.

Regardless of the number of layers, failure of the specimens in this series was gradual, and it was observed that only the outer layer (with unidirectional fibers aligned in the hoop direction) of the jacket was opened up and 100% of crushed concrete stayed in the jacket (**Figure 5-13**), which is different to the observation made in Series 4A (**Figure 5-13)**.

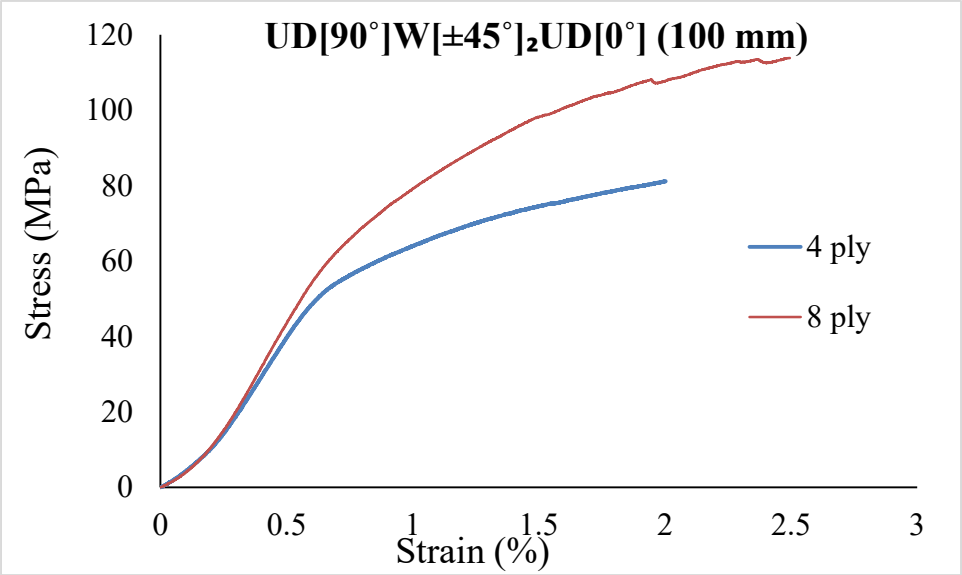

Figure 5-15 Stress-Strain Curves (UD [90˚] W [±45˚]$_2$ UD [0˚] 100 mm)

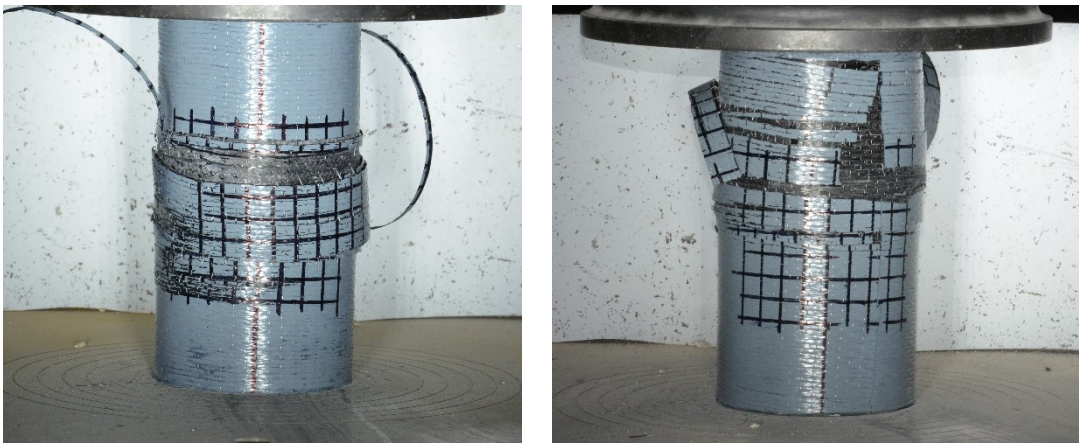

4 layers 8 layers

Figure 5-16 Post failure photos of CFRP confined cylinders (series 4B (100 mm))

Table 5-6 Results of specimens tested in series 4B

Orientation	Experiment			%Increase in Strength			%Increase in Strain					
	Specimen #	Size(mm)	$f_{cc}{}'$	$\left(\frac{f'_{cc}}{f_{co}}\right)$	f_l (MPa)	$\varepsilon_{cc}{}'$	$\left(\frac{\varepsilon'_{cc}}{\varepsilon_{co}}\right)$	ε_1	k_1	μ_{cu}	e_{cu}	w_{cu}
UD[90˚]W[±45˚]$_2$UD[0˚]	1.0	100.0	78.6	82.7	15.2	0.025	942.265	0.002	2.35	15.16	1.45	11.02
	2.0	100.0	75.8	76.2	15.2	0.024	871.892	0.002	2.16	11.51	1.26	8.10
	3.0	100.0	87.2	102.7	15.2	0.022	802.954	0.002	2.91	13.92	1.31	9.48
	4.0	100.0	83.7	94.4	15.2	0.021	780.796	0.002	2.68	11.69	1.24	8.09
	AVG	**100.0**	**81.3**	**89.0**	**15.2**	**0.023**	**849.477**	**0.002**	**2.52**	**13.07**	**1.32**	**9.17**
UD[90˚]$_2$W[±45˚]$_4$UD[0˚]$_2$	1.0	100.0	115.8	169.2	25.0	0.033	1265.613	0.012	2.91	2.86	2.70	2.01
	2.0	100.0	119.9	178.7	25.0	0.026	974.887	0.017	3.08	1.57	1.99	0.99
	3.0	100.0	103.8	141.1	25.0	0.042	1641.896	0.015	2.43	2.75	3.12	1.94
	4.0	100.0	115.9	169.3	25.0	0.037	1430.981	0.014	2.91	2.62	2.97	1.80
	AVG	**100.0**	**113.9**	**164.6**	**25.0**	**0.035**	**1328.344**	**0.015**	**2.83**	**2.45**	**2.70**	**1.69**

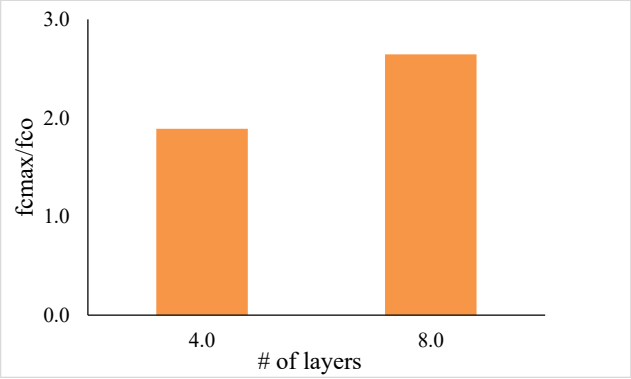

Increase in stress

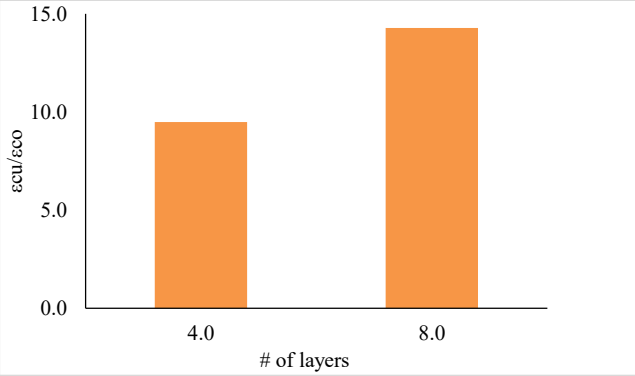

Increase in strain

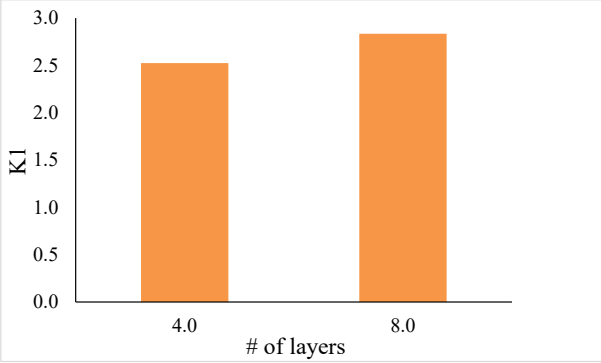

Strength effectiveness

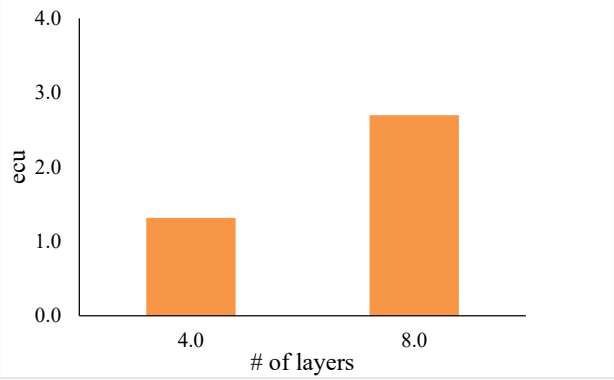

Energy absorption capacity

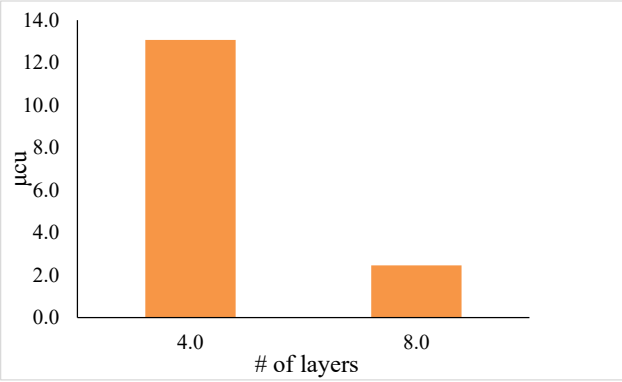

Ductility factor

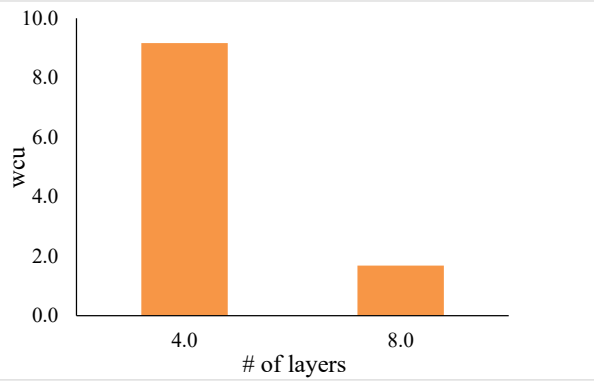

Work index

Figure 5-17 Effect of number of layers on different factors (series 4B (100 mm))

5.3.6 Series 5A (UD [0°]$_2$ W [±45°]$_2$)

Specimens in series 5A were wrapped with 4 and 8 layer of 0^0 unidirectional and woven $\pm45^0$ CFRP. For the 4 ply specimens, the first 2 layers consisted of unidirectional CFRP at 0^0, followed by 2 layers of woven $\pm45^0$ CFRP. The 8 ply specimens were first confined with 4 layers of UD [0^0], followed by 4 layers of W [$\pm45^0$] CFRP. Stress-strain results for this series are summarized in **Figure 5-18**, **Table 5-7** and **Figure 5-20**. Failure photos for typical cylinders in this series are shown in **Figure 5-19.**

Increase in both stress and strain was expected in this series due to the provision of CFRP with fibers aligned in the 0^0 and $\pm45^0$ directions, and these increases were proportional to the number of layers. Cylinders wrapped with 4 layers of CFRP showed enhancement in strength (f'_{cc}/f_{co}) of roughly 182.2%, with a considerable increase in strain ($\varepsilon'_{cc}/\varepsilon_{co}$) of approximately 1714.8%. Specimens with 8 plies had average percent increase in strength and strain of 315.7% and 2300.8% for cylinders with 8 layers, demonstrating an important enhancement in both strength and strain capacity as the number of plies was doubled.

The average strength effectiveness factors (k_1) for this series were approximately 3.13 and 2.92, pointing to a relative reduction in confinement efficiency as the number of plies is doubled. On the other hand, the energy absorption capacity (e_{cu}) was found to increase from of 3.75 to 6.74 for cylinders with 4 and 8 layers of CFRP, respectively. **Table 5-7** shows that the number of plies had no significant effect on the work index (w_{cu}) and ductility factor (μ_{cu}) with average values near 1.8 and 2.7, respectively.

Figure 5-18 shows that stress-strain curves show a similar response to those observed in Series 1, an indicator that the UD [0^0] fibers dominate the response for this layup configuration. In

terms of failure mode, jacket damage was observed to be more significant in cylinders with 4 vs. 8 plies. Moreover, jacket rupture occurred along the entire cylinder height in specimens with 4 plies, while jacket rupture was concentrated near the mid-region in the shape of wings at the mid-height of the cylinder with 8 plies, an indicator of reduced damage with the increase in the amount of confinement layers.

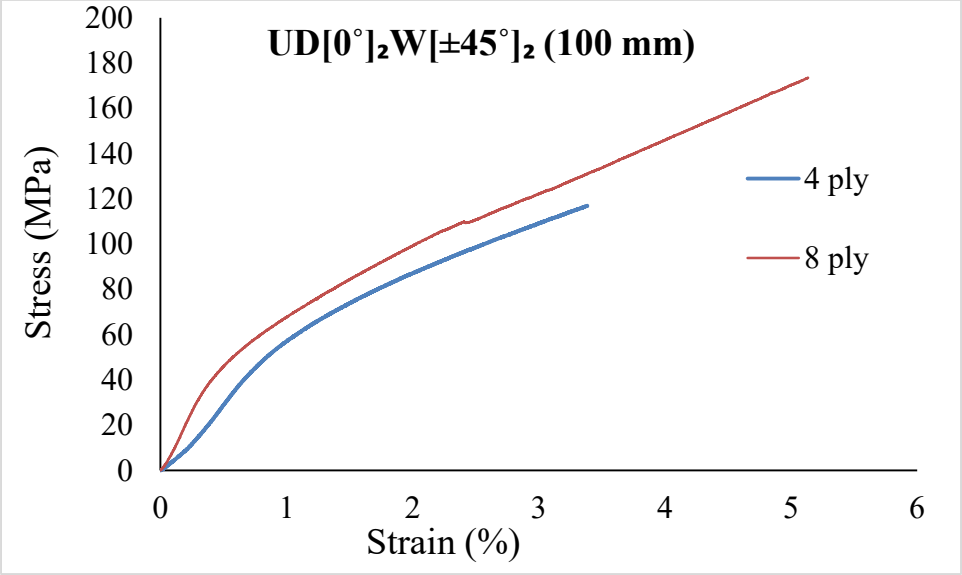

Figure 5-18 Stress-strain curves (UD [0°]₂ W [±45°]₂ 100 mm)

4 layers 8 layers

Figure 5-19 Post failure photos of CFRP confined cylinders (series 5 (100 mm))

Table 5-7 Results of specimens tested in series 5A

Orientation	Experiment			%Increase in Strength			%Increase in Strain					
	Specimen #	Size(mm)	$f_{cc}{}'$	$\left(\frac{f'_{cc}}{f_{co}}\right)$	f_l (MPa)	$\varepsilon_{cc}{}'$	$\left(\frac{\varepsilon'_{cc}}{\varepsilon_{co}}\right)$	ε_1	k_1	μ_{cu}	e_{cu}	w_{cu}
UD[0˚]$_2$W[±45˚]$_2$	1.0	100.0	122.0	183.5	25.0	0.039	1510.382	0.015	3.15	2.67	3.18	1.77
	2.0	100.0	122.5	184.6	25.0	0.040	1548.133	0.022	3.17	1.86	3.06	1.16
	3.0	100.0	117.7	173.5	25.0	0.036	1381.330	0.017	2.98	2.11	2.70	1.34
	4.0	100.0	123.5	187.1	25.0	0.061	2419.696	0.016	3.21	3.84	6.05	3.06
	AVG	**100.0**	**121.4**	**182.2**	**25.0**	**0.044**	**1714.885**	**0.017**	**3.13**	**2.62**	**3.75**	**1.83**
UD[0˚]$_4$W[±45˚]$_4$	1.0	100.0	177.1	311.4	46.6	0.054	2099.220	0.020	2.88	2.69	5.98	1.70
	2.0	100.0	169.5	293.8	46.6	0.059	2340.295	0.020	2.72	3.02	6.48	1.94
	3.0	100.0	174.6	305.7	46.6	0.063	2471.810	0.024	2.83	2.57	7.12	1.67
	4.0	100.0	194.5	352.0	46.6	0.058	2291.875	0.022	3.25	2.61	7.38	1.70
	AVG	**100.0**	**178.9**	**315.7**	**46.6**	**0.059**	**2300.800**	**0.022**	**2.92**	**2.72**	**6.74**	**1.75**

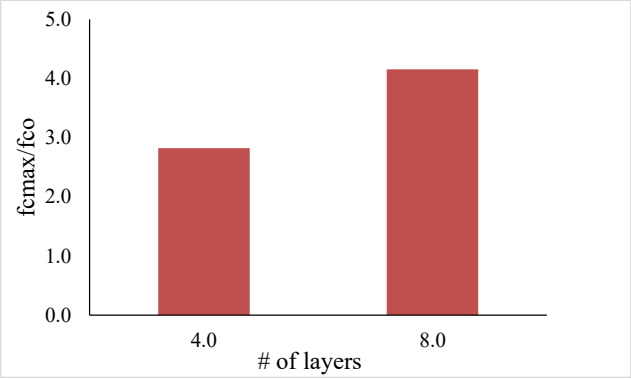

Increase in stress

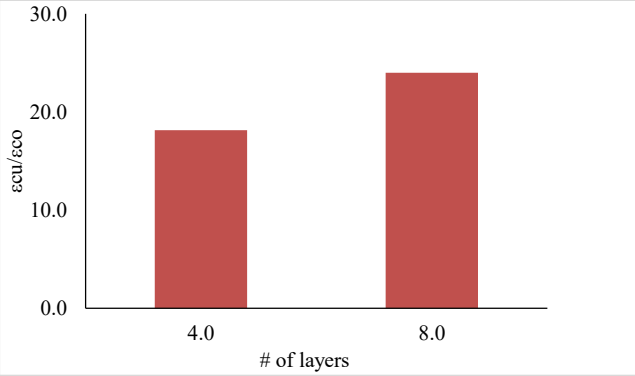

Increase in strain

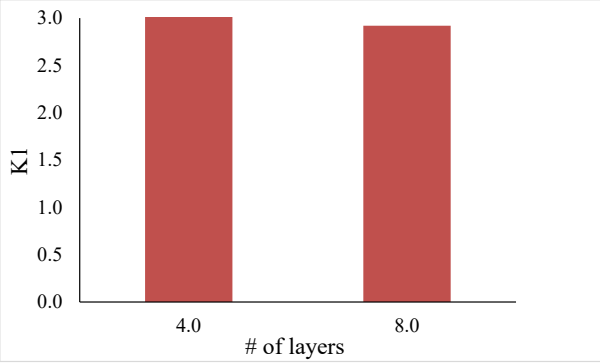

Strength effectiveness

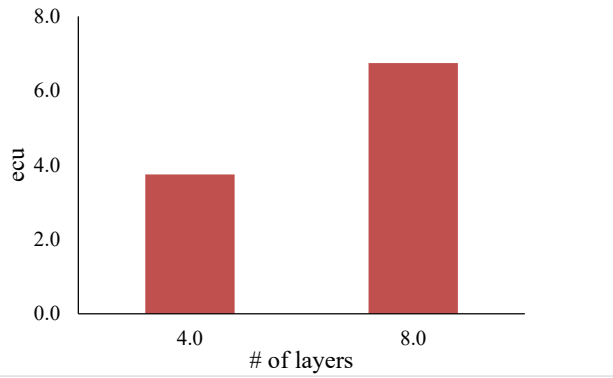

Energy absorption capacity

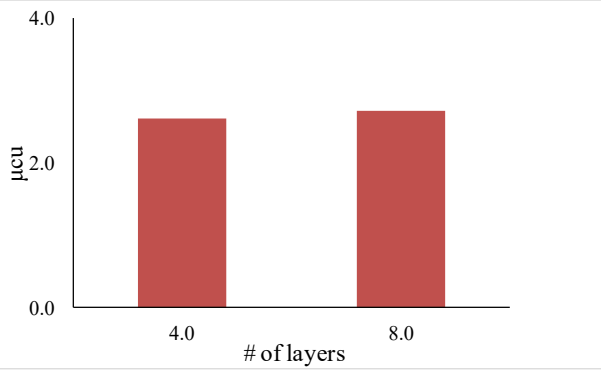

Ductility factor

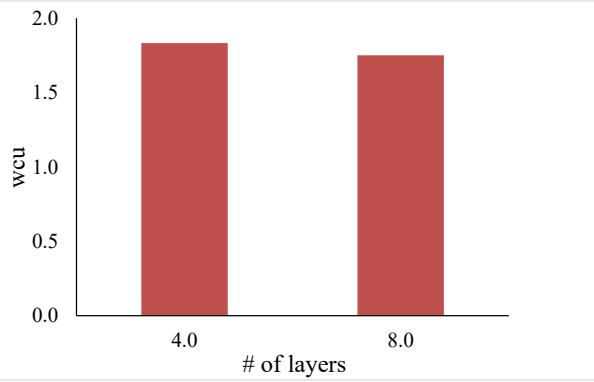

Work index

Figure 5-20 Effect of number of layers on different factors (series 5A (100 mm))

5.3.7 Series 5B (W [±45°]$_2$ UD [0°]$_2$)

Series 5B was constructed with same CFRP layup used in Series 5A, however the order of ply application was reversed to W [±45°] - UD [0°] (i.e. woven sheets = innermost layers and unidirectional sheets = outermost layers). Stress-strain results are summarized in **Figure 5-21**, **Table 5-8** and **Figure 5-23**. Failure photos for typical cylinders in this series are shown in **Figure 5-19**. As with Series 5A, enhancements in both strength and strain capacity result as the number of plies are increased from 4 to 8. Cylinders with 4 plies of CFRP showed enhancement in strength (f'_{cc}/f_{co}) of 141.9%, with a considerable increase in maximum strain ($\varepsilon'_{cc}/\varepsilon_{co}$) of 1130.2%. Comparatively, specimens with 8 plies showed average increase in strength and strain of 279.9% and 2445.7%. It is noted that when compared to companion specimens in Series 5A, the average increase in stress is found to be 40.3 % and 35.8 % lower for the cylinders confined with 4 and 8 layers of CFRP. The increase in strain is also different when compared to Series 5A; in the case of cylinders with 4 layers the increase in strain is 51.68 % lower than that of series 5A, while no significant difference is observed when comparing companion specimens with 8 layers of CFRP.

The strength effectiveness factor (k_1) shows average values of 2.44 and 2.59 for specimens with 4 and 8 plies, respectively. Conversely, energy absorption capacity (e_{cu}) nearly triples (from 2.13 to 6.22) as the number of CFRP plies is increased from 4 to 8. The effect of number of layers is less significant when comparing the average work index (w_{cu}) and ductility factors (μ_{cu}) in **Table 5-8**.

The stress-strain curves of the specimens in Series 5B show an initially steep parabolic ascending branch and a quasi-linear second branch (**Figure 5-21**), an indicator that the unidirectional fibers are dominating the stress-strain behavior in this layup configuration.

The failure mode of specimens with 4 and 8 plies was similar. Both the outer and inner layers of the CFRP jackets opened up at failure, however the outer layer experienced more damage (see **Figure 5-22**). The layup sequence also had an effect on failure mode, with the overall level of damage being less significant in this series when compared to the companion 5A series (compare damage in **Figure 5-18** and **Figure 5-22**), indicating that the provision of woven angular fibers on the innermost layer is one way to control the explosive concrete failures associated with cylinders confined with unidirectional fibers.

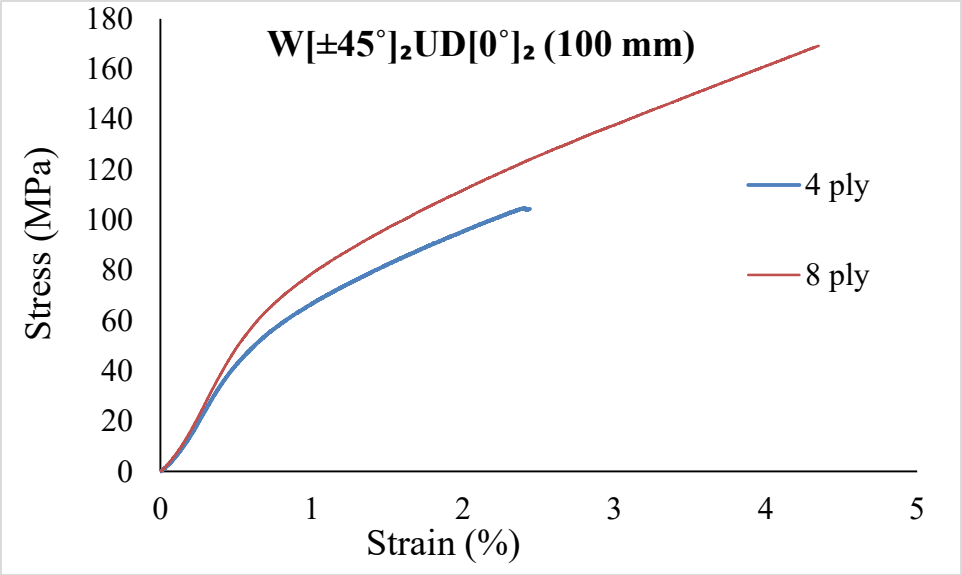

Figure 5-21 Stress-strain curves (W [±45°]₂ UD [0°]₂ 100 mm)

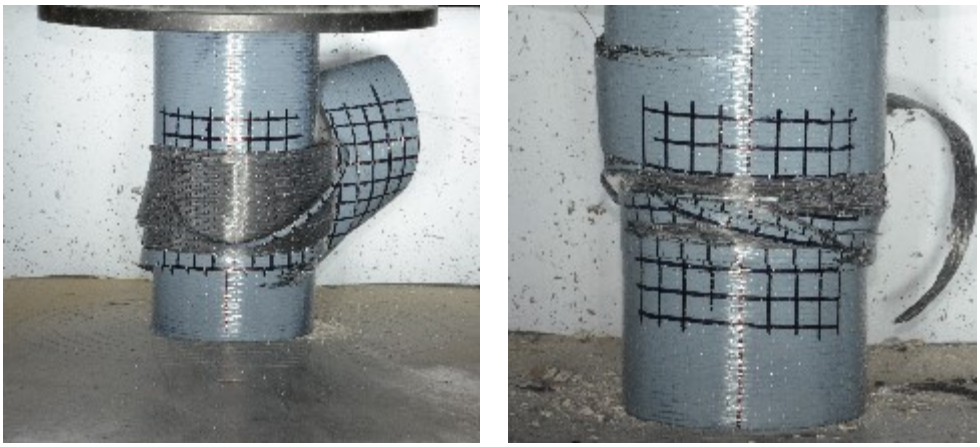

4 layers 8 layers

Figure 5-22 Post failure photos of CFRP confined cylinders (series 5B (100 mm))

Table 5-8 Results of specimens tested in series 5B

Orientation	Experiment			%Increase in Strength			%Increase in Strain					
	Specimen #	Size(mm)	f_{cc}'	$\left(\frac{f_{cc}'}{f_{co}}\right)$	f_l (MPa)	ε_{cc}'	$\left(\frac{\varepsilon_{cc}'}{\varepsilon_{co}}\right)$	ε_1	k_1	μ_{cu}	e_{cu}	w_{cu}
W[±45°]$_2$UD[0°]$_2$	1.0	100.0	106.2	146.8	25.0	0.029	1093.476	0.012	2.52	2.50	2.08	1.69
	2.0	100.0	103.4	140.3	25.0	0.027	1004.842	0.011	2.41	2.39	1.95	1.67
	3.0	100.0	107.9	150.7	25.0	0.030	1128.560	0.012	2.59	2.58	2.12	1.69
	4.0	100.0	99.0	130.0	25.0	0.034	1293.927	0.009	2.23	3.65	2.38	2.59
	AVG	**100.0**	**104.1**	**141.9**	**25.0**	**0.030**	**1130.201**	**0.011**	**2.44**	**2.78**	**2.13**	**1.91**
W[±45°]$_4$UD[0°]$_4$	1.0	100.0	170.8	296.8	46.6	0.050	1935.084	0.015	2.74	3.23	5.89	2.25
	2.0	100.0	150.0	248.6	46.6	0.057	2250.226	0.021	2.30	2.78	5.63	1.82
	3.0	100.0	158.9	269.2	46.6	0.050	1944.112	0.018	2.49	2.78	5.09	1.79
	4.0	100.0	174.2	304.8	46.6	0.091	3653.385	0.015	2.82	6.27	8.25	3.24
	AVG	**100.0**	**163.5**	**279.9**	**46.6**	**0.062**	**2445.702**	**0.017**	**2.59**	**3.76**	**6.22**	**2.27**

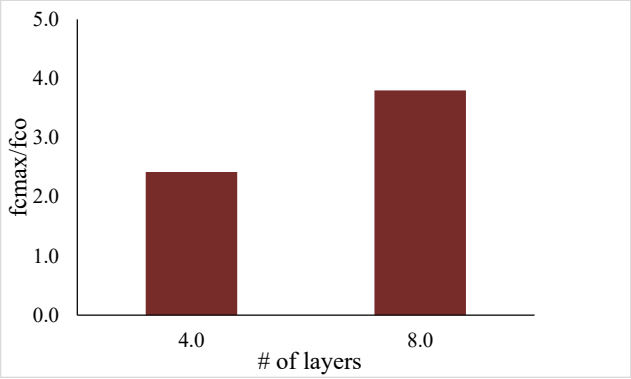

Increase in stress

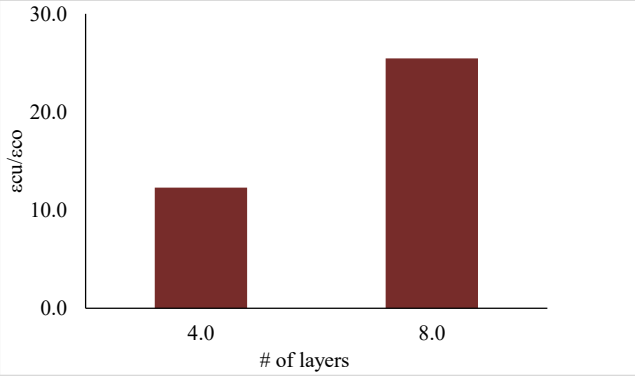

Increase in strain

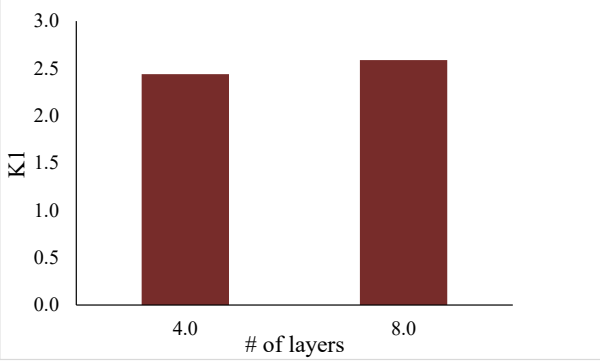

Strength effectiveness

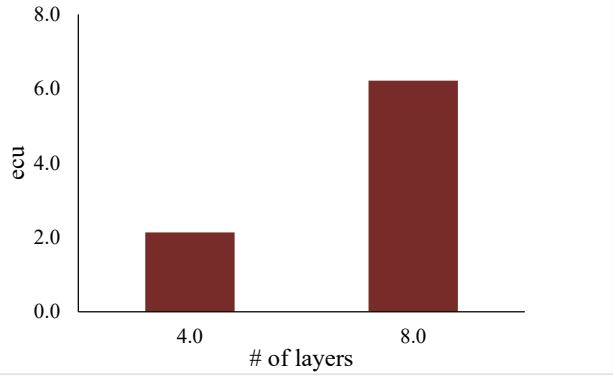

Energy absorption capacity

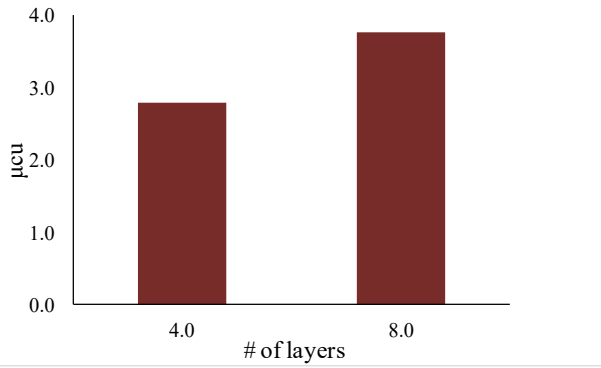

Ductility factor

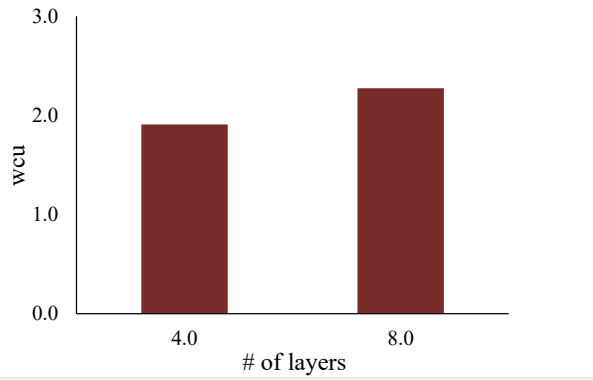

Work index

Figure 5-23 Effect of number of layers on different factors (series 5B (100 mm))

5.3.8 Series 6 (UD [90˚x/0˚x])

Cylinders in this series were confined with unidirectional CFRP sheets placed at 90° and 0°. The series differs from series 2, in that the first set of plies was applied at 90° followed by the remaining set applied at 0° (e.g. for 4 plies: 2 x UD [90°] followed by 2 x UD [0°]). Typical stress-strain plots for this series are shown in **Figure 5-24**, while **Table 5-9** and **Figure 5-26** summarize the various stress-strain parameters for this series. Photos of typical specimens at failure are shown in **Figure 5-25**.

As it is clearly demonstrated in **Figure 5-24**, both maximum strength and strain of specimens confined using the UD [90˚x/0˚x] layup were observed to increase proportionally to the number of CFRP layers. The increase in strength (f'_{cc}/f_{co}) and strain ($\varepsilon'_{cc}/\varepsilon_{co}$) were found to be 145.0% and 1257.0%, 180.8% and 1508.2%, as well as 229.8% and 1684.2%, for cylinders confined with 4, 6, and 8 layers of CFRP, respectively. As previously reported for Series 2, the amount of confinement showed no positive effect on the strength effectiveness factor (k_1), with average values of 2.58, 2.39 and 2.17 reported for specimens with 4, 6 and 8 plies, indicating a loss of confinement efficiency as the number of plies is increased. Energy absorption capacity (e_{cu}) is found to increase proportionally with the number of layers; for example, e_{cu} increased from 2.48 to 4.47 when the number of CFRP layers jumped from 4 to 8 layers. Increasing the number of plies displayed no considerable influence on the ductility factor (μ_{cu}) and work index factor (w_{cu}). Specimens confined with 4, 6, and 8 layers of CFRP presented ductility factors (μ_{cu}) of 2.58, 2.79, and 2.70, respectively. These specimens also exhibited work index factors (w_{cu}) of 1.84, 1.92, and 1.96, respectively.

As with other layups with unidirectional fibers in the hoop direction, **Figure 5-24** shows that the stress-strain response of the specimens follows a parabolic ascending branch with a quasi-linear secondary branch until failure, although the transition is more rounded and not as clearly defined due to the influence of the 90^0 fibers.

Failure of these specimens occurred in a relatively brittle manner with rupture of the CFRP jacket, with disintegration of core concrete and expulsion of particles of crushed concrete at failure. It was noticed that rupture of the CFRP jacket happened in both 90^0 and 0^0 orientations, for all layups in this series. However, the concrete core experienced more damage in specimens with more plies; see **Figure 5-25** which shows more significant release of crushed concrete particles outside the jacket in cylinders with 8 layers of CFRP.

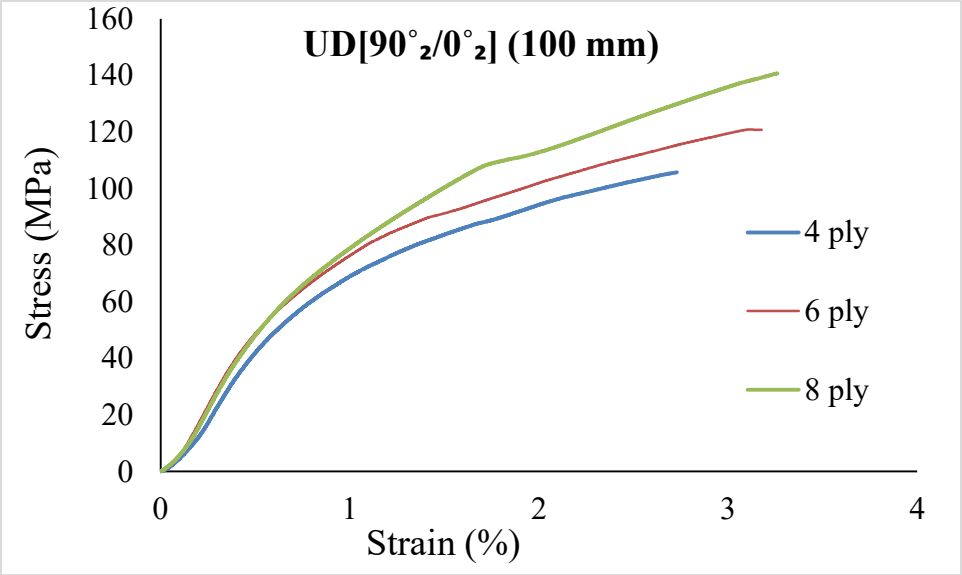

Figure 5-24 Stress-Strain Curves (UD [90˚x/0˚x] 100 mm)

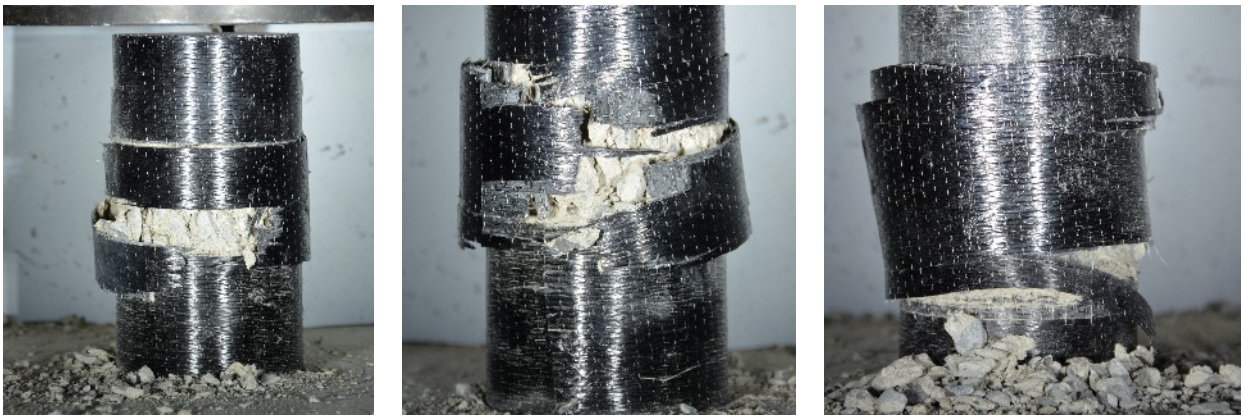

4 layers 6 layers 8 layers

Figure 5-25 Post failure photos of CFRP confined cylinders (series 6 (100 mm))

Table 5-9 Results of specimens tested in series 6

Orientation	Experiment			%Increase in Strength			%Increase in Strain					
	Specimen #	Size(mm)	f_{cc}'	$\left(\frac{f_{cc}'}{f_{co}}\right)$	f_l (MPa)	ε_{cc}'	$\left(\frac{\varepsilon_{cc}'}{\varepsilon_{co}}\right)$	ε_1	k_1	μ_{cu}	e_{cu}	w_{cu}
UD[90°$_2$/0°$_2$]	1.0	100.0	104.7	143.3	24.2	0.032	1228.888	0.013	2.55	2.43	2.37	1.70
	2.0	100.0	100.9	134.5	24.2	0.032	1228.888	0.013	2.39	2.45	2.30	1.72
	3.0	100.0	106.1	146.5	24.2	0.034	1278.334	0.011	2.60	3.06	2.65	2.27
	4.0	100.0	108.7	152.7	24.2	0.034	1300.698	0.015	2.71	2.22	2.58	1.54
	5.0	100.0	106.6	147.8	24.2	0.033	1248.379	0.012	2.63	2.74	2.50	1.96
	AVG	**100.0**	**105.4**	**145.0**	**24.2**	**0.033**	**1257.037**	**0.013**	**2.58**	**2.58**	**2.48**	**1.84**
UD[90°$_3$/0°$_3$]	1.0	100.0	121.6	182.7	32.5	0.035	1324.087	0.011	2.42	3.02	3.09	2.21
	2.0	100.0	122.6	184.8	32.5	0.039	1498.482	0.021	2.45	1.83	3.17	1.22
	3.0	100.0	108.0	150.9	32.5	0.037	1410.053	0.014	2.00	2.60	2.46	1.61
	4.0	100.0	129.8	201.6	32.5	0.047	1821.830	0.014	2.67	3.29	4.06	2.20
	5.0	100.0	122.2	184.0	32.5	0.039	1486.787	0.012	2.43	3.22	3.45	2.35
	AVG	**100.0**	**120.8**	**180.8**	**32.5**	**0.039**	**1508.248**	**0.015**	**2.39**	**2.79**	**3.25**	**1.92**
UD[90°$_4$/0°$_4$]	1.0	100.0	137.6	219.8	45.7	0.047	1829.421	0.021	2.07	2.29	4.53	1.60
	2.0	100.0	141.1	227.8	45.7	0.041	1576.652	0.016	2.15	2.54	4.23	1.87
	3.0	100.0	148.8	245.8	45.7	0.043	1680.878	0.016	2.32	2.73	4.72	1.99
	4.0	100.0	142.9	232.0	45.7	0.040	1555.724	0.015	2.19	2.70	4.14	1.94
	5.0	100.0	139.3	223.7	45.7	0.046	1778.539	0.014	2.11	3.25	4.74	2.42
	AVG	**100.0**	**141.9**	**229.8**	**45.7**	**0.043**	**1684.243**	**0.016**	**2.17**	**2.70**	**4.47**	**1.96**

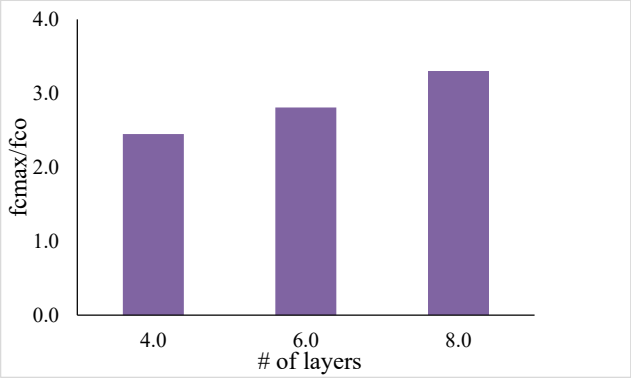

Increase in stress

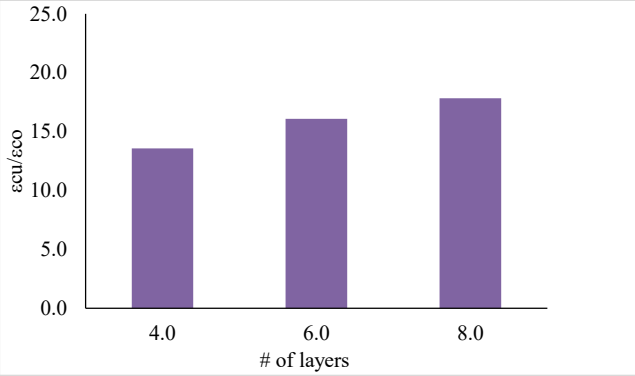

Increase in strain

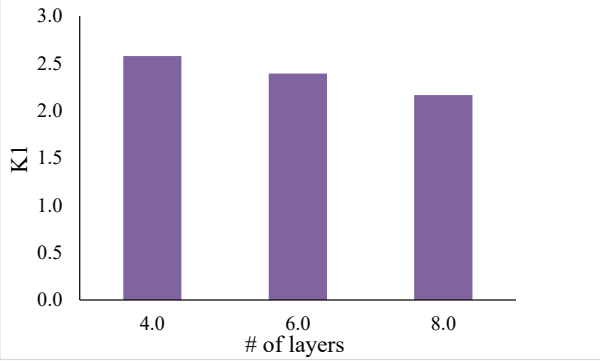

Strength effectiveness

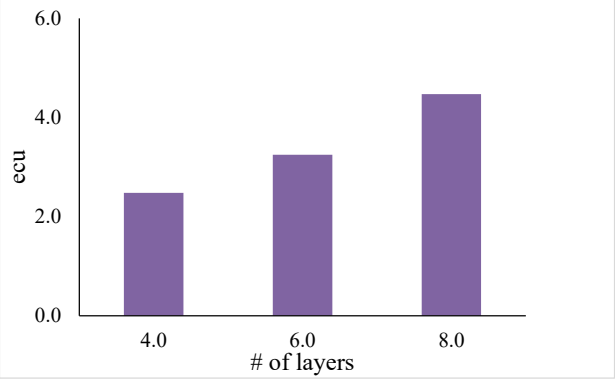

Energy absorption capacity

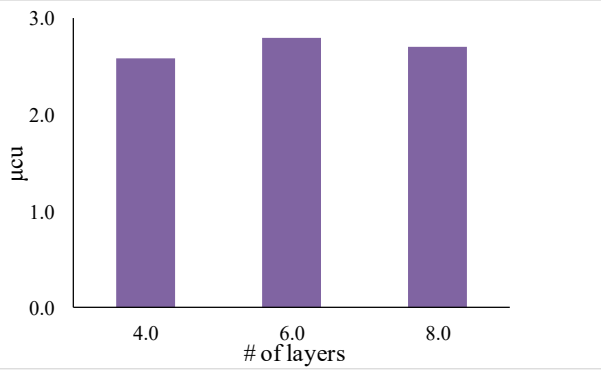

Ductility factor

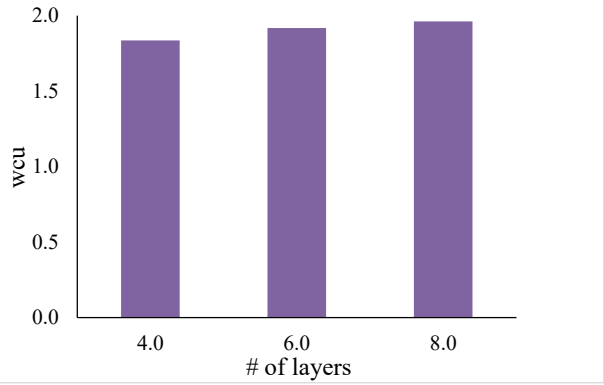

Work index

Figure 5-26 Effect of number of layers on different factors (series 6 (100 mm))

5.3.9 Series 7 (W [±45˚])

The W [±45˚] series was the last series investigated in this research program. Specimens in this series were confined with 4, 6, or 8 layers of woven ±45° CFRP fabric (differs from Series 3 in that woven fibers are used in this series). Typical stress-strain plots for specimens having 4, 6 and 8 layers of woven CFRP are shown in **Figure 5-27**, while **Table 5-10** and **Figure 5-29** summarize the various stress-strain parameters for this series. Photos of typical specimens at failure are shown in **Figure 5-28**.

As with Series 3, a large increase in maximum strain was expected for specimens in this series, while the increase in maximum stress was expected to be negligible. Cylinders wrapped with 4 layers of CFRP showed a small enhancement in strength (f'_{cc}/f_{co}) of roughly 1.7%, while a considerable increase in strain ($\varepsilon'_{cc}/\varepsilon_{co}$) of 1567.7% was reached. The percent increase in strength and strain were 14.8% & 5767.1% for cylinders with 6 layers, and 31.2% & 6240.2% for cylinders with 8 layers. One can note a significant increase in strain capacity when going from 4 to 6 layers, an indicator that provision 4 layers of woven CFRP may not be the optimal amount of confinement to achieve satisfactory performance with woven angular fibers. The strength effectiveness factor (k_1) obtained in the W [±45˚] series is less than 1 for this series (except when cylinder is confined with 8 layers of CFRP) which further indicates that this fiber configuration has a negligible influence on strength enhancement; that is, while the woven CFRP have some tensile resistance (see coupon test results), this tensile resistance does not result in a confining pressure (f_l) which significantly contributes to enhancing strength, particular when a lower amount of plies are applied.

The provision of W [±45˚] CFRP resulted in a significant enhancement in energy absorption and ductility, which improved as the number of plies was increased. For example, energy absorption capacity (e_{cu}) for cylinders confined with 4, 6 and 8 layers reached average values of 1.47, 5.56, and 7.43, respectively. The added confinement also improved the work index (w_{cu}) and ductility factor (μ_{cu}) as the number of layers increased from 4 to 6, while both factors showed small increases as the number of layers went from 6 to 8 (see **Table 5-10** and **Figure 5-29**).

Figure 5-27 shows that peak stress, overall toughness and ductility improved proportionally with the number of layers, with a significant increase in strain capacity as the number of plies went from 4 to 6, and a lesser effect as the number of plies went from 6 to 8. It is noted that the stress-strain response is different than in other series, with a load drop after the first branch followed by a plateau, which turns into another ascending branch in the case of specimens with 6 and 8 plies (it is noted that the failure stress is higher than the first peak in the case of 8 plies). It is also noted that the drop in stress after the first branch was not observed in the companion series with unidirectional 45˚ fibers.

All specimens in this series showed ductile and gradual failures. Failure of the jacket occurred along the entire height of the specimens and the tear line seemed to be more vertical (and not at 45˚) when compared to failures observed in Series 3 (compare **Figure 5-28** and **Figure 5-10**). It was also noticed that the concrete core experienced more damage in cylinders with more layers (see **Figure 5-28**).

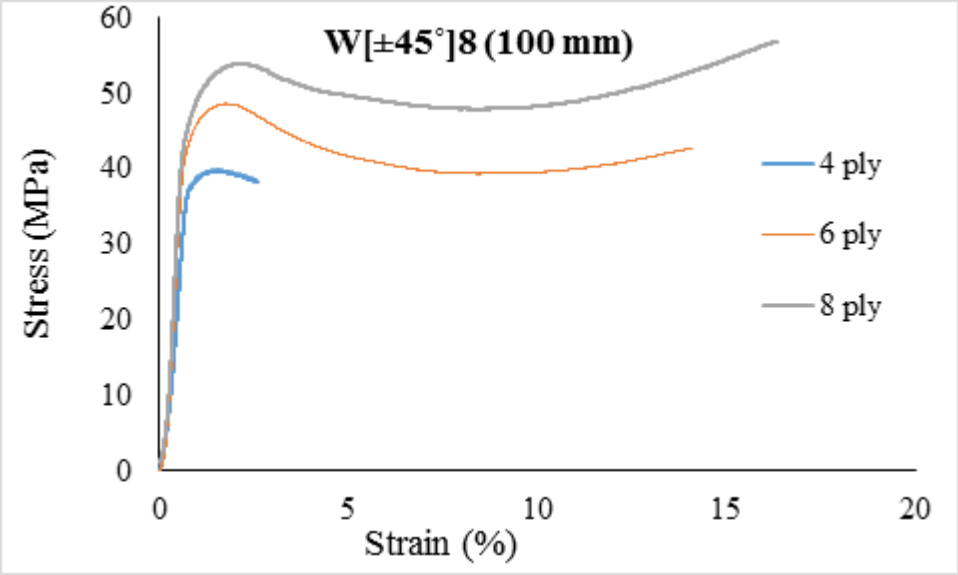

Figure 5-27 Stress-Strain Curves (W [±45°] 100 mm)

4 layers 6 layers 8 layers

Figure 5-28 Post failure photos of CFRP confined cylinders (series 7 (100 mm))

Table 5-10 Results of specimens tested in series 7

Orientation	Experiment			%Increase in Strength			%Increase in Strain					
	Specimen #	Size(mm)	f_{cc}'	$\left(\frac{f'_{cc}}{f_{co}}\right)$	f_l (MPa)	ε_{cc}'	$\left(\frac{\varepsilon'_{cc}}{\varepsilon_{co}}\right)$	ε_1	k_1	μ_{cu}	e_{cu}	w_{cu}
W[±45°]$_4$	1.0	100.0	42.1	-2.2	5.7	0.028	1033.361	0.009	-0.16	3.25	0.95	2.67
	2.0	100.0	41.5	-3.5	5.7	0.039	1496.430	0.009	-0.26	4.25	1.33	3.49
	3.0	100.0	48.3	12.2	5.7	0.039	1492.121	0.007	0.92	5.58	1.49	4.45
	4.0	100.0	43.1	0.2	5.7	0.057	2248.995	0.008	0.02	7.42	2.09	6.28
	AVG	**100.0**	**43.8**	**1.7**	**5.7**	**0.041**	**1567.727**	**0.008**	**0.13**	**5.13**	**1.47**	**4.22**
W[±45°]$_6$	1.0	100.0	46.9	9.0	8.6	0.166	6719.040	0.013	0.45	13.28	6.26	10.68
	2.0	100.0	55.2	28.3	8.6	0.137	5511.202	0.007	1.41	18.63	5.52	13.61
	3.0	100.0	48.6	13.0	8.6	0.143	5783.668	0.008	0.65	18.82	5.84	15.76
	4.0	100.0	46.9	9.1	8.6	0.125	5034.387	0.008	0.45	15.22	4.63	12.00
	AVG	**100.0**	**49.4**	**14.8**	**8.6**	**0.143**	**5762.074**	**0.009**	**0.74**	**16.49**	**5.56**	**13.01**
W[±45°]$_8$	1.0	100.0	56.9	32.3	11.5	0.167	6732.171	0.010	1.21	16.90	8.23	14.67
	2.0	100.0	62.0	44.2	11.5	0.182	7367.788	0.009	1.65	20.99	9.31	17.31
	3.0	100.0	54.6	26.8	11.5	0.176	7104.555	0.009	1.01	19.15	8.20	16.39
	4.0	100.0	52.3	21.6	11.5	0.094	3756.381	0.008	0.81	12.50	3.98	10.12
	AVG	**100.0**	**56.5**	**31.2**	**11.5**	**0.155**	**6240.224**	**0.009**	**1.17**	**17.38**	**7.43**	**14.62**

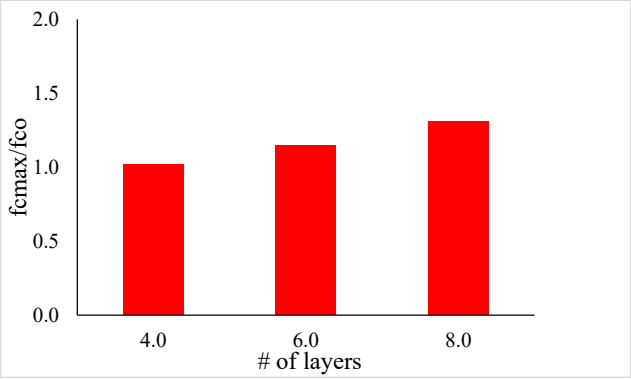

Increase in stress

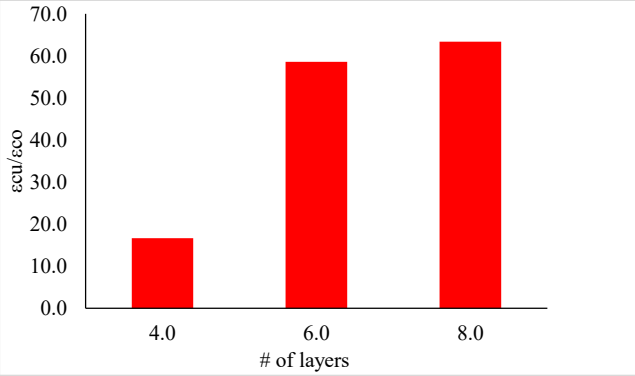

Increase in strain

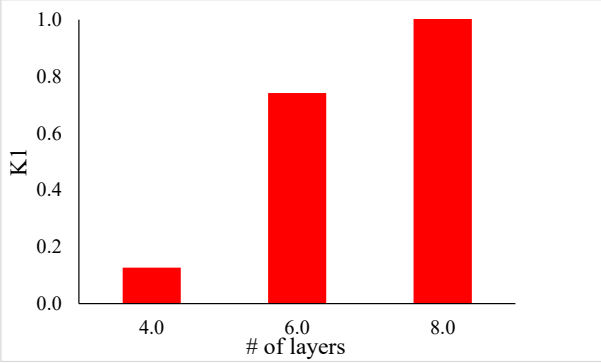

Strength effectiveness

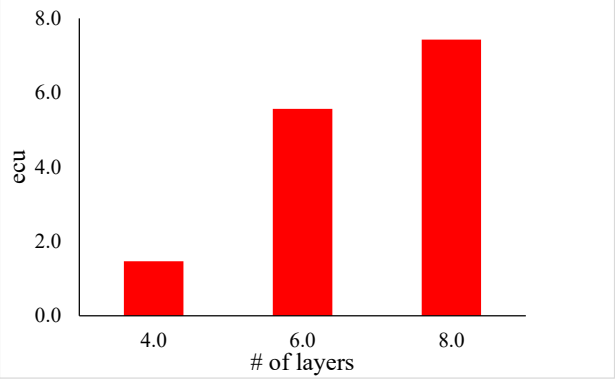

Energy absorption capacity

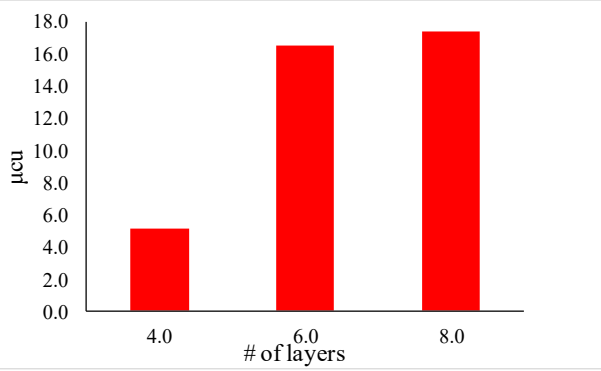

Ductility factor

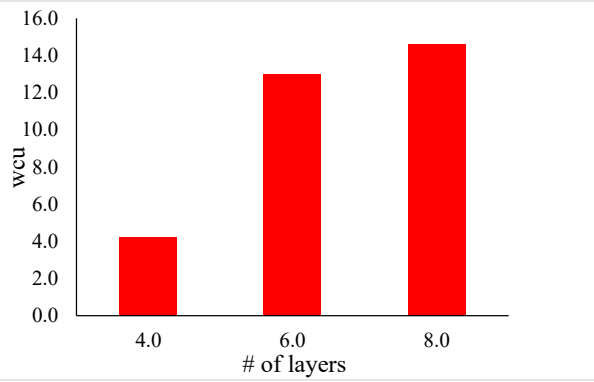

Work index

Figure 5-29 Effect of number of layers on different factors (series 7 (100 mm))

5.4 Overall summary - effect of number of layers

As discussed in the foregoing sections, the stress-strain behavior of the unconfined concrete was altered and improved with the provision of CFRP confinement, and the number of CFRP plies had a strong influence on this improvement. However, fiber orientation and stacking sequence had a considerable effect on the effect of the number of layers on stress-strain response. **Figure 5-30a** demonstrates that, ignoring the fiber orientation and stacking sequence, all specimens gained strength when the number of CFRP plies was increased, although specimens confined with hoop direction fibers (0°) displayed the largest enhancement in strength. Likewise, strain capacity was affected by the number of CFRP layers in all series; however, **Figure 5-30b** shows that specimens confined with angular fibers (±45°) achieved the maximum enhancement in strain resistance as the number of plies was increased. **Figure 5-30c** shows that number of plies did not have a significant influence on the strength effectiveness factor (k_1), which fluctuated between 2 and 3. An exception was noted in specimens confined with woven angular fibers (±45°) that displayed a k_1 less than 1. **Figure 5-30d** illustrates that the energy absorption capacity factor (e_{cu}) generally improved when the amount of confinement layers was increased from 4 to 6 layers, where it almost doubled in most series (with an even greater enhancement for Series 1), and experienced relatively smaller increase when the number of layers went up to 8 layers. This observation demonstrates that there is an optimal amount of layers for each CFRP layup configuration, beyond which improvements in mechanical performance do not justify increased costs associated with applying additional layers of CFRP. The number of layers exhibited some impact on the ductility factor (μ_{cu}) and the work index (w_{cu}), similar to the observations that were noted for energy absorption capacity, although the trends are sometimes conflicting and less clear for these parameters. The effect of number of layers on both ductility factor and work

index were more pronounced in cylinders with 6 layers of CFRP, except for series 1 and series 4B which showed decrease in these parameters when the number of layers were increased (see **Figure 5-30e & f**).

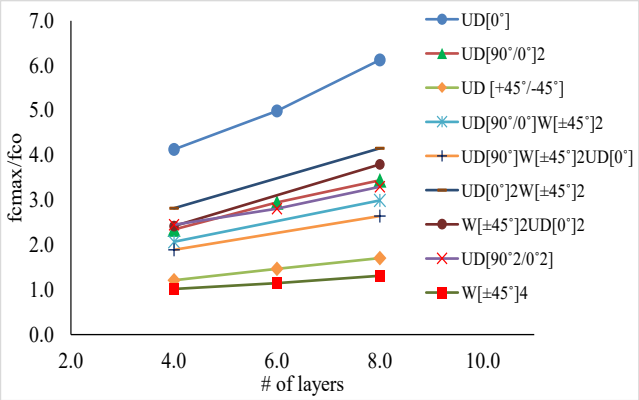

a) Stress ratio

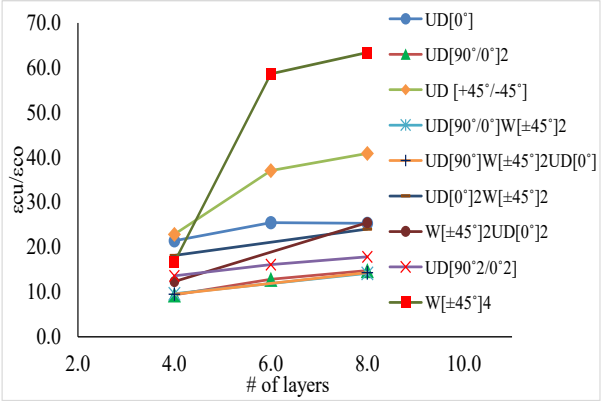

b) Strain ratio

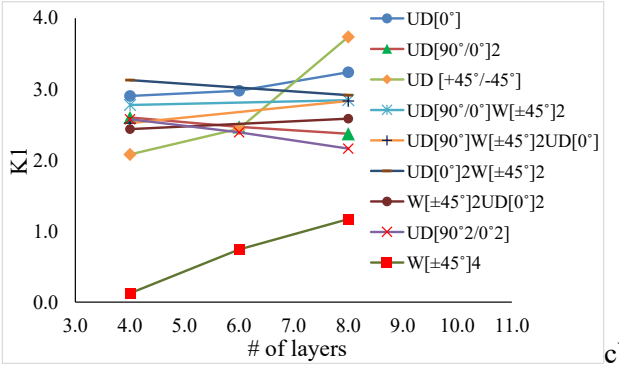

c) Strength effectiveness

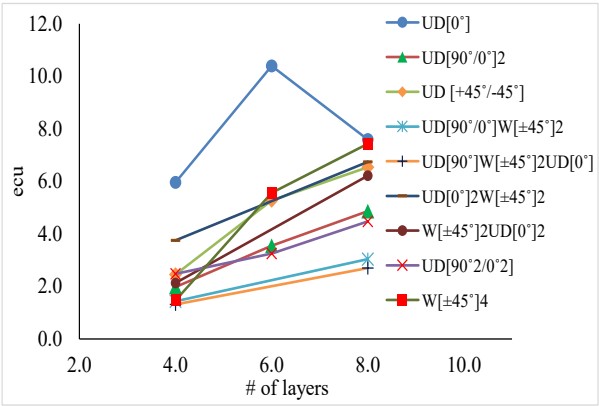

d) Energy absorption capacity

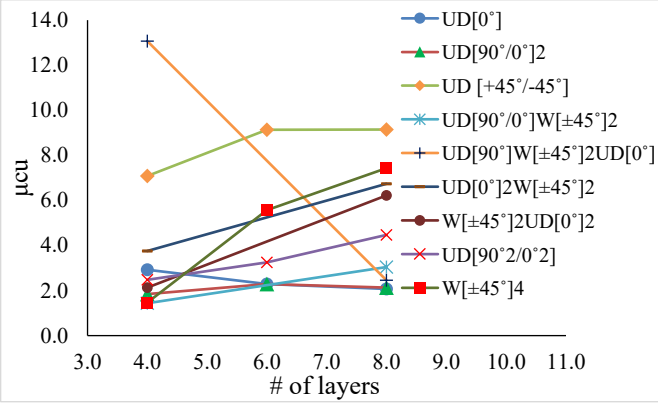

e) Ductility factor

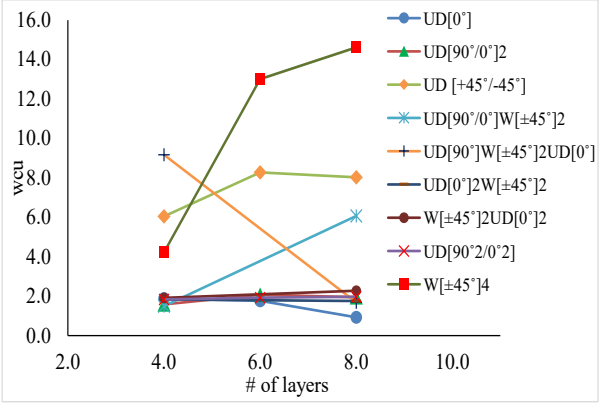

f) Work index

Figure 5-30 Effect of number of layers on different stress-strain parameters

5.5 Size effect

In this section effect of size on the stress-strain behavior of the CFRP confined cylinders is examined by comparing the stress-train response of the "small" (100 mm) and "large" (150 mm) specimens in each series.

5.5.1 Series 1 (UD [0˚])

Figure 5-31 clearly shows that the effectiveness of confinement on the increase in strength and strain of CFRP wrapped cylinders decreases as the specimen size is increased. For example, “small” size specimens confined with 4 layers of CFRP showed an increase in strength (f'_{cc}/f_{co}) of 313.41% while “large” size specimens with the same amount of confinement had a strength improvement of roughly 212.90%, which is over 100% above the gain in strength observed for the “large” size specimens. This fact is due to inversely relationship of CFRP lateral confining pressure ($f_l = 2.f_{FRP}.n_{FRP}/D$) to the diameter of the cylinder.

In terms of the effect on strain capacity, “small” size specimens confined with 4, 6, and 8 layers of CFRP showed average percent increases in strain ($\varepsilon'_{cc}/\varepsilon_{co}$) of approximately 2043.17%, 2447.02%, and 2427.14% respectively, while “large” size specimens confined with same amount of CFRP showed average increases of about 1139.60%, 1769.44%, and 2098.69%, respectively. These values demonstrate that the “small” size specimens gained more strain capacity when compared to companion “large” size specimens. It’s worth noting that increasing the number of plies from 6 to 8 did not result in further enhancement in strain for the “small” size cylinders, while the increase in strain is more significant in the case of the companion “large” size specimens, which indicates that the "optimal" number of CFRP plies varies based on cross-section size (i.e. 6 plies may be optimal for 100 mm, whereas 8 plies may be justified at 150 mm).

An insignificant variation was observed between the different specimen sizes in the cases of strength effectiveness factor (k_1). In the case of energy absorption capacity (e_{cu}) “small” size cylinders showed better performance as it is obvious from the results presented in **Table 5-1**. The “large” size specimens showed more "ductile" performance when evaluated quantitatively with the ductility factor (μ_{cu}), although this is not as clear when qualitatively examining the stress-strain curves. For example “small” size cylinders confined with 4, 6, and 8 layers of CFRP sheets experienced ductility factors of 2.92, 2.29, and 2.07 respectively. However, “large” size cylinders with same amount of confinement showed ductility factors of 2.61, 3.42, and 3.23 respectively. In the case of work index (w_{cu}), better results were achieved by “large” size specimens. For example, work index factors of 1.87, 1.76, and 1.24 were obtained by “small” size cylinders, while work index factors of 1.75, 1.53, and 2.04 were achieved by “large” size specimens confined with 4, 6, and 8 layers of CFRP respectively.

Based on the experimental results presented in **Table 5-1**, one can see that the size effect for CFRP placed in a UD [0˚] configuration is more clear and significant when evaluated in terms of the percentage increase in maximum stress and strain

It can be seen in **Figure 5-32** that no significant differences were observed in the mode failure of the “small” and “large” size specimens which sudden and explosive failures. During testing it was noticed that more time was needed to cause failure in the “large” size specimens, which is to be expected, since more length of CFRP needs to rupture before the cylinder fail.

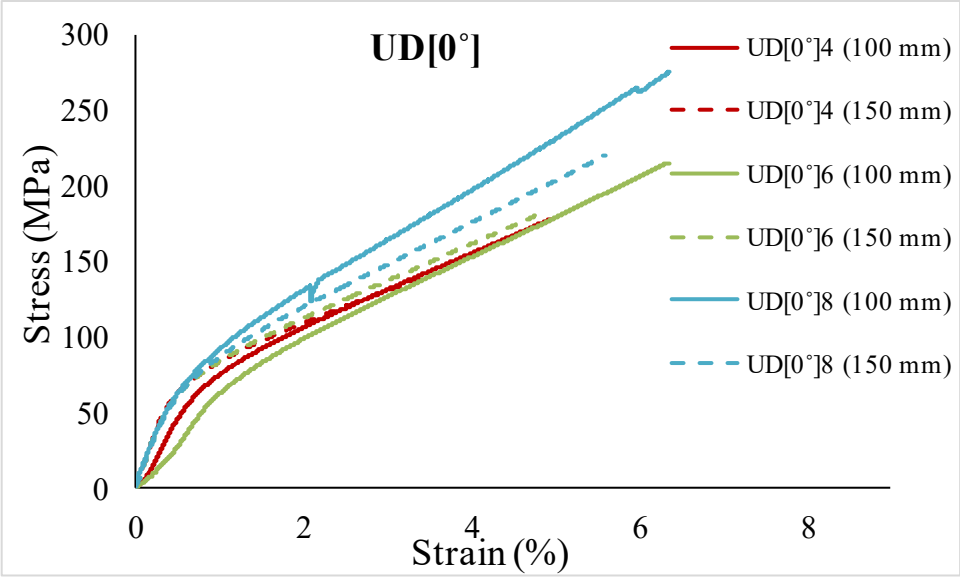

Figure 5-31 Size effect on confined specimens with UD [0˚] fiber configuration

4 Layers (100mm) | 6 Layers (100mm) | 8 Layers (100mm)

4 Layers (150mm) | 6 Layers (150mm) | 8 Layers (150mm)

Figure 5-32 Post failure photos of "small" and "large" size confined cylinders

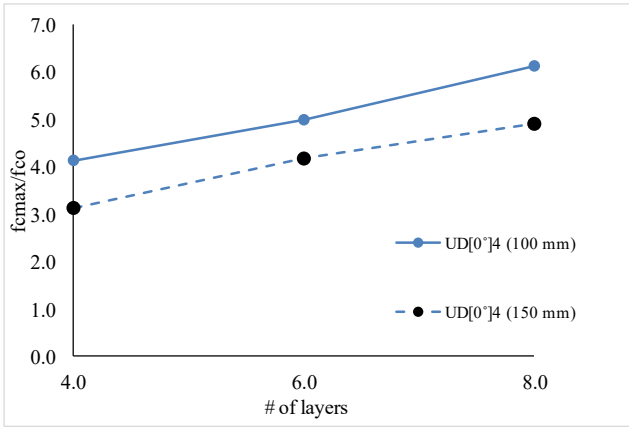

a) Stress ratio

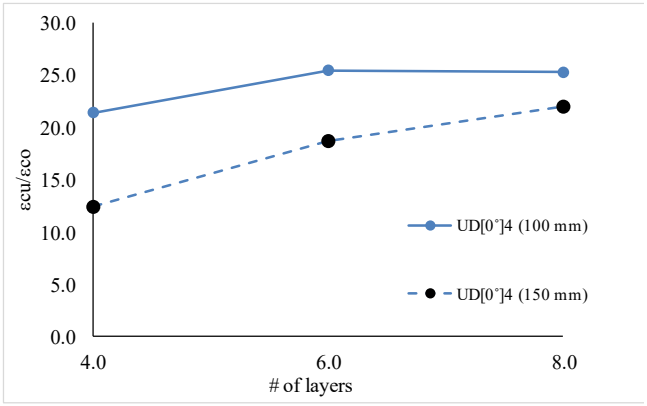

b) Strain ratio

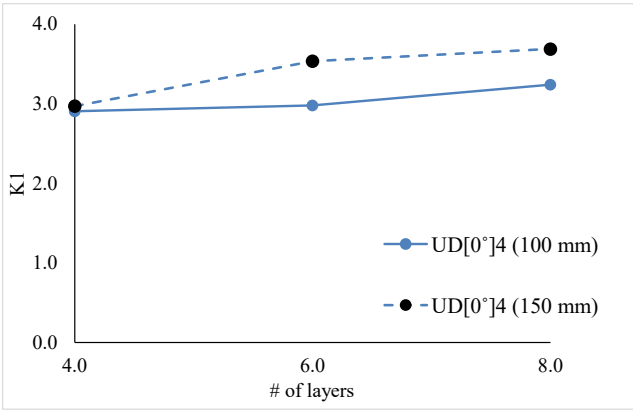

c) Strength effectiveness

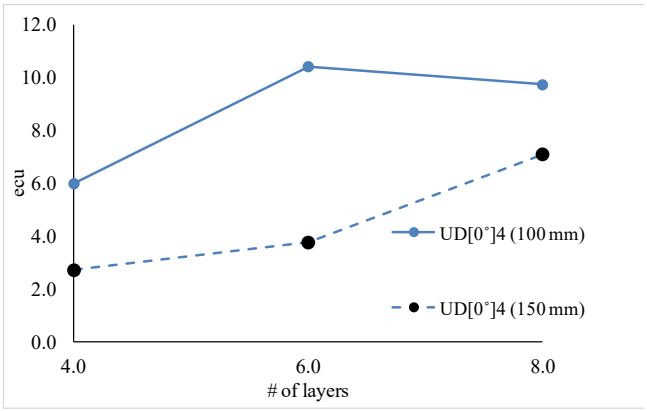

d) Energy absorption capacity

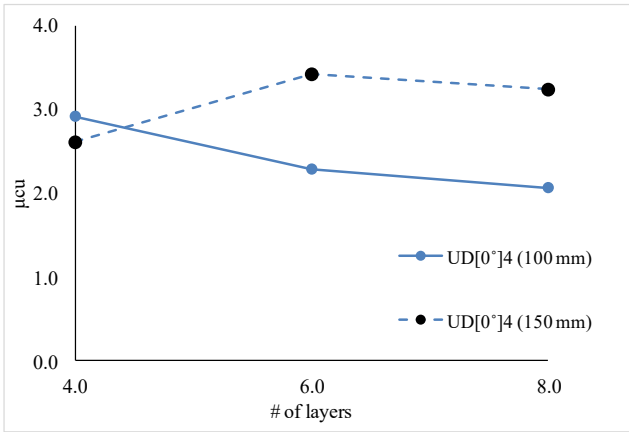

e) Ductility factor

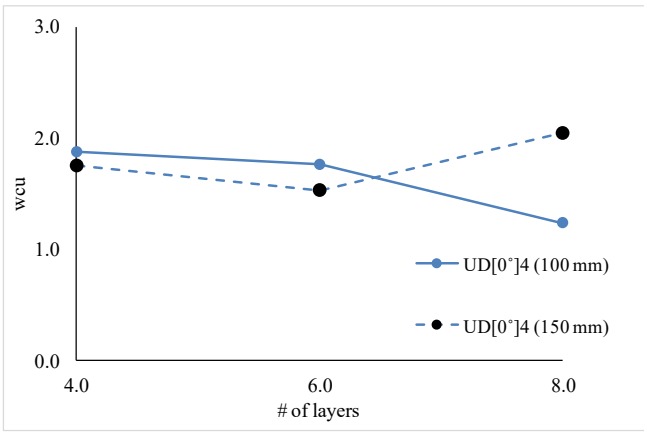

f) Work index

Figure 5-33 Size effect on different stress-strain parameters (Series 1)

5.5.2 Series 2 (UD [90˚/0˚])

As with Series 1, **Figure 5-34** shows that the relative increase in strength of the CFRP wrapped cylinders in Series 2 decreases with an enlargement of the specimen size. For example, "small" size specimens confined with 4 layers of CFRP showed an increase in strength (f'_{cc}/f_{co}) of 134.44% while "large" size specimens with the same amount of confinement had a strength improvement of roughly 96.38%, which is 38% lower than the gain in strength observed for the "small" size specimens. Similar results are observed for the increase in strain; "small" size specimens with 4, 6, and 8 layers of CFRP show average percent increases in strain ($\varepsilon'_{cc}/\varepsilon_{co}$) of 836.72%, 1183.87%, and 1377.14% respectively, while "large" size specimens confined with same amount of CFRP showed average increase of 743.80%, 824.23%, and 954.05, respectively. These values demonstrate that the "small" size specimens showed greater strain capacity when compared to companion "large" size specimens.

An insignificant variation was observed between the different specimen sizes in the cases of strength effectiveness factor (k_1). In the case of energy absorption capacity (e_{cu}) "small" size cylinders showed better performance as shown in **Table 5-1** and **Figure 5-33**. When the ductility is evaluated using the ductility factors (μ_{cu}), the "large" size specimens show more ductile performance. For example "small" size cylinders confined with 4, 6, and 8 layers of CFRP sheets experienced ductility factors of 1.84, 2.29, and 2.13, while "large" size cylinders with same amount of confinement showed ductility factors of 2.12, 2.08, and 2.98, respectively. A similar observation is made when examining the work index (w_{cu}), where better results are achieved by the "large" size specimens. For example, work index factors of 1.58, 2.07, and 1.95 were obtained by "small" size cylinders, while values of 2.95, 3.06, and 2.11 were achieved by "large" size specimens confined with 4, 6, and 8 layers of CFRP, respectively.

Based on the experimental results presented in **Table 5-1** and **Figure 5-36**, one can see that the size effect for CFRP placed in a UD [90˚/0˚] configuration is more clear and significant when evaluated in terms of the percentage increase in maximum stress and strain.

In terms of the effect of size on failure mode, **Figure 5-35** shows that the "large" size specimens experienced more damage in the jacket and concrete core, with the damage in the 150 mm cylinders becoming somewhat more significant as the number of CFRP layers reached 8.

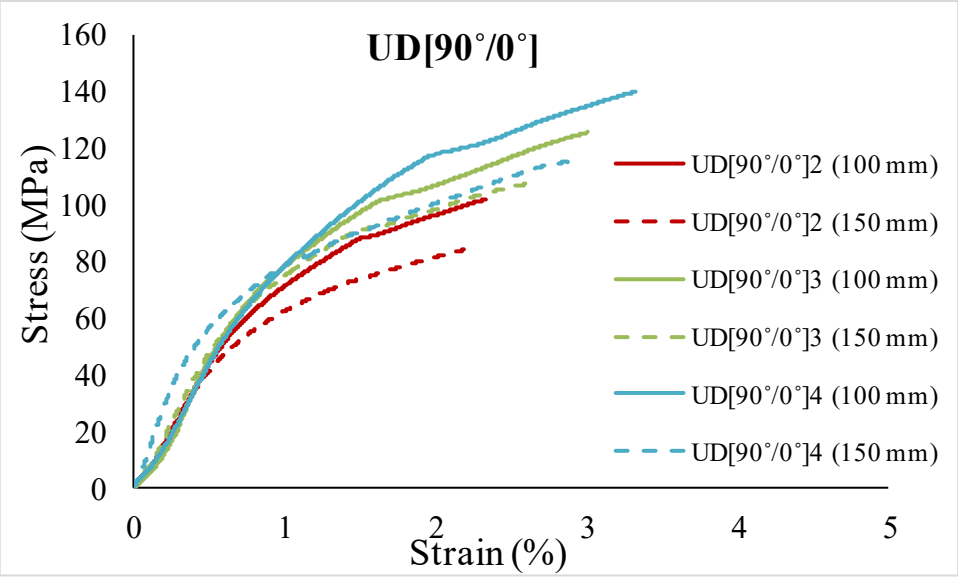

Figure 5-34 Size effect on confined specimens with UD [90˚/0˚] fiber configuration

4 layers (100mm) 6 Layers (100mm) 8 Layers (100mm)

4 Layers (150mm) 6 Layers (150mm) 8 Layers (150mm)

Figure 5-35 Post failure photos of "small" and "large" size confined cylinders

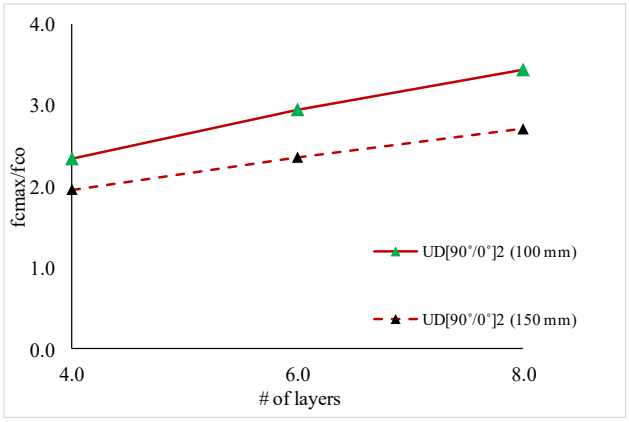

a) Stress ratio

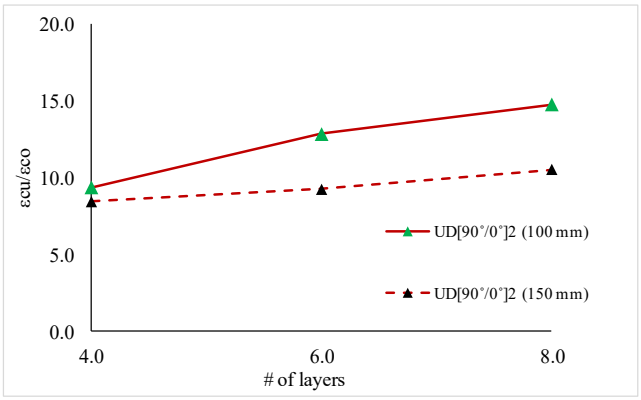

b) Strain ratio

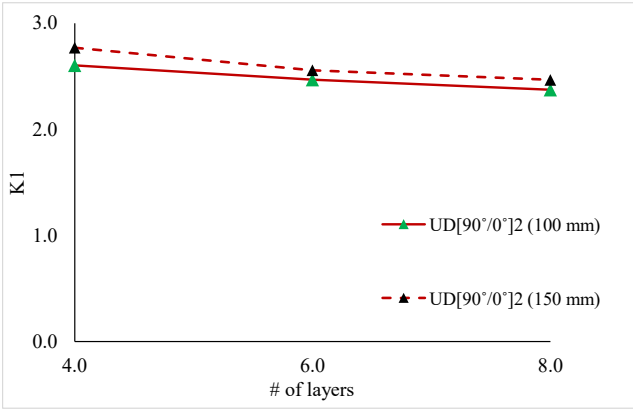

c) Strength effectiveness

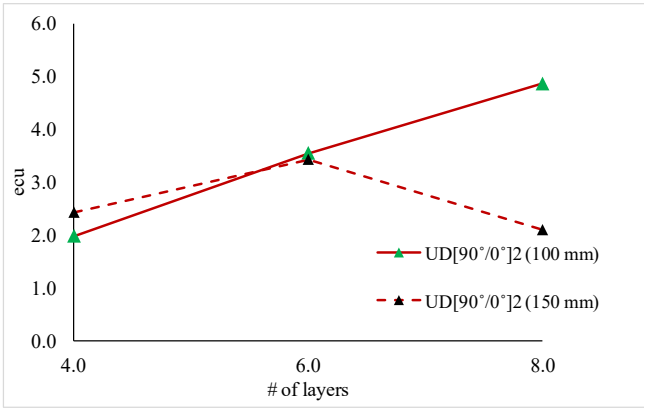

d) Energy absorption capacity

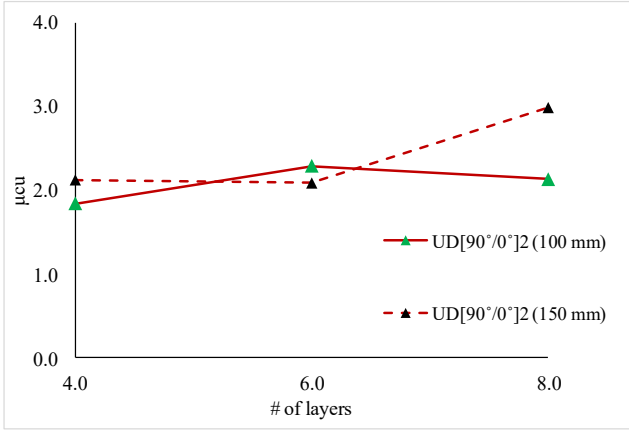

e) Ductility factor

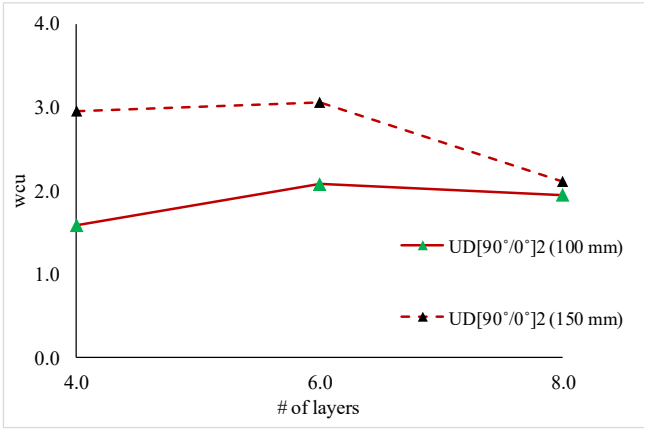

f) Work index

Figure 5-36 Size effect on different stress-strain parameters (Series 2)

5.5.3 Series 3 (UD [+45˚/-45˚])

Although strength enhancement was less significant in Series 3, where confinement was provided by fibers in a UD [+45˚/-45˚] orientation, the relative increase in strength decreased as the specimen size went from 100 to 150 mm. For example, "small" size specimens confined with 6 layers of CFRP exhibited an increase in strength (f'_{cc}/f_{co}) of 47.02 %, while "large" size cylinders confined with the same amount of CFRP had an increase in strength of 28.07%. A similar trend is found in the case of the increase in strain ($\varepsilon'_{cc}/\varepsilon_{co}$); as shown in **Figure 5-37**, "small" size specimens more strain capacity when compared to companion "large" size cylinders, regardless of the number of CFRP layers.

No reliable trend emerges when examining the effect of size on the strength effectiveness factor (k_1). In the case of energy absorption capacity (e_{cu}) "small" size cylinders showed better performance as it is obvious from the results presented in **Table 5-1** and **Figure 5-39**. In the case of the work index (w_{cu}), different results are observed for companion cylinders confined with 4 layers of CFRP, while companion cylinders with 6 and 8 layers have similar results. For example, work index factors of 6.04, 8.28, and 8.03 were obtained for "small" size cylinders, while the corresponding factors were 5.10, 8.50, and 8.71 for "large" size companions with 4, 6, and 8 layers of CFRP. The "large" size specimens confined with 4 layers of CFRP showed less ductile performance compare to "small" size companion, when ductility is evaluated using the ductility factors (μ_{cu}). However, the values are similar in the case of companion small/large specimens with 6 and 8 layers of CFRP. For example "small" size cylinders confined with 4, 6, and 8 layers of CFRP sheets experienced ductility factors of 7.08, 9.14, and 9.15 while "large" size companions showed ductility factors of 4.85, 9.60, and 9.58, respectively. **Figure 5-38** shows that no important difference is observed in the mode failure of the "small" and "large"

size specimens in this series, with ductile and gradual failures for all cylinders owing to the provision of angular fibers. In all cases final failure was associated with diagonal tearing of CFRP sheets along specimen height, regardless of the cylinder size and the number of layers.

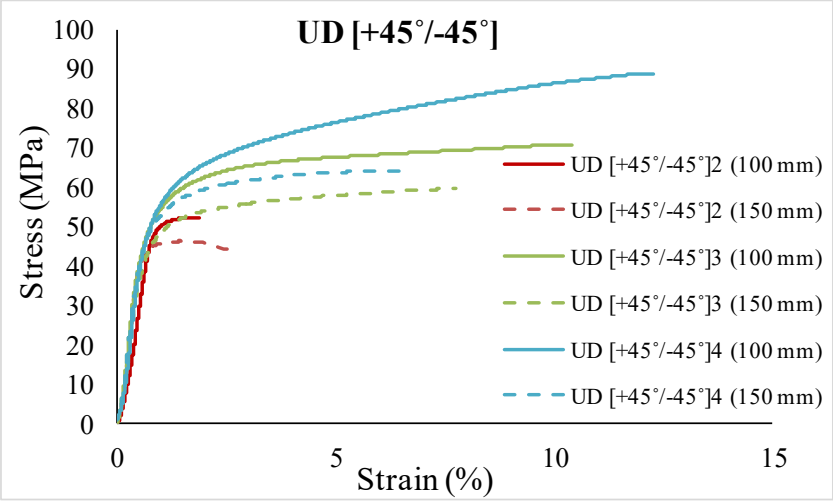

Figure 5-37 Size effect on confined specimens with UD [+45°/-45°] fiber configuration

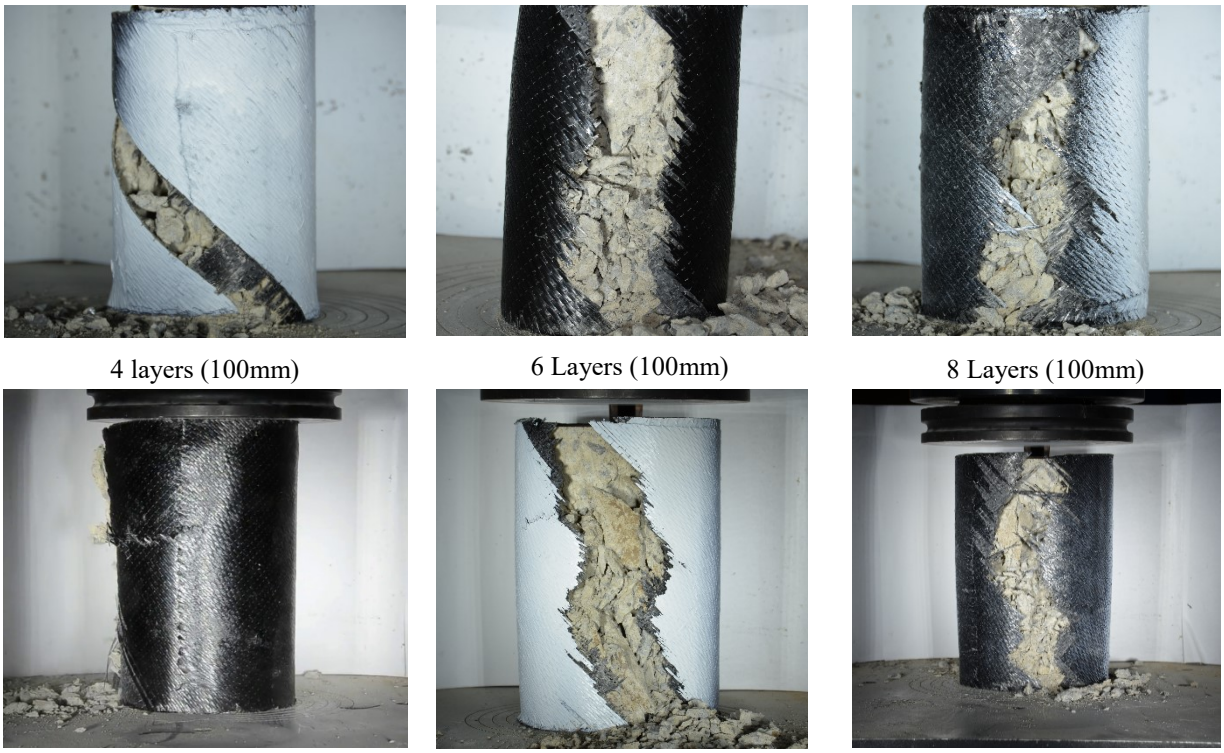

Figure 5-38 Post failure photos of "small" and "big" size confined cylinders

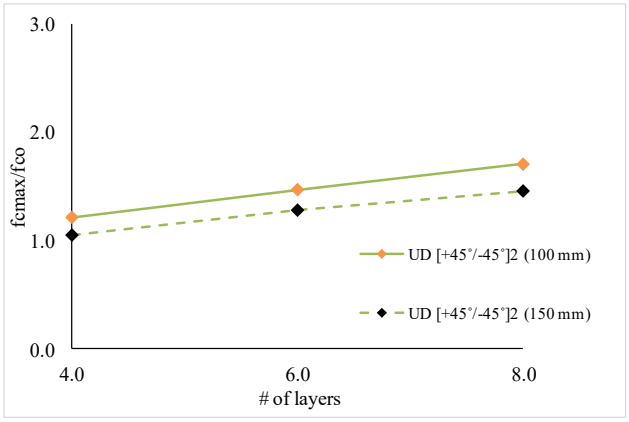

a) Stress ratio

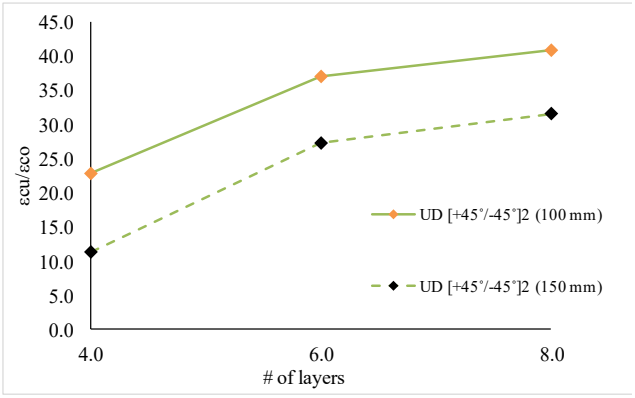

b) Strain ratio

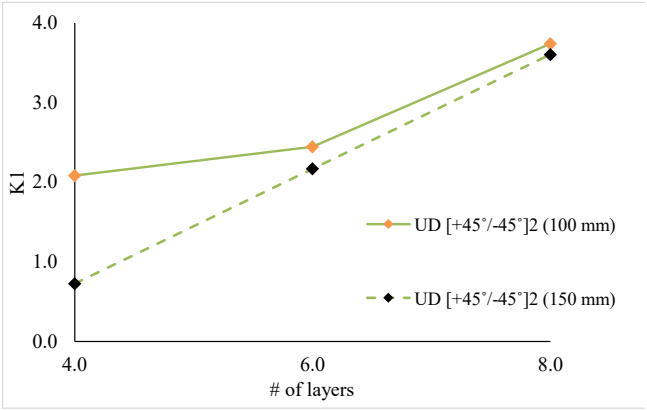

c) Strength effectiveness

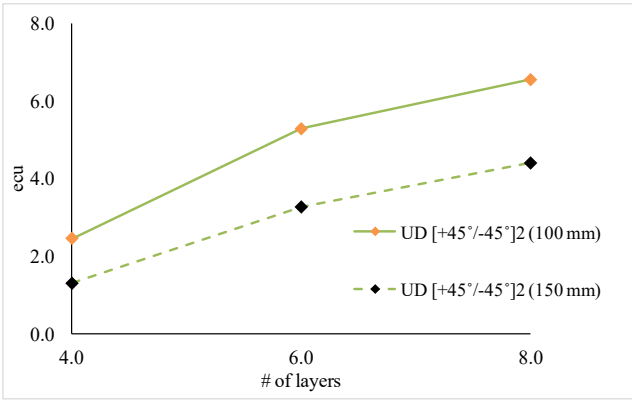

d) Energy absorption capacity

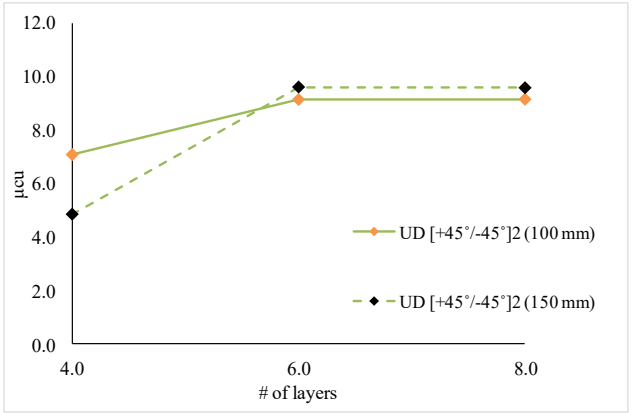

e) Ductility factor

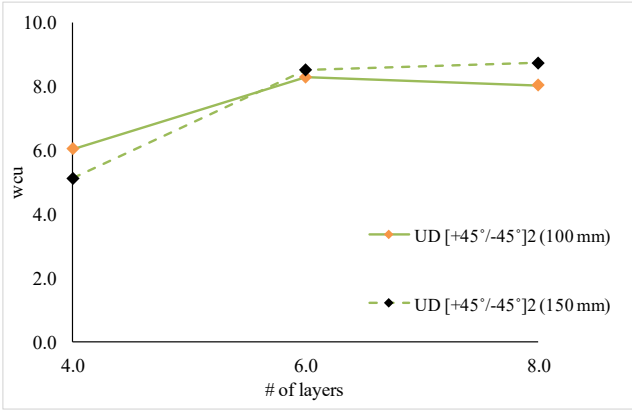

f) Work index

Figure 5-39 Size effect on different stress-strain parameters (Series 3)

5.5.4 Series 4A (UD [90˚/0˚] W [±45˚])

Continuing with the trends observed in Series 1-2, **Figure 5-40** shows that the effectiveness of confinement on strength decreases with an expansion of specimen size for cylinders confined with the UD [90˚/0˚] W [±45˚] stacking sequence. For example in terms of the effect on strength, "small" size specimens confined with 4 layers of CFRP showed a f'_{cc}/f_{co} ratio of 107.14% while companion "large" size cylinders had an average strength improvement of 67.31%, a relative reduction of 40% with the increase in specimen size.

Increase in strain ($\varepsilon'_{cc}/\varepsilon_{co}$) in "small" size specimens was proportional to number of CFRP layers, while the same ratio decreases by increasing the number of CFRP layers in the "large" size specimens. For instance, "small" specimens confined with 4 and 8 layers of CFRP show average strain ratios ($\varepsilon'_{cc}/\varepsilon_{co}$) of 859.58% and 1316.19%, while "large" size cylinders confined with same amount of CFRP show ratios of 759.80% and 694.25%, respectively.

As in the previous series, no significant no significant trend related to size effect is observed when comparing the strength effectiveness factors (k_1).

In the case of energy absorption capacity (e_{cu}), "small" size cylinders showed better overall toughness as seen **Table 5-1**. For example, in "small" size cylinders energy absorption capacity is increased from 1.43 to 3.04 by increasing the number of layers from 4 to 8, while in "large" size cylinders this factor increased from 1.08 to 1.32 for the same amount of confinement. Furthermore, "small" cylinders showed a relative increase in energy absorption as more layers of CFRP were added, while the "large" size cylinders experienced insignificant change in energy absorption capacity with the increase in number of layers. When toughness is normalized and evaluated in terms of the work index (w_{cu}), better results are achieved for "large" vs. "small"

size specimens with 4 layers of CFRP, however, the trend is reversed at 8 layers. For example, work index factors of 1.49 and 6.06 were obtained for the “small” size cylinders with 4 and 8 layers of CFRP, while the corresponding factors were 1.80 and 1.50 for companion “large” cylinders.

The ductility factor (μ_{cu}) increases proportionally with the number of layers in the “small” size cylinders, while no significant change is observed in the "large" cylinders as the number of plies is increased. For example “small” size cylinders confined with 4 and 8 layers of CFRP sheets experienced ductility factors of 2.17 and 8.90, while “large” size cylinders with same amount of confinement showed ductility factors of 2.50 and 2.19 respectively.

Based on the experimental results presented in **Table 5-1** and **Figure 4-18**, one can see that the size effect for CFRP placed in a UD [90˚/0˚] W [±45˚] configuration is more clear and significant when evaluated in terms of the increase in stress and strain.

As shown in **Figure 5-41** the failure mode of the various cylinders in this series is similar with alternating diagonal tears of the jackets along the specimen height, however “large” specimens experienced more damage in the jacket and concrete core, when compared to the "small" size companions.

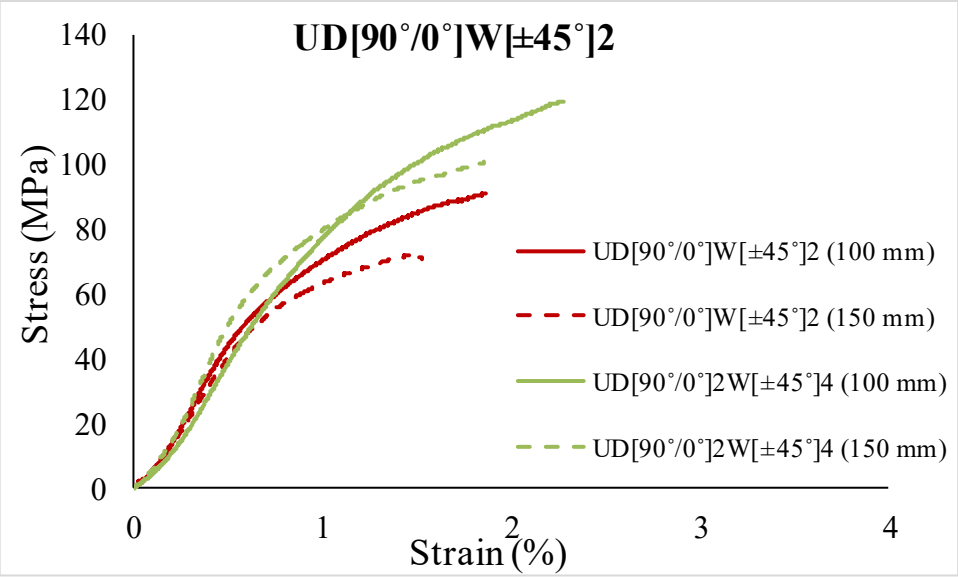

Figure 5-40 Size effect on confined specimens with UD [90˚/0˚] W [±45˚] fiber configuration

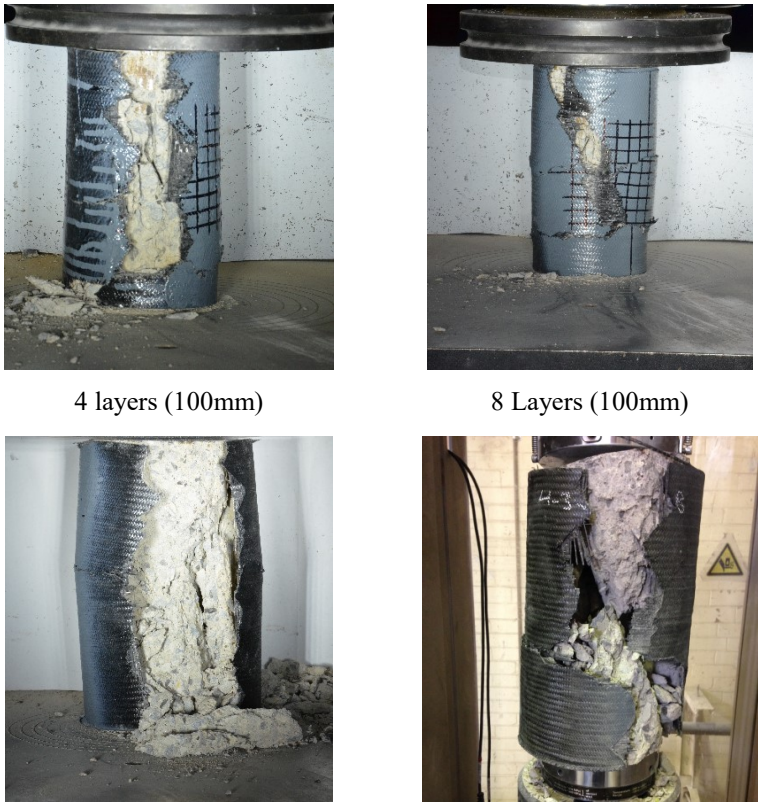

4 layers (100mm) 8 Layers (100mm)

4 Layers (150mm) 8 Layers (150mm)

Figure 5-41 Post failure photos of "small" and "large" size confined cylinders

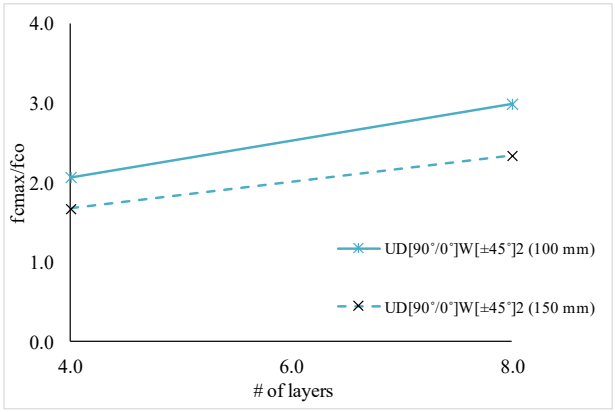

a) Stress ratio

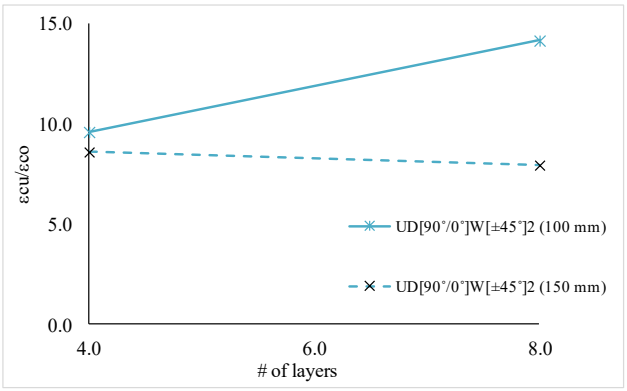

b) Strain ratio

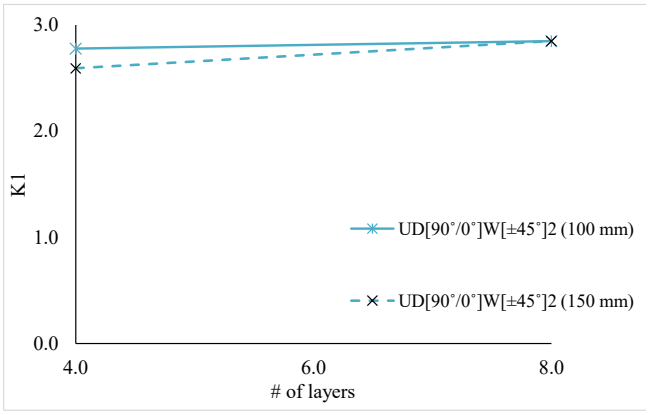

c) Strength effectiveness

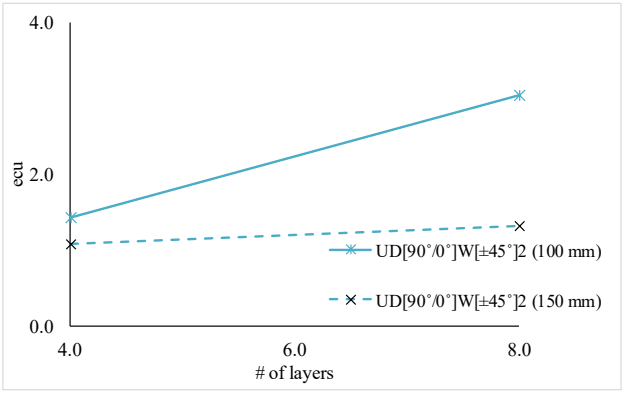

d) Energy absorption capacity

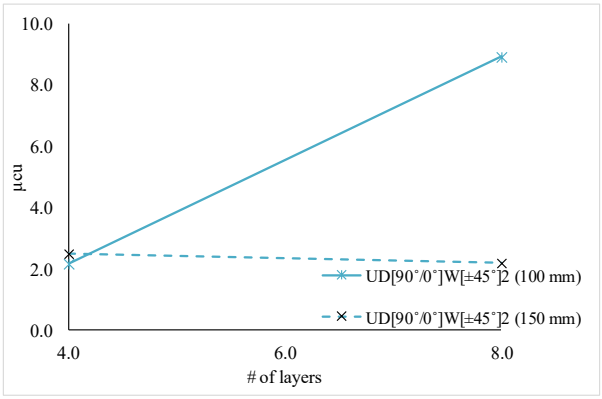

e) Ductility factor

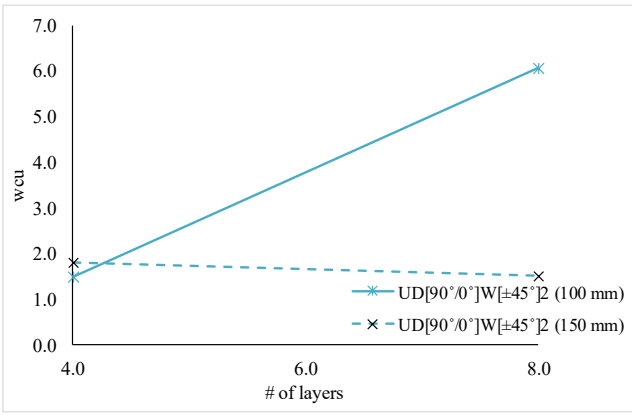

f) Work index

Figure 5-42 Size effect on different stress-strain parameters (Series 4A)

5.5.5 Series 4B (UD [90˚] W [±45˚]$_2$ UD [0˚])

As shown in **Figure 5-43**, the effectiveness of confinement on the increase in strength and strain of CFRP wrapped cylinders in Series 4B was similar up to the end of the first ascending branch of the stress-strain response, after which the “small” size specimens showed improved performance. When evaluated in terms of the strength enhancement, the “small” size specimens confined with 4 layers of CFRP showed average strength ratio (f'_{cc}/f_{co}) of 88.99% while “large” size specimens with the same amount of confinement had a corresponding ratio of 70.25%, a 19% decrease in strength enhancement when compared to the "small" cylinders. Increase in strain ($\varepsilon'_{cc}/\varepsilon_{co}$) in “small” size specimens increased proportionally to the number of CFRP layers, while the strain ratio decreases by increasing the number of CFRP layers in “large” size specimens. For example, “small” specimens confined with 4 and 8 layers of CFRP had average percent increase in strain ($\varepsilon'_{cc}/\varepsilon_{co}$) of 849.48% and 1328.34% respectively, while companion “large” size specimens showed average ratios of 882.90% and 741.68%. Comparing Series 4A and 4B, one can see that in the case of the "small" cylinders, the relative increase in strength was more obvious in 4A, while no big difference was observed in the case of the increase in strain. For “large” specimens the increase in strength was more pronounced 4A, while the inverse is observed in the case of increase in strain.

No significant variation is observed between the different specimen sizes in the cases of strength effectiveness factor (k_1). In the case of energy absorption capacity (e_{cu}) “small” size cylinders showed better toughness as shown in **Table 5-1** and **Figure 5-45**. As in Series 4A, the toughness increases with the addition of layers in the case of the “small” cylinders, while the effect is insignificant in the “large” size cylinders. In the case of the work index (w_{cu}), “small” size specimens with 4 layers of CFRP show larger values when compared to those of the "large"

specimens, while the values are similar at 8 layers. For example, work index factors of 9.17 and 1.69 were obtained for the "small" cylinders confined with 4 and 8 layers of CFRP, while the corresponding factors were 2.05 and 1.70 in the "large" size companions.

The ductility factor (μ_{cu}) decrease in the "small" size cylinders as the number of layers are increased, while no significant changes result in the "large" cylinders as the number of plies goes up. For example "small" size cylinders confined with 4 and 8 layers of CFRP sheets had ductility factors of 13.07 and 2.45, while, "large" size companions showed ductility factors of 2.87 and 2.36.

As with the previous series, one can see that the size effect is more distinguishable for the UD [90˚] W $[\pm 45^{\circ}]_2$ UD [0˚] configuration when evaluated in terms of the percentage increase in maximum stress and strain.

As shown in **Figure 5-44** all cylinders in this series, regardless of specimen size and number of layers, had gradual and controlled failures with large plastic deformations before rupture of the CFRP jackets. The final failure mode was similar in most specimens, with rupture of fibers in the outer UD [0˚] layers and crushed concrete retained by the inner CFRP layers; the exception being the "large" size specimen confined with 4 layers, which experienced complete jacket rupture, which can point to insufficient amount of CFRP confinement for this cylinder.

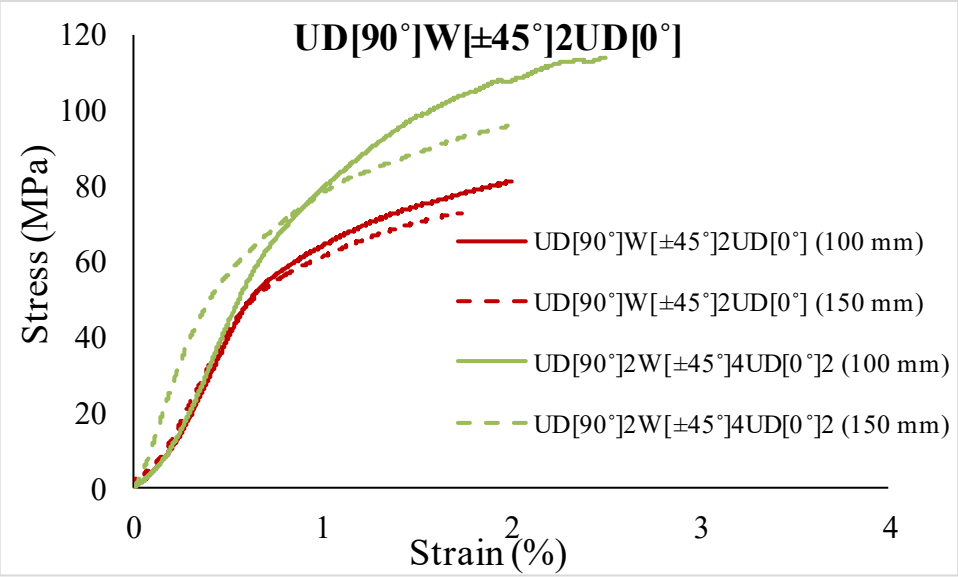

Figure 5-43 Size effect on confined specimens with UD [90˚] W $[\pm 45^{\circ}]_2$ UD [0˚] fiber configuration

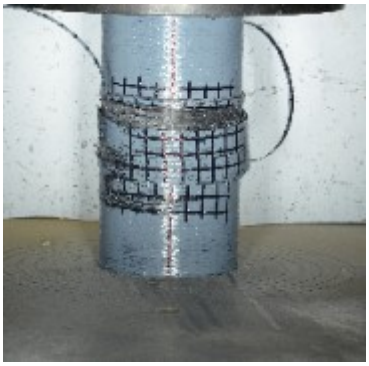

4 layers (100mm)

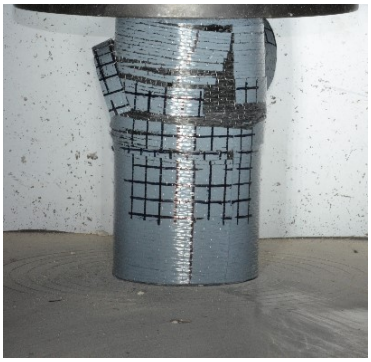

8 Layers (100mm)

4 Layers (150 mm)

8 Layers (150 mm)

Figure 5-44 Post failure photos of "small" and "large" size confined cylinders

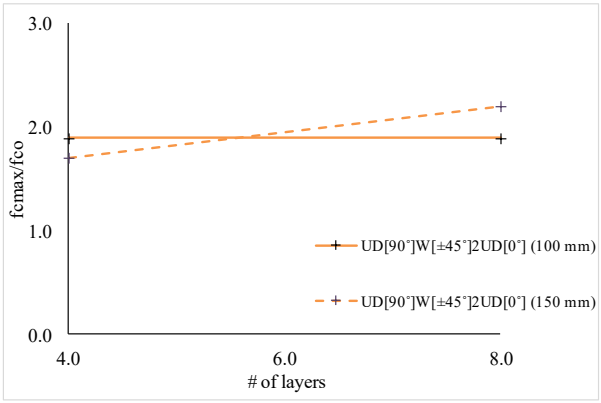

a) Stress ratio

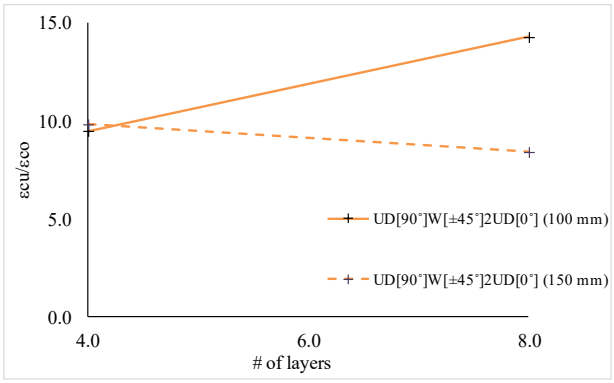

b) Strain ratio

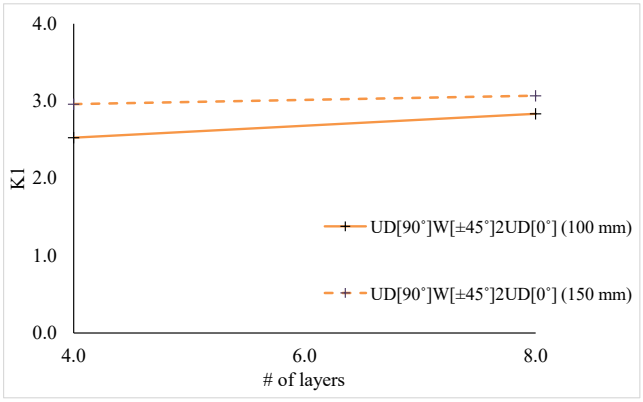

c) Strength effectiveness

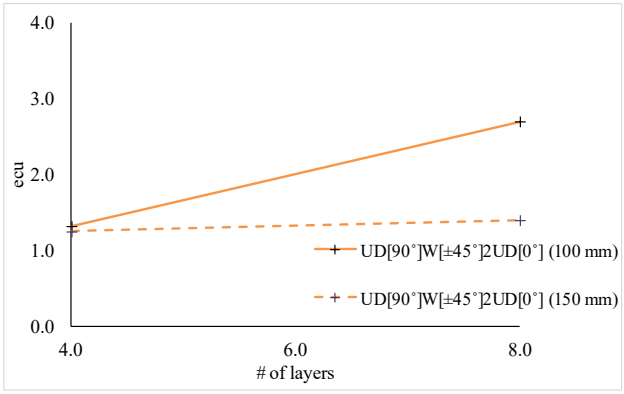

d) Energy absorption capacity

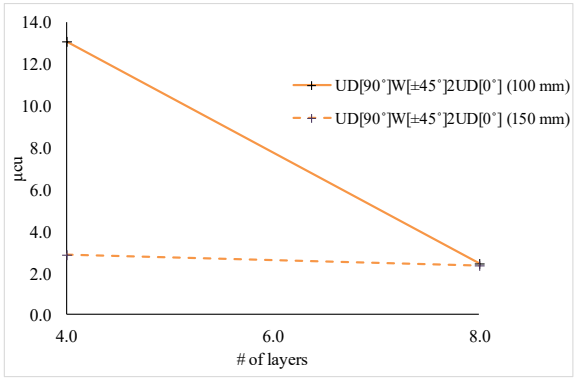

e) Ductility factor

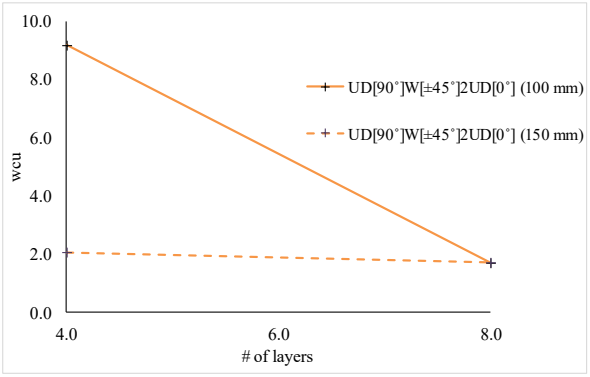

f) Work index

Figure 5-45 Size effect on different stress-strain parameters (Series 4B)

5.5.6 Series 5A (UD [0˚] W [±45˚])

This section evaluates the size effect in the Series 5A specimens. As shown in **Figure 5-46** the stress-strain response of the "large" size specimens shows a stiffer ascending branch and larger stresses in the early stages of loading, although the "small" size specimens performed better in the case of maximum increase in strength and strain. Thus, as with the previous series, it can be claimed that strength effectiveness decreases by increasing the specimen size. For example, "small" size specimens confined with 4 layers of CFRP showed an increase in strength (f'_{cc}/f_{co}) of 182.17% while "large" size specimens with the same amount of confinement had an average strength improvement of 128.27%, which is 54% lower. Increase in strain ($\varepsilon'_{cc}/\varepsilon_{co}$) in the "small" size specimens was proportional to the number of CFRP layers, while percentage the strain ratio reduces as the number of layers increase in the "large" specimens. For instance, "small" size specimens confined with 4 and 8 layers of CFRP provided an average percent increase in strain ($\varepsilon'_{cc}/\varepsilon_{co}$) of 1714.88% and 2300.80% respectively, while "large" size companions showed an average increases of 2849.39% and 1399.67%, respectively. This comparison also shows that the "large" size specimens with 4 layers of CFRP observed better increase in strain compared to the "small" size companions.

No significant variation related to specimen size is observed for the strength effectiveness factor (k_1), however it can be noticed that larger factors are obtained in specimens with lesser number of layers in both sizes as it is presented in **Figure 5-48**. "Small" size specimens confined with 4 and 8 layers of CFRP s showed strength effectiveness factors of 1.98 and 1.50 respectively, while companion "large" size specimens showed factors of 2.07 and 1.74.

Energy absorption capacity (e_{cu}) increased in the "small" size cylinders by increasing the number of plies, while no important changes are observed in "large" size cylinders as the

quantity of plies is varied. For instance, “small” size cylinders confined with 4 and 8 layers of CFRP sheets showed energy absorption capacities of 3.75 and 6.74, while the corresponding values were 3.57 and 3.60 for “large” size specimens with the same number of layers. In the case of work index (w_{cu}), the values are higher for the "large" cylinders, while in both “small” and “large” cylinders, the index is found to decrease as the number of layers are increased. For example, work indices of 1.83 and 1.75 were obtained for the “small” size cylinders confined with 4 and 8 layers of CFRP, while the corresponding indices were 2.77 and 1.83 for “large” specimens with the same number of plies.

The ductility factors (μ_{cu}) show insignificant difference with the increase in ply thickness in the case of the “small” size cylinders while the ductility factors decreases as the number of confinement layers are increased in “large” size specimens. For example “small” size cylinders confined with 4 and 8 layers of CFRP achieved ductility factors of 2.62 and 2.72, while “large” cylinders with the same amount of confinement showed ductility factors of 5.40 and 2.74.

Based on the above discussions, one can conclude that the size effect for CFRP placed in a UD [0˚] W [±45˚] pattern is more apparent when comparing the increase in maximum stress.

The use of UD [0˚] fabric in the innermost layers (with the W [±45˚] sheets placed on the outside) led to somewhat brittle failures for all specimens in this series, however as shown in **Figure 5-47,** the “large” size specimens experienced more explosive failures and more severe damage in the jacket and concrete core, due to the placement order of the confinement layers.

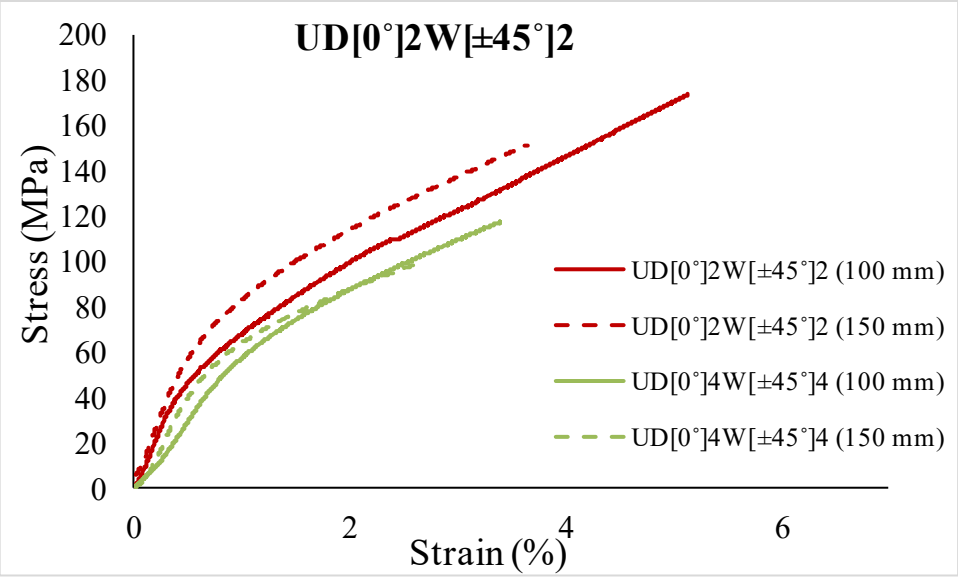

Figure 5-46 Size effect on confined specimens with UD [0˚] W [±45˚] fiber configuration

4 layers (100mm) 8 Layers (100mm)

4 Layers (150mm) 8 Layers (150mm)

Figure 5-47 Post failure photos of "small" and "large" size confined cylinders

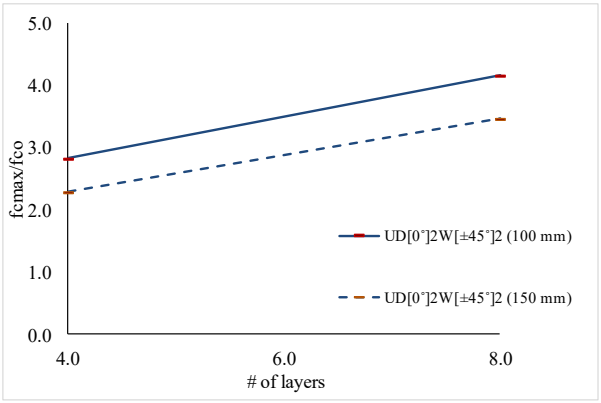

a) Stress ratio

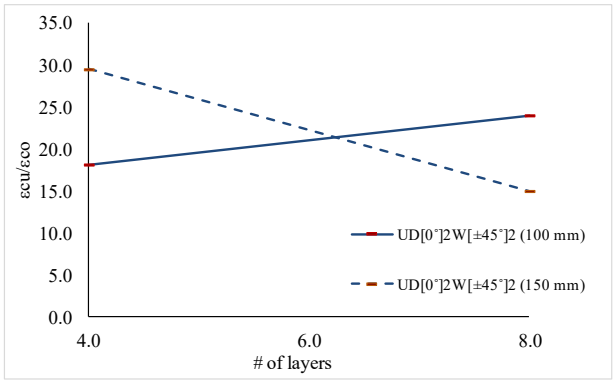

b) Strain ratio

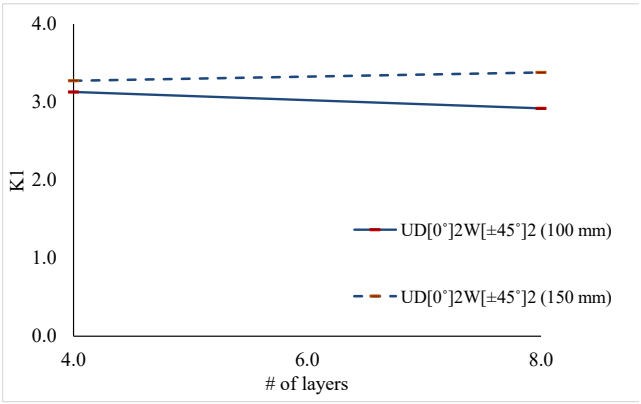

c) Strength effectiveness

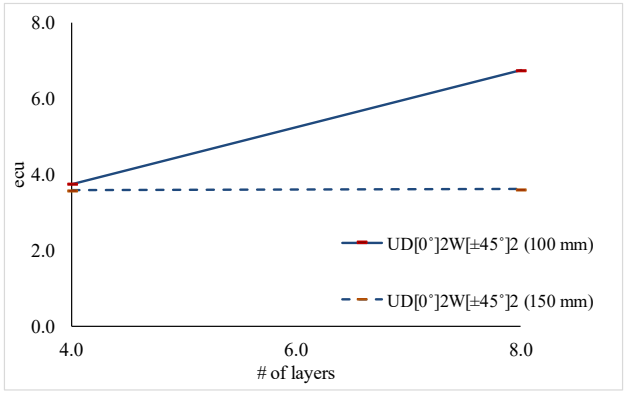

d) Energy absorption capacity

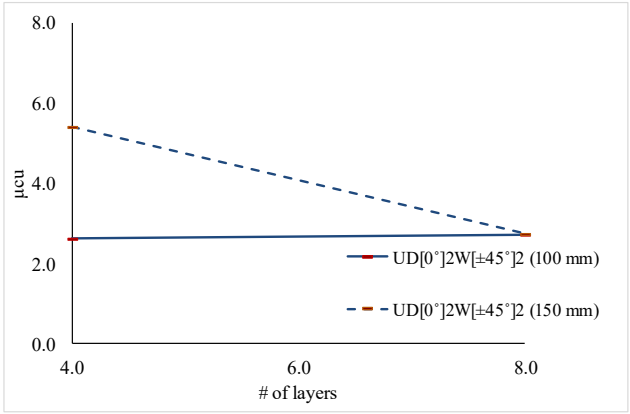

e) Ductility factor

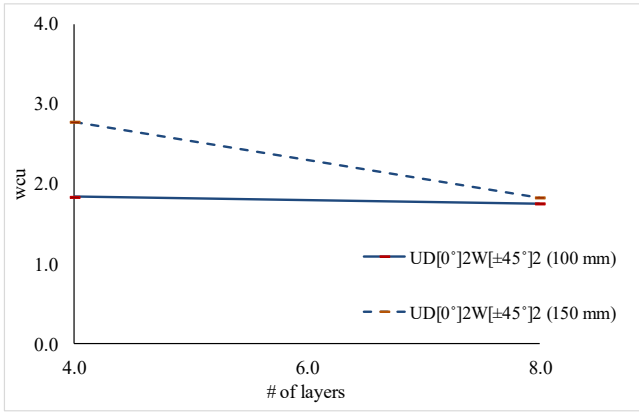

f) Work index

Figure 5-48 Size effect on different stress-strain parameters (Series 5A)

5.5.7 Series 5B (W [±45˚] UD [0˚])

Series 5B had a similar layup to that of Series 5A however the order of sheet application was reversed. **Figure 5-49** shows that the stress-train response of the different size companion specimens shows similar behavior at early stages of loading. However it can be seen that the overall effectiveness of confinement on increasing maximum strength and strain decreases with an expansion of the specimen size. For example, “small” size specimens confined with 4 layers of CFRP showed an increase in strength (f'_{cc}/f_{co}) of 141.92% while “large” size specimens with the same amount of confinement had a strength improvement of 90.05%, a relative reduction in confinement efficiency of 52%. Increase in strain ($\varepsilon'_{cc}/\varepsilon_{co}$) was proportional to the number of CFRP layers disregarding the specimen size; however the strain ratios are higher for the "small" size specimens. "Small” cylinders confined with 4 and 8 layers resulted in an average percent increase in strain ($\varepsilon'_{cc}/\varepsilon_{co}$) of 1130.20% and 2445.70%, while “large” cylinders confined with same amount of CFRP showed average ratios of 836.67% and 1472.58%.

Significant variation was not observed between the different specimen sizes in the case of the strength effectiveness factors (k_1). The ductility factor (μ_{cu}) was found to increase by increasing the number of CFRP layers in both “small” and “large” size specimens, however the values are greater as the cylinder size is reduced. For example, “small” cylinders confined with 4 and 8 layers of CFRP sheets experienced ductility factors of 2.78 and 3.76, while “large” companions showed ductility factors of 1.88 and 2.66 respectively. Similarly energy absorption capacity (e_{cu}) “small” increased by adding more layers, however “small” size cylinders showed better overall toughness as seen in **Table 5-1** and **Figure 5-51**. For instance, “small” size cylinders confined with 4 and 8 layers of showed energy absorption capacity of 2.13 and 6.21, respectively. On the other hand “large” size cylinders with same amount of CFRP layers displayed energy absorption

capacities of 1.24 and 3.43. The same trend is observed when examining the work index (w_{cu}) results. For example, work index factors of 1.91 and 2.27 were obtained for "small" size cylinders at 4 and 8 layers, while "large" size specimens show factors of 1.25 and 1.73.

As with most other series, the size effect is most clear when the maximum stress and strain values are compared in specimens witch the W [±45˚] UD [0˚] layup configuration.

Examining the failure photos in **Figure 5-50**, it can be seen that "large" size specimens experienced more damage in the jacket (and concrete core for specimens with 4 layers), when compared to the 100 mm companions.

Comparing series 5A and series 5B it can be noticed that the layup sequence used in series 5A resulted in greater strength increase due to applying the UD [0˚] sheets in the innermost layers (this may be because passive confinement is activated first in the inner layers). Similar results were observed in the case of energy absorption due to high energy absorption capacity of the unidirectional FRP sheets. However, specimens in Series 5B showed better performance in the case of the ductility factor. Similarly, these specimens showed generally more ductile failure modes (rupture of external layers only in most specimens) and these results can be attributed to application of the W [±45˚] sheets in the innermost layers.

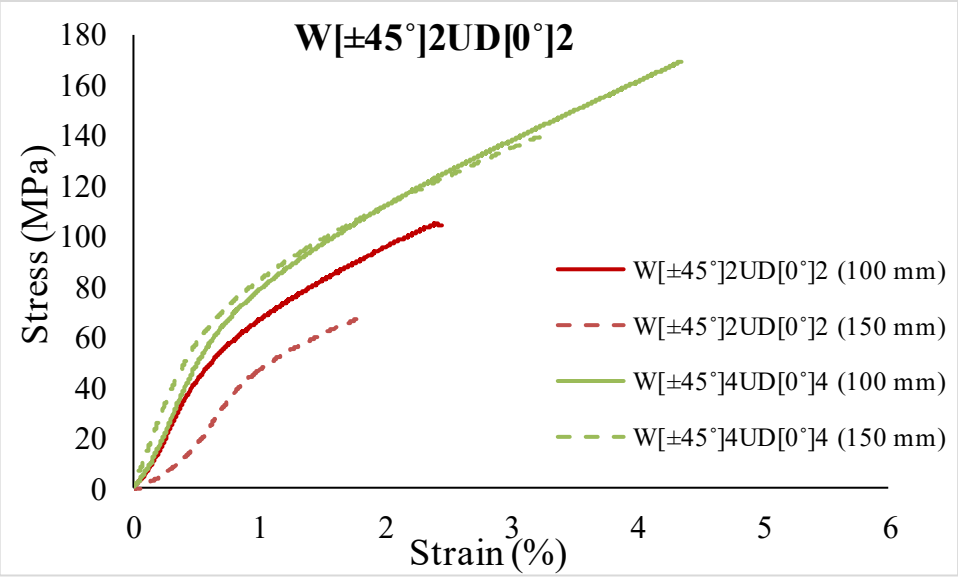

Figure 5-49 Size effect on confined specimens with W [±45˚] UD [0˚] fiber configuration

4 layers (100mm)

8 Layers (100mm)

4 Layers (150 mm)

8 Layers (150 mm)

Figure 5-50 Post failure photos of "small" and "large" size confined cylinders

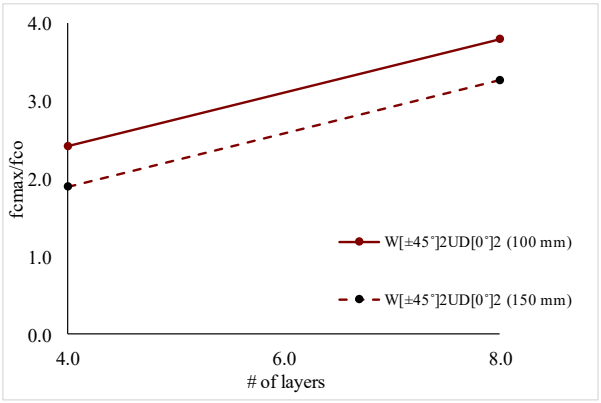

a) Stress ratio

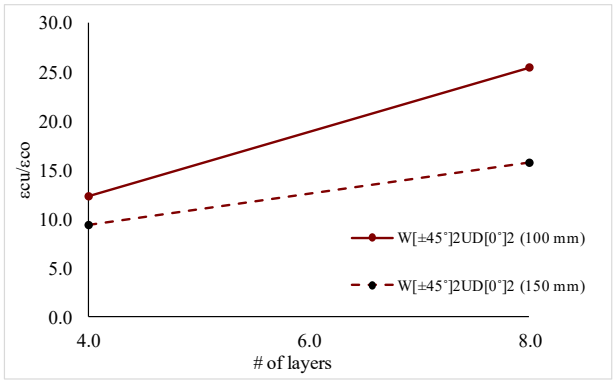

b) Strain ratio

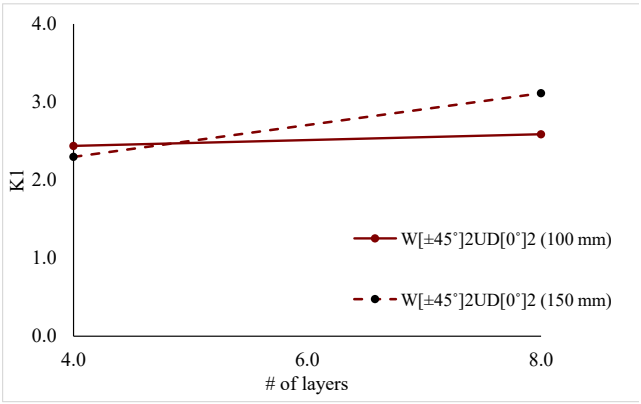

c) Strength effectiveness

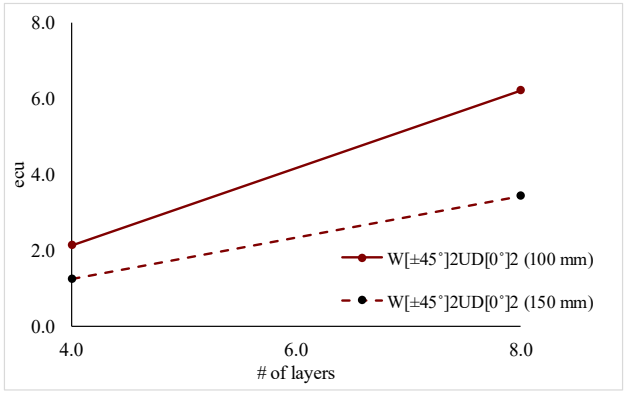

d) Energy absorption capacity

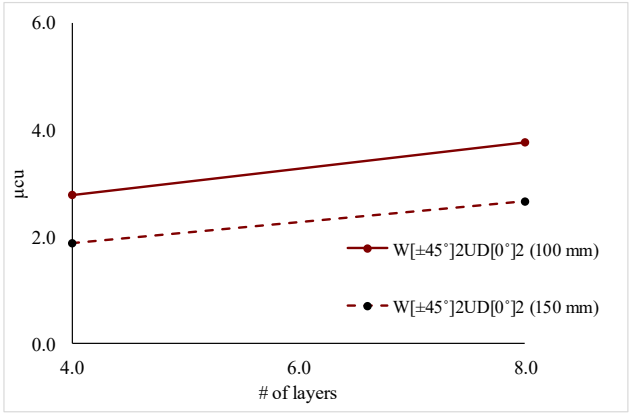

e) Ductility factor

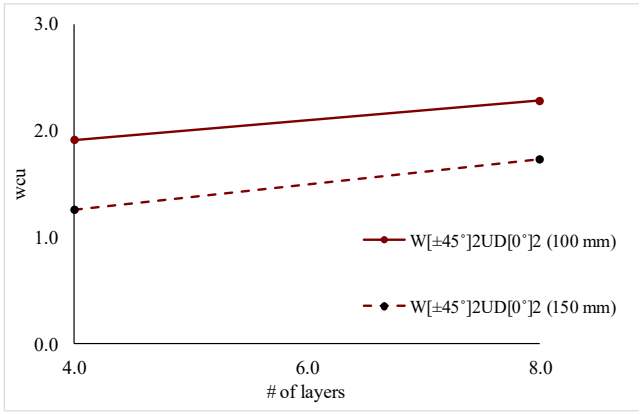

f) Work index

Figure 5-51 Size effect on different stress-strain parameters (Series 5B)

5.5.8 Series 6 (UD [90$_x$˚/0$_x$˚])

Figure 5-52 shows the stress-strain comparisons of small and large specimens in Series 6. Continuing the trend from the preceding discussions, the confinement effectiveness of the UD [90x˚/0x˚] sheets decreased with an enlargement of cylinder size. In terms of the strength enhancement, the "small" size cylinders confined with 4 layers of CFRP showed an increase in strength (f'_{cc}/f_{co}) of 144.96%, while "large" size companions had an average strength improvement 82.88%, which is 62% below the gain in strength observed for the "small" size specimens. Increase in strain ($\varepsilon'_{cc}/\varepsilon_{co}$) was also affected by specimen size, with ratios of 1257.04%, 1508.25%, and 1684.24% for the "small" series cylinders with 4, 6 and 8 plies and corresponding strain increase ratios of 1152.04%, 1188.38%, and 881.77% for the companion "large" cylinders. It is noted that the ratios reduce as the number of layers go from 6 to 8 in the "large" specimens.

Insignificant variation was observed between the different specimen sizes in the cases of strength effectiveness factor (k_1). Higher ductility factors (μ_{cu}) were observed in "large" size cylinders as it can be seen in **Table 5-1**. For example "small" size cylinders confined with 4, 6, and 8 layers of CFRP sheets experienced ductility factors of 2.58, 2.79 and 2.70, while the factors for the larger cylinders with same amount of plies were 3.47, 2.58 and 3.10, respectively. In the case of energy absorption capacity (e_{cu}), the increase in toughness was proportional to the number of CFRP layers for the "small" cylinders, while the effect is only seen up to 6 layers in the "large" size cylinders as shown in **Figure 5-54**. "Small" size cylinders confined with 4, 6, and 8 layers of CFRP achieved energy absorption capacities of 2.48, 3.25, and 4.47, while these factors were 1.55, 2.25, and 1.85 in the companion 150 mm cylinders. The work index (w_{cu}) factors are somewhat similar (at ~ 2) for all cylinders, regardless of size or number of layers.

Continuing the trend from previous series, evaluation of the results shows that size effect is more apparent when evaluated in terms of the percentage increase in stress and strain in the [90x˚/0x˚] series.

Figure 5-53 shows that the “large” size specimens experienced more damage in the jacket and concrete core, when compared to their smaller size companions.

Comparing Series 2 with Series 6, which had similar fiber orientation but a different layup sequence, it can be noticed that “small” size cylinders in Series 2 showed better performance in the case of the increase in strength, while better performance was observed with “large” size cylinders in the case of increase in strain. Insignificant variation was observed in the case of strength effectiveness factor in both sizes in both series. Cylinders in Series 6 showed more "ductile" behavior compared to those of Series 2, when ductility was evaluated in terms of the ductility factor. However, improved energy absorption capacity was seen in specimens in Series 2. It should however be noted that although the Series 2 showed comparatively better stress-strain performance, these specimens experienced more catastrophic failures.

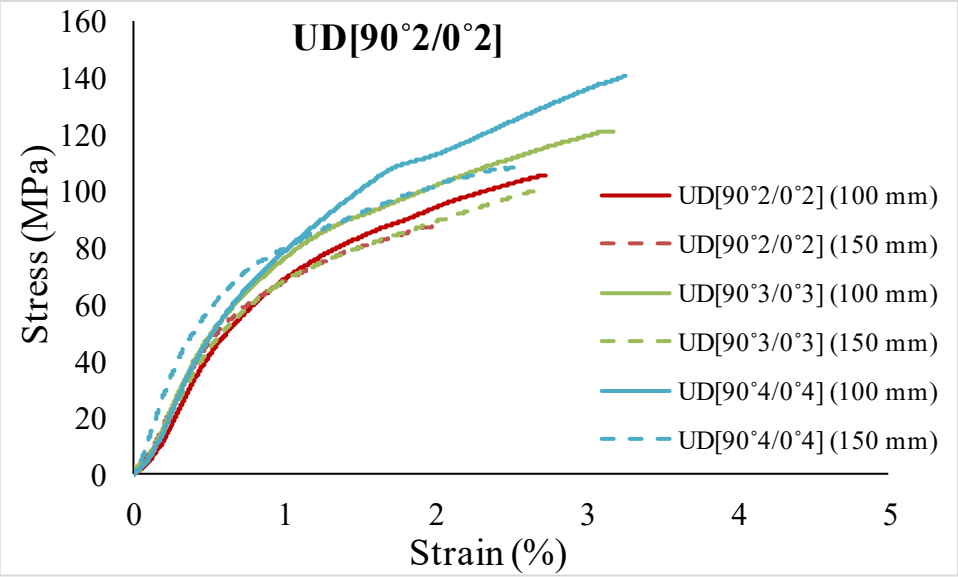

Figure 5-52 Size effect on confined specimens with UD [90_x˚/0_x˚] fiber configuration

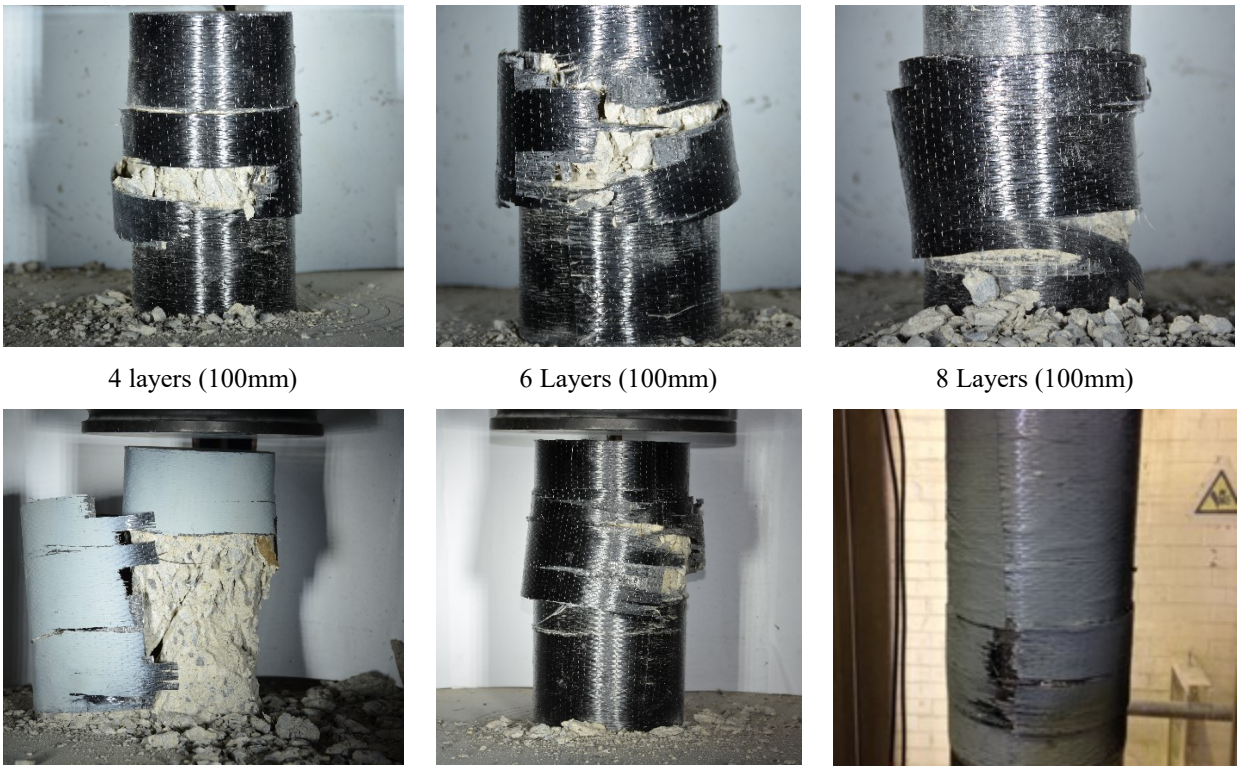

4 layers (100mm) | 6 Layers (100mm) | 8 Layers (100mm)

4 Layers (150mm) | 6 Layers (150mm) | 8 Layers (150mm)

Figure 5-53 Post failure photos of "small" and "big" size confined cylinders

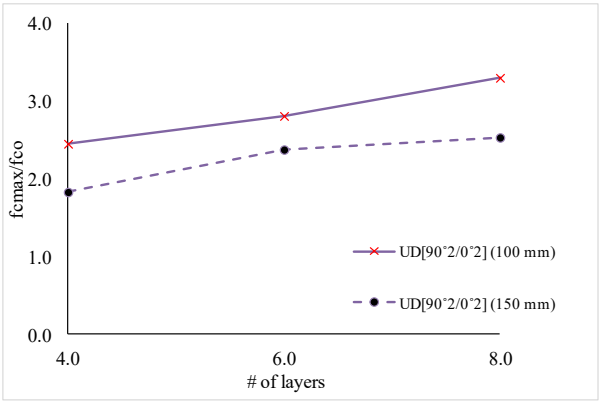

a) Stress ratio

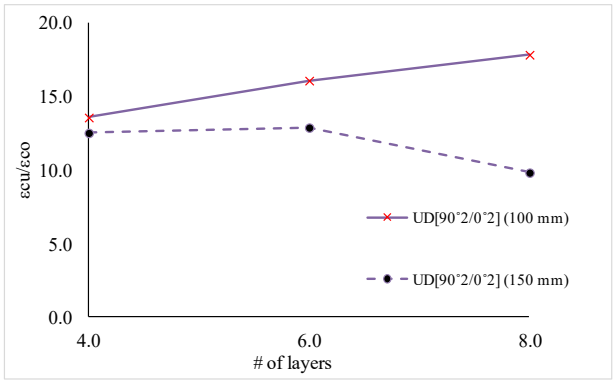

b) Strain ratio

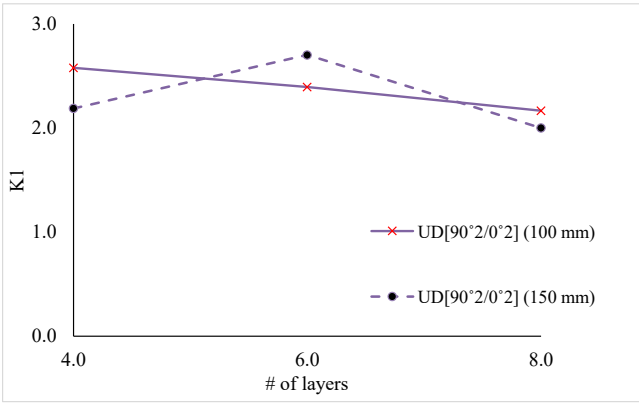

c) Strength effectiveness

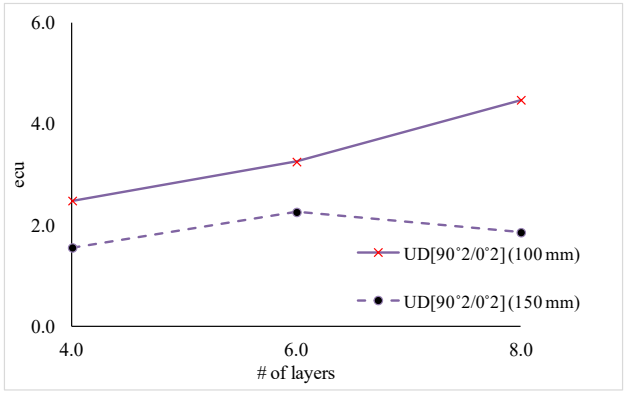

d) Energy absorption capacity

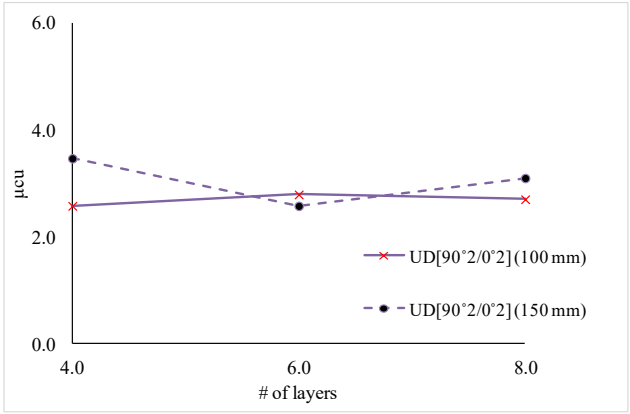

e) Ductility factor

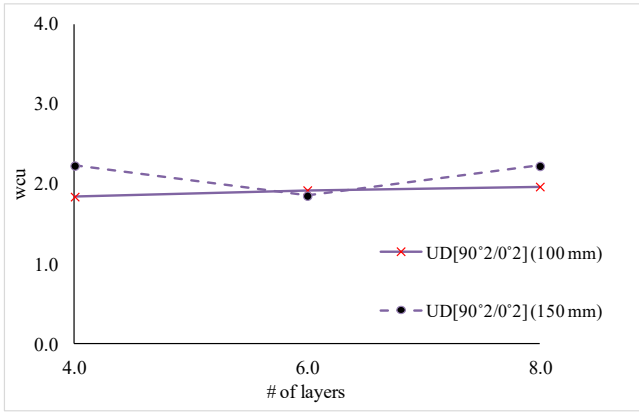

f) Work index

Figure 5-54 Size effect on different stress-strain parameters (Series 6)

5.6 Summary

The effect of size on the behavior of the FRP-confined concrete specimens has been studied in this section. It has been established that larger specimens experienced relatively lower strength enhancements when compared to smaller sized specimens as it is shown in **Figure 5-55a**. **Figure 5-55b** also shows that in most of the cases "small" size cylinders showed better performance in the case of increase in strain. Based on the test results presented in **Figure** 5-55**c**, an unimportant difference results in the case of the strength effectiveness factor (k_1) between small and large specimens. The influence of specimen size was also found to vary in the case of energy absorption capacity factor (e_{cu}) except in series 1 which clearly shows better results for the "small" size cylinders (see **Figure 5-55d**). The impact of specimen size on the ductility factor (μ_{cu}) and work index (w_{cu}), is unclear as shown in **Figure 5-55e & f**, except for Series 3 (UD [+45˚/-45˚]).

Further research is recommended on specimens with greater size differences to effectively evaluate the size effect on the overall stress-strain behavior of CFRP confined concrete, as both cylinders sizes can be considered relatively small when compared to reinforced concrete columns found in buildings and bridges .

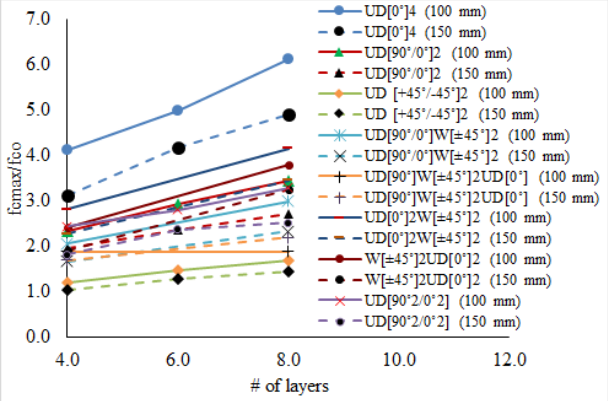

a) Stress ratio

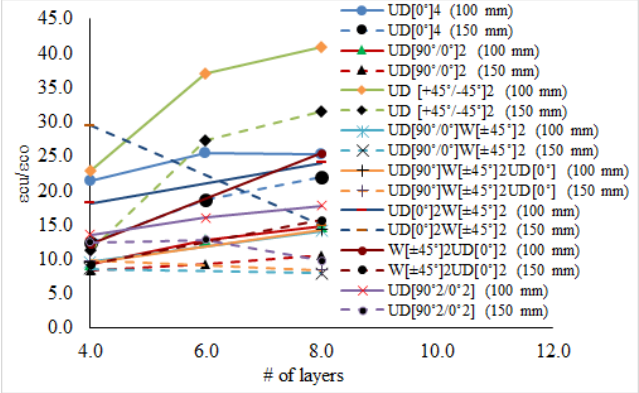

c) Strain ratio

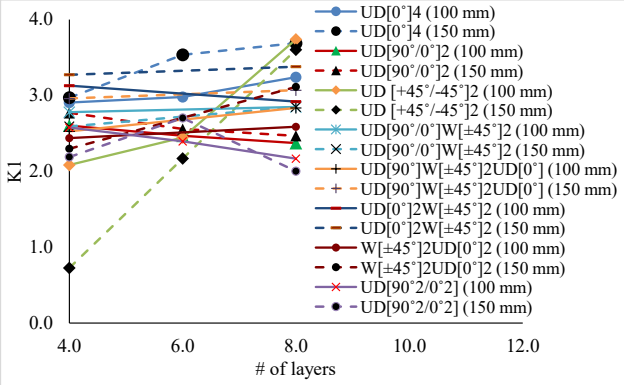

c) Strength effectiveness

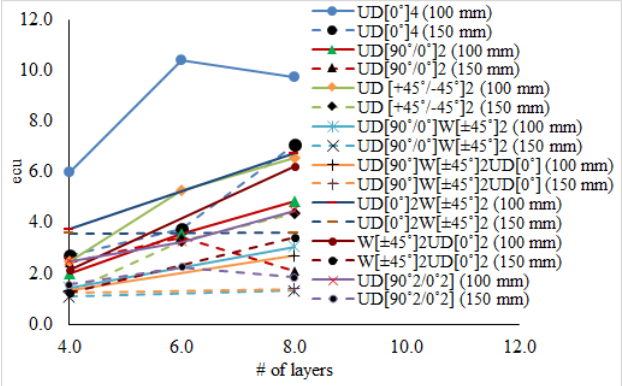

d) Energy absorption capacity

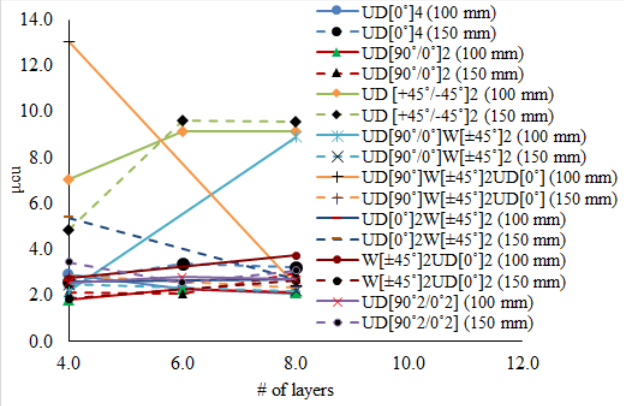

e) Ductility factor

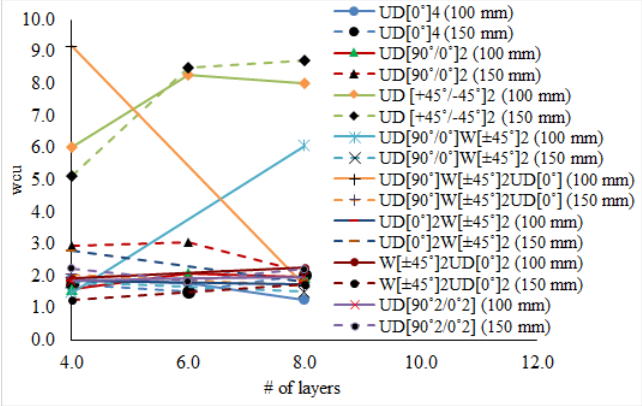

f) Work index

Figure 5-55 Size effect on different parameters

5.7 Effect of fiber orientation and stacking sequence

5.7.1 4 layers of CFRP

5.7.1.1 Coupons

Figure 5-56 shows the effect of stacking sequence on the stress-strain behavior of flat CFRP coupons. It is clear that the highest stiffness and strength was recorded for Series 1 which had fibers in UD [0º], parallel to the loading axis, while the maximum ductility was achieved for Series 3 and 7 which had fibers in angular direction (+/- 45º). Linear-elastic behavior is obvious in those series with unidirectional UD [0º] fibers. On the other hand, non-linear behavior was observed in the coupons with fibers aligned in angular directions. Other combinations show a hybrid of both behaviors, although the unidirectional fibers tend to dominate response. For example, coupons with combination of fibers in UD [0º] and angle direction showed limited nonlinear behavior up to the rupture strength of angular fibers followed by linear behavior due to unidirectional direction fibers until final rupture of the coupon. Post failure photos from coupons are presented in **Figure 5-59**. No significant difference is observed in the failure photos, where specimens fail at a critical section (either at the middle or edges) since they are flat samples which are tested in direct tension, nonetheless more brittle failures occurred for those specimens with larger amounts of unidirectional fibers parallel to the loading axis. Coupons in series 3 and series 7 showed different failure patterns due to use of 45 degree fibers in these series.

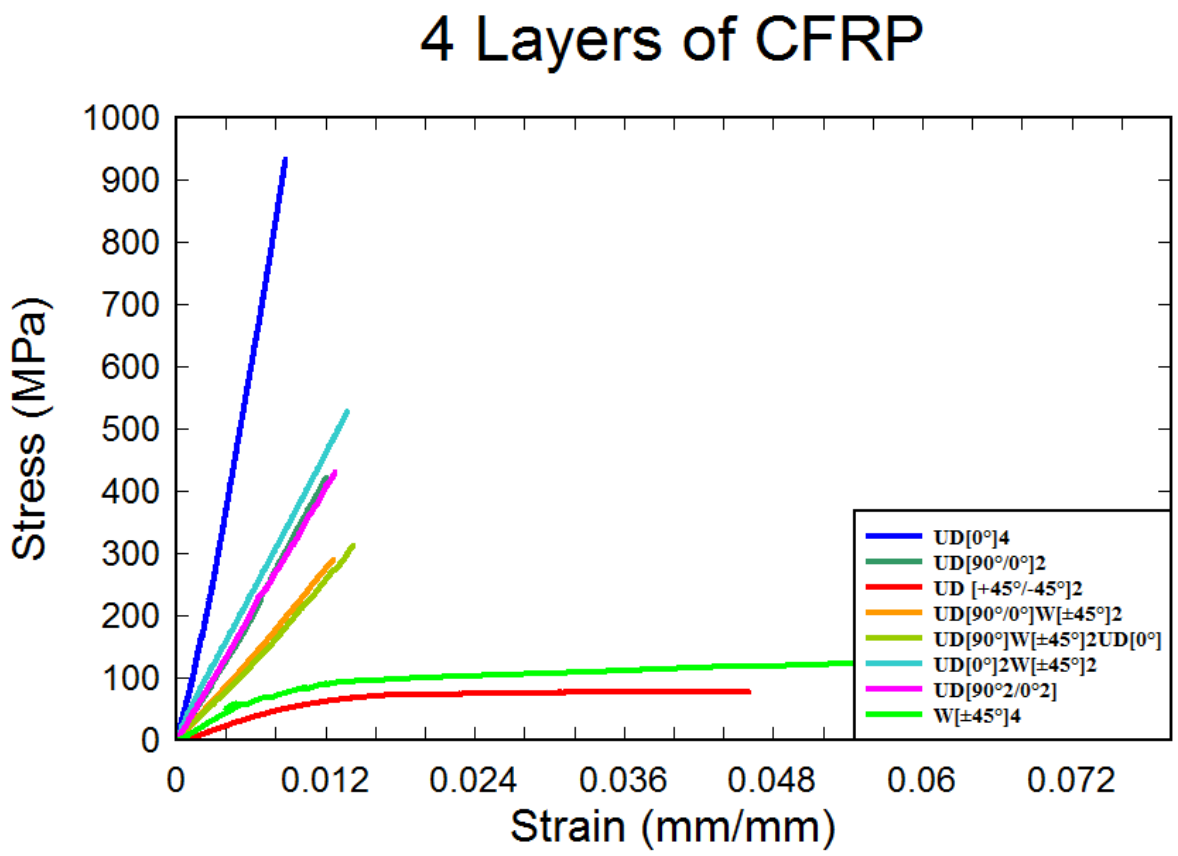

Figure 5-56 Effect of stacking sequence on stress-strain behavior of CFRP coupons

5.7.1.2 Cylinders

The effect of fiber orientation for 4 layers of CFRP on the strength of confined concrete is shown in **Figure 5-57**. Comparison of various stress-strain parameters is also shown in **Figure 5-60**. It can be observed that specimens confined in the hoop direction (0°) experienced a more important strength increase. In contrast, specimens confined in with angular fibers demonstrated a greater increase in strain capacity. The percentage of strength increase (f'_{cc}/f_{co}) for specimens with 4 plies of CFRP were determined as 313.4%, 134.4%, 21.5%, 107.1, 88.9, 182.1, 141.9, 144.9, and 1.7% for the UD[0˚] (Series 1), UD[90˚/0˚] (Series 2), UD [+45˚/-45˚] (Series 3), UD[90˚/0˚]W[±45˚]$_2$ (Series 4A), UD[90˚]W[±45˚]$_2$UD[0˚] (Series 4B), UD[0˚]$_2$W[±45˚]$_2$

(Series 5A), W[±45˚]$_2$UD[0˚]$_2$ (Series5B), UD[90˚$_2$/0˚$_2$] (Series 6), and W[±45˚]$_4$ (Series 7), respectively. It can be seen that the largest values are reported for specimens with a greater amount of UD[0˚] sheets. As can be seen in **Table 5-1** and **Figure 5-60**, the strain increase ratio ($\varepsilon'_{cc}/\varepsilon_{co}$) was most significant for cylinders confined with W [±45˚] sheets. When considering all specimens, the maximum increase in strain-ratio was obtained for specimens confined with the woven angular sheet, with an average ratio of 1567.7%, a substantial improvement.

It was observed that the fiber orientation did not have a significant impact on the strength effectiveness factor (k_1) which fluctuated around a value of 3, except for CFRP jackets placed in W [±45˚] which had a (k_1) value less than 1 because of a small gain in strength.

The influence of orientation on energy absorption capacity factor (e_{cu}) was found to be largest for the UD [0°] pattern, with the various series having the following sequence of decreasing energy absorption: UD [0˚] > UD [0˚]$_2$ W [±45˚]$_2$ > UD [90˚$_2$/0˚$_2$] > UD [+45˚/-45˚] > W [±45˚]$_2$ UD [0˚]$_2$ > UD [90˚/0˚] > W [±45˚]$_4$ > UD [90˚/0˚] W [±45˚]$_2$ > UD [90˚] W [±45˚]$_2$ UD [0˚].

Maximum values of 13.1 and 9.2 for the ductility factor (μ_{cu}) and the work index (w_{cu}), were achieved for specimens in Series 4B (UD [90˚] W [±45˚]$_2$ UD [0˚]). This layup sequence showed moderate increase in stress and strain, with additional benefits in terms of failure mode as discussed in the previous sections.

Figure 5-58 shows that the type of CFRP sheets and stacking sequence had a direct impact on the failure mode with more brittle failures observed in the case of specimens with large amount of UD [0˚] fibers and ductile failures in specimens having large amount of angular fibers. Combination of both fiber types resulted in a hybrid of both responses.

In summary, despite the differences in stress-strain response and failure mode, confinement of specimens with unidirectional fibers aligned purely in the hoop direction (UD [0˚]) as in Series 1 resulted in the best overall stress-strain performance at 4 layers, with largest increase in strength, and overall toughness, with a stress-strain response which enveloped all other series. On the other hand the use of angular fibers n series 3 and 7 resulted in increased strain capacity, although the use of this type of CFRP may require a greater amount of layers to achieve satisfactory performance (see next section). The response of other series showed a hybrid response due to the combined effect of different fiber orientation, however the response was generally dominated by the influence of the unidirectional hoop fibers with some changes in the shape of the transition point and ductility as 90˚ and 45˚ CFRP sheets were added.

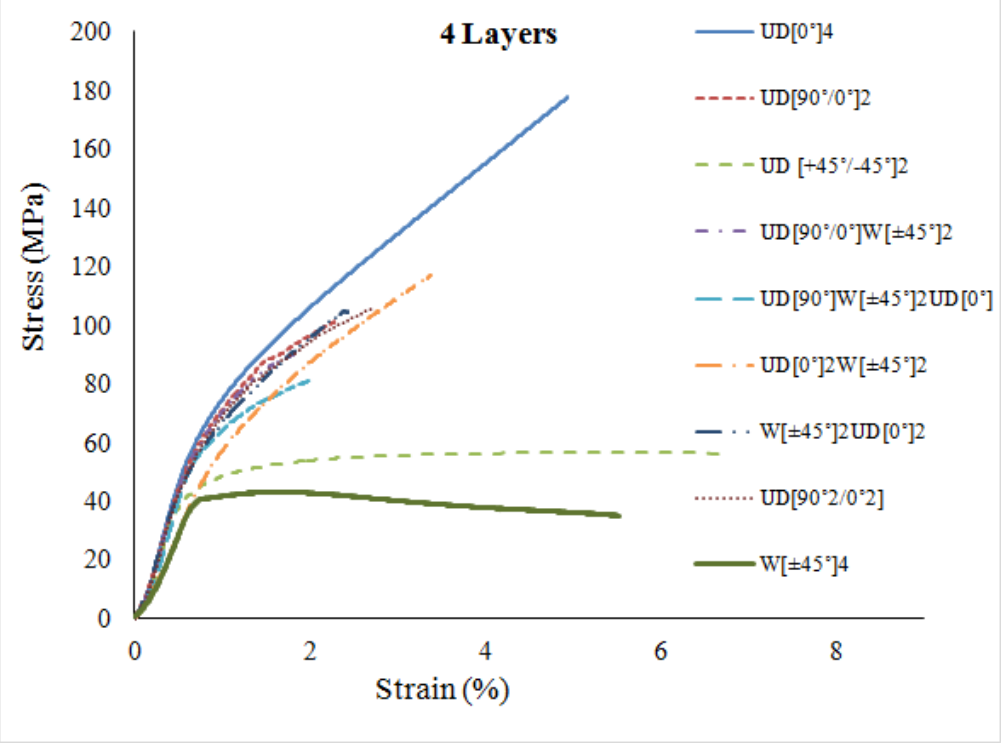

Figure 5-57 Effect of fiber orientation on stress-strain behavior of confined concrete

UD[90˚/0˚]$_2$

UD[90˚$_2$/0˚$_2$]

UD [+45˚/-45˚]$_2$

W[±45˚]$_4$

UD[90˚/0˚]W[±45˚]$_2$

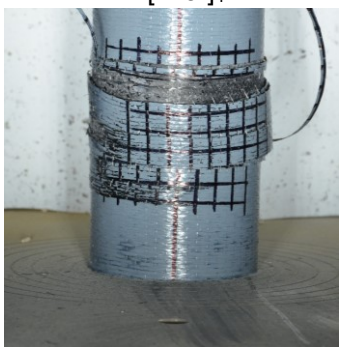

UD[90˚]W[±45˚]$_2$UD[0˚]

UD[0˚]$_2$W[±45˚]$_2$

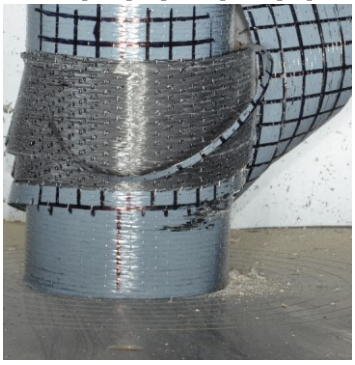

W[±45˚]$_2$UD[0˚]$_2$

Figure 5-58 Post failure photos of cylinders with different stacking sequences (4 layers)

UD[90˚/0˚]$_2$

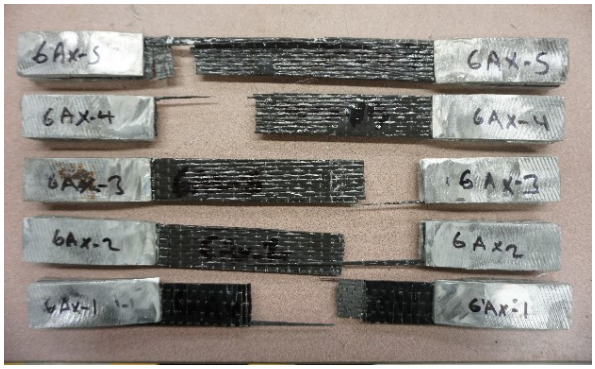

UD[90˚$_2$/0˚$_2$]

UD [+45˚/-45˚]$_2$

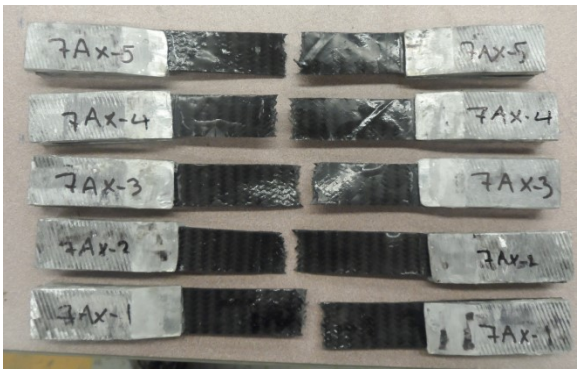

W[±45˚]$_4$

UD[90˚/0˚]W[±45˚]$_2$

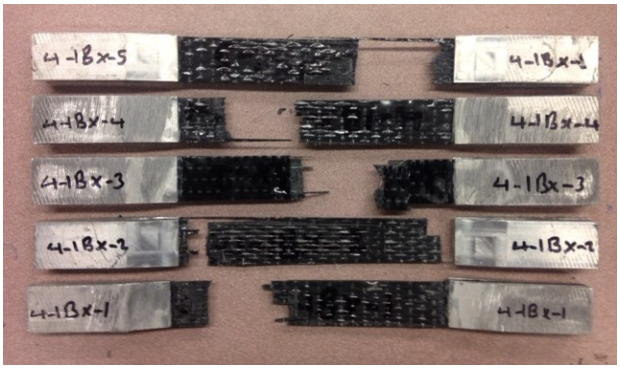

UD[90˚]W[±45˚]$_2$UD[0˚]

Figure 5-59 Post failure photos of coupons with different stacking sequences (4 layers)

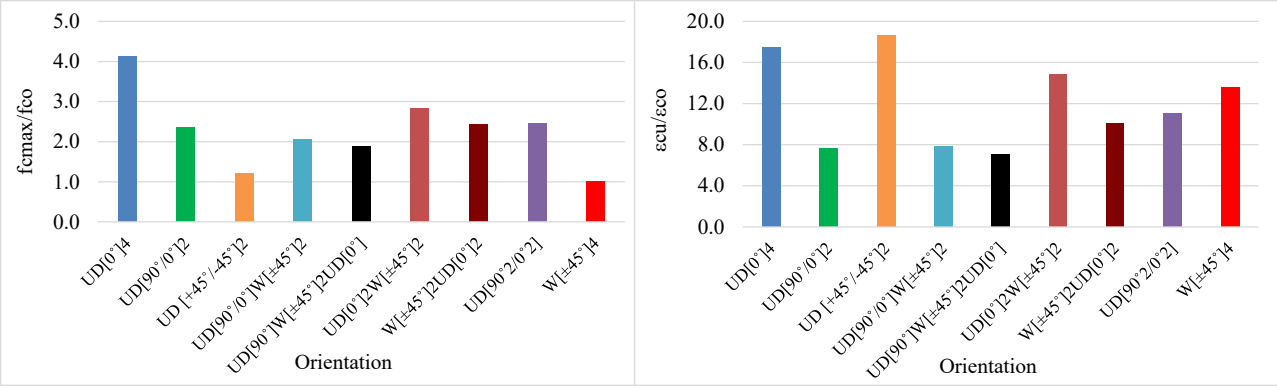

a) Stress ratio

b) Strain ratio

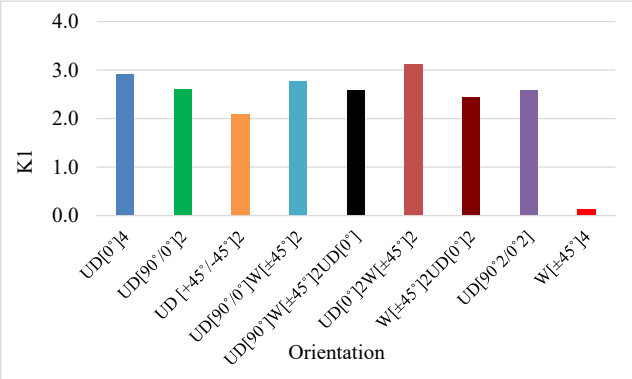

c) Strength effectiveness

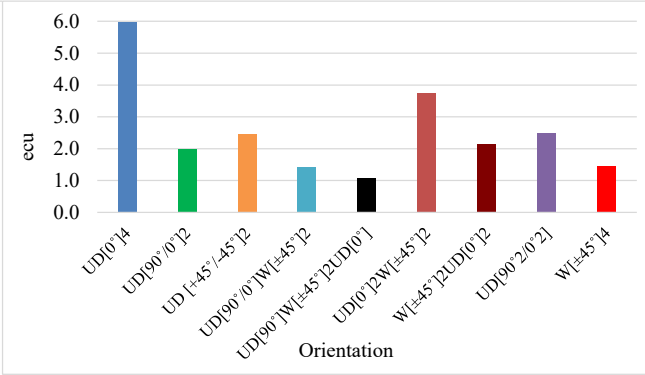

d) Energy absorption capacity

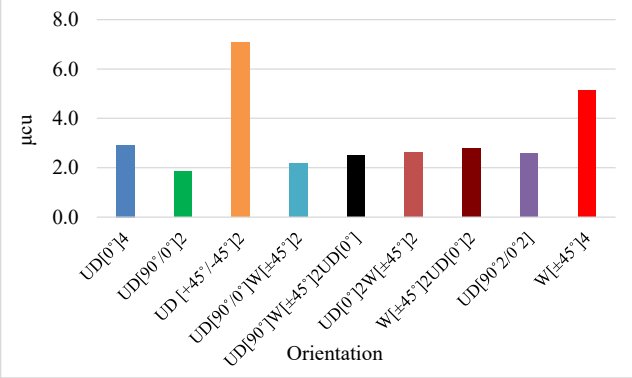

e) Ductility factor

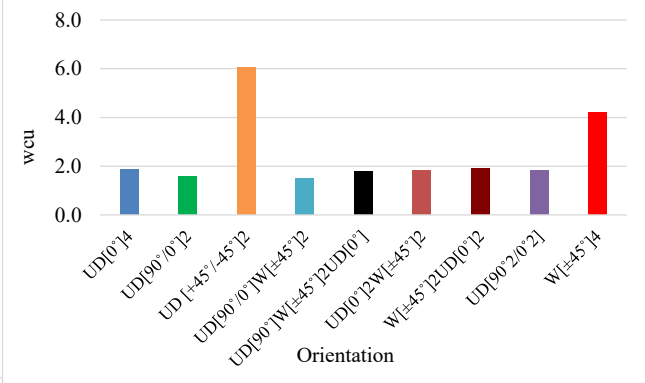

f) Work index

Figure 5-60 Effect of fiber orientation and stacking sequence on different parameters

5.7.2 6 layers of CFRP

5.7.2.1 Coupons

Figure 5-61 shows the effect of stacking sequence on the stress-strain behavior of CFRP coupons with 6 layers of CFRP. As previously discussed maximum strength and stiffness was achieved by coupons in Series 1 (fibers parallel to load axis), while maximum ductility was obtained by coupons having fibers in angle direction (Series 3 and 7). All other combinations were in between these two extremes. By comparing the CFRP coupons with 4 and 6 layers, the stress enhancement was lower in coupons having UD[0º] fibers, while no noticeable difference is observed companion coupons in other series. The failure mode of coupons was similar to the mode at 4 layers as shown **Figure 5-64**.

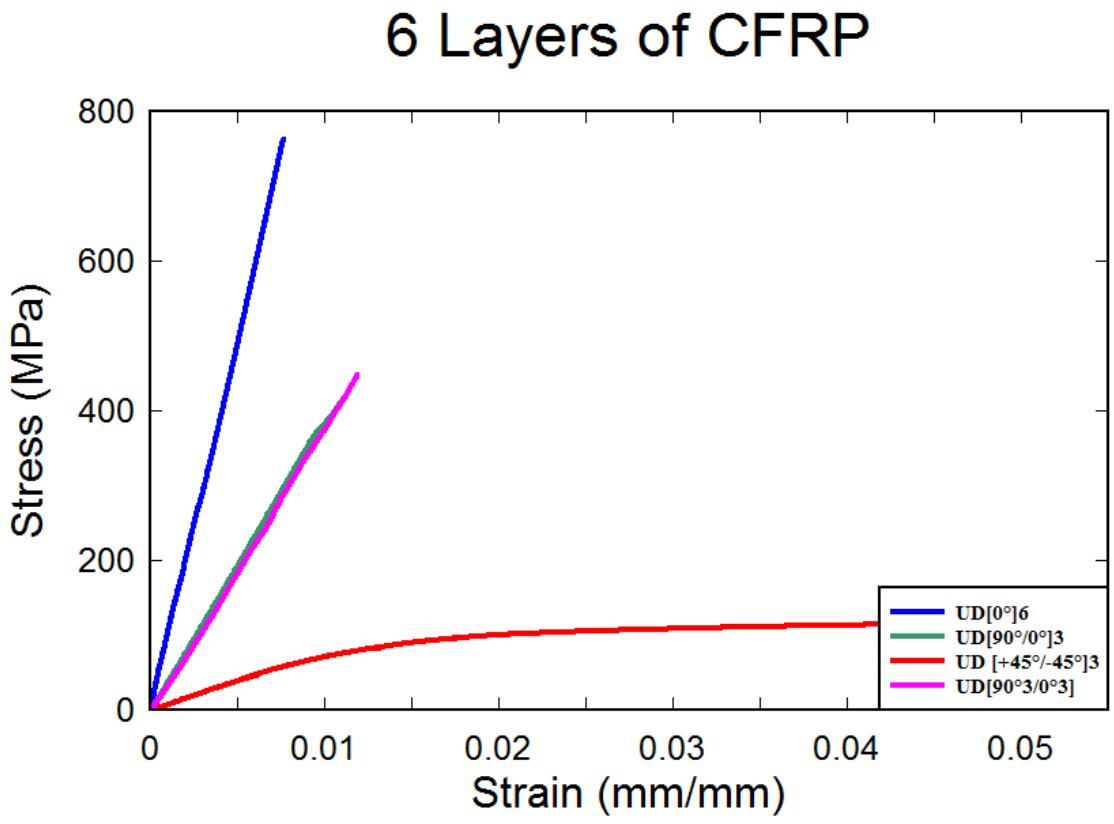

Figure 5-61 Effect of stacking sequence on stress-strain behavior of CFRP coupons

5.7.2.2 Cylinders

Figure 5-62 compares the stress-strain response of cylinders with 6 layers of CFRP but having different stacking sequence. The comparison of strength, ductility and toughness indicators is presented in **Table 5-1** and **Figure 5-65**. In terms of the increase in stress (f'_{cc}/f_{co}) and strain ($\varepsilon'_{cc}/\varepsilon_{co}$), the sequence among series at 6 layers generally follows the same trend as was observed with 4 layers. Although, in the case of the UD [90˚/0˚] and UD [90˚$_x$/0˚$_x$], the specimens confined in the UD [90˚/0˚] direction were found to have a higher gain in strength and strain than those in the UD [90˚$_x$/0˚$_x$] pattern (opposite to observation at 4 layers). The most important strength increase of 399.1% was achieved by specimens having hoop fibers (UD [0˚]) only, while the maximum gain in strain of 5762.1% was reached by specimens with a ±45° fiber orientation (Series 3 and 7). An average increase in strength of 195.01% and 180.78% was observed for specimens confined in UD [90˚/0˚] and UD [90˚$_x$/0˚$_x$], respectively, while the same specimens exhibited an average increase in strain of approximately 1183.87% and 1508.25%. Specimens confined in the hoop direction (UD [0˚]) displayed the greatest energy absorption capacity factor (e_{cu}) of 10.40, and specimens confined with CFRP sheets in the UD [90˚$_x$/0˚$_x$] pattern demonstrated the lowest energy absorption capacity factor (e_{cu}) of 3.25. Those confined by sheets with fibers in the woven angled direction (W [±45˚]) provided a maximum ductility factor (μ_{cu}) of roughly 16.49. As also presented in **Table 5-1** and **Figure 5-65**, a minimum ductility factor of approximately 2.28 was attained by specimens confined with the UD [0˚] pattern. **Figure 5-63** shows the effect of stacking sequence on the failure mode of confined concrete cylinders. It is obvious jacket rupture and concrete core crushing varies by changing the stacking sequence.

In summary, the stress-strain curve of cylinders is affected by fiber orientation and stacking sequence with the greatest increase in strength associated with series having hoop direction fibers, while more ductile behavior is obtained in series with angular fibers.

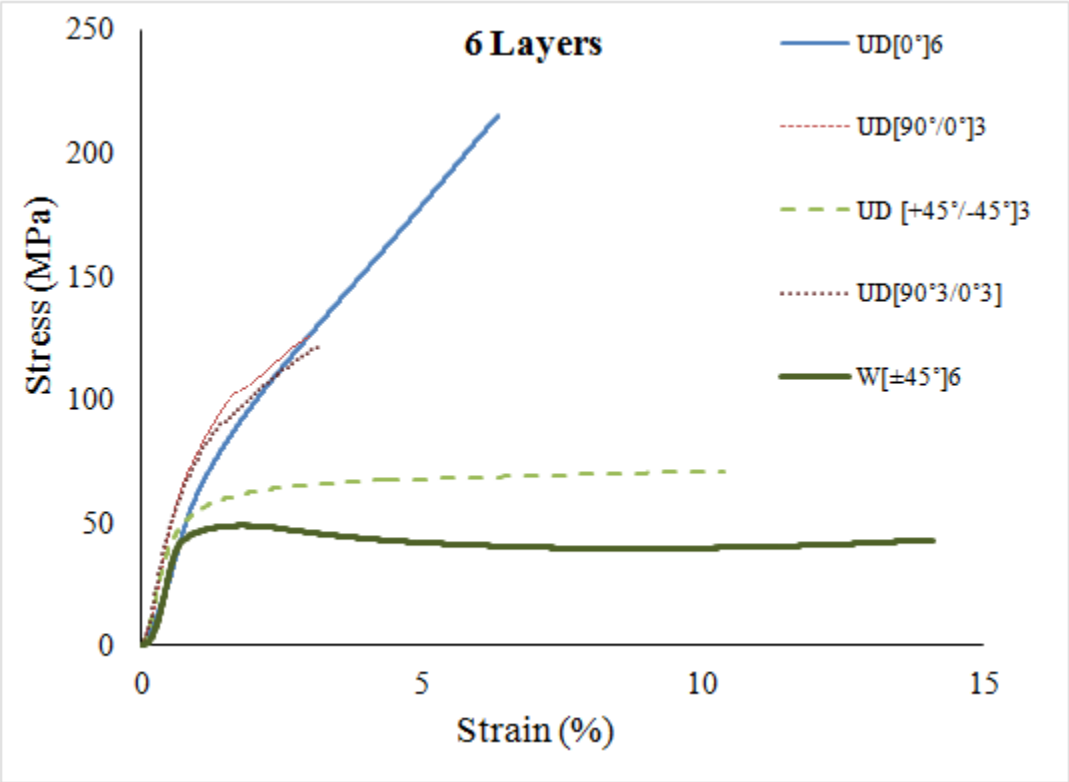

Figure 5-62 Effect of fiber orientation on stress-strain behavior of confined concrete

UD[90˚/0˚]$_3$

UD[90˚$_3$/0˚$_3$]

UD [+45˚/-45˚]$_3$

W[±45˚]$_6$

Figure 5-63 Post failure photos of cylinders with different stacking sequences (6 layers)

UD[90˚/0˚]$_3$

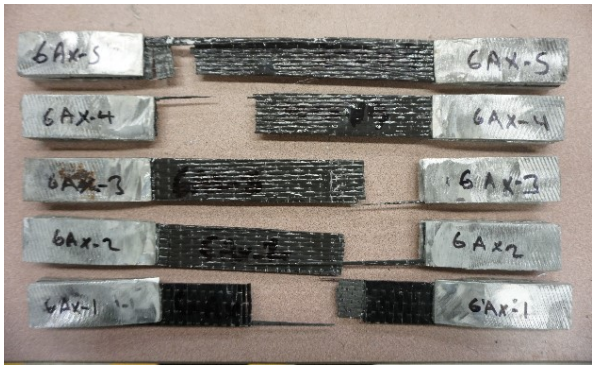

UD[90˚$_3$/0˚$_3$]

Figure 5-64 Post failure photos of coupons with different stacking sequences (6 layers)

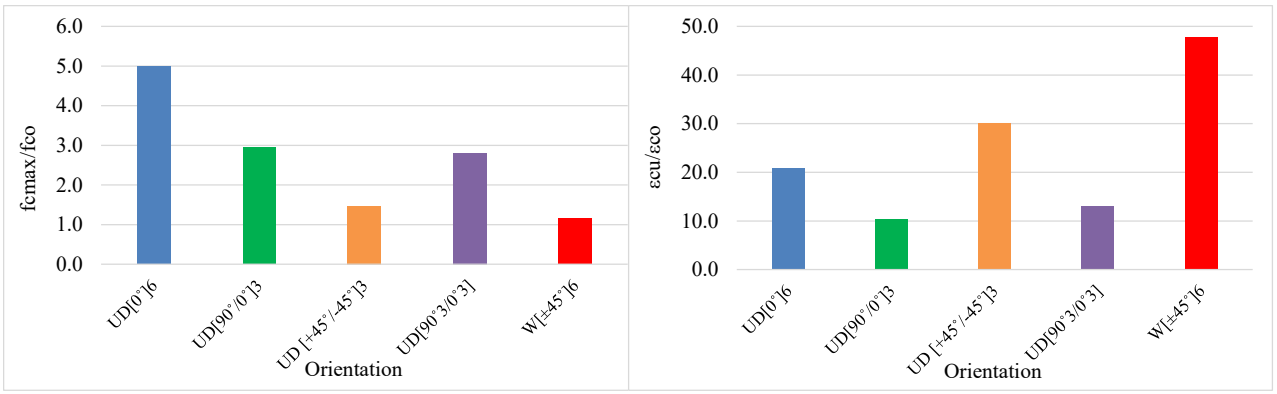

a) Stress ratio

b) Strain ratio

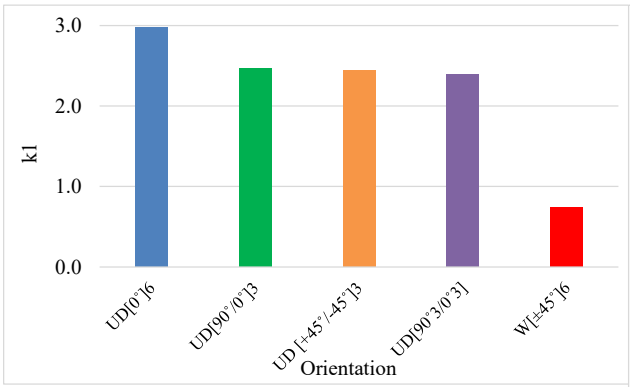

c) Strength effectiveness

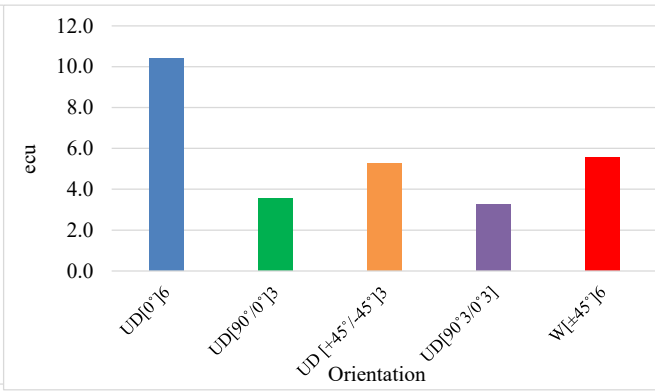

d) Energy absorption capacity

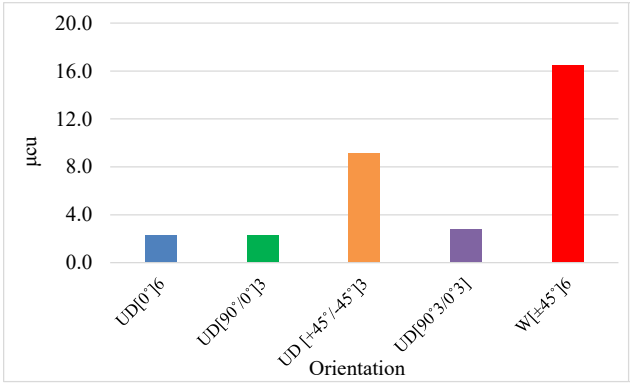

e) Ductility factor

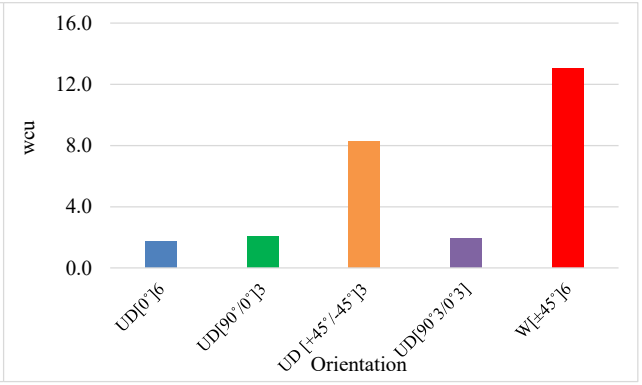

f) Work index

Figure 5-65 Effect of fiber orientation and stacking sequence on different parameters

5.7.3 8 layers of CFRP

5.7.3.1 Coupons

Similar trends are observed for the results of coupons with 8 layers when compared to the results in the 4 and 6 layer series. However examining **Figure 5-66** it can be noticed that the coupons show somewhat reduced ductility for those specimens with angular fibers when compared to companion coupons with lesser layers. In summary, the results from the specimens with 4, 6 and 8 layers demonstrate that stacking sequence has significant impact on the tensile stress-strain behavior of CFRP laminates.

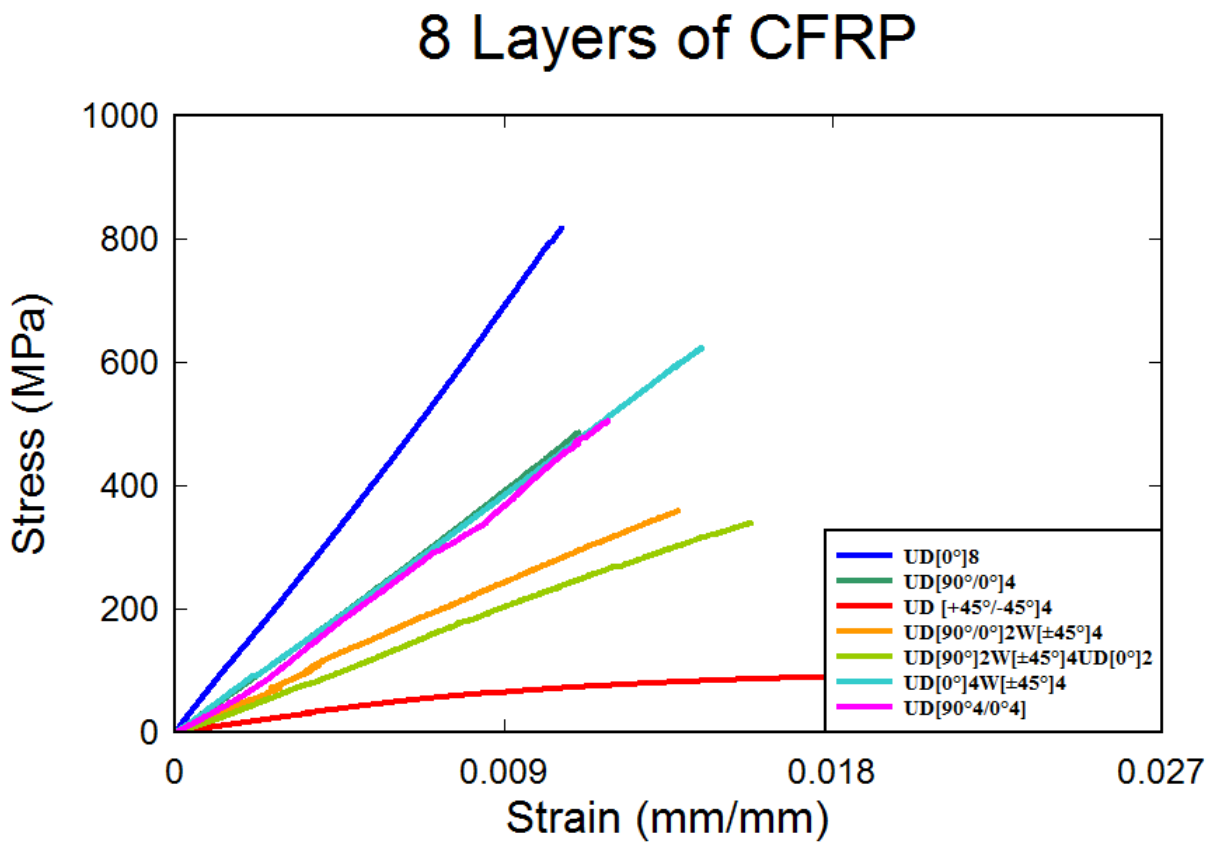

Figure 5-66 Effect of stacking sequence on stress-strain behavior of CFRP coupons

5.7.3.2 Cylinders

Figure 5-67 shows specimens with 8 layers similar trends to those observed in 4 and 6 layer cylinder series. In general the best overall stress-strain performance is observed for specimens confined with 8 layers of CFRP having fibers in the hoop direction (UD [0˚]), or a matrix of fibers in the hoop (UD [0˚]) and other directions, which means the stress-train response in all combinations is dominated by the fibers in hoop direction, particularly in the case of increase in maximum confined stress. The largest and smallest enhancements in peak stress (512.75 % and 31.23 %, respectively) were obtained for cylinders confined with UD[0˚]$_{8,}$ and W[±45˚]$_{8,}$ respectively. No clear trend is observed in the case of the strength effectiveness factor (k_1). Specimens confined with hoop direction CFRP showed a maximum energy absorption capacity (e_{cu}) of about 7.59 as shown in **Table 5-1**. The ductility (μ_{cu}) and work index (w_{cu}) factors are further indicators of ductility and toughness of the confined specimens. These factors were found to be sensitive to stacking sequence, with specimen with woven angled direction (W [±45˚]) presenting the best ductility (μ_{cu}= 17.38), when compared to those jacketed in all other directions. In terms of the effect of layup sequence, most stress-strain factors were similar for cylinders confined with UD[90˚/0˚]$_4$ and UD[90˚$_4$/0˚$_4$], except in the case of increase in strain. For example, a relative increase in maximum strain of 1377.14 % was experienced in cylinders confined with 8 layers of CFRP in UD[90˚/0˚]$_4$ direction, while cylinders with the same amount of confinement with the UD[90˚$_4$/0˚$_4$] layup showed 1684.24 % increase. Similarly, comparing cylinders confined with UD[0˚]$_4$W[±45˚]$_4$ and W[±45˚]$_4$UD[0˚]$_4$, one can see energy absorption capacity is affected by layup sequence.

As discussed previously and shown in **Figure 5-69** no significant difference in failure mode due to were observed in the case of coupons with different stacking sequences. **Figure 5-68** shows

how stacking sequence effect the mode of failure in the cylinders. Examining the failure photos one can see how changing the layup order of CFRP layers has an important effect on final failure mode (compare photos on the left and right for companion series). Better behavior was achieved in the right-hand photos, where concrete spalling is reduced as the sheet is changed from unidirectional or woven (e.g. Series 3 vs. 7) and were innermost fibers are angular and outermost fibers are unidirectional (e.g. series 5A vs. 5B).

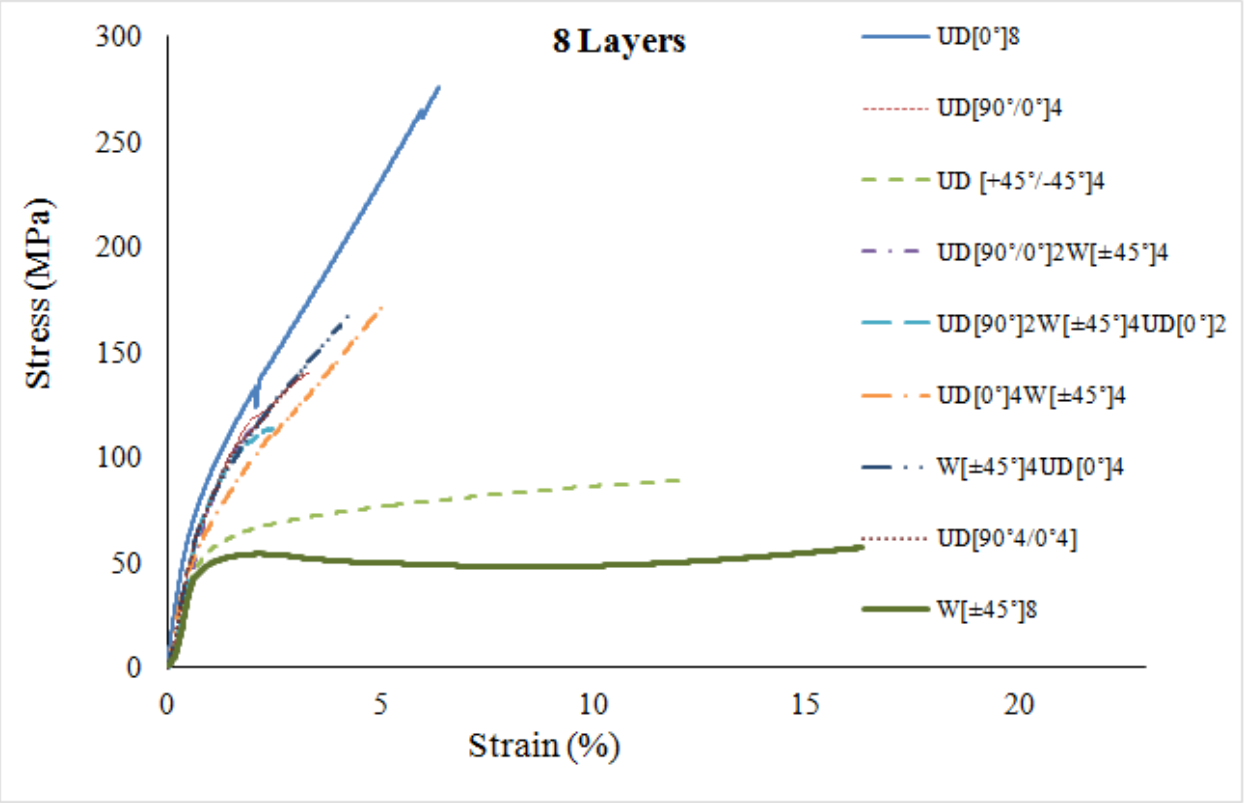

Figure 5-67 Effect of fiber orientation on stress-strain behavior of confined concrete

UD[90˚/0˚]$_4$

UD[90˚$_4$/0˚$_4$]

UD [+45˚/-45˚]$_4$

W[±45˚]$_8$

UD[90˚/0˚]$_2$W[±45˚]$_4$

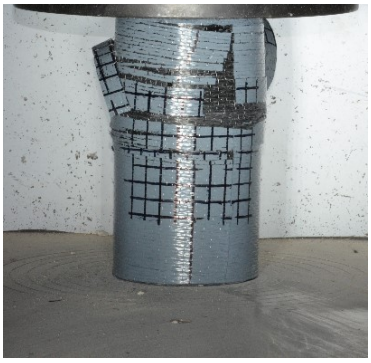

UD[90˚]$_2$W[±45˚]$_4$UD[0˚]$_2$

UD[0˚]$_4$W[±45˚]$_4$

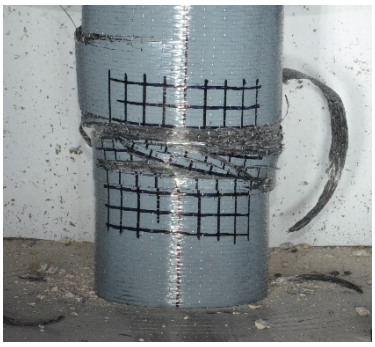

W[±45˚]$_4$UD[0˚]$_4$

Figure 5-68 Post failure photos of cylinders with different stacking sequences (8 layers)

UD[90˚/0˚]$_4$

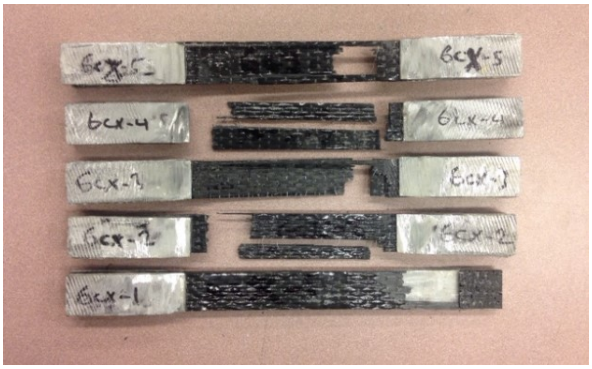

UD[90˚$_4$/0˚$_4$]

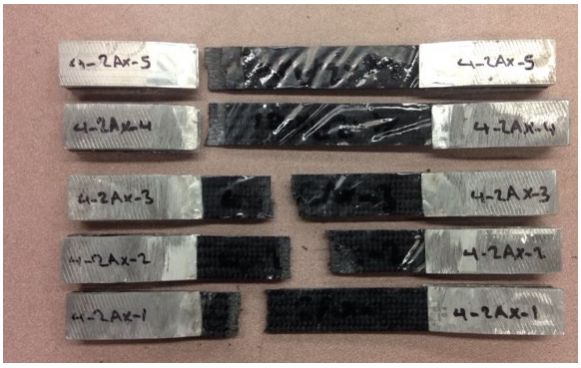

UD[90˚/0˚]$_2$W[±45˚]$_4$

UD[90˚]$_2$W[±45˚]$_4$UD[0˚]$_2$

Figure 5-69 Post failure photos of coupons with different stacking sequences (8 layers)

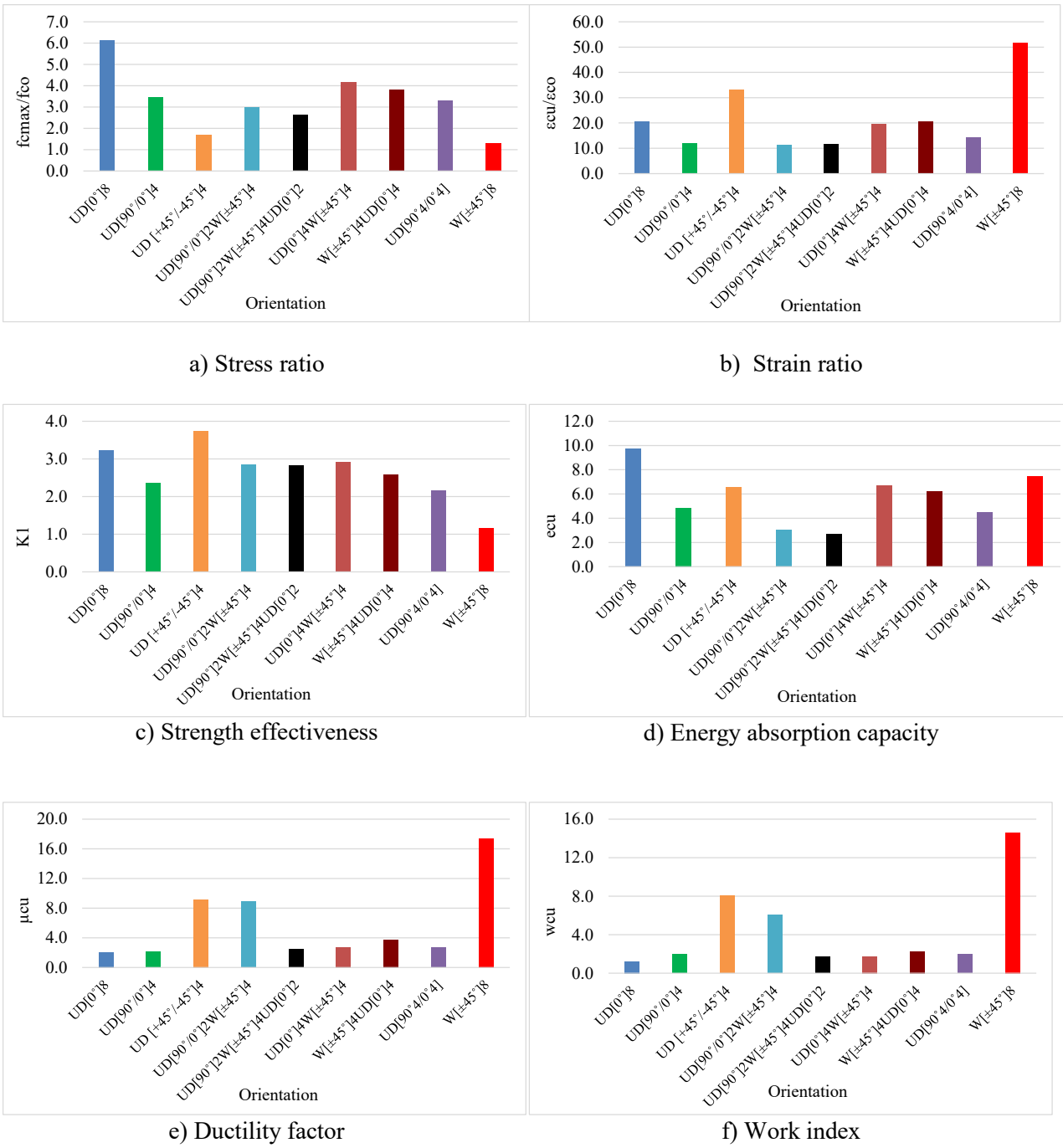

a) Stress ratio

b) Strain ratio

c) Strength effectiveness

d) Energy absorption capacity

e) Ductility factor

f) Work index

Figure 5-70 Effect of fiber orientation and stacking sequence on different parameters

5.8 Summary

Previous researchers have noted that fiber orientation and stacking sequence have direct impacts on the behavior of confined concrete (Parretti and Naani 2002; Li et al. 2005; Au and Buyukozturk 2005; Sadeghian (2009 and 2010); Vincent and Ozbakkaloglu 2013). These researchers have concluded that concrete specimens confined with FRP having fibers aligned in the hoop direction (UD [0˚]) experience a maximum increase in strength, while those confined with angular fibers achieve greater increase in strain. These characteristics were also evident in this study and are clear when examining the results in **Figure 5-60**, **Figure 5-65**, and **Figure 5-70** for cylinders confined with 4, 6, and 8 layers of CFRP sheets, where maximum strength improvements are reported for the UD [0˚] series, and maximum increase in strain capacity. For specimens with large amounts of CFRP having fibers aligned in the angled directions.

The influence of fiber orientation on energy absorption capacity (e_{cu}) (i.e. overall toughness) was greatest for cylinders confined in the hoop direction (UD [0˚]) due to the large increases in maximum stress and strain. The ductility factor (μ_{cu}) and work index (w_{cu}) were also used to assess the ductility of the tested specimens. Consulting **Figure 5-60**, **Figure 5-65**, and **Figure 5-70** one can see that in general, specimens confined with 4 layers of UD [+45˚/-45˚] sheets provided better ductility, while by increasing the number of layers to 6 and 8 layers this behavior inverted to cylinders confined with W [±45˚] CFRP sheets.

The stacking sequence also had a significant impact on the failure mode of the CFRP confined concrete cylinders. It was found that confining cylinders with unidirectional CFRP sheets with fibers aligned in the hoop direction gives the best increase in strength; however this also results in very catastrophic failures, due to the large release of energy as the FRP jacket fails. Cylinders confined with CFRP sheets having fibers aligned in the angular direction led to more ductile and

gradual failures. The results also demonstrate that by applying the angular CFRP sheets as an inner layer and hoop direction sheets in outermost layers is one strategy that can prevent catastrophic brittle failures, with concrete crushing in the concrete core confined within the FRP jacket, preventing the violent expulsion of concrete fragments.

6 Chapter 6: Analysis

6.1 General

Over the past few decades researchers have conducted extensive experimental research related to the compressive behavior of concrete confined with FRP jacketing. Based on this experimental work, researchers have proposed constitutive models for predicting the stress-strain behavior FRP-confined concrete. Most of these models have been calibrated based on experimental programs where limited variables have been considered (i.e. FRP type, number of layers, concrete strength (Cui and Sheikh 2010)). As was demonstrated in the current study, the behavior of FRP-confined concrete is altered when using different FRP fiber orientation and layup arrangements. This chapter will examine the ability of models proposed in the literature to predict the stress-strain response of the cylinders tested in this research program and will give insight into the need to develop new constitutive models which take into account the effect of FRP fiber orientation on stress-strain response.

The models proposed in the literature can be classified into two groups: 1) Design-oriented models and 2) analysis-oriented models (Lam and Teng 2003, Cui 2010). In the first category experimental results are used to derive empirical equations that can predict stress-strain response, while in the second category an incremental procedure, where axial stress and strain are evaluated at a given confining stress, is used to develop the models (with consideration of strain compatibility and force equilibrium) (Cui and Sheikh 2010). In this chapter, various models from the first category are evaluated. In the sections that follow each model is briefly described, thereafter the models are used to predict the results from the current experimental program. The accuracy of the models is assessed by comparing experimental and analytical stress-strain curves

and comparing experimental and analytical predictions for peak stress, peak strain as well as using the strength, toughness and ductility stress-strain indicators described in Chapter 5.

6.2 Constitutive Models Description

6.2.1 Confinement pressure due to FRP jacketing

The majority of the models in design-oriented empirical models modify the stress-strain behavior of concrete based on the confinement pressure exerted by the FRP-jacketing (f_l). For circular cross-sections, the maximum confining pressure is obtained assuming uniform confinement pressure and assuming the FRP jacket reaches is tensile rupture strength:

$$f_l = \frac{2 \, . \, f_{FRP} \, . n_{frp}}{D} \qquad \textbf{Eq. 6-1}$$

Where D = diameter of circular specimen; n_{FRP} = total thickness of the FRP jacket (number of layers multiplied by the thickness per layer); f_{FRP} = tensile strength of FRP material; and f_l = maximum confining pressure exerted by FRP jacket

The tensile strength of the FRP material is calculated using Hooke's law and assumes the FRP material has linear-elastic stress-strain behavior up to failure:

$$f_{FRP=} \, E_{FRP} . \, \varepsilon_{FRP} \qquad \textbf{Eq. 6-2}$$

Where $E_{FRP=}$ Modulus of elasticity of FRP in fiber direction; $\varepsilon_{FRP=}$ Rupture strain of FRP. In the current study the FRP material properties for different jacket layups were obtained from the coupon test data presented in Chapter 4.

In the next section the constitutive models which were taken from the literature are described and compared to the experimental test data from each series (further discussion will be provided in **Section** 6.3) will be discussed.

6.2.2 Design-oriented empirical models

6.2.3 Fardis and khalili (1982)

This early model was developed using the data from experimental program where the authors tested 46 small size cylinders confined with GFRP jackets under pure compressive loading. Two cylinders sizes with dimensions of (75 x 150 mm) and (100 x 200 mm) were tested, with two batches of normal-strength concrete having unconfined strength of 34.5 MPa and 31 MPa. Specimens were confined with 1 to 5 layers of GFRP jackets. Based on this data the authors suggested that the simple tri-axial failure criterion proposed by Richart et al. (1929) and later modified by Newman and Newman (1971), can be used to estimate the maximum strength of FRP-confined concrete, as shown in **Eq**. **6-3** and **Eq**. **6-4**:

$$f_{cc'=}\ f_{co}\left(1+k_1\frac{f_l}{f_{co}}\right) \qquad \textbf{Eq. 6-3}$$

$$f_{cc'=}\ f_{co}\left[1+3.7(\frac{f_l}{f_{co}})^{0.86}\right] \qquad \textbf{Eq. 6-4}$$

Where $f_{cc'=}$ peak strength of FRP-confined concrete; f_{co} = unconfined concrete strength; and k_1= Strength effectiveness factor assigned to be 4.1 by Richart et al. (1929). Using the data generated in their experimental study the authors proposed an equation to predict the maximum strain of FRP-confined concrete at failure:

$$\varepsilon_{cc}^{'} = 0.002+0.001\frac{E_{FRP}\, n_{FRP}}{D\, f_{co}} \qquad \textbf{Eq. 6-5}$$

Where $\varepsilon_{cc}^{'} =$ Axial strain corresponding to $f_{cc'}$ and the remaining parameters are as defined previously. The following hyperbolic equation is then used to predict the complete stress-strain response of the FRP-confined concrete:

$$f_c = \frac{E_{co}\, \varepsilon_c}{1+\varepsilon_c\left(\frac{f_{cc}^{'}}{E_{co}}-\frac{1}{\varepsilon_{cc}^{'}}\right)} \qquad \textbf{Eq. 6-6}$$

Where $E_{co} =$ initial tangent modulus of unconfined concrete; and f_c = stress at any given strainε_c . **Figure 6-1** shows how the model predicts the stress-strain response of the FRP-confined concrete cylinders tested in the current study (results shown for 100 mm cylinders with 4 layers of CFRP). In general it can be seen that model over-predicts the stress-strain curves in most series, while poor results are observed in complex layups which contain angular FRP layers. Further discussion is provided in **Section** 6.3.

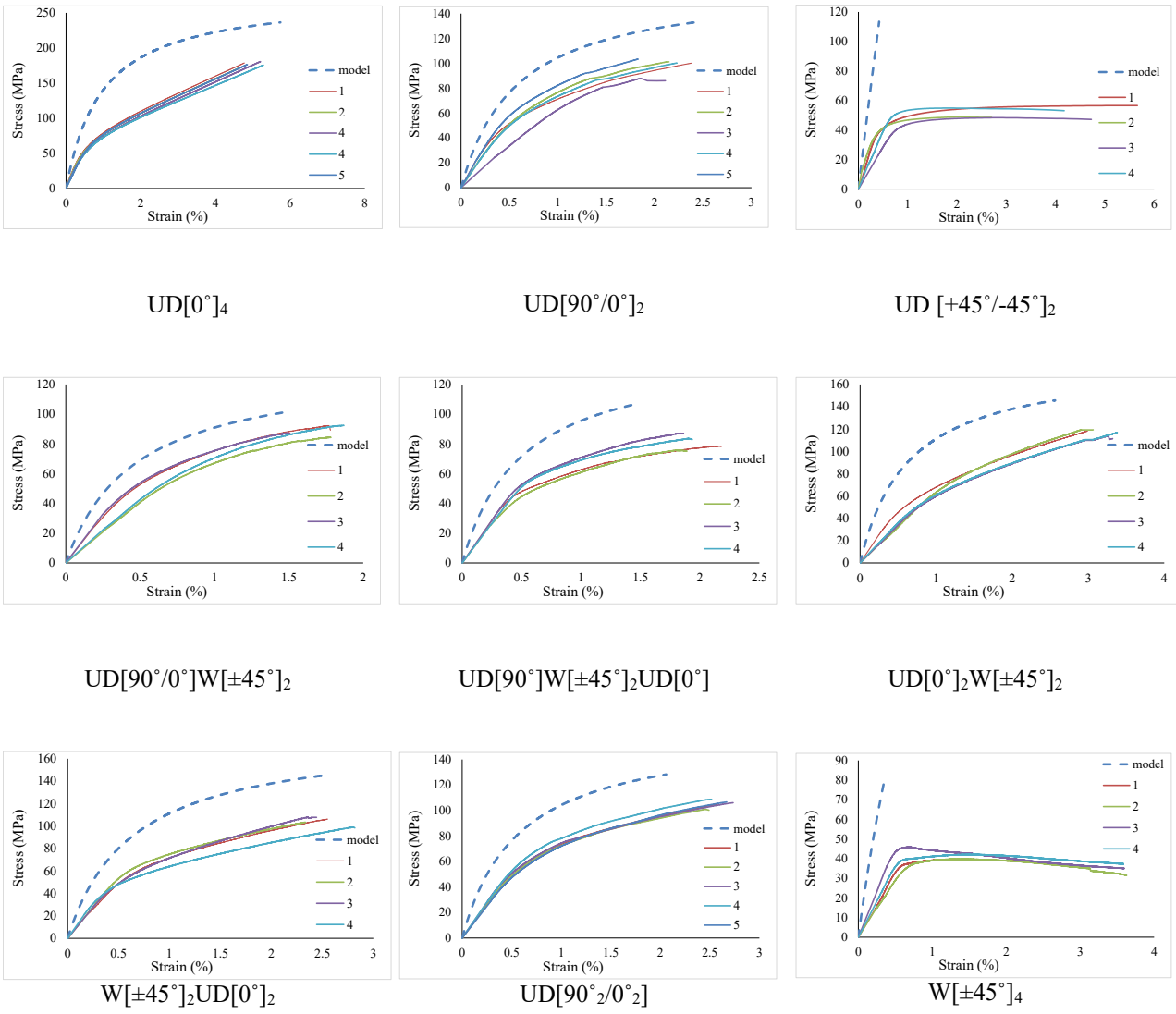

Figure 6-1 prediction of stress-strain behavior of FRP-confined concrete columns (Fardis and khalili (1982))

6.2.4 Miyauchi et al. (1999)

This model was derived based on data generated from a study were a large series of cylinders confined with unidirectional CFRP sheets in the hoop direction were tested under uniaxial

compression load. Two specimen sizes of 100 x 200 mm and 150 x 300 mm were considered and test variables included concrete strength (20MPa, 30MPa, 50MPa and 100MPa) and the number of CFRP layers. In most of the cases the authors observed bilinear stress-strain responses for the CFRP-confined concrete, with the exception of those samples with 100MPa concrete, which experienced post-peak softening. Based on the results, the authors proposed two types of stress-strain relationships: 1) increasing type and 2) decreasing type, as shown in **Figure 6-2**. The equations used to predict the curves consist of parabolic functions for the first branch and a linear equation in the second branch.

For the increasing type these equations are defined as follows:

$$f_c = f_{co}\left[2\frac{\varepsilon_c}{\varepsilon_{co}} - (\frac{\varepsilon_c}{\varepsilon_{co}})^2\right] \qquad 0 \le \varepsilon_c \le \varepsilon_{c\lambda} \qquad \textbf{Eq. 6-7}$$

$$f_c = f_{cu} - \lambda(\varepsilon_{cu} - \varepsilon_c) \qquad \varepsilon_{c\lambda} \le \varepsilon_c \le \varepsilon_{cu} \qquad \textbf{Eq. 6-8}$$

Where ε_{co} = the peak strain of unconfined concrete, taken as 0.002; f_{cu}= concrete stress at failure (where f_{cu}= $f_{cc}^{'}$ in the increasing type) and ε_{cu}= concrete axial strain corresponding to f_{cu}. The parameter λ is defined using the following empirical relationship:

$$\lambda = \frac{-2f_{co}(\varepsilon_{cu} - \varepsilon_{co}) + \sqrt{4f_{co}(f_{co}\varepsilon_{cu}^2 - 2f_{co}\varepsilon_{co}\varepsilon_{cu} + f_{cu}\varepsilon_{co}^2)}}{\varepsilon_{co}^2} \qquad \textbf{Eq. 6-9}$$

The limiting strain and stress between branch 1 and 2 ($\varepsilon_{c\lambda}$, $f_{c\lambda}$) are defined as follows:

$$\varepsilon_{c\lambda} = \varepsilon_{co} - \lambda\frac{\varepsilon_{co}^2}{2f_{co}} \qquad \textbf{Eq. 6-10}$$

$$f_{c\lambda} = f_{co}\left[2\frac{\varepsilon_{c\lambda}}{\varepsilon_{co}} - (\frac{\varepsilon_{c\lambda}}{\varepsilon_{co}})^2\right] \quad \textbf{Eq. 6-11}$$

In the case of the decreasing type curve, the relationships for the first and second branch of the stress-strain curve are defined as follows:

$$f_c = f_{co}\left[2\frac{\varepsilon_c}{\varepsilon_{co}} - (\frac{\varepsilon_c}{\varepsilon_{co}})^2\right] \qquad 0 \leq \varepsilon_c \leq \varepsilon_{co} \quad \textbf{Eq. 6-12}$$

$$f_c = f_{co} + \frac{(\varepsilon_c - \varepsilon_{co})(f_{cu} - f_{co})}{\varepsilon_{cu} - \varepsilon_{co}} \qquad \varepsilon_{co} \leq \varepsilon_c \leq \varepsilon_{cu} \quad \textbf{Eq. 6-13}$$

Based on the experimental data generated in their study, the authors proposed an empirical relationship for the failure stress of FRP-confined concrete (f_{cu}) and corresponding strain (ε_{cu}):

$$f_{cu} = f_{co}\left(1 + 2.98\frac{f_l}{f_{co}}\right) \quad \textbf{Eq. 6-14}$$

$$\varepsilon_{cu} = \varepsilon_{co}\left[1 + a_1(\frac{f_l}{f_{co}})^{b_1}\right] \quad \textbf{Eq. 6-15}$$

Where the parameters a_1 and b_1 are calculated as follows:

$$a_1 = 15.87 - 0.093 f_{co} \quad \textbf{Eq. 6-16}$$

$$b_1 = 0.246 - 0.0064 f_{co}$$ **Eq. 6-17**

Figure 6-3 presents how the model predicts the stress-strain behavior of FRP-confined concrete columns with different stacking sequences tested in the current study. It can be seen that the model does not accurately capture failure stress and strain in most series, with poor correlation between experimental and analytical results for layups containing angular CFRP.

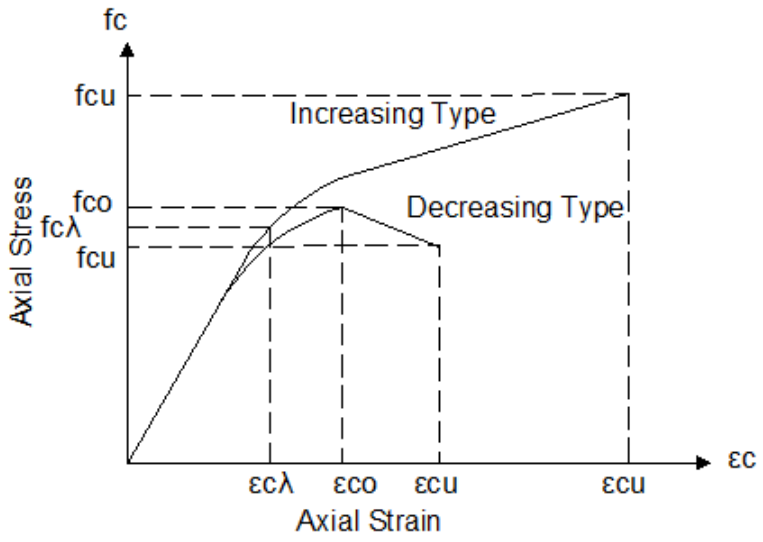

Figure 6-2 Increasing and decreasing stress-strain curves for FRP confined concrete (Miyauchi et al. (1999))

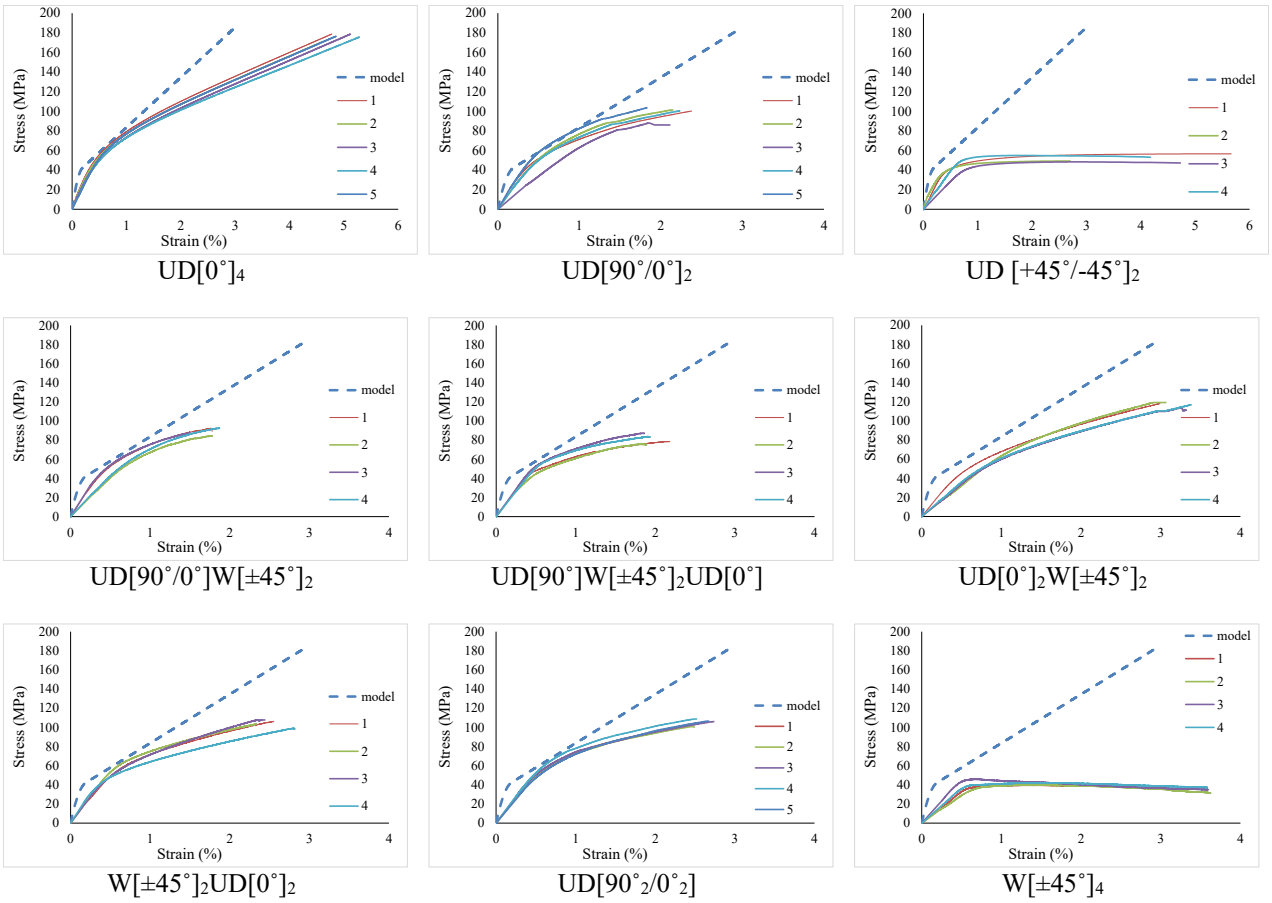

Figure 6-3 prediction of stress-strain behavior of FRP-confined concrete columns (Miyauchi et al. (1999))

6.2.5 Campione and Miraglia (2003)

This model was derived based on experimental work FRP confined concrete specimens. Having both circular and square cross-sections (where square sections had rounded corners). Using data from this study an analytical model was developed using the closed form equation of Pinto and Giuffre (1970) which was originally proposed to predict the stress-strain behavior of concrete confined with steel jacketing. The authors proposed the following expression to model the complete stress-strain response of FRP-confined concrete specimens having circular cross-section similar to a four parameters model previously proposed by Richard and Abbott (1975):

$$f_c = f_{co}\left[\frac{E_2}{E_1}\cdot\frac{\varepsilon_c}{\varepsilon_{co}} + \frac{\left(1-\frac{E_2}{E_1}\right)\frac{\varepsilon_c}{\varepsilon_{co}}}{\left[1+\left(\frac{\varepsilon_c}{\varepsilon_{co}}\right)^n\right]^{\frac{1}{n}}}\right] \quad \textbf{Eq. 6-18}$$

Where the parameters E_2 and E_1 are taken as:

$$E_2 = \frac{f_{cc}^{'} - f_{co}}{\varepsilon_{cc}^{'} - \varepsilon_{co}} \quad \textbf{Eq. 6-19}$$

E_1 =Initial concrete modulus of elasticity

The shape of the stress-strain curve in the transition zone was controlled by n factor which was suggested to be taken as equal to 3. A schematic description of the resulting stress-strain curve is in **Figure 6-4**. The maximum confined concrete stress is approximated using the expression and below which takes into account the confining pressure provided by the FRP:

$$f_{cc}^{'} = f_{co} + 2\,f_l \quad \textbf{Eq. 6-20}$$

The maximum strain at failure is approximated using the following expression which is derived based on the energy balance method proposed by Mander et al. (1988):

$$\varepsilon_{cc}^{'} = \frac{8t_{FRP}}{D}\frac{f_{FRP}^2}{E_{FRP}}\frac{1}{f_{co}+f_l} \quad \textbf{Eq. 6-21}$$

t_{FRP} = Total thickness of FRP jacket

Figure 6-5 compares the predictions using this model with the experimental results from the current study. It can be seen that the model provides accurate predictions for Series 1 which had unidirectional fibers and captures the general shape of the stress-strain curves for the FRP-

confined concrete cylinders with fibers aligned in different orientations, although maximum stress and failure strain are not always accurately predicted.

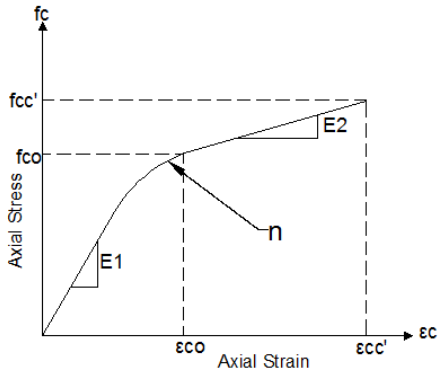

Figure 6-4 Stress-strain curve for FRP confined concrete (Campione and Miraglia (2003))

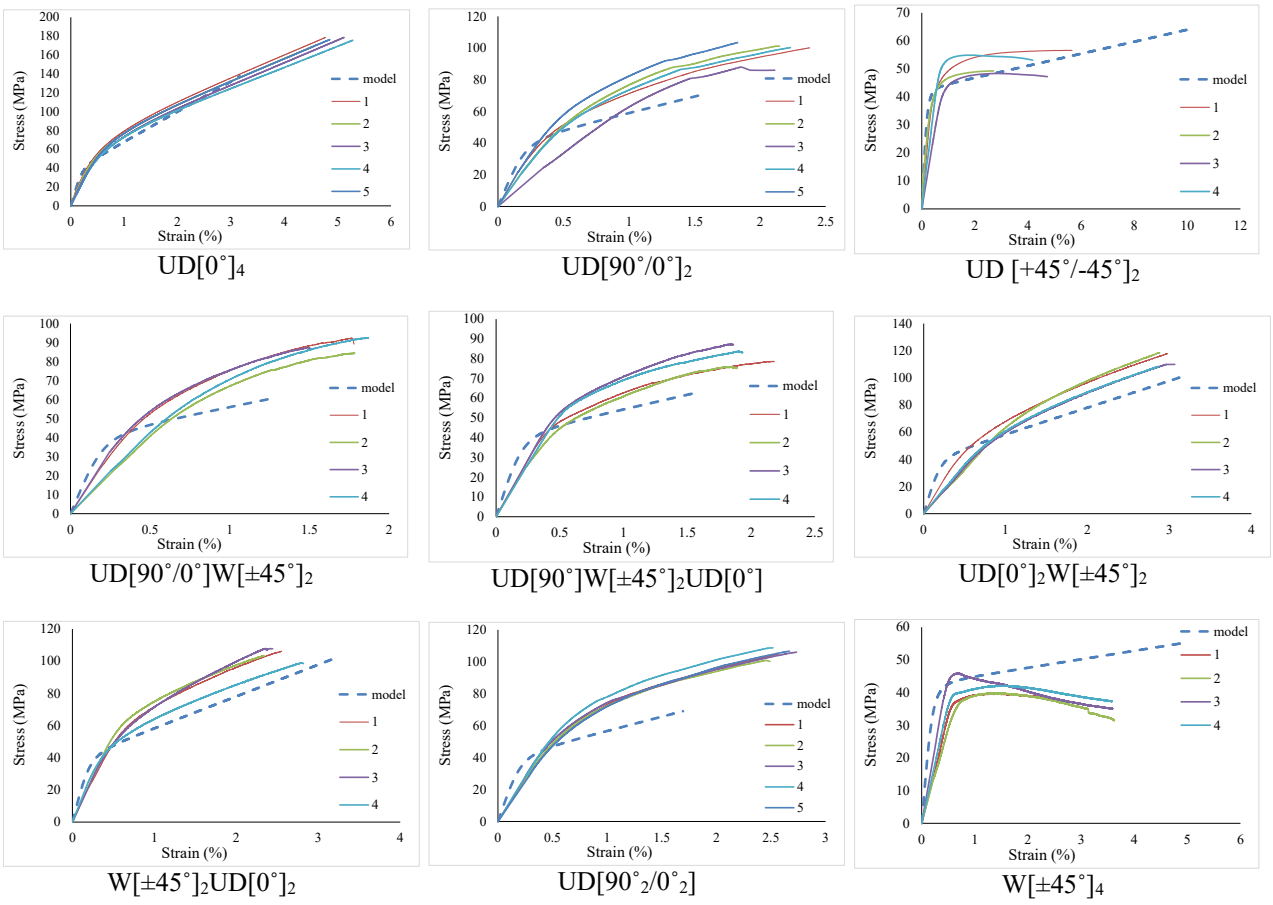

Figure 6-5 Prediction of stress-strain behavior of FRP-confined concrete columns ((Campione and Miraglia (2003))

6.2.6 Lam and Teng (2003)

Based on a database of experimental results from other researchers, Lam and Teng (2003) proposed the stress-strain shown schematically in **Figure 6-6** to predict the stress-strain response of FRP-confined concrete. The model consists of a bilinear curve with two branches, consisting of an initial parabolic ascending branch followed by a second linear branch as defined in the expressions below:

$$f_{c=} E_c \varepsilon_c - \frac{(E_c - E_2)^2}{4 f_{co}} \varepsilon_c^2 \qquad \text{For } 0 < \varepsilon_c < \varepsilon_o \text{ (parabolic portions)} \qquad \textbf{Eq. 6-22}$$

$$f_c = f_o + E_2 \varepsilon_c \qquad \text{For } \varepsilon_o < \varepsilon_c < \varepsilon_{cc}^{'} \text{ (linear portion)} \qquad \textbf{Eq. 6-23}$$

Where f_o is taken as the strength of unconfined concrete (f_{co}) for simplicity, and where the modulus of elasticity of the unconfined concrete is approximated as E_c= 4730$\sqrt{f_{co}}$. Strain ε_o is the axial strain at which the parabolic portion meets the linear portion and is defined as follows.

$$\varepsilon_o = \frac{2 f_o}{E_c - E_2} \qquad \textbf{Eq. 6-24}$$

The secant modulus (E_2) is calculated as follows:

$$E_2 = \frac{f_{cc}^{'} - f_o}{\varepsilon_{cc}^{'}} \qquad \textbf{Eq. 6-25}$$

The authors proposed empirical equations for the peak stress and peak strain, which are given as:

$$f_{cc'=}\ f_{co} + \left(3.3 \frac{f_{lu,a}}{f_{co}}\right) \qquad \textbf{Eq. 6-26}$$

$$\varepsilon_{cc}^{'} = \varepsilon_{co}\left[1.75 + 12\left(\frac{f_{lu,a}}{f_{co}}\right)\left(\frac{\varepsilon_{h,rup}}{\varepsilon_{co}}\right)^{0.45}\right] \quad \textbf{Eq. 6-27}$$

Where ε_{co} = 0.002; $\varepsilon_{h,rup}$ = measured hoop rupture strain of FRP jacket; and $f_{lu,a}$= actual lateral confining pressure at ultimate condition. The authors reported that the measured rupture strain of FRP jacket ($\varepsilon_{h,rup}$) is generally lower than the one which is obtained from coupon tests, thus adjusted strain and confining pressure values defined as $\varepsilon_{h,rup}$ and $f_{lu,a}$ are utilized in the model expression for peak stress and strain. Based on data from the literature an efficiency factor of 0.586 was suggested to modify the CFRP rupture strain obtained from coupon tests.

The comparison between the stress-strain curves from the current experimental tests and the predictions using the Lam and Teng (2003) model are shown in **Figure 6-7**. The models accurately predicts the response of specimens in Series 1 which had unidirectional fibers in the hoop direction and captures the general shape of the stress-strain response in other series with complex layups, although the stiffness of the first branch is generally over-predicted.

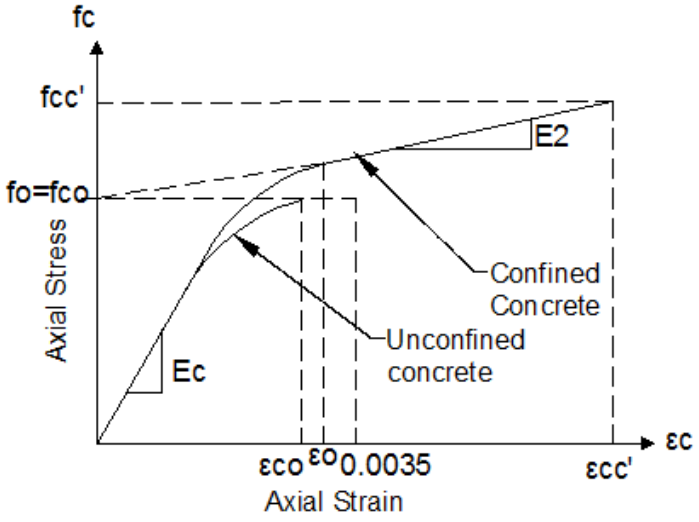

Figure 6-6 Axial stress-strain curve for FRP confined concrete (Lam and Teng (2003))

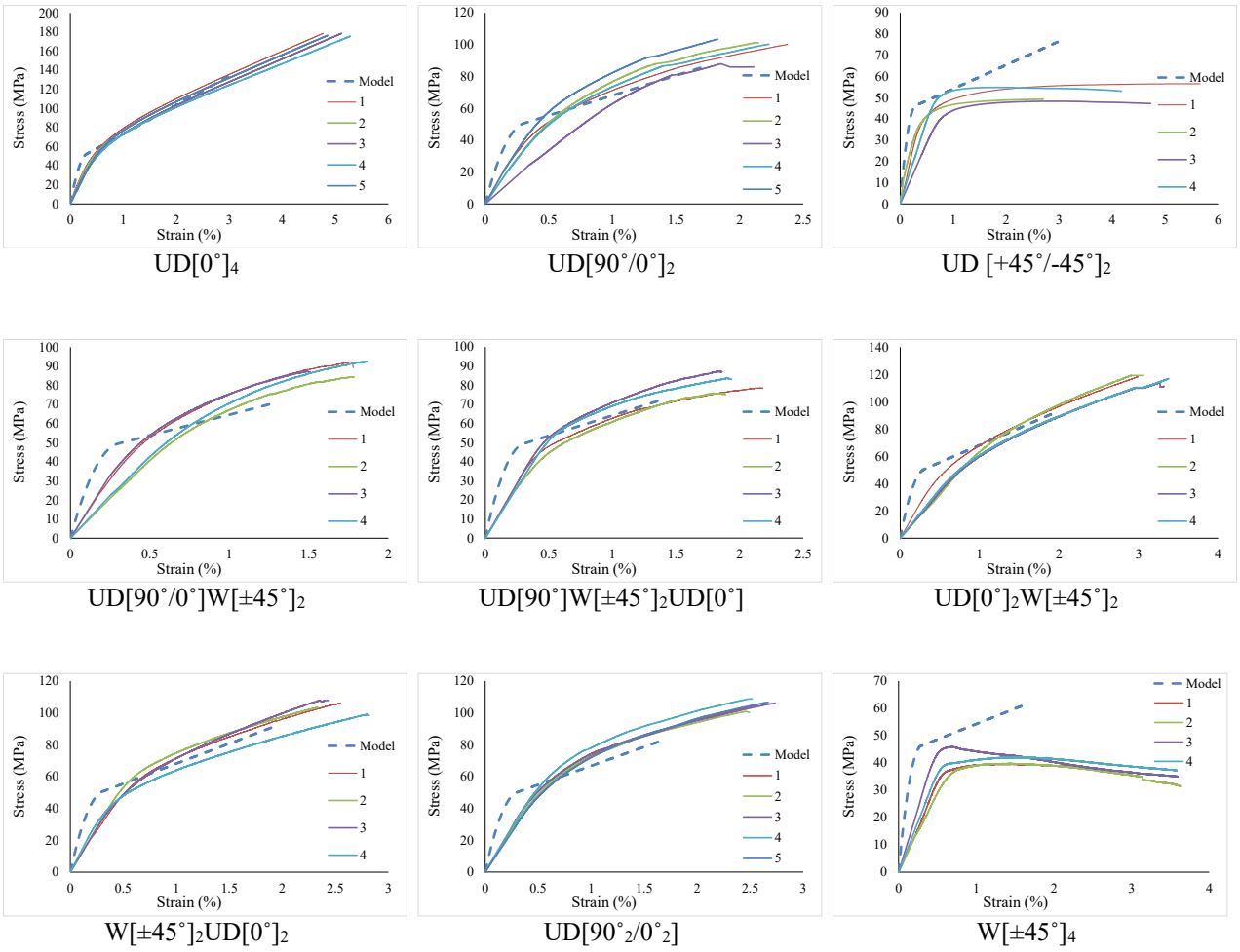

Figure 6-7 prediction of stress-strain behavior of FRP-confined concrete columns (Lam and Teng (2003))

6.2.7 Xiao and Wu (2003)

This model uses a bilinear stress-strain expression which is based on the work of Richard and Abbott (1975) to predict the stress-strain response of FRP-confined concrete:

$$f_c = \frac{(E_1 - E_2)\varepsilon_c}{\{1+[\frac{(E_1 - E_2)\varepsilon_c}{f_o}]^n\}^{\frac{1}{n}}} \qquad \textbf{Eq. 6-28}$$

Where E_1 and E_2 are the first and second slope of the stress-strain curve and n is a shape factor which is suggested to be taken as 2. The first and second slopes are obtained using the following expressions:

$$E_1 = 4733\sqrt{f_{co}} \quad \textbf{Eq. 6-29}$$

$$E_2 = k_1 E_l \mu_{tu} \quad \textbf{Eq. 6-30}$$

All other factors in the original Richard and Abbott (1975) model were re-calibrated based on regression analysis of a large database of test results from the literature as defined below:

$$k_1 = 4.1 - 0.45\left(\frac{f_{co}^2}{E_l}\right)^{1.4} \quad \textbf{Eq. 6-31}$$

$$\mu_{tu} = 10\left(\frac{f_{co}}{E_l}\right)^{0.9} \quad \textbf{Eq. 6-32}$$

$$f_o = \left(1 + 4.8x10^{-4}E_l^{0.85}\right).f_{co} \quad \textbf{Eq. 6-33}$$

$$f_{cc}^{'} = f_{co} + k_1 f_l \quad \textbf{Eq. 6-34}$$

The predictions of the experimental results using this recalibrated model are shown in **Figure 6-8**. It can be seen that the model predicts the stress-strain behavior of cylinders having different CFRP layups with reasonable accuracy, although the model becomes unstable for Series 3 and 7 which were confined with CFRP having only angular fibers.

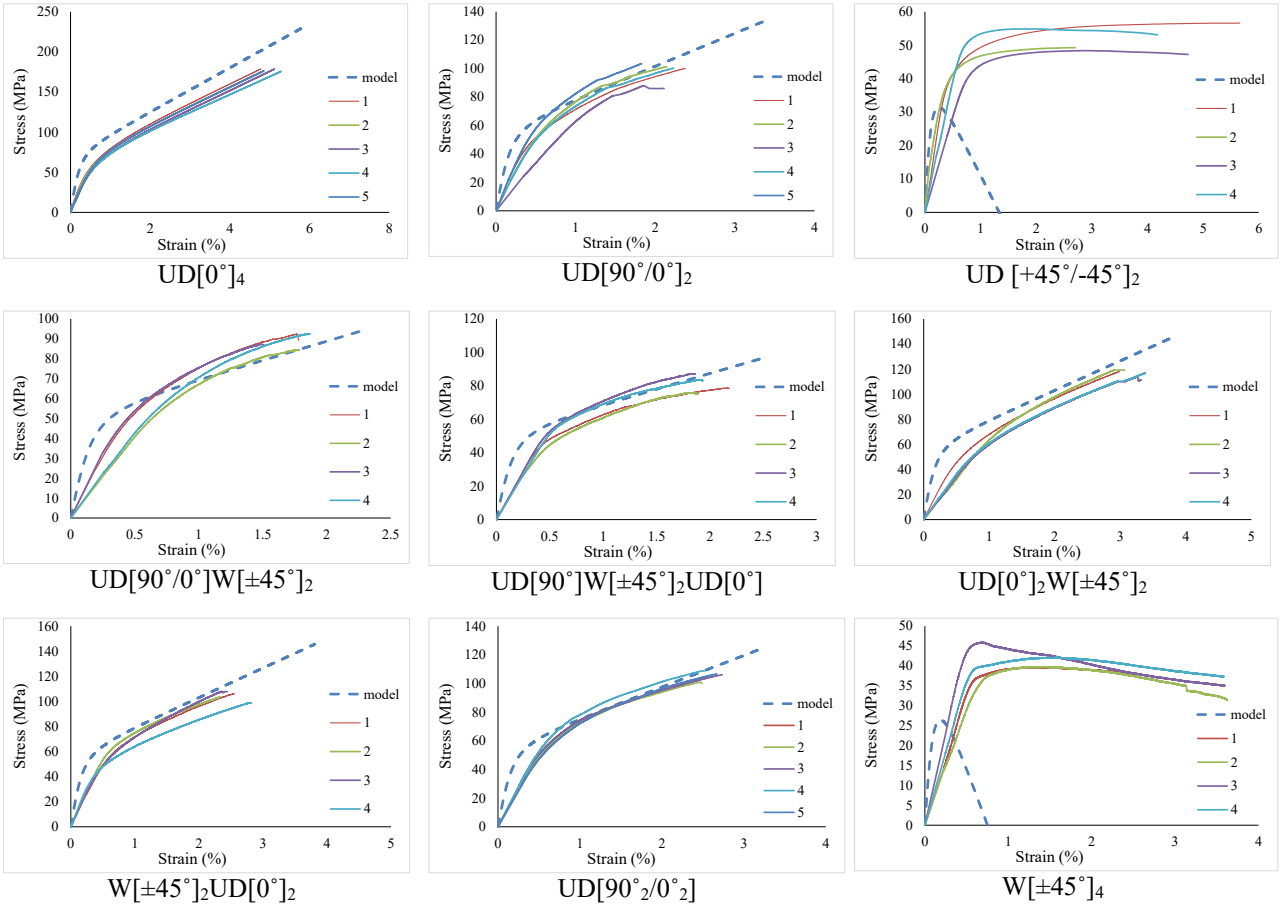

Figure 6-8 prediction of stress-strain behavior of FRP-confined concrete columns (Xiao and Wu (2003))

6.2.8 Jiang and Teng (2006)

The Jiang and Teng (2006) model uses the same stress-strain curve described by Lam and Teng (2003), however this model proposed new expressions for peak stress and corresponding peak strain as follows:

$$f_{cc}^{'} = f_{co}\left[1 + 3.5\left(\frac{E_l}{\frac{f_{co}}{\varepsilon_{co}}} - 0.01\right)\left(\frac{\varepsilon_{h,rup}}{\varepsilon_{co}}\right)\right] \qquad \text{if } \frac{E_l}{f_{co}/\varepsilon_{co}} \geq 0.01 \qquad \textbf{Eq. 6-35}$$

$$\text{and } \frac{f_{cc}^{'}}{f_{co}} = 1 \qquad \text{if } \frac{E_l}{f_{co}/\varepsilon_{co}} < 0.01 \qquad \textbf{Eq. 6-36}$$

$$\varepsilon_{cc}^{'} = \varepsilon_{co}\left[1.65 + 6.5\left(\frac{E_l}{\frac{f_{co}}{\varepsilon_{co}}}\right)^{0.8}\left(\frac{\varepsilon_{h,rup}}{\varepsilon_{co}}\right)^{1.45}\right] \qquad \textbf{Eq. 6-37}$$

Where $E_l = \frac{2\,.\,E_{FRP}\,.t_{FRP}}{D}$ and $\varepsilon_{h,rup} =$ The rupture strain of the FRP jacket.

Figure 6-9 shows how this re-calibrated model, with new expressions for peak stress and strain, predicts the stress-strain behavior of FRP-confined concrete cylinders tested in the current study. It can be seen that the model predicts the stress-strain response of most series with reasonable accuracy, with improved results when compared to the original Lam and Teng (2003) model.

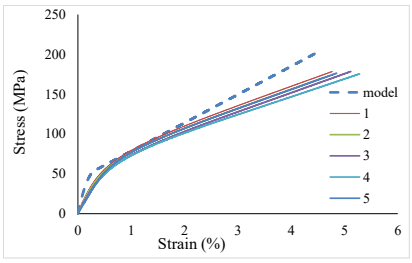

$UD[0^\circ]_4$

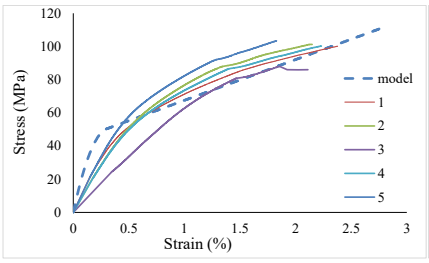

$UD[90^\circ/0^\circ]_2$

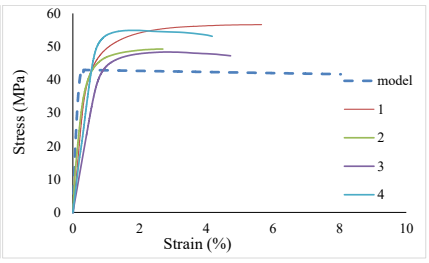

$UD\ [+45^\circ/-45^\circ]_2$

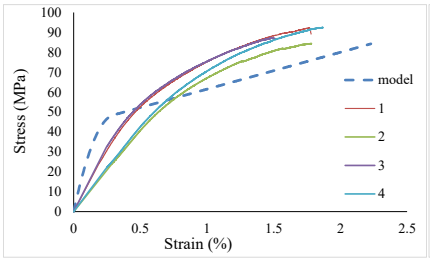

$UD[90^\circ/0^\circ]W[\pm45^\circ]_2$

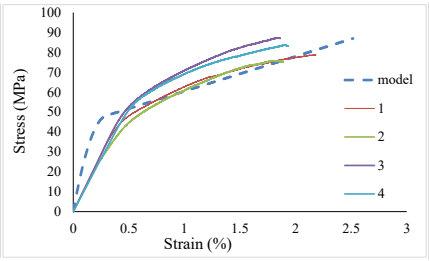

$UD[90^\circ]W[\pm45^\circ]_2UD[0^\circ]$

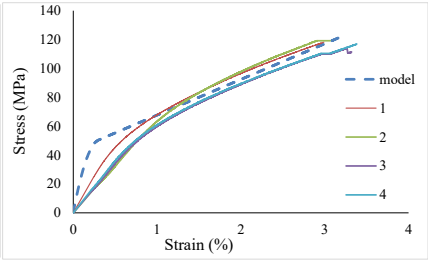

$UD[0^\circ]_2W[\pm45^\circ]_2$

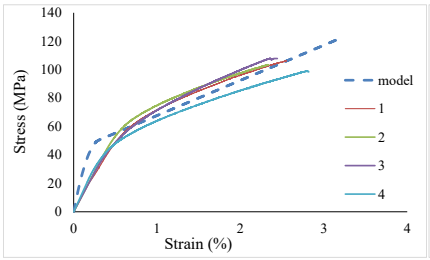

$W[\pm45^\circ]_2UD[0^\circ]_2$

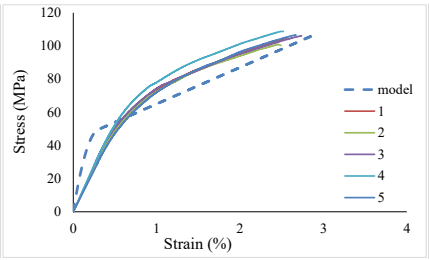

$UD[90^\circ_2/0^\circ_2]$

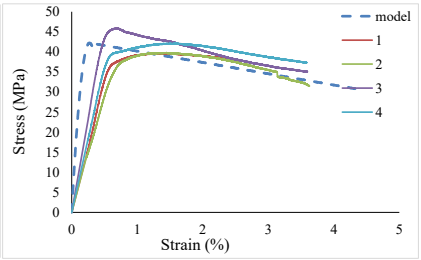

$W[\pm45^\circ]_4$

Figure 6-9 prediction of stress-strain behavior of FRP-confined concrete columns Xiao and Wu (2003)

6.2.9 Youssef et al. (2007)

The authors of this study proposed an analytical model based on the results of a comprehensive experimental program which included large scale specimens having circular, square and rectangular cross sections. The experimental stress-strain curves of FRP-confined concrete tested in this study showed bilinear behavior. In the model the first portion of the curve follows the response of unconfined concrete until the jacket becomes active. After this point, the curve performs shows ascending or descending behavior based on the amount of confinement and the geometry of the cross section. These two types of behaviors are shown in **Figure 6-10**.

The expressions used for these two stress-strain branches are shown below:

$$f_c = E_c\varepsilon_c\left[1-\frac{1}{m}\left(\frac{\varepsilon_c}{\varepsilon_{c1}}\right)^{m-1}\right] \qquad \text{If } 0 \le \varepsilon_c \le \varepsilon_{c1} \qquad \textbf{Eq. 6-38}$$

$$f_c = f_{c1} + E_2(\varepsilon_c - \varepsilon_{c1}) \qquad \text{If } \varepsilon_c > \varepsilon_{c1} \qquad \textbf{Eq. 6-39}$$

Where $E_2 =$ slope of the second branch and is calculated is defined as followed:

$$E_2 = \frac{f'_{cc} - f_o}{\varepsilon'_{cc}} \qquad \textbf{Eq. 6-40}$$

Parameter m, and the transition stress and strain (f_{c1} and ε_{c1}) are calculated as follows:

$$m = \frac{E_c\varepsilon_{c1}}{E_c\varepsilon_{c1} - f_{c1}} \qquad \textbf{Eq. 6-41}$$

$$f_{c1} = f_{co}\left[1 + 3\left(\frac{4t_{FRP}E_{FRP}\varepsilon_{l1}}{Df_{co}}\right)^{\frac{5}{4}}\right] \qquad \textbf{Eq. 6-42}$$

$$\varepsilon_{c1} = 0.002748 + 0.1169\left(\frac{4t_{FRP}E_{FRP}\varepsilon_{l1}}{f_{co}}\right)^{\frac{6}{7}}\left(\frac{f_{FRP}}{E_{FRP}}\right)^{\frac{1}{2}} \quad \textbf{Eq. 6-43}$$

Where the strain $\varepsilon_{l1} = 0.002$. The authors also propose expressions for peak stress and peak strain based on the confinement ratio as follows:

$$f'_{cc} = f_{co}[1 + 2.25]\left(\frac{f_{lu}}{f_{co}}\right)^{\frac{5}{4}} \quad \textbf{Eq. 6-44}$$

$$\varepsilon'_{cc} = 0.003368 + 0.2590\left(\frac{f_{lu}}{f_{co}}\right)\left(\frac{f_{FRP}}{E_{FRP}}\right)^{\frac{1}{2}} \quad \textbf{Eq. 6-45}$$

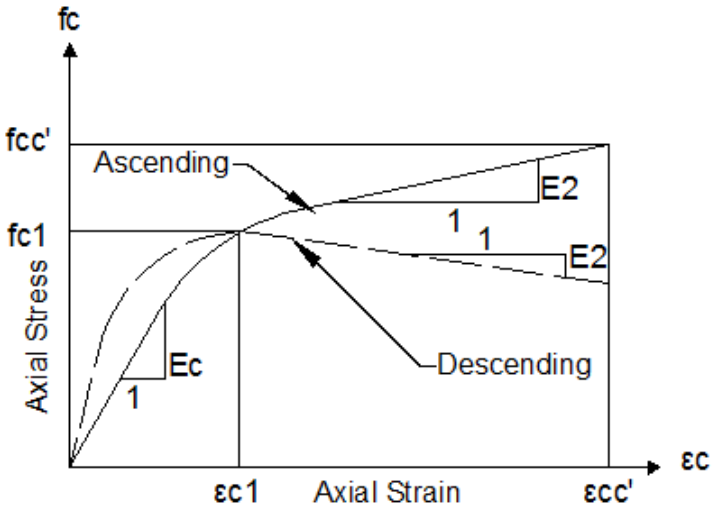

Figure 6-10 Stress-strain curves of FRP confined concrete (Youssef et al. (2007))

Figure 6-11 shows predictions obtained using the Youssef et al. (2007) model. It can be seen that the model predicts the stress-strain behavior of FRP-confined concrete cylinders with different stacking sequences with reasonable accuracy, particularly in the case of the shape of the stress-strain curves, although failure strains are under-predicted for most series.

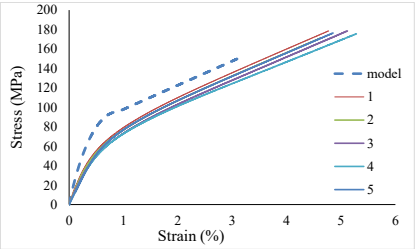

UD[0˚]$_4$

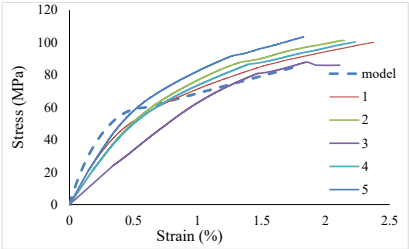

UD[90˚/0˚]$_2$

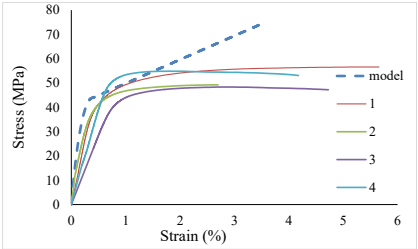

UD [+45˚/-45˚]$_2$

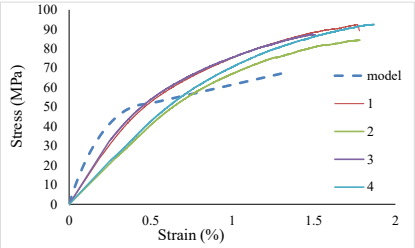

UD[90˚/0˚]W[±45˚]$_2$

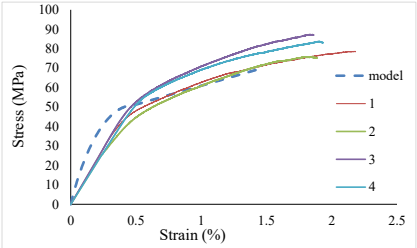

UD[90˚]W[±45˚]$_2$UD[0˚]

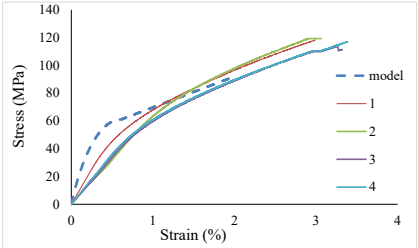

UD[0˚]$_2$W[±45˚]$_2$

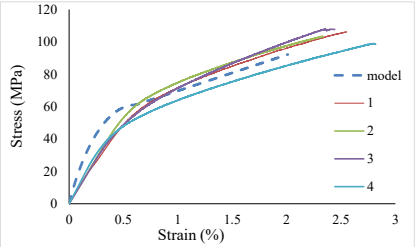

W[±45˚]$_2$UD[0˚]$_2$

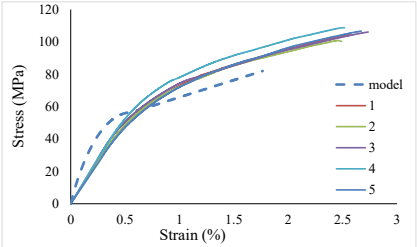

UD[90˚$_2$/0˚$_2$]

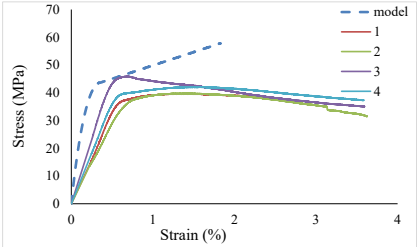

W[±45˚]$_4$

Figure 6-11 prediction of stress-strain behavior of FRP-confined concrete columns

6.2.10 Wu et al. (2009)

Wu et al (2009) propose a model for predicting the stress-strain behavior of FRP-confined concrete with circular cross-sections which re-calibrates models proposed by Samaan et al. (1998) for high-strength concrete (HSC) columns confined with aramid fiber reinforced polymer (AFRP). In this model, a single expression is used to model the complete stress-strain response of FRP-confined concrete:

$$f_c = \frac{(E_1 - E_2)\varepsilon_c}{\left[1 + \left(\frac{(E_1 - E_2)\varepsilon_c}{f_0}\right)^n\right]^{\frac{1}{n}}} + E_c\varepsilon_c \qquad \textbf{Eq. 6-46}$$

Where E_1 and E_2 are the first and the second slope of the stress-strain curve which are calculated using the following expressions:

$$E_1 = 3320\sqrt{f_{co}} + 6900 \qquad \textbf{Eq. 6-47}$$

$$E_2 = \frac{f'_{cc} - f_{co}}{\varepsilon'_{cc}} \qquad \textbf{Eq. 6-48}$$

A schematic representation of the stress-strain model and its parameters is shown in **Figure 6-12**. The stress f_o is calculated using the following expression below, while $n =$ Shape factor, suggested to be taken as 2.5.

$$f_o = 0.872f_{co} + 0.371f_l + 6.258 \qquad \textbf{Eq. 6-49}$$

Based on regression analysis of available data the authors propose the following expressions to predict the peak stress and strain of confined concrete:

$$f'_{cc} = f_{co}(1 + 3.2\frac{f_l}{f_{co}}) \quad \textbf{Eq. 6-50}$$

$$\varepsilon'_{cc} = \varepsilon_{co}(1 + 9.5\frac{f_l}{f_{co}}) \quad \textbf{Eq. 6-51}$$

Comparison between the predictions made using the Wu et al (2009) model and the experimental results is presented in **Figure 6-13**. It can be seen that the model generally over-predicts the peak stress, while peak strain generally under-predicted in most series.

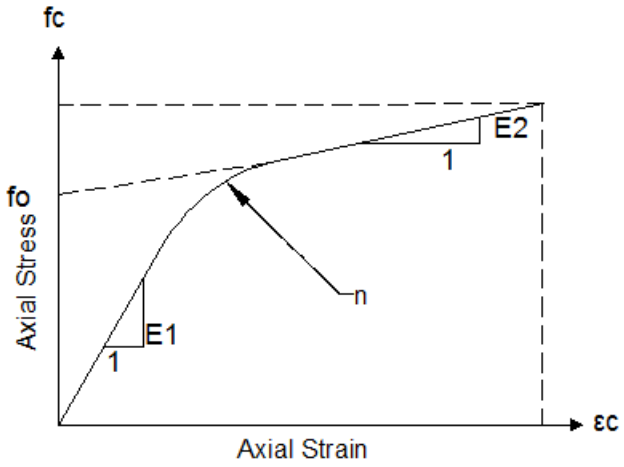

Figure 6-12 Parameters on proposed stress-strain model (Wu et al. (2009))

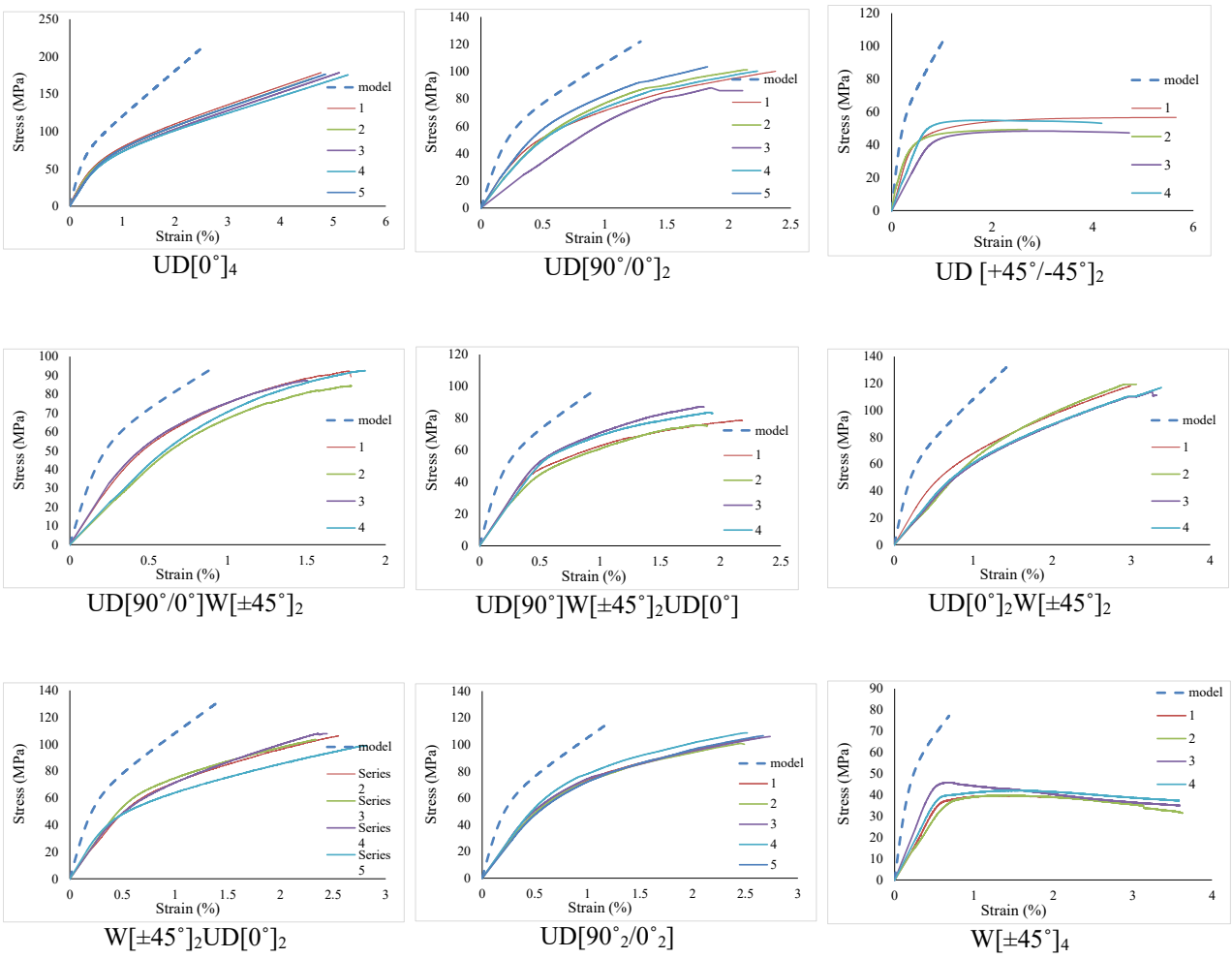

Figure 6-13 prediction of stress-strain behavior of FRP-confined concrete columns (Wu et al. (2009))

6.2.11 Fahmy and Wu (2010)

Fahmy and Wu (2010) propose a model which modifies the model originally proposed by Lam and Teng (2003). The model expressions are recalibrated based on a large database of data in the literature encompassing multiple variables, including type of FRP (which previous models generally do not consider during calibration). Consistent with the Lam and Teng (2003) model the stress-strain curve follows an initial ascending parabolic branch followed by a linear branch:

$$f_{c=} E_c \varepsilon_c \frac{(E_c - E_2)^2}{4 f_{co}} \varepsilon_c^2 \qquad \text{For } 0 < \varepsilon_c < \varepsilon_o \text{ (parabolic portions)} \qquad \textbf{Eq. 6-52}$$

$$f_c = f_o + E_2 \varepsilon_c \qquad \text{For } \varepsilon_o < \varepsilon_c < \varepsilon'_{cc} \text{ (linear portion)} \qquad \textbf{Eq. 6-53}$$

Where the slope of the second branch E_2 is modified from Samaan et al. (1998) as:

$$E_c = m_2\left(245.61 f_{co}^{m_1} + 0.6728 E_l\right)$$

$$m_1 = 0.5,\ m_2 = 0.83 \quad \text{If} \quad f_{co} \leq 40 \text{ MPa} \qquad \textbf{Eq. 6-54}$$

$$m_1 = 0.2,\ m_2 = 1.73 \quad \text{If} \quad f_{co} > 40 \text{ MPa}$$

The peak confined stress is calculated based on a strength effectiveness factor (k_1) which is function of the strength of the unconfined concrete, and the confinement pressure as follows:

$$f'_{cc} = f_{co} + k_1 f_{lu} \qquad \textbf{Eq. 6-55}$$

$$k_1 = 4.5 f_{lu}^{-0.3} \qquad \text{If} \quad f_{co} \leq 40 \text{ MPa} \qquad \textbf{Eq. 6-56}$$

$$k_1 = 3.75 f_{lu}^{-0.3} \qquad \text{If} \quad f_{co} > 40 \text{ MPa} \qquad \textbf{Eq. 6-57}$$

While peak confined strain is calculated using the linear shape of the second branch as follows:

$$\varepsilon'_{cc} = \frac{f'_{cc} - f_{co}}{E_2} \qquad \textbf{Eq. 6-58}$$

A schematic of the stress-strain curve used in this model is shown in **Figure 6-14.**

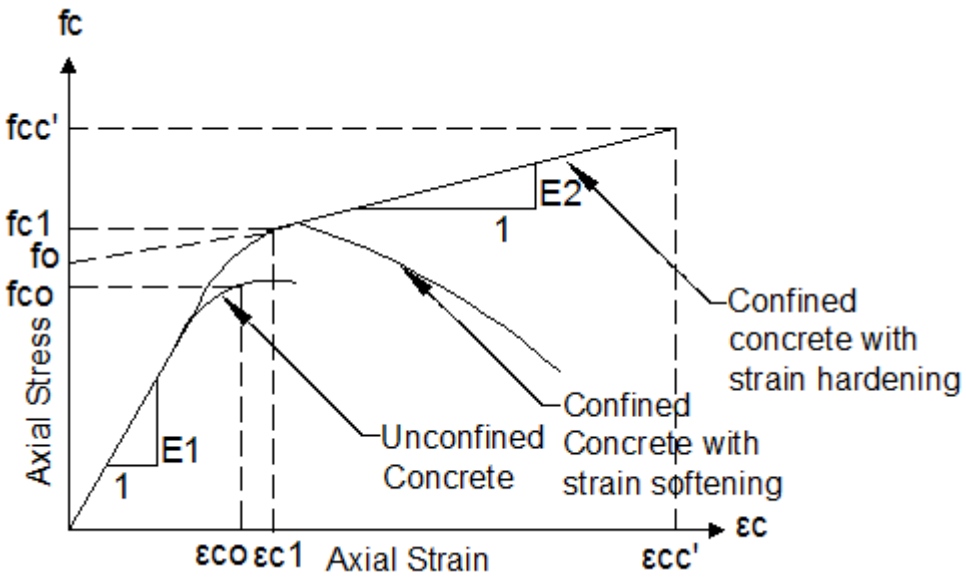

Figure 6-14 Typical stress-strain responses for unconfined and FRP confined concrete (Fahmy and Wu (2010))

Figure 6-15 shows the stress-strain predictions made using the Fahmy and Wu (2010) and compares the results to the experimental data from this study. It can be seen that the model predictions are not very accurate for layup configurations where the UD[0˚] fibers dominate the response, with under estimation of failure strain in most series.

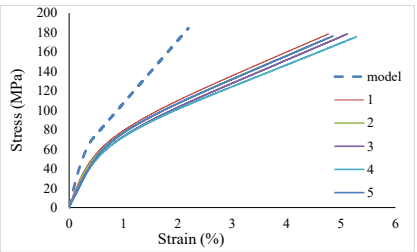

$UD[0^{\circ}]_4$

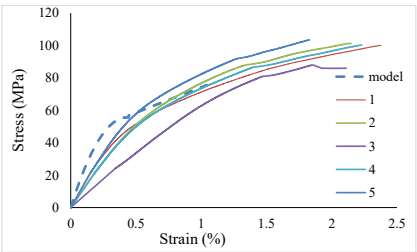

$UD[90^{\circ}/0^{\circ}]_2$

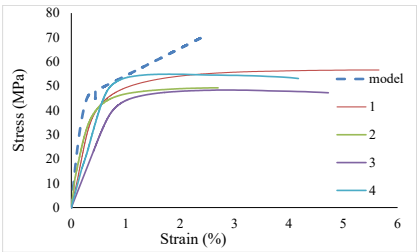

$UD\ [+45^{\circ}/-45^{\circ}]_2$

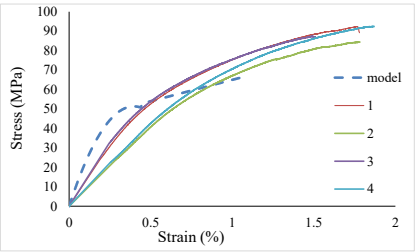

$UD[90^{\circ}/0^{\circ}]W[\pm45^{\circ}]_2$

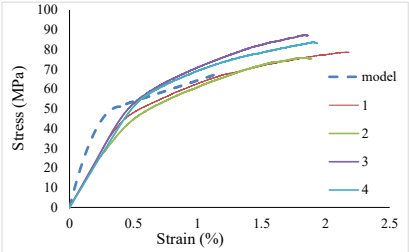

$UD[90^{\circ}]W[\pm45^{\circ}]_2UD[0^{\circ}]$

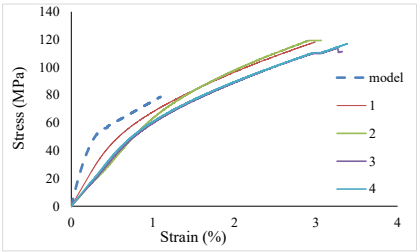

$UD[0^{\circ}]_2W[\pm45^{\circ}]_2$

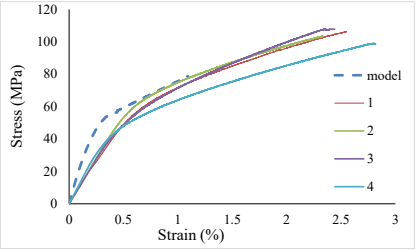

$W[\pm45^{\circ}]_2UD[0^{\circ}]_2$

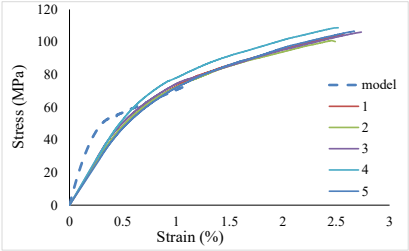

$UD[90^{\circ}_2/0^{\circ}_2]$

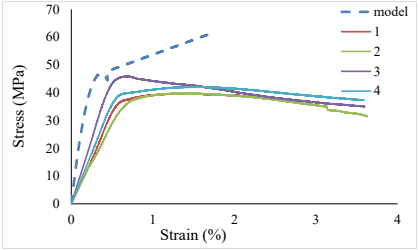

$W[\pm45^{\circ}]_4$

Figure 6-15 prediction of stress-strain behavior of FRP-confined concrete columns (Fahmy and Wu (2010))

6.2.12 Pellegrino and Modena (2010)

Following the approach of other researchers Pellegrino and Modena (2010) propose a stress-strain model which consists of a parabolic ascending branch and linear secondary branch to predict the stress-strain response of FRP-confined concrete. The analytical model, which is based

on the four parameter bilinear model of Richard and Abbott (1975) used in previous studies is shown in **Figure 6-16** and defined using the following expressions:

$$f_c = \frac{(E_1 - E_2)\varepsilon_c}{\left[1 + \left(\frac{(E_1 - E_2)\varepsilon_c}{f_0}\right)^n\right]^{\frac{1}{n}}} + E_c\varepsilon_c \qquad \textbf{Eq. 6-59}$$

Where the four parameters used to define the curve are: E_1 = slope of the first branch of the stress-strain curve which corresponds to the modulus of elasticity of unconfined concrete; E_2 = slope of the second branch of the stress-strain curve as defined in; **Eq**. **6-60** f_o = stress which corresponds to the intersection of the line corresponding to the second branch of the curve and the vertical axis as defined in **Eq**. **6-61** and $n =$ parameter related to the curvature of the transition zone between two branches of the curve calculated using **Eq**. **6-62**.

$$E_2 = \frac{f'_{cc} - f_{co}}{\varepsilon'_{cc} - \varepsilon_{co}} \qquad \textbf{Eq. 6-60}$$

$$f_o = f'_{cc} - E_2\varepsilon'_{cc} \qquad \textbf{Eq. 6-61}$$

:

$$n = 1 + \frac{1}{\frac{E_1}{E_{co}} - 1} \qquad \textbf{Eq. 6-62}$$

The parameter E_{co} represents the slope of the line passing from the origin to the transition point:

$$E_{co} = \frac{f_{co}}{\varepsilon_{co}} \qquad \textbf{Eq. 6-63}$$

Figure 6-17 shows the comparison between the predictions made using the Pellegrino and Modena (2010) model and the experimental results. It can be seen the model provides reasonable

predictions for most series with the exception of the cylinders in Series 3 and 7 which were confined with angular CFRP sheets.

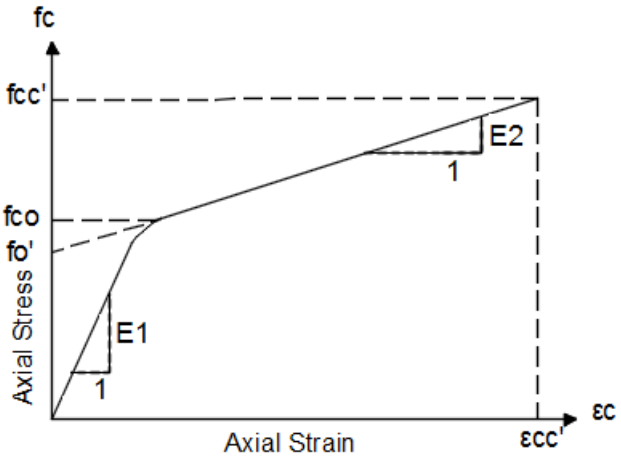

Figure 6-16 Stress-strain model for FRP confined columns (Pellegrino and Modena (2010))

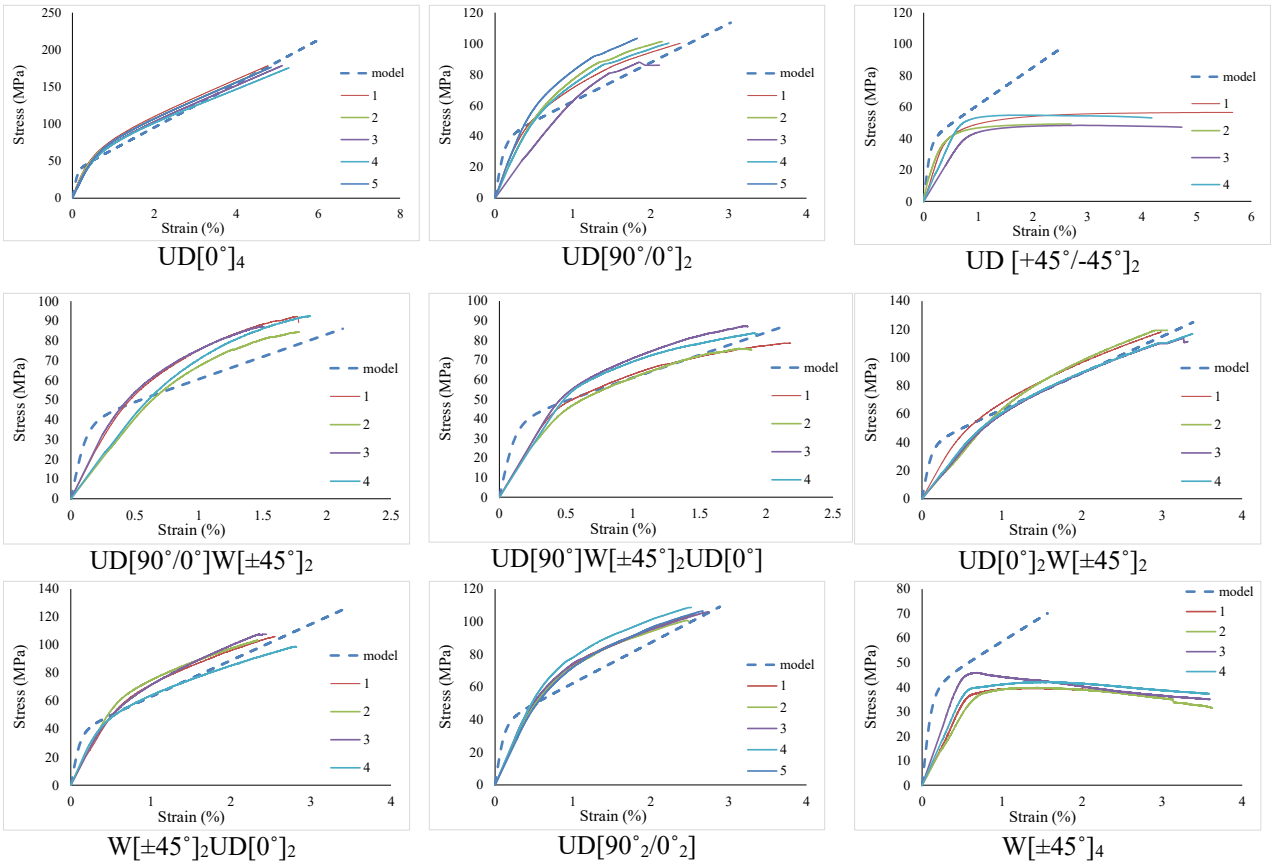

Figure 6-17 prediction of stress-strain behavior of FRP-confined concrete columns (Pellegrino and Modena (2010))

6.2.13 Liu et al. (2013)

Liu et al. (2013) propose a constitutive model for predicting the stress-strain response of FRP-confined concrete having circular sections. This model modifies the Lam and Teng (2003) expressions. The modifications include new expressions for FRP rupture strain; peak confined stress and strain, intercept stress. The stress-strain curve follows the same branches used in the Lam and Teng (2003) model:

$$f_{c=} E_c\varepsilon_c - \frac{(E_1 - E_2)^2}{4f_{co}}\varepsilon_c^2 \qquad \text{For } 0 < \varepsilon_c < \varepsilon_o \text{ (parabolic portions)} \qquad \textbf{Eq. 6-64}$$

$$f_c = f_o + E_2\varepsilon_c \qquad \text{For } \varepsilon_o < \varepsilon_c < \varepsilon'_{cc} \text{ (linear portion)} \qquad \textbf{Eq. 6-65}$$

Where the slopes of two branches are taken as defined previously:

$$E_1 = 4750\sqrt{f_{co}} \qquad \textbf{Eq. 6-66}$$

$$E_2 = \frac{f'_{cc} - f_{co}}{\varepsilon'_{cc}} \qquad \textbf{Eq. 6-67}$$

In this model the stress f_o is calculated using the following expression which is function of the unconfined concrete strength (f_{co}):

$$f_o = 1.105 f_{co} \qquad \textbf{Eq. 6-68}$$

The authors propose the following expressions for predicting the peak confined stress and strain.

$$f'_{cc} = (c_1\, f_{co}) + \left(\frac{2\, f_{lu}\, k_1}{k_\varepsilon}\right) \qquad \textbf{Eq. 6-69}$$

$$\varepsilon'_{cc} = \varepsilon_{co} c_2 + 12\left(\frac{f_{lu}}{f_{co}}\right)\left(\varepsilon_{hrup}^{0.45}\right)\left(\varepsilon_{co}^{0.55}\right) \qquad \textbf{Eq. 6-70}$$

The expressions for peak stress and strain are function of the actual confined pressure provided by the FRP (f_{lu}), which is smaller than the ideal maximum FRP confining pressure (f_l), and the FRP rupture strain (ε_{hrup}), which is reduced when compared to maximum FRP strain (ε_{FRP}) obtained from coupon testing. The parameter k_ε is the ratio between these two strains and is calculated as follows:

$$k_\varepsilon = 0.9 - 2.3xf_{co}x10^{-3} - 0.75x10^{-6} \quad \textbf{Eq. 6-71}$$

With parameter K_1 taken as follows:

$$K_1 = \frac{2E_{FRP}t_{FRP}}{D} \quad \textbf{Eq. 6-72}$$

The parameters c_1 and c_2 and strain values ε_{l1} and f_{lo} are calculated as follows:

$$c_1 = 1 + 0.0058\left(\frac{K_1}{f_{co}}\right) \quad \textbf{Eq. 6-73}$$

$$c_2 = 2 - 0.01(f_{co} - 20) \quad \textbf{Eq. 6-74}$$

$$\varepsilon_{l1} = \left(0.43 + \left(\frac{0.009K_1}{f_{co}}\right)\right)f_{co} \quad \textbf{Eq. 6-75}$$

$$f_{lo} = K_1\varepsilon_{l1} \quad \textbf{Eq. 6-76}$$

$$k_2 = 0.263$$

$$k_{lo} = f_{co}^{1.65}$$

$$\varepsilon_t = \frac{2f_o}{(E_c - E_2)} \qquad \textbf{Eq. 6-77}$$

Figure 6-18 shows comparison between the predictions made using the Liu et al. (2013) model and the experimental stress-strain curves for FRP-confined cylinders tested in this study. It can be seen that the model captures the general shape of the stress-strain curve in most series with reasonable predictions for the different layup configurations.

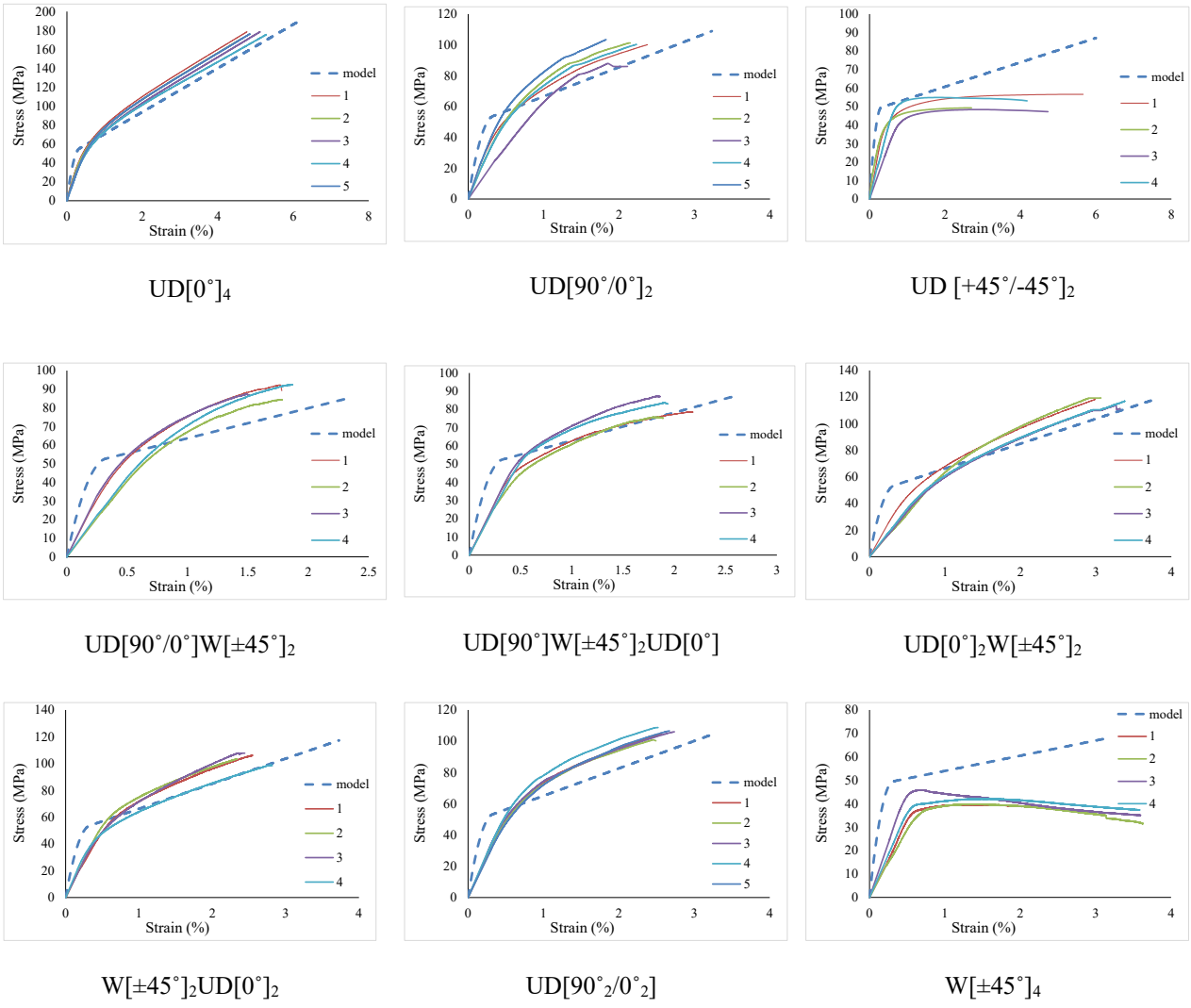

Figure 6-18 prediction of stress-strain behavior of FRP-confined concrete columns (Liu et al. (2013))

6.3 Prediction of stress-strain

In this section the performance of the models discussed in **Section** 6.2 are examined by comparing the predictions with the experimental results within each series. The accuracy of the models is assessed by comparing experimental and analytical stress-strain curves and comparing experimental and analytical predictions for peak stress, peak strain as well as using the strength, toughness and ductility stress-strain indicators described in **Chapter 5**.

6.3.1 Predictions for Series 1: UD[0˚]

Figure 6-19, **Figure 6-20** and **Figure 6-21** show comparisons between experimental and analytical responses for the Series 1 specimens having 4, 6 and 8 layers of CFRP. **Table 6-1** compares the peak stress, peak strain, strength, ductility and toughness parameters obtained from the analytical and experimental stress-strain curves, based on the average of 5 samples. Examining the stress-strain prediction for the case of 4 layers of CFRP in **Figure 6-19** it can be seen that better predictions are provided by some of the more recent models, while earlier models such as the one proposed by Fardis and khalili (1982) overestimates the stress-strain response and stiffness as has been mentioned by other researchers as well. In the case of the overall trend of the stress-strain curves the best results are obtained using the models proposed by Pellegrino and Modena (2010) and Liu et al. (2013). However, these models over-predicted the stiffness of the first ascending branch of the experimental stress-train curve. One can see in **Figure 6-20** and **Figure 6-21** most of the models showed better predictions of the first branch of the curve as the number of layers is increased to 6 and 8, while the slope of the second branch of the experimental curves is over-predicted as the number of layers is increased. In general, models which modify the four parameter model of Richard and Abbott 1975, such as those of such as Lam and Teng (2003), Xiao and Wu (2003), Jiang and Teng (2006), Wu et al (2009), Fahmy and

Wu (2010), Pellegrino and Modena (2010), and Liu et al. (2013)**,** showed a relatively better ability to predict the experimental stress-strain curves in this series. Examining **Table 6-1** it can be seen that most of the models showed reasonable percentage of error in predicting the peak stress($f_{cc}^{'}$), with the best results obtained using the models proposed by Jiang and Teng (2006), Wu et al (2009), Pellegrino and Modena (2010), and Liu et al. (2013). In terms of energy absorption capacity (e_{cu}), most models generally provide poor predictions, particularly as the number of layers are increased. At 4 layers, the best predictions are achieved by the models of Pellegrino and Modena (2010) and Liu et al. (2013) which have error percentages of 19.64 and 5.92. The correlation of experimental and analytical predictions of the remaining ductility and toughness factors is not acceptable for most models.

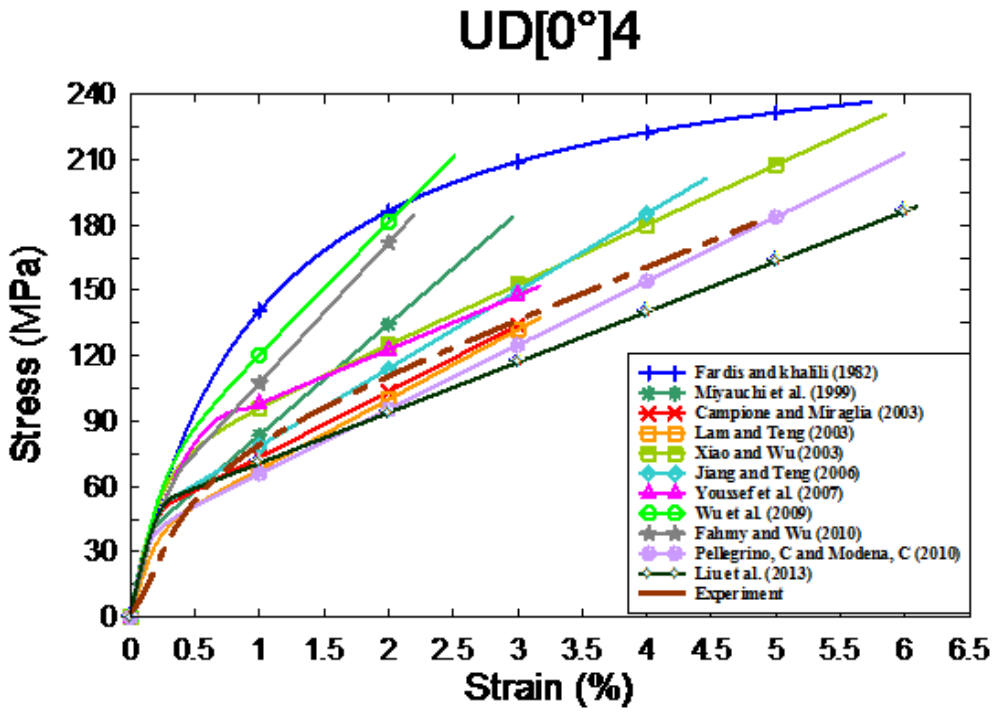

Figure 6-19 Stress-strain prediction of different models (4 layers)

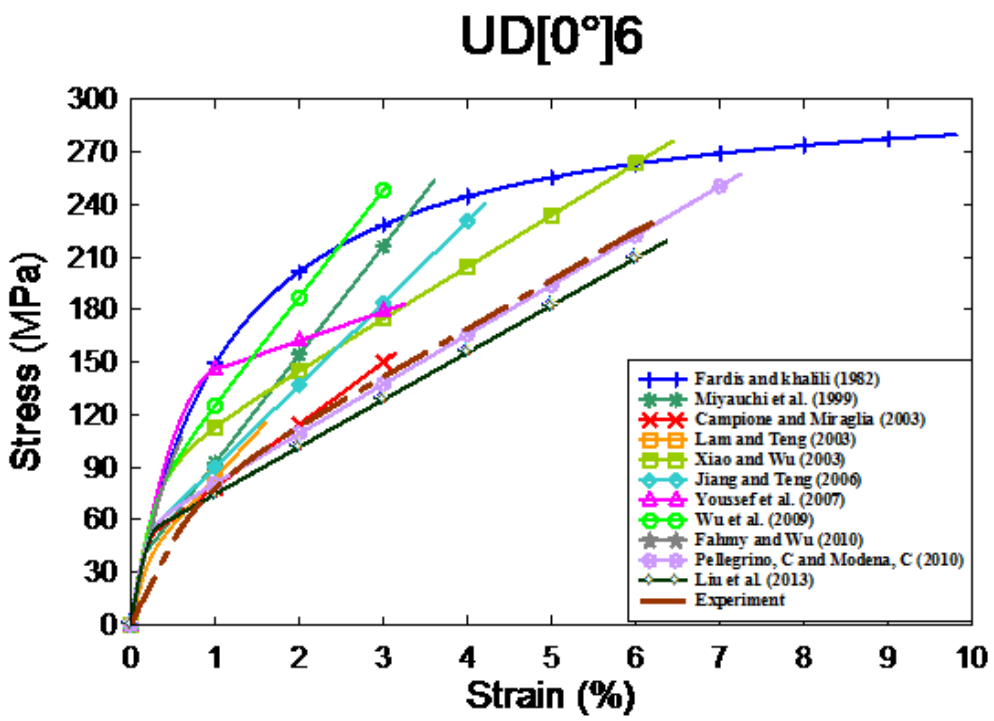

Figure 6-20 Stress-strain prediction of different models (6 layers)

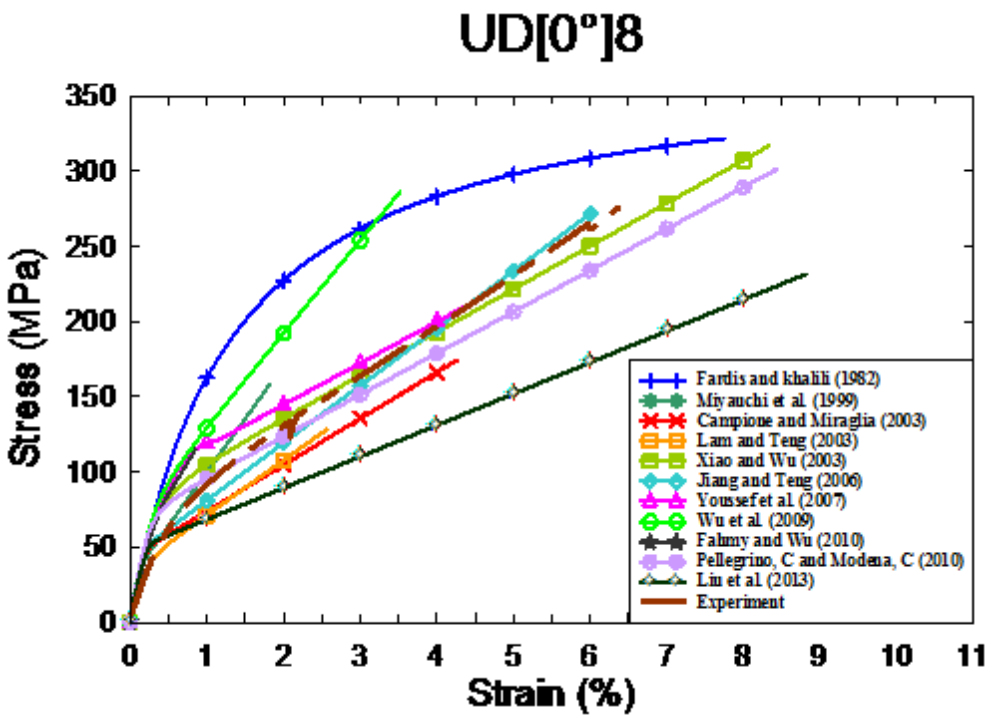

Figure 6-21 Stress-strain prediction of different models (8 layers)

Table 6-1 Prediction of different factors by existing proposed models

Author	# Layer	UD[0°]							
		f'_{cc}	ε'_{cc}	K_1	μ_{cu}	e_{cu}	w_{cu}	f_l	ε_1
Experiment	4	177.91	0.05	2.91	2.92	5.96	1.87	46.40	0.02
	6	214.77	0.06	2.98	2.29	10.39	1.76	57.65	0.03
	8	263.69	0.06	3.24	2.07	7.59	0.92	68.10	0.46
Fardis and Khalili 1982	4	236.44	0.06	4.10	4.42	10.69	3.48	47.18	0.01
	Error (%)	32.90	9.92	40.89	51.39	79.36	85.98	1.68	-29.19
	6	279.99	0.10	4.10	4.90	22.70	4.05	57.80	0.02
	Error (%)	30.37	57.92	37.58	114.30	118.48	130.32	0.27	-28.12
	8	321.67	0.08	4.10	4.12	19.60	3.24	67.97	0.02
	Error (%)	21.99	25.75	26.54	99.40	158.23	252.29	-0.19	-95.92
Miyauchi et al. 1999	4	183.60	0.03	2.98	15.48	3.18	9.05	47.18	0.00
	Error (%)	3.20	-43.31	2.40	430.62	-46.64	384.17	1.68	-89.58
	6	253.90	0.04	2.98	19.48	5.11	10.87	70.77	0.00
	Error (%)	18.22	-41.90	0.00	751.83	-50.82	517.79	22.76	-93.35
	8	324.20	0.04	2.98	23.07	7.31	12.53	94.36	0.00
	Error (%)	22.95	-32.57	-8.03	1016.76	-3.69	1261.58	38.57	-99.61
Campione and Miraglia 2003	4	137.36	0.02	2.00	5.02	2.69	4.75	47.18	0.00
	Error (%)	-22.79	-60.35	-31.27	72.12	-54.87	153.88	1.68	-77.53
	6	158.60	0.02	2.00	3.69	1.13	1.64	57.80	0.00
	Error (%)	-26.15	-74.14	-32.89	61.33	-89.12	-6.94	0.27	-84.37
	8	178.94	0.03	2.00	3.67	2.04	1.63	67.97	0.01
	Error (%)	-32.14	-58.34	-38.27	77.43	-73.12	77.03	-0.19	-98.48
Lam and Teng 2003	4	134.24	0.03	3.30	9.87	2.62	6.40	27.65	0.00
	Error (%)	-24.54	-42.35	13.40	238.32	-56.04	242.09	-40.41	-83.38
	6	154.78	0.03	3.30	10.22	3.06	6.44	33.87	0.00
	Error (%)	-27.93	-49.46	10.74	346.94	-70.55	266.01	-41.24	-88.97
	8	174.44	0.04	3.30	13.85	4.59	8.55	39.83	0.00
	Error (%)	-33.85	-30.75	1.85	570.47	-39.53	828.90	-41.51	-99.33
Xiao and Wu 2003	4	230.80	0.07	3.98	9.92	8.64	5.69	47.18	0.01
	Error (%)	29.73	24.97	36.78	240.06	44.97	204.24	1.68	-64.16
	6	279.79	0.07	4.10	9.53	11.45	5.26	57.80	0.01
	Error (%)	30.27	19.41	37.46	316.57	10.20	198.87	0.27	-72.04
	8	316.40	0.09	4.02	11.12	16.28	6.26	67.97	0.01
	Error (%)	19.99	48.43	24.15	438.32	114.49	580.39	-0.19	-98.21
Jiang and Teng 2006	4	201.36	0.04	3.36	14.49	5.40	8.72	47.18	0.00
	Error (%)	13.18	-14.67	15.34	396.73	-9.40	366.22	1.68	-83.24
	6	240.52	0.04	2.56	13.47	5.92	7.88	77.07	0.00
	Error (%)	11.99	-32.22	-14.00	488.84	-43.02	347.66	33.69	-88.77
	8	273.73	0.06	3.39	19.15	9.53	11.02	67.97	0.00
	Error (%)	3.81	-1.77	4.77	826.99	25.56	1097.93	-0.19	-99.31

Author	# Layer	UD[0°]							
		f'_{cc}	ε'_{cc}	K_1	μ_{cu}	e_{cu}	w_{cu}	f_l	ε_1
Youssef 2007	4	151.65	0.03	2.30	4.28	3.40	3.03	47.18	0.01
	Error (%)	-14.76	-39.42	-20.87	46.62	-42.95	62.06	1.68	-59.70
	6	183.04	0.03	2.42	3.48	4.64	2.72	57.80	0.01
	Error (%)	-14.77	-47.66	-18.70	52.27	-55.34	54.38	0.27	-66.47
	8	214.48	0.05	2.52	4.05	6.64	2.77	67.97	0.01
	Error (%)	-18.66	-26.51	-22.13	96.12	-12.52	201.26	-0.19	-97.57
Wu et al. 2009	4	193.98	0.03	3.20	5.43	3.31	3.69	47.18	0.00
	Error (%)	9.04	-51.94	9.96	86.25	-44.46	97.51	1.68	-74.83
	6	227.97	0.03	3.20	6.84	4.63	4.58	57.80	0.00
	Error (%)	6.15	-51.20	7.38	198.97	-55.44	160.49	0.27	-84.08
	8	260.50	0.04	3.20	7.73	6.10	5.14	67.97	0.00
	Error (%)	-1.21	-42.80	-1.24	273.95	-19.63	458.17	-0.19	-99.01
Fahmy and Wu 2010	4	98.67	0.01	1.18	2.13	2.43	6.08	47.18	0.00
	Error (%)	-44.54	-83.47	-59.45	-26.95	-59.23	225.02	1.68	-77.93
	6	107.18	0.01	1.11	1.37	0.38	0.80	57.80	0.00
	Error (%)	-50.10	-90.16	-62.74	-39.99	-96.34	-54.71	0.27	-84.01
	8	114.88	0.01	1.06	1.73	0.60	1.06	67.97	0.00
	Error (%)	-56.43	-86.19	-67.36	-16.50	-92.09	15.18	-0.19	-98.93
Pellegrino and Modena 2010	4	212.84	0.06	3.60	14.40	7.44	8.40	47.18	0.00
	Error (%)	19.64	14.72	23.70	393.79	24.83	349.35	1.68	-77.34
	6	257.51	0.07	4.08	11.89	11.15	7.11	52.54	0.01
	Error (%)	19.90	16.67	36.99	419.97	7.31	303.97	-8.86	-78.11
	8	301.45	0.08	3.80	12.50	15.49	7.61	67.97	0.01
	Error (%)	14.32	37.00	17.36	505.07	104.08	727.46	-0.19	-98.53
Liu et al. 2013	4	188.43	0.06	3.08	15.86	7.13	9.85	47.18	0.00
	Error (%)	5.92	16.58	5.92	443.60	19.63	426.95	1.68	-79.08
	6	219.24	0.06	3.05	12.36	8.43	7.47	57.80	0.01
	Error (%)	2.08	2.51	2.31	440.24	-18.86	324.22	0.27	-81.49
	8	231.51	0.09	2.77	23.75	12.24	14.25	67.97	0.00
	Error (%)	-12.20	43.06	-14.40	1049.53	61.26	1448.99	-0.19	-99.19

6.3.2 Predictions for Series 2 UD[90˚/0˚]

Figure 6-22, Figure 6-23 and Figure 6-24 show comparisons between experimental and analytical responses for the Series 2 specimens having 4, 6 and 8 layers of CFRP. **Table 6-2** compares the peak stress, peak strain, strength, ductility and toughness parameters obtained from the analytical and experimental stress-strain curves, based on the average of 5 samples. Examining the stress-strain prediction for the case of 4 layers of CFRP in **Figure 6-22** it can be seen that better predictions are provided by the same models which performed well in Series 0. In the case of the overall trend of the stress-strain curves the best results are obtained using the models proposed by Xiao and Wu (2003) and Jiang and Teng (2006) even though they overestimate the peak strain. However, these models over-predicted the stiffness of the first ascending branch of the experimental stress-train curve. One can see in **Figure 6-23** and **Figure 6-24** most of the models showed better predictions of the first branch of the curve as the number of layers is increased to 6 and 8, while the slope of the second branch of the experimental curves is over-predicted as the number of layers is increased. In the case of prediction of the stress-strain curve trend, most of the models failed to predict the first branch of the stress-strain curve as it can be seen from **Figure 6-22,** while most of them showed acceptable results in the prediction of the second branch of the curve. Existing models showed stiffer performance in the first branch of the curve, which is known as the unconfined concrete stress-strain branch. Examining **Table 6-2** it can be seen that in the case of peak stress, Liu et al. (2013) model showed the best prediction. The correlation of experimental and analytical predictions of the remaining ductility and toughness factors is not acceptable for most models.

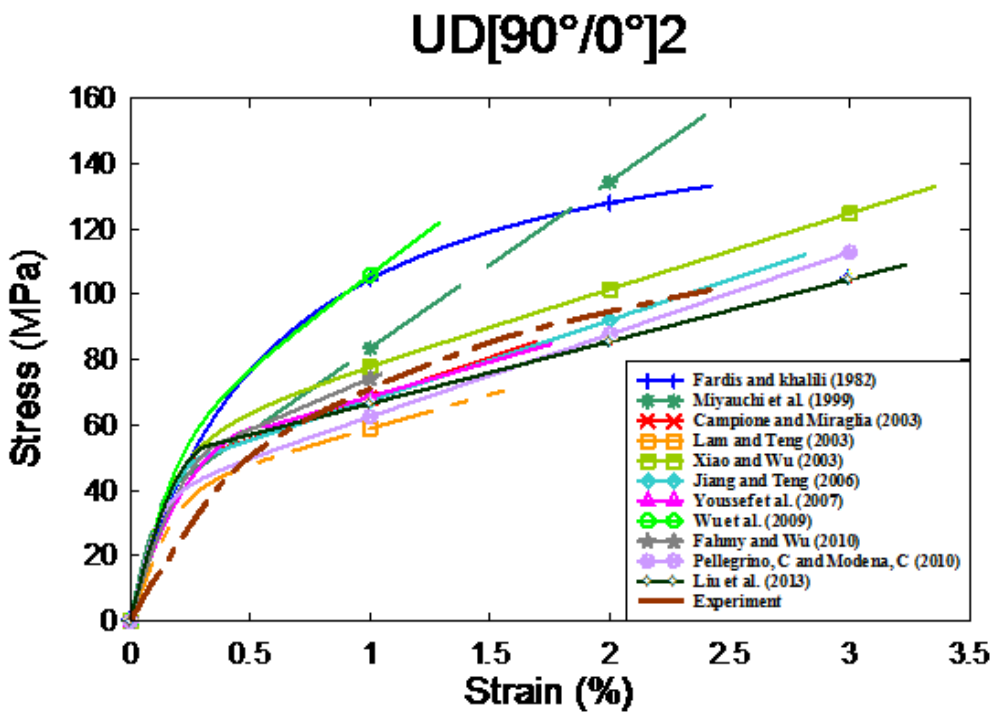

Figure 6-22 Stress-strain prediction of different models (4 layers)

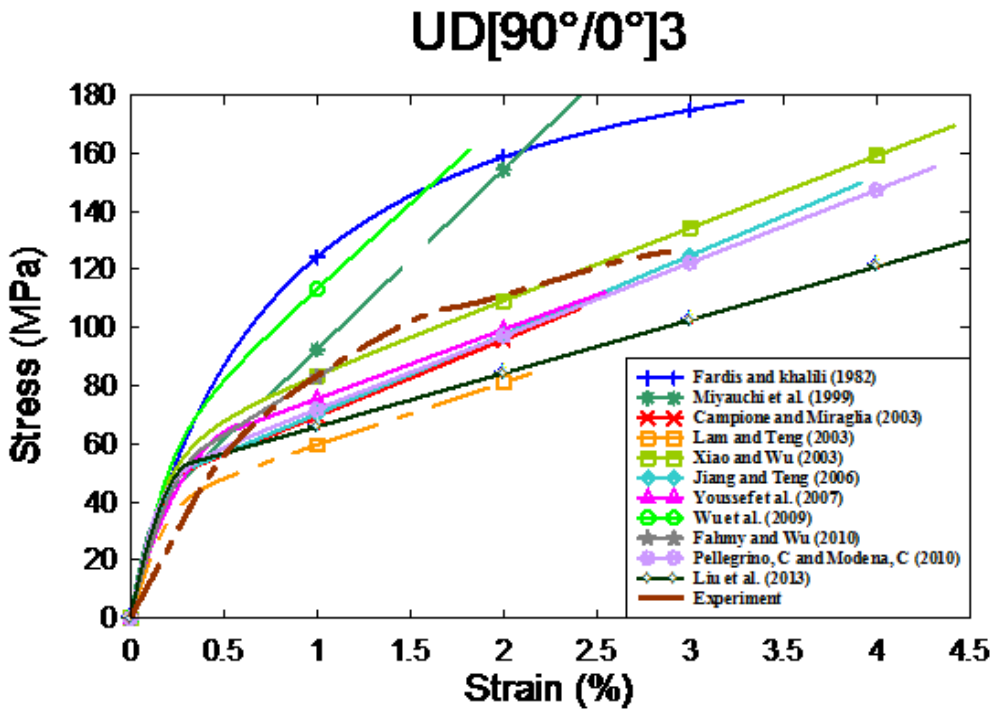

Figure 6-23 Stress-strain prediction of different models (6 layers)

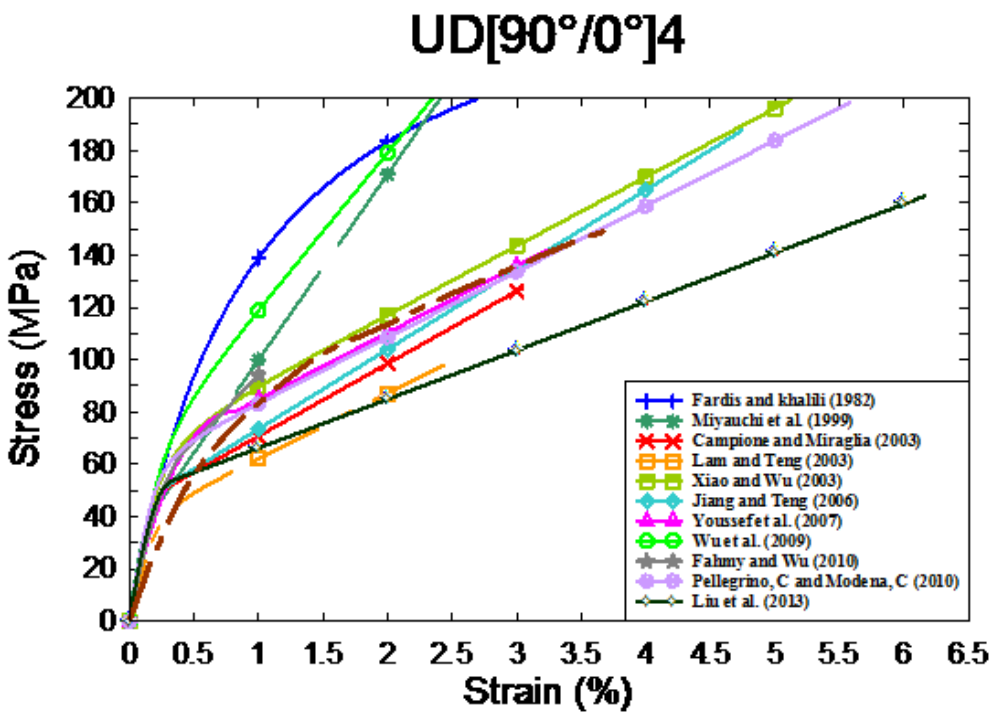

Figure 6-24 Stress-strain prediction of different models (8 layers)

Table 6-2 Prediction of different factors by existing proposed models

Author	# Layers	UD[90˚/0˚]							
		f'_{cc}	ε'_{cc}	K_1	μ_{cu}	e_{cu}	w_{cu}	f_l	ε_1
Experiment	4	100.89	0.02	2.60	1.84	1.98	1.58	22.22	0.01
	6	126.96	0.03	2.47	2.29	3.55	2.07	33.99	0.01
	8	148.10	0.04	2.37	2.13	4.86	1.95	44.29	0.02
Fardis and Khalili 1982	4	133.13	0.02	4.10	3.51	2.43	2.65	21.98	0.01
	Error (%)	31.96	6.10	57.68	90.40	22.84	67.23	-1.06	-46.05
	6	178.02	0.03	4.10	3.72	4.41	2.80	32.93	0.01
	Error (%)	40.22	5.09	65.99	62.34	24.28	35.08	-3.11	-36.54
	8	222.14	0.04	4.10	3.71	7.47	2.83	43.69	0.01
	Error (%)	50.00	22.39	73.00	73.87	53.67	45.23	-1.35	-29.74
Miyauchi et al. 1999	4	183.60	0.03	2.98	15.48	3.18	9.05	47.18	0.00
	Error (%)	81.98	29.71	14.61	739.59	60.75	472.38	112.34	-85.04
	6	253.90	0.04	2.98	19.48	5.11	10.87	70.77	0.00
	Error (%)	99.99	15.25	20.65	750.29	44.01	424.09	108.22	-86.71
	8	324.20	0.04	2.98	23.08	7.31	12.53	94.36	0.00
	Error (%)	118.91	15.39	25.74	982.83	50.38	543.27	113.06	-89.36
Campione and Miraglia 2003	4	86.96	0.02	2.00	3.86	0.79	2.25	21.95	0.00
	Error (%)	-13.81	-31.84	-22.99	109.18	-60.07	42.33	-1.20	-68.45
	6	108.86	0.02	2.00	5.93	1.26	3.19	32.93	0.00
	Error (%)	-14.25	-31.25	-19.03	158.64	-64.49	53.69	-3.11	-73.94
	8	130.39	0.02	1.99	5.22	1.59	2.61	43.91	0.00
	Error (%)	-11.96	-32.35	-16.02	144.96	-67.29	34.24	-0.86	-72.43
Lam and Teng 2003	4	85.51	0.02	3.30	5.61	1.04	4.03	12.87	0.00
	Error (%)	-15.24	-25.79	27.09	204.57	-47.43	154.85	-42.10	-76.41
	6	106.68	0.02	3.30	7.96	1.76	5.44	19.30	0.00
	Error (%)	-15.97	-22.87	33.60	247.52	-50.40	162.36	-43.23	-78.24
	8	127.50	0.03	3.28	10.00	2.55	6.57	25.73	0.00
	Error (%)	-13.91	-15.42	38.56	369.20	-47.54	237.31	-41.91	-82.01
Xiao and Wu 2003	4	123.69	0.03	3.68	8.24	3.06	6.08	21.95	0.00
	Error (%)	22.60	46.97	41.36	347.14	54.68	284.27	-1.20	-68.18
	6	169.09	0.05	3.83	8.44	4.94	5.05	32.93	0.01
	Error (%)	33.19	55.92	55.02	268.38	39.22	143.63	-3.11	-58.51
	8	214.46	0.06	3.90	9.98	7.84	5.82	43.91	0.01
	Error (%)	44.81	74.16	64.77	368.44	61.28	198.93	-0.86	-62.89
Jiang and Teng 2006	4	112.07	0.03	3.15	9.35	2.14	6.35	21.95	0.00
	Error (%)	11.08	23.18	21.00	406.92	8.18	301.18	-1.20	-76.47
	6	149.78	0.04	3.24	12.90	3.73	8.20	32.93	0.00
	Error (%)	17.97	25.21	31.27	462.83	5.12	295.13	-3.11	-78.19
	8	187.66	0.05	3.29	15.44	5.43	9.42	43.91	0.00
	Error (%)	26.72	31.81	39.02	624.52	11.70	383.53	-0.86	-81.84

Author	# Layers	UD[90˚/0˚]							
		f'_{cc}	ε'_{cc}	K_1	μ_{cu}	e_{cu}	w_{cu}	f_l	ε_1
Youssef 2007	4	84.82	0.02	1.90	3.00	1.09	2.20	21.95	0.01
	Error (%)	-15.93	-23.08	-26.74	62.99	-44.90	39.01	-1.20	-54.31
	6	112.31	0.03	2.10	3.63	2.00	2.54	32.93	0.01
	Error (%)	-11.53	-18.64	-14.78	58.51	-43.64	22.46	-3.11	-49.68
	8	141.71	0.03	2.25	3.92	3.13	2.68	43.91	0.01
	Error (%)	-4.32	-10.29	-5.15	84.14	-35.61	37.84	-0.86	-51.37
Wu et al. 2009	4	113.34	0.01	3.20	4.03	1.03	2.84	21.95	0.00
	Error (%)	12.34	-43.58	23.23	118.33	-47.93	79.53	-1.20	-74.98
	6	148.38	0.02	3.20	4.02	1.87	2.78	32.93	0.00
	Error (%)	16.87	-41.81	29.55	75.41	-47.30	34.10	-3.11	-67.48
	8	182.82	0.02	3.18	6.04	2.92	4.12	43.91	0.00
	Error (%)	23.45	-34.89	34.36	183.44	-39.93	111.39	-0.86	-77.07
Fahmy and Wu 2010	4	75.62	0.01	1.49	2.77	0.56	1.96	21.95	0.00
	Error (%)	-25.05	-54.31	-42.85	50.07	-71.69	24.18	-1.20	-70.52
	6	86.29	0.01	1.31	2.76	0.64	1.89	32.93	0.00
	Error (%)	-32.03	-65.35	-46.78	20.56	-81.96	-8.91	-3.11	-71.82
	8	95.76	0.01	1.20	2.50	0.66	1.67	43.91	0.00
	Error (%)	-35.34	-71.33	-49.30	17.08	-86.42	-14.45	-0.86	-75.55
Pellegrino and Modena 2010	4	113.57	0.03	3.21	9.83	2.25	6.43	21.95	0.00
	Error (%)	12.57	32.60	23.63	433.10	13.74	306.64	-1.20	-75.92
	6	155.32	0.04	3.41	10.58	4.30	6.79	32.93	0.00
	Error (%)	22.34	37.92	38.09	361.61	21.18	227.07	-3.11	-70.71
	8	198.49	0.06	3.54	10.90	7.08	6.97	43.91	0.01
	Error (%)	34.02	55.05	49.42	411.54	45.65	257.77	-0.86	-69.75
Liu et al. 2013	4	108.97	0.03	3.00	10.77	2.48	7.59	21.95	0.00
	Error (%)	8.01	41.49	15.57	484.02	25.36	379.58	-1.20	-76.54
	6	135.48	0.05	2.81	14.78	17.32	39.43	32.93	0.00
	Error (%)	6.72	53.15	13.70	545.10	388.11	1800.66	-3.11	-76.73
	8	162.57	0.06	2.72	18.99	6.42	12.17	43.91	0.00
	Error (%)	9.78	71.19	14.91	791.08	32.07	524.93	-0.86	-80.82

6.3.3 Predictions for Series 3 UD [+45˚/-45˚]

Figure 6-25, Figure 6-26, and **Figure 6-27** show comparisons between experimental and analytical responses for the Series 2 specimens having 4, 6 and 8 layers of CFRP. **Table 6-3** compares the peak stress, peak strain, strength, ductility and toughness parameters obtained from the analytical and experimental stress-strain curves, based on the average of 5 samples. Examining the stress-strain prediction for the case of 4 layers of CFRP in **Figure 6-25** it can be seen that better predictions are provided by some of the same models discussed in Series 1, even in the case of specimens with angular fibers. In the case of the overall trend of the stress-strain curves Lam and Teng (2003), Jiang and Teng (2006), and Liu et al. (2013) tend to predict the trend of the stress strain curve even though these models were developed based on FRP confinement in hoop direction. Percentage of error in prediction of the peak stress and peak strain are large which means more refinement is needed to predict the stress-strain behaviour of FRP confined concrete with fibers aligned in angle (UD [+45˚/-45˚]) direction. None of the models showed reasonable error percentage in the case of peak stress and peak strain, however, it's worth mentioning that by increasing the amount of confinement, the error percentage decreases as seen in **Table 6-3**. Results are not acceptable in the case of prediction of strength effectiveness factor K_1 (as it can be seen in **Table 6-3**, existing models either overestimates or underestimates the factor). Most models underestimate the energy absorption capacity e_{cu} of the FRP confined concrete columns as it is obvious in **Table 6-3**.

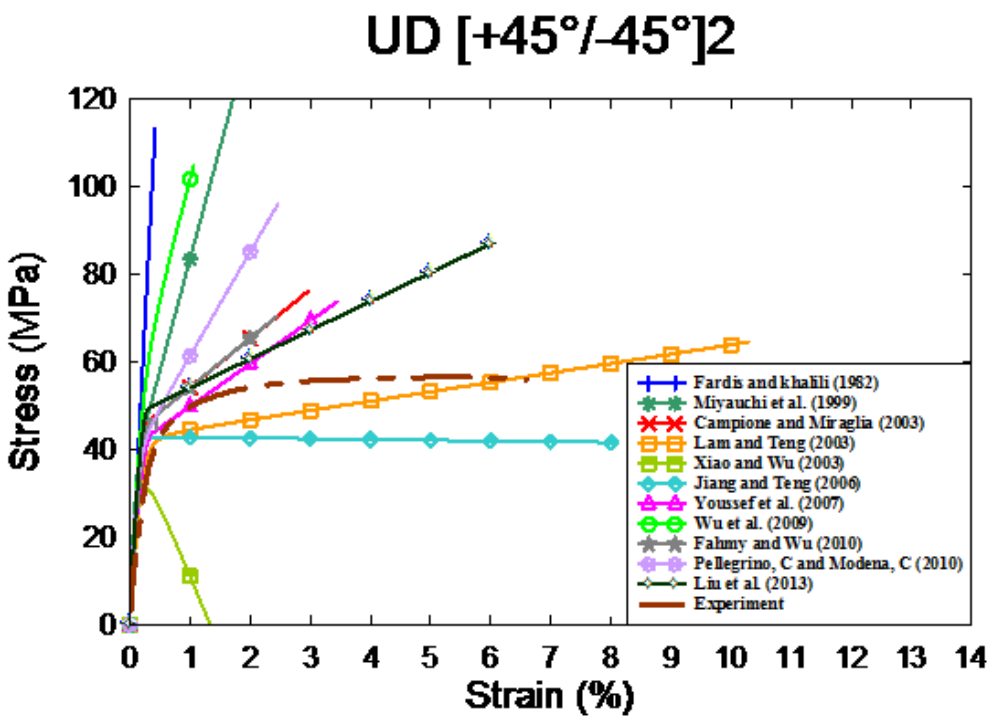

Figure 6-25 Stress-strain prediction of different models (4 layers)

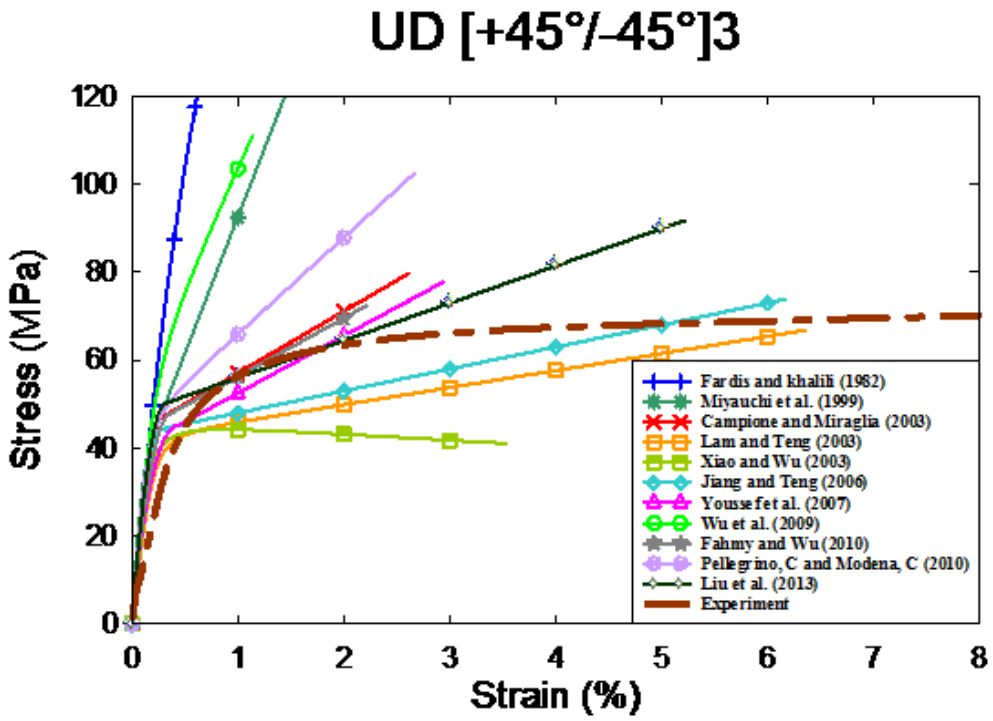

Figure 6-26 Stress-strain prediction of different models (6 layers)

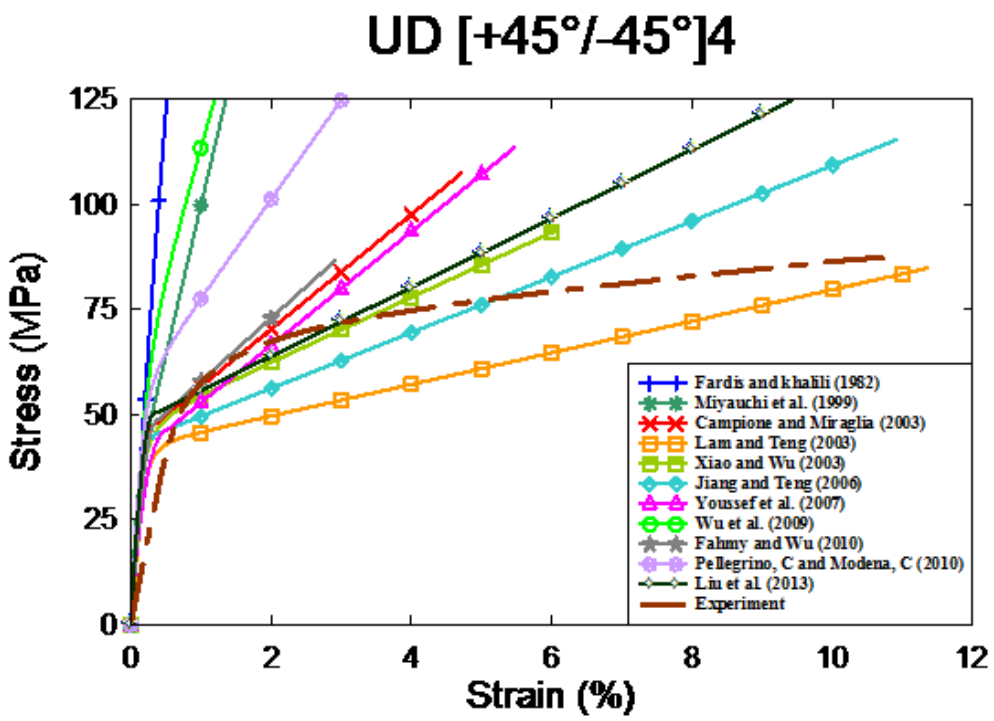

Figure 6-27 Stress-strain prediction of different models (8 layers)

Table 6-3 Prediction of different factors by existing proposed models

Author	# Layers	UD [+45°/-45°]							
		f'_{cc}	ε'_{cc}	K_1	μ_{cu}	e_{cu}	w_{cu}	f_l	ε_1
Experiment	4	52.27	0.06	2.08	7.08	2.45	6.04	4.44	0.01
	6	63.27	0.09	2.45	9.14	5.27	8.28	8.28	0.01
	8	73.39	0.10	3.74	9.15	6.54	8.03	8.12	0.01
Fardis and Khalili 1982	4	113.55	0.00	4.10	1.00	0.24	0.51	17.21	0.00
	Error (%)	117.24	-92.41	97.12	-85.87	-90.03	-91.57	287.57	-48.35
	6	120.78	0.01	4.10	1.31	0.43	0.75	18.97	0.00
	Error (%)	90.90	-93.09	67.35	-85.65	-91.85	-90.96	129.10	-52.52
	8	179.96	0.01	4.10	1.56	0.77	0.84	33.40	0.01
	Error (%)	145.20	-92.00	9.63	-82.93	-88.23	-89.57	311.39	-54.17
Miyauchi et al. 1999	4	183.60	0.03	2.98	15.48	3.18	9.05	47.18	0.00
	Error (%)	251.25	-46.77	43.27	118.62	29.88	49.93	962.65	-76.59
	6	253.90	0.04	2.98	19.48	5.11	10.87	70.77	0.00
	Error (%)	301.31	-60.06	21.63	113.22	-3.10	31.35	754.74	-81.54
	8	324.20	0.04	2.98	23.08	7.31	12.53	94.36	0.00
	Error (%)	341.73	-58.32	-20.32	152.31	11.76	56.00	1062.11	-83.86
Campione and Miraglia 2003	4	77.42	0.10	2.00	16.28	5.45	11.14	17.21	0.01
	Error (%)	48.10	84.96	-3.85	129.94	122.59	84.46	287.57	-22.64
	6	80.94	0.06	2.00	9.55	3.40	6.30	18.97	0.01
	Error (%)	27.93	-29.47	-18.37	4.55	-35.52	-23.86	129.10	-33.52
	8	109.81	0.11	2.00	17.54	7.16	10.06	33.40	0.01
	Error (%)	49.62	14.07	-46.52	91.80	9.47	25.31	311.39	-41.88
Lam and Teng 2003	4	76.28	0.03	3.30	10.33	1.73	7.88	10.08	0.00
	Error (%)	45.92	-46.59	58.65	45.86	-29.34	30.55	127.11	-64.79
	6	79.68	0.03	3.30	9.00	1.56	6.74	11.12	0.00
	Error (%)	25.95	-71.07	34.69	-1.55	-70.42	-18.56	34.25	-71.04
	8	107.60	0.05	3.30	16.27	3.51	11.24	19.58	0.00
	Error (%)	46.60	-52.62	-11.76	77.94	-46.34	40.04	141.07	-73.98
Xiao and Wu 2003	4	-72.04	0.03	-6.69	19.60	-0.48	3.81	17.21	0.00
	Error (%)	-237.83	-38.36	-421.42	176.76	-119.60	-36.95	287.57	-78.58
	6	37.96	0.04	-0.27	5.82	1.47	6.38	18.97	0.01
	Error (%)	-40.00	-60.90	-110.84	-36.30	-72.12	-22.87	129.10	-39.51
	8	89.70	0.06	1.40	7.71	4.16	5.94	33.40	0.01
	Error (%)	22.22	-39.61	-62.62	-15.75	-36.40	-26.05	311.39	-29.96
Jiang and Teng 2006	4	41.66	0.08	-0.08	29.01	3.36	29.13	17.21	0.00
	Error (%)	-20.30	44.42	-103.74	309.77	37.23	382.35	287.57	-66.11
	6	73.82	0.06	1.62	21.90	3.56	17.13	18.97	0.00
	Error (%)	16.68	-31.67	-33.68	139.74	-32.49	106.89	129.10	-71.91
	8	115.45	0.11	2.17	38.56	8.61	26.34	33.40	0.00
	Error (%)	57.30	9.56	-42.01	321.62	31.63	228.07	311.39	-74.61

Author	# Layers	UD [+45°/-45°]							
		f'_{cc}	ε'_{cc}	K_1	μ_{cu}	e_{cu}	w_{cu}	f_l	ε_1
Youssef 2007	4	73.79	0.03	1.79	8.72	1.92	6.58	17.21	0.00
	Error (%)	41.18	-38.05	-13.96	23.16	-21.58	9.02	287.57	-51.63
	6	77.78	0.03	1.83	6.78	1.68	4.98	18.97	0.00
	Error (%)	22.94	-67.41	-25.15	-25.80	-68.14	-39.88	129.10	-56.71
	8	113.56	0.05	2.11	10.65	4.12	7.07	33.40	0.01
	Error (%)	54.73	-45.14	-43.52	16.39	-37.01	-12.01	311.39	-53.95
Wu et al. 2009	4	98.07	0.01	3.20	2.28	0.74	1.63	17.21	0.00
	Error (%)	87.61	-81.01	53.85	-67.77	-69.78	-73.01	287.57	-43.33
	6	103.70	0.01	3.20	3.37	0.84	2.39	18.97	0.00
	Error (%)	63.91	-87.35	30.61	-63.13	-84.07	-71.13	129.10	-66.19
	8	149.90	0.02	3.20	4.64	1.91	3.21	33.40	0.00
	Error (%)	104.23	-81.50	-14.44	-49.23	-70.80	-60.03	311.39	-64.39
Fahmy and Wu 2010	4	70.48	0.02	1.60	7.04	1.34	5.48	17.21	0.00
	Error (%)	34.84	-56.05	-23.22	-0.52	-45.27	-9.29	287.57	-57.52
	6	72.42	0.02	1.55	6.34	1.23	4.85	18.97	0.00
	Error (%)	14.47	-75.43	-36.69	-30.60	-76.67	-41.36	129.10	-65.10
	8	86.72	0.03	1.31	8.27	1.84	6.02	33.40	0.00
	Error (%)	18.16	-70.74	-65.00	-9.55	-71.87	-25.02	311.39	-68.39
Pellegrino and Modena 2010	4	96.25	0.02	3.09	6.70	1.61	4.55	17.21	0.00
	Error (%)	84.13	-55.69	48.77	-5.40	-34.24	-24.72	287.57	-54.96
	6	102.56	0.03	3.14	5.45	1.91	3.80	18.97	0.00
	Error (%)	62.11	-70.40	28.16	-40.31	-63.78	-54.09	129.10	-51.13
	8	157.18	0.04	3.42	9.20	4.54	6.08	33.40	0.00
	Error (%)	114.16	-56.14	-8.61	0.61	-30.59	-24.27	311.39	-57.40
Liu et al. 2013	4	87.07	0.06	2.56	19.26	3.99	14.70	17.21	0.00
	Error (%)	66.57	7.90	23.13	171.98	62.96	143.46	287.57	-61.85
	6	91.77	0.05	2.57	16.66	3.59	12.47	18.97	0.00
	Error (%)	45.05	-42.14	4.94	82.30	-31.92	50.70	129.10	-68.72
	8	127.89	0.10	2.54	31.28	8.55	21.34	33.40	0.00
	Error (%)	74.25	-1.65	-32.05	242.03	30.72	165.75	311.39	-71.90

6.3.4 Predictions for Series 4A UD[90˚/0˚]W[±45˚]

Figure 6-28 and **Figure 6-29** show comparisons between experimental and analytical responses for the Series 2 specimens having 4, 6 and 8 layers of CFRP. **Table 6-4** compares the peak stress, peak strain, strength, ductility and toughness parameters obtained from the analytical and experimental stress-strain curves, based on the average of 5 samples. Examining the stress-strain prediction for the case of 4 layers of CFRP in **Figure 6-28** it can be seen that relatively better predictions are provided by some of the same "accurate" models discussed in previous series, and this is to be expected because the unidirectional 0˚ fibers dominate the response of this series The earlier Fardis and Khalili (1982) and Wu et al (2009) follow a similar stress-strain pattern when compared to the experimental stress-strain curves (where rounding of the curve at transition is captured), however stiffer behavior was shown with both models. Percentage of error in most of the models was increased by increasing the number of layers except for the Fardis and Khalili (1982) in the case of the predictions for peak stress. The Xiao and Wu (2003), Jiang and Teng (2006), Wu et al (2009), Pellegrino and Modena (2010), and Liu et al. (2013) experienced error percentage of -0.64, -5.54, -0.41, -3.46, and -4.45 respectively, for specimens confined with 4 layers of CFRP sheets. However, the percentage of error increased to -6.31, -14.41, -12.37, -12.25, and -19.44 respectively, by increasing the number of layers to 8 layers. All of the models underestimate the peak strain except the Miyauchi et al. (1999) model which overestimates the peak strain as seen in **Table 6-4**. Percentage of error in predicting the strength effectiveness factor amongst the models ranged from -61% to 45%. Error percentage of all other factors is presented in **Table 6-4** in details.

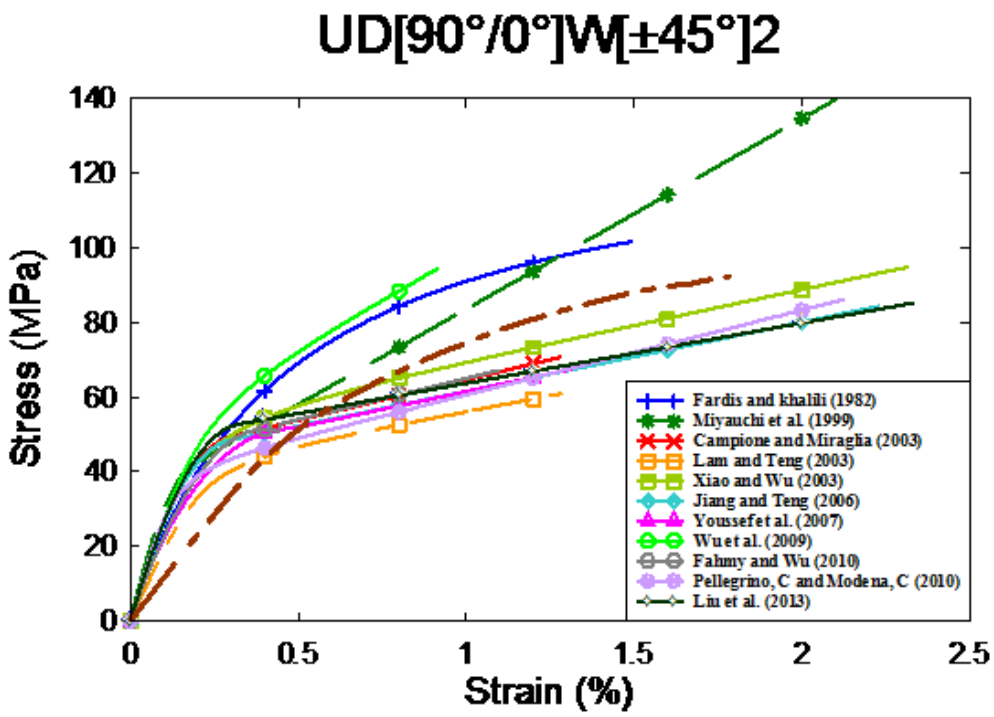

Figure 6-28 Stress-strain prediction of different models (4 layers)

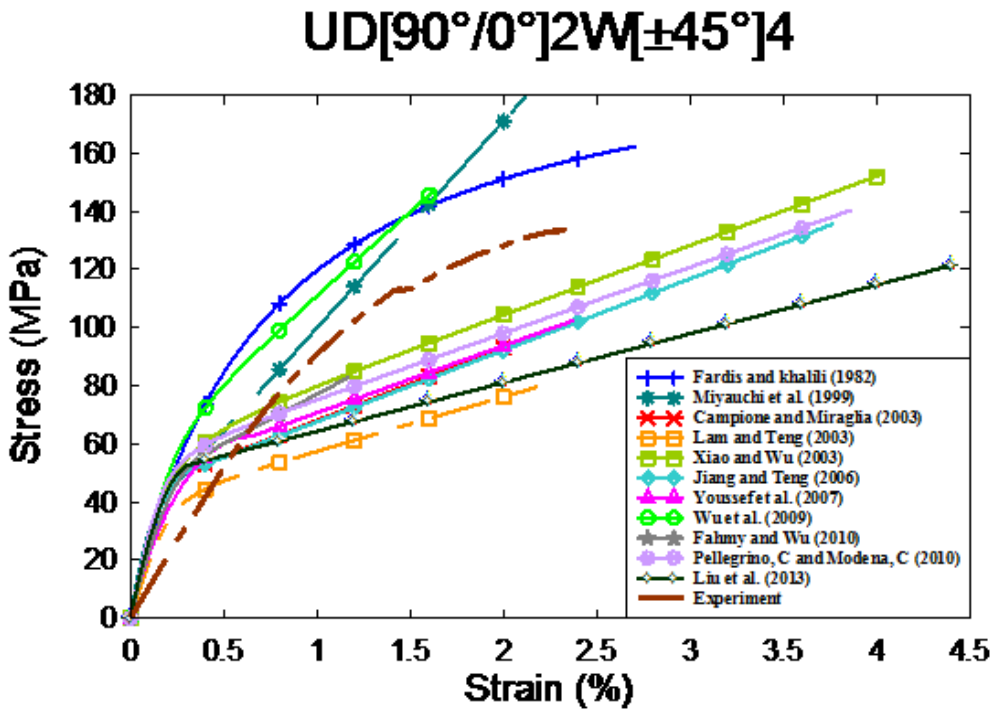

Figure 6-29 Stress-strain prediction of different models (8 layers)

Table 6-4 Prediction of different factors by existing proposed models

Author	# Layers	UD[90˚/0˚]W[±45˚]							
		f'_{cc}	ε'_{cc}	K_1	μ_{cu}	e_{cu}	w_{cu}	f_l	ε_1
Experiment	4	89.14	0.02	2.78	2.17	1.43	1.49	16.60	0.02
	8	128.78	0.03	2.85	8.91	3.04	6.06	30.12	0.03
Fardis and Khalili 1982	4	101.65	0.01	4.03	2.82	1.10	2.04	14.55	0.01
	Error (%)	14.04	-36.05	44.98	29.84	-23.08	37.04	-12.33	-77.29
	8	132.50	0.02	3.08	2.08	3.26	2.46	29.11	0.01
	Error (%)	2.89	-39.73	7.89	-76.64	7.16	-59.41	-3.37	-71.02
Miyauchi et al. 1999	4	183.60	0.03	2.98	15.48	3.18	9.05	47.18	0.00
	Error (%)	105.97	26.62	7.19	613.54	122.37	508.86	184.23	-91.82
	8	253.90	0.04	2.24	20.03	7.31	15.99	94.36	0.00
	Error (%)	97.16	4.49	-21.58	124.97	140.28	163.87	213.29	-94.78
Campione and Miraglia 2003	4	71.61	0.01	1.97	3.27	0.58	2.07	14.55	0.00
	Error (%)	-19.66	-45.17	-29.28	50.78	-59.44	38.94	-12.33	-83.24
	8	86.66	0.02	1.50	4.41	1.23	3.44	29.11	0.00
	Error (%)	-32.71	-47.31	-47.37	-50.50	-59.57	-43.23	-3.37	-88.05
Lam and Teng 2003	4	70.67	0.01	3.24	4.30	0.68	3.23	8.53	0.00
	Error (%)	-20.73	-45.26	16.69	98.02	-52.45	117.15	-48.63	-87.26
	8	85.21	0.02	2.48	5.94	1.55	6.06	17.06	0.00
	Error (%)	-33.83	-48.37	-13.16	-33.34	-49.05	-0.04	-43.37	-91.30
Xiao and Wu 2003	4	88.57	0.02	3.13	5.35	1.60	4.17	14.55	0.00
	Error (%)	-0.64	-1.01	12.64	146.44	11.89	180.55	-12.33	-81.48
	8	120.65	0.03	2.67	6.63	4.11	6.63	29.11	0.01
	Error (%)	-6.31	-1.22	-6.39	-25.52	35.09	9.34	-3.37	-85.11
Jiang and Teng 2006	4	84.29	0.02	2.84	7.56	1.38	5.56	14.55	0.00
	Error (%)	-5.45	-4.67	2.05	248.71	-3.50	273.61	-12.33	-87.40
	8	110.17	0.03	2.31	10.19	3.32	10.02	29.11	0.00
	Error (%)	-14.45	-11.15	-19.03	14.44	9.13	65.22	-3.37	-91.28
Youssef 2007	4	67.45	0.01	1.68	2.73	0.67	2.07	14.55	0.00
	Error (%)	-24.34	-43.84	-39.57	25.94	-53.15	38.97	-12.33	-79.44
	8	84.46	0.02	1.42	2.88	1.71	3.13	29.11	0.01
	Error (%)	-34.42	-45.98	-50.02	-67.62	-43.79	-48.35	-3.37	-81.26
Wu et al. 2009	4	88.78	0.01	3.15	2.68	0.58	1.91	14.55	0.00
	Error (%)	-0.41	-60.86	13.15	23.38	-59.44	28.46	-12.33	-85.38
	8	112.85	0.01	2.40	2.88	1.55	3.09	29.11	0.00
	Error (%)	-12.37	-62.88	-15.79	-67.67	-49.05	-49.08	-3.37	-87.11
Fahmy and Wu 2010	4	67.15	0.01	1.66	3.03	0.55	2.26	14.55	0.00
	Error (%)	-24.67	-53.03	-40.31	39.58	-61.54	51.82	-12.33	-84.49
	8	75.46	0.01	1.12	3.05	0.68	2.36	29.11	0.00
	Error (%)	-41.40	-66.21	-60.87	-65.76	-77.65	-61.12	-3.37	-88.92
Pellegrino and Modena 2010	4	86.06	0.02	2.96	6.05	1.28	4.24	14.55	0.00
	Error (%)	-3.46	-9.20	6.43	178.88	-10.49	184.96	-12.33	-84.99
	8	113.00	0.03	2.41	5.26	3.66	5.67	29.11	0.01
	Error (%)	-12.25	-12.82	-15.61	-40.88	20.30	-6.50	-3.37	-83.44
Liu et al. 2013	4	85.18	0.02	2.90	7.25	1.50	5.47	14.55	0.00
	Error (%)	-4.45	-0.27	4.25	234.09	4.89	268.01	-12.33	-86.24
	8	103.75	0.03	2.09	10.61	3.70	11.06	29.11	0.00
	Error (%)	-19.44	-0.86	-26.76	19.13	21.62	82.43	-3.37	-90.66

6.3.5 Predictions for Series 4B UD[90˚]W[±45˚]UD[0˚]

Figure 6-30 and **Figure 6-31** show comparisons between experimental and analytical responses for the Series 2 specimens having 4, 6 and 8 layers of CFRP. Table 6-5 compares the peak stress, peak strain, strength, ductility and toughness parameters obtained from the analytical and experimental stress-strain curves, based on the average of 5 samples. Examining the stress-strain prediction for the case of 4 layers of CFRP in **Figure 6-30** it can be seen that better predictions are provided by the same "accurate" models discussed in previous sections. One can see in **Figure 6-31** most of the models showed better predictions of the first branch of the curve as the number of layers is increased to 6 and 8, while the slope of the second branch of the experimental curves is over-predicted as the number of layers is increased. Fardis and khalili (1982) model showed the best ability to capture in the trend of the stress-strain response, however, it's worth mentioning that this model showed the same pattern for all types of confinement. In the case of peak stress most of the models displayed reasonable results except Fardis and khalili (1982) and Miyauchi et al. (1999) which significantly overestimate peak stress. Table 6-5 shows that the best predictions of peak strain was achieved by Pellegrino and Modena (2010) model which experienced 7.74% and 6.18% error in specimens confined with 4 and 8 layers of CFRP sheets. Similarly this model predicted the energy absorption capacity, which is the area under the stress-strain curve with the minimum percentage of error compare to all other models presented in this study. Nonetheless, in general, none of the models were able to predict the stress-strain behavior for this layup pattern, particularly in the case of peak stress, and peak strain.

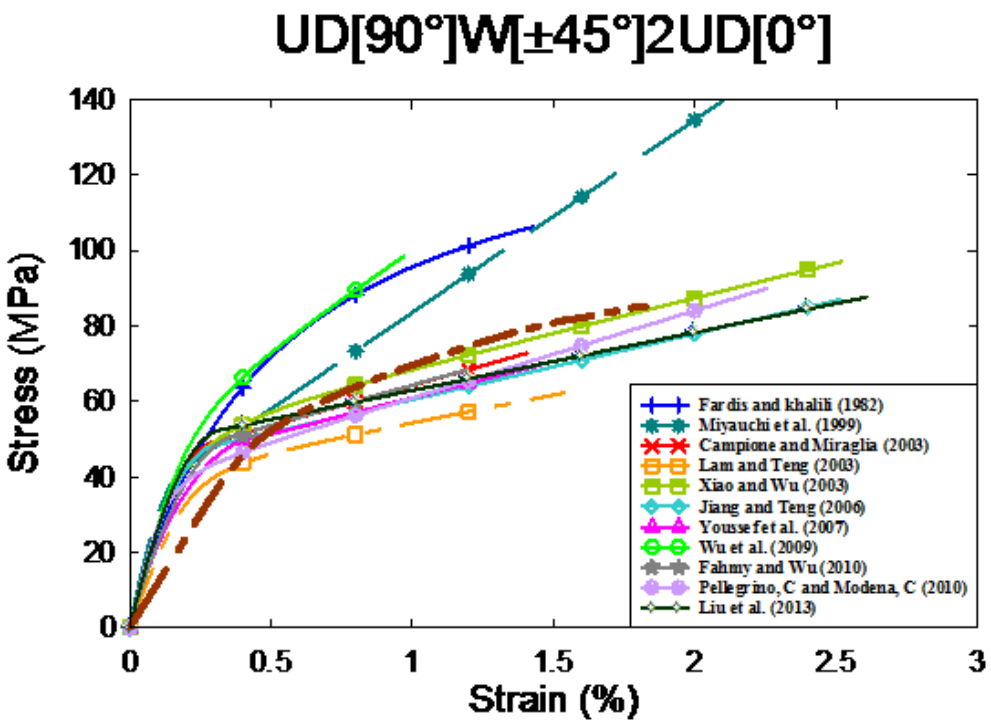

Figure 6-30 Stress-strain prediction of different models (4 layers)

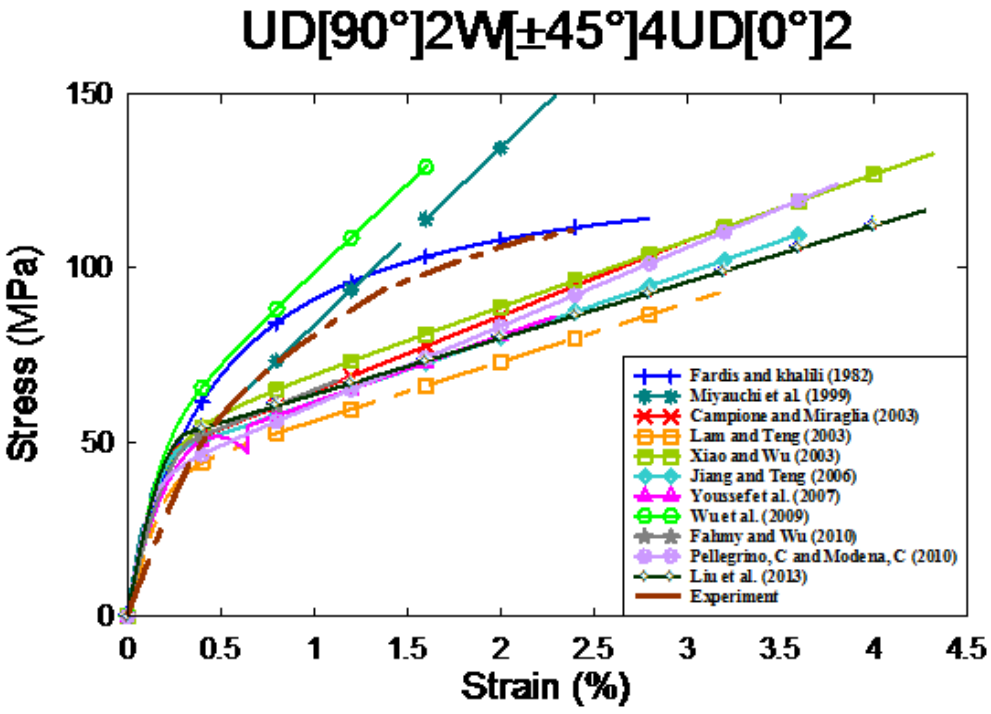

Figure 6-31 Stress-strain prediction of different models (8 layers)

Table 6-5 Prediction of different factors by existing proposed models

Author	# Layers	UD[90°]W[±45°]UD[0°]							
		f'_{cc}	ε'_{cc}	K_1	μ_{cu}	e_{cu}	w_{cu}	f_l	ε_1
Experiment	4	81.33	0.02	2.52	2.50	1.08	1.80	15.17	0.00
	8	113.86	0.03	2.83	2.45	2.70	1.69	24.99	0.01
Fardis and Khalili 1982	4	106.23	0.01	4.34	0.98	1.08	2.02	14.55	0.01
	Error (%)	30.62	-31.84	72.41	-60.58	0.16	12.06	-4.07	181.92
	8	160.31	0.03	4.03	4.34	2.51	2.44	29.11	0.01
	Error (%)	40.80	-19.82	42.42	77.19	-6.93	44.31	16.47	-55.68
Miyauchi et al. 1999	4	183.60	0.03	2.98	15.48	3.18	9.05	47.18	0.00
	Error (%)	125.75	41.32	18.25	519.82	194.90	402.99	211.02	7.01
	8	324.20	0.04	2.98	23.08	5.73	9.82	94.36	0.00
	Error (%)	184.75	19.33	5.30	841.97	112.47	481.90	277.60	-87.59
Campione and Miraglia 2003	4	73.84	0.02	2.12	4.35	0.73	2.79	14.55	0.00
	Error (%)	-9.20	-26.43	-15.90	74.38	-32.30	55.14	-4.07	98.01
	8	100.22	0.02	1.97	5.76	2.04	5.72	29.11	0.00
	Error (%)	-11.97	-41.05	-30.53	135.29	-24.36	238.84	16.47	-75.46
Lam and Teng 2003	4	72.82	0.01	3.50	4.73	0.77	3.55	8.53	0.00
	Error (%)	-10.46	-32.83	38.77	89.37	-28.59	97.38	-43.78	66.47
	8	98.33	0.02	3.24	7.20	2.23	7.51	17.06	0.00
	Error (%)	-13.64	-37.51	14.63	194.01	-17.31	345.03	-31.75	-79.18
Xiao and Wu 2003	4	91.03	0.03	3.30	7.73	1.78	6.00	14.55	0.00
	Error (%)	11.93	20.28	30.98	209.56	65.07	233.21	-4.07	82.35
	8	150.39	0.04	3.69	9.07	3.88	5.41	29.11	0.00
	Error (%)	32.09	24.09	30.38	270.03	43.87	220.86	16.47	-67.15
Jiang and Teng 2006	4	86.99	0.03	3.02	8.57	1.59	6.23	14.55	0.00
	Error (%)	6.96	20.14	19.95	243.35	47.45	245.86	-4.07	64.23
	8	134.36	0.04	3.14	11.97	2.72	6.71	29.11	0.00
	Error (%)	18.01	3.78	10.91	388.74	0.86	297.66	16.47	-79.20
Youssef 2007	4	69.85	0.01	1.85	3.01	0.76	2.25	14.55	0.00
	Error (%)	-14.11	-30.36	-26.78	20.58	-29.52	24.73	-4.07	171.07
	8	101.14	0.02	2.00	3.53	1.41	2.15	29.11	0.01
	Error (%)	-11.17	-34.22	-29.41	44.25	-47.72	27.51	16.47	-55.34
Wu et al. 2009	4	92.35	0.01	3.39	2.79	0.64	2.00	14.55	0.00
	Error (%)	13.55	-53.73	34.57	11.89	-40.65	10.95	-4.07	94.10
	8	134.56	0.02	3.15	4.51	1.36	2.83	29.11	0.00
	Error (%)	18.18	-53.73	11.16	84.16	-49.57	67.78	16.47	-75.39
Fahmy and Wu 2010	4	68.45	0.01	1.75	3.30	0.61	2.46	14.55	0.00
	Error (%)	-15.83	-43.00	-30.60	32.19	-43.43	36.83	-4.07	102.38
	8	82.23	0.01	1.35	2.92	0.57	1.81	29.11	0.00
	Error (%)	-27.78	-67.76	-52.37	19.37	-78.86	7.03	16.47	-73.54
Pellegrino and Modena 2010	4	89.94	0.02	3.23	7.18	1.40	4.96	14.55	0.00
	Error (%)	10.59	7.61	28.00	187.55	29.83	175.39	-4.07	75.64
	8	138.55	0.04	3.28	11.54	3.05	6.67	29.11	0.00
	Error (%)	21.69	9.37	16.00	370.89	13.09	295.33	16.47	-77.25
Liu et al. 2013	4	87.63	0.03	3.07	8.13	1.71	6.08	14.55	0.00
	Error (%)	7.74	24.48	21.69	225.48	58.58	237.83	-4.07	79.50
	8	120.89	0.04	2.68	13.24	3.45	8.84	29.11	0.00
	Error (%)	6.18	22.81	-5.43	440.41	27.92	423.75	16.47	-77.74

6.3.6 Predictions for Series 5A UD[0˚]W[±45˚]

Figure 6-32 and **Figure 6-33** show comparisons between experimental and analytical responses for the Series 2 specimens having 4, 6 and 8 layers of CFRP. **Table 6-6** compares the peak stress, peak strain, strength, ductility and toughness parameters obtained from the analytical and experimental stress-strain curves, based on the average of 5 samples. The models which had good predictions in Series 1 (UD[0˚]) showed reasonable predictions for this series as well. This is to be expected; as shown in **Figure 6-32** and **Figure 6-33** , even though W[±45˚] CFRP sheets were used in this series, stress-strain response is dominated by fibers in the hoop direction UD[0˚] and follows the same trend observed in Series 1. Continuing the observation made in previous series, most of the models showed reasonable prediction for the second branch of the stress-strain curve while overestimating the stiffness of the first branch of the curve. **Table 6-6** shows that the percentage of error in predicting peak stress increases with the increase in the amount of confinement. For example, in the Liu et al. (2013) model which showed the minimum percentage of error amongst all other models, percentage of error increases from -3.36 to -5.41 by increasing the number of CFRP layers from 4 to 8 layers. No reliable predictions are obtained when comparing all other factors in **Table 6-6** since the percentage of error in predicting peak strain is very high in most models. In addition to this, the shape of the stress-strain curve is not captured by most models, which explains the poor predictions for energy absorption capacity and ductility factors.

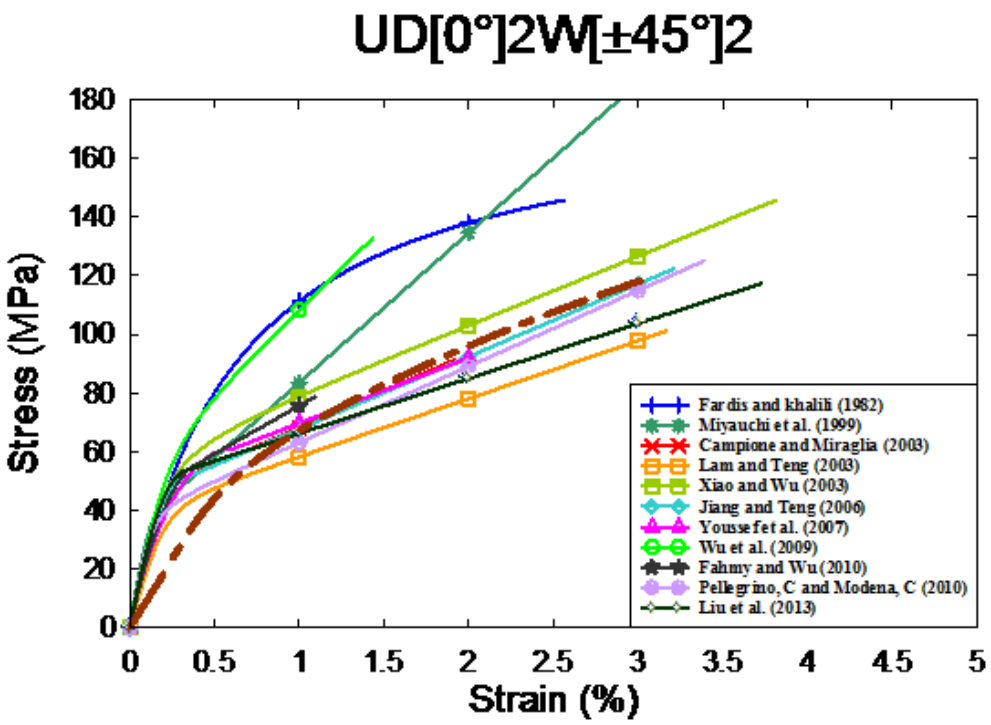

Figure 6-32 Stress-strain prediction of different models (4 layers)

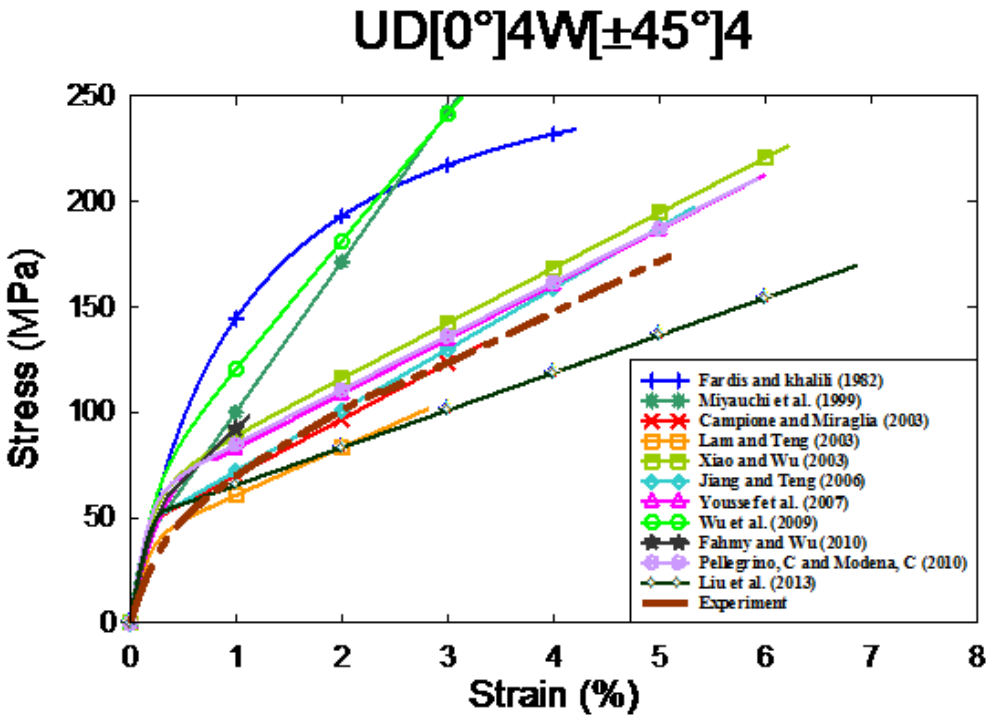

Figure 6-33 Stress-strain prediction of different models (8 layers)

Table 6-6 Prediction of different factors by existing proposed models

Author	# Layers	UD[0°]W[±45°]							
		f'_{cc}	ε'_{cc}	K_1	μ_{cu}	e_{cu}	w_{cu}	f_l	ε_1
Experiment	4	121.43	0.04	3.13	2.62	3.75	1.83	25.05	0.02
	8	178.90	0.06	2.92	2.72	6.74	1.75	46.56	0.02
Fardis and Khalili 1982	4	145.72	0.03	4.41	1.19	2.80	2.69	23.28	0.01
	Error (%)	20.01	-42.01	40.97	-54.63	-25.31	46.80	-7.06	-58.87
	8	233.90	0.04	4.10	4.20	7.38	3.16	46.56	0.01
	Error (%)	30.74	-28.14	40.41	54.43	9.50	80.08	0.00	-53.67
Miyauchi et al. 1999	4	183.60	0.03	2.98	15.48	3.18	9.05	47.18	0.00
	Error (%)	51.20	-33.05	-4.79	491.06	-15.18	393.87	88.35	-88.98
	8	324.20	0.04	2.98	23.08	7.31	12.53	94.36	0.00
	Error (%)	81.22	-29.00	2.05	747.57	8.46	614.95	102.67	-91.66
Campione and Miraglia 2003	4	93.11	0.02	2.15	3.73	2.16	4.77	23.28	0.00
	Error (%)	-23.32	-58.98	-31.24	42.55	-42.38	160.38	-7.06	-72.00
	8	136.12	0.03	2.00	5.41	1.90	2.68	46.56	0.01
	Error (%)	-23.91	-51.95	-31.51	98.58	-71.81	53.20	0.00	-75.91
Lam and Teng 2003	4	91.45	0.02	3.30	6.37	1.25	4.53	14.68	0.00
	Error (%)	-24.69	-56.51	5.43	143.39	-66.66	147.05	-41.39	-82.61
	8	133.04	0.03	3.07	11.10	2.92	7.23	29.36	0.00
	Error (%)	-25.64	-42.46	5.01	307.56	-56.68	312.89	-36.93	-85.94
Xiao and Wu 2003	4	135.85	0.04	3.99	6.13	3.74	4.43	23.28	0.01
	Error (%)	11.88	-13.83	27.43	133.96	-0.24	141.43	-7.06	-64.17
	8	225.13	0.07	3.91	10.05	8.86	5.87	46.56	0.01
	Error (%)	25.84	15.24	33.96	269.07	31.46	234.75	0.00	-68.91
Jiang and Teng 2006	4	122.26	0.03	3.40	10.65	2.61	7.09	23.28	0.00
	Error (%)	0.69	-27.48	8.77	306.76	-30.38	286.74	-7.06	-82.65
	8	196.72	0.05	3.30	17.43	6.33	10.53	46.56	0.00
	Error (%)	9.96	-9.01	13.06	540.04	-6.08	501.17	0.00	-85.85
Youssef 2007	4	92.25	0.02	2.12	3.28	1.33	2.35	23.28	0.01
	Error (%)	-24.03	-54.51	-32.41	25.38	-64.52	28.35	-7.06	-64.70
	8	149.87	0.04	2.30	4.33	7.94	6.38	46.56	0.01
	Error (%)	-16.23	-38.51	-21.40	59.05	17.81	263.97	0.00	-61.51
Wu et al. 2009	4	123.17	0.01	3.44	3.59	1.24	2.52	23.28	0.00
	Error (%)	1.44	-67.49	10.02	37.25	-66.92	37.29	-7.06	-76.96
	8	192.00	0.02	3.20	4.69	9.73	9.56	46.56	0.01
	Error (%)	7.32	-57.56	9.59	72.08	44.36	445.74	0.00	-75.45
Fahmy and Wu 2010	4	78.75	0.01	1.54	2.88	0.61	2.04	23.28	0.00
	Error (%)	-35.15	-75.27	-50.94	9.90	-83.73	11.20	-7.06	-78.11
	8	98.16	0.01	1.18	2.74	0.73	1.82	46.56	0.00
	Error (%)	-45.13	-80.80	-59.43	0.72	-89.12	4.02	0.00	-81.02
Pellegrino and Modena 2010	4	125.02	0.03	3.52	8.30	2.71	5.31	23.28	0.00
	Error (%)	2.96	-23.39	12.56	217.11	-27.71	189.81	-7.06	-76.49
	8	210.28	0.06	3.59	10.38	7.89	6.58	46.56	0.01
	Error (%)	17.54	1.17	23.04	281.40	17.06	275.71	0.00	-73.59
Liu et al. 2013	4	117.34	0.04	3.19	11.49	3.02	7.93	23.28	0.00
	Error (%)	-3.36	-15.69	2.02	338.68	-19.44	332.49	-7.06	-81.30
	8	169.23	0.07	2.71	21.21	7.38	13.48	46.56	0.00
	Error (%)	-5.41	17.27	-7.16	678.96	9.50	669.39	0.00	-85.01

6.3.7 Predictions for Series 5B W[±45˚]UD[0˚]

It is clear from the comparison of **Figure 6-34** and **Figure 6-35** , as the number of CFRP sheets with UD[0˚] increase, the behavior of the stress-strain curves gets closer to the one observed in Series 1. As a result models which were modified based on the four parameter model of Richard and Abbott (1975) displayed the best performance in predicting in the stress-strain behavior of the CFRP confined concrete cylinders in this series. Error percentage related to peak stress were reasonable for all models except for the Fardis and khalili (1982) and Miyauchi et al. (1999) models. The errors associated with the predictions of peak strain are higher when compared to predictions for peak stress. As it was discussed poor predictions for strain affect the accuracy of predictions of overall energy absorption capacity. It is also noted that error associated with ε_1 is high which can be due to how it is defined in different models. This factor in some models is calculated based on the ratio of the unconfined concrete strength to the difference between the two slopes of the stress-strain curve, while in others it is obtained from the intersection of the tangent of both first and second slope of the stress-strain curve ($E_1$and E_2).

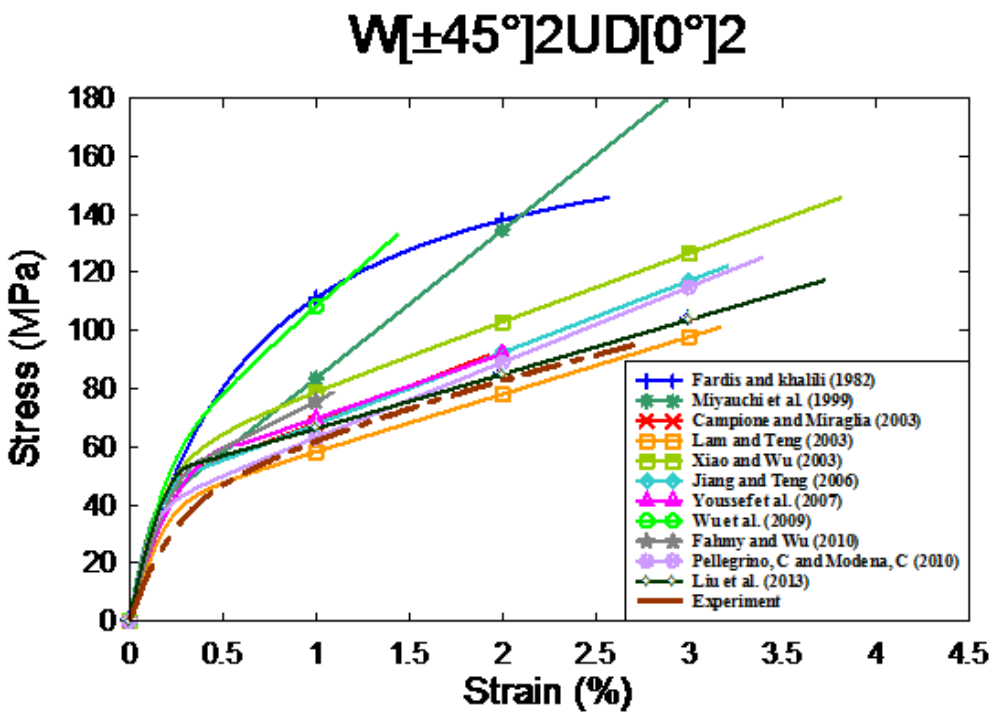

Figure 6-34 Stress-strain prediction of different models (4 layers)

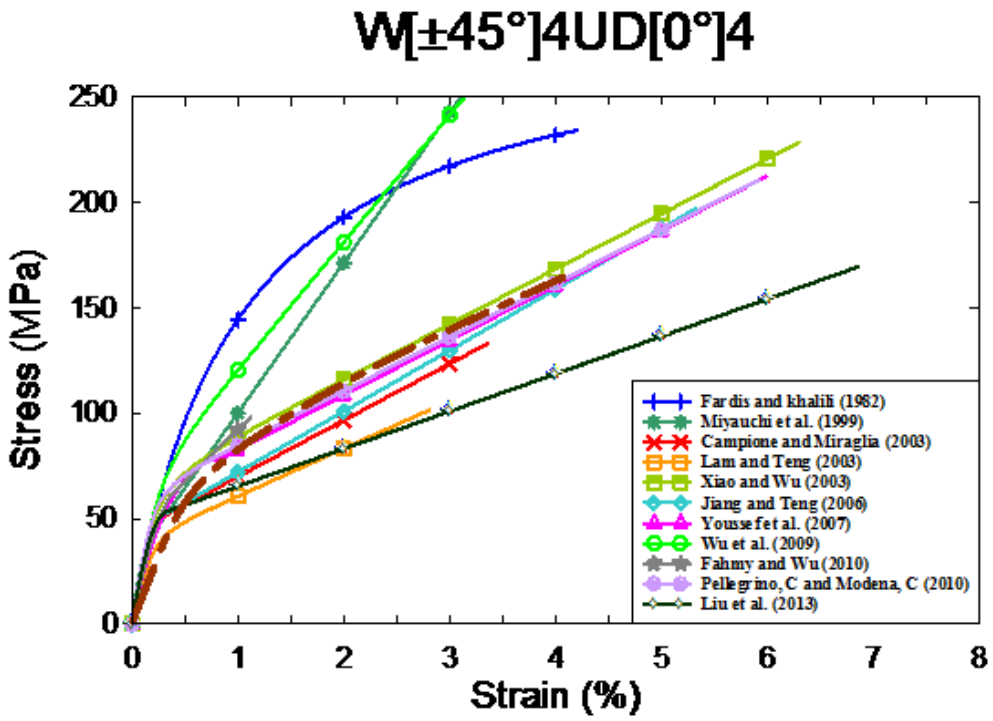

Figure 6-35 Stress-strain prediction of different models (8 layers)

Table 6-7 Prediction of different factors by existing proposed models

Author	# Layers	W[±45˚]UD[0˚]							
		f'_{cc}	ε'_{cc}	K_1	μ_{cu}	e_{cu}	w_{cu}	f_l	ε_1
Experiment	4	104.11	0.03	2.44	2.78	2.13	1.91	25.05	0.01
	8	163.47	0.06	2.59	3.76	6.22	2.27	46.56	0.02
Fardis and Khalili 1982	4	145.72	0.03	4.41	1.50	2.80	3.05	23.28	0.01
	Error (%)	39.97	-14.45	80.83	-46.14	31.29	59.49	-7.06	-42.39
	8	233.90	0.04	4.10	4.67	7.38	3.51	46.56	0.01
	Error (%)	43.08	-32.23	58.30	24.15	18.74	54.15	0.00	-47.45
Miyauchi et al. 1999	4	183.60	0.03	2.98	15.48	3.18	9.05	47.18	0.00
	Error (%)	76.36	-1.23	22.13	456.71	49.10	374.22	88.35	-82.53
	8	324.20	0.04	2.98	23.08	7.31	12.53	94.36	0.00
	Error (%)	98.32	-33.04	15.06	513.29	17.62	450.78	102.67	-89.49
Campione and Miraglia 2003	4	93.11	0.02	2.15	4.72	2.16	6.04	23.28	0.00
	Error (%)	-10.57	-39.49	-11.79	69.93	1.28	216.43	-7.06	-64.94
	8	136.12	0.03	2.00	6.42	1.90	3.19	46.56	0.00
	Error (%)	-16.73	-54.68	-22.78	70.59	-69.43	40.12	0.00	-74.43
Lam and Teng 2003	4	91.45	0.02	3.30	6.37	1.25	4.53	14.68	0.00
	Error (%)	-12.16	-35.83	35.25	129.25	-41.39	137.22	-41.39	-72.44
	8	133.04	0.03	3.07	11.10	2.92	7.23	29.36	0.00
	Error (%)	-18.62	-45.73	18.40	194.90	-53.02	218.08	-36.93	-82.29
Xiao and Wu 2003	4	135.85	0.04	3.99	8.41	3.74	6.08	23.28	0.00
	Error (%)	30.49	27.12	63.46	202.58	75.36	218.30	-7.06	-58.64
	8	225.13	0.07	3.91	11.57	9.06	6.90	46.56	0.01
	Error (%)	37.72	8.69	51.03	207.36	45.77	203.51	0.00	-65.96
Jiang and Teng 2006	4	122.26	0.03	3.40	10.65	2.61	7.09	23.28	0.00
	Error (%)	17.44	6.98	39.53	283.12	22.38	271.35	-7.06	-72.51
	8	196.72	0.05	3.30	17.43	6.33	10.53	46.56	0.00
	Error (%)	20.34	-14.19	27.47	363.12	1.85	363.13	0.00	-82.16
Youssef 2007	4	92.25	0.02	2.12	3.28	1.33	2.35	23.28	0.01
	Error (%)	-11.39	-32.90	-13.30	18.10	-37.64	23.25	-7.06	-44.06
	8	149.87	0.04	2.30	4.33	7.94	6.38	46.56	0.01
	Error (%)	-8.32	-42.01	-11.38	15.09	27.75	180.39	0.00	-51.49
Wu et al. 2009	4	123.17	0.01	3.44	4.19	1.24	2.94	23.28	0.00
	Error (%)	18.31	-52.04	41.14	50.76	-41.86	53.73	-7.06	-68.68
	8	192.00	0.02	3.20	4.64	9.73	9.47	46.56	0.01
	Error (%)	17.45	-59.98	23.55	23.35	56.55	316.50	0.00	-68.76
Fahmy and Wu 2010	4	78.75	0.01	1.54	2.88	0.61	2.04	23.28	0.00
	Error (%)	-24.36	-63.52	-37.07	3.52	-71.40	6.77	-7.06	-65.30
	8	98.16	0.01	1.18	2.74	0.73	1.82	46.56	0.00
	Error (%)	-39.95	-81.89	-54.26	-27.12	-88.25	-20.19	0.00	-76.08
Pellegrino and Modena 2010	4	125.02	0.03	3.52	10.46	2.71	6.69	23.28	0.00
	Error (%)	20.09	13.02	44.39	276.12	27.07	250.42	-7.06	-70.42
	8	210.28	0.06	3.59	10.90	7.89	6.91	46.56	0.01
	Error (%)	28.63	-4.59	38.71	189.70	26.95	203.83	0.00	-68.30
Liu et al. 2013	4	117.34	0.04	3.19	11.49	3.02	7.93	23.28	0.00
	Error (%)	12.71	24.38	30.88	313.19	41.60	315.28	-7.06	-70.36
	8	169.23	0.07	2.71	21.21	7.38	13.48	46.56	0.00
	Error (%)	3.52	10.59	4.67	463.64	18.74	492.73	0.00	-81.11

6.3.8 Predictions for Series 6 UD[90˚$_x$/0˚$_x$]

Figure 6-36, Figure 6-37, and **Figure 6-38** show comparisons between experimental and analytical responses for the Series 6 specimens having 4, 6 and 8 layers of CFRP. **Table 6-8** compares the peak stress, peak strain, strength, ductility and toughness parameters obtained from the analytical and experimental stress-strain curves, based on the average of 5 samples. It is obvious from **Figure 6-36**, **Figure 6-37**, and **Figure 6-38** the trend of the stress-strain curve follows that the response is generally dominated by the unidirectional 0˚ fibers, with similar trend to the one observed in series 1. Thus the same models which provide accurate predictions in series 1 show relatively better predictions in Series 6. All of the models showed stiffer behavior in the first part of the curve with the predicted response getting closer to the experimental response as number of layers increased. As seen in **Table 6-8** errors associated with peak stress, increase as amount of confinement increases. For example, the error percentages from the Liu et al. (2013) models are -1.14%, 13.24%, and 17.44% for specimens confined with 4, 6, and 8 layers of CFRP sheets, respectively. In the case of peak strain most of the models underestimate the peak strain especially for specimens with lower number of CFRP sheets. Almost all of the models overestimate the ductility factor (μ_{cu}). Similarly the error in predicting the energy absorption capacity was not reasonable in most models, where **Table 6-8,** shows errors over 30% at 6 and 8 layers, except for the Jiang and Teng (2006) model. The other factors showed high percentage of error for all models.

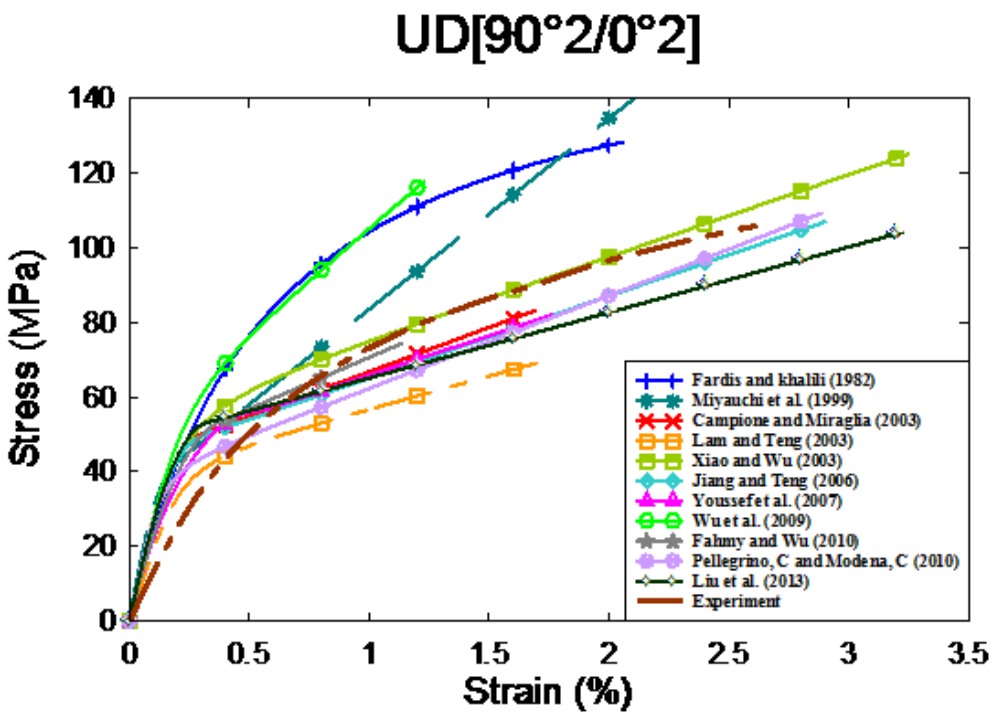

Figure 6-36 Stress-strain prediction of different models (4 layers)

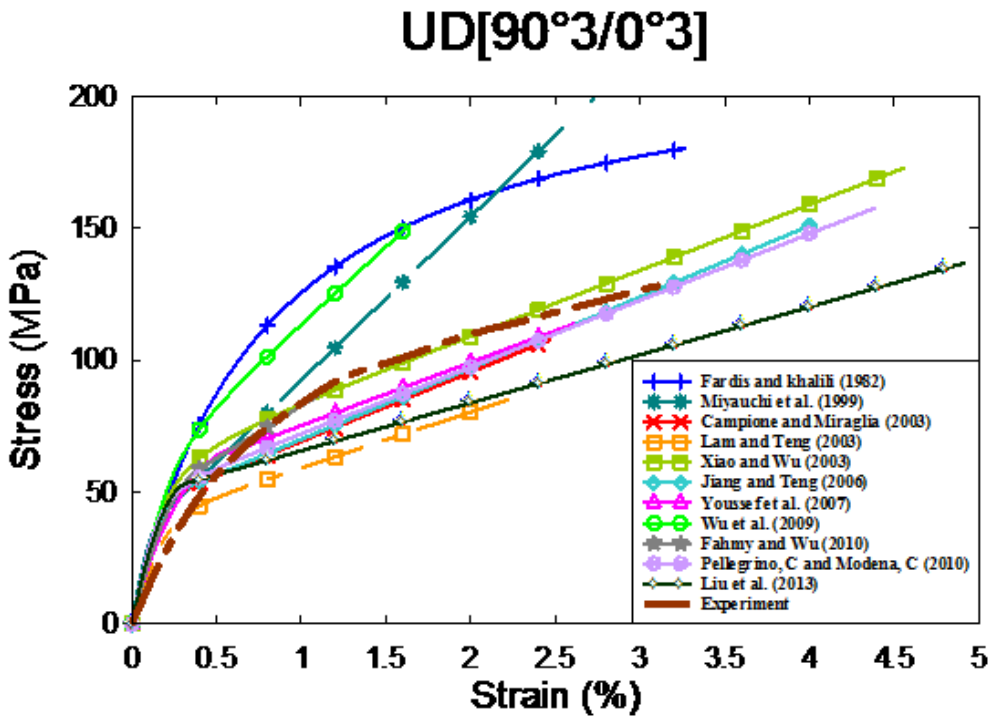

Figure 6-37 Stress-strain prediction of different models (6 layers)

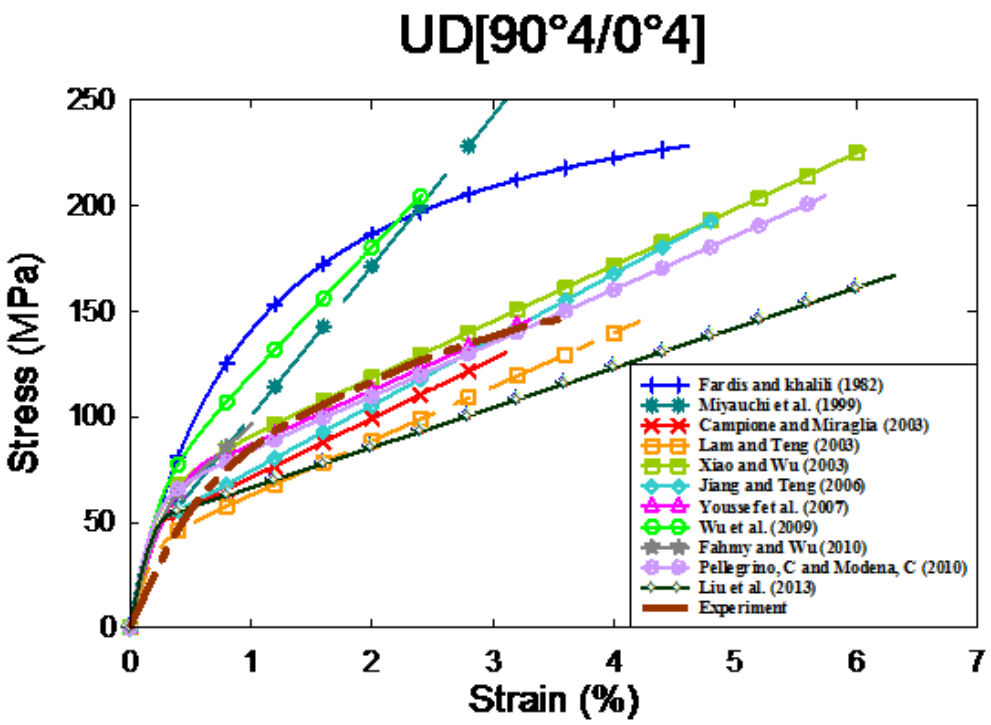

Figure 6-38 Stress-strain prediction of different models (8 layers)

Table 6-8 Prediction of different factors by existing proposed models

Author	# Layers	UD[90˚x/0˚x]							
		f'_{cc}	ε'_{cc}	K_1	μ_{cu}	e_{cu}	w_{cu}	f_l	ε_1
Experiment	4	105.42	0.03	2.58	2.58	2.48	1.84	24.21	0.01
	6	120.83	0.04	2.39	2.79	3.25	1.92	32.51	0.01
	8	141.94	0.04	2.17	2.70	4.47	1.96	45.68	0.02
Fardis and Khalili 1982	4	128.28	0.02	3.82	3.10	1.94	2.27	22.33	0.01
	Error (%)	21.69	-37.70	48.00	20.15	-21.71	23.80	-7.75	-48.78
	6	180.35	0.03	4.10	3.87	4.43	2.91	33.50	0.01
	Error (%)	49.26	-16.64	71.55	38.65	36.38	51.74	3.05	-42.33
	8	228.07	0.05	4.14	3.84	8.05	2.94	44.67	0.01
	Error (%)	60.69	6.04	90.94	42.19	80.07	49.84	-2.22	-26.42
Miyauchi et al. 1999	4	183.60	0.03	2.98	15.48	3.17	9.03	47.18	0.00
	Error (%)	74.17	-10.46	15.50	500.23	27.93	391.34	94.88	-85.27
	6	253.90	0.04	2.98	19.48	5.11	10.87	70.77	0.00
	Error (%)	110.13	-7.99	24.69	597.77	57.32	466.89	117.69	-87.35
	8	324.20	0.04	2.98	23.08	7.31	12.53	94.36	0.00
	Error (%)	128.41	-4.47	37.33	753.99	63.51	538.14	106.57	-88.96
Campione and Miraglia 2003	4	84.60	0.02	1.86	4.91	0.86	2.95	22.33	0.00
	Error (%)	-19.75	-48.74	-27.80	90.55	-65.29	60.41	-7.75	-73.43
	6	110.00	0.02	2.00	5.35	1.31	2.87	33.50	0.00
	Error (%)	-8.96	-43.24	-16.32	91.76	-59.67	49.44	3.05	-71.61
	8	133.28	0.02	2.02	4.95	3.77	5.75	44.67	0.00
	Error (%)	-6.10	-43.94	-6.86	83.36	-15.67	192.89	-2.22	-69.83
Lam and Teng 2003	4	83.22	0.02	3.07	5.64	1.02	4.08	13.09	0.00
	Error (%)	-21.05	-48.79	19.12	118.71	-58.84	122.18	-45.94	-76.87
	6	107.78	0.02	3.30	8.16	1.82	5.57	19.63	0.00
	Error (%)	-10.80	-36.96	38.08	192.16	-43.97	190.65	-39.61	-79.30
	8	130.29	0.03	3.33	10.22	2.65	6.67	26.18	0.00
	Error (%)	-8.21	-28.38	53.68	278.11	-40.72	239.94	-42.70	-81.31
Xiao and Wu 2003	4	116.82	0.03	3.31	6.27	2.81	4.64	22.33	0.01
	Error (%)	10.82	-1.80	28.11	143.10	13.41	152.80	-7.75	-60.10
	6	171.19	0.05	3.83	8.97	5.18	5.46	33.50	0.01
	Error (%)	41.67	26.83	60.10	221.37	59.47	184.78	3.05	-62.14
	8	220.64	0.06	3.98	10.31	8.73	6.33	44.67	0.01
	Error (%)	55.45	48.16	83.27	281.44	95.28	222.50	-2.22	-61.68
Jiang and Teng 2006	4	106.91	0.03	2.86	9.73	2.13	6.68	22.33	0.00
	Error (%)	1.41	-12.28	10.91	277.13	-14.04	263.61	-7.75	-77.03
	6	151.56	0.04	3.24	13.26	3.87	8.41	33.50	0.00
	Error (%)	25.43	2.65	35.59	374.78	19.14	338.64	3.05	-79.26
	8	192.85	0.05	3.35	15.64	5.63	9.48	44.67	0.00
	Error (%)	35.87	10.78	54.59	478.75	25.93	382.88	-2.22	-81.11

Author	# Layers	UD[90˚x/0˚x]							
		f'_{cc}	ε'_{cc}	K_1	μ_{cu}	e_{cu}	w_{cu}	f_l	ε_1
Youssef 2007	4	82.03	0.02	1.75	3.17	1.06	2.32	22.33	0.01
	Error (%)	-22.18	-46.62	-32.26	22.81	-57.22	26.21	-7.75	-57.07
	6	113.82	0.03	2.11	3.71	2.07	2.59	33.50	0.01
	Error (%)	-5.81	-33.39	-11.55	32.92	-36.27	34.79	3.05	-51.93
	8	145.80	0.03	2.30	3.93	3.30	2.69	44.67	0.01
	Error (%)	2.72	-24.04	6.06	45.26	-26.18	37.04	-2.22	-48.41
Wu et al. 2009	4	109.56	0.01	2.98	3.78	0.95	2.66	22.33	0.00
	Error (%)	3.93	-62.78	15.51	46.43	-61.66	44.80	-7.75	-74.89
	6	150.20	0.02	3.20	4.31	1.92	2.98	33.50	0.00
	Error (%)	24.31	-52.84	33.89	54.31	-40.89	55.35	3.05	-70.68
	8	187.45	0.02	3.23	4.26	3.08	2.90	44.67	0.01
	Error (%)	32.06	-44.48	49.02	57.55	-31.11	47.63	-2.22	-65.23
Fahmy and Wu 2010	4	74.38	0.01	1.41	3.05	0.61	2.21	22.33	0.00
	Error (%)	-29.44	-65.67	-45.54	18.46	-75.38	20.11	-7.75	-71.37
	6	86.81	0.01	1.31	2.81	0.66	1.94	33.50	0.00
	Error (%)	-28.16	-71.86	-45.28	0.73	-79.68	1.07	3.05	-73.20
	8	96.98	0.01	1.21	2.43	0.65	1.60	44.67	0.00
	Error (%)	-31.67	-76.65	-44.31	-10.07	-85.46	-18.27	-2.22	-74.38
Pellegrino and Modena 2010	4	109.22	0.03	2.96	9.14	2.08	6.03	22.33	0.00
	Error (%)	3.61	-12.68	14.92	254.36	-16.06	228.09	-7.75	-75.66
	6	157.56	0.04	3.42	10.26	4.42	6.57	33.50	0.00
	Error (%)	30.39	11.81	43.08	267.58	36.07	242.54	3.05	-70.82
	8	204.41	0.06	3.61	8.85	7.48	5.63	44.67	0.01
	Error (%)	44.02	32.28	66.53	227.46	67.32	186.79	-2.22	-60.14
Liu et al. 2013	4	104.21	0.03	2.74	9.99	2.40	7.12	22.33	0.00
	Error (%)	-1.14	-2.34	6.23	287.40	-3.14	287.81	-7.75	-75.10
	6	136.84	0.05	2.80	15.17	4.48	10.10	33.50	0.00
	Error (%)	13.24	25.44	17.20	443.48	37.92	426.85	3.05	-77.86
	8	166.69	0.06	2.77	19.44	6.71	12.39	44.67	0.00
	Error (%)	17.44	45.19	27.61	619.30	50.09	531.36	-2.22	-80.08

6.3.9 Predictions for Series 7 W[±45˚]

Figure 6-39, Figure 6-40 and **Figure 6-41** show comparisons between experimental and analytical responses for the Series 2 specimens having 4, 6 and 8 layers of CFRP. **Table 6-9** compares the peak stress, peak strain, strength, ductility and toughness parameters obtained from the analytical and experimental stress-strain curves, based on the average of 5 samples. **Figure 6-39** shows that the best overall predictions were obtained for the Lam and Teng (2003) and Jiang and Teng (2006) models. The predictions from these models were better in specimens with 4 layers of CFRP. It is clear from **Figure 6-40** and **Figure 6-41,** stiffness of the second branch of the curve is increasing in all the models, whereas this is not observed in the experimental curves. Most models failed to predict the peak stress as it is clear from the results in **Table 6-9.** The provision of fibers aligned in angle direction (±45º) allowed for high strain capacity in this series and this was not captured by most of the models which underestimate the peak strain. Since the errors are high for peak stress and strain, the remaining stress-strain factors showed poor predictions.

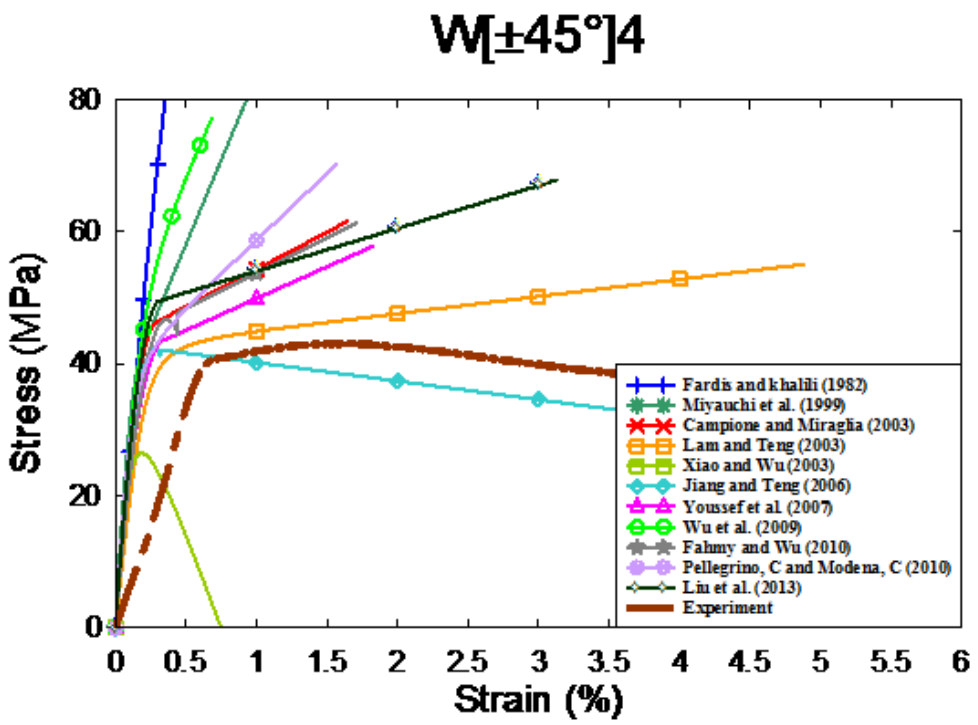

Figure 6-39 Stress-strain prediction of different models (4 layers)

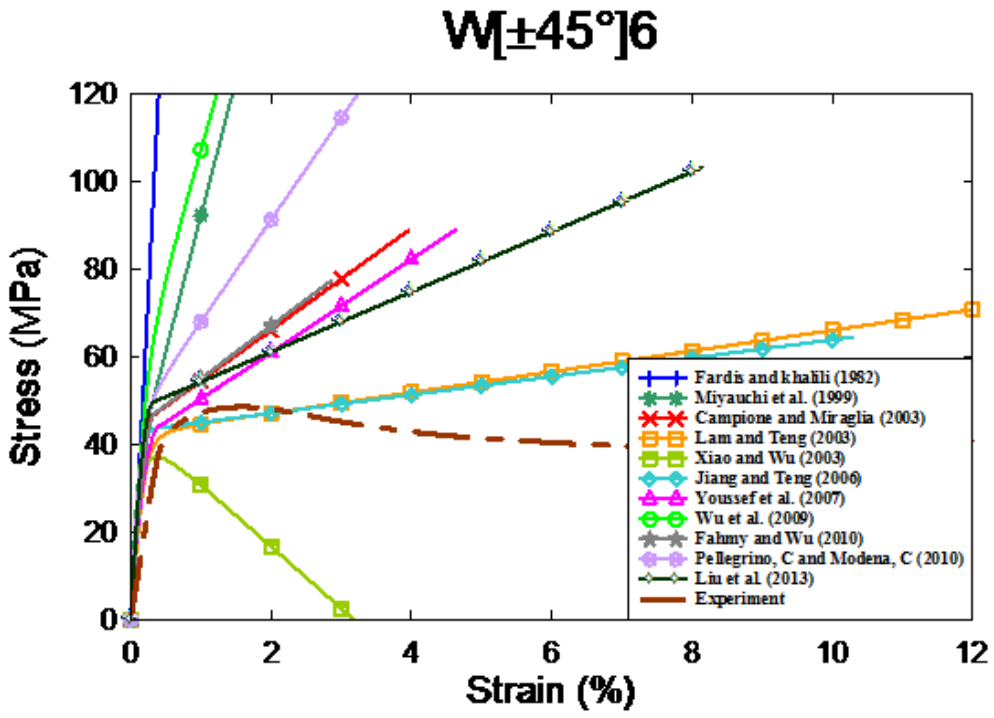

Figure 6-40 Stress-strain prediction of different models (6 layers)

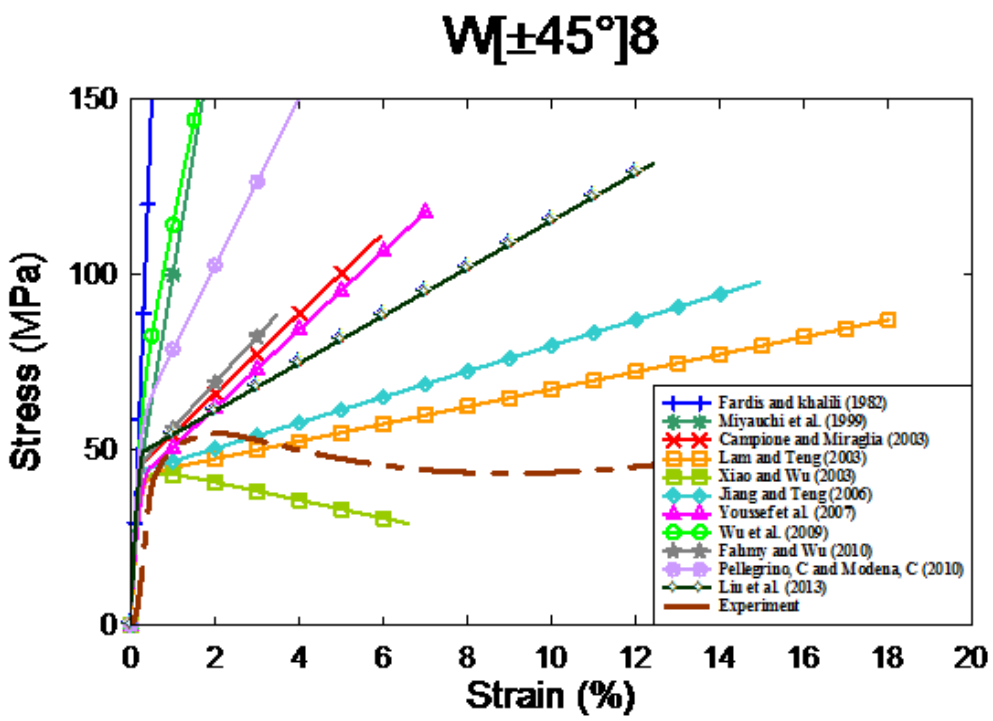

Figure 6-41 Stress-strain prediction of different models (8 layers)

Table 6-9 Prediction of different factors by existing proposed models

Author	# Layers	W[±45°]							
		f'_{cc}	ε'_{cc}	K_1	μ_{cu}	e_{cu}	w_{cu}	f_l	ε_1
Experiment	4	43.76	0.04	0.13	5.13	1.47	4.22	5.74	0.01
	6	49.42	0.14	0.74	16.49	5.56	13.01	8.61	0.01
	8	56.48	0.15	1.17	17.38	7.43	14.62	11.49	0.01
Fardis and Khalili 1982	4	82.32	0.00	4.10	1.09	0.16	0.58	9.59	0.00
	Error (%)	88.12	-90.98	3053.85	-78.71	-89.08	-86.30	67.08	-58.40
	6	140.42	0.00	4.10	1.31	0.24	0.49	23.76	0.00
	Error (%)	184.11	-96.81	454.05	-92.03	-95.69	-96.21	175.96	-61.11
	8	187.32	0.01	4.10	1.56	0.01	0.01	35.20	0.00
	Error (%)	231.69	-96.06	250.43	-91.04	-99.92	-99.95	206.35	-55.58
Miyauchi et al. 1999	4	183.60	0.03	2.98	15.48	3.18	9.05	47.18	0.00
	Error (%)	319.56	-27.14	2192.31	201.89	116.94	114.42	721.98	-76.32
	6	253.90	0.04	2.98	19.48	5.11	10.87	70.77	0.00
	Error (%)	413.73	-74.76	302.70	18.16	-8.14	-16.44	721.98	-79.25
	8	324.20	0.04	2.98	23.08	7.31	12.53	94.36	0.00
	Error (%)	474.06	-73.12	154.70	32.74	-1.61	-14.31	721.26	-79.55
Campione and Miraglia 2003	4	62.18	0.05	2.00	8.12	2.31	6.19	9.59	0.01
	Error (%)	42.10	20.00	1438.46	58.40	57.59	46.51	67.08	-25.66
	6	90.52	0.13	2.00	15.59	7.32	9.84	23.76	0.01
	Error (%)	83.15	-10.31	170.27	-5.47	31.59	-24.40	175.96	-7.87
	8	113.40	0.18	2.00	32.98	11.61	18.75	35.20	0.01
	Error (%)	100.80	16.53	70.94	89.69	56.27	28.27	206.35	-37.97
Lam and Teng 2003	4	61.55	0.02	3.30	5.72	0.82	4.63	5.62	0.00
	Error (%)	40.64	-59.50	2438.46	11.57	-44.06	9.67	-2.09	-64.38
	6	88.95	0.04	3.30	13.73	2.57	10.03	13.92	0.00
	Error (%)	79.97	-72.31	345.95	-16.73	-53.80	-22.93	61.71	-67.71
	8	111.07	0.06	3.30	10.26	4.53	7.06	20.63	0.01
	Error (%)	96.67	-61.61	182.05	-40.97	-39.02	-51.73	79.52	-34.34
Xiao and Wu 2003	4	-72.36	0.02	-12.03	8.92	-0.30	1.88	9.59	0.00
	Error (%)	-265.35	-51.69	-9352.46	74.05	-120.47	-55.37	67.08	-72.76
	6	-22.71	0.05	-2.77	7.81	0.52	-3.90	23.76	0.01
	Error (%)	-145.95	-67.91	-473.73	-52.63	-90.65	-129.98	175.96	-34.21
	8	25.77	0.07	-0.49	12.83	2.40	18.10	35.20	0.01
	Error (%)	-54.37	-57.27	-141.84	-26.18	-67.70	23.83	206.35	-41.55
Jiang and Teng 2006	4	30.83	0.04	-1.27	15.75	1.56	18.43	9.59	0.00
	Error (%)	-29.55	6.39	-1076.29	207.12	6.42	336.41	67.08	-66.00
	6	64.59	0.10	0.91	36.89	5.50	30.52	23.76	0.00
	Error (%)	30.69	-27.95	22.80	123.74	-1.13	134.55	175.96	-68.73
	8	97.79	0.15	1.56	53.23	10.47	38.18	35.20	0.00
	Error (%)	73.16	-3.41	33.04	206.18	40.93	161.20	206.35	-68.15

Author	# Layers	W[±45°]							
		f'_{cc}	ε'_{cc}	K_1	μ_{cu}	e_{cu}	w_{cu}	f_l	ε_1
Youssef 2007	4	57.83	0.02	1.55	5.14	0.85	4.13	9.59	0.00
	Error (%)	32.15	-54.96	1089.41	0.31	-42.01	-2.19	67.08	-55.94
	6	89.09	0.05	1.94	10.68	2.94	7.61	23.76	0.00
	Error (%)	80.26	-67.59	162.15	-35.22	-47.15	-41.50	175.96	-51.41
	8	118.33	0.07	2.14	14.40	5.51	9.52	35.20	0.00
	Error (%)	109.53	-54.43	82.92	-17.15	-25.83	-34.85	206.35	-44.46
Wu et al. 2009	4	73.69	0.01	3.20	2.71	0.36	1.93	9.59	0.00
	Error (%)	68.39	-83.12	2361.54	-47.11	-75.44	-54.27	67.08	-68.68
	6	119.03	0.01	3.20	3.50	1.15	2.46	23.76	0.00
	Error (%)	140.84	-90.38	332.43	-78.78	-79.33	-81.11	175.96	-55.95
	8	155.64	0.02	3.20	5.63	2.07	3.88	35.20	0.00
	Error (%)	175.59	-87.50	173.50	-67.62	-72.14	-73.48	206.35	-61.03
Fahmy and Wu 2010	4	61.25	0.02	1.90	4.93	0.84	3.96	9.59	0.00
	Error (%)	39.97	-57.97	1363.99	-3.79	-42.70	-6.22	67.08	-57.13
	6	77.44	0.03	1.45	8.18	1.66	6.15	23.76	0.00
	Error (%)	56.70	-80.05	95.91	-50.38	-70.16	-52.71	175.96	-60.96
	8	88.35	0.03	1.29	9.89	2.22	7.19	35.20	0.00
	Error (%)	56.45	-77.61	10.12	-43.11	-70.12	-50.85	206.35	-60.27
Pellegrino and Modena 2010	4	70.18	0.02	2.83	5.25	0.81	3.86	9.59	0.00
	Error (%)	60.39	-61.41	2080.42	2.32	-44.74	-8.59	67.08	-62.98
	6	120.17	0.03	3.25	5.48	2.62	3.70	23.76	0.01
	Error (%)	143.14	-77.35	338.89	-66.74	-52.90	-71.60	175.96	-33.88
	8	164.26	0.05	3.45	9.22	4.94	6.05	35.20	0.00
	Error (%)	190.86	-70.34	194.44	-46.97	-33.51	-58.61	206.35	-43.54
Liu et al. 2013	4	67.78	0.03	2.58	10.03	1.75	8.29	9.59	0.00
	Error (%)	54.88	-23.09	1887.17	95.66	19.38	96.24	67.08	-61.42
	6	103.34	0.08	2.54	26.09	6.09	18.89	23.76	0.00
	Error (%)	109.09	-43.02	243.18	58.22	9.47	45.16	175.96	-65.03
	8	131.90	0.12	2.53	39.85	11.10	26.98	35.20	0.00
	Error (%)	133.55	-19.56	115.86	129.21	49.41	84.57	206.35	-64.57

7 Chapter 7: Conclusions

7.1 Summary

This thesis presented the results of a research program investigating examining the effect of parameters such as fiber orientation, amount of confinement, and specimen size on the behavior of FRP-confined concrete. As part of the experimental study, a large set of concrete cylinders having two different sizes were confined with carbon fiber reinforced polymer (CFRP) sheets having various orientations and tested under pure axial compressive loading. The specimens were confined using various CFRP stacking sequences, with fibers oriented at 0°, 90°, and ±45° (both unidirectional and woven). Furthermore, within each stacking sequence, the numbers of layers was varied between 4, 6, and 8 to examine the impact of number of plies on the behavior of the FRP-confined concrete cylinders. In addition, the research program included a large of CFRP coupons made from CFRP laminates having the same properties as the CFRP jackets used in the strengthening of the cylinder series. The analytical program assessed the accuracy and suitability of using various FRP confinements to predict the stress-strain response of the confined cylinders tested in the experimental program. This chapter provides a summary of the findings from this research program as well as the recommendations for the future work.

7.2 Conclusions

7.2.1 Experimental program

The results from the experimental program indicate that parameters such as fiber orientation, stacking sequence, number of confinement layers and specimen size have a direct impact on the strength, ductility and stress-strain behavior of CFRP confined concrete. However, the level of influence varies from one parameter to the other, with the results demonstrating that fiber orientation has a more noticeable effect when compared to the other parameters.

7.2.1.1 Coupon tests

The following conclusions can be drawn based on the findings from the coupon tests:

1- Effect of stacking sequence

Coupons with fibers aligned in hoop direction showed the best overall behavior in terms of maximum strength. On the other hand maximum ductility was obtained by coupons having fibers in the angular direction. All other stacking orders fall in between these two extremes. In addition to that, coupons with unidirectional 0^o fibers showed linear elastic behavior while coupons with angular fibers showed non-linear behavior.

2- Effect of number of layers

Load carrying capacity increased by adding more CFRP sheets, however no significant changes were observed in the case of maximum deformation.

3- Effect of X vs Y

Coupons were cut in both X and Y direction to have better insight on the stress-strain behavior of CFRP coupons in different direction. The trends varied from one series to the other were observed, although the variations in X and Y were relatively small.

4- Effect of parameters on failure mode

In all the cases failure mode the various series with different stacking sequence, even by increasing the number of layers, was generally the same consisting of lateral rupture either in the middle or end regions, however angular failures were observed in those series with purely +45 and -45^o fibers .

7.2.1.2 Cylinder tests

The following conclusions can be drawn based on the findings from the cylinder tests:

1- The stress-strain behavior of FRP-confined concrete is strongly influenced FRP fiber orientation and stacking sequence;

2- Cylinders confined with unidirectional fibers aligned in the hoop direction (UD [0^o]) show a bilinear response which has been reported by other researchers, with an initial ascending parabolic branch, followed by a quasi-linear secondary branch with increase in stress and strain until brittle failure of the FRP jacket.

3- Cylinders confined with angular fibers (45^o) show a different response, with limited increase in peak stress and significant increase in strain capacity, with a distinct stress-strain plateau after peak stress. The response of cylinders with angular unidirectional (UD[+45˚/-45˚]) vs. woven CFRP (W[±45˚]) was similar, although some changes in the post-peak response was observed in the case of specimens confined with woven CFRP;

4- In this study it was observed that the stress–strain curves of cylinders with different layup configurations follow the trend of the strongest fibers. For example, in the case of UD[90˚/0˚], UD[90˚/0˚]W[±45˚], UD[0˚]$_2$W[±45˚]$_2$, the curve trend was found to be dominated by the UD[0˚] sheets, although the other fiber orientations modify some aspects of the stress-strain response (e.g. rounding of transition point when 90˚ CFRP sheets are added, and effects on strength, stiffness and strain capacity when 45˚ CFRP sheets are used);

5- Peak stress and strain capacity of CFRP-confined concrete increases proportionally with the number of CFRP layers, although the efficiency and contribution of additional CFRP sheets reduces once the number of sheets reaches a certain threshold (for example the

specimens generally showed increases in strength or toughness when going from 4 to 6 sheets, with limited supplementary improvements when going to 8 sheets);

6- A similar observation was made in the case of energy absorption capacity, with the overall toughness increasing with the number of CFRP layers, up to a certain ply limit, which depended on the FRP stacking sequence. Less significance was observed due to increase in the number CFRP layers in the case of ductility enhancement;

7- Size is an important parameter affecting the stress-strain response of CFRP-confined concrete, with peak stress, failure strain and overall toughness generally reduced when the cylinder size is increased from 100 mm to 150 mm. The results indicate the need for further studies examining the effect of size on the response of larger scale columns;

8- Cylinders confined with composite layups having higher modulus of elasticity showed steeper response in the second branch of the stress-strain curve. CFRP jackets with higher rupture strains generally showed improved toughness and greater ductility improvement;

9- Different stress-strain responses were observed in series with identical CFRP sheets but configured using different stacking sequence/order;

10- Brittle fracture of CFRP jackets was experienced in specimens confined with unidirectional fibers aligned in the hoop direction due to radial expansion of concrete core under axial loading. The failures became more brittle and explosive as the number of UD[0˚] CFRP plies was increased.

11- Specimens having layups with unidirectional fibers aligned in the vertical direction showed signs buckling in the CFRP jacket even though fibers were not loaded directly;

12- Specimens confined with angular fibers showed gradual and ductile failures, avoiding brittle fiber fractions since they are not loaded to their elastic limits. Eventual failures

were controlled, with gradual tearing of the CFRP jacket and minimal expulsion of core concrete at failure.

13- Specimens confined with layups consisting of multiple fiber orientations, showed a hybrid failure response with failure mode affected by the type and combination of CFRP orientations as well as sequence of stacking. For example cylinders with angular CFRP in the innermost layers and unidirectional fibers on the outermost layers showed more ductile failures where angular fibers prevented concrete fragmentation and spalling, while hoop direction fibers increase strength significantly.

7.2.2 Conclusions from analytical program

The following conclusions can be drawn based on the findings of the analytical study and the comparisons between experimental and analytical stress-strain curves:

1- Researchers have proposed a large number of analytical models to predict the stress-strain response of FRP-confined concrete, however most models, which have been calibrated based on data from cylinders confined with FRP having fibers aligned in the hoop direction, are not suitable to predict the stress-strain behavior of concrete cylinders retrofitted with CFRP jackets with varying orientations and layup sequences;

2- Most existing models over predict the stress especially at the presence of angular fibers. In overall, none of the models are capable to predict the stress-strain precisely. Most models provide reasonable accurate prediction in the case of cylinders confined with unidirectional fibers in the hoop direction. The accuracy of models becomes less as the number of layers increased or other fiber orientations are introduced. Similar observations were achieved in the case of prediction of peak strain with a less accuracy compare to prediction of peak stress.

3- Overall, the following models provide relatively more accurate predictions of stress-strain behavior of cylinders confined with different CFRP layup configurations: Jiang and Teng (2006), Pellegrino and Modena (2010) and Liu et al. (2013)
4- Finally, there is a need for further research to develop new stress-strain models (or re-calibrate existing models) to account for the effect of FRP fiber orientation and stacking sequence.

7.3 Recommendation for future work

The following research is recommended to further understanding related to the stress-strain behavior of FRP-confined concrete having various parameters:

1- This study showed that size effect is an important parameter affecting the stress-strain response of FRP-confined concrete. While two cylinders sizes were considered in this study, both can be categorized as "small" when compared to practical columns in structures; there is a need for further experimental research on larger scale columns having practical dimensions to investigate the effect of various parameters such as number of layers, fiber orientation and stacking sequence on column performance;
2- Further investigations are required to investigate the effect of stacking sequence and fiber orientation to evaluate possible benefits associated with different fiber orientations, particularly in the case of fibers aligned in the vertical direction. This can include tests on more slender columns, columns tested under eccentric loads, beams tested under combined axial and quasi-static lateral loads, and columns tested under simulated earthquake or blast loads;
3- Existing analytical models need to refined and re-calibrated in order to properly predict the compressive stress-strain behavior of FRP-confined concrete having various fiber

orientations and stacking sequences. There is a need for both experimental data to calibrate these models as well as analytical studies to redefine model parameters that can affect the stress-strain response;

4- The cylinders and coupons in this research study were tested with minimal instrumentation. Further testing should be conducted with specimens using advanced instrumentation and testing techniques to capture important parameters such actual confining pressure and rupture strains in CFRP jackets, with comparison to data gathered from coupon testing.

5- Further research on cylinders and structural components with different fiber orientations and stacking sequences but manufactured using different fibers materials (glass - GFRP, aramid - AFRP), resin (matrix) types and sheet type (unidirectional and woven).

8 References

Abbasnia, R., Ahmadi, R., and Ziaadiny, H. (2012). “Effect of Confinement Level, Aspect Ratio and concrete strength on the Cyclic Stress-Strain Behavior of FRP-Confined Concrete Prisms”. Composites, Part B: Engineering, 43(2), 825-831.

Abbasnia, R., and Holakoo, A. (2012).”An Investigation of Stress-Strain Behavior of FRP-Confined Concrete under Cyclic Compressive Loading.” International Journal of Civil Engineering, 10(3), 201-209.

Abbasnia, R., Hosseinpour, F., Rostamian, M., and Ziaadiny, H. (2013).”Cyclic and Monotonic Behavior of FRP Confined Concrete Rectangular Prisms with Different Aspect Ratios.” Construction and Building Materials, 40, 118-125.

Aire, C., Gettu, R., Casas, J. R., Marques, S., and Marques, D. (2010). “Concrete Laterally Confined with Fiber-Reinforced polymers (FRP): Experimental Study and Theoretical Model.” Materials de Construccion, 60(297), 19-31.

Au, C., and Buyukozturk, O. (2005). “Effect of Fiber orientation and Ply Mix on Fiber Reinforced Polymer-Confined Concrete.” Journal of Composites for Construction, 9(5), 397-407.

Benzaid, R., Chikh, N.E., and Mesbah, H. (2008). “Behavior of Square Concrete Column Confined with GFRP Composite warp.” Journal of Civil Engineering and Management, 14(2), 115-120.

Campione, G., & Miraglia, N. (2003). Strength and strain capacities of concrete compression members reinforced with FRP. Cement and Concrete Composites, 25(1), 31-41.

Considere, A. (1902). “Experimental Research on Reinforced Concrete.” Translated and Arranged by Leon S, Moisseiff, McGraw Publishing Co., New York.

Csuka, B., & Kollár, L. P. (2010).FRP-confined circular concrete columns subjected to concentric loading. Journal of Reinforced Plastics and Composites, 29(23), 3504-3520.

Cui, C. (2009). Behaviour of normal and high strength concrete confined with fibre reinforced polymers (FRP) (Doctoral dissertation, University of Toronto).

Cui, C., and Sheikh, S.A. (2010).”Experimental Study of Normal-and High-Strength Concrete Confined with Fiber-Reinforced Polymers.” Journal of Composites for Construction, 14(5), 553-561.

El-Hacha, R., and Mashrik, M.A. (2012).”Effect of SFRP Confinement on Circular and Square Concrete Columns.” Engineering Structures, 36, 379-393.

Elsanadedy, H.M., Al-Salloum, Y.A., Alsayed, S.H., and Iqbal, R.A. (2012).”Experimental and Numerical Investigation of Size Effects in FRP-Wrapped Concrete Columns.” Construction and Building Materials, 29, 56-72.

Fardis, M.N. and Khalili, H.H. (1981). “Concrete Encased in Fiberglass-Reinforced Plastic.” ACI Journal. (78)6, 440-446.

Fardis, M.N. and Khalili, H.H. (1982). “FRP-Encased Concrete as a Structural Material.” Magazine of Concrete Research. 34(121), 191-202.

Gajdosova, K., and Bilcik, J. (2013).”Full-Scale Testing of CFRP-Strengthened Slender Reinforced Concrete Columns.” Journal of Composites for Construction, 17(2), 239-248.

Gernouti, Y., and Rabehi, B. (2010).”FRP-Confined Short Concrete Columns under Compressive Loading: Experimental and Modeling Investigation.” Journal of Reinforced Plastics and Composites, 0731684410393054.

Hadi, M.N.S., and Le, T.D. (2014).”Behavior of Hollow Core Square Reinforced Concrete Columns Wrapped with CFRP with Different Fiber Orientations.” Construction and Building Materials, 50, 62-73.

Han, Y.Y., Zhang, H., Li, Y.Q., Yao, J., and Hu, X.P. (2012, March).”Experimental Study on Axial Compression of FRP Confined Concrete Column.” In Advanced Materials Research, (vol. 461, pp. 682-685).

Harries, K.A., and Kharel, G. (2002). “Behavior and Modelling of Concrete Subject to Variable Confining Pressure.” ACI Materials Journal, 99(2), 180-189.

Hong, W. K., & Kim, H. C. (2004). “Behavior of Concrete Columns Confined by Carbon Composite Tubes”. Canadian Journal of Civil Engineering, 31(2), 178-188.

Hoshikuma, J., K. Kawashima, K. Nagaye and A. W. Taylor. (1997). “Stress-Strain Model for Confined Reinforced Concrete in Bridge Pier.” Journal of Structural Engineering, ASCE, 123(5):624-633.

Ilki, A. Kumbasar, N., and Koc, V. (2002). “Strength and Deformability of Low Strength Concrete Confined by Carbon Fiber Composite Sheets.” In proceedings of the 15th ASCE Engineering Mechanics Conference, New York, On CD. Paper (No. 101).

Ilki, A., Peker, O., Karamuk, E., Demir, C., and Kumbasar, N. (2008). “FRP Retrofit of Low and Medium Strength Circular and Rectangular Reinforced Concrete Columns.”Journal of Materials in Civil Engineering, 20(2), 169-188.

Kestner, J., Harries, K.A., Pessiki, S.P., Sause, R., and Ricles, J. (1998).”Rehabilitation of Reinforced Concrete Columns Using Fiber Reinforced Polymer Composite Jackets.” ATLSS, Rep. No. 97-07, Lehigh University, Bethlehem, Pa.

Kumutha, R., & Palanichamy, M. S. (2006). “Investigation of reinforced concrete columns confined using glass fiber-reinforced polymers”. Journal of reinforced plastics and composites, 25(16), 1669-1678.

Kumutha, R., Vaidyanathan, R., and Palanichamy, M. S. (2007). “Behavior of Reinforced Concrete Rectangular Columns Strengthened using GFRP. Cement and Concrete Composites, 29(8), 609-615.

Li, G. (2006).”Experimental Study of FRP Confined Concrete Cylinders.” Engineering Structures, 28(7), 1001-1008.

Li, G., Maricherla, D., Singh, K., Pang, S. S., and John, M. (2005). “Effect of Fiber Orientation on the Structural Behavior of FRP Wrapped Concrete Cylinders.” Composite Structures, 74(4), 475-483.

Li, Y., Lin, C., and Sung, Y. (2003). “A Constitute Model for Concrete Confined with Carbon Fiber Reinforced Plastics.” Mechanics of Materials, 35(6), 603-619.

Liang, M., Wu, Z.M., Ueda, T., Zhang, J.J., and Akogbe, R. (2012).”Experiment and Modeling on Axial Behavior of Carbon Fiber Reinforced Polymer Confined Concrete Cylinders with Different Sizes.” Journal of Reinforced Plastics and Composites, 31(6), 389-403.

Long, Y.L., and Zhu, J. (2014).”Experimental Study on Concrete Columns with Various Sizes Confined by BFRP and Hybrid FRP under Axial Compression.” Advanced Materials Research, 838, 407-411.

Martines, S., A. H. Nilson, and F. O. Slate. (1984). “Spirally In forced High-Strength Concrete Column.” ACI Journal, 81: 431-442.

Masia, M. J., Gale, T. N., and Shrive, N. G. (2004). “Size Effects in Axially Loaded Square-Section Concrete Prisms Strengthened Using Carbon Fiber Reinforced Polymer Wrapping”. Canadian Journal of Civil Engineering, 31(1), 1-13.

Mirmiran, A., & Shahawy, M. (1997). “Behavior of Concrete Columns Confined by Fiber Composites”. Journal of Structural Engineering, 123(5), 583-590.

Mohamed, H. M., & Masmoudi, R. (2010). “Axial Load Capacity of Concrete-Filled FRP Tube Columns: Experimental Versus Theoretical Predictions”. Journal of Composites for Construction, 14(2), 231-243.

Ozbakkaloglu, T. (2013). “Compressive Behavior of Concrete-Filled FRP Tube Columns: Assessment of Critical Column Parameters”. Engineering Structures, 51, 188-199.

Ozbakkaloglu, T. and Oehlers, D. J. (2008). “Concrete-Filled Square and Rectangular FRP Tubes under Axial Compression”. Journal of Composites for Construction, 12(4), 469-477.

Ozbakkaloglu, T., and Akin, E. (2011). “Behavior of FRP-Confined Normal-and High-Strength Concrete under Cyclic Axial Compression.” Journal of Composites for Construction, 16(4), 451-463.

Pantelides, C. P., & Yan, Z. (2007). Confinement model of concrete with externally bonded FRP jackets or posttensioned FRP shells. Journal of Structural Engineering, 133(9), 1288-1296.

Park, R., Priestley, M.J.N., and Gill, W.D. (1982). “Ductility of Square-Confined Concrete Columns.” Journal of the Structural Division, ASCE, 108(4), 929-950.

Parretti, R., and Nanni, A. (2002). “Axial Testing of Concrete Columns Confined with Carbon FRP: Effect of Fiber Orientation.” In CD Proc. Of the Third International Conference on Composites in Infrastructure.

Pellegrino, C., & Modena, C. (2010). Analytical model for FRP confinement of concrete columns with and without internal steel reinforcement. Journal of Composites for Construction, 14(6), 693-705.

Pham, T.M., Doan, L.V., and Hadi, M.N. (2013).”Strengthening Square Reinforced Concrete Columns by Circularisation and FRP Confinement.” Construction and Building Materials, 49, 490-499.

Purba, B. K., & Mufti, A. A. (1999). Investigation of the behavior of circular concrete columns reinforced with carbon fiber reinforced polymer (CFRP) jackets. Canadian Journal of Civil Engineering, 26(5), 590-596.

Rajappa, R.R. (2004).”Behavior of FRP Wrapped Concrete Cylinders.” ProQuest.

Richart, F. E., Brandtzaeg, A., and Brown, R. L. (1928). “A Study of the Failure of Concrete under Combined Compressive Stresses.” Bulletin No. 185, Engineering Experimental Station, University of Illinois, Urbana.

Rousakis, T.C., and Karabinis, A.I. (2012).”Adequately FRP Confined Reinforced Concrete Columns under Axial Compressive Monotonic or Cyclic Loading.” Materials and Structures, 45(7), 957-975.

Sadeghian, P., Rahai, A. R., and Ehsani, M. R. (2009). “Effect of Fiber Orientation on Nonlinear Behavior of CFRP composites.” Journal of Reinforced Plastics and Composites.

Sadeghian, P., Rahai, A. R., and Ehsani, M. R. (2010). “Effect of Fiber orientation on Compressive Behavior of CFRP-Confined Concrete Columns.” Journal of Reinforced Plastics and Composites, 29(9), 1335-1346.

Sheikh, S. A., and Uzummeri, S. M. (1982). “Analytical Model for Concrete Confinement in Tied Columns.” Journal of the Structural Division, 108(12), 2703-2722.

Song, X., Gu, X., Li, Y., Chen, T., and Zhang, W. (2012).”Mechanical Behavior of FRP-Strengthened Concrete Columns Subjected to Concentric and Eccentric Compression Loading.” Journal of Composites for Construction, 17(3), 336-346.

Tao, Z., Yu, Q., & Zhong, Y. Z. (2008). “Compressive Behavior of CFRP-Confined Rectangular Concrete Columns”. Magazine of Concrete Research, 60(10), 735-745.

Toutanji, H.A. (1999). “Stress-Strain Characteristics of Concrete Columns Externally Confined with Advanced Fiber Composite Sheets.” ACI Material Journal, 96(3), 397-404.

Vincent, T., and Ozbakkaloglu, T. (2013). “Influence of Fiber Orientation and Specimen End Condition on Axial compressive Behavior of FRP-Confined Concrete.” Construction and Building Materials, 47, 814-826.

Vincent, T., Ozbakkaloglu, T. (2013).”Influence of Concrete Strength and Confinement Method on Axial Compressive Behavior of FRP Confined High-and Ultra High-Strength Concrete.” Composites Part B: Engineering, 50, 413-428.

Wang, L. M., & Wu, Y. F. (2008). “Effect of Corner Radius on the Performance of CFRP-Confined Square Concrete Columns: Test”. Engineering Structures, 30(2), 493-505.

Wang, Y.F., and Wu, H.L. (2010).”Size Effect of Concrete Short Columns Confined with Aramid FRP Jackets.” Journal of Composites for Construction, 15(4), 535-544.

Wang, Z., Wang, D., Smith, S.T., and Lu, D. (2012). “Experimental Testing and Analytical Modeling of CFRP-Confined Large Circular RC Columns Subjected to Cyclic Axial Compression.” Engineering Structures, 40, 64-74.

Wei, Y. Y., & Wu, Y. F. (2012). Unified stress–strain model of concrete for FRP-confined columns. Construction and Building Materials, 26(1), 381-392.

Wu, H. L., Wang, Y. F., Yu, L., and Li, X. R. (2009). “Experimental and Computational Studies on High-Strength Concrete Circular Columns Confined by Aramid Fiber-Reinforced Polymer Sheets.” Journal of Composites for Construction, 13(2), 125-134.

Wu, Y. F., and Wei, Y. Y. (2010). “Effect of Cross-Sectional Aspect Ratio on the Strength of CFRP-Confined Rectangular Concrete Columns”. Engineering Structures, 32(1), 32-45.

Xiao, Q. G., Teng, J. G., and Yu, T. (2010). “Behavior and Modeling of Confined High-Strength Concrete.” Journal of Composites for Construction, 14(3), 249-259.

Xiao, Y., and Wu, H. (2000). “Compressive Behavior of Concrete Confined by Carbon Fiber Composite Jackets.” Journal of Materials in Civil Engineering, 12(2), 139-145.

Youssef, M.N., Feng, M.Q., and Mosallam, A.S. (2007).”Stress-Strain Model for Concrete Confined by FRP Composites.” Composites Part B: Engineering, 38(5), 614-628.

Zhou, C., Lu, X., Li, H., and Tian, T. (2013).”Experimental Study on Seismic Behavior of Circular RC Columns Strengthened with Pre-Stressed FRP Strips.” Earthquake Engineering and Engineering Vibration, 12(4), 625-642.